P.O.Box 2345, Beijing 100023,China
Fax: +86-10-85381893
E-mail: wjg@wjgnet.com www.wjgnet.com

World J Gastroenterol 2003;9(11):2385-2389
World Journal of Gastroenterology
 ISSN 1007-9327

• REVIEW •

Gut in diseases: Physiological elements and their clinical significance

Lian-An Ding, Jie-Shou Li

Lian-An Ding, Department of General Surgery, Affiliated Hospital of Medical School, Qingdao University, Qingdao 266003, Shandong Province, China
Jie-Shou Li, Institute of General Surgery, Clinical Medical College of Nanjing University, Nanjing 210002, Jiangsu Province, China
Correspondence to: Lian-An Ding, Male, Associate Professor of Medical School, Qingdao University, 16 Jiangsu Road, Qingdao 266003, Shandong Province, China. dlahaolq@hotmail.com
Telephone: +86-532-5646006 **Fax:** +86-532-2911840
Received: 2003-03-05 **Accepted:** 2003-06-02

Abstract

The intestinal barrier function of GI tract is very important in the body except for the function of digestion and absorption. The functional status of gut barrier basically reflects the stress severity when body suffers from trauma and various stimulations. Many harmful factors such as drugs, illnesses, trauma and burns can damage the gut barrier, which can lead to the barrier dysfunction and bacterial/endotoxin translocation. The paper discusses and reviews the concepts, anatomy, pathophysiology of gut barrier and its clinical relations.

Ding LA, Li JS. Gut in diseases: Physiological elements and their clinical significance. *World J Gastroenterol* 2003; 9(11): 2385-2389

http://www.wjgnet.com/1007-9327/9/2385.asp

INTRODUCTION

The gut has long been thought to be quiescent or inactive during illnesses. It has not been paid much attention and not protected just like other organs such as the heart, lung, and kidney in ICU patients. It is generally considered that biochemical metabolism of the body takes place mainly in the liver. Developments in studying technology and advances in surgical skills have led to a better understanding of nutrients metabolism, anatomic architecture and physiological functions of the gut. Gastrointestinal (GI) tract has functions not only to digest and absorb nutrients, but also to modulate systemic immunity and to prevent enteric bacterial/endotoxin' s invasion, so-called gut barrier function. Functional status of the gut sometimes determines the patients' prognosis and recovery from diseases. Some traditional managements are not beneficial or completely harmful to intestinal barrier capability, and aggravate the primary diseases the body suffers. There is a practical significance to further study the physiological functions of GI tract. An overall understanding of the mechanisms of pathophysiological changes of the gut in illness would make us take measurable treatments to patients clinically. This review deals with a series of new concepts and advances in research of intestinal barrier that might be helpful to clinicians.

INTESTINAL BARRIER AND RELATED CONCEPTS

Intestinal barrier function

The definition of intestinal barrier function means that the gut can prevent the harmful materials in intestinal lumen such as bacteria and endotoxin from entering other aseptic organs, tissues and blood circulation through intestinal mucous membrane. The gut barrier is chiefly composed of three components: mucous epithelia, intestinal flora, and secreting immunoglobulin and gut associated lymphatic tissues (GALT)[1], namely the ecological barrier (normal inhabitant flora within intestine), mechanical barrier (mucous epithelia) and immune barrier (or secreting IgA, miscellaneous immune cells including intraepithelial lymphocytes and macrophages, neutrophils, natural killer cells underlying the mucous membrane, Payer' s nodes and mesenteric lymph node). Among them mucous epithelium is the most important one that establishes a mechanical barrier between the lumen and blood circulation. The gut barrier in general term means this structural epithelia[2-5].

Architecture of intestinal barrier

There are two pathways for materials in the lumen when entering into the blood circulation through mucous membrane. One is the transcellular route, the other is the paracellular route, which occupies 5 % of the total intestinal surface area. These two configurations are the main constituents of epithelial barrier[3,6]. It is considered that there are dispersively nonpolarized holes which are full of water and have a radius of 0.3-0.8 nm on the top of villous cells and a tight-junction of 0.95 nm in radius between villous cells. Substances with different sizes of radius get across intestinal epithelia through transcellular or paracellular way when entering into the body. Molecules smaller than 0.3-0.8 nm in radius could enter into the mucous membrane through these holes. Molecules bigger than those such as disaccharides (lactulose and cellobiose etc) and ^{51}Cr-EDTA seem to enter into epithelia through paracellular tight-junctions. Based on this mechanism the intestinal permeability is measured by combining the smaller (such as monosaccharide) and bigger molecules (such as disaccharide) clinically and experimentally[3,6,7]. The two accesses are influenced by alterations of absorbing intestinal area. Substanecs absorbed by the intestine would reduce after atrophy of villi or bowel resection[3, 5-7].

Bacterial translocation

Bacteria come into aseptic tissues from the bowel lumen through mucosal barrier and colonize in tissues such as mesenteric lymph node, liver, spleen and blood. This process is called bacterial translocation (BT). Studies in experimental rodents showed that translocated bacteria seen most oftenly within intact epithelial cells were *Candida*, *E. coli*, *Proteus mirabilis*, *Enterococcus faecalis* and so on, whereas *E. coli* was common and anaerobes and fungi were rare in human beings[1,8]. Endotoxin could pass through bowel wall into the body easier than bacteria in the lumen[9].

Mechanisms of intestinal barrier damage

Hunger, malnutrition and longer parenteral nutrition could cause intestinal mucosa atrophy and impair the mechanical bowel barrier[1,3,10,11]. Shock, ischemia/reperfusion damage, endotoxin of bacteria are the factors that lead to deterioration of intestinal barrier[4,12]. It was found that changes in

prostaglandin and related enzymes-Ca^{++} and cAMP system within cells affected significantly the structure of gut barrier. Non-steroid anti-inflammatory drugs (NSAIDs) could destroy the system and increase the intestinal permeability. Thus it caused bacteria/endotoxin translocating from intestinal lumen into blood circulation and other aseptic tissues, and sepsis would ensue[2,6]. Because of the increments of intestinal permeability, a series of alterations occurred, such as edema of tissues underlaid mucous membrane, microvasculature compression, stasis of blood circulation and thrombosis in microvasculature system. These patho-physiological changes impaired the microvasculature underlaid mucosa and aggravated further the damage of mucosal barrier[2]. Animal experiments showed that treatment with non-steroid anti-inflammatory drugs in aseptic rats did not cause impairment of intestinal mucous membrane. The clinical symptoms were remitted evidently by treatment with metronidazol to human bowel lesions caused by NSAIDs[13]. Managements with antibiotics in rats (it decreased the bacteria load within the intestine) also prevented NSAIDs from inducing intestine inflammation. In addition, the method of fasting for reducing bacterial antigen in alimentary tract could counteract inflammatory intestinal lesions that caused by NSAIDs either[2,14]. Studies showed that factors causing alterations in hormones secreted by mucous enterocytes and changes of related enzymatic system caused damage of intestinal barrier, and the enteric bacteria and endotoxin reinforced the damage. Prabhu *et al*[15] concluded from researches in rats that surgical stress in the small intestine caused structural and functional alterations in the brush border membrane (BBM) through oxidative stress which could affect gut barrier integrity and the generation of arachidonic acid, might mediate distal organ dysfunction. Activation of phospholipase A2 during the process was considered as a pivotal step. Other investigations discovered that the increment of intestinal permeability was mainly due to the relaxation of the tight-junction between intestinal epithelial cells, indicating that there are close connections between changes in tight-junction and cytoskeleton. Any drugs or chemical materials that could impact on cytoskeleton such as lipopolysaccharide, growth factors, cytokines, and hormones, would affect the intestinal permeability[16].

Nitric oxide and intestinal barrier

Nadler *et al*[12] considered that various insults working on human body could cause overexpression of inducible nitric oxide synthase (iNOS) and hence a redundant production of nitrix oxide (NO) occurred. This higher concentration of NO could lead to deposition of protein salts of nitrite-peroxide (and nitric-peroxide) on mitochondrial membrane, impair mitochondrial membrane potential (or permeability) or decrease ATP production. It would destroy the cellular respiratory function and aggravate cellular apoptosis, thus resulting in a breakage in mucous epithelial continuity and "bare area". Bacteria entering through the "bare area", so-called bacterial translocation takes place. A number of researches have shown that endotoxin increases NO over-production with intestinal barrier damages[17-20]. Our animal experiments confirmed this finding (data not published).

Gut is a central organ for surgical stress

The gut has long been thought to be quiescent or inactive during illnesses[29]. A large number of animal experiments and clinical investigations have suggested that functional changes in gastrointestinal mucous mumbrane occur during illness. Bacteria and endotoxin within the lumen enter into the other aseptic tissues and blood circulation through disordered functional and/or disorganized structural mucous epithelia, which influence greatly on occurrence, progress and transformation of illnesses[1-4,6,10-12,21-30]. In recent decades based on large amounts of animal experiments and clinical investigations, a series of new functions concerning gut metabolism and nutrition, intestinal barrier and immunity function, have been recognized. Following the elucidation on mechanisms of systemic inflammatory response syndrome (SIRS) and multiple-organ dysfunction syndrome (MODS)[4,11,29,31-37], the action of the gut as a central organ for surgical stress has also been put forward[29,30,32,35]. It is now known that the gastrointestinal tract contains about 50 % of reticular endothelia and other immune cells, and occupies about 80 % of the total humoral immunity of a human body. It is therefore the largest immune organ of the body[32-35]. Various insults such as trauma, burn, infection, shock, ischemia/reperfusion, irradiation therapy, chemical therapeutical medicines, and SIRS, could directly or indirectly cause an overgrowth of bacteria in bowel and lead to deterioration of intestinal barrier. Hence translocation of enteric bacteria and/or endotoxin, SIRS, sepsis and even MODS ensue[8,38-40], suggesting that the function of the gut in illness determines the patient' s prognosis[38, 41]. Based on this theory and clinical practice above, Wilmore *et al* put forward that gut was a reservoir of pathogens in illness and a central organ for surgical stress[29, 41]. This has been accepted by most scholars[8,38].

EVALUATION OF GUT BARRIER

There are many ways for measuring intestinal barrier function, but no one is perfect. Three regular approaches are often used to measure the function of gut barrier. The first is to examine the morphologies of mucous membrane such as thickness of mucosa, depth of crypts, architecture of villi, proliferating cellular nuclear antigen (PCNA) and intraepithelial lymphocytes (IELs). The second is to test translocation of bacteria/endotoxin, or bacteria growth and endotoxin concentration in mesenteric lymph node (MLN), liver, spleen, portal vein and/or systemic circulation. The third is to measure intestinal permeability[5,6], which is often carried out by using some labeling substances in experimental and clinical researches. Such substances could be water-soluble, nontoxic, and freely permeated through numerous small ' water pores' in the cell membranes of mucosal enterocytes. There is few or no such substances in body tissues that could not be metabolized. They should be excreted rapidly in an easily measured form. The substances matching with conditions mentioned above are lactulose, mannitol, ^{51}Cr-EDTA, PEG400 and inulin[2,6,42]. The approches that are most frequently used to examine intestinal permeability are the two-sugar test, or lactulose/mannitol test. There are two pathways for the subtances to get across the bowel mucous membrane, transcellular (through plasma membrane of enterocyte in the tip) and paracellular (the tight-junction between cells) routes. Smaller molecular substances (such as monosaccharide) pass through enterocytes by transcellular route, whereas bigger molecules (such as disaccharide) get across enterocytes by paracellular pathway. Thus, the increase of small intestinal permeability reflects the "leakeage degree" of mucous enterocytes [2,5-7].

DISEASES AND FACTORS CAUSING GUT BARRIER DYSFUNCTION

Any insults that lead to an overgrowth of enteric bacteria, an impairment of immune defence function and a damage to mechanical barrier of the gut would result in disorders of the intestinal barrier, and bacteria/endotoxin translocation would ensue[1,4,6,10,11,27]. Followings are the causes that lead to an increase of intestinal permeability.

Infection
This includes intestinal and intraperitoneal infections[38] and infections out of the intestinal tract (such as pneumonia)[43].

Parenteral nutrition
The issue has been confirmed by many animal experiments and clinical researches[10,11,21,25,44,45]. The reason is that 70 % of nutrients are absorbed directly from gut lumen, whereas only 30 % is provided by arterial blood supply[1]. Thus parenteral nutrition makes intestinal mucous membrane in a hunger state and leads to gut mucosa atrophy.

Mulnutrition
Mulnutrition could cause atrophy of intestinal mucosa, an insufficiency of protein synthesis and deficiency of body immunity. These would impair the gut barrier[3-27,28,32,34].

Overgrowth of enteric bacteria
Drugs or infection caused by some pathogens could lead to the overgrowth of intestinal bacteria and hence injures the gut barrier[8,27,39,45, 46].

Endotoxin
Endotoxin could increase NO production in the body and lead to impairment of intestinal barrier function[27,46,47]. Our animal experiments were in accordance with this (not shown).

Surgical stress
Various injuries such as burn/scald[10], organ transplantation (reperfusion injury), surgery and trauma[48-50], haemorrhagic shock and many other insults that lead to SIRS, would bring about an increment of intestinal permeability and damage of gut barrier[4,21].

Drugs
Oral administration of castor oil would cause a physical damage of intestinal mucous membrane in mice. Diabetes mellitus induced by streptozotocin in mice caused an overgrowth of enteric bacteria and an immunity injury of the body. Cyclo-oxygenase inhibitors of prostglandin such as mezolin can block production of prostacyclin in bowel mucous membrane, which increases the permeability of mucous epithelium and bacterial translocation[2,14]. It can also bring about intestinal pathological changes[13,51]. Immunosupressive agents such as chemotherapy drugs, anti-transplant rejection drugs[4,52], and antiacids can destroy gut mucosal barrier[53].

Multiple illnesses
Various abdominal diseases could cause an increase of intestinal permeability. One of these is inflammatory bowel disease (IBD)[2,9,42]. Others are intestinal obstruction, biliary block[4,9], leukemia, endotoxemia, parenteral and enteral nutrition[1, 4,10,11].

Physical injury
It includes radioactive intestinal damage[54].

AGENTS DECREASING INTESTINAL PERMEABILITY
Enteral nutrition could alleviate intestinal atrophy of mucous membrane during stress and could lower gut permeability, improve mucosal immunity. These have been confirmed by experiments and clinical practices[11,37]. Treatments with some special nutrients or immune-modulating drugs for patients with parenteral nutrition could also ameliorate intestinal barrier function[2,3,21].

Glutamine
Except for nutrient digestion and absorption, one of the functions of intestinal mucosa is to prevent enteric bacteria and endotoxin from entering into other parts and blood circulation of the body. It is now considered that gut barrier dysfunction is an important cause for infectious complications when patients suffer from hyper-metabolism after surgery and trauma[1,4,10,27,29,31]. It is still unclear what pathological mechanisms lead to gut barrier failure. It is taken for granted that two important factors causing intestinal barrier failure are the damage of intestinal blood supply and the lack of nutrient support[21]. It has been discovered from animal models and septic patients that the state is associated with insufficiency of perfusion (including disorders of microcirculation) and lack of essential nutrients (including glutamine) in their mucosa[2, 21]. Except for antimicrobial therapy of selective decontamination aiming at getting rid of enteric pathogens, it has been carried out to protect gut barrier function from being injured or have been injured in patients threatened by enterogenous infection. A promising approach is to use glutamine parenterally, which is an essential nutrient for the gut in stress and decreases sharply in illness. A series of experiments and clinical researches showed that nutritional support supplemented with glutamine could improve gut barrier function and enhence the body immunity[8,10,21,32,34,42,44,55-58].

Glutamine exerts its effects on the body in many ways. It supplies fuels for mucous enterocytes and strengthens the barrier structure of the gut on the one hand, and increases secretion of IgA by regulating IL-4 and IL-10 on the other hand, thus preventing enteric bacteria from adhesion to intestinal mucosa and subsequent bacterial translocation[59].

Arginine
Arginine influences the body immune system extensively. First, it is the precursor of polyamines and nucleic acids, which are essential for cell hyperplasia and differentiation. Second, it can produce hydroxyproline through metabolism to promote collagenation. Third, it can stimulate different human cells to secrete hormones such as growth hormone, glycagon, insulin-like growth factor 1 and insulin etc., which have various effects on the immune reactions of the body. In addition, arginine is also a precursor of nitric oxide, an important immune molecule[32,44], and has functions to kill bacteria, protect or impair intestinal barrier[32,44,60,61]. Some scholars reported that arginine could alleviate the secondary damage of gut barrier[62,63], whereas others held a completely different opinion, which had also confirmative evidences[50, 64]. Further investigations on the effects and mechanisms of arginine on the body are needed.

Recombinant human growth hormone (rhGH)
Growth hormone has many biological functions[22,44,64-66]. It could decrease intestinal permeability and improve gut barrier function in illness[39,58,69-71]. Possible mechanism of this may be that it promotes hyperplasia of intestinal epithelia[72], or enhances the mechanical barrier of mucous membrane.

Insulin-like growth factor-(IGF-I)
The main effects of IGF-I on the body are basically the same as rhGH[73, 74]. It promotes hyperplasia of mucous membrane of the intestine, and increase the uptake and utilization of glutamine by the bowel when in sepsis[70].

Nucleic acid
Kishibuchi *et al*[75] observed the alterations of cellular ultrastructure under electronic microscope, variations of intestinal permeability and changes of protease in bowel

mucous membrane, which showed that intestinal barrier function was significantly improved.

Others

Epidermal growth factors (EGF) have positive effects on the proliferation of mucous epithelia[76].

REFERENCES

1 **MacFie J**. Enteral versus parenteral nutrition: the significance of bacterial translocation and gut-barrier function. *Nutrition* 2000; **16**: 606-611
2 **Mohajer B**, Ma TY. Eicosanoids and the small intestine. *Prostaglandins Other Lipid Mediat* 2000; **61**: 125-143
3 **Van Der Hulst RR**, Von Meyenfeldt MF, Van Kreel BK, Thunnissen FB, Brummer RJ, Arends JW, Soeters PB. Gut permeability, intestinal morphology, and nutritional depletion. *Nutrition* 1998; **14**: 1-6
4 **Berg RD**. Bacterial translocation from the gastrointestinal tract. *Trends in Microbiol* 1995; **3**: 149-154
5 **Daugherty AL**, Mrsny RJ. Regulation of the intestinal epithelial paracellular barrier. *Pharm Sci Technol Today* 1999; **2**: 281-287
6 **Travis S**, Menzies I. Intestinal permeability: functional assessment and significance. *Clin Sci* 1992; **82**: 471-488
7 **Bijlsma PB**, Peeters RA, Groot JA, Dekker PR, Taminiau JA, Van Der Meer R. Differential *in vivo* and *in vitro* intestinal permeability to lactulose and mannitol in animals and humans: a hypothesis. *Gastroenterology* 1995; **108**: 687-696
8 **MacFie J,** O'Boyle C, Mitchell CJ, Buckley PM, Johnstone D, Sudworth P. Gut origin of sepsis: a prospective study investigating associations between bacterial translocation, gastric microflora, and septic morbidity. *Gut* 1999; **45**: 223-228
9 **Van Deventer SJ**, ten Cate JW, Tytgat GN. Intestinal endotoxemia. Clinical significance. *Gastroenterology* 1988; **94**: 825-831
10 **Sugiura T**, Tashiro T, Yamamori H, Takagi K, Hayashi N, Itabashi T, Toyoda Y, Sano W, Nitta H, Hirano J, Nakajima N, Ito I. Effects of total parenteral nutrition on endotoxin translocation and extent of the stress response in burned rats. *Nutrition* 1999; **15**: 570-575
11 **Kompan L**, Kremzar B, Gadzijev E, Prosek M. Effects of early enteral nutrition on intestinal prmeability and the development of multiple organ failure after multiple injury. *Intensive Care Med* 1999; **25**: 157-161
12 **Nadler EP,** Ford HR. Regulation of bacterial translocation by nitric oxide. *Pediatr Surg Int* 2000; **16**: 165-168
13 **Bjarnason I**, Hayllar J, Smethurst P, Price A, Gumpel MJ. Metronidazole reduces intestinal inflammation and blood loss in nonsteroidal anti-inflammatory drug induced enteropathy. *Gut* 1992; **33**: 1204-1208
14 **Robert A**, Asano T. Resistance of germ freerats to indomethacin-induced intestinal lesions. *Prostaglandins* 1977; **14**: 331-341
15 **Prabhu R**, Anup R, Balasubramanian KA. Surgical stress induces phospholipid degradation in the intestinal brush border membrane. *J Surg Res* 2000; **94**: 178-184
16 **Gasbarrini G**, Montalto M. Structure and function of tight junctions. Role in intestinal barrier. *Ital J Gastroenterol Hepatol* 1999; **31**: 481-488
17 **Dickinson E**, Tuncer R, Nadler E, Boyle P, Alber S, Watkins S, Ford H. NOX, a novel nitric oxide scavenger, reduces bacterial translocation in rats after endotoxin challenge. *Am J Physiol* 1999; **277**(6 Pt1): G1281-1287
18 **Unno N**, Wang H, Menconi MJ, Tytgat SH, Larkin V, Smith M, Morin MJ, Chavez A, Hodin RA, Fink MP. inhibition of inducible nitric oxide synthase ameliorates endotoxin-induced gut mucosal barrier dysfunction in rats. *Gastroenterology* 1997; **113**: 1246-1257
19 **Mishima S**, Xu D, Deitch EA. Increase in endotoxin-induced mucosal permeability is related to increased nitric oxide synthase activity using the Ussing chamber. *Crit Care Med* 1999; **27**: 880-886
20 **Forsythe RM**, Xu DZ, Lu Q, Deitch EA. Lipopolysaccharide-induced enterocyte-derived nitric oxide induces intestinal monolayer permeability in an autocrine fashion. *Shock* 2002; **17**: 180-184
21 **Foitzik T**, Kruschewski M, Kroesen AJ, Hotz HG, Eibl G, Buhr HJ. Does glutamine reduce bacterial translocation? A study in two animal models with impaired gut barrier. *Int J Colorectal Dis* 1999; **14**: 143-149
22 **Eizaguirre I**, Aldazabal P, Barrena MJ, Garcia-Arenzana JM, Ariz C, Candelas S, Tovar JA. Effect of growth hormone on bacterial translocation in experimental short-bowel syndrome. *Pediatr Surg Int* 1999; **15**: 160-163
23 **O'Boyle CJ**, MacFie J, Dave K, Sagar PS, Poon P, Mitchell CJ. Alterations in intestinal barrier function do not predispose to translocation of enteric bacteria in gastroenterologic patients. *Nutrition* 1998; **14**: 358-362
24 **Heys SD**, Ashkanani F. Glutamine. *Br J Surg* 1999; **86**: 289-290
25 **Pierro A**, van Saene HK, Donnell SC, Hughes J, Ewan C, Nunn AJ, Lloyd DA. Microbial translocation in neonates and infants receiving long-term parenteral nutrition. *Arch Surg* 1996; **131**: 176-179
26 **O'Dwyer ST**, Michie HR, Ziegler TR, Revhaug A, Smith RJ, Wilmore DW. A single dose of endotoxin increases intestinal permeability in healthy humans. *Arch Surg* 1988; **123**: 1459-1464
27 **Deith EA**, Ma WJ, Ma L, Berg RD, Specian RD. Protein malnutrition predisposes to inflammatory-induced gut-origin septic states. *Ann Surg* 1990; **211**: 560-567
28 **Welsh FK**, Farmery SM, MacLennan K, Sheridan MB, Barclay GR, Guillou PJ, Reynolds JV. Gut barrier function in malnourished patients. *Gut* 1998; **42**: 396-401
29 **Wilmore DW**, Smith RJ, O'Dwyer ST, Jacobs DO, Ziegler TR, Wang XD. The gut: a central organ after surgical stress. *Surgery* 1988; **104**: 917-923
30 **Marshall JC**, Christou NV, Meakins JL. Immunomodulation by altered gastrointestinal tract flora. The effects of orally administered, killed Staphylococcus epidermidis, Candida, and pseudomonas on systemic immune responses. *Arch Surg* 1988; **123**: 1465-1469
31 **Bengmark S**, Gianotti L. Nutritional support to prevent and treat multiple organ failure. *World J Surg* 1996; **20**: 474-481
32 **Hulswe KW**, Van Acker BA, von Meyenfeldt MF, Soeters PB. Nutritional depletion and dietary manipulation: effects on the immune response. *World J Surg* 1999; **23**: 536-544
33 **Goris RJ**, te Boekhorst TP, Nuytinck JK, Gimbrere JS. Multiple-organ failure. Generalized autodestructive inflammation? *Arch Surg* 1985; **120**: 1109-1115
34 **McCauley R**, Kong SE, Heel K, Hall JC. The role of glutaminase in the small intestine. *Int J Biochem Cell Biol* 1999; **31**: 405-413
35 **Brandtzaeg P**, Halstensen TS, Kett K, Krajci P, Kvale D, Rognum TO, Scott H, Sollid LM. Immunobiology and immunopathology of human gut mucosa: humoral immunity and intraepithelial lymphocytes. *Gastroenterology* 1989; **97:** 1562-1584
36 **Alverdy J**, Stern E, Poticha S, Baunoch D, Adrian T. Cholecystokinin modulates mucosal immunoglobulin A function. *Surgery* 1997; **122**: 386-393
37 **Keith Hanna M**, Zarzaur BL Jr, Fukatsu K, Chance DeWitt R, Renegar KB, Sherrell C, Wu Y, Kudsk KA. Individual neuropeptides regulate gut-associated lymphoid tissue integrity, intestinal immunoglobulin A levels, and respiratory antibacterial immunity. *J Parenter Enteral Nutr* 2000; **24**: 261-269
38 **Marshall JC**, Christou NV, Meakins JL. Small-bowel bacterial overgrowth and systemic immunosuppression in experimental peritonitis. *Surgery* 1988; **104**: 404-411
39 **Fukushima R**, Saito H, Inoue T, Fukatsu K, Inaba T, Han I, Furukawa S, Lin MT, Muto T. Prophylactic treatment with growth hormone and insulin-like growth factor I improve systemic bacterial clearance and survival in a murine model of burn-induced gut-derived sepsis. *Burns* 1999; **25**: 425-430
40 **Swank GM**, Deitch EA. Role of the gut in multiple organ failure: bacterial translocation and permeability changes. *World J Surg* 1996; **20**: 411-417
41 **Carrico CJ**, Meakins JL, Marshall JC, Fry D, Maier RV. Multiple-Organ-Failure Syndrome. *Arch Surg* 1986; **121**: 196-208
42 **Juby LD**, Rothwell J, Axon AT. Lactulose/mannitol test: an ideal screen for celiac disease. *Gastroenterology* 1989; **96**: 79-85
43 **Yu P**, Martin CM. Increased gut permeability and bacterial translocation in *Pseudomonas* pneumonia-induced sepsis. *Crit Care Med* 2000; **28**: 2573-2577
44 **Ziegler TR**, Leader LM, Jonas CR, Griffith DP. Adjunctive therapies in nutritional support. *Nutrition* 1997; **13** (9 Suppl): 64S-72S
45 **Pappo I**, Polacheck I, Zmora O, Feigin E, Freund HR. Altered

gut barrier function to candida during parenteral nutrition. *Nutrition* 1994; **10:** 151-154
46 **Mishima S**, Xu D, Lu Q, Deitch EA. Bacterial translocation is inhibited in inducible nitric oxide synthase knockout mice after endotoxin challenge but not in a model of bacterial overgrowth. *Arch Surg* 1997; **132**: 1190-1195
47 **Steinberg S**, Flynn W, Kelly K, Bitzer L, Sharma P, Gutierrez C, Baxter J, Lalka D, Sands A, Van Liew J, Hassett J, Price R, Beam T, Flint L. Development of a bacteria-independent model of the multiple organ failure syndrome. *Arch Surg* 1989; **124:** 1390-1395
48 **Reynolds JV**, Kanwar S, Welsh FK, Windsor AC, Murchan P, Barclay GR, Guillou PJ. Does the route of feeding modify gut barrier function and clinical outcome in patients after major upper gastrointestinal surgery? *J Parenter Enteral Nutr* 1997; **21**: 196-201
49 **Anup R**, Aprana V, Pulimood A, Balasubramanian KA. Surgical stress and the small intestine: Role of oxygen free radicals. *Surgery* 1999; **125**: 560-569
50 **Baue AE**. The role of the gut in the development of multiple organ dysfunction in cardiothoracic patients. *Ann Thorac Surg* 1993; **55**: 822-829
51 **Allison MC**, Howatson AG, Torrance CJ, Lee FD, Russell RI. Gastrointestinal damage associated with the use of nonsteroidal antiinflammatory drugs. *N Engl J Med* 1992; **327**: 749-754
52 **Nakamaru M**, Masubuchi Y, Narimatsu S, Awazu S, Horie T. Evaluation of damaged small intestine of mouse following methotrexate administration. *Cancer Chemother Pharmacol* 1998; **41**: 98-102
53 **Basaran UN,** Celayir S, Eray N, Ozturk R, Senyuz OF. The effect of an H_2-receptor antagonist on small-bowel colonization and bacterial translocation in newborn rats. *Pediatr Surg Int* 1998; **13**: 118-120
54 **Vazquez I**, Gomez-de-Segura IA, Grande AG, Escribano A, Gonz áez-Gancedo P, Gomez A, Diez R, De Miguel E. Protective effect of enriched diet plus growth hormone administration on radiation-induced intestinal injury and on its evolutionary pattern in the rat. *Dig Dis Sci* 1999; **44**: 2350-2358
55 **Van Der Hulst RR**, Van Kreel BK, Von Meyenfeldt MF, Brummer RJ, Arends JW, Deutz NE, Soeters PB. Glutamine and the preservation of gut integrity. *Lancet* 1993; **341**: 1363-1365
56 **Burke DJ**, Alverdy JC, Aoys E, Moss GS. Glutamine-supplemented total parenteral nutrition improves gut immune function. *Arch Surg* 1989; **124**: 1396-1399
57 **Li JY**, Lu Y, Hu S, Sun D, Yao YM. Preventive effect of glutamine on intestinal barrier dysfunction induced by severe trauma. *World J Gastroenterol* 2002; **8**: 168-171
58 **Gu Y**, Wu ZH. The anabolic effects of recombinant human growth hormone and glutamine on parenterally fed, short bowel rats. *World J Gastroenterol* 2002; **8**: 752-757
59 **Kudsk KA**, Wu Y, Fukatsu K, Zarzaur BL, Johnson CD, Wang R, Hanna MK. Glutamine-enriched total parenteral nutrition maintains intestinal interleukin-4 and mucosal immunoglobulin A levels. *J Parenter Enteral Nutr* 2000; **24**: 270-275
60 **Moncada S**, Higgs EA. Endogenous nitric oxide: physiology, pathology and clinical relevance. *Eur J Clil Inves* 1991; **21**: 361-374
61 **Nadler EP**, Ford HR. Regulation of bacterial translocation by nitric oxide. *Pediatr Surg Int* 2000; **16**: 165-168
62 **Hutcheson IR**, Whittle BJ, Boughton-Smith NK. Role of nitric oxide in maintaining vascular integrity in endotoxin-induced acute intestinal damage in the rat. *Br J Pharmacol* 1990; **101**: 815-820
63 **Brooks EC**, Mahr NN, Radisavljevic Z, Jacobson ED, Terada LS. Nitric oxide attenuates and xanthine oxidase exaggerates lung damage-induced gut injury. *Am J Physioly* 1997; **272**(4Pt1): G845-852
64 **Mishima S**, Xu D, Deitch EA. Increase in endotoxin-induced mucosal permeability is related to increased nitric oxide synthase activity using the Ussing chamber. *Crit Care Med* 1999; **27**: 880-886
65 **Tritos NA**, Mantzoros CS. Recombinant human growth hormone: old and novel uses. *Am J Med* 1998; **105**: 44-57
66 **Inoue Y**, Copeland EM, Souba WW. Growth hormone enhances amino acid uptake by the human small intestine. *Ann Surg* 1994; **219**: 715-724
67 **Byrne TA**, Morrissey TB, Nattakom TV, Ziegler TR, Wilmore DW. Growth hormone, glutamine, and a modified diet enhance nutrient absorption in patients with severe short bowel syndrome. *J Parenter Enteral Nutr* 1995; **19**: 296-302
68 **Zhou X,** Li YX, Li N, Li JS. Effect of bowel rehabilitative therapy on structural adaptation of remnant small intestine: animal experiment. *World J Gastroenterol* 2001; **7**: 66-73
69 **Scopa CD**, Koureleas S, Tsamandas AC, Spiliopoulou I, Alexandrides T, Filos KS, Vagianos CE. Beneficial effects of growth hormone and insulin-like growth factor I on intestinal bacterial translocation, endotoxemia, and apoptosis in experimentally jaundiced rats. *J Am Coll Surge* 2000; **190**: 423-431
70 **Balteskard L,** Unneberg K, Mjaaland M, Jenssen TG, Revhaug A. Growth hormone and insulinlike growth factor 1 promote intestinal uptake and hepatic release of glutamine in sepsis. *Ann Surg* 1998; **228**: 131-139
71 **Chen K**, Nezu R, Inoue M, Wasa M, Iiboshi Y, Fukuzawa M, Kamata S, Takagi Y, Okada A. Beneficial effects of growth hormone combined with parenteral nutrition in the management of inflammatory bowel desease: An experimental study. *Surgery* 1997; **14**: 212-218
72 **Zhou X**, Li N, Li JS. Growth hormone stimulates remnant small bowel epithelial cell proliferation. *World J Gastroenterol* 2000; **6**: 909-913
73 **Huang KF**, Chung HD, Herndon DN. Insulinlike growth factor 1 (IGF-1) reduces gut atrophy and bacterial translocation after severe burn injury. *Arch Surg* 1993; **128**: 47-53
74 **Chen K**, Okuma T, Okamura K, Tabira Y, Kaneko H, Miyauchi Y. Insulin-like growth factor-I prevents gur atrophy and maintains intestinal integrity in septic rats. *J Parenter Enteral Nutr* 1995; **19**: 119-124
75 **Kishibuchi M**, Tsujinaka T, Yano M, Morimoto T, Iijima S, Ogawa A, Shiozaki H, Monden M. Effects of nucleosides and a nucleotide mixture on gut mucosal barrier function on parenteral nutrition in rats. *J Parenter Enteral Nutr* 1997; **21**: 104-111
76 **Chen DL**, Wang WZ, Wang JY. Epidermal growth factor prevents gut atrophy and maintains intestinal integrity in rats with acute pancreatitis. *World J Gastroenterol* 2000; **6**: 762-765

Edited by Zhang JZ and Wang XL

P.O.Box 2345, Beijing 100023,China
Fax: +86-10-85381893
E-mail: wjg@wjgnet.com www.wjgnet.com

World J Gastroenterol 2003;9(11):2390-2394
World Journal of Gastroenterology
 ISSN 1007-9327

• REVIEW •

Gene therapy for gastric cancer: A review

Chao Zhang, Zhan-Kui Liu

Chao Zhang, Zhan-Kui Liu, Department of General Surgery, Southwest Hospital, Third Military Medical University, Gaotan Yan, Chongqing 400038, China
Correspondence to: Dr. Chao Zhang, M.D. Department of General Surgery, Southwest Hospital, Third Military Medical University, Gaotan Yan, Chongqing 400038, China. meizhang6688@yahoo.com.cn
Telephone: +86-23-68773074
Received: 2002-10-05 **Accepted:** 2003-04-11

Abstract

Gastric cancer is common in China, and its early diagnosis and treatment are difficult. In recent years great progress has been achieved in gene therapy, and a wide array of gene therapy systems for gastric cancer has been investigated. The present article deals with the general principles of gene therapy and then focuses on how these principles may be applied to gastric cancer.

Zhang C, Liu ZK. Gene therapy for gastric cancer: A review. *World J Gastroenterol* 2003; 9(11): 2390-2394
http://www.wjgnet.com/1007-9327/9/2390.asp

INTRODUCTION

Enormous progress has been seen in molecular genetics over the past few decades. It has given us insights at the molecular level, into vital progresses in living organisms, such as embryonic development, growth regulation, differentiation, pathogenesis and carcinogenesis. Insights into the mechanism of pathologic progresses such as developmental disorders and carcinogenesis, have stimulated efforts to develop therapeutic approaches to prevent or correct these processes. Techniques to directly change the genetic information of a cell have greatly improved expectations of the therapeutic potential of genetic manipulation. These developments have raised hopes that diseases appearing to be incurable can soon be cured. Especially for cancer such as gastric cancer, which is common in China. It is well established that most cancers result from a series of accumulated, acquired genetic lesions in somatic cells that are faithfully reproduced until a malignant clone is created, which is ultimately able to destroy the host. Gene therapy has emerged as a new method of therapeutic and possibly preventive intervention against cancer at the level of cellular gene expression[1-14]. Generally speaking, gene therapy can be defined as the introduction and expression of an exogenous gene into human cells for therapeutic benefit, and is conventionally restricted to human diseases associated with single gene defects[15].

In oncology, it can be defined as the introduction of DNA into cells (either neoplastic or normal) in order to shrink or eliminate a malignant tumor. This may be achieved by means of directly inducing malignant cell death, modulating immune response to tumors or reversing the malignant process by correcting genetic abnormalities. It may also be possible to enhance a tumor's responsiveness to conventional treatments such as chemotherapy and radiotherapy, and to protect normal tissue by introduction of genetic materials that confers resistance to the toxic effects of such treatment[16, 17]. A number of strategies have been developed to accomplish cancer gene therapy. These approaches included cytotoxic gene therapy, antisense therapy, and immunotherapy[18-22]. However, despite progress in the field, wide clinical applications and success have not been achieved[23,24]. As with all forms of gene therapy in cancer, the main problems to overcome will be optimizing delivery in order to maximize the proportion of successfully transduced cancer cells, In treatment of human malignant tumours, several obstacles explain the limitations of currently available treatments for achieving definitive cures in most cases of advanced disease. There are some problems in gene therapy. A combination of new chemotherapy drugs, higher doses of drugs, novel cytokines, improved regimens of radiotherapy, and more sophisticated surgery can achieve incremental improvements in cancer treatment. But these therapies do not address critical biological obstacles, and thus, probably will not bring about the much-needed radical advances in the implementation and results of cancer treatment. In contrast, gene therapy offers the potential for overcoming some of these fundamental barriers.

APPROACHES TO GENE THERAPY

Vector

One of the major problems in gene therapy is difficulty in delivering appropriate nucleic acid sequences to target cells. Various strategies have been evolved, which can be essentially divided into two types. One use viral vectors while the other uses non-viral vectors.

Viruses vector The main viruses which have been studied as potential vectors for transducing genes into cancer cells are retrovirus and adenovirus. Retroviruses are single-stranded RNA viruses, and after deletion of one or more structural genes, a foreign gene can be incorporated forming a "recombinant" retrovirus. This could then be used to infect a cell so that it integrates into the host cell's genome which then expresses viral genes as well as the "therapeutic" gene[25,26]. Adenoviruses consist of a core containing double-stranded DNA surrounded by a protein capsid. When an adenovirus vector is created, E1 genes are deleted in order to render the virus incapable of replication, thereby obviating the risk of transforming healthy host cells[27]. Adenoviruses have a greater potential than retroviruses in that they have a higher efficiency of infection and it is possible to incorporate larger segments of DNA. Weber *et al*[28] thought that oncoretrovirus-based vector was a safe and reliable vector system that could achieve permanent integration of delivered transgenes. Successful application of these vectors for gene therapy has proven difficult due to their relatively low transduction efficiency. However, cumulative improvements in methodology have recently yielded promising clinical results. Furthermore, significant improvements in basic retrovirus vector technology now can revitalize the field. But they do induce antiviral immune responses that may compromise the ability to treat an immunocompetent host on more than one occasions. Other viruses which have been used in this context include herpes virus, vaccinia virus and adenovirus-associated virus. Pieroni *et al*[29] found the use of baculovirus vectors for gene expression in mammalian cells was in continuous expansion. These vectors do not replicate in mammalian cells, do not cause a cytopathic effect upon

infection and are able to carry large DNA inserts. Baculovirus vectors have been shown to transduce various cell types *in vitro* and *in vivo* with significant efficiency leading to stable gene expression. This review focuses on recent the developments in baculovirus vector that highlight its potential use for new gene therapy strategies. Okada *et al*[30]. have done something about adeno-associated viral vector-mediated gene therapy for ischemia-induced neuronal death.

Non-viral vector The most widely studied non-viral vector is liposome. Liposome is a positively charged lipid membrane which can be complexed with DNA, and fusion of liposome-DNA complex with a negatively charged membrane leads to transfer of DNA into cells. Lasic *et al*[31] reviewed stabilized liposomes in cancer therapy and gene delivery. Unfortunately, the efficiency of gene transduction using liposomes was currently much lower than that achieved by viral vectors[32].

Other approach

Another approach is to use direct injection of plasmid DNA, but this technique can only transfect cells immediately adjacent to the injection site so that only a small number of cells can be treated[33].Vanden *et al*[34] found that oncoretroviral vectors and lentiviral vectors offered the potential for long-term gene expression by virtue of their stable chromosomal integration and lack of viral gene expression. Gomez *et al*[35]analyzed conditionally replicative adenoviral vectors. Liu *et al*[19] described that the successful transformation of C. sporogenes, a clostridial strain with the highest reported tumor colonization efficiency, with *E. coli* cytosine deaminase (CD) gene and showed that systemically injected spores of these bacteria expressed CD only in the tumor.

It is hoped, however, that by complexing adenovirus and plasmid DNA with protein ligands which bind to specific receptors, enhanced gene transfer into specific cellular targets might be achieved[36]. An example of this is the argenine-glycine-aspartic acid motif that targets integrin receptors[37]. Aside from different approaches to introducing genetic material into cells, gene therapy can be classified according to the different end results. The main aims in this respect are gene replacement, antisense therapy, cytotoxic gene therapy, immunotherapy and drug resistance transfer.

Cytotoxic gene therapy

One of the most promising strategies for gene therapy against various types of cancer is the introduction of a suicide gene, which is transduction of a gene that transforms a non- toxic "pro-drug" into a toxic substance. One approach to this general concept is the transfer of the gene for HSV thymidine kinase (HSV-tk), as this phosphorylates nucleoside analogues such as acyclovir and ganciclovir which are then incorporated into DNA as it replicates[38]. Floeth *et al*[39] analyzed the mechanisms of the "bystander effect" in VPC-mediated HSV-Tk/GCV gene therapy. Thus, these compounds are only toxic to cells expressing HSV-tk, although the bystander effect has also been noted in this type of gene therapy[40]. This is presumably due to release of toxic metabolites produced by the prodrug-activating enzymes which then kill surrounding non-transduced cells. A similar type of cytotoxic gene therapy involves an adenovirus carrying cDNA for cytosine deaminase enzyme of *E.coli* and prodrug 5-fluorocytosine. The prodrug is given orally and converted to 5-fluorouracil in the cells containing cytosine deaminase[41,42].

Antisense therapy

When oligonucleotides bind to their complementary RNA or DNA, they prevent translation or transcription, respectively. This process, known as "anti-sense", is a theoretically attractive method for inactivating oncogenes which are overexpressed in tumors[43,44]. Tang *et al*[45] amplified the 200 VEGF cDNA fragment and inserted it into human U6 gene cassette in the reverse orientation transcribing small antisense RNA which could specifically interact with VEGF165 and VEGF121 mRNA. Their conclusion was expression of antisense VEGF RNA in SMMC-7721 cells could decrease tumorigenicity and antisense-VEGF gene therapy might be an adjuvant treatment for hepatoma. Like gene replacement therapy, however, it would seem that all cells in tumors would have to be transduced, and oligonucleotides would have to last long enough to down-regulate the appropriate genes. Nonetheless, this approach did seem to be effective in certain animal models[46-48]. Kumai *et al*[49] investigated the effect of antisense oligodeoxynucleotides (AS ODN) against tyrosine hydroxylase (TH) on hypertension and sympathetic nervous system activity in spontaneously hypertensive rats (SHR). Systolic blood pressure (SBP) in SHR treated with TH AS ODN (50, 200 mg/rat, i.v.) was significantly lower than that in control SHR. Epinephrine and norepinephrine levels, TH activity, and TH protein levels in adrenal medulla of SHR were reduced concomitantly with TH AS ODN treatment-induced changes in SBP. In contrast, TH AS ODN (200 mg/rat) had no effect on SBP in Wistar-Kyoto rats (WKY), though catecholamine levels, TH activity, and TH protein levels were significantly decreased. These findings suggest that peripheral systemic injection of TH AS ODN may be effective as hypotensive therapy in SHR. Marchand *et al*[50] found the use of miniosmotic pumps, phosphate-buffered saline, VEGF, or VEGF combined with AS-Flk-1, AS-Flt-1, or AS-scrambled oligonucleotides were released in mouse testis for 14 days. VEGF (1, 2.5, and 5 mg) increased the formation of new capillary blood vessels by 236 %, 246 %, and 287 %, respectively. The combination of AS-Flk-1 or AS-Flt-1 (200 mg) to VEGF (2.5 mg) reduced by 87 % and 85 % of new blood vessel formation, respectively, and the expression of their corresponding proteins. These data demonstrate the therapeutical potential of AS-Flk-1 or AS-Flt-1 to prevent VEGF-mediated angiogenesis *in vivo*.

Immunotherapy

The main principle of genetic immunotherapy is to improve the host' s immune response to a particular tumor. One approach is to employ intramuscular injection of DNA which encodes a tumor-associated antigen such as CEA either directly or in form of a viral vaccine[51]. Cheng *et al*[52] have developed a new strategy to enhance nucleic acid vaccine potency by linking VP22, a herpes simplex virus type 1 (HSV-1) tegument protein, to a model antigen. This strategy facilitated the spread of linked E7 antigen to neighboring cells. In their study, they created a recombinant Sindbis virus (SIN)-based replicon particle encoding VP22 linked to a model tumor antigen, human papillomavirus type 16 (HPV-16) E7, using a stable SIN PCL. The linkage of VP22 to E7 in these SIN replicon particles resulted in a significant increase in the number of E7-specific CD8(+) T cell precursors and a strong antitumor effect against E7-expressing tumors in vaccinated C57BL/6 mice relative to wild-type E7 SIN replicon particles. Furthermore, a head-to-head comparison of VP22-E7-containing naked DNA, naked RNA replicons, or RNA replicon particle vaccines indicated that SINrep5-VP22/E7 replicon particles generated the most potent therapeutic antitumor effect. By leading to an active immune response, this was thought to be more effective than passive immunisation using specific antibodies against the antigen in question. Another way was to enhance immunity by using genes for cytokines such as interleukins (IL) which could recruit and stimulate appropriate effector cells[53,54]. Nishioka *et al*[55] have done something about genetic modification of dendritic cells and its application to cancer

immunotherapy. Although the results in the experimental systems were promising, the clinical application of gene-modified DCs had several problems such as the standardization of methods of manipulation and gene-transduction of DCs. Approaches to solve them require further studies. Takemura *et al*[56] have previously produced an anti-MUC1 x anti-CD3 diabody (Mx3 diabody) in an Escherichia coli (*E. coli*) expression system, other approaches have been found, for instance, Vonderheide *et al*[57] applied telomerase as a universal tumor-associated antigen. Schadendorf *et al*[58] reviewed the use of histamine in cancer immunotherapy.

APPLICATION OF GNEE THERAPY FOR GASTRIC CANCER

p53 gene

About 60 % of human gastric cancers carry point mutations of p53 gene, and because of its central role,this nuclear protein is believed to play a role in the regulation of cellular response to DNA damage. Wild-type p53 replacement therapy is an attractive concept in this disease. The responses of human gastric cancer cell lines to recombinant adenovirus encoding wild-type p53 gene have been analysed *in vitro* and *in vivo*[59]. In that study, growth inhibition was observed in cell lines expressing p53 mutations, but not in lines with wild-type p53. Furthermore, the mechanism of cell killing was found to be apoptosis. Thus, it seems that p53 replacement therapy has potential as a therapeutic strategy for human gastric cancer.

Antisense therapy

Antisense therapy has also been used in gastric cancer cell line. Proliferating cell nuclear antigen (PCNA) has been shown to stimulate DNA synthesis by DNA polymerase delta, and to be strongly expressed by gastric cancer cells with a high proliferative activity. Antisense oligonucleotides specific for PCNA mRNA have been shown to inhibit the growth of all gastric cancer cell lines tested, whereas random sequence oligonucleotides had no effect.

Cytotoxic gene therapy

Gastrointestinal cancer is the most important clinical target of gene therapy. Suicide gene therapy with herpes simplex virus type 1 thymidine kinase (HSV-TK) gene, has been shown to exert antitumor efficacy in various cancer models *in vitro*. A modificiation of this approach has been madee to insert carcinoembryonic antigen (CEA) promoter into the viral vector to increase the efficiency of transfection of HSV-tk into cells expressing CEA. When compared with transduction of HSV-tk with a ubiquitous promoter, the use of CEA promoter enhanced the killing effect of ganciclovir in CEA producing cells. While in colorectal cancer, about 40 % of gastric cancer expressed CEA, and CEA producing gastric cancer cell lines were susceptible to this treatment. Okino *et al*[60] described the sequential histopathological changes after suicide gene therapy of N-methyl-N' -nitro-N-nitrosoguanidine (MNNG)-induced gastric cancer in rats. Gastric tumors were induced by MNNG in 38/73 (52 %) of Wistar strain rats. The suicide gene therapy group (14 rats) was subjected to *in situ* gene transfer with a recombinant adenovirus vector carrying the HSV-TK gene driven by CAG promoter (Ad.CAGHSV-TK) in gastric tumor, followed by the antiviral drug ganciclovir (GCV). They observed the histopathological changes at various times after HSV-TK/GCV gene therapy, groups of animals were sacrificed at 3, 8, and 30 days after gene transfer. Apoptosis in gastric tumors was detected by the TUNEL method to assess the efficacy of HSV-TK/GCV gene therapy, and it was markable in the 8- and 30-day treatment groups compared to the sham operation controls (P<0.001). Various histopathological changes, degeneration of cancer tissue and fibrosis after necrosis and apoptosis were significantly greater in the 30-day treatment group. The HSV-TK gene was detectable in peripheral blood by PCR until 30 days after gene transfer. These results might be useful in devising a method of suicide gene therapy for humans.

Other forms of cytotoxic gene therapy which have been used with success in gastric cancer cell lines include transfection of E.coli phosphoribosyltransferase (UPRT) which could catalyse the synthesis of UMP from uracil and 5-phosphoribosyl-alpha-1-diphosphate, thereby sensitising the cell to 5-fluorouracil (5-FU). This has been shown to enhance the cell killing effect of 5-FU in gastric cell lines both *in vitro* and *in vivo*. Shimizu *et al*[61] have generated a recombinant adenovirus encoding the UP gene (AxCA.UP) which has been applied in gastric cancer gene therapy to sensitize cancer cells to lower concentrations of 5-FU.

Immunotherapy

Genetic immunotherapy is another area of active research, and work with severe combined immunodeficiency (SCID) mice given human peripheral lymphocytes and autologous human tumour cells from patients with gastric cancer has yielded interesting results. In one study, administration of an adenovirus vector expressing IL-6 cDNA-induced CD8+cytotoxic T-lymphocytes specific for tumour cells from the precursor human T-lymphocytes *in vivo*, inhibited growth and metastasis of autologous human tumours. In another study, SCID mice reconstituted with peripheral blood cells containing CD34+cells were inoculated with human gastric cancer cell lines transduced with cytokine genes including IL-2 and IL-6. It was found that the tumourigenicity of IL-2 producing tumour cells was significantly reduced in the CD34+ reconstituted but not in the non-reconstituted mice, whereas transduction of IL-6 did not affect tumourigenicity, irrespective of the reconstitution status of the mice. This system could provide a model for investigating the utility of transfecting tumours with individual cytokines. Yu *et al*[62] described the bioactivity of MG7 scFv for its application as a targeting mediator in gene therapy of gastric cancer. Two positive recombinant phage clones have been found to contain the exogenous scFv gene. ELISA showed that MG7 scFv had a strong antigen-binding affinity. Immunodotting assay showed that transfected E.coli HB2151 could successfully produce soluble MG7scFv with a high yield via induction by IPTG. The molecular mass of MG7 scFv was 30 kDa by Western blot. DNA sequencing demonstrated that VH and VL genes of MG7 scFv were 363 bp and 321 bp, respectively.

PROSPECT

With development of the genomic research, more and more individual patients have benefited from the revolution so far. Thus, despite a paucity of clinical information, gene therapy for gastric cancer is on the horizon. As with all forms of gene therapy in cancer, the main problems are to optimize delivery in order to maximize the proportion of successfully transduced cancer cells, and to choose the most appropriate targets for an individual tumor. There is no doubt that human cancers are heterogeneous in terms of genetic abnormality, and a better understanding of the mutational spectrum associated with a cancer type along with the ability to obtain mutation profiles for individual tumors is an important step to successful gene replacement and antisense therapy[63-68].

One factor critical to successful human gene therapy is the development of efficient gene delivery systems. Although numerous vector systems for gene transfer have been developed, a perfect vector system has not yet been constructed. Difficulties of *in vivo* gene transfer appear to be due to

resistance of living cells to invasion by foreign materials and interference of cellular functions. We should analyze what barriers in tissues affect *in vivo* gene transfection and focus on how to solve these problems for gene therapy[68-71].

REFERENCES

1 **Wadhwa PD**, Zielske SP, Roth JC, Ballas CB, Bowman JE, Gerson SL. Cancer gene therapy: scientific basis. *Annu Rev Med* 2002; **53**: 437-452
2 **Otsu M**, Wada T, Candotti F. Gene therapy for primary immune deficiencies. *Curr Opin Allergy Clin Immunol* 2001; **1**: 497-501
3 **Cupp CL**, Bloom DC. Gene therapy, electroporation, and the future of wound-healing therapies. *Facial Plast Surg* 2002; **18**: 53-57
4 **Yamaoka T**. Gene therapy for diabetes mellitus. *Curr Mol Med* 2001; **1**: 325-327
5 **Seto M**, Yamazaki T, Sonsda J, Matsumine A, Shinto Y, Uchida A. Suppression of tumor growth and pulmonary metastasis in murine osteosarcoma using gene therapy. *Oncol Rep* 2002; **9**: 337-340
6 **Englemann C**, Heslan JM, Fabre M, Lagarde JP, Klatzmann D, Panis Y. Importance, mechanisms and limitations of the distant bystander effect in cancer gene therapy of experimental liver tumors. *Cancer Lett* 2002; **179**: 59-69
7 **Okada Y**, Okada N, Nakagawa S, Mizuguchi H, Kanehira M, Nishino N, Takahashi K, Mizuno N, Hayakawa T, Mayumi T. Fiber-mutant technique can augment gene transduction efficacy and anti-tumor effects against established murine melanoma by cytokine-gene therapy using adenovirus vectors. *Cancer Lett* 2002; **177**: 57-63
8 **Ruiz J**, Mazzolini G, Sangro B, Qian C, Prieto J. Gene therapy of hepatocellular carcinoma. *Dig Dis* 2001; **19**: 324-332
9 **Li S**, Zhang X, Xia X. Regression of tumor growth and induction of long-term antitumor memory by interleukin 12 electro-gene therapy. *J Natl Cancer Inst* 2002; **94**: 762-768
10 **Manninen HI**, Makinen K. Gene therapy techniques for peripheral arterial disease. *Cardiovasc Intervent Radiol* 2002; **25**: 98-108
11 **Adachi O**, Nakano A, Sato O, Kawamoto S, Tahara H, Toyoda N, Yamato E, Matsumori A, Tabayashi K, Miyazaki J. Gene transfer of Fc-fusion cytokine by *in vivo* electroporation: application to gene therapy for viral myocarditis. *Gene Ther* 2002; **9**: 577-582
12 **Johnson-Saliba M**, Jans DA. Gene therapy: optimising DNA delivery to the nucleus. *Curr Drug Targets* 2001; **2**: 371-399
13 **Baum BJ**, Kok M, Tran SD, Yamano S. The impact of gene therapy on dentistry: a revisiting after six years. *J Am Dent Assoc* 2002; **133**: 35-44
14 **Havlik R**, Jiao LR, Nicholls J, Jensen SL, Habib NA. Gene therapy for liver metastases. *Semin Oncol* 2002; **29**: 202-208
15 **Li Y**, Okegawa T, Lombardi DP, Frenkel EP, Hsieh JT. Enhanced transgene expression in androgen independent prostate cancer gene therapy by taxane chemotherapeutic agents. *J Urol* 2002; **167**: 339-346
16 **Rieger PT**. The role of oncology nurses in gene therapy. *Lancet Oncol* 2001; **2**: 233-238
17 **Ohana P**, Bibi O, Matouk I, Levy C, Birman T, Ariel I, SchneiderY, Ayesh S, Giladi H, Laster M, De Groot N, Hochberg A. Use of H19 regulatory sequences for targeted gene therapy in cancer. *Int J Cancer* 2002; **98**: 645-650
18 **Huh WK**, Barnes MN, Kelley FJ, Alvarez RD. Gene therapy. *Cancer Treat Res* 2002; **107**: 133-157
19 **Liu SC**, Minton NP, Giaccia AJ, Brown JM. Anticancer efficacy of systemically delivered anaerobic bacteria as gene therapy vectors targeting tumor hypoxia / necrosis. *Gene Ther* 2002; **9**: 291-296
20 **Kaneko S**, Tamaoki T. Gene therapy vectors harboring AFP regulatory sequences. Preparation of an adenoviral vector. *Mol Biotechnol* 2001; **19**: 323-330
21 **Mc CF**. Cancer gene therapy: fringe or cutting edge? *Nature Rev Cancer* 2001; **1**: 130-141
22 **Chang LJ**, He J. Retroviral vectors for gene therapy of AIDS and cancer. *Curr Opin Mol Ther* 2001; **3**: 468-475
23 **Richardson PD**, Augustin LB, Kren BT, Steer CJ. Gene repair and transposon-mediated gene therapy. *Stem Cells* 2002; **20**: 105-118
24 **Xu AG**, Li SG, Liu JH, Gan AH. Function of apoptosis and expression of proteins Bcl-2, p53 and C-myc in the development of gastric cancer. *World J Gastroenterol* 2001; **7**: 403-406
25 **Roth JA**, Cristiano RJ. Gene therapy for cancer: what have we done and where are we going? *J Nat Cancer Inst* 1997; **89:** 21-39
26 **Brenner MK.** Genetic marking and manipulation of hematopoietic progenitor cells using retroviral vectors. *Immunomethod*s 1994; **5**: 204-210
27 **Mitani K,** Graham FL, Caskey CT. Transduction of human bone marrow by adenoviral vector. *Hum Gene Ther* 1994; **5**: 941-948
28 **Weber E**, Anderson WF, Kasahara N. Recent advances in retrovirus vector-mediated gene therapy: teaching an old vector new tricks. *Curr Opin Mol Ther* 2001; **3**: 439-453
29 **Pieroni L**, La Monica N. Towards the use of baculovirus as a gene therapy vector. *Curr Opin Mol Ther* 2001; **3**: 464-467
30 **Okada T**, Sakai T, Murata T, Kako K, Sakamoto K, Ohtomi M, Katsura T, Ishida N. Promoter analysis for daily expression of Drosophila timeless gene. *Biochem Biophys Res Commun* 2001; **283**: 577-582
31 **Lasic DD**, Vallner JJ, Working PK. Sterically stabilized liposomes in cancer therapy and gene delivery. *Curr Opin Mol Ther* 1999; **1**: 177-185
32 **Manthorpe M**, Cornefert-Jensen F, Hartikka J, Felgner J, Rundell A, Margalith M, Dwarki V. Gene therapy by intrmuscular injection of plasmid DNA: studies on firefly luciferase gene expression in mice. *Human Gene Therapy* 1993; **4**: 419-431
33 **Michael SI**, Curiel DT. Strategies to achieve targeted gene delivery via the receptor-mediated endocytosis pathway. *Gene Ther* 1994; **1**: 223-232
34 **Vanden Driessche T**, Naldini L, Collen D, Chuah MK. Oncoretroviral and lentiviral vector-mediated gene therapy. *Methods Enzymol* 2002; **346**: 573-579
35 **Gomez NJ**, Curiel DT. Conditionally replicative adenoviral vectors for cancer gene therapy. *Lancet Oncol* 2000; **1**: 148-158
36 **Simko V**, Michael S. Effect of ursodeoxycholic acid on *in vivo* and in vitro toxic liver injury in rats. *Aliment Pharmacol Ther* 1994; **8:** 315-322
37 **Hart SL**, Knight AM, Harbottle RP, Mistry A, Hunger HD, Cutler DF, Williamson R, Coutelle C. Cell binding and internalization by filamentous phage displaying a cyclic Arg-Gly-Asp-containing peptide. *J Bio Chem* 1994; **269**: 12468-12474
38 **Moolten FL**. Tumour chemosensitivity conferred by inserted herpes thymidine kinase genes: paradigm for a prospective cancer control strategy. *Cancer Research* 1986; **46**: 5276-5281
39 **Floeth FW**, Shand N, Bojar H, Prisack HB, Felsberg J, Neuen-Jacob E, Aulich A, Burger KJ, Bock WJ, Weber F. Local inflammation and devascularization-*in vivo* mechanisms of the "bystander effect" in VPC-mediated HSV-Tk / GCV gene therapy for human malignant glioma. *Cancer Gene Ther* 2001; **8**: 843-851
40 **Freeman SM**, Abboud CN, Whartenby KA, Packman CH, Koeplin DS, Moolten FL, Abraham GN. The "bystander effect": tumour regression when a fraction of the tumor mass is genetically modified. *Cancer Research* 1993; **53**: 5274-5283
41 **Huber BE**, Austin EA, Good SS, Knick VC, Tibbels S, Richards CA. *In vivo* antitumor activity of 5-fluorocytosine on human colorectal carcinoma cells genetically modified to express cytosine deaminase. *Cancer Research* 1993;**53**: 4619-4626
42 **Crystal RG,** Hirschowitz E, Lieberman M, Daly J, Kazam E, Henschke C, Yankelevitz D, Kemeny N< Silverstein R, Ohwada A, Russ T, Mastrangeli A, Sanders A, Cooke J, Harvey BG. Phase 1 study of direct administration of a replication deficient adenovirus vector containing the E. coli cytosine deaminase gene to metastatic colon carcinoma of the liver in association with the oral administration of the pro-drug 5-fluorocytosine. *Human Gene Therapy* 1997; **8**: 985-1001
43 **Milligan JF**, Matteucci MD, Martin JC. Current concepts in antisense drug design. *J Med Chem* 1993; **36**: 1923-1937
44 **Chen L**. Antibody gene therapy: old wine in a new bottle. *Nat Med* 2002; **8**: 333-334
45 **Tang YC**, Li Y, Qian GX. Reduction of tumorigenicity of SMMC-7721 hepatoma cells by vascular endothelial growth factor antisense gene therapy. *World J Gastroenterol* 2001; **7**: 22-27
46 **Sacco MG**, Barbieri O, Piccini D, Noviello E, Zoppe M, Zucchi I, Frattini A, Villa A, Vezzoni P. *In vitro* and *in vivo* antisense-me-

diated growth inhibition of a mammary adenocarcinoma from MMTV-neu transgenic mice. *Gene Therapy* 1998; **5**: 388-393

47 **Wagner RW.** Gene inhibition using antisense oligodeoxynucleotides. *Nature* 1994; **372**: 333-335

48 **Cotter FE**, Johnson P, Hall P, Pocock C, Al Mahdi N, Cowell JK, Morgan G. Antisense oligonucleotides suppress B-cell lymphoma growth in a SCID-hu mouse model. *Oncogene* 1994; **9**: 3049-3055

49 **Kumai T**, Tateishi T, Tanaka M, Watanabe M, Shimizu H, Kobayashi S. Tyrosine hydroxylase antisense gene therapy causes hypotensive effects in the spontaneously hypertensive rats. *J Hypertens* 2001; **19**: 1769-1773

50 **Marchand GS**, Noiseux N, Tanguay JF, Sirois MG. Blockade of *in vivo* VEGF-mediated angiogenesis by antisense gene therapy: role of Flk-1 and Flt-1 receptors. *Am J Physiol Heart Circ Physiol* 2002; **282**: H194-204

51 **Tsang KY**, Zaremba S, Nieroda CA, Zhu MZ, Hamilton JM, Scholm J. Generation of human cytotoxic T cells specific for human carcinoembryonic antigen epitopes from patients immunised with recombinant vaccinia-CEA vaccine. *J Nat Cancer Inst* 1995; **87**: 982-990

52 **Cheng WF**, Hung CF, Hsu KF, Chai CY, He L, Polo JM, Slater LA, Ling M, Wu TC. Cancer immunotherapy using Sindbis virus replicon particles encoding a VP22-antigen fusion. *Hum Gene Ther* 2002; **13**: 553-568

53 **Wei MX**, Tamiya T, Hurford JR, Boviatsis EJ, Tepper RI, Chiacca EA. Enhancement of interleukin-4-mediated tumour regression in athymic mice by in situ retroviral gene transfer. *Human Gene Therapy* 1995; **6**: 437-443

54 **Steele RJ**, Thompson AM, Hall PA, Lane DP. The p53 tumour suppressor gene. *British J Surgery* 1998; **85**: 1460-1467

55 **Nishioka Y**, Hua W, Nishimura N, Sone S. Genetic modification of dendritic cells and its application for cancer immunotherapy. *J Med Invest* 2002; **49**: 7-17

56 **Takemura S**, Kudo T, Asano R, Suzuki M, Tsumoto K, Sakurai N, Katayose Y, Kodama H, Yoshida H, Ebara S, Saeki H, Imai K, Matsuno S, Kumagai I. A mutated superantigen SEA D227A fusion diabody specific to MUC1 and CD3 in targeted cancer immunotherapy for bile duct carcinoma. *Cancee Immunol Immunother* 2002; **51**: 33-44

57 **Vonderheide RH**. Telomerase as a universal tumor-associated antigen for cancer immunotherapy. *Oncogene* 2002; **21**: 674-679

58 **Schadendorf D**. The use of histamine in cancer immunotherapy. *J Invest Dermatol* 2002; **118**: 560-561

59 **Ohashi M**, Kanai F, Ueno H, Tanaka T, Tateishi K, Kawakami T, Koike Y, Ikenoue T, Shiratori Y, Hamada H, Omata M. Adenovirus mediated p53 tumour suppressor gene therapy for human gastric cancer cells *in vitro* and *in vivo*. *Gut* 1999; **44**: 366-371

60 **Okino T**, Onda M, Matsukura N, Inada KI, Tatematsu M, Suzuki S, Shimada T. Sequential histopathological changes *in vivo* after suicide gene therapy of gastric cancer induced by N-methyl-N'-nitro-N-nitrosoguanidine in rats. *Jpn J Cancer Res* 2001; **92**: 673-679

61 **Shimizu T**, Shimada H, Ochiai T, Hamada H. Enhanced growth suppression in esophageal carcinoma cells using adenovirus-mediated fusion gene transfer (uracil phosphoribosyl transferase and herpes simplex virus thymidine kinase). *Cancer Gene Ther* 2001; **8**: 512-521

62 **Yu ZC**, Ding J, Pan BR, Fan DM, Zhang XY. Expression and bioactivity identification of soluble MG7 scFv. *World J Gastroenterol* 2002; **8**: 99-102

63 **Robbins PD**, Evans CH, Chernajovsky Y. Gene therapy for arthritis. *Gene Ther* 2003; **10**: 902-911

64 **Baker D**, Hankey DJ. Gene therapy in autoimmune, demyelinating disease of the central nervous system. *Gene Ther* 2003; **10**: 844-853

65 **Thomas CE**, Ehrhardt A, Kay MA. Progress and problems with the use of viral vectors for gene therapy. *Nat Rev Genet* 2003; **4**: 346-358

66 **Bagley J**, Iacomini J. Gene Therapy Progress and Prospects: Gene therapy in organ transplantation. *Gene Ther* 2003; **10**: 605-711

67 **Guarini S.** New gene therapy for the treatment of burn wounds. *Crit Care Med* 2003; **31**: 1280-1281

68 **Kaneda Y**. Gene therapy: a battle against biological barriers. *Curr Mol Med* 2001; **1**: 493-499

69 **Denny WA**. Prodrugs for gene-firected rnzyme-prodrug therapy (suicide gene therapy). *J Biomed Biotechnol* 2003; **2003**:48-70

70 **Scholl SM**, Michaelis S, McDermott R. Gene Therapy Applications to Cancer Treatment. *J Biomed Biotechnol* 2003; **2003**: 35-47

71 **Lundstrom K**. Latest development in viral vectors for gene therapy. *Trends Biotechnol* 2003; **21**: 117-122

Edited by Zhu LH and Wang XL

P.O.Box 2345, Beijing 100023,China
Fax: +86-10-85381893
E-mail: wjg@wjgnet.com www.wjgnet.com

World J Gastroenterol 2003;9(11):2395-2399
World Journal of Gastroenterology
 ISSN 1007-9327

• ESOPHAGEAL CANCER •

Correlation between expression of human telomerase subunits and telomerase activity in esophageal squamous cell carcinoma

Chun Li, Ming-Yao Wu, Ying-Rui Liang, Xian-Ying Wu

Chun Li, Ming-Yao Wu, Xian-Ying Wu, Department of Pathology, Medical College, Shantou University, Shantou 515031, Guangdong Province, China
Ying-Rui Liang, Department of Pathology, Foshan First People' s Hospital, Foshan 528000, Guangdong Province, China
Supported by the Medical Science Research Foundation of Guangdong Province, No.A2001413
Correspondence to: Dr. Chun Li, Department of Pathology, Medical College, Shantou University, Shantou, 515031 Guangdong Province, China. chli@stu.edu.cn
Telephone: +86-754-8900486
Received: 2003-05-12 **Accepted:** 2003-06-27

Abstract

AIM: To investigate telomerase activity and hTERT, TP-1 expression and their relationships in esophageal squamous cell carcinoma (ESCC).

METHODS: Telomerase activity was measured in 60 ESCC tissues using telomeric repeat amplification protocol (TRAP) assay by silver staining. *In situ* hybridization was used for detecting hTERT and TP-1mRNA.

RESULTS: The telomerase activity was detected in 83.3 % of ESCC tissues. The difference of telomerase activity was significant between well and poorly cancer differentiated lesions ($P<0.05$). The positive rate of telomerase activity was higher in patients with lymphatic metastasis than in patients without lymphatic metastasis. In cancer tissues hTERT mRNA expression was 75 % and TP-1 mRNA expression was 71.7 %. The expression of hTERT, TP-1 mRNA in well and poorly differentiated carcinoma was not significant. The expression of hTERT mRNA was correlated with telomerase activity, but TP-1 mRNA expression was not correlated with it.

CONCLUSION: Telomerase activity and hTERT, TP-1 mRNA expression are up-regulated in ESCC. Telomerase activity in ESCC is correlated with lymphatic metastasis and cancer differentiation. Telomerase activity may be used as a prognostic marker in ESCC. hTERT mRNA expression is correlated with telomerase activity. Enhanced hTERT mRNA expression may initially comprehend the telomerase activity level, but it is less sensitive than TRAP assay.

Li C, Wu MY, Liang YR, Wu XY. Correlation between expression of human telomerase subunits and telomerase activity in esophageal squamous cell carcinoma. *World J Gastroenterol* 2003; 9(11): 2395-2399
http://www.wjgnet.com/1007-9327/9/2395.asp

INTRODUCTION

Repetitive telomere sequences are present at the ends of eukaryotic chromosomes that protect the ends from damage and rearrangement. Progressive shortening of telomeric sequences is associated with cell division owing to the end replication involved in DNA replication. Telomerase is a special type of reverse transcriptase that stabilizes the telomeric ends of chomosome by adding TTAGGG repeats onto the chromosome ends. In humans, telomerase is composed of at least two components. hTR containing the template for reverse transcription[1], and telomerase associated proteins. Telomerase associated protein consists of hTP-1[2,3] and human telomerase reverse transcriptase (hTERT). hTERT is thought to be a enzyme' s catalytic subunit. In human, telomerase was active during embryonic development, and it was active in adult germ-line tissues, immortal cell[4,5] and most malignant tumors[6,7]. We have reported that telomerase activities were high both in esophageal squamous cell carcinoma (ESCC) and in their preneoplasia lesions[8]. This study was to examine telomerase activity, expression of hTERT mRNA, and hTP-1 mRNA in ESCC tissues and to analyze the relationship between teolmerase activity and its associated proteins.

MATERIALS AND METHODS

Materials

Esophageal squamous cell carcinoma tissues from 60 patients (40 men and 20 female, aged from 34 to 70 years) undergone surgical resection in Tumor Hospital of Medical College Shantou University from 1999 to 2001 were analyzed. All fresh tissues were taken immediately after operation and stored at -70 ℃.

TRAP-silver staining for telomerase activity

We used $TRAP_{EZE}$ telomerase detection kit (Intergen Company). After addition of 10-20 μl telomerase assay lysis buffer (1×CHAPS), the cells were lysed on ice. The lysate was incubated on ice for 30 min and then centrifuged at 12 000 r/min for 20 min at 4 ℃. The supernatant was collected and the protein concentration was determined by standard procedures (BCA protein assay). A volume of 0.6 μg protein equivalent was added to 48 μl reaction solution containing TRAP buffer, dNTP Mix, TS primer, RP primer, K_1 primer and 2 units Taq polymerase. PCR condition was 33 cycles at 94 ℃ for 30 s, at 59 ℃ for 30 s. PCR products were loaded and run on 12.5 % non-denaturing polyacrylamide gel. After electrophoresis, the gel was stained with silver.

In situ hybridization for hTERT and TP-1 mRNA expression

Samples were frozen and serially cut into 5 μm thick sections. One section was stained by hematoxylin and eosin (HE) for microscopic examination. Another was detected for hTERT and TP-1 mRNA expression. Expression of hTERT mRNA and hTP-1 mRNA was detected by digoxigenin-labeked gene probe which form a commercial kit (Boster Company, China) according to the manufacturer' s instructions. The hTERT oligonucleotides probes were 5' -AGTCA GGCTG GGCCT CAGAGAGCTG AGTAG GAAGG-3' , 5' -GCATG TACGG CTGGA GGTCT GTCAA GGTAG AGACG-3' , and 5' -AGCCA AGGTT CCAGG CAGCT CACTG ACCCT-3' . The hTP-1 oligonucleotides probes were 5' -ATATC TGAGT

GGGTA GATAC ATGCT GATGT-3', 5'-GTCAG ATAGA CCAAG ACAGT GCGGC CTGGC CTGGC-3', and 5'-AGCCA AGGTT CCAGG CAGCT CACTG ACCCT-3'. The positive expression showed brown staining signals in cytoplasm. The positive cancer cells constituted more than 75 % of all cancer cells on the section were defined as a score of 3+ (strong), about 25-75 % of positive cells had a score of 2+ (moderate), and less than 25 % had a score of 1+ (weak). The score of - (negative) had no positive cancer cell.

Controls

TRAP telomerase activity analysis: Esophageal cancer cell line EC109 was used as positive telomerase control, which was identified to be telomerase positive by our laboratory. Negative control was to perform a $TRAP_{EZE}$ kit assay with 1×CHAPS lysis buffer substituted for the cell extract. Heat-treatment of each sample by incubating at 85 ℃ for 20 minutes prior to $TRAP_{EZE}$ kit assay to inactivate telomerase served as a heat inactivation control. The $TRAP_{EZE}$ primer Mix contains internal control, which produce a 36 bp band (S-IC) in every lane to monitor PCR inhibition. If the extract with telomerase activity, a ladder of products with 6 bp increment starting at 50 bp nucleotide and a 36 bp internal control band could be seen. If the extract was telomerase negative, there was only a 36 bp internal control band (S-IC) (Figure1).

In situ hybridization: Positive control section was provided with the kit. Negative control included using incubation solution instead of the probe or the sections digested with ribonucleases (RNase) (10 mg· L^{-1}) before hTERT or hTP-1 detection.

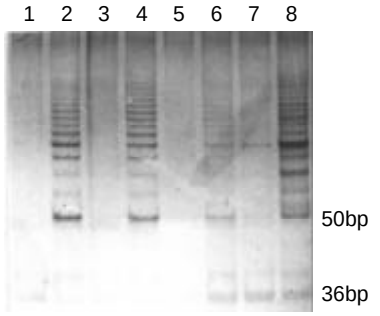

Figure 1 Carcinoma telomerase activity detected by TRAP-silver assay and separated on a 12.5 % polyacrylamide gel. Lane 1: primer-dimer/PCR contamination control, Lane 2: telomerase positive control, Lanes 4, 6 and 8: telomerase positive samples, Lanes 3, 5 and 7: heat-treated controls.

Statistical analysis

Statistical significance was tested using rectified chi-square test and exact method.

RESULTS

Relationship between telomerase activity and cancer differentiation

Histopathologically, the study population (n=60) was divided into 3 categories according to cancer differentiation as follows: grade I (n=15), grade II (n=33), and grade III (n=12). In 60 cases of esophageal SCC, telomerase activity was detected in 50 cases. The positive rate was 83.3 %. As showed in Table 1, the positive rates of telomerase activity were low in grade I and progressively increased from grade I to grade III. The significant difference of telomerase activity rate was found between grade I and grade II (χ^2=4.597, P<0.05), while, there was no significant differences between grade II and grade III (χ^2=0.263, P>0.05).

Table 1 Relationship between differentiation degree and telomerase activity in 60 cases of ESCC

Tumor stage	Sample (n)	Positive (n)	Prositive rate (%)	P value
I	15	9	60	
II	33	30	90.9	P<0.05
III	12	11	91.6	

Relationship between telomerase activity and lymphatic metastasis

There were 41 patients with lymph node metastasis out of the 60 patients. Telomerase activity rates were higher in patients with lymphatic metastasis (90.2 %) than in those without (63.2 %) (Table 2), and this difference was significant (χ^2=4.68, P<0.05).

Table 2 Relationship between telomerase activity and lymphatic metastasis

Sample (n)	Lymphatic metastasis	Telomerase activity		P value
		+	-	
41	+	37	4	P<0.05
19	-	12	7	

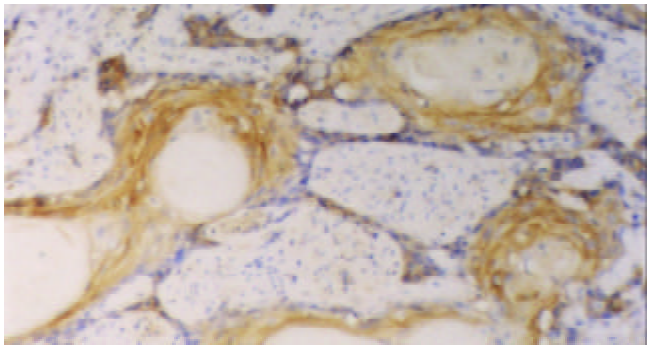

Figure 2 Esophageal squamous cell carcinoma (grade I). expression of hTERT mRNA was limited to the basaloid cell nests (40×).

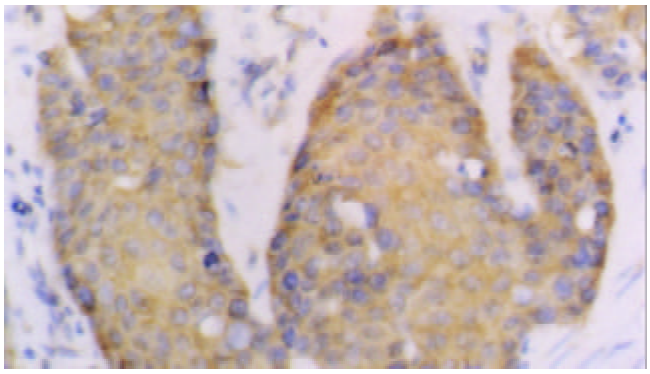

Figure 3 Poorly-differentiated esophageal squamous cell carcinoma. The expression of TP-1 mRNA was diffuse in cancer cells (40×).

Expression of hTERT and hTP-1 mRNA in esophageal squamous cell cacinoma

The positive rates of hTERT and hTP-1 mRNA expression were 75 % and 71.7 % respectively. The expression of hTERT and hTP-1 in well-differentiated carcinoma was limited to the basaloid cell nests (Figure 2). In the poorly-differentiated carcinoma, most tumor cells showed diffuse or occasionally

Table 3 Intensity of hTERT and hTP-1 mRNA expression in esophageal carcinoma tissues

Tumor stage	hTERT						*P* value	hTP-1					*P* value
	n	-	+	++	+++	Positive rate (%)		-	+	++	+++	Positive rate (%)	
I	15	7	4	3	1	53.3		7	5	3	0	53.3	
II	33	6	7	11	9	81.8	*P*>0.05	8	6	12	7	75.8	*P*>0.05
III	12	2	2	4	4	83.3		2	2	5	3	83.3	

Table 4 Relationship between hTERT, hTP-1 expression and telomerase activity

Telomerase activity	hTERT		*P* value	TP-1		*P* value
	+	-		+	-	
+	41	9	*P*<0.05	38	12	*P*>0.05
-	4	6		5	5	

focal expression (Figure 3). As showed in Table 3, the positive intensity and the positive rate of hTERT and hTP-1 expression progressively increased from grade I to grade III, but no significant differences existed between them (hTERT: χ^2=4.95, *P*>0.05; TP-1: χ^2=3.49, *P*>0.05).

Relationship between hTERT, hTP-1 expression and telomerase activity

Relationship between hTERT and hTP-1 expression and telomerase activity are summarized in Table 4. By statistical analyses, the expression of hTERT mRNA was correlated with telomerase activity (χ^2=5.76, *P*<0.05), but the expression of hTP-1 mRNA was no correlated with telomerase activity (χ^2=1.64, *P*>0.05).

DISCUSSION

Telomerase is a ribonucleoprotein reverse transcriptase that utilizes its own RNA template for the addition of telomeric sequences to chromosomal ends in order to maintain telomeric length. *In vivo* and *in vitro* studies suggested that telomerase was associated with cellular immortality and malignance, indicating that activation of telomerase might play an important role in tumorigenesis and immortalization. Telomerase activation has been demonstrated in many types of human tumors, including tumors in breast[9], nasopharynx[10,11], stomach[12-14], prostate[15], urinary bladder[16], skin[17], cervix[18], lung[19,20] and brain[21]. Some scientists suggested that telomerase activity was a diagnostic and prognostic marker for malignant tumors[22,23]. Previous research suggested that the positive rate of telomerase activity in esophageal carcinoma was 79-87 %, but there were different conclusions regarding the relationship between telomerase activity and cancer differentiation in esophageal cacinoma. Asai *et al*[24] reported that well-differentiated cancer had higher detectable telomerase activity, but Ikeguchi *et al*[25] found the opposite result. Zhao *et al*[26] concluded that telomerase activity had no correlation with cancer differentiation. Our present study results suggested that the detectable rate of telomerase activity was gradually increased from well-differentiated carcinoma to poorly-differentiated one. The difference between grade I and grade II was significant, while the difference between grade II and grade III was not significant. This result gave more evidences that telomerase activity was correlated with differentiation in esophageal SCC. The presence of telomerase activity in esophageal SCC with lymphatic metastasis suggested that the telomerase activity in patients with lymphatic metastasis was higher than that in patients without lymphatic metastasis.

Collins *et al*[27,28] first purified tetrahymena telomease protein p80. The p80 components could be specifically cross-linked to telomerase RNA. Then, the mammalian (mouse and human) homology of p80 was found, and termed telomerase-associated protein 1 (TP-1)[29]. The sequence of TP-1 showed most homology to tetrahymena p80. *In vitro* experiments suggested that TP-1 interacted specifically with telomerase RNA and that TP-1 was associated with telomerase activity. However, expression of TP-1 did not reflect the level of telomerase activity[30-32]. In the present study, we found that TP-1 expression was high in esophageal squamous cell carcinoma, but it was not correlated with telomerase activity. The specific mechanism by which the protein participated in telomerase function has not been defined.

Two related proteins, Est2p from the yeast *Saccharomyces cerevisiae* and p123 from the ciliate Euplotes aediculatus, have been identified as the catalytic subunits of telomerase in their respective species[33-36]. Est2 was first identified as a gene required for telomere maintenance in yeast[37] and was essential for telomerase activity. Then, a human gene, hEST2/hTERT (human telomerase reverse transcriptase), sharing significant sequence similarity with telomerase catalytic subunit genes of lower eukaryotes was cloned and the protein was identified[38]. Studies suggested that hTERT expression was correlated with telomerase activity. The expression of hTERT was up-regulated concomitantly with the activation of telomerase during the immortalization of cultured cells and down-regulated during *in vivo* cellular differentiation[39]. *In vitro*, changes in the sequence of hTERT amino acid might reduce telomerase activity, and transfer of hTERT into normal human cell might resurrect telomease[40]. Designing a ribozyme targeting hTERT also reduced telomerase activity[41]. However, some studies revealed that the levels of hTERT expression and detectable telomerase activity were not concomitant[42-48]. The present experiment suggested that hTERT mRNA expression was correlated with telomeras activity in esophageal SCC. But we found that the positive rate of hTERT mRNA expression was lower than detectable telomerase activity. The positive intensity and the positive rate of hTERT expression were progressively increased from grade I to grade III, but the differences between them was not significant. In 50 detectable telomerase activity cases, just 41 cases expressed hTERT mRNA, 9 cases had negatively expression of hTERT mRNA. There were 4 hTERT positive cases without detectable telomerase activity. It indicated that hTERT gene expression was an important factor to resurrect telomease, but not the only one. There was a possibility that other mechanisms were intervened to modulate telomerase activity. The reasons why the tissue had expression of hTERT mRNA without detectable telomerase activity are not clear. Following might be the explanations. Posttranscriptional modification of telomerase subunits would modulate telomerase activity, and there were some inhibitors in telomerase extract solution to reduce its activity. Using *in situ* hybiridization assay detected hTERT

expression might initially comprehend telomerase activity level. However, the result of hTERT expression and detectable telomerase activity were not identical. It was less sensitive than TRAP assay.

In summary, detectable telomerase activity and telomerase subunit expression are high in esophageal squamous cell carcinoma. Telomerase activity is related to tumor differentiation and lymphatic metastasis, which may provide a new marker for evaluating the prognosis of patients with esophageal SCC. Expression of hTERT mRNA is correlated with telomerase activity, but the expression of TP-1 mRNA is not correlated with telomerase activity.

REFERENCES

1 **Feng J**, Funk WD, Wang SS, Weinrich SL, Avilion AA, Chiu CP, Adams RR, Chang E, Allsopp RC, Yu J. The RNA component of human telomerase. *Science* 1995; **269:** 1236-1241

2 **Nakayama J**, Saito M, Nakamura H, Matsuura A, Ishikawa F. TLP1: a gene encoding a protein component of mammalian telomerase is a novel member of WD repeats family. *Cell* 1997; **88:** 875-884

3 **Harrington L**, Mcphail T, Mar V, Zhou W, Oulton R, Bass MB, Arruda I, Robinson MO. A mammalian telomerase-associated protein. *Science* 1997; **275:** 973-977

4 **Shen ZY,** Xu LY, Chen MH, Shen J, Cai WJ, Zeng Y. Progressive transformation of immortalized esophageal epithelial cells. *World J Gastroenterol* 2002; **8:** 976-981

5 **Shen ZY**, Xu LY, Li EM, Cai WJ, Chen MH, Shen J, Zeng Y. Telomere and telomerase in the initial stage of immortalization of esophageal epithelial cell. *World J Gastroenterol* 2002; **8:** 357-362

6 **Kim NW**, Piatyszek MA, Prowse KR, Harley CB, West MD, Ho PL, Coviello GM, Wright WE, Weinrich SL, Shay JW. Specific association of human telomerase activity with immortal cells and cancer. *Science* 1994; **266:** 2011-2015

7 **Hiyama E**, Hiyama K. Clinical utility of telomerase in cancer. *Oncogene* 2002; **21:** 643-649

8 **Li C**, Liang YR, Wu MY, Xu LY, Cai WJ. Telomerase activity analysis of esophageal carcinoma using microdissection-TRAP assay. *Chinese Med J* 2002; **115:** 1405-1408

9 **Hiyama E**, Gollahon L, Kataoka T, Kuroi, K, Yokoyama T, Gazdar AF, Hiyama K, Piatyszek MA, Shay JW. Telomerase activity in human breast tumors. *J Natl Cancer Inst* 1996; **88:** 116-122

10 **Cheng RY**, Yuen PW, Nicholls JM, Zheng Z, Wei W, Sham JS, Yang XH, Cao L, Huang DP, Tsao SW. Telomerase activation in nasopharyngeal carcinomas. *Br J Cancer* 1998; **77:** 456-460

11 **Tsao SW**, Zhang DK, Cheng RY, Wan TS. Telomerase activation in human cancers. *Chin Med J (Engl)* 1998; **111:** 745-750

12 **Hiyama E**, Yokoyama T, Tatsumoto N, Hiyama K, Imamura Y, Murakami Y, Kodama T, Piatyszek MA, Shay JW, Matsuura Y. Telomerase activity in gastric cancer. *Cancer Res* 1995; **55:** 3258-3262

13 **Yakoob J**, Hu GL, Fan XG, Zhang Z. Telomere, telomerase and digestive cancer. *World J Gastroenterol* 1999; **5:** 334-337

14 **Zhan WH**, Ma JP, Peng JS, Gao JS, Cai SR, Wang JP, Zheng ZQ, Wang L. Telomerase activity in gastric cancer and its clinical implications. *World J Gastroenterol* 1999; **5:** 316-319

15 **Sommerfeld HJ**, Meeker AK, Piatyszek MA, Bova GS, Shay JW, Coffey DS. Telomerase activity: a prevalemt marker of malignant human prostate tissue. *Cancer Res* 1996; **56:** 218-222

16 **Lin Y**, Miyamoto H, Fujinami K, Uemura H, Hosaka M, Iwasaki Y, Kubota Y. Telomerase activity in human bladder cancer. *Clin Cancer Res* 1996; **2:** 929-932

17 **Taylor RS**, Ramirez RD, Ogoshi M, Chaffins M, Piatyszek MA, Shay JW. Detection of telomerase activity in malignant and nonmalignant skin conditions. *J Invest Dermatol* 1996; **106:** 759-765

18 **Zhang DK**, Ngan HY, Cheng RY, Cheung AN, Liu SS, Tsao SW. Clinical significance of telomerase activation and telomeric restriction fragment (TRF) in cervical cancer. *Eur J Cancer* 1999; **35:** 154-160

19 **Wu TC,** Lin P, Hsu CP, Huang YJ, Chen CY, Chung WC, Lee H, Ko JL. Loss of telomerase activity may be a potential favorable prognostic marker in lung carcinomas. *Lung Cancer* 2003; **41:** 163-169

20 **Hiyama K**, Hiyama E, Ishioka S, Yamakido M, Inai K, Gazdar AF, Piatyszek MA, Shay JW. Telomerase activity in small-cell and non-small-cell lung cancers. *J Natl Cancer Inst* 1995; **87:** 895-902

21 **Sano T**, Asai A, Mishima K, Fujimaki T, Kirino T. Telomerase activity in 144 brain tumours. *Br J Cancer* 1998; **77:** 1633-1637

22 **Zhang YL**, Zhang ZS, Wu BP, Zhou DY. Early diagnosis for colorectal cancer in China. *World J Gastroenterol* 2002; **8:** 21-25

23 **Qin LX**, Tang ZY. The prognostic molecular markers in hepatocellular carcinoma. *World J Gastroenterol* 2002; **8:** 385-392

24 **Asai A**, Kiyozuka Y, Yoshida R, Fujii T, Hioki K, Tsubura A. Telomere length, telomerase activity and telomerase RNA expression in human esophageal cancer cells: correlation with cell proliferation, differentiation and chemosensitivity to anticancer drugs. *Anticancer Res* 1998; **18:** 1465-1472

25 **Ikeguchi M**, Kaibara N. Telomerase activity in esophageal squamous cell carcinoma and in normal esophageal epithelium adjacent to carcinoma. *Nippon Rinsho* 1998; **56:** 1176-1180

26 **Zhao CF**, Chen CL. Detection of telomerase activity in tumor tissues from patients with esophageal carcinoma. *Chin J Cancer* 2000; **19:** 131-133

27 **Collins K,** Kobayashi R, Greider CW. Purification of Tetrahymena telomerase and cloning of genes encoding the two protein components of the enzyme. *Cell* 1995; **81:** 677-686

28 **Kickhoefer VA**, Stephen AG, Harrington L, Robinson MO, Rome LH. Vaults and telomerase share a common subunit, TEP1. *J Biol Chem* 1999; **274:** 32712-32717

29 **Harrington L,** Mcphail T, Mar V, Zhou W, Oulton R, Bass MB, Arruda I, Robinson MO. A mammalian telomerase-associated protein. *Science* 1997; **275:** 973-977

30 **Harrington L**, Zhou W, McPhail T, Oulton R, Yeung DS, Mar V, Bass MB, Robinson MO. Human telomerase contains evolutionarily conserved catalytic and structural subunits. *Genes Dev* 1997; **11:** 3109-3115

31 **Nakayama J,** Saito M, Nakamura H, Matsuura A, Ishikawa F. TLP1: a gene encoding a protein component of mammalian telomerase is a novel member of WD repeats family. *Cell* 1997; **88:** 875-884

32 **Saito T**, Matsuda Y, Suzuki T, Hayashi A, Yuan X, Saito M, Nakayama J, Hori T, Ishikawa F. Comparative gene mapping of the human and mouse TEP1 genes, which encode one protein component of telomerases. *Genomics* 1997; **46:** 46-50

33 **Counter CM,** Meyerson M, Eaton EN, Weinberg RA. The catalytic subunit of yeast telomerase. *Proc Natl Acad Sci U S A* 1997; **94:** 9202-9207

34 **Lingner J**, Cech TR, Hughes TR, Lundblad V. Three Ever Shorter Telomere (EST) genes are dispensable for *in vitro* yeast telomerase activity. *Proc Natl Acad Sci U S A* 1997; **94:** 11190-11195

35 **Nakamura TM**, Morin GB, Chapman KB, Weinrich SL, Andrews WH, Lingner J, Harley CB, Cech TR. Telomerase catalytic subunit homologs from fission yeast and human. *Science* 1997; **277:** 955-959

36 **Lingner J,** Hughes TR, Shevchenko A, Mann M, Lundblad V, Cech TR. Reverse transcriptase motifs in the catalytic subunit of telomerase. *Science* 1997; **276:** 561-567

37 **Lendvay TS**, Morris DK, Sah J, Balasubramanian B, Lundblad V. Senescence mutants of Saccharomyces cerevisiae with a defect in telomere replication identify three additional EST genes. *Genetics* 1996; **144:** 1399-1412

38 **Meyerson M**, Counter CM, Eaton EN, Ellisen LW, Steiner P, Caddle SD, Ziaugra L, Beijersbergen RL, Davidoff MJ, Liu Q, Bacchetti S, Haber DA, Weinberg RA. hEST2 the putative human telomerase catalytic subunit gene, is up-regulated in tumor cells and during immortalization. *Cell* 1997; **90:** 785-795

39 **Counter CM**, Meyerson M, Eaton EN, Ellisen LW, Caddle SD, Haber DA, Weinberg RA. Telomerase activity is restored in human cells by ectopic expression of hTERT (hEST2), the catalytic subunit of telomerase. *Oncogene* 1998; **16:** 1217-1222

40 **Ramakrishnan S**, Eppenberger U, Mueller H, Shinkai Y, Narayanan R. Expression profile of the putative catalytic subunit of the telomerase gene. *Cancer Res* 1998; **58:** 622-625

41 **Hao ZM,** Luo JY, Cheng J, Wang QY, Yang GX. Design of a

ribozyme targeting human telomerase reverse transcriptase and cloning of it's gene. *World J Gastroenterol* 2003; **9:** 104-107

42 **Ulaner GA**, Hu JF, Vu TH, Giudice LC, Hoffman AR. Telomerase activity in human development is regulated by human telomerase reverse transcriptase (hTERT) transcription and by alternate splicing of hTERT transcripts. *Cancer Res* 1998; **58**: 4168-4172

43 **Liu K,** Schoonmaker MM, Levine BL, June CH, Hodes RJ, Weng NP. Constitutive and regulated expression of telomerase reverse transcriptase (hTERT) in human lymphocytes. *Proc Natl Acad Sci U S A* 1999; **96:** 5147-5152

44 **Hara T,** Noma T, Yamashiro Y, Naito K, Nakazawa A. Quantitative analysis of telomerase activity and telomerase reverse transcriptase expression in renal cell carcinoma. *Urol Res* 2001; **29:** 1-6

45 **Kameshima H,** Yagihashi A, Yajima T, Kobayashi D, Hirata K, Watanabe N. Expression of telomerase-associated genes: reflection of telomerase activity in gastric cancer. *World J Surg* 2001; **25:** 285-289

46 **Zhang RG,** Guo LX, Wang XW, Xie H. Telomerase inhibition and telomere loss in BEL-7404 human hepatoma cells treated with doxorubicin. *World J Gastroenterol* 2002; **8:** 827-831

47 **Yajima T,** Yagihashi A, Kameshima H, Kobayashi D, Hirata K, Watanabe N. Telomerase reverse transcriptase and telomeric-repeat binding factor protein 1 as regulators of telomerase activity in pancreatic cancer cells. *Br J Cancer* 2001; **85:** 752-757

48 **Tominaga T,** Kashimura H, Suzuki K, Nakahara A, Tanaka N, Noguchi M, Itabashi M, Ohkawa J. Telomerase activity and expression of human telomerase catalytic subunit gene in esophageal tissues. *J Gastroenterol* 2002; **37:** 418-427

Edited by Zhang JZ and Wang XL

P.O.Box 2345, Beijing 100023,China
Fax: +86-10-85381893
E-mail: wjg@wjgnet.com www.wjgnet.com

World J Gastroenterol 2003;9(11):2400-2403
World Journal of Gastroenterology
 ISSN 1007-9327

• ESOPHAGEAL CANCER •

Epidemiology of gastroenterologic cancer in Henan Province, China

Jian-Bang Lu, Xi-Bin Sun, Di-Xin Dai, Shi-Kuan Zhu, Qiu-Ling Chang, Shu-Zheng Liu, Wen-Jie Duan

Jian-Bang Lu, Xi-Bin Sun, Qiu-Ling Chang, Wen-Jie Duan, Henan Cancer Research Institute, Zhengzhou 450003, Henan Province, China
Di-Xin Dai, Shi-Kuan Zhu, Shu-Zheng Liu, Henan Tumor Hospital, Zhengzhou 450003, Henan Province, China
Supported by the National Medical Science and Technique Foundation of China during the 9th Five-Year Plan Period, No.96-906-01-01 and Science Research Fund of Henan Province, No. 971200101
Correspondence to: Dr. Jian-Bang Lu, Department of Epidemiology, Henan Cancer Research Institute, Dongming Road 127, Zhengzhou 450003, Henna Province, China. hncjbl@sohu.com
Telephone: +86-371-5962654
Received: 2002-07-23 **Accepted:** 2002-10-17

Abstract

AIM: To estimate the mortality rates of gastroenterologic cancers for the period between 1974 and 1999, in Henan Province, China and its epidemiologic features.

METHODS: Information on death of patients with cancer was provided by the county-city registries. Population data were provided by the local police bureau. All the deaths of cancer registered were classified according to the three-digit rubric of the ICD-9. Cancer mortality rates reported herein were age-adjusted, using the world population as standard and weighted piecewise linear regression analysis.

RESULTS: Total cancer age-adjusted mortality rates were 195.91 per 100 000 for males and 124.36 per 100 000 for females between 1996 and 1998. During the period of 1974-1999, a remarkable decrease took place in esophageal carcinoma, stomach cancer remained essentially stable and liver cancer, a moderate increase. Colorectal cancer was slightly increased over the last two decades.

CONCLUSION: The population-based cancer registry can give an accurate picture of cancer in Henan Province, by providing a set of analyses of selected cancer mortality data as a source of reference for researchers in cancer, public health and health care services.

Lu JB, Sun XB, Dai DX, Zhu SK, Chang QL, Liu SZ, Duan WJ. Epidemiology of gastroenterologic cancer in Henan Province, China. *World J Gastroenterol* 2003; 9(11): 2400-2403
http://www.wjgnet.com/1007-9327/9/2400.asp

INTRODUCTION

China is one of the countries with the highest esophageal cancer and gastric cancer risk over the past century which is still the leading cause of deaths worldwide[1-9]. The aim of this study was to estimate the mortality of digestive tract cancers in Henan Province.

Promotion of cancer control programs requires accurate data on cancer incidence and mortality from population-based registries. In 1977, we reviewed all causes of death between 1974 and 1976 retrospectly and enlisted the participation in this survey of the 15 cancer registries from 1983 to 1999 in Henan Province which was inhabited with about 9 million people, one-tenth of the province's total population. The geographical locations of these units are shown in Figure 1.

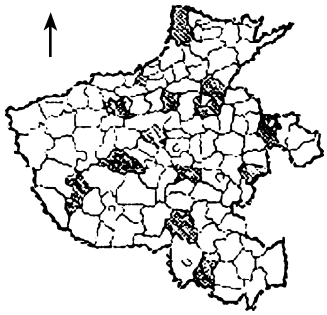

Figure 1 Geographical locations of the participating county and city registries of Henan Province, China.

MATERIALS AND METHODS

Information on death of patients with cancer was provided by the county-city registries, that consisted of the rural doctors and the local hospital doctors. Information was requested on demographic factors such as place of residence, age, sex, date of birth, and primary site of cancer as well as different diagnostic methods used such as radiology, cytology, and histology. Population data were provided by the local police bureau, consisting of the total population and the age-sex structure at the end of each year in each site studied.

All cancer deaths registered were classified according to the three-digit rubric of the ICD-9[10]. To facilitate comparison on an international basis, cancer mortality rates reported herein were age-adjusted, using the world population as standard. The direct standardization method was used to calculate various age groups from 5-years to 80 years and older. Cancer mortality trends from 1974 to 1999 were determined for more than 4 anatomic sites in males and females using weighted piecewise linear regression analysis.

RESULTS

The total cancer age-adjusted mortality rates were 193.68 per 100 000 for males and 133.29 per 100 000 for females in 1974-1976, and 218.29 per 100 000 and 125.52 per 100 000 in 1986-1988, and 195.91 per 100 000 and 124.36 per 100 000 in 1996-1998, respectively, accounting for 13.12 % for males and 10.71 % for females in 1974-1976, and 19.78 % and 15.82 % in 1986-1988, and 22.37 % and 17.25 % in 1996-1998, respectively of all cancer deaths. The major cancers diagnosed in Henan Province among males and femals are presented in Table 1. The main cancers in men included esophagus, stomach, liver and lung cancers, and the main cancers in women included esophagus, stomach, liver, lung, cervical and breast cancers. In general in Henan Province, men had higher mortality rates than women.

Table 1 Estimated cancer mortality rates[1] for males and females in Henan Province based on 15 selected registries

Site[2]	Years	Male		Female	
		ADM[1]	%	ADM[1]	%
All sites	1974-76	193.68	100.00	133.29	100.00
(140-208)	1986-88	218.29	100.00	125.52	100.00
	1996-98	195.91	100.00	124.36	100.00
Esophagus	1974-76	70.06	45.62	36.34	36.65
(150)	1986-88	67.78	31.04	35.99	32.14
	1996-98	43.77	25.70	25.73	24.19
Stomach	1974-76	36.02	19.89	19.79	15.01
(151)	1986-88	63.45	30.39	31.90	24.97
	1996-98	51.56	26.85	31.71	24.19
Colon / rectum	1974-76	6.47	3.92	6.14	4.48
(153-154)	1986-88	6.33	3.36	6.23	4.83
	1996-98	7.89	4.12	8.41	5.04
Liver (155)	1974-76	17.54	11.53	8.21	7.70
	1986-88	26.63	14.96	11.48	10.93
	1996-98	32.02	16.37	16.16	14.58

1: Age-adjusted mortality, standardized using world standard population. 2: Numbers in parentheses are ICD-9.

Table 2 illustrates urban-rural comparisons for selected cancer deaths from 1983 -1985 and 1997 in Henan Province, which included 12 counties and three cities. In Henan Province, rural areas had higher cancer mortality rates than urban areas, except for liver cancer in males.

Table 2 Urban and rural differences in mortality rates[1] of cancer from selected sites in Henan Province, China (1980's and 1990's)

Site[2]	Sex	Urban area		Rural area	
		1983-85	1997	1983-85	1997
All sites	M	170.09	149.52	208.80	190.34
(140-208)	F	99.89	52.83	126.99	103.07
Esophagus	M	78.74	12.10	87.63	50.03
(150)	F	45.62	5.48	57.29	25.58
Stomach	M	35.13	21.01	54.06	49.66
(151)	F	17.35	4.05	31.86	23.52
Colon / Rectum	M	8.10	8.92	6.38	9.17
(153-154)	F	5.48	2.36	4.36	4.81
Liver (155)	M	30.47	38.48	23.40	36.10
	F	11.11	9.43	11.28	17.06

1: Age-adjusted mortality, standardized using world standard population. 2: Numbers in parentheses are ICD- 9.

Cancer mortality rates at all sites did not change over the past two decades (Figure 2). During the period of 1974 -1999, marked changes took place in Henan Province in cancer mortality rates at certain sites. Esophageal carcinoma markedly declined, esophageal cancer mortality rates decreased over the period studied for males from approximately 70 per 100 000 in 1974-1976 to 43 per 100 000 in 1996-1998, and for females from approximately 36 per 100 000 to 25 per 100 000, respectively (Figure 3). Stomach cancer remained essentially stable (Figure 4), liver cancer have markedly increased (Figure 5). Colorectal cancer was the fifth most frequently diagnosed cancer in Henan Province. Men were diagnosed with this cancer slightly more frequently than women. Mortality rates for colorectal cancer have slightly increased over the last two decades (Table 1).

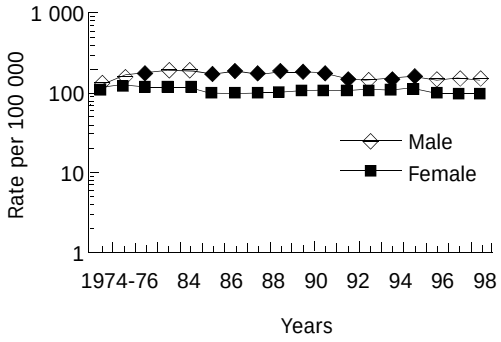

Figure 2 Total cancer mortality in Henan Province, China,1974-1999.

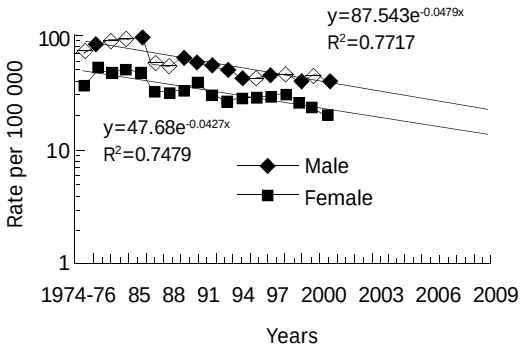

Figure 3 Age-adjusted mortality of esophageal cancer in Henan Province, China, 1974-1999.

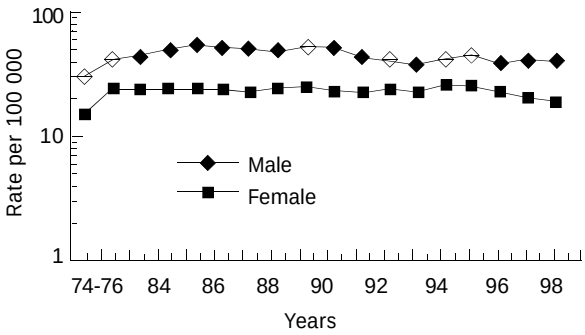

Figure 4 Age-adjusted mortality of stomach cancer in Henan Province, China, 1974-1999.

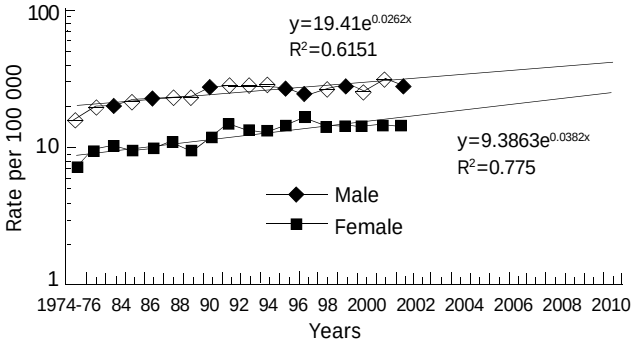

Figure 5 Age-adjusted mortality of liver cancer in Henan Province, China, 1974-1999.

DISCUSSION

Generally, genetic factors, per se, do not produce marked mortality changes over a short period of time, unless a specific

genetic factor present in the population interacts with a newly introduced agent in the environment. Thus marked changes in mortality rates, either increased or decreased, usually indicate that a new environmental agent has been introduced into or removed from the population in question. Compared with many other countries[11-18], all cancer mortality in Henan Province varied slightly over the past 25 years. Although mortality rates varied widely in specific cancers, cancers of the esophagus, stomach, liver and lung accounted for over 86 % of all cancer deaths in Henan Province. Cervical cancer and breast cancer made up 81 % of deaths in women. In general in Henan Province, men had higher mortality rates than women, and rural areas had higher mortality rates than urban areas, except for lung cancer.

Cancer mortality rates at all sites have been associated with many factors, including diet and nutrition[19-23], occupational exposure to toxic chemicals, tobacco and alcohol use, and certain viruses[24-31]. We found that lower socio-economic status, environmental pollution around the residential areas, lampblack in rooms, lower body mass index (BMI), more pickled food intake, cigarette smoking, alcohol drinking, mental-trauma and depression were risk factors of esophageal cancer. It also showed that the subjects having histories of upper digestive tract operation, dysplasia of esophagus and family histories of carcinoma had markedly increased risks for developing esophageal cancer[32]. Over the last 20 years, the dietary change occurred in Linzhou which was associated with the incidence and mortality decrease of esophageal cancer in the past ten years[33,34]. Cancer mortality rates at all sites remained essentially stable for males during the period studied, from approximately 193 per 100 000 in 1974-1976 to 195 per 100 000 in 1996-1998. Cancer mortality rates of females decreased over the last two decades from 133.29 per 100 000 in 1974-1976 to 124.36 per 100 000 in 1996-1998.

At the time of this study, esophageal cancer mortality rates decreased over the period studied for males, from approximately 70 per 100 000 in 1974-1976 to 43 per 100 000 in 1996-1998, and for females, from 36 per 100 000 in 1974-1976 to 24 per 100 000 in 1996-1998. Stomach cancer mortality rates did not change substantially during the period studied. Inversely, gastric cancer incidence and mortality rates showed a consistent decline in recent decades world-wide[12-15,21,22,35]. Liver cancer mortality rates for males markedly increased over the last two decades, from 17 per 100 000 in 1974-1976 to 32 per 100 000 in 1996-1998, for females from 8 per 100 000 in 1974-1976 to 16 per 100 000 in 1996-1998. Primary liver carcinoma (PLC) incidence and death rates in Australia increased in the past two decades[36]. Based on selected cancer registries around the world, developing countries have experienced PLC increases in incidence wherease developed countries have experienced declines[37].

The data analyzed in this report were age-adjusted using world standard population and stratified for sex and places. In temporary variation, the patterns presented were descriptive in nature. Secular trend in esophageal cancer and live cancer for both sexes in 1974-2010 with regression was used for spatial analysis.

At the end of the 20th century, cancer was the second leading cause of death in Henan Province. In the new century cancer will be the number one killer in Chinese.

Future cancer control research must aim to reduce cancer risk, incidence and mortality, and improve the quality of life[38].

CONCLUSIONS

The role of population-based cancer registry is to collect the data which give an accurate picture of cancer in a population, in order to understand and control the impact of cancer on that population. The cancer registry data can also be used to plan medical facilities and requirements needed for cancer control.

ACKNOWLEDGEMENTS

We thank the doctors from the 15 counties and cities for their assistance in data collection.

REFERENCES

1 **Ke L.** Mortality and incidence trends from esophagus cancer in selected geographic areas of China circa 1970-90. *Int J Cancer* 2002; **102**: 271-274
2 **Zhang W,** An F, Lin H. A case-control study on the risk factors of esophageal cancer in Jieyang City of Guangdong in China. *Zhonghua Liuxing Bingxue Zazhi* 2001; **22**: 442-445
3 **Botterweck AA,** Schouten LJ, Volovics A, Dorant E, van Den Brandt P. Trends in incidence of adenocarcinoma of the oesophagus and gastric cardia in ten European countries. *Int J Epidemiol* 2000; **29**: 645-654
4 **Desoubeaux N,** Le Prieur A, Launoy G, Maurel J, Lefevre H, Guillois JM, Gignoux M. Recent time trends in cancer of the oesophagus and gastric cardia in the region of Calvados in France, 1978-1995; a population based study. *Eur J Cancer Prev* 1999**; 8**: 479-486
5 **Adanja B,** Gledovic Z, Pekmezovic T, Vlajinac H, Jarebinski M, Zivaljevic V, Pavlovic M. Mortality trends of malignant tumours of digestive organ in Belgrade, Yugoslavia, 1975-1997. *Dig Liver Dis* 2000; **32**: 386-391
6 **Wijnhoven BP**, Louwman MW, Tilanus HW, Goebergh JW. Increased incidence of adenocarcinomas at the gastro-oesophageal junction in Dutch males since the 1990s. *Eur J Gastroenterol Hepatol* 2002; **14**: 115-122
7 **Blaser MJ,** Saito D. Trends in reported adenocarcinomas of the oesophagus and gastric cardia in Japan. *Eur J Gastroenterol Hepatol* 2002; **14**: 107-113
8 **Hansen S,** Wiig JN, Giercksky KE, Tretli S. Esophageal and gastric carcinoma in Norway 1958-1992: incidence time trend variability according to morphological subtypes and organ subsites. *Int J Cancer* 1997; **71**: 340-344
9 **Wolfgarten E,** Rosendahl U, Nowroth T, Leers J, Metzger R, Holscher AH, Bollschweiler E. Coincidence of nutritional habits and esophageal cancer in Germany. *Onkologie* 2001; **24**: 546-551
10 **World Health Organization**: International classification of diseases (ICD-9); 1 st ed. *Geneva: WHO* 1976
11 **Coleman MP,** Esteve J, Damiecki P, Arslan A, Renaard H. Trends in cancer incidence and mortality. *Lyon IARC Scientific Publications* 1993
12 **Newnham A,** Quinn MJ, Babb P, Kang JY, Majeed A. Trends in oesophageal and gastric cancer incidence, mortality and survival in England and Wales 1971-1998 / 1999. *Aliment Pharmacol Ther* 2003; **17**: 655-664
13 **Ruiz Ramos M,** Nieto Garcia MA, Mayoral Cortes JM. Mortality caused by cancer in Andalusia: trends and geographic distribution. *Aten Primaria* 2001; **28**: 634-641
14 **Corella D,** Guillen M. Dietary habits and epidemiolgy of gastric carcinoma. *Hepatogastroenterology* 2001; **48**: 1537-1543
15 **Gaudi I,** Kasler M. The course of cancer mortality in Hungary between 1975-2001. *Magy Onkol* 2002; **46**: 291-295
16 **Terry MB,** Gaudet MM, Gammon MD. The epidemiology of gastric cancer. *Sem in Radiat Oncol* 2002; **12**: 111-127
17 **Brooks-Brunn JA.** Esophageal cancer: an overview. *Medsurg Nurs* 2000; **9**: 248-254
18 **Bae JM,** Jung KM, Won YJ. Estimation of cancer deaths in Korea for the upcoming years. *J Korean Med Sci* 2002; **17**: 611-615
19 **Harvard Center for Cancer Prevention, Harvard School of Public Health**. Harvard report on cancer prevention. Volume 1. Causes of human cancer. *Cancer Causes Control* 1996; **7**: 3-59
20 **Palli D**, Russo A, Decarli A. Dietary patterns, nutrient intake and gastric cancer in a high-risk area of Italy. *Cancer Causes Control* 2001; **12**: 163-172
21 **Brown LM,** Devesa SS. Epidemiologic trends in esophageal and gastric cancer in United States. *Surg Oncol Clin N Am* 2002; **11**:

235-256
22 **Holtmann G**. Reflux disease: the disorder of the third millennium. *Eur J Gastroenterol Hepatol* 2001; **13**(Suppl 1): S5-11
23 **Mayne ST,** Navarro SA. Diet, obesity and reflux in the etiology of adenocarcinomas of the esophagus and gastric cardia in humans. *J Nutr* 2002; **132**(11Suppl): 3467S-3470S
24 Waste-mnnagement Education & Research Consortium (WERC), Collegge of Engineering, New Mexico State University (NMSU). *Cancer incidence rates in Eddy and Lea counties New Mexico* 1970-1994. 1998
25 **Tomeo CA**, Colditz GA, Willett WC, Giovannucci E, Platz E, Rockhill B, Dart H, Huneter DJ. Harvard report on cancer prevention Volume 3. Prevention of colon cancer in the United States. *Cancer Causes Control* 1999; **10**:167-180
26 **Colditz GA**, Atwood KA, Emmons RR, Nonson WC, Willett D, Trichopoulos Hunter DJ. Harvard report on cancer prevention. Volume 4. Harvard cancer risk index. *Cancer Causes Control* 2000; **11**: 477-488
27 **Bulbulyan MA,** Iiychova SA, Zahm SH, Astashevsky SV, Zaridze DG. Cancer mortality among women in the Russian printing industry. *Am J Ind Med* 1999; **36**: 166-171
28 **Tovar-Guzman VJ,** Barquera S, Lopez-Antunano FJ. Mortality trends in cancer attributable to tobacco in Mexico. *Salud Publica Mex* 2002; **44**(Suppl 1): S20-28
29 **Yu MC,** Yuan JM, Govindarajan S, Ross RK. Epidemiology of hepatocellular carcinoma. *Can J Gastroenterol* 2000; **14**: 703-709
30 **Cacoub P,** Geffray L, Rosenthal E, Perronne C, Veyssier P, Raguin G. Mortality among human immunodeficiency virus-infected patients with cirrhosis or hepatocellular carcinoma due to hepatitis C virus in Frence Departments of Internal Medicine / Infections Diseases, in 1995 and 1997. *Clin Infect Dis* 2001; **32**: 1207-1214
31 **El-Serag HB.** Epidemiology of hepatocellular carcinoma. *Clin Liver Dis* 2001; **5**: 87-107
32 **Lu JB**, Lian SY, Sun XB, Zhang ZX, Dai DX, Li BY, Cheng LP, Wei JR, Duan WJ. A case-control study on the risk factors of esophageal cancer in Linzhou. *Zhouhua Liuxingbingxue Zazhi* 2000; **21**: 434-436
33 **Lu JB**, Lian SY, Sun XB, Zhang ZX, Dai DX, Li BY, Cheng LP, Wei JR, Duan WJ. Dietary changes and the trends in morbidity and mortality on esophageal cancer in Linzhou. *Zhongguo Gonggong Weisheng* 2001; **17**: 60-61
34 **Lu JB**, Sun XB, Dai DX, Lian SY, Chang QL, Liu SZ, Li BY. Prevalence trends of esophageal cancer in Henan in 1974-1999. *Zhongliu Fangzhi Zazhi* 2002; **9**: 118-120
35 **Parkin DM**, Whelan SL, Ferlay J, Young J, eds. Cancer incidence In Five Continents, *IARC Scientific Publications* No.**143**. Lyon: International Agency for Research on Cancer, 1997
36 **Law MG,** Roberts SK, Dore GJ, Kaldor JM. Primary hepatocellular carcinoma in Australia, 1978-1997: increasing incidence and mortality. *Med J Aust* 2000; **173**: 403-405
37 **McGlynn KA,** Tsao L, Hsing AM, Devesa SS, Praumeni JF Jr. International trends and patterns of primary liver cancer. *Int J Cancer* 2001; **94**: 290-296
38 **Barbara K**. Rimer. Cancer control research 2001. *Cancer Causes Control* 2000; **11**: 257-270

Edited by Ma JY and Wang XL

P.O.Box 2345, Beijing 100023,China
Fax: +86-10-85381893
E-mail: wjg@wjgnet.com www.wjgnet.com

World J Gastroenterol 2003;9(11):2404-2408
World Journal of Gastroenterology
 ISSN 1007-9327

• ESOPHAGEAL CANCER •

Inhibition of adenovirus-mediated p27kip1 gene on growth of esophageal carcinoma cell strain

Qing-Ming Wu, Jie-Ping Yu, Qiang Tong, Xiao-Hu Wang, Guo-Jian Xie

Qing-Ming Wu, Jie-Ping Yu, Department of Gastroenterology, Renmin Hospital of Wuhan University, Wuhan 430060, Hubei Province, China
Qiang Tong, Xiao-Hu Wang, Guo-Jian Xie, Department of Gastroenterology, Taihe Hospital of Yunyang Medical College, Shiyan 442000, Hubei Province, China
Correspondence to: Dr. Qing-Ming Wu, Department of Gastroenterology, Taihe Hospital of Yunyang Medical College, 29 Renmin Road, Shiyan 442000, Hubei Province, China. wuhe9224@sina.com
Telephone: +86-719-8801431 **Fax:** +86-719-8883809
Received: 2003-03-04 **Accepted:** 2003-06-02

Abstract

AIM: To investigate the inhibition of p27kip1 gene on the growth of esophageal carcinoma cell strain (EC9706).

METHODS: Recombinant adenovirus Ad-p27kip1 was constructed and transfected into esophageal carcinoma cell EC-9706, and its effect on p27kip1 expression, the growth of esophageal carcinoma cell, DNA replication, protein synthesis, cell multiplication and apoptosis were explored by means of cell growth count, ^{3}H-TdR, ^{3}H-Leucine incorporation, flow cytometry, DNA fragment analysis and TUNEL.

RESULTS: Recombinant adenovirus Ad-p27kip1 was successfully constructed with a virus titer of 1.24×10^{12} pfu/ml. p27kip protein expression increased markedly after EC-9706 transfection, while incorporation quantity of ^{3}H-TdR and ^{3}H-Leucine decreased significantly. The growth of esophageal carcinoma cell was inhibited obviously. Testing of flow cytometry displayed a typical apoptosis peak, and DNA gel electrophoresis showed a typical apoptosis ladder. TUNEL showed the apoptosis rate of Ad-p27kip1 group and control group to be 37.3 % and 1.26 % ($P<0.001$) respectively.

CONCLUSION: Ad-p27kip1 can inhibit the growth and multiplication of esophageal carcinoma cells and induce apoptosis. Therefore, enhanced p27kip1 expression may be a new way to treat esophageal carcinoma.

Wu QM, Yu JP, Tong Q, Wang XH, Xie GJ. Inhibition of adenovirus-mediated p27kip1 gene on growth of esophageal carcinoma cell strain. *World J Gastroenterol* 2003; 9(11): 2404-2408
http://www.wjgnet.com/1007-9327/9/2404.asp

INTRODUCTION

As a kind of thermostable cell cycle inhibitive protein, p27 (mol. wt=27 KD) can inhibit CDK activity and consequently regulate cell cycle negatively when combined with CyclinE-CDK2 or CyclinE-CDK4[1]. The expression level and activity of p27 protein are associated with the formation of tumor. p27 protein quantity in tumor is markedly lower than that in normal cells level and its content is also closely related to the degree of differentiation, action of molecular biology and prognosis of tumor[2-7]. In the present study, we aim to give a tentative answer to whether enhanced expression of p27 protein inhibit the growth of cancer cell?

MATERIALS AND METHODS

Materials

Reagent p27kip1SP reagent was obtained from Beijing Zhongshan Biology Company. Endoenzyme, KpnI, BamHI and T4 DNA ligase were purchased from Huamei Biological Engineering Company. DMEM, RPMI1640, Lipofectamine were purchased from GIBCO/BRL Company. Low melting-temperature agarose and X-gal were obtained from Promega Company. CsCl was from Sigma Company. And high-grade neogenetic bovine serum from Hangzhou Sijiqing Biological Engineering Material Co. Ltd. p27kiplcDNA and adenovirus PCR primer were designed and synthesized by Saibaisheng Biological Company. And tryPsase from Shanghai Biological Products Company. ^{3}H-TDR and ^{3}H-Leucine were provided by Beijing Atomic Power Research Institute. DNA-PREPTMLPR and DNA-PREPTMstain were obtained from America Beckman Coulter Company.

Plasmid, strain, adenovirus and cell line PCMV5p27kip1 was presented by Dr. Wang Gang, Urinary Surgery Research Institute of the First Hospital of Beijing Medical University. PAACCMVPLPA and PJM17 were presented by academician Wu Zhuze, No. 2 Research Institute of Military Academy of Medical Science. DH 5a was presented by Dr. Peng Xu, Endocardial Department of the First Hospital of Beijing Medical University. Recombinant adenovirus was constructed by Molecular Biology Laboratory of Taihe Hospital. 293 cell was Hek cell line transferred from the gene of adenovirus E1 region, esophageal carcinoma cell strain EC9706 was presented by professor Wang Mingrong, China Academy of Medical Sciences.

Methods

Construction of adenovirus shuttle plasmid carrying p27kip1 Double enzyme cut was performed on pCMV5 p27kip1 and pACCMVPLPA with KpnI and BamHI respectively, and the fragments were separated at low melting-temperature agarose gel electrophoresis. The recovered p27kiplcDNA and adenovirus fragments were connected overnight with T_4DNA ligase at 4 ℃ by directional clone, and then transferred into receptive colibacillus DH_{5a}. From the selection of colonial amplification, a small quantity of plasmid was extracted and double cut with KpnI and BamHI. The presence of 690 bp and 8 800 bp in agarose gel after electrophoresis indicated that p27kip1cDNA had been inserted into adenovirus shuttle vector, hence successful construction of adenovirus shuttle plasmid pAd-p27kip1 carrying p27kip1.

Transfection of 293 cell by Lipofectamine-mediated pAd-p27kip1 and pJM17, and preparation of adenovirus recombinant Ad-p27kip1 (1) 293 cell was inoculated in a 9 cm plat, cultured in an incubator at 37 ℃ and 5 % CO_2, and transfected at 80 % fusion. (2) DNA-lipofectamine compound was dripped in an Eppendorf tube. Plasmid pAd-p27kip1 and pJM17 were diluted in 1 ml DMEM culture fluid, and revolved

for 1 s, then lipofectamine suspension was added uniformly. It was kept at room temperature for 30 minutes. (3) DNA-lipofectamine compound was dripped in culture flasks, and cultured in an incubator at 37 ℃ and 5 % CO_2. 0.5 % agarose was added for covering (0.5 % agarose contains 1×DMEM, 10 % Fcs), and cultured in an incubator with 37 ℃ and 5 % CO_2 after its coagulation, then pathological changes of 293 cell were observed.

PCR appraisal of recombinant adenovirus Ad-p27kip1[8] From 293 cell undergone pathologic changes after common transfection, culture supernate 100 μl was drawn, form which cell chip was removed centrifugally, and DNA was extracted and precipitated, then PCR amplification was performed on this DNA model. Primers 1 and 2 were used for amplifying p27kip1 gene, primer 3 and primer 4 for amplifying adenovirus skeleton gene fragments. The product of PCR amplification was appraised with 0.8 % agarose through electrophoresis, and held to be recombinant adenovirus Ad-p27kip1 containing human p27kip1 if gene fragments of 275 bp and 860 bp were both amplified. The sequence of primers was as follows.

Primer 1: 5' CCTAGAGGGCAAAGTACGAGTA 3'
Primer 2: 5' GAAGAATCGTCGGTTGCAGGTCGCT 3'
Primer 3: 5' TCGTTTCTCAGCAAGCTGTTG 3'
Primer 4: 5' CAATCTGAACTCAAAGCGTGG 3'

Amplification, purification and titer of recombinant adenovirus Ad-p27kip1 Recombinant adenovirus supernate 500 ul was added to 293 cell with 80 % fusion, and cultured in an incubator at 37 ℃ and 5 % CO_2. Ultracentrifugation in CsCl gradient and purification were performed on the adenovirus supernate by Graham method[8]. Then purified virus fluid 100 ul, 10 % SDS 20 ul, PBS 880 ul were taken to test light absorption value of OD_{260}nm and OD_{280} nm of the DNA of virus gene group, and accordingly to calculate the grannule quantity and purity of the virus. $1OD_{260}=10^{12}$pfu/ml, $OD_{260}/OD_{280}>1.3$ showed the purity was fairly high, virus titer pfu/ml=A260 ×dilution×10^{12}.

Transduction efficiency test of adenovirus Recombinant adenovirus Ad-LacZ was used to infect cells of esophageal carcinoma EC-9706 respectively by MOI 25, 50, 100 and 200. When X-gal was dyed, the cells dyed blue under microscope were positive cells expressed by LacZ gene, then the percentage of the cells dyed blue was calculated.

Influence of Ad-p27kip1 on growth curve of esophageal carcinoma cell 1×10^4/ml cell suspension was made of the cultured esophageal carcinoma cells (5 % FcsRPMI1640) after digestion and collection. The cells of esophageal carcinoma were inoculated in 4 pieces of culture boards with 24 holes/piece according to the quantity of 1 ml/hole, cultured for 24 h. When in 40-50 % fusion, cells were rinsed with RPMI1640, and went on culture for 24 h for synchronization. The test was divided into three groups: experimental group: Ad-p27kip1, negative control groups: Ad-LacZ ,blank group: free-virus.The test groups were infected with the cells of esophageal carcinoma (RPMI1640) for 2 h with 100 MOI, during which the culture fluid was shaken every 15 min, and two hours later exchanged with 5 % Fcs RPMI1640 for culture. Prior to the transfection of esophageal carcinoma cells by virus, three holes were taken as cell count to obtain the average value, afterwards daily cell count was collected for 4 days, and the changes of growth curve of esophageal carcinoma cell were recorded.

Incorporation test of ^{3}H-TdR and ^{3}H-leucine As described above, the experimental group and control group were cultured for 3 h with 5 % Fcs RPMI1640, and then for 12 h with free-Fcs RPMI1640. Each group was added 1 μ Ci ^{3}H-TdR or ^{3}H-leucine, which was rinsed with PBS at the 24th, 48th and 72th hour and fixed with methyl alcohol for 10 min and absolute ethyl alcohol for 10 min. Finally, 0.1M NaOH 200 μl was added. 200 μl of each was taken after blowing, and mixed in 5 ml scintillation liquid for overnight. On the following day, the CPM of ^{3}H was tested, three times for each group with three wells.

Change of p27 protein expression of cell of esophageal carcinoma p27 protein expression of the three groups was detected by immunohistochemical SP method.

FCM detection after occurrence Ad-p27kip1 effect on esophageal carcinoma cell After 48 h effect, cells from the three groups were collected, centrifugated under digestion (1 000 rpm, 5 min). PBS was added for regulating the cell density to 10^6/ml with supernates removed. 100 ul cell suspension was put in a preparatory tube, and mixed with DNA-PREPTMLPR 200 ul. Half a minute later DNA-PREPTM stain reagent (PI staining) 2 ml was added for mixing. After staying static for half an hour, cell cycle and apoptosis were detected with FCM, and processed by SYSTEM II TM software from Coulter Company.

Apoptosis detected with DNA fragment analysis and TUENL method From the experimental group after the above-mentioned effect, genome DNA was extracted regularly. DNA fragment was analyzed by agarose gel electrophoresis. At the same time, apoptosis was detected by TUNEL method, and contrasted with that in the blank group.

RESULTS

Construction of pAd-p27kip1 shuttle plasmid

Double enzyme cutting was performed on pCMV5p27kip1 and pACCMVpLpA with KpnI and BamHI, then 690 bp fragment and 8 800 bp fragment were collected respectively at low melting-temprature agarose gel electrophoresis, for the production of plasmid pAd-p27kip1 with coupled reaction. Through transformation, amplification and extraction of colibacillus, enzyme cutting appraisal were conducted to approve that pAd-p27kip1 contained p27kip1 and adenovirus carrier skeleton (Figure 1).

Figure 1 pAd-p27kip1 appraisal 1 200 bp ladder Marker: 200, 400, 600, 800, 1 000, 1 200, 1 400, 1 600, 1 800, 2 000 bp. 2, pCMV5p27kip1 (kpnI+BamHI): 690 bp segment. 3, pAd-p27kip1(kpnI+BamHI): 690 bp and 8 800 bp segment. 4, pACCMVPLPA (kpnI+BamHI): 8 800 bp segment. 5, Hind III marker: 2 027, 2 322, 4 361, 6 557, 9 416, 23 130 bp.

Construction, amplification, purification, titer test of Ad-p27kip1 and PCR appraisal

When contransfected with the above synthesized pAd-p27kip1 and pJM17, 293 cells underwent pathologic changes and floated as in grape clusters, which suggested that Ad-p27kip1 was produced through homologous recombinant, ultracentrifugation in CsCl gradient and purification. Spectrophotometer detection showed that the virus titer was 1.24×10^{12} pfu/ml, $OD_{260}/OD_{280}>1.3$, which suggested that both the virus titer and the purity were fairly high. The extracted Ad-p27kip1 adenovirus DNA underwent PCR amplification for a contrast between PCMV5p27kip1 and pACCMVpLpA, with 275 bp and 860 bp as the amplification products (Figure 2).

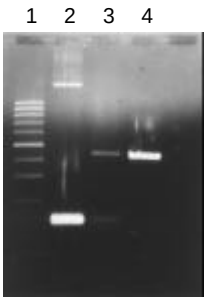

Figure 2 Ad-p27kip1 PCR appraisal 1 200 bp ladder Marker: 200, 400, 600, 800, 1 000, 1 200, 1 400, 1 600, 1 800, 2 000 bp, 2, pCMV5p27kip1model, 275 bp gene segament, 3, Ad-p27kip1 model: 275 bp and 860 bp gene segament, 4, PAVVMVPLPA model, 860 bp gene segament.

Transfection efficiency of recombinant adenovirus

Cells of esophageal carcinoma were infected with Ad-LacZ by MOI 25, 50, 100, 200 respectively, then stained with X-gal 48 h later. The transfection efficiency (%) was found to be 90, 100, 100, 100 respectively. It was concluded that 100 % transduction efficiency could be achieved with MOI $\geqslant$50, hence MOI 100 should be adopted for EC-9706 in the fellowing experiments.

Growth curve of esophageal carcinoma cell

Cell growth curve showed that the count of cancer cell in the experimental group declined over time, reached the bottom on the fourth day, but in Ad-Lacz group and blank group, it was just the opposite (Figure 3).

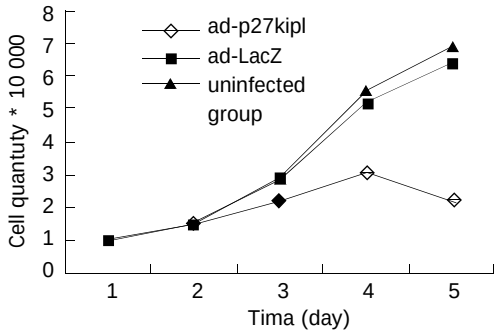

Figure 3 Growth curve of cell of esophageal carcinoma.

Table 1 ^{3}H-TdR incorporation quantity ($\bar{x}\pm s$ CPM / Well)

Group	2nd day	3rd day	4th day
Ad-p27kip1	2 013.42±84.38[a]	1 546.54±104.14[a]	244.22±39.62[a]
Ad-LacZ	3 316.81±96.37[b]	3 574.21±68.58[b]	4 451.38±154.67[b]
Blank	3 564.34±72.82	3 685.72±122.23	4 468.65±237.36

[a]P<0.001 *vs* Blank group, [b]P>0.05 Ad-LacZ group *vs* Blank group.

Table 2 Incorporation quantity of ^{3}H-Leucine ($\bar{x}\pm s$ CPM / Well)

Group	2nd day	3rd day	4th day
Ad-p27kip1	595.16±57.06[a]	422.82±45.81[a]	267.58±37.56[a]
Ad-LacZ	886.47±48.47[b]	915.44±93.58[b]	1 139.46±89.24[b]
Blank	895.21±967.52	967.52±78.35	1 243.95±06.72

[a]P<0.001 *vs* Blank group, [b]P>0.05 Ad-LacZ group *vs* Blank group.

Effect of Ad-p27kip1 on incorporation quantity of esophageal carcinoma cells ^{3}H-TdR and ^{3}H-leuine

The incorporation quantity of experimental group was markedly lower than that of the control group (P<0.001), declined over time as against the rise in Ad-LacZ group and blank group. There was no statistical difference (Table 1 and Table 2) between them.

Influence of Ad-p27kip1 on p27 expression of esophageal carcinoma cell

Immunocytochemical staining after virus transfection of esophageal carcinoma cells for 24 h showed that p27 expression increased clearly in experimental group, whereas there was not any change in control group (Figure 4 and 5).

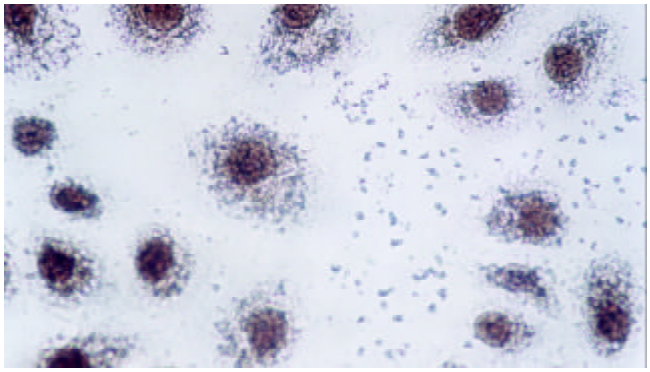

Figure 4 p27kip1 overexpression in transfection group ×200.

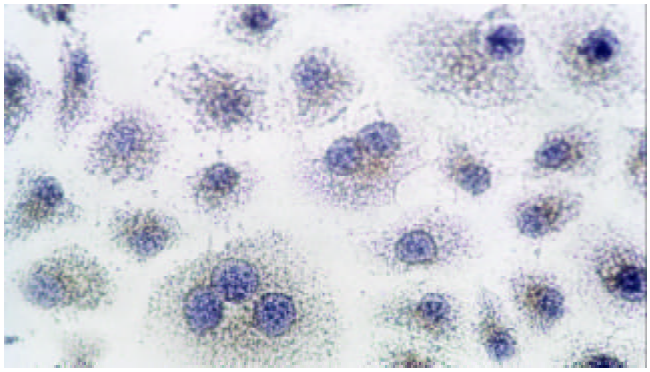

Figure 5 p27 negative expression in control group ×200.

Induction and quantitative detection of apoptosis esophageal carcinoma cells by Ad-p27kip1

Forty-eight hours after Ad-p27kip1, Ad-Lacz and blank management for EC-9706 cell, FCM determination showed that apoptotic cells took on an obvious apoptosis peak prior to G0/G1 peak. The apoptosis value of Ad-p27kip1, Ad-LacZ and blank group was 32.7 %, 5.72 % and 0.05 % respectively. Ad-p27kip1 group had the highest rate of apoptosis whereas blank group had the lowest rate.

Influence of Ad-p27kip on cell cycle of esophageal carcinoma

Cell cycle from FCM is listed in Table 3. In Ad-LacZ and blank control group, G1/G0 stage ratio decreased gradually whereas S stage increased, which indicated a rapidly changing G1/G0→S procedure and active cell multiplication. However, in the experimental group, G1/G0 stage ratio was fairly high and S stage decreased. There was a significant difference from control group (P<0.05). Cell cycle arrested G1 and inhibited cell multiplication.

Table 3 Effect of Ad-p27 on EC9706 cell cycle through fluid cell meter

Group	Distribution of cell cycle (%)		
	G0/G1	S	G2/M
Blank	40.39±3.86	49.61±4.27	13.10±1.03
Ad-LacZ	44.17±2.63	39.56±3.39	16.27±2.85
Ad-p27kip1	66.52±5.48[a,b]	21.15±3.26[a,b]	12.33±2.72

[a]P<0.05 *vs* Blank group, [b]P<0.05 *vs* Ad-LacZ group.

Analysis of DNA fragment

After cell EC-9706 was processed by Ad-p27kip1, gel electrophoresis of genome DNA displayed a clear ladder band, but no ladder band was found in contrasting group (Figure 6).

Figure 6 DNA fragment analysis 1 200 bp ladder marker: 200, 400, 600, 800, 1 000, 1 200, 1 400, 1 600, 1 800, 2 000 bp. 2, Ad-p27kip1group: 2 μg. 3, Ad-p27kip1group: 1 μg. 4. Blank group.

Detection of cell apoptosis by TUNEL Method

If brownish yellow color of karyon was found with TUNEL, it showed positive apoptosis, and no color was negative. The apoptosis rate of Ad-p27kip1 group and control group was 37.3 % and 1.26 % respectively, and there was obvious difference X^2 testing (P<0.01).

DISCUSSION

Advances in cellular biology of tumor and molecular biology have found that the occurrence of esophageal carcinoma is a comprehensive pathologic process with multifunction, multistage and multigene variations. Activation of various oncogenes and inactivation of anti-oncogene may be the major factors for normal epithelial canceration. Genetic treatment aimed to import objective genes into gene mutation or lost cells with the use of gene engineering technology, and to have functional expression replacing the original genes in order to recover the functions and effects of original genes and correct genetic distortion or genetic loss resulted from cellular developmental disturbance and realize the treatment[9]. p53, p21, Egr-1, FHIT, VEGF, E2F-1and hIFN-beta have been used as target genes in the treatment of esophagus carcinoma both *in vivo* and *in vitro*, and certain efficacy has been obtained[10-18]. Currently the analysis on esophagus carcinoma treatment through gene recombinant adenovirus p53 has entered the clinical stage[19], which will provide a bright future for tumor treatment.

P27 as candidate objective gene for tumor genetic treatment.

The key to genetic treatment is the correct selection of exogenous objective genes, its import into target cells and steady expression. Koguchi[20] used adenovirus carrier to pack p27 gene to transfect astrocytes, and found its overexpression inhibited multiplication activity of astrocytes. Katner[21] used adenovirus carrier containing p27kiplcDNA to transfect human 786-0 renal carcinoma cells, and found that the cell with p27kip1 overexpression lost the growth features of tumor cells, and that CDK activity of transfected cells was inhibited obviously, and that the multiplication time was extended. Patel[22] used p27kip gene to transfect human tumor cell line AV-W9 to induce cell death.The study of p27 gene in human breast cancer cells[23], neuroblastoma cells[24], prostate carcinoma cells[25]and lymphoma[26] showed the similar results, suggesting that p27 gene could be used as an objective gene for genetic treatment of tumor.

Construction of recombinant adenovirus carrier Ad-p27kip1 and its influence on p27 expression

Adenovirus carrier is of small pathogenicity and low genetic toxicity. With its wide host range, adenovirus can infect not only duplicated cells or cleavage cells, but also resting cells. Its huge package volume allows the insertion of 7.5kb exogenic gene fragment without any active carcinogene or insertion mutation within non-integral host chromosome. The virus can reach a high titer and 100 % infection rate through reproduction and purification. With its stable properties and safety for the human, it was considered as a gene conversion carrier of highly efficient expression[27] and most promising for genetic treatment[28].

Ad-p27kip1 constructed in the present study is a kind of replication of E1-deleted adenovirus vector. pJM17, the adenovirus skeleton with E1 region removed, can produce homologous recombinant with shuttle plasmids for producing infective adenovirus. Gene in E1 region is needed for adenovirus duplication, which requires that the duplication of intact adenovirus should be carried out in cell transfected by gene of E1 region. But since 293 cell is the right packaging cell for the transfection, replication of defective adenovirus has only one opportunity for infection in target cell without any duplication ability to fulfil the functions of adenovirus carrier, avoid damage of adenovirus itself to target cells and reach gene conversion.

Ad-p27kip1 containing human p27kip1 can positively connect p27kip1cDNA to CMV promoter of adenovirus. And as appraised by PCR amplification, p27 expression increased markedly after transfection of esophageal carcinoma cell. Contrasting adenovirus Ad-LacZ used in our study achieved 100 % induction efficiency with MOI=50. Ad-p27kip1 virus titer was 1.24×10^{12} pfu/ml, OD_{260}/OD_{280}>1.3, virus titer and purity were fairly high. This suggests that high expression of p27 after transfection is related to high induction efficiency and high purity, it can meet the demands of genetic treatment.

Inhibition of Ad-p27kip1 on growth of esophageal carcinoma

Studies demonstrated that declination of p27kip1 expression was an early event of esophageal carcinoma genesis, and also an independent prognostic factor of esophageal carcinoma[29-32]. We imported human p27kip1 gene into esophageal carcinoma cell EC9706 and analyzed its biological properties through cell growth curve, ^{3}H-TdR and ^{3}H-Leucine incorporation experiment, FCM and DNA fragment analysis. We found that esophageal carcinoma cell displayed G1 stage block after import of the gene, and that p27 inhibited cell multiplication of esophageal carcinoma obviously, and that from G1 stage to S stage, the self-multiplication ability of the control cell decreased, and the apoptosis rate increased to 32.7 %, a significant difference (P<0.01) compared with that of control group and Ad-LacZ group. It may be concluded p27kip1 gene is an important gene for occurrence of esophageal carcinoma, decreased p27 expression may be a major factor to cell differentiation and death disturbance, while increased of p27 expression can promote

cell death of esophageal carcinoma, which offers a new perspective on treating esophageal carcinoma.

REFERENCES

1 **Polyak K,** Kato JY, Solomon MJ, Sherr CJ, Massague J, Roberts JM, Koff A. p27kip1, a cyclin-Cdk inhibitor,links transforming growth factor-β and contact inhibiton to cell cycle arrest. *Genes Dev* 1994; **8**: 9-22

2 **Harada K**, Supriatno Yoshida H, Sato M. Low p27Kip1 expression is associated with poor prognosis in oral squamous cell carcinoma. *Anticancer Res* 2002; **22**: 2985-2989

3 **Chen AJ**, Meng QH, Long B, Yang GL. Relationship between p27 expression and prognosis of colorectal carcinoma. *Ai Zheng* 2002; **21**: 1075-1077

4 **Myung N**, Kim MR, Chung IP, Kim H, Jang JJ. Loss of p16 and p27 is associated with progression of human gastric cancer. *Cancer Lett* 2000; **153**: 129-136

5 **Lacoste-Collin L**, Gomez-Brouchet A, Escourrou G, Delisle MB, Levade T, Uro-Coste E. Expression of p27(Kip1) in bladder cancers: immunohistochemical study and prognostic value in a series of 95 cases. *Cancer Lett* 2002; **186**: 115-120

6 **Schwerer MJ**, Sailer A, Kraft K, Maier H. Cell proliferation and p27Kip1 expression in endophytic schneiderian papillomas. *Laryngoscope* 2002; **112**: 852-857

7 **Cesinaro AM**, Migaldi M, Corrado S, Maiorana A. Expression of p27kip1 in basal cell carcinomas and trichoepitheliomas. *Am J Dermatopathol* 2002; **24**: 313-318

8 **Zhang X**, Liu S, Liang C, Yang H. Adenovirus-mediated Rb gene transfect for head and neck cancer. *Huaxi Yike Daxue Xuebao* 2001; **32**: 194-195

9 **Roth JA**, Cristiano RJ. Gene therapy for cancer: what have we done and where are we going? *J Nat Cancer Inst* 1997; **89**: 21-39

10 **Matsubara H**, Maeda T, Gunji Y, Koide Y, Asano T, Ochiai T, Sakiyama S, Tagawa M. Combinatory anti-tumor effects of electroporation-mediated chemotherapy and wild-type p53 gene transfer to human esophageal cancer cells. *Int J Oncol* 2001; **18**: 825-829

11 **Shimada H**, Shimizu T, Ochiai T, Liu TL, Sashiyama H, Nakamura A, Matsubara H, Gunji Y, Kobayashi S, Tagawa M, Sakiyama S, Hiwasa T. Preclinical study of adenoviral p53 gene therapy for esophageal cancer. *Surg Today* 2001; **31**: 597-604

12 **Fujii T**, Tanaka Y, Tanaka T, Matono S, Sueyoshi S, Fujita H, Shirouzu K, Kato S, Yamana H. Experimental gene therapy using p21/WAF1 gene in esophageal squamous cell carcinoma-adenovirus infection and gene gun technology. *Gan To Kagaku Ryoho* 2001; **28**: 1651-1654

13 **Wu MY**, Chen MH, Liang YR, Meng GZ, Yang HX, Zhuang CX. Experimental and clinicopathologic study on the relationship between transcription factor Egr-1 and esophageal carcinoma. *World J Gastroenterol* 2001; **7**: 490-495

14 **Ishii H**, Dumon KR, Vecchione A, Trapasso F, Mimori K, Alder H, Mori M, Sozzi G, Baffa R, Huebner K, Croce CM. Effect of adenoviral transduction of the fragile histidine triad gene into esophageal cancer cells. *Cancer Res* 2001; **61**: 1578-1584

15 **Gu ZP**, Wang YJ, Li JG, Zhou YA. VEGF165 antisense RNA suppresses oncogenic properties of human esophageal squamous cell carcinoma. *World J Gastroenterol* 2002; **8**: 44-48

16 **Yang HL**, Dong YB, Elliott MJ, Liu TJ, McMasters KM. Caspase activation and changes in Bcl-2 family member protein expression associated with E2F-1-mediated apoptosis in human esophageal cancer cells. *Clin Cancer Res* 2000; **6**: 1579-1589

17 **Guo WZ**, Ran YL, Liu J, Yu L, Sun LX, Yang ZH. Enhancement by hypoxia of antisense VEGF(165) gene expression in esophageal cancer cells. *Shengwu Huaxue Yushengwu Wuli Xuebao (Shanghai)* 2002; **34**: 625-629

18 **Tsunoo H**, Komura S, Ohishi N, Yajima H, Akiyama S, Kasai Y, Ito K, Nakao A, Yagi K. Effect of transfection with human interferon-beta gene entrapped in cationic multilamellar liposomes in combination with 5-fluorouracil on the growth of human esophageal cancer cells *in vitro*. *Anticancer Res* 2002; **22**: 1537-1543

19 **Shimada H**, Matsubara H, Ochiai T. Gene therapy for esophageal cancer. *Nippon Geka Gakkai Zasshi* 2002; **103**: 371-375

20 **Koguchi K**, Nakatsuji Y, Nakayama K, Sakoda S. Modulation of astrocyte proliferation by cyclin-dependent kinase inhibitor p27 (Kip1). *Glia* 2002; **37**: 93-104

21 **Katner AL**, Gootam P, Hoang QB, Gnarra JR, Rayford W. A recombinant adenovirus expressing p27(Kip1) induces cell cycle arrest and apoptosis in human 786-0 renal carcinoma cells. *J Urol* 2002; **168**: 766-773

22 **Patel SD**, Tran AC, Ge Y, Moskalenko M, Tsui L, Banik G, Tom W, Scott M, Chen L, Van Roey M, Rivkin M, Mendez M, Gyuris J, McArthur JG. The p53-independent tumoricidal activity of an adenoviral vector encoding a p27-p16 fusion tumor suppressor gene. *Mol Ther* 2000; **2**: 161-169

23 **Craig C**, Wersto R, Kim M, Ohri E, Li Z, Katayose D, Lee SJ, Trepel J, Cowan K, Seth P. A recombinant adenovirus expressing p27Kip1 induces cell cycle arrest and loss of cyclin-Cdk activity in human breast cancer cells. *Oncogene* 1997; **14**: 2283-2289

24 **Matsuo T**, Seth P, Thiele CJ. Increased expression of p27Kip1 arrests neuroblastoma cell growth. *Med Pediatr Oncol* 2001; **36**: 97-99

25 **Katner AL**, Hoang QB, Gootam P, Jaruga E, Ma Q, Gnarra J, Rayford W. Induction of cell cycle arrest and apoptosis in human prostate carcinoma cells by a recombinant adenovirus expressing p27(Kip1). *Prostate* 2002; **53**: 77-87

26 **Turturro F**, Seth P. Prolonged adenovirus-mediated expression of p27(kip1) unveils unexpected effects of this protein on the phenotype of SUDHL-1 cells derived from t(2;5)-anaplastic large cell lymphoma. *Leuk Res* 2003; **27**: 329-335

27 **Zhang WW**. Development and application of adenoviral vectors for gene therapy of cancer. *Cancer Gene Ther* 1999; **6**: 113-138

28 **Tseng JF**, Farnebo FA, Kisker O, Becker CM, Kuo CJ, Folkman J, Mulligan RC. Adenovirus-mediated delivery of a soluble form of the VEGF receptor Flk1 delays the growth of murine and human pancreatic adenocarcinoma in mice. *Surgery* 2002; **132**: 857-865

29 **Yasunaga M**, Tabira Y, Nakano K, Iida S, Ichimaru N, Nagamoto N, Sakaguchi T. Accelerated growth signals and low tumor-infiltrating lymphocyte levels predict poor outcome in T4 esophageal squamous cell carcinoma. *Ann Thorac Surg* 2000;**70**: 1634-1640

30 **Shamma A**, Doki Y, Tsujinaka T, Shiozaki H, Inoue M, Yano M, Kawanishi K, Monden M. Loss of p27(KIP1) expression predicts poor prognosis in patients with esophageal squamous cell carcinoma. *Oncology* 2000; **58**: 152-158

31 **Shibata H**, Matsubara O, Wakiyama H, Tanaka S. The role of cyclin-dependent kinase inhibitor p27 in squamous cell carcinoma of the esophagus. *Pathol Res Pract* 2001; **197**: 157-164

32 **Taniere P**, Martel-Planche G, Saurin JC, Lombard-Bohas C, Berger F, Scoazec JY, Hainaut P. TP53 mutations, amplification of P63 and expression of cell cycle proteins in squamous cell carcinoma of the oesophagus from a low incidence area in Western Europe. *Br J Cancer* 2001; **85**: 721-726

Edited by Bo XN and Wang XL

P.O.Box 2345, Beijing 100023,China
Fax: +86-10-85381893
E-mail: wjg@wjgnet.com www.wjgnet.com

World J Gastroenterol 2003;9(11):2409-2412
World Journal of Gastroenterology
 ISSN 1007-9327

Flow cytometric analysis of DNA, telomerase content and multi-gene expression in esophageal epithelial dysplasia

Lian-Fu Zuo, Pei-Zhong Lin, Fing-Ying Qi, Jian-Wen Guo, Jiang-Hui Liu

Lian-Fu Zuo, Jian-Wen Guo, Jiang-Hui Liu, Hebei Provincial Tumor Institute, Shijiazhuang 050011, Hebei Province, China
Pei-Zhong Lin, Department of Pathology, Tumor Institute, Chinese Academy of Medical Sciences, Beijing 100021,China
Feng-Ying Qi, Department of Pathology, Hebei Medical University, Shijiazhuang 050017, Hebei Province,China
Supported by the National Key Technologies Research and Development Program of China during the 9th Five-year Plan Period, No.96-906-01-02
Correspondence to: Lian-Fu Zuo, Hebei Provincial Tumor Institute, Shijiazhuang 050011, Hebei Province, China. zuolianfu@sina.com
Telephone: +86-311-6033511 **Fax**: +86-311-6077634
Received: 2003-05-10 **Accepted:** 2003-06-19

Abstract

AIM: To investigate the alteration of molecular events and the early carcinogenesis mechanism of esophageal epithelial cells in the high incidence area of esophageal cancer.

METHODS: Esophageal epithelial cells of esophageal cancer patients were collected from the high incidence area in China. Content of DNA and telomerase as well as multi-gene expressions such as p^{53}, p^{21} and cyclin D_1 in esophageal precancer cells were quantitatively analysed by flow cytometry (FCM) with indirect immunofluorescence technique and DNA propidium iodide fluorescence staining.

RESULTS: FCM analysis results showed the DNA content increased significantly and the heteroploid rate was 87.9 % in occurred carcinogenesis. P^{53} protein accumulation and ras p^{21} increase were seen in the early carcinogenesis of the esophagus. The positive rate of p^{53} and ras p^{21} was 100 % (5/5, 4/4 respectively) in the cancer group. Telomerase and oncogene cyclin D_1 were over- expressed in all of the cancer patients.

CONCLUSION: Increased DNA content and heteroploid rate, accumulation of p53 protein, and over-expression of p21, telomerase and cyclin D_1 proteins were early molecular events during the development of esophageal cancer.

Zuo LF, Lin PZ, Qi FY, Guo JW, Liu JH. Flow cytometric analysis of DNA, telomerase content and multi-gene expression in esophageal epithelial dysplasia. *World J Gastroenterol* 2003; 9 (11): 2409-2412
http://www.wjgnet.com/1007-9327/9/2409.asp

INTRODUCTION

Esophageal cancer is one of the most common malignant tumors, and many studies have been made on it[1-3]. Former studies focused primarily on precancerous lesions and carcinogenesis of esophagus. But early carcinogenesis of esophageal cancer is unclear. In the present study, we investigated the DNA, telomerase content and P^{53}, ras P^{21} and cyclin D_1 multi-gene product of exfoliated cell samples from Cixian County, a high incidence area of esophageal cancer in Hebei Province of China with flow cytometry. It may provide a theoretic basis for under standing the carcinogenesis of esophageal epithelial cells and early diagnosis of esophageal cancer.

MATERIALS AND METHODS

Specimen collection

All samples were collected from Cixian County, a high incidence area of esophageal cancer, Hebei Province, China. One thousand nine hundred and sixteen cases of exfoliated cell specimens of esophagus were obtained with a mesh saccule. The exfoliated cell sample in each case was divided into two parts. One part was used for smear preparation on slides with papanicolaou stain for cytologic diagnosis, another part was used for preparation of a single cell suspension for flow cytometry analysis.

Specimen preparation for FCM DNA analysis

Exfoliated cells from 1916 cases for DNA analysis were obtained as follows. The exfoliated cells were washed out from the saccule with 0.9 % NaCl solution, centrifuged and fixed in 70 % ethanol. Before DNA analysis the cell samples were washed off 70 % ethanol in 0.9 % NaCl solution. Cell suspension (1×10^6 cells/ml) was centrifuged (5 min, 1 000 r/min) and washed twice with 0.9 % NaCl solution. After centrifugation the cells were stained in one million of propidium iodid (PI) solution (PI 50 μg/ml with triton-x-100 and RNase) for 30 minutes and filtered through a 47 μm nylon mesh to remove cellular fragments and clusters. Chicken red blood cells were added to the sample before stained as an internal standard for calibration of the FCM instrument.

The antibodies for immunofluorescence detection of telomerase, P^{53}, P^{21} and cyclin D1 protein were described as below: (1) Monoclonal antibody (MoAb) P^{53} was a mouse antibody against human P^{53} protein (Clone PAB1801, Oncogene Science, Inc. U S. working concentration 1:100). (2) MoAb P^{21} was a mouse antibody against human pan-ras P^{21} protein (Clone F-132, Santa Cruz, US, working concentration 1:100). (3) MoAb cyclin D1 was a mouse antibody against human cyclin D1 protein (Clone DCS-6, Santa Cruz, US, working concentration 1:100). (4) Telomerase was rabbit antibody against human telomerase associated protein (TP1) polyclonal antibody (Clone C-20, Stanta Cruz, US, working concentration 1:50). (5) The second antibody was used with FITC-conjugated goat anti-mouse/anti-rabbit IgG (Tackson Immunoresearch Laboratories Inc, code number 115-095-003/115095, working concentration 1:100).

Labeling method

The sample fluorescence staining was performed using indirect immunofluorescence labeling method. Samples from 100 cases were randomly selected for each antibody labeling. Each sample (10^6 cells/ml) was washed twice with PBS and incubated in water-bath for 30-min at 37 ℃ with 100 μl antibody (p53, p21, cyclin D1, telomerase). The samples were then washed twice with PBS and incubated in water-bath for 30 min at 37 ℃ with 100 μl of the second antibody of FITC-conjugated goat anti-mouse/rabbit IgG. The cell suspension

was washed, and resuspended in l.0 ml PBS, filtered through a 47 μm nylon mesh, analyzed by flow cytometry, before the samples were analyzed.

Three control samples were used. One sample was used as negative control with PBS replacing the first/second antibody. Another sample was used as positive isotype control with only the first antibody incubated. The remaining sample was incubated only with the second fluorescence antibody as positive isotype control.

Flow cytometry measurement of DNA and immunofluoresence

The stained samples were analyzed in a FACS 420 flow cytometer (FACS 420 Fluorescence Activated Cell Sorting, Becton. Dickinson, Sunnyvale. California, U S A). The light source was a 2w argon ion laser using a wave-length of 488 nm. The working power was 300 mw. Single parameter was measured respectively in DNA (with a liner mode) and each protein (with a Log mode). Usually, 10 000 cells for each sample were analyzed. The analytic data were processed with a HP-300 consort 300 computer. The coefficient of variation (CV)of the instrument was adjusted within 5 % using PI staining chicken red blood cells.

Measured data analysis

DNA ploid analysis DNA content was presented as the DNA index (DI), DI=G0/1 peak average channel value in experimental sample DNA histogram / G0/1 peak average channel value in normal cell sample DNA histogram. DNA ploids were judged according to DI value. The normal epithelial cells in each sample were used as internal standard reference cell for diploid DNA value, DI in diploid cell was 1.0. A diploid DNA histogram was defined as DI=1.0±2 cv. An aneuploid DNA histogram was defined as DI≠1.0±2 cv.

Cell cycle analysis DNA cell cycle was analyzed using a software of DNA histogram distribution (sum of broadened retangled model). The phases in G0/1.S.G2M were calculated according to DNA content distribution histogram. The proliferation index (PI) was used to present cell proliferation activity PI(%)=S+G2M/G0/1+S+G2M.

Quantitative analysis of P^{53}, rasP^{21}, cyclin D1 and telomerase expression Fluorescence index (FI) was used to describe P^{53}, P^{21}, cyclin D1 and telomerase expression. Following FI calculated formulation: FI=average fluorescence intensity of sample protein expression - average fluorescence intensity of isotype control/average fluorescence intensity of normal control. The sample was considered positive when FI was above 1.0.

Statistical analyses

Chi- square test and *t* test were used for statistical analysis of the results. The study was double blind with a group of cytologists making cytologic diagnosis, while another group performed DNA analysis.

RESULTS

Cytologic diagnosis

The cytologic observation showed that among the 1 916 cases of exfoliated cell smears, 217 were normal, 306 were mild dysplasia, 952 were moderate dysplasia, 349 were severe dysplasia and 92 were esophageal cancer.

Relationship between DI and cytologic diagnosis

The FCM DI value and corresponding cytologic diagnosis of 1916 samples are presented in Table 1. Table 1 shows that cellular DNA content was closely related to epithelial changes in esophagus. DI increased as the grade of dysplasia increased. Significant differences in DI were found in the mild, moderate and severe dysplasia groups. There was no significant difference in DI between the normal and mild dysplasia groups.

Table 1 Relationship between cellular DNA content and cytologic diagnosis

Cellular diagnosis	No.of cases	DI value ($\bar{x}$±s)	*P* value (*t* test)
Normal	217	1.01±0.06	>0.2
Mild dysplasia	306	1.03±0.10	<0.01
Moderte dysplasia	952	1.06±0.27	<0.01
Severe dysplasia	349	1.09±0.14	<0.01
Cancer	92	1.24±0.18	<0.01

Relationship between DNA ploid and cytologic diagnosis

The results of DNA ploid status in different cytologic groups of exfoliated esophageal cells are shown in Table 2, which shows that 21 cases in normal group were DNA heteroploid, but none became cancerous in follow-up. Thus, DNA heteroploidy in normal group was defined as false heteroploid. The rate of DNA heteroploid in dysplasia increased as the dysplasia lesion progressed. The difference in DNA heteroploid among three dysplasia groups was statistically significant (P<0.01).

Relationship between PI value and cytologic diagnosis

The results of cell cycle analysis showed that cell proliferation activity was closely related to epithelial changes in esophagus, PI value was 13.8±4.3 % in normal group, 16.4±2.5 % in mild dysplasia group, 17.9±4.1 % in moderate dysplasia group, 19.8±2.9 % in severe dysplasia group, 24.6±4.2 % in cancer group, respectively. PI value increased as dysplasia lesion progressed. The difference in PI value between normal group and the three dysplasia groups had a statistical significance (P<0.05).

Table 2 Relationship between DNA ploid and cytologic diagnosis

Cellular diagnosis	No.of cases	DNA ploidy pattern		Rate of heteroploid (%)	*P* value x^2 test
		diploid	heteroploid		
Normal	217	196	21	9.7	>0.05
Mild dysplasia	306	280	26	8.5	>0.01
Moderate dysplasia	952	791	161	16.9	<0.01
Severe dysplasia	349	229	120	34.4	<0.01
Cancer	92	20	72	78.3	<0.01

Relationship between P^{53}, P^{21} protein expression and cytologic grade

The results of P^{53}, P^{21} protein expression are shown in Table 3.

Table 3 Expression of P^{53}, P^{21} in various lesions of esophageal epithelial cells

Cytological group	No.of cases	P^{53} FI ($\bar{x}$±s)	P^{53+}cases (%)	P^{21} FI ($\bar{x}$±s)	P^{21+} cases (%)
Normal	10	1.00±0.11	0	1.00±0.19	0
Mild dysplasia	24	1.10±0.15	5 (20.8 %)	1.09±0.21	6 (25.0 %)
Severe dysplasia	61	1.36±0.32	34 (54.8 %)	1.34±0.35	35 (57.4 %)
Cancer	5	2.28±0.20	5 (100 %)	1.82±0.24	5 (100 %)

Expression of P^{53} and ras P^{21} in Table 3 showed that FI value increased as the grade of cytologic diagnosis of the esophageal epithelia increased. The differences in FI values among the normal, mild and severe dysplasia and cancer groups were statistically significant (P<0.01). The positive

rate of P^{53} and ras P^{21} expression among the four groups of esophageal epithelial lesion was also statistically significant ($P<0.01$).

Correlation of cyclin D1 and telomerase associated protein (TP1) expression with cytologic diagnosis grading

Table 4 Results of cyclin D1 and TP1 expression in various lesions of esophageal epithelia

Cytologic diagnosis	No.of cases	Cyclin D1, FI ($\bar{x}\pm s$)	Cyclin D_1^+ cases	TP FI ($\bar{x}\pm s$)	TP_1^+ cases
Normal	7	1.00±0.07	0	0.99±0.07	0
Mild dysplasia	11	0.97±0.12	1 (9.1 %)	1.22±0.15	7 (63.6 %)
Severe dysplasia	76	1.21±0.22	45 (59.2 %)	1.33±0.27	64 (84.2 %)
Cancer	6	1.84±0.18	6 (100 %)	1.70±0.15	6 (100 %)

Table 4 contains the cyclin D1 and TP1 expression data from 100 cases of esophageal epithelial lesion. The results showed that the cyclin D1 and TP1 protein expression level was correlated with cytologic diagnosis grading. FI values of cyclin D1 in normal group were not significantly different from that in mild esophageal dysplasia group. But FI values of TP1 between normal group and mild dysplasia group were significantly different ($P<0.05$).

The difference in FI value of cyclin D1 and TP1 among the mild, severe dysplasia and cancer groups was markedly significant ($P<0.01$), and the positive rate of cyclin D1 and TP1 protein expression among the four groups was also significantly different ($P<0.01$).

DISCUSSION

The results of this study showed that alteration of multiple molecular events occurred during esophageal epithelial carcinogenesis.

In this study, we found that the increased DI value was correlated with the precancerous lesion progression. Cellular DNA content and DNA ploid status were closely related to the severity of epithelial dysplasia. The rate of FCM DNA heteroploid increased significantly in the transition of dysplasia from mild to severe. Thus it is clear that cellular DNA content could reflect the pathologic changes in the epithelium of esophagus[4]. DNA content increase and DNA heteroploidy were the very important early signals of carcinogenesis[3,4].

Detection of FCM DNA heteroploidy might provide early cancerous information, before the morphologic evidence of cancer occurred[3,4]. It has been proved in previous studies that proliferation index (PI) is an indicator to reflect cell proliferation activity. In our study, the cell proliferation activity was closely related to the dysplasia degree of esophagus. PI was 16.4 % in mild dysplasia group, 17.9 % in moderate dysplasia group, 19.8 % in severe dysplasia group. The results proved that the rate and speed in cell proliferation were obviously increased during esophageal epithelial carcinogenesis.

In carcinogenesis, the precancerous cell lesion resulted in not only abnormal DNA change but also abnormal change in multiple genes and its product expression[3-14]. Previous studies demonstrated that lots of genetic alteration existed in esophageal precancer cells. P^{53} mutation in tumor-suppressor gene and ras P^{21} activated in tumor gene were revealed to be early molecular events during esophageal carcinogenesis[5,9,10,16]. In our studies, expression of P^{53} and P^{21} protein varied with dysplasia degree, FI value increased significantly from mild to severe dysplasia. Overexpression of P^{53} and P^{21} was closely related to early stages of esophageal carcinogenesis. The studies by Yasuda' s group also revealed that P^{53} mutation was a key molecular event in esophageal carcinogenesis[6]. The expression of P^{53} protein in our study accumulated at early stages of esophageal carcinogenesis.

The ras gene in normal cells possesses an important effect on cell growth and proliferation. The ras gene activation can speed up cell proliferation and malignant transformation. Overexpression of ras gene (P^{21}) occurred frequently in precancerous lesion of esophagus[15]. In our studies, expression of ras P^{21} varied with dysplasia degree. FI of ras P^{21} expression was significant among the normal, mild, severe dysplasia and cancer groups ($P<0.01$). It is suggested that ras P^{21} overexpression may be an important factor during esophageal epithelial carcinogenesis, and ras P^{21} may be a valuable marker at the early stages of carcinogenesis.

Recent studies have indicated that cyclin D1 is an oncogene which is related to the regulation of cell cycle[17-21]. The cyclin D1 gene product is a key protein which makes cells enter into proliferation condition, and cyclin D1 and CDK4 are composed of a complex which could functionally inhibit tumor suppressor gene P^{16} and Rb activity[23], thus promoting the cell proliferation ability. Many cells could enter into proliferation stage from G1 to S,G2M phase, so that excessive cell proliferation could cause carcinogenesis[19,23]. In this study, the expression of cyclin D1 protein increased in severe degree of esophageal epithelial dysplasia. The results indicate that overexpression of cyclin D1 plays an important role during esophageal carcinogenesis. An increase in cyclin D1 might result in an oncogene[22-25].

Recently, it has become a new research target of telomerase activity and its relation to carcinogenesis. It has been demonstrated that telomerase activity is increased in esophageal carcinoma. Telomerase activity could be used as an early stage marker of esophageal epithelial carcinogenesis[25-27]. Telomerase quantitative analysis of esophageal precancerous lesion has not been reported. In this study, telomerase content in esophageal epithelial dysplasia cells was quantitatively analyzed by flow cytometry. The results showed that telomerase content obviously increased in severe dysplasia group and cancer group. The positive rate of telomerase expression was 83.1 % in severe dysplasia group and 100 % in cancer group. Overexpression of telomerase might be an important factor and early molecular event to monitor the patients with high-risk of precancerous lesion during esophageal epithelial carcinogenesis[28-31]. Therefore, quantitative detection of telomerase content might be an early diagnostic method for esophageal cancer[27]. It is suggested that inhibition of telomerase activity might be a new therapy for cancer[29-31].

In summary, the DNA content, P^{53}, ras P^{21}, cyclin D1 and telomerase content showed significant changes during esophageal epithelial carcinogenesis, they could also become biomarkers to identify precancerous lesions in high-risk population at high incidence areas of esophageal cancer. These results indicate that combined analysis of multiple parameters can greatly increase the accuracy of early identification of esophageal cancer in the high risk population.

REFERENCES

1 **Moreto M**. Diagnosis of esophagogastric tumors. *Endoscopy* 2001; **33**: 1-7

2 **Bektas A**, Yasa MH, Kuzu I, Dogan I, Unal S, Ormeci N. Flow cytometric DNA analysis and immunohistochemical P^{53}, PCNA and histopathologic study in primary achalasia: preliminary results. *Hepatogastroenterology* 2001; **48**: 408-412

3 **Ma P**, Song M, Ren CS. Significance of P^{27} expressio and DNA contents in esophagus carcinoma. *Shiyong Aizheng Zazhi* 2001; **16**: 262-263

4 **Zuo LF**, Ling PZ, Qi FY, Wang JX, Ding ZW, Guo JW, Liu JH. Flow cytometric DNA analyses of epithelial dysplasia of the esophagus. *Analyt Quant Cytol Histol* 2000; **22**: 175-177

5 **Zhu MH**. Research advance and significance in biologic function of P^{53}. *Zhonghuan Binglixue Zazhi* 2000; **29**: 60-62

6 **Jin YL**, Zhang W, Liu BQ, Wang HP, Han SK, Han ST, Qu P, Li M, Ding ZW, Lin PZ. Abnormal expression of P^{53} Ki67, and iNOS in human esophageal carci moma in situ and pre-maligrant lesions. *Zhonghua Zhongliu Zazhi* 2001; **23**: 129-132

7 **Zuo LF**, Qi FY, Zhang LX, Lin PZ, Liu JH, Guo JW. The role of tumor suppressor gene P^{53} and cell-cycle relatedgene produces in the carcinogenesis of esophageal epithelia. *Zhonghua Xin Yixue* 2003; **4**: 1345-1347

8 **Yasuda M**, Kuwano H, Watanabe M, Toh Y, Ohno S, Suqimachi K. P^{53} expression in squamous dysplasia associated with carcinoma of the oesophagus: evidence for field carcinogenesis. *Br J Cancer* 2000; **83**: 1033-1038

9 **Geboes K**, Van Eyken P. The diagnosis of dysplasia and malignancy in Barrett's oesophagus. *Histophathology* 2000; **37**: 99-107

10 **Shimada Y**, Imamura M, Watanbae G, Uchida S, Harada H, Makino T, Kano M. Prognositic factors of oesophageal squamous cell carcinoma from the perspective of molecular biology. *Br J Cancer* 1999; **80**: 1281-1288

11 **Zhan XM**, Wang GX, Sun CW, Wang JY, Li L. Expression of P16, P21, P53 and cyclin D1, and their significance in esophageal carcinoma.*Shiyong Aizheng Zazhi* 2001; **16**: 36-38

12 **Itoshima T**, Fujiwara T, Waku T, Shao J, Kataoka M, Yarbrough WG, Liu TJ, Roth JA, Tanaka N, Kodama M. Induction of apoptosis in human esophageal cancer cells by sequential transfer of the wild-type P53and E2F-1 genes: involvement of P53 accumulation via ARF-mediated MDM2 down-regulation. *Clin Cancer Res* 2000; **6**: 2851-2859

13 **Kato H**, Yoshikawa M, Fukai Y, Tajima K, Masuda N, Tsukada K, Kuwano H, Nakajima T. An immunohistochemical study of P16. PRb. P21 and P53 proteins in human esophageal cancers. *Anticancer Res* 2000; **20**: 345-349

14 **Xu M**, Jin YL, Fu J, Huang H, Chen SZ, Qu P, Tian HM, Liu ZY, Zhang W. The abnormal expression of retinoic acid receptor-β, P53 and Ki 67 protein in normal, premalignant and malignant esophageal tissues .*World J Gastroenterol* 2002; **8**: 200-202

15 **Galiana C**, Fusco A, Martel N, Nishihira T, Hirohashi S, Yamasaki H. Possible role of activated ras genes in human esophageal carcinogenesis. *Int J Cancer* 1993; **54**: 978-982

16 **Qiao GB**, Han CL, Jiang RC, Sun CS, Wang Y, Wang YJ. Overexpression of P53 and its risk factors in esophageal cancer in urban areas of Xi'an. *World J Gastroenterol* 1998; **4**: 57-60

17 **Ikeda G**, Isaji S, Chandra B, Watanbe M, Kawarada Y. Prognostic significance of biologic factors in squamous cell carcinoma of the esophagus. *Cancer* 1999; **86**: 1396-1405

18 **Shinohara M**, Aoki T, Sato S, Takagi Y, Osaka Y, Koyanagi Y, Hatooka S, Shinoda M. Cell-cycle regulated factors in esophageal cancer. *Dis Esophagus* 2002; **15**: 149-154

19 **Ohbu M**, Kobayashi N, Okayasu I. Expression of cell cycle regulatory proteins in the multistep process of oesophageal carcinogenesis: stepwise over-expression of cyclin E and P53, reduction of P21(WAF1 / CIP1) and dysregulation of cyclin D1 and P27 (KIP1) . *Histopathology* 2001; **39**: 589-596

20 **Saeki H**, Ohno S, Miyazaki M, Araki K, Egashira A, Kawaguchi H, Watanabe M, Morita M, Sugimachi K. P53 protein accumulation in multiple oesophageal squamous cell carcinoma: Relationship to risk factors. *Oncology* 2002; **62**: 175-179

21 **Fujii S,** Tominaga O, Nagawa H, Tsuno N, Nita ME, Tsuruo T, Muto T. Quantitative analysis of the cyclin expression in human esophageal cancer cell lines. *J Exp clin Cancer Res* 1998; **17**: 491-496

22 **Shamma A**, Doki Y, Shiozaki H, Tsujinaka T, Yamamoto M, Inoue M, Yano M, Monden M. Cyclin D1 overexpression in esophageal dysplasia:a possible biomarker for carcinogenesis of esophageal squamous cell Carcinoma. *Int J Oncol* 2000; **16**: 261-266

23 **Liu SX**, Zuo LF, Zhang JY, Guo JW, Liu JH, Li YM. The expression of Rb, P21 and cyclin D1 in 41 esophageal cancers. *Zhonghua Xin Yixue* 2002; **3**: 97-99

24 **Toyoda H**, Nakamura T, Shinoda M, Suzuki T, Hatooka S, Kobayashi S, Ohashi K, Seto M, Shiku H, Nakamura S. Cyclin D1 expression is useful as a prognostic indicator for advanced esophageal Carcinomas bu not for superficial tumors. *Dig Dis Sci* 2000; **45**: 864-869

25 **Zhang LX**, Qi FY, Zuo LF, Lin PZ, Guo JW, Liu JH. The expression of $P^{16,}$ cyclin D1 and DNA content analysis in the carcinogenesis of esophageal epithelial cells. *Zhonghua Xin Yixue* 2001; **2**: 1-3

26 **Wu MY**, Wu XY, Zhuang CX. The expression of human telomerase reverse transcriptase in esophageal squamous cell carcinoma and paracancerous esophageal epithelium. *Shiyong Aizheng Zazhi* 2003; **18**: 132-134

27 **Zhang LX**, Qi FY, Zuo LF, Lin PZ, Guo JW, Liu JH. The quantitative analysis of telomerase and DNA ploid in the carcinogenesis of esophageal epithelium. *Zhonghua Xin Yixue* 2001; **2**: 193-195

28 **Shen ZY**, Xu LY, Li EM, Cai WJ, Chen MH, Shen J, Zeng Y. Telomere and telomerase in the initial stage of immortalization of esophageal epithelial cell. *World J Gastroenterol* 2002; **8**: 357-362

29 **Koyanagi K**, Ozawa S, Ando N, Takeuchi H, Ueda M, Kitajima M. Clinical significance of telomerase activity in the non cancerous epithelial region of oesophageal squamous cell carcinoma. *Br J Surg* 1999; **86**: 674-679

30 **Koyanagi K**, Ozawa S, Ando N, Mukai M, Kitagawa Y, Ueda M, Kitajima M. Telomerase activity as an indicator of malignany potential in iodine-nonreactive lesion of the esophagus. *Cancer* 2000; **88**: 1524-1529

31 **Rudolph P**, Schubert C, Tamm S, Heidorm K, Hauschild A, Michalska I, Majewski S, Krupp G, Jablonska S, Parwaresch R. Telomerase activity in melanocytic lesions: A potential marker of tumor biology. *Am J Path* 2000; **156**: 1425-1432

Edited by Wang XL and Zhu LH

P.O.Box 2345, Beijing 100023,China
Fax: +86-10-85381893
E-mail: wjg@wjgnet.com www.wjgnet.com

World J Gastroenterol 2003;9(11):2413-2418
World Journal of Gastroenterology
 ISSN 1007-9327

• GASTRIC CANCER •

Roles of PLC-g2 and PKCa in TPA-induced apoptosis of gastric cancer cells

Bing Zhang, Qiao Wu, Xiao-Feng Ye, Su Liu, Xiao-Feng Lin, Mu-Chuan Chen

Bing Zhang, Qiao Wu, Xiao-Feng Ye, Su Liu, Xiao-Feng Lin, Mu-Chuan Chen, Key Laboratory of the Ministry of Education for Cell Biology and Tumor Cell Engineering, School of Life Sciences, Xiamen University, Xiamen 361005, Fujian Province, China
Bing Zhang, Medical school, Xiamen University, Xiamen 361005, Fujian Province, China
Supported by the National Natural Science Foundation of China (No. 30170477), the National Outstanding Youth Science Foundation of China (No.39825502), and the Natural Science Foundation of Fujian Province (C0110004)
Correspondence to: Dr. Qiao Wu, Key Laboratory of the Ministry of Education for Cell Biology and Tumor Cell Engineering, School of Life Sciences, Xiamen University, Xiamen 361005, Fujian Province, China. xgwu@xmu.edu.cn
Telephone: +86-592-2182542 **Fax:** +86-592-2086630
Received: 2003-05-13 **Accepted:** 2003-06-27

Abstract

AIM: To investigate the roles of PLCγ2 and PKCα in TPA-induced apoptosis of gastric cancer cells.

METHODS: Human gastric cancer cell line MGC80-3 was used. Protein expression levels of PLCγ2 and PKCα were detected by Western blot. Protein localization of PLCγ2 and PKCα was shown by immunofluoscence analysis under laser-scanning confocal microscope. Apoptotic morphology was observed by DAPI fluorescence staining, and apoptotic index was counted among 1 000 cells randomly.

RESULTS: Treatment of gastric cancer cells MGC80-3 with TPA not only up-regulated expression of PLC-γ2 protein, but also induced PLC-γ2 translocation from the cytoplasm to the nucleus. However, this process was not directly associated with apoptosis induction. Further investigation showed that PKCa translocation from the cytoplasm to the nucleus was correlated with initiation of apoptosis. To explore the inevitable linkage between PLC-γ2 and PKCα during apoptosis induction, PLC inhibitor U73122 was used to block PLC-γ2 translocation, in which neither stimulating PKCα translocation nor inducing apoptosis occurred in MGC80-3 cells. However, when U73122-treated cells were exposed to TPA, not only PLC-γ2, but also PKCα was redistributed. On the other hand, when cells were treated with PKC inhibitor alone, PLC-γ2 protein was still located in the cytoplasm. However, redistribution of PLC-γ2 protein occurred in the presence of TPA, no matter whether PKC inhibitor existed or not.

CONCLUSION: PLC-γ2 translocation is critical in transmitting TPA signal to its downstream molecule PKCα. As an effector, PKCα directly promotes apoptosis of MGC80-3 cells. Therefore, protein translocation of PLCγ2 and PKCα is critical event in the process of apoptosis induction.

Zhang B, Wu Q, Ye XF, Liu S, Lin XF, Chen MC. Roles of PLC-γ2 and PKCα in TPA-induced apoptosis of gastric cancer cells. *World J Gastroenterol* 2003; 9(11): 2413-2418
http://www.wjgnet.com/1007-9327/9/2413.asp

INTRODUCTION

Once binding to the cell surface receptors, many extracellular signaling molecules could elicit intracellular responses by activating inositol phospholipid-specific phopholipase C (PLC)[1,2]. Activated PLC could catalyze the hydrolysis of phosphatidylinositol 4,5-biphosphate (PIP_2) to diacylglycerol (DAG) and inositol 1, 4, 5-triphosphate (IP_3). DAG and IP3 are second messengers, the former could function to activate protein kinase C (PKC), and the latter could stimulate release of Ca^{2+} from internal stores[1,3-5]. This bifurcating pathway constitutes the cornerstone of a transmembrane signal transduction mechanism that was known to regulate a large array of cellular processes[5-9].

Ten types of PLC isoform have been divided into three types, β, γ and δ[4-6,10,11]. One PLC isoform, PLC-γ, is a substrate of epidermal growth factor (EGF) receptor, and its catalytic activity could be stimulated by tyrosine phosphorylation[12]. PLC-γ has been implicated in mitogenic signaling by platelet-derived growth factor (PDGF) receptor. Through the pleiotropic actions of IP_3 and DAG, PLC-γ could participate in regulation of cell proliferation and differentiation[13]. PLC-γ overexpression could favor cell survival in response to acute oxidative stress[14,15]. In rat pheochromocytoma PC12 cells, overexpression of PLC-γ could inhibit apoptosis induced by short wave length ultraviolet radiation[16].

Protein kinase C (PKC) could play a variety of regulatory roles in proliferation, differentiation, apoptosis, gene expression, membrane transportation, and signal transduction[17-19]. There have been at least 11 distinct PKC isoforms[20]. In many tissues, both PKC activation and Ca2+ mobilization could act synergistically to evoke some cellular responses[21-24]. For example, activation of PKC and increase in Ca^{2+} were the "on" signals for T-cell activation[27,28]. By contrast, this PKC activator could also act as a negative regulator of T-cell activation[27,28]. Thus, PKC activation in T-cells has bidirectional effects on the cellular activation process.

Several evidences suggest that activation of PKC could attenuate receptor-coupled PLC activity in certain types of cell, providing a negative feedback signal to limit the magnitude and duration of receptor signaling[3,5]. Although such a regulatory mechanism has not been fully understood, it is possible that the targets might include receptors, G protein, PTK, protein tyrosine phosphatase and PLC itself[5]. Phosphorylation of Thr-654 of the EGF receptor by PKC reduced the ability of the receptor tyrosine kinase to phosphorylate PLC-γ, thereby preventing PLC-γ activation[29]. A decrease in the extent of tyrosine phosphorylation of PLC-γ has also been proved to be the mechanism by which the PKC activator, TPA and cAMP could attenuate the PIP2 hydrolysis induced by TCR[30]. Thus, interaction between PLC-γ and PKC is related to PLC-γ phosphorylation.

To date, little is known about the molecular event of PLC-γ translocation, and the functional consequences of PLC-γ in response to extracellular signal stimulation. It is generally accepted that PLC-γ localizes and functions in cytosol. EGF or PDGF treatment of cells could induce translocation of PLC-γ1 from a predominantly cytosolic localization to membrane

fraction[31], showing a preliminary clue that the function of PLC-γ may be in relation with its intracellular changes. In this study, we found that 12-O-tetradecanoylphorbol-1, 3-acetate (TPA) not only up-regulated the expression level of PLC-γ2, but also induced PLC-γ2 translocation from the cytoplasm to the nucleus in gastric cancer cells MGC80-3. In addition, according to our previous studies concerning the critical role of PKC-associated signaling pathway in promoting apoptosis of gastric cancer cell[32], we hypothesized that PLC-γ2 may play an important role in transmitting TPA signal to PKCα, which finally lead to apoptosis induction in gastric cancer cells. This notion may provide a novel strategy for exploring the cross-talk between PLC-γ2 and PKCα in apoptosis.

MATERIALS AND METHODS

Cell line and culture condition

Human gastric cancer cell line, MGC80-3 was established by Cancer Research Center, Xiamen University[33]. The cells were maintained in RPMI-1640 medium, supplemented with 10 % FCS, 1 mmol/L glutamine, and 100 U/ml penicillin.

Western blot analysis[34]

The cells were harvested, and suspended in RIPA buffer (10 mmol/L Tris (pH7.4), 150 mmol/L NaCl, 1 % Triton X-100, 1 % deoxycholic acid, 0.1 % SDS, 5 mmol/L EDTA (pH8.0), 1 mmol/L PMSF). Protein concentration was determined using the Bio-Rad protein assay system according to the manufacturer' s instructions (Bio-Rad Hereules, CA). 50 μg protein was subjected to SDS-PAGE and transferred to nitrocellulose membrane for Western blot analysis. The membrane was subsequently blocked with 5 % dry milk in TBS-T and then immunnoblotted with the responding antibody. Binding was detected by using the ECL kit (Pierce) according to the manufacturer' s instructions.

Apoptosis analysis[32]

The cells were trypsinized, and washed in PBS. The harvested cells were fixed in 3.7 % paraformaldehyde on ice, washed in PBS and stained with 50 μg/ml of 4, 6-diamidino-2-phenylindole (DAPI, Sigma) containing 100 μg/ml of DNase-free RNase A per ml. The cells were observed under fluorescence microscope. Apoptotic cells were counted among 1 000 cells randomly. The apoptotic index was the mean of three independent experiments.

Immunofluorescence analysis[35]

The cells were cultured on a cover glass overnight. After washed in PBS, the cells were fixed in 4 % paraformaldehyde. To display PLC-γ2 or PKCα protein, the cells were incubated first with anti-PLC-γ2 or anti-PKCα antibody (Santa Cruz), and then reacted with their corresponding FITC-conjugated anti-IgG (Pharmingen) as secondary antibodies. To visualize the nuclei, the cells were stained with propidium iodine (PI, 50 μg/ml) containing 100 μg of DNase-free RNase A per ml. Fluorescent image was observed under laser-scanning confocal microscope (Bio-Rad MRC-1024ES).

RESULTS

Expression and translocation of PLC-g2 in response to TPA

To determine the effect of TPA on PLC-γ2 protein expression, Western blot analysis was carried out. As shown in Figure 1A, PLC-γ2 protein was normally expressed in MGC80-3 cells. When exposed to TPA for different time, expression level of PLC-γ2 protein was increased in a time-dependent manner (Figure 1A), implying that PLC-γ2 might play a role in response to TPA. To examine whether redistribution of PLC-γ2 protein also occurred in response to TPA, immunofluorescent localization of PLC-γ2 protein was conducted and observed by laser-scanning confocal microscope. The result illustrated that in intact MGC80-3 cells, PLC-γ2 protein was more abundant in cytoplasm, and formed a much brighter circle a round the nuclear membrane (Figure 1B). After treatment of TPA for different time, PLC-γ2 protein was translocated from the cytoplasm to the nucleus by degrees (Figure 1B). To further confirm this translocation, cytoplasmic and nuclear protein fractions were prepared, and expression level of PLC-γ2 protein was analyzed by Western blot. Figure 1C shows that PLC-γ2 protein in intact cells mainly appears in the cytoplasmic fraction, and only a trace amount in the nuclear fraction. However, TPA-treatment changed the proportion of PLC-γ2 protein between the two fractions and such a change was time-dependent. After 48 hr TPA treatment, PLC-γ2 protein could only be detected in the nuclear fraction (Figure 1C). Clearly, this result was in accordance with that of Figure 1B, indicating that transloation of PLC-γ2 protein by TPA occurred in MGC80-3 cells.

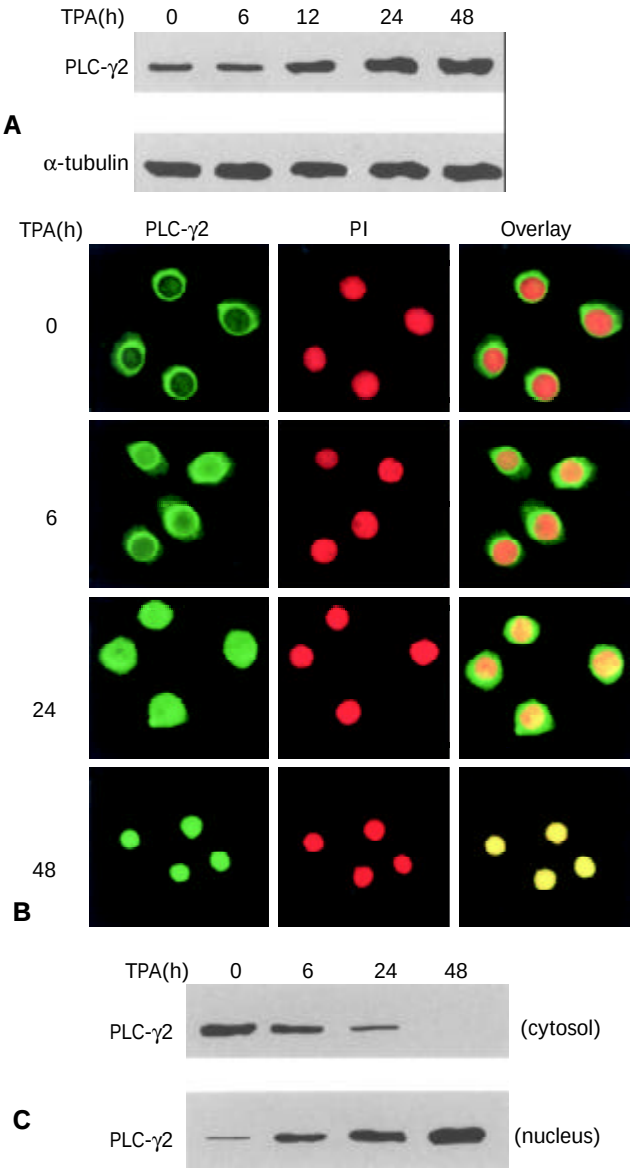

Figure 1 Expression and redistribution of PLC-γ2 in response to TPA. A: Effect of TPA on PLC-γ2 protein expression. Cells were treated with TPA (100 ng/ml) for indicated time, and expression level of PLC-γ2 protein was analyzed by Western blot. α-tubulin was used as a control to quantify the amount of

protein used in each lane. B: Translocation of PLC-γ2 in response to TPA. Cells were treated with TPA for indicated time, then immunostained with corresponding antibodies or dye as described in Materials and Methods. The fluorescent images were observed under laser-scanning confocal microscope. C: Redistribution of PLC-γ2 protein in response to TPA. The nuclear and cytosolic fractions were prepared as described in Materials and Methods.

PLC-γ2 expression was not required for apoptosis induction by TPA

Since TPA could induce apoptosis in many types of cancer cell lines[32,35-37], it would be interesting to know whether activation of PLC-γ2 was a necessary link for apoptosis induction by TPA. A PLC-specific inhibitor U73122[38] was thus used upon gastric cancer cells. Prior to be stimulated with TPA, U73122 partially repressed the expression level of PLC-γ2 protein (Figure 2A). In the presence of U73122, TPA-induced increase of PLC-γ2 expression was also blocked. Even after TPA treatment was prolonged for 48 hr, the expression level of PLC-γ2 was always lower than the control or TPA treatment alone (Figure 2A). In parallel, apoptosis of MGC80-3 cells was examined by DAPI staining. When the cells were treated with TPA alone, apoptotic cells became smaller, the nuclei became condensed and fragmented with bright chromatins. Importantly, an increased apoptotic index was clearly shown with the extension of TPA treatment (Figure2B: TPA). However, no such a change was observed in cells treated with U73122 alone (Figure 2B: U73122). By contrast, when cells pretreated with U73122, followed by TPA stimulation, many apoptotic cells were still seen, which not only showed morphological changes similar to those treated with TPA alone, but also had an increased apoptotic index with the extension of TPA treatment (Figure 2B: U73122+TPA). Therefore, these results showed that additional expression of PLC-γ2 protein was not required for TPA-induced apoptosis in MGC80-3 cells.

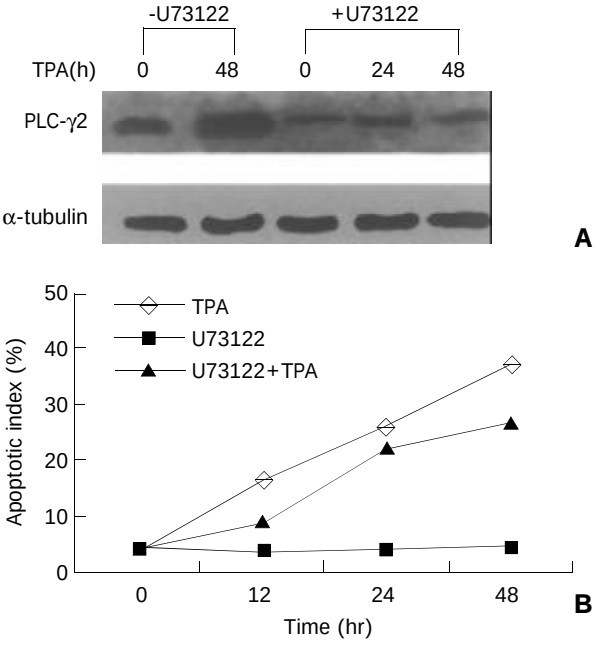

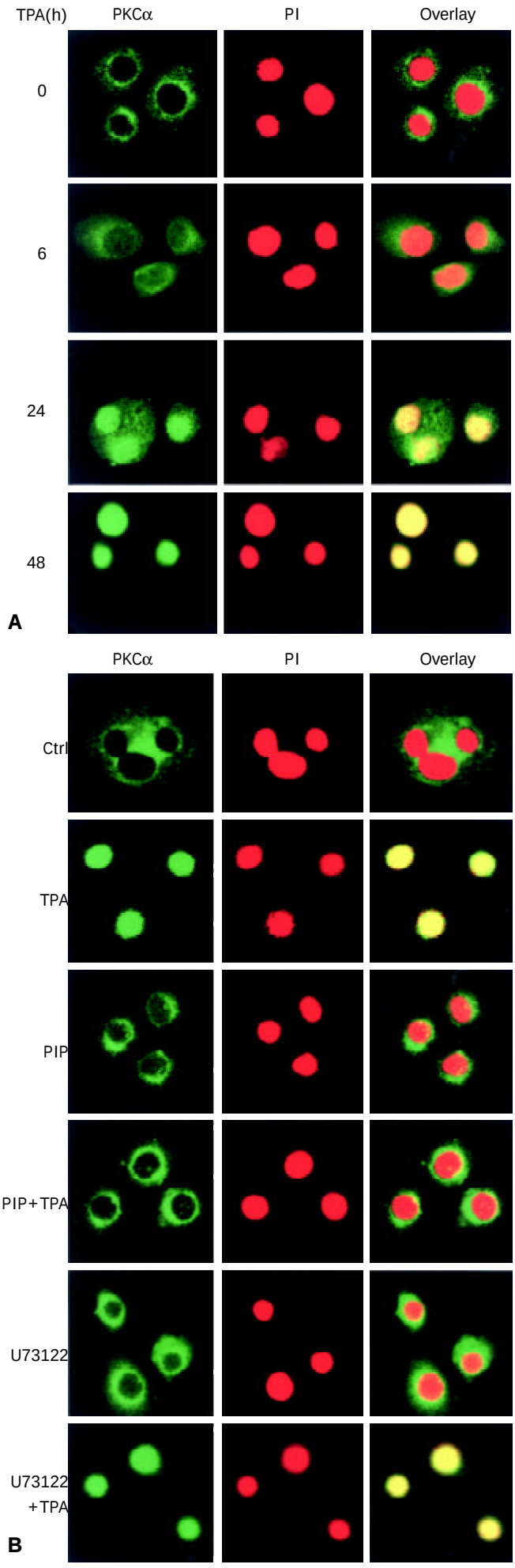

Figure 2 Effect of PLC-γ2 protein expression on apoptosis inducted by TPA. A: Effect of PLC-specific inhibitor U73122 on PLC-γ2 protein expression detected by Western blot. Cells were pretreated with or without U73122 (10^{-3} mmol/L) for 3 hr, and followed by TPA for indicated time. B: Analysis of apoptotic index. Cells were pretreated with or without U73122 for 3 hr, and then exposed to TPA for indicated time. Apoptotic cells were counted among 1 000 cells randomly.

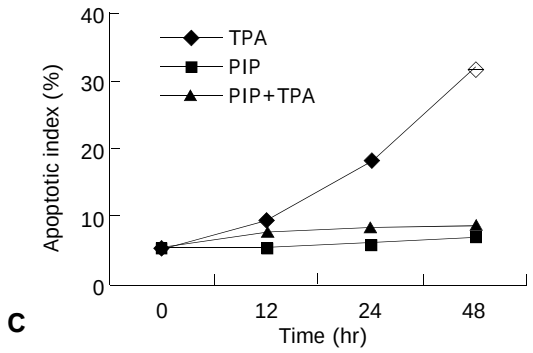

Figure 3 Translocation of PKCα protein in the process of apoptosis induced by TPA. A: Redistribution of PKCα protein. Cells were treated with TPA for indicated time, then immunostained with corresponding antibodies or dye as described in Materials and Methods. The images were observed under laser-scanning confocal microscope. B: Effects of various inhibitors, including PKC-specific inhibitor (PIP., 12 μmol/L) and PLC-specific inhibitor (U73122), on redistribution of PKCα. The detecting method was the same as described in Figure 3A. C: Analysis of apoptotic index. The method was similar as in Figure 2B.

PKCα translocation was directly associated with induction of apoptosis by TPA

The consequent question was that since TPA could induce rapid expression of PLC-γ2 protein which seemed to be not critical in TPA-induced apoptosis in MGC80-3 cells, then, what was the role of rapidly expressed PLC-γ2 protein in TPA-induced event? As PKC was a downstream molecule of PLC[3,4], it was inferred that PLC-γ2 might indirectly play its final effect through the downstream PKC signaling pathway in relation to TPA-induced apoptosis. To test this possibility, the effects of TPA on PKCα were investigated. Firstly, the expression of PKCα protein was determined by Western blot analysis. The result showed that PKCα was intrinsically expressed in MGC80-3 cells, but its expression was not changeable by TPA (data not shown). Secondly, the possible TPA-induced translocation of PKC in MGC80-3 cells was observed. PKCα protein was shown to localize in cytoplasm (Figure 3A). However, TPA treatment stimulated the translocation of PKCα protein from cytoplasm to nucleus in a time-dependent manner. After 48 hr of TPA treatment, cellular PKCα protein was completely translocated into the nucleus, showing a unique yellow color (Figure 3A). Finally, to investigate the behavior of PKCα translocation, PKC-specific inhibitor, a PKC inhibitor peptide(PIP)[39], was used. As expected, PKC inhibitor peptide could not induce PKCα protein translocated to the nucleus (Figure 3B, PIP.), even plus TPA for 48 hr it no longer initiated PKCα protein translocation (Figure 3B, PIP+TPA).

Since TPA could regulate redistribution, but not expression of PKCα protein, it would be attractive to ask whether redistribution of PKCα was in action in TPA-induced apoptosis. The results showed that TPA could no longer induce apoptosis when translocation of PKCα was blocked by PKC inhibitor peptide. Even though these cells were subsequently treated by TPA for 48 hr, the apoptotic index was obviously reduced reduced as compared with the TPA treatment alone (Figure 3C), suggesting that translocation of PKCα protein into the nucleus might be intrinsic in the mechanism of TPA-induced apoptosis.

PKCα was a downstream factor of PLC-γ2

It was then necessary to probe into the intrinsic mechanism of whether there was some inevitable linkage between PLC-γ2 and PKCα in the process of TPA-induced apoptosis. Since enhanced expression of PLCγ2 protein was not required for apoptosis induction (Figure 2), we therefore focused on the translocation behavior of PLC-γ2 with regard to the TPA-induced apoptosis effect. Out of our expectation, when cells were pre-treated with PLC-specific inhibitor U73122 for 3 hr alone, both PLC-γ2 and PKCα proteins did not redistribute (Figures 3B and 4A, U73122). However, when cells were exposing to TPA for 48 hr, not only PLC-γ2 protein but also PKCα protein were translocated into the nucleus (Figures 3B and 4A, U73122+TPA), although expression level of PKCα protein was not changed (Figure 4B). Together with the results in Figure 2, it was suggested that PLC-γ2 might function in passing TPA message to its downstream molecule PKCα in gastric cancer cells.

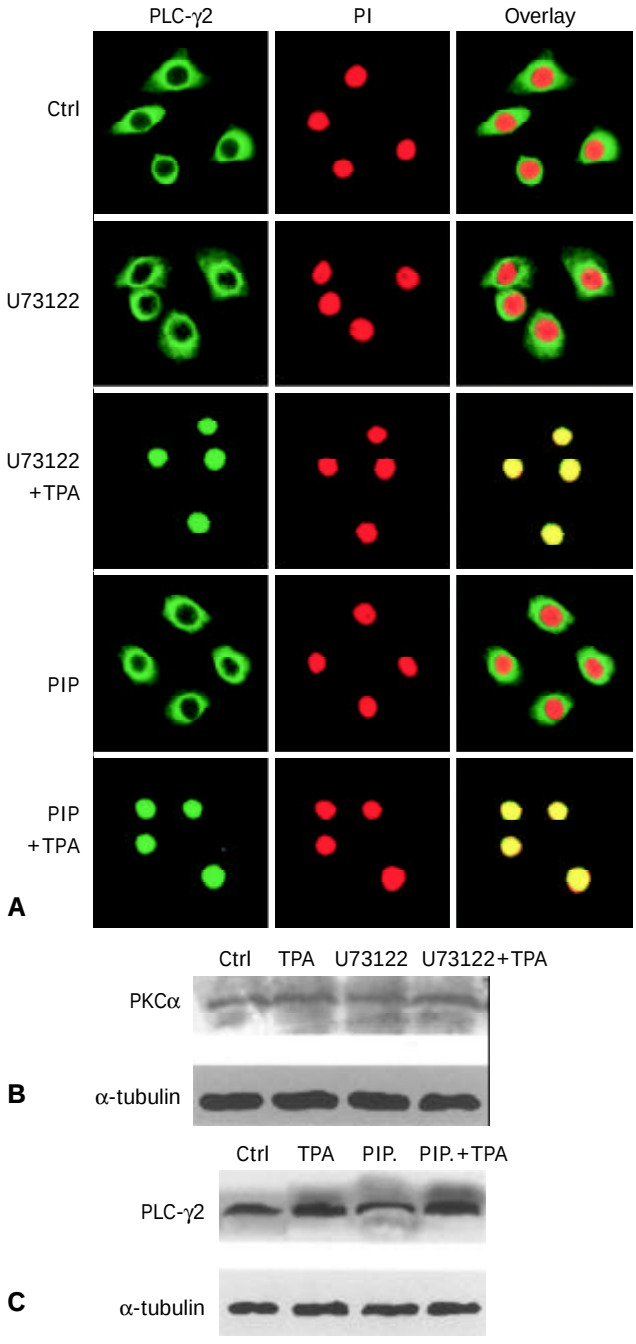

Figure 4 Correlation between PLC-γ2 and PKCα in their redistribution. A: Effects of PKC- and PLC-specific inhibitors on PLC-γs redistribution. The Method was as described in Figure 3B. B: Effects of PKC- and PLC-specific inhibitors on PKCα expression detected by Western blot. C: Effects of PKC- and PLC-specific inhibitors on PLC-γ2 expression.

On the other hand, PKC-specific inhibitor was also used to test its role in the expression of PLC-γ2 protein. When cells were treated with PKC inhibitor peptide (PIP) for 2 hr, PLC-γ2 protein was still located in the cytoplasm (Figure 4A, PIP). However, followed by TPA treatment for 48 hr, translocation of PLC-γ2 protein into the nucleus was not blocked by this inhibitor (Figure 4A: PIP+TPA). Similar result was observed in Western blot analysis, in which the expression level of PLC-γ2 protein was enhanced by TPA, no matter whether PKC inhibitor existed or not (Figure 4C). Taken together, all these findings above convincingly indicated that PKC inhibitor-induced inhibition of PKCα protein (mainly its translocation) and TPA-induced PLC-γ2 protein expression and translocation were two separate events. It also suggested that induction of PLC-γ2 protein translocation was a critical event in signal transmission between TPA and PKCα.

DISCUSSION

PLC-γ has been reported to be activated and up-regulated in response to external signals[13,15,40-44]. Most of these previous studies focused on PLC-γ2 phosphorylation and the relevant growth factor receptor(s), but its physiologic function and signaling pathway were rarely concerned. In the present study, we found that the enhanced expression of PLC-γ2 by TPA was not directly correlated to apoptosis induction. PLC-γ exerted its influence on intracellular process largely through the initiation of second messengers IP3 and DAG, and the subsequent Ca^{2+} mobilization and PKC activation. More importantly, these PLC-γ-induced chain reactions could be stimulated by some external stimuli[40,41]. Taking this fact into account, we therefore turned to investigate the possible regulatory mechanism of PLC-γ2 not correlated with its expression level.

PLC-specific inhibitor U73122 alone could partially suppress the expression of PLC-γ2 protein, but not induce apoptosis in MGC80-3 cells. However, TPA could still induce apoptosis in U73122-pretreated MGC80-3 cells, even though the expression of PLC-γ2 was in its supressed state, indicating that up-regulation of PLCγ2 expression was not required for apoptosis induced by TPA. However, TPA-induced apoptosis in MGC80-3 cells depended on PKCα protein translocation from cytoplasm into nucleus. When translocation of PKCα protein was blocked by its specific inhibitor PKC inhibitor peptide, the apoptosis decreased dramatically even in the presence of TPA. Therefore, these evidences strongly suggest that PLC-γ2 and PKCα can exert distinct effects in response to TPA, and regulation of PKCα protein translocation is closely associated with apoptosis induction.

We have indicated that TPA could promote PLC-γ2 translocation from cytoplasm to nucleus in a time-dependent manner, so it is interesting to figure out why PLC-γ2 is regulated (particularly its translocation) in response to TPA, and what the underlying functional implication is. Recently, some important evidences revealed that PLC-γ2 was critical for transmission of the B-cell antigen receptor complex (BCR)-dependent signals that led to the nuclear translocation of NF-κB[45], and PLC-γ1 was important for transducing survival signals against the cytotoxic effect of oxidant exposure[15]. These studies strongly imply that PLC-γ is capable of transducting signal, leading to translocation of its downstream molecule. To clarify whether TPA-induced apoptosis via PKC pathway was correlated with PLC-γ2, we investigated the effect of PLC-γ2 protein translocation on promoting PKCa translocation and initiating apoptosis. PLC-inhibitor U73122 alone could block the expression of PLC-γ2, but did not initiate the translocation of PLC-γ2 protein and induce PKCα expression, in which neither PKCα translocation nor apoptotic process could be detected. It is thus conceivable that PKCα translocation and cell apoptosis induced by TPA are PLC-γ2 translocation dependent in gastric cancer cells. Furthermore, our present study strongly supports the view that protein redistribution is an important event, which is critical for the function of protein.

Some literatures pointed out that down regulation of surface receptor expression represented an obvious mechanism by which PKC might block PLC activation[29,30]. For example, in Jurkat T cells, activation of PKC by PKC-stimulating agonists resulted in a decrease in its tyrosine phosphorylation, which was responsible for the apparently decreased PLC activity[5]. By contrast, in the present study, the relation between PLC-γ2 and PKCα seemed to be inter-dependent and synergistic. Our results showed a definite linkage between PLC-γ2 and PKCα translocation, and the synergistic effect of PLC-γ2 and PKCα in the initiation of apoptosis in MGC80-3 cells induced by TPA. In addition, the fact that pretreatment of cells with PKC inhibitor did not affect PLC-γ2 activation and translocation by TPA was consistent with the observation in which pretreatment of 293 cells for 30 min with PKC inhibitor Gö6976 did not stimulate PLC activation by EGF[46], demonstrating that PKC is a downstream molecule of PLCγ pathway. Taken together, PLC-γ2 functions in signal transmission to initiate TPA-induced apoptosis via PKCα pathway.

In summary, PLC-γ2 and its downstream molecule PKCα are essential for initiating TPA-induced apoptosis in gastric cancer cells. Translocation of PLC-γ2 and PKCα proteins is critical events in the process of apoptosis. In the cross-talk between TPA, PLC-γ2 and PKCα, PLCγ2 receives TPA message, then transmits it to PKCα. PKCα functions as an effector, directly promoting apoptosis of MGC80-3 cells. This is a novel concept for PLC-γ2 and PKCα functions, which will help us to get further insights into the relationship between PLC-γ2/PKCα and the subsequent cellular events.

REFERENCES

1 **Rana RS**, Hokin LE. Role of phosphoinositides in transmembrane signaling. *Physiol Rev* 1990; **70**: 115-164

2 **Majerus PW**. Inositol phosphate biochemistry. *Annu Rev Biochem* 1992; **61**: 225-250

3 **Rhee SG**, Bae YS. Regulation of phosphoinositide-specific phospholipase C isozymes. *J Biol Chem* 1997; **272**: 15045-15048

4 **Noh DY**, Shin SL, Rhee SG. Phosphoinositide-specific phospholipase C and mitogenic signaling. *Biochim Biophys Acta* 1995; **1242**: 99-113

5 **Rhee SG**, Choi KD. Regulation of inositol ignalingids-specific phospholipase C Isozymes. *J Biol Chem* 1992; **267**: 12393-12396

6 **Berridge MJ**. Inositol trisphosphate and calcium signaling. *Nature* 1993; **361**: 315-325

7 **Nishizuka Y**. Protein kinase C and lipid signaling for sustained cellular responses. *FASEB J* 1995; **9**: 484-496

8 **Berridge MJ**. Neuronal calcium signaling. *Neuron* 1998; **21**: 13-26

9 **Ji QS**, Winnier GE, Niswender KD, Horstman D, Wisdom R, Magnuson MA, Carpenter G. Essential role of the tyrosine kinase substrate phospholipase C-γ1 in mammalian growth and development. *Proc Natl Acad Sci U S A* 1997; **94**: 2999-3003

10 **Cockcroft S**, Thomas GMH. Inositol-lipid-specific phospholipase C isoenzymes and their differential regulation by receptors. *Biochem J* 1992; **288**: 1-14

11 **Lee SB**, Rhee SG. Significance of PIP2 hydrolysis and regulation of phospholipase C isozymes. *Curr Opin Cell Biol* 1995; **7:** 183-189

12 **Nishibe S**, Wahl MI, Wedegaertner PB, Kim JW, Rhee SG, Carpenter G, Kim KJW. Selectivity of phospholipase C phosphorylation by the epidermal growth factor receptor, the insulin receptor, and their cytoplasmic domains. *Proc Natl Acad Sci U S A* 1990; **87**: 424-428

13 **Kayali AG**, Eichhorn J, Haruta T, Morris AJ, Nelson JG, Vollenweider P, Olefsky JM, Webster NJG. Association of the insulin receptor with phospholipase C-γ(PLC-γ1) in 3T3-L1 adipocytes suggests a role for PLCr in metabolic signaling by

insulin. *J Biol Chem* 1998; **273**: 13808-13818
14 **Lee YH**, Kim SY, Kim JR, Yoh KT, Baek SH, Kim MJ, Ryu SH, Suh PG, Kim JH. Overexpression of phospholipase C beta-1 protects NIH3T3 cells from oxidative stress-induced cell death. *Life Sci* 2000; **67**: 827-837
15 **Wang XT**, McCullough KD, Wang XJ, Carpenter G, Holbrook NJ. Oxidative stress-induced phospholipase C-γ1 activation enhances cell survival. *J Biol Chem* 2001; **276**: 28364-28371
16 **Lee YH**, Kim S, Kim J, Young KK, Kim MJ, Ryu SIL, Suh P. Overexpression of phospholipase C-gamma1 suppresses UVC-induced apoptosis through inhibition of c-fos accumulation and c-Jun N-terminal kinase activation in PC12 cells. *Biochim Biophys Acta* 1999; **1440**: 235-243
17 **Han Y**, Han ZY, Zhou XM, Shi R, Zheng Y, Shi YQ, Miao JY, Pan BR, Fan DM. Expression and function of classical protein kinase C isoenzymes in gastric cancer cell line and its drug-resistant sublines. *World J Gastroenterol* 2002; **8**: 441-445
18 **Chen Y**, Wu Q, Song SY, Su WJ. Activation of JNK by TPA promotes apoptosis via PKC pathway in gastric cancer cells. *World J Gastroenterol* 2002; **8**: 1014-1018
19 **Joanne G**, Harald M, Walter K, Frederic Mushinski J. Immunocytochemical localization of eight protein kinase C isozymes overexpressed in NIH 3T3 fibroblasts. Isoform-specific association with microfilaments, Golgi, endoplasmic reticulum, and nuclear and cell membranes. *J Biol Chem* 1995; **270**: 9991-10001
20 **Shao RG**, Cao CX, Pommier Y. Activation of PKCa downstream from caspases during apoptosis induced by 7-hydroxystaurosporine or the topoisomerase inhibitors, camptothecin and etoposide, in human myeloid leukemia HL-60 cells. *J Biol Chem* 1997; **272**: 31321-31325
21 **Nishizuka Y**. Turnover of inositol phospholipids and signal transduction. *Science* 1984; **225**: 1365-1370
22 **Majerus PW**, Connolly TM, Dickmyn H, Ross TS, Bross TE, Ishii H, Bansal VS, Wilson DB. The Metabolism of phosphoinositide-derived messenger molecules. *Science* 1986; **234**: 1519-1526
23 **Isokov N**, Mally MI, Scholz W, Altman A. T-lymphocyte activation: the role of protein kinase C and the bifurcating inositol phospholipid signal transduction pathway. *Immunol Rev* 1987; **95**: 89-111
24 **Kaibuchi K**, Takai Y, Nishizuka Y. Protein kinase C and calcium ion in mitogenic response of macrophage- depleted human peripheral lymphocytes. *J Biol Chem* 1985; **260**: 1366-1369
25 **Albert F**, Hua C, Truneh A, Pierres M, Schmitt-Verhulst AM. Distinction between antigen receptor and IL2 receptor triggering events in the activation of alloreactive T cell clones with calcium ionophore and phorbol ester. *J Immunol* 1985; **134**: 3649-3655
26 **Isakov N**, Altman A. Human T lymphocyte activation by tumor promoters: role of protein kinase C. *J Immunol* 1987; **138**: 3100-3107
27 **Abraham RT**, Ho SN, Harna TJ, Rusovick KM, McKean D. Inhibition of T-cell antigen receptor-mediated transmembrane signaling by protein kinase C activation. *Mol Cell Biol* 1988; **8**: 5448-5458
28 **Mills GB**, May C, Hill M, Ebanks R, Roifman C, Mellors A, Gelfand EW. Physiologic activation of protein kinase C limits IL-2 secretion. *J Immunol* 1989; **142**: 1995-2003
29 **Decker SJ,** Ellis C, Pawson T, Velu T. Effects of substitution of threonine 654 of the epidermal growth factor receptor on epidermal growth factor-mediated activation of phospholipase C. *J Biol Chem* 1990; **265**: 7009-7015
30 **Park DJ**, Min HK, Rhee SG. Inhibition of CD3-linked phospholipase C by phorbol ester and by camp is associated with decreased phosphotyrosine and increased phosphoserine contents of PLC-1. *J Biol Chem* 1992; **267**: 1496-1501
31 **Todderud G**, Wahl MI, Rhee SG, Carpenter G. Stimulastion of phospholipase C-gamma 1 memebrane association by epidermal growth factor. *Science* 1990; **249**: 296-299
32 **Wu Q**, Liu S, Ding L, Ye XF, Su WJ. PKCα translocation from mitochondria to nucleus is closely related to induction of apoptosis in gastric cancer cells. *Science In China* 2002; **45:** 237-244
33 **Wang KH**. An in vitro cell line (MGc80-3) of a pooly differentiated mucoid adenocarcinoma of human stomach. *Shiyan Shengwu Xiebao* 1983; **16**: 257-267
34 **Wu Q,** Chen ZM, Su WJ. Growth inhibition of gastric cancer cells by all-trans retinoic acid through arresting cell cycle progression. *Chinese Med J* 2001; **114**: 958-961
35 **Wu Q**, Liu S, Ye XF, Huang ZW, Su WJ. Dual roles of Nur77 in selective regulation of apoptosis and cell cycle by TPA and ATRA in gastric cancer cells. *Carcinogenesis* 2002; **21**: 1583-1592
36 **Champelovier P**, Richard MJ, Seigneurin D. Autocrine regulation of TPA-induced apoptosis in monoblastic cell-line U-937: role for TNF-alpha, MnSOD and IL-6. *Anticancer Res* 2000; **20**: 451-458
37 Li Y, Bhuiyan M, Mohammad RM, Sarkar FH. Induction of apoptosis in breast cancer cells by TPA. *Oncogene* 1998; **17**: 2915-2920
38 **Bleasdale JE,** Bundy GL, Bunting S, Filzpatrick FA, Huff RM, Sun FF, Pike JE. Inhibition of phospholipase C dependent processes by U-73122. *Adv Prostaglandin Thromboxane Leukot Res* 1989; **19**: 590-593
39 **House C**, Kemp BE. Protein kinase C contains a pseudosubstrate prototope in its regulatory domain. *Science* 1987; **238**: 1726-1728
40 **Mclaughlin AP**, De Vries GW. Role of PLC gamma and Ca(2+) in VEGF- and FGF-induced choroidal andothelial cell proliferation. *Am J Physiol Cell Physiol* 2001; **281**: 1448-1456
41 **Doong H**, Prise J, Kim YS, Gasbarre C, Probst J, Liotta LA, Blanchette J, Rizzo K, Kohn E. CAIR-1/BAG-3 forms an EGF-regulated ternary complex with phospholipase C-gamma and Hsp70/Hsc70. *Oncogene* 2000; **19**: 4385-4395
42 **Jilek F**, Huttelova R, Petr J, Holubova M, Rozinek J. Activation of pig oocytes using calcium ionophore: effect of protein synthesis inhibitor cycloheximide. *Anim Reprod Sci* 2000; **63**: 101-111
43 **Kurosaki T**, Maeda A, Ishiai M, Hashioto A, Inabe K, Takata M. Regulation of the phospholipase C-gamma2 pathway in B cells. *Immunol Rev* 2000; **176**: 19-29
44 **Carpenter G**, Ji Q. Phospholipase C-gamma as a signal-transducing element. *Exp Cell Res* 1999; **253**: 15-24
45 **Petro JB**, Khant WN. Phospholipase C-γ2 Couples Bruton's Tyrosine Kinase to the NF-κB Signaling Pathway in B Lymphocytes. *J Biol Chem* 2001; **276**: 1715-1719
46 **Schmidt M,** Frings M, Mono ML, Guo Y, Oude Weernink PA, Evellin S, Han L, Jakobs KH. G Protein-coupled Receptor-induced Sensitization of Phospholipase C Stimulation by Receptor Tyrosine Kinases. *J Biol Chem* 2000; **275**: 32603-32610

Edited by Zhang JZ and Wang XL

P.O.Box 2345, Beijing 100023,China
Fax: +86-10-85381893
E-mail: wjg@wjgnet.com www.wjgnet.com

World J Gastroenterol 2003;9(11):2419-2423
World Journal of Gastroenterology
 ISSN 1007-9327

• GASTRIC CANCER •

Construction and analysis of SSH cDNA library of human vascular endothelial cells related to gastrocarcinoma

Yong-Bo Liu, Zhao-Xia Wei, Li Li, Hang-Sheng Li, Hui Chen, Xiao-Wen Li

Yong-Bo Liu, Hui Chen, Xiao-Wen Li, Department of Cell Biology and Medical Genetics, Medical College of Zhengzhou University, Zhengzhou, 450052, Henan Province, China
Zhao-Xia Wei, Department of Anatomy, Henan Medical College for Enterprise Employees, Zhengzhou 450003, Henan Province, China
Li Li, Department of Cardiovascular Disease, People' Hospital of Henan Province, Zhengzhou 450003, Henan Province, China
Hang-Sheng Li, Department of Gynecology and Obstetrics, Henan Medical College for Enterprise Employees, Zhengzhou 450003, Henan Province, China
Correspondence to: Yong-Bo Liu, Department of Cell Biology and Medical Genetics, Medical College of Zhengzhou University, Zhengzhou, 450052, Henan Province, China. liuyb415@163.net
Telephone: +86-371-6974324
Received: 2003-05-11 **Accepted:** 2003-06-04

Abstract

AIM: To construct subtracted cDNA libraries of human vascular endothelial cells (VECs) related to gastrocarcinoma using suppression substractive hybridization (SSH) and to analyze cDNA libraries of gastrocarcinoma and VECs in Cancer Gene Anatomy Project (CGAP) database.

METHODS: Human VECs related to gastric adenocarcinoma and corresponding normal tissue were separated by magnetic beads coupled with antibody CD31 (Dynabeads CD31). A few amount of total RNA were synthesized and amplified by SMART™ PCR cDNA Synthesis Kit. Then, using SSH and T/A cloning techniques, cDNA fragments of differentially expressed genes in human VECs of gastric adenocarcinoma were inserted into JM109 bacteria. One hundred positive bacteria clones were randomly picked and identified by colony PCR method. To analyze cDNA libraries of gastrocarcinoma and VECs in CGAP database, the tools of Library Finder, cDNA xProfiler, Digital GENE Expression Displayer (DGED), and Digital Differential Display (DDD) were used.

RESULTS: Forward and reverse subtraction cDNA libraries of human VECs related to gastrocarcinoma were constructed successfully with SSH and T/A cloning techniques. Analysis of CGAP database indicated that no appropriate library of VECs related to carcinoma was constructed.

CONCLUSION: Construction of subtraction cDNA libraries of human VECs related to gastrocarcinoma was successful and necessary, which laid a foundation for screening and cloning new and specific genes of VECs related to gastrocarcinoma.

Liu YB, Wei ZX, Li L, Li HS, Chen H, Li XW. Construction and analysis of SSH cDNA library of human vascular endothelial cells related to gastrocarcinoma. *World J Gastroenterol* 2003; 9(11): 2419-2423
http://www.wjgnet.com/1007-9327/9/2419.asp

INTRODUCTION

The microvascular system is indispensable throughout the full life span of an organism. Malformation and / or malfunction of VECs contribute to numerous human pathologies including various congenital abnormalities, arteriosclerosis, benign tumors, and cancer. Angiogenesis, the development of new blood vessels by sprouting from the preexisting vasculature, plays an important role in a number of physiological and pathological processes. Stimulated growth or strengthening of so-called collateral vascular branches might circumvent areas with obstructed blood flow in the case of stroke or coronary heart disease. On the other hand, there is substantial evidence suggesting that inhibition of tumor vascular rise might slow down, stop or eventually even reverse tumor growth and could thus become an important part of cancer therapy. The growth of micro vessel accompanying tumor development has, in particular, aroused greater interest and helped improve our understanding of the central role of Vices. Suppression subtractive hybridization (SSH), a PCR-based coda subtracted method, is an important method to reach this aim[1-4]. Because it still needs a lot of initiating RNA, bulk tissues (normal and cancerous) instead of individual cells are routinely used in the analysis. In recent two years, many articles have been publicized employing this method using various tissues[5,6] or cell lines[7,8]. However, bulk tissue contains many different cell types, which will burden the latter work for identifying special genes, and cell lines are different from cells *in vivo* especially for disease cells. With the introduction of Laser Capture Microdissection (LCM), the quantity and purity of RNA from either malignant or benign individual cells invariably yield more reliable and comprehensive experimental results[9-12]. But cell selection and extraction by LCM is currently a manual process, and at most only a few thousand cells can be extracted in an amount of time necessary to limit RNA degradation, and the machine is too expensive for average laboratory. Gastrocarcinoma, one of the most common human malignant tumors, ranks worldwide as the first leading cause of cancer-related mortality. A great deal of articles have been publicized about differentially expressed genes in normal and tumor gastric tissues[13-15]. Some researchers used cells separated from tissues digested with collagenase or cultured cells as material[16-18]. However, with cell culture even primary cell culture, the expressed gene map may change a lot. Likewise, in cells treated with collagenase at 37 ℃ for 30 minutes for separating the target cells from tissue, the specially expressed genes may lose before disposal or new genes may appear after disposal. The Cancer Gene Anatomy Project (CGAP) database of the National Cancer Institute has thousands of expressed sequences, derived from diverse normal and tumor cDNA libraries, but has no appropriate VECs cDNA library related to tumor. The aim of the present study was to select all genes specially expressed in VECs related to gastrocarcinoma rather than in normal gastric tissue. Using VECs mechanically separated by Dynabeads CD31 as materials without collagenase and culture, we built a cDNA library through SSH method, thus paved the way for further research on changes of VECs in gastrocarcinoma.

MATERIALS AND METHODS

Materials

The resected specimens about 2 cm^3 from gastric adenocarcinoma

confirmed pathologically and from normal gastric tissues 7 cm away from the edge of the adenocarcinoma in same patients who were admitted to Henan Provincial Hospital were put into RNA protecting solution (RNAlater™, Ambion Company) after being rinsed with PBS immediately after resection.

Methods

Separation of ECs with Dynabeads CD31 About 1 cm^3 of tissue cut from tissues stabilized by RNA*later* was put into a mortar with a little RNA*later* RNA Stabilization Reagent, and then was scissored and ground with scissors and pestle. To make cell suspension, 1 ml RNA*later* RNA Stabilization Reagent was added to it, then filtered through a sterile 80-μm-nylon filter. 25 μl washed Dynabeads®CD31 beads were added to the suspension for 30 minutes at 2-8 ℃. For identification, slide was made with one drop of this mixture and stained with hematoxylin and eosin (H&E). Then bead-bound cells were separated in a magnetic device (Dynal MPC®).

Isolation of total RNA

Rnaeasy Mini Kit and Rnase-Free Dnase set (QIAGEN Company) were used to extract the total RNA from bead-bound cells. RNA purified by Rnaeasy Column was analyzed for integrity and size by formaldehyde agarose gel electrophoresis and quantification and purity of RNA by OD value.

Synthesis, amplification and purification of cDNA

About 100 ng total RNA was used to synthesize the first strand of cDNA with SMART™ PCR cDNA Synthesis Kit (Clontech Company), then amplified by LD-PCR with 15, 18, 21, 24, 27 cycles separately and analyzed through 1.2 % agarose gel electrophoresis in order to get the perfect cycle number with which we harvested a suitable amount rather than a superfluous one to build the library. Placental total RNA was performed as control. CHROMA SPIN-100 Column was used to purify the cDNA.

Digestion with RsaI and purification of digested products

SampleI, cDNA from VECs of gastrocarcinoma, and sample II, cDNA from VECs of normal stomach tissue, and sample III, cDNA from VECs of placental tissue were treated with enzyme RsaI respectively. From each sample, 10-μl solutions was taken before digestion and 1 h, 3 h and 3.5 h after digestion, and 1.2 % agarose gel electrophoresis was performed for identification of digestion efficiency. Digested products were purified by QIAquick PCR purification Kit (QIAGEN Company), and subsequently concentrated to 6.7 μl by ethanol precipitation method.

Isolation of specially expressed cDNA fragments

Based on the instructions of Clontech PCR-Select™ cDNA Subtraction Kit, sample I and sample II were used as test 1 and driver 1, correspondingly sample II and sample I were used as test 2 and driver 2. Mixture of sample III and ω×174/Hae III DNA was treated as test 3, correspondingly sample III alone was performed as driver 3. Each sample test was divided into two parts, and each part was ligated separately with Adaptor 1 and Adaptor 2, and then hybridized with the corresponding sample driver. The mixture of two parts was hybridized with corresponding sample driver again. The fragments with both Adaptor 1 and Adaptor 2, namely specially expressed cDNA fragments in sample test rather than in sample driver, were amplified by nested PCR. Adeptors possessed outside primer and inside primer. So forward and reverse subtraction fragments were obtained. Subtraction efficiency was checked by G3PDH, a housekeeping gene, according to PCR cycles needed in subtracted sample and unsubtracted sample, with which the gene could be observed on agarose/EtBr gel.

Purification of subtraction fragments

QIAquick PCR Purification Kit was utilized to purify the subtraction fragments.

Clone and screening of subtraction fragments

1 μl, 2 μl, 3 μl PCR fragments of subtraction and non-subtraction and 2 μl control DNA were respectively taken to ligate with 1 μl pGEM-T easy Vector. 10-μl ligation reaction solutions were transformed into 150 μl competent cells JM109. Background control was set up by pGEM-T easy Vector without any insert, and transformation control was also set up by an uncut plasmid pGEM@-5Zf (+) Vector. The transformation culture was plated on petri dishes containing LB/ampicillin/IPTG/X-Gal, and then screened white colony for inset fragment.

Identification of positive recombination of vector

Select 100 white colonies separately from forward and reverse library and replant 5 ml LB/Amp solution. Then it was shaken at 37 ℃ overnight. Take 1 μg culture solution as model and Nested Primer 1 and Nested Primer 2R to amplify the insert and test it by electrophoresis.

Storage of library

Select white colonies separately from forward and reverse library and inoculate 5 ml LB/Amp solution. Then it was shaken at 37 ℃ overnight. Add 700 μl culture solution into 1.5 ml EP tube containing 50 % glycerin and keep it at -80 ℃.

Analysis of related library

cDNA library of stomach cancer tissue, normal stomach tissue and vascular endothelial cell were analyzed using GLS, cDNA xProfiler, DDD, DGED and Library Finder in Cancer Genome Anatomy Project (CGAP). dbEST was categorized using the GLS tool of CGAP. We considered precancer libraries as cancer libraries. All of the cDNA libraries were categorized according to tissue type (tissue origin), tissue histology (cancerous, normal, or fetal), and the library preparation method (microdissected, bulk, cell line, or flow cytometric sorted).

RESULTS

Through Dynabeads®CD31, about 8×10^6 endothelial cells were obtained with almost 100 % purity. Slides were made and stained with H&E (Figure 1).

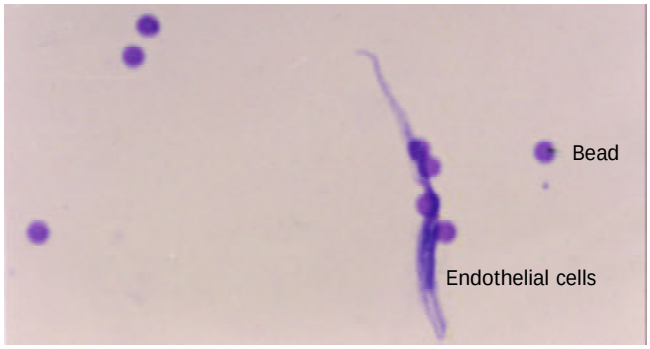

Figure 1 Endothelial cell attached with several beads.

The amount of RNA extracted from stomach cancer and normal stomach tissue was respectively 1.0 μg and 0.85 μg with OD_{260}/OD_{280} ratio 2.10 and 1.96. By formaldehyde agarose gel electrophoresis, the integrity and size were analyzed and clear bands of 18s and 28s were seen (Figure 2).

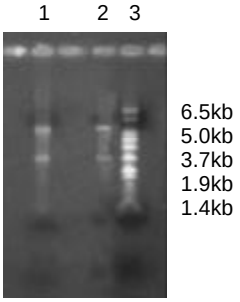

Figure 2 Lane 1, total RNA of stomach cancer. Lane 2, total RNA of normal stomach tissue. Lane 3, marker.

Figure 3 Lanes 1, 2, 3 demonstrate 21, 24, 27 PCR cycles of cDNA products of stomach cancer tissue. Lanes 4, 5, 6 demonstrate 21, 24, 27 PCR cycles of cDNA products of normal stomach tissue. Lanes 7, 8, 9 demonstrate 15, 18, 21 PCR cycles of cDNA products of placental tissue. Lane 10, marker.

Synthesis and amplification of cDNA

The first strands of cDNA have been amplified by LD-PCR with different cycles: 15, 18, 21, 24, and 27. The products could be viewed on 2 % agarose gel electrophoresis (Figure 3). For both normal tissue and cancer tissue, a total of 27 cycles were performed, respectively, and for placental tissue, totally 18 cycles were performed.

Analysis of RsaI digestion efficiency

cDNA, before digestion with *RsaI*, appeared as a smear of 0.5-10 kb on 1 % agarose gel electrophoresis, and after digestion the average cDNA size was smaller (0.1-2 kb) (Figure 4).

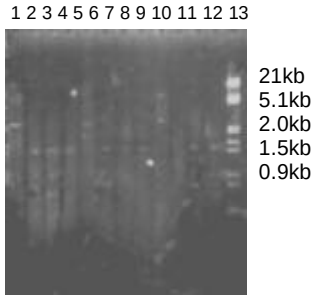

Figure 4 Lanes 1, 2, 3, 4: sampleI. Lanes 5, 6, 7, 8: sampleII. Lanes 9, 10, 11, 12: sample III. Lane 13, marker. Lanes 1, 5, 9: cDNA undigested. Lanes 2, 6, 10: cDNA digested for 1 h. Lanes 3, 7, 11: cDNA digested for 3 h. Lanes 4, 8, 12: cDNA digested for 3.5 h.

Analysis of ligation efficiency

That the intensity ratio of PCR products determined by G3PD primer 3' and Adaptor primer 1 to PCR products determined by G3PD primer 3' and 5' was over 1:4 on 2.0 % agarose/EB gel showed that ligation efficiency was above 25 % (Figure 5).

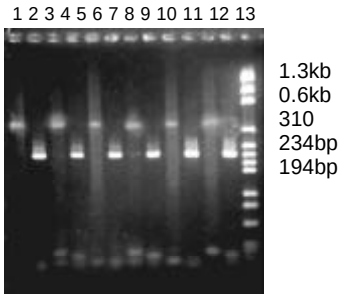

Figure 5 Lanes 1, 2, 3, 4 : sampleI. Lanes 5, 6, 7, 8: sample II. Lanes 9, 10, 11, 12: sample III. Lane 13, marker. Lanes 1, 5, 9: PCR products using cDNA ligated Adaptor 1 as model, and G3PDH 3' primer and PCR Primer 1. Lanes 2, 6, 10: PCR products using cDNA ligated Adaptor 1 as model, and G3PDH 3'primer and G3PDH 5'primer; Lanes 3, 7, 11: PCR products using cDNA ligated Adaptor 2 as model, and G3PDH 3' primer and primer 1. Lanes 4, 8, 12: PCR products using cDNA ligatefd Adaptor 2 as model, and G3PDH 3' primer and G3PDH 5' primer.

Analysis of differentially expressed cDNA with nest PCR

The second hybridization products were amplified by outside primers. The products presented unclear smear on 2 % agarose/EB gel. After second PCR with inside primers, several bands could be seen clearly among the smears. Based on the manual, the experiment was successful (Figure 6).

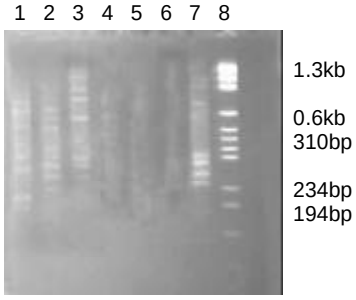

Figure 6 Lanes 1, 2, 3 indicated subtracted samples I, II, III. Lanes 4, 5, 6 indicated unsubtracted sample I, II, III. Lane 7 showed the subtracted control provided by the kit. Lane 8: Marker.

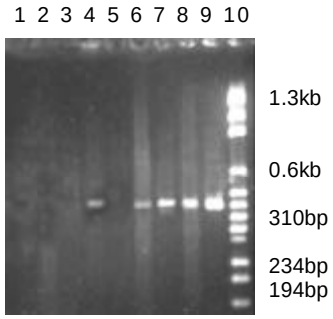

Figure 7 Lanes 1, 2, 3, 4 indicated the subtracted sample I was amplified by PCR wth different cycles: 18, 23, 28, 33. Lanes 6, 7, 8, 9 indicated the unsubtracted sample I was amplified by PCR wth different cycles: 18, 23, 28, 33. Lane 10: Marker.

PCR analysis of subtraction efficiency

After PCR amplification, the housekeeping gene G3PDHs appeared at 18 cycles in unsubtraction samples and at 33 cycles in subtraction samples. This result indicated that G3PDHs expressed in both parts have been greatly decreased

through the subtraction method. If five cycles corresponded roughly to 20-fold cDNA enrichment, G3PDHs would have been decreased almost 300 times. It implied that other genes expressed in both tissues have been reduced the same fold and the specially expressed genes in the test sample were selected (Figure 7).

Screening transformants for inserts

720 white colonies were observed on two petri dishes of positive control with 7 % presence ratio of blue colony. Two white colonies were observed on one petri dish of background control with 15 blue colonies. On one petri dish of transformation control, 160 white colonies without blue colony were observed. 992 white colonies appeared on 5 petri dishes of forward subtraction, and 890 white colonies appeared on 5 petri dishes of reverse subtraction. 60 white colonies were selected from forward and reverse subtractions, and amplified with nested Primer 1 and nested Primer 2R. 54 and 50 fragments ranged from 100 bp to 1 000 bp were selected from the corresponding forward and reverse subtraction libraries.

Analysis of CGAP database

dbEST was categorized using the GLS tool of the CGAP. All of the cDNA libraries were categorized according to tissue type (tissue origin), tissue histology (cancerous, normal, or fetal), and the library preparation method (microdissected, bulk, cell line, or flow cytometric sorted). Among 319 stomach cDNA libraries, all 73 libraries of normal stomach were from bulk tissues instead of cells and none was established by SSH method except those without label. Among the 245-cDNA libraries of stomach cancer, 28 originated from cell lines with 9 libraries built by SSH, and none of the other 217 libraries originating from tissue was built by SSH. All 15 vascular cDNA libraries came from normal tissue or cell line or cultured cells, and SSH method was not used. And appropriate VECs related to tumor have not been built into cDNA library. Among the libraries derived from cell lines, two derived from umbilical vein endothelium, one derived from aortic endothelium, another one came from endothelial cells of foreskin through primary culture of dermal microvascular endothelial cells. Among the 11 non-cell line libraries, 6 were from aorta, 2 umbilical veins, 1 unlabeled vein; another two were from choroidal plexus and basilar artery.

DISCUSSION

Bio-behavior such as growth and metastasis of cancer is closely related with proliferation of microvessel. Newborn capillaries of cancer differ from normal ones in growth process or distribution. For instance, VECs of breast cancer can grow 50 times faster than VEC in normal tissue[19] and vascular endothelial growth factors (VEGFs) play an important role in tumor angiogenesis[20,21], and their over- expression is closely related to clinical staging, lymph node metastasis and recurrence of gastric carcinoma[22]. So increasing attention has been paid to VECs[23].

Differentially expressed genes between the corresponding normal and cancer tissue can help us understand the molecular basis of malignancy and potentially serve as biomarkers or prognostic markers of malignancy. The identification and characterization of human genes expressed exclusively or preferentially in microvascular system of tumor will hopefully shed light on the mechanisms of tumor development and provide useful genetic markers for screening, diagnosis, prognosis, therapeutic monitoring and development of therapeutic vaccines. There are many techniques that aim at producing an inventory of differential transcripts between two populations of mRNAs. High-throughput gene expression techniques (microarrays, genechips) to identify cancer-specific genes are becoming available[24-26], however, the technology is not cost effective for average laboratories. SSH method allows identifying overexpressed genes (designated forward +SSH) but also underexpressed genes (designated reverse -SSH) by exchanging the driver and tester populations during the procedure (Clontech, Palo Alto, USA). Since this technique was established by Diatchenko, many new genes have been separated from almost all tissues, such as renal cell cancer, lung cancer, liver cancer[27-30], etc.

The CGAP database of the National Cancer Institute has thousands of expressed sequences, both known and novel, in the form of expressed sequence tags (ESTs). These ESTs derive from diverse normal and tumor cDNA libraries. In CGAP database, there are 8 221 libraries from various tissues. Among these libraries, 54 libraries are based on SSH method, and 69 material samples are prepared through microdissection. Among those 54 libraries with SSH method, none of the material sample has been prepared through microdissection.

CGAP also offers different data-mining tools: tools of the GLS, the cDNA xProfiler, the DDD, and the DGED. With these tools and database in CGAP, differently expressed genes can be predicted too[31-33]. Using DGED tool to compare normal stomach libraries and cancer libraries, 117 differently expressed genes can be found. But endothelial cells related to cancer have no appropriate library that can be matched and compared. So cDNA library of endothelial cells related to cancer needs to be built, and the more the better, just like prostate libraries.

TO separate VECs from microvessel, tissues were usually treated with collagenase at 37 ℃ for 30 minutes according to present common techniques, and magnetic beads coupled with monoclonal antibody CD31(Dynabeads CD31) have also been used[34,35]. VECs separated by monoclonal antibody have been identified without change[36]. Instead of using collagenase and cell culture, we separated VECs with Dynalbeads CD31 after mechanically grinding tissue and filtering through a sterile 80-μm-nylon filter. In this way, we obtained about 10^6 VECs, from which 1 μg total RNA was harvested. Although the amount of the cells was limited and even some cells were connected by fibers, they were relatively pure. The process of separating VECs from tissue with Danalbeads CD31 lasted almost 1 h, as a result RNAlater, solution-inhibiting degradation of RNA, has been used to substitute PBS required by the Danalbeads CD31 Kit. Because the amount was far from 1-2 mg total RNA required by SSH method, Smart cDNA Synthesis Kit was introduced to synthesize and amplify cDNA from the relatively few RNA, which requires only 50 ng total RNA. In the process of amplification, after the first 15 cycles, for each three more cycles, a little sample was taken and tested in order to get suitable copies of cDNA, as more copies would add burden to later screening work.

In performing SSH, each step was operated exactly according to the manual of the kit and the results were verified correct before each following step. G3PDH was used to identify the forward and reverse subtractions. On agarose/EB gel, appearance of G3PDH band was 15 PCR cycles later in subtraction sample than in unsubtraction sample. It implied the amount of G3PDH decreased 300 times by subtraction technique. Finally, with T/A technique, subtracted PCR products were ligated to T vector and transformed into bacteria JM109. So, both the forward subtraction cDNA library containing cDNA fragments only expressed in VECs of stomach cancer but not normal stomach tissue, and the reverse subtraction cDNA library containing cDNA fragments not expressed in VECs of stomach cancer tissue but normal stomach tissue were built up successfully, which was a good beginning for researching into new genes of VECs related to gastrocarcinoma and gene therapy of gastrocarcinoma.

ACKNOWLEDGEMENT

We thank Dr. Xu ZF, Dr. Pan Wi, Dr. Wang XL, from the Life Science Academy of Zhongshan University; and Mr. Zhang QX, Mr. Ding Y, Mr. Jin H, from the Histological Department of Medical College of Zhengzhou University.

REFERENCES

1 **Diatchenko L**, Lau YF, Campbell AP, Chenchik A, Moqadam F, Huang B, Lukyanov S, Lukyanov K, Gurskaya N, Sverdlov ED, Siebert PD. Suppression subtractive hybridization: a method for generating differentially regulated or tissue-specific cDNA probes and libraries. *Proc Natl Acad Sci U S A* 1996; **93**: 6025-6030

2 **Diatchenko L**, Lukyanov S, Lau YF, Siebert PD. Suppression subtractive hybridization: a versatile method for identifying differentially expressed genes. *Methods Enzymol* 1999; **303**: 349-380

3 **Ji W**, Wright MB, Cai L, Flament A, Lindpaintner K. Efficacy of SSH PCR in isolating differentially expressed genes. *BMC Genomics* 2002; **3**: 12

4 **Wang X**, Feuerstein GZ. Suppression subtractive hybridisation: application in the discovery of novel pharmacological targets. *Pharmacogenomics* 2000; **1**: 101-108

5 **Villalva C**, Trempat P, Zenou RC, Delsol G, Brousset P. Gene expression profiling by suppression subtractive hybridization (SSH): a example for its application to the study of lymphomas. *Bull Cancer* 2001; **88**: 315-319

6 **Li YJ**, Tian F, Chen ZC, Guan YJ, He CM, Yang XM, Xie DH. Isolation and Identification of cDNA Sequences Differentially Expressed in Laryngeal Carcinoma. *Shengwu Huaxue Yu Shengwu WuLi Xuebao* 2000; **32:** 153-157

7 **Eleveld-Trancikova D**, Kudela P, Majerciak V, Regendova M, Zelnik V, Pastorek J, Pastorekova S, Bizik J. Suppression subtractive hybridisation to isolate differentially expressed genes involved in invasiveness of melanoma cell line cultured under different conditions. *Int J Oncol* 2002; **20**: 501-508

8 **Langley RR**, Ramirez KM, Tsan RZ, Van Arsdall M, Nilsson MB, Fidler IJ. Tissue-specific Microvascular Endothelial Cell Lines from H-2K (b)-tsA58 Mice for Studies of Angiogenesis and Metastasis. *Cancer Res* 2003; **63:** 2971-2976

9 **Fend F**, Emmert-Buck MR, Chuaqui R, Cole K, Lee J, Liotta LA, Raffeld M. Immuno-LCM: laser capture microdissection of immunostained frozen sections for mRNA analysis. *Am J Pathol* 1999; **154**: 61-66

10 **Kerk NM**, Ceserani T, Tausta SL, Sussex IM, Nelson TM. Laser capture microdissection of cells from plant tissues. *Plant Physiol* 2003; **132:** 27-35

11 **Pedersen TX**, Leethanakul C, Patel V, Mitola D, Lund LR, Dano K, Johnsen M, Gutkind JS, Bugge TH. Laser capture microdissection-based *in vivo* genomic profiling of wound keratinocytes identifies similarities and differences to squamous cell carcinoma. *Oncogene* 2003; **22:** 3964-3976

12 **Yim SH,** Ward JM, Dragan Y, Yamada A, Scacheri PC, Kimura S, Gonzalez FJ. Microarray analysis using amplified mRNA from laser capture microdissection of microscopic hepatocellular precancerous lesions and frozen hepatocellular carcinomas reveals unique and consistent gene expression profiles. *Toxicol Pathol* 2003; **31**: 295-303

13 **Mori M**, Mimori K, Yoshikawa Y, Shibuta K, Utsunomiya T, Sadanaga N, Tanaka F, Matsuyama A, Inoue H, Sugimachi K. Analysis of the gene-expression profile regarding the progression of human gastric carcinoma. *Surgery* 2002; **131**(Suppl 1): S39-47

14 **Jung MH**, Kim SC, Jeon GA, Kim SH, Kim Y, Choi KS, Park SI, Joe MK, Kimm K. Identification of differentially expressed genes in normal and tumor human gastric tissue. *Genomics* 2000; **69**: 281-286

15 **Yoshikawa Y,** Mukai H, Hino F, Asada K, Kato I. Isolation of two novel genes, down-regulated in gastric cancer. *Jpn J Cancer Res* 2000; **91**: 459-463

16 **Su N,** Yan H**,** Li YP. Isolation, purification, identification and gene transfer of microvascular endothelial cells. *Xibao Shengwuxue Zazhi* 2000; **22**: 94-98

17 **Muczynski KA,** Ekle DM, Coder DM, Anderson SK. Normal human kidney HLA-DR-expressing renal microvascular endothelial cells: characterization, isolation, and regulation of MHC class II expression. *J Am Soc Nephrol* 2003; **14:** 1336-1348

18 **Stier S,** Totzke G, Grunewald E, Neuhaus T, Fronhoffs S, Sachinidis A, Vetter H, Schulze-Osthoff K, Ko Y. Identification of syntenin and other TNF-inducible genes in human umbilical arterial endothelial cells by suppression subtractive hybridization. *FEBS Lett* 2000; **467**: 299-304

19 **Jin HM,** Li XT. Neovascularization and disease. *Zhongguo Weixunhuan* 2001; **5**: 173-177

20 **Liu DH**, Zhang XY, Fan DM, Huang YX, Zhang JS, Huang WQ, Zhang YQ, Huang QS, Ma WY, Chai YB, Jin M. Expression of vascular endothelial growth factor and its role in oncogenesis of human gastric carcinoma. *World J Gastroenterol* 2001; **7**: 500-505

21 **Tao HQ**, Lin YZ, Wang RN. Significance of vascular endothelial growth factor messenger RNA expression in gastric cancer. *World J Gastroenterol* 1998; **4:** 10-13

22 **Konno H**, Baba M, Tanaka T, Kamiya K, Ota M, Oba K, Shoji A, Kaneko T, Nakamura S. Overexpression of vascular endothelial growth factor is responsible for the hematogenous recurrence of early-stage gastric carcinoma. *Eur Surg Res* 2000; **32**: 177-181

23 **Liu C**, Zhang L, Shao ZM, Beatty P, Sartippour M, Lane TF, Barsky SH, Livingston E, Nguyen M. Identification of a novel endothelial-derived gene EG-1. *Biochem Biophys Res Commun* 2002; **290**: 602-612

24 **Khan J**, Bittner ML, Saal LH, Teichmann U, Azorsa DO, Gooden GC, Pavan WJ, Trent JM, Meltzer PS. cDNA microarrays detect activation of a myogenic transcription program by the PAX3-FKHR fusion oncogene. *Proc Natl Acad Sci U S A* 1999; **23:** 13264-13269

25 **Elek J**, Park KH, Narayanan R. Microarray-based expression profiling in prostate tumors. *In Vivo* 2000; **14**: 173-182

26 **Wikman H,** Kettunen E, Seppanen JK, Karjalainen A, Hollmen J, Anttila S, Knuutila S. Identification of differentially expressed genes in pulmonary adenocarcinoma by using cDNA array. *Oncogene* 2002; **21**: 5804-5813

27 **Pitzer C,** Stassar M, Zoller M. Identification of renal-cell-carcinoma-related cDNA clones by suppression subtractive hybridization. *J Cancer Res Clin Oncol* 1999; **125:** 487-492

28 **Ai JK**, Huang X, Wang YJ, Bai Y, Lu YQ, Ye XJ, Xin DQ, Na YQ, Zhang ZW, Guo YL. Screening of novel genes differentially expressed in human renal cell carcinoma by suppression subtractive hybridization. *Ai Zheng* 2002; **21:** 1065-1069

29 **Zhang L**, Cilley RE, Chinoy MR. Suppression subtractive hybridization to identify gene expressions in variant and classic small cell lung cancer cell lines. *J Surg Res* 2000; **93:** 108-119

30 **Li J**, Han B, Huang G, Qian G, Liang P, Yang T, Chen J. Screening and identification for cDNA of differentially expressed genes in human primary hepatocellular carcinoma. *Zhonghua Yixue Yichuanxue Zazhi* 2003; **20:** 49-52

31 **Schmitt AO**, Specht T, Beckmann G, Dahl E, Pilarsky CP, Hinzmann B, Rosenthal A. Exhaustive mining of EST libraries for genes differentially expressed in normal and tumour tissues. *Nucleic Acids Res* 1999; **27**: 4251-4260

32 **Scheurle D**, De Young MP, Binninger DM, Page H, Jahanzeb M, Narayanan R. Cancer gene discovery using digital differential display. *Cancer Res* 2000; **60**: 4037-4043

33 **Asmann YW**, Kosari F, Wang K, Cheville JC, Vasmatzis G. Identification of differentially expressed genes in normal and malignant prostate by electronic profiling of expressed sequence tags. *Cancer Res* 2002; **62**: 3308-3314

34 **Zhou H**, Xu GW, Sheng ML, Tang J. Construction of human vascular endothelial cell database. *Shengwu Huaxue Zazhi* 1993; **9**: 507-509

35 **Van Leeuwen EB,** Molema G, de Jong KP, van Luyn MJ, Dijk F, Slooff MJ, Ruiters MH, van der Meer J. One-Step Method for Endothelial cell isolation from large human blood vessels using fibrin glue. *Lab Invest* 2000; **80**: 987-989

36 **Su X**, Sorenson CM, Sheibani N. Isolation and characterization of murine retinal endothelial cells. *Mol Vis* 2003; **9**: 171-178

Edited by Zhu LH

P.O.Box 2345, Beijing 100023,China
Fax: +86-10-85381893
E-mail: wjg@wjgnet.com www.wjgnet.com

World J Gastroenterol 2003;9(11):2424-2427
World Journal of Gastroenterology
 ISSN 1007-9327

• GASTRIC CANCER •

Therapeutic mechanism of ginkgo biloba exocarp polysaccharides on gastric cancer

Ai-Hua Xu, Hua-Sheng Chen, Bu-Chan Sun, Xiao-Ren Xiang, Yun-Fei Chu, Fan Zhai, Ling-Chang Jia

Ai-Hua Xu, Hua-Sheng Chen, Bu-Chan Sun, Medical College, Yangzhou University, Yangzhou 225001, Jiangsu Province, China
Xiao-Ren Xiang, Nanjing University of Traditional Chinese Medicine, Nanjing 210029, Jiangsu Province, China
Yun-Fei Chu, The First People Hospital of Yangzhou, Yangzhou 225002, Jiangsu Province, China
Fan Zhai, Ling-Chang Jia, Jiangsu Provincial Subei People Hospital, Yangzhou 225001, Jiangsu Province, China
Supported by the Society Development Foundation of Jiangsu Province, No. BS 2000086
Correspondence to: Ai-Hua Xu, Medical College, Yangzhou University, Yangzhou 225001, Jiangsu Province, China. yzxih@21cn.com
Telephone: +86-514-7310741 **Fax:** +86-514-7341733
Received: 2003-05-13 **Accepted:** 2003-06-02

Abstract

AIM: To study the therapeutic mechanism of Ginkgo biloba exocarp polysaccharides (GBEP) on gastric cancer.

METHODS: Thirty patients with gastric cancer were treated with oral GBEP capsules. The area of tumors was measured by electron gastroscope before and after treatment, then the inhibitory and effective rates were calculated. The ultrastructures of tumor cells were examined by transmissional electron microscope. Cell culture, MTT, flow cytometry were performed to observe proliferation, apoptosis and changes of relevant gene expression of human gastric cancer SGC-7901 cells.

RESULTS: Compared with the statement before treatment, GBEP capsules could reduce the area of tumors, and the effective rate was 73.4 %. Ultrastructural changes of the cells indicated that GBEP could induce apoptosis and differentiation in tumor cells of patients with gastric cancer. GBEP could inhibit the growth of human gastric cancer SGC-7901 cells following 24-72 h treatment *in vitro* at 10-320 mg/L, which was dose- and time-dependent. GBEP was able to elevate the apoptosis rate and expression of c-fos gene, but reduce the expression of c-myc and bcl-2 genes also in a dose-dependent manner.

CONCLUSION: The therapeutic mechanism of GBEP on human gastric cancer may relate to its effects on the expression of c-myc, bcl-2 and c-fos genes, which can inhibit proliferation and induce apoptosis and differentiation of tumor cells.

Xu AH, Chen HS, Sun BC, Xiang XR, Chu YF, Zhai F, Jia LC. Therapeutic mechanism of ginkgo biloba exocarp polysaccharides on gastric cancer. *World J Gastroenterol* 2003; 9(11): 2424-2427
http://www.wjgnet.com/1007-9327/9/2424.asp

INTRODUCTION

Ginkgo biloba exocarp polysaccharide (GBEP) is polysaccharides isolated from ginkgo biloba exocarp. Many studies showed that GBEP was able to inhibit tumors and enhance immune function of tumor bearing mice. Clinical studies showed that GBEP had certain therapeutic effects but few toxic side-effects on patients with tumors, and had good prospects in clinical application[1-4]. This study was to investigate the therapeutic effect and mechanism of GBEP on human gastric cancer.

MATERIALS AND METHODS

Patients

A total of 30 patients with gastric adenocarcinoma (20 males aged from 28 to 81 years old, 10 females aged from 52 to 75 years old) were all ascertained by the pathological examination in Jiangsu Provincial Subei People Hospital or the First People Hospital of Yangzhou, China. Their Karnofsky scores were all above 60. All the patients did not receive any other anti-tumor treatments recently.

Cell line

Human gastric cancer cells (SGC-7901) purchased from Department of Cellular and Molecular Biology, Shanghai Institute of Biochemistry and Cell Biology Academia Sinica, were sub-cultured every 2 or 3 days.

Reagents

GBEP was extracted from exocarp of ripe ginkgo biloba. The content of polysaccharides was higher than 80 %. RPMI 1640 was from GibcoBRL(Maryland, USA). MTT and trypsin (1:250) were from Sigma (ST. Louis, USA). Monoclonal mouse anti-human c-myc and bcl-2 were purchased from Antibody Diagnostica Inc., USA. Monoclonal rabbit anti-human c-fos was from Santa Cruz (Santa Cruz, USA).

Methods

Influence of GBEP on gastric carcinoma patients GBEP capsules are composed of GBEP dry powder and a certain proportion of excipient, and 0.25 g per capsule. Each patient with gastric carcinoma was treated with oral GBEP capsule, 2 pills each time, twice a day, for over 30 d. Changes of tumor size were measured by electron gastroscope. The inhibitory rates (IR) were calculated according to the formula: IR=(tumor area before treatment - tumor area after treatment) ÷ tumor area before treatment×100 %, which is used in the assessment of therapeutic effects. The assessment followed the clinical assessment standards for solid tumors made by WHO, which are classified as complete response (CR), partial response (PR), stable disease (SD) or no change (NC), and progressive disease (PD). The effective rate equals CR plus PR. At the meantime tumor biopsies were obtained for ultrastructural examination by transmissional electron microscope (HV-300). Images captured by transmissional electron microscope were analysed, and the nucleocytoplasmic ratio as well as the surface density of heterochromatin in the tumor cells were calculated before and after treatment.

MTT experiment SGC-7901 cells growing exponentially were digested by 0.25 % trypsin for 1-2 minutes, then washed in Hanks' balanced salt solution (HBSS) for 2 times, and RPMI

1640 containing 10 % new born bovine serum medium was added to adjust the cell density to 1×10^8 cells/L. After addition of the final cell suspensions of 100 μl/well, 96-well plates were put into an incubator containing 5 % CO_2, and incubated at 37 ℃ for 24 hours. Then, 100 μl RPMI 1640 containing different concentrations of GBEP was added to each well. Each concentration had 3 wells, and the control was added with 100 μl RPMI 1640. They were cultured for 24 hours, 48 hours and/or 72 hours. Fresh medium was changed per 24 hours, and GBEP was added. Four hours before the end of culture, 10 μl MTT (the final concentration was 5 g/L) was added, and cultured for 4 hours. Optical density (OD) values for each well were measured at 570 nm with the enzyme linked immunosorbent assay meter[5,6]. The inhibitory rates were calculated according to the formula: IR=[1-(the mean of treated group)/(the mean of control group)]×100 %.

Measurement of cell apoptosis SGC-7901 cells growing exponentially were digested with 0.25 % trypsin for 1-2 minutes. After that, the cells were washed 2 times with PBS buffer (pH 7.2), counted and mixed with RPMI 1640 containing 10 % new born bovine serum to create a final cell density of 2×10^8 cells/L. Four ml final cell suspension was added into each culture bottle, and cultured for 24 h in the condition of 5 % CO_2, at 37 ℃. Then the culture bottles were randomly mixed with different concentrations of GBEP or a positive control drug adriamycin. The negative control group was mixed with an equal volume of RPMI 1640. Then, all the culture bottles were cultured for another 48 h. After that, they were digested and washed. At last they were fixed with alcohol and kept at 4 ℃. The tumor cells were fixed with alcohol and kept in citrate buffer for at least 1 hour after washed in PBS to create a final cell density of 1×10^9 cells/L, they were then centrifuged and mixed with 1 800 μl solution A (trypsinization solution). After 10 minutes, they were mixed with 1 500 μl solution B (RNASE) for 20 minutes, then mixed with 1 500 μl solution C (PI) and filtered by a nylon net after 15 minutes. Finally, the apoptotic rate of the cells was examined.

Analysis of protein content Cell culture was carried out as previously described. The SGC-7901 cells were centrifuged (2 000 ω/minute for 5 minutes) after washed in PBS, mixed with monoclonal mouse anti-human c-myc, or bcl-2, or rabbit anti-human c-fos, and kept at 4 ℃ for 45 minutes. The cells were washed in PBS and mixed with sheep anti-mouse or sheep anti-rabbit IgG and kept at 4 ℃ for another 45 minutes. After washed in PBS and centrifugation, the cells were mixed with 300 μl PBS in sediment and the rate of positive protein for c-myc, bcl-2 and c-fos gene was measured by flow cytometry.

RESULTS

Effect of GBEP capsules on gastric cancer cells

Compared with that before treatment, the tumor area was apparently reduced, which was further proved by electron gastroscopy, and the inhibitory rate of GBEP on tumors was 53.5 %. According to the standards proposed by WHO for the short-term therapeutic effectiveness of solid tumors, there were 2 cases of CR (6.7 %), 20 PR (66.7 %), 5 SD (16.7 %), 3 PD (10 %) in the 30 cases, and the total effective rate was 73.4 %. Images captured by transmissional electron microscope showed that most of the cancer cells had sufficient euchromatins but deficient heterochromatins in the nuclei, the cancer cells had sufficient free ribosomes and deficient glycogens in the cytoplasm before treatment. After treatment with GBEP, most of the cancer cells had sufficient heterochromatins in the nuclei. Some cancer cells became pyknosis. Heterochromatin margination was seen in some of the cancer cells (in the course of apoptosis). Some euchromatins were dissolved, mitochondria were swollen, and rough endoplasmic reticulum was dilated. The results of image analysis showed that nucleocytoplasmic ratio in most of the cancer cells was reduced, surface density of heterochromatin was increased. Influence of GBEP capsules on the tumor area of gastric cancer, on the tumor cells' nucleocytoplasmic ratio and the surface density are shown in Figure 1.

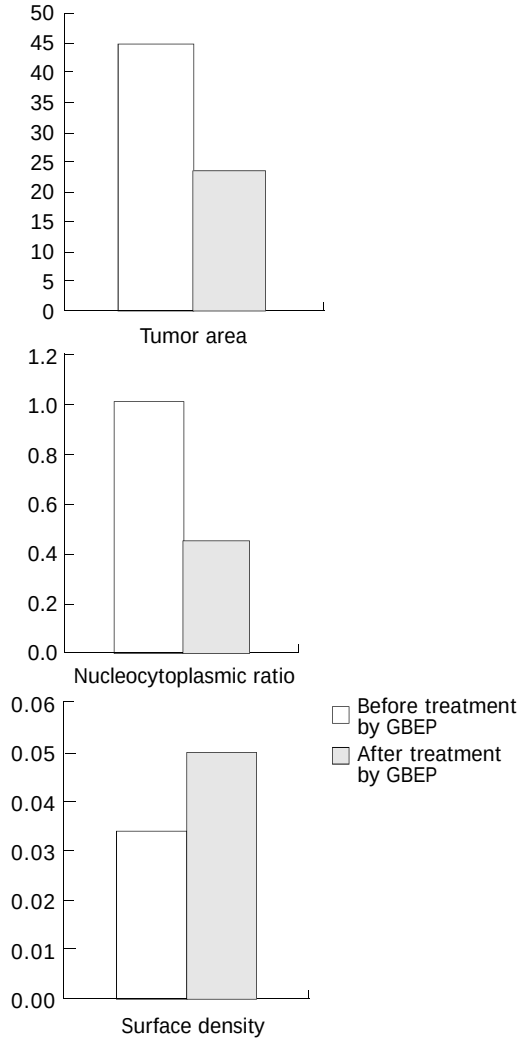

Figure 1 Influence of GBEP capsules on tumor area of gastric cancer, and on tumor cells' nucleocytoplasmic ratio and surface density.

Inhibition of GBEP on human gastric cancer SGC-7901 cells

GBEP could inhibit SGC-7901 cell proliferation following 24-72 hours treatment *in vitro* at 10-320 mg/L. Compared with the control group, the inhibition of SGC-7901 cell proliferation by GBEP was dose- and time-dependent ($P<0.01$) (Figure 2).

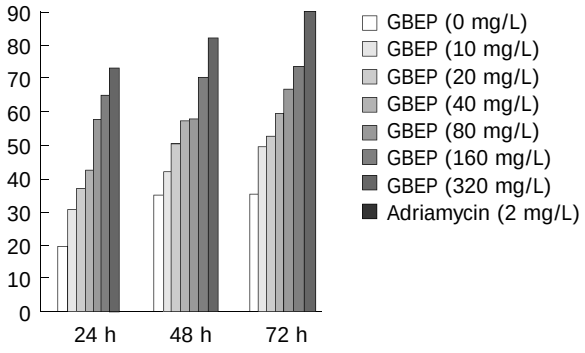

Figure 2 Inhibition of GBEP on human gastric cancer SGC-7901 cell proliferation *in vitro*.

Effects of GBEP on human gastric cancer SGC-7901 cell apoptosis

DNA contents of human gastric cancer SGC-7901 cells were analysed by flow cytometry. The results showed that GBEP could induce apoptosis in SGC-7901 cells at a certain degree (Figure 3).

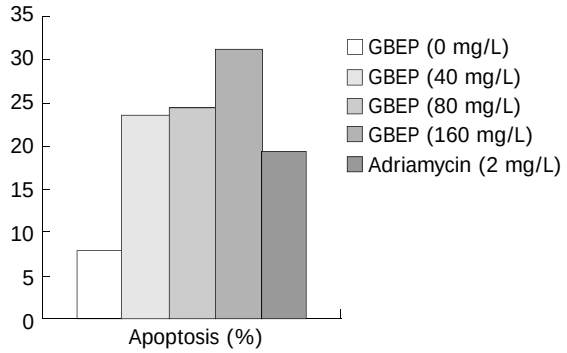

Figure 3 Effects of GBEP on human gastric cancer SGC-7901 cell apoptosis.

Effect of GBEP on expression of c-myc, bcl-2 and c-fos genes in SGC-7901 cells

Protein contents of human gastric cancer SGC-7901 cells were analysed by flow cytometry. The results showed that GBEP could inhibit the expression of c-myc and bcl-2 genes, but enhance the expression of c-fos in SGC-7901 cells (Table 1).

Table 1 Effect of GBEP on expression of c-myc, bcl-2 and c-fos genes in SGC-7901 cells

Group	Dose (mg/L)	Rate of positive protein sign (%)		
		c-myc	bcl-2	c-fos
RPMI 1640	-	22.05	19.35	12.68
GBEP	40	20.33	15.29	17.35
GBEP	80	12.50	11.74	24.96
GBEP	160	7.34	7.17	45.26
Adriamycin	2	9.67	9.31	68.01

DISCUSSION

Gastric cancer is one of the most common malignant tumors in China. Surgical treatment is the main therapy of it. Anti-tumor drugs still play an important role in comprehensive therapy. Now cytotoxic compounds remain the main part of the chemotherapy drugs. The main defects of the cytotoxic compounds are the poor therapeutic effects on solid tumors, higher toxic side-effects and easy occurrence of drug resistance. Many Chinese drugs can enhance the immune function of the body. When used in the treatment, they showed less toxic side-effects but lower inhibitory rate on tumors.

Polysaccharides are big molecules linked by monosaccharides. The sugar-chain of polysaccharides can regulate cell proliferation, differentiation, growth and aging. They showed definite therapeutic effectiveness in anti-tumor therapy, and the ability to enhance body' s immune function, as well as a lower toxic side-effect[7-10]. For example, mushroom polysaccharides have already been used as a drug to regulate the organism reaction in clinical therapy and to prevent tumors in Japan. Umbellate pore fungus polysaccharides which were developed and used in clinical therapy in China, could reduce side-effects of chemotherapy and enhance the effects of chemotherapy against tumors.

We performed this clinical experiment by treating 30 gastric cancer patients with oral GBEP capsules. The images captured by electron gastroscope showed the average inhibitory rate of its capsules on gastric tumor was 53.5 %. The effective rate was 73.4 %. It indicated that GBEP had good clinical therapeutic effectiveness on gastric cancer.

Apoptosis is an active cellular process whereby individual cells are triggered to undergo self-destruction. Recent studies showed apoptosis played a main role in the prevention and treatment of tumors[11-13]. Anti-tumor effect of many chemotherapy drugs could induce apoptosis in tumor cells[14,15]. Cell apoptosis was regulated by genes[16,17]. We have known that apoptosis regulators can be divided into two kinds, namely apoptosis-inducing genes and apoptosis-inhibitory genes. Up-regulation of apoptosis-inducing gene expression could elevate the sensitivity of cells to factors or signals inducing apoptosis, and trigger apoptosis in this way. Up-regulation of apoptosis-inhibitory gene expression could reduce the sensitivity of cells to factors or signals inducing apoptosis, and apoptosis could be inhibited or delayed in this way. Bcl-2 was an important apoptosis-inhibitory gene[18-20], it included a nucleus molecule that can block cell apoptosis, prolong cell lives, accelerate DNA repairing, and thus promoting tumor genesis and development. So it could down-regulate cell apoptosis[21-25]. This clinical study and examination of cellular ultrastructures showed clues of apoptosis induced by GBEP in human gastric cancer cells. Using techniques of cell culture *in vitro* and flow cytometry, the contents of DNA and protein of human gastric cancer SGC-7901 cells were analysed. The results showed GBEP could increase SGC-7901 cell apoptosis rate, down-regulate bcl-2 at concentrations of 40-160 mg/L. It indicated that one of the therapeutic mechanisms of GBEP on gastric cancers might be that it induced tumor cell apoptosis. It also indicated that bcl-2 was involved in this process.

Malignant cells are similar to undifferentiated embryonic cells in morphology, function and metabolism. When tissue changes into malignancy, many phenotypes of the cells go back to the embryonic cell phenotypes, which is called de-differentiation or retro-differentiation. Malignant cells can be induced to differentiate towards normal cells in the presence of differentiation-inducer. Many malignant cells can approach to normal cells, even transform into normal cells completely, which is called re-differentiation or reversion. Change of cells from normal to malignancy is a break of the balance between proliferation and differentiation. Uncontrollable proliferation and de-differentiation are the characteristics of most malignant tumors. Differentiation-inducers can decelerate proliferation, enhance differentiation, thus creating a new normal balance. Like apoptosis, proliferation and differentiation are regulated by genes. C-myc is an important gene involved in the control of cell proliferation, and could up-regulate cell cycle progression, and induce cell proliferation[26-29]. C-fos gene is considered as an early response gene, and its expression level was in proportion to the differentiation degree of gastric cancer[30-32]. This clinical study and results of the cell ultrastructural examination showed clues of apoptosis induced by GBEP in human gastric cancer cells. The results of MTT experiment *in vitro* showed GBEP could inhibit the proliferation of human gastric cancer SGC-7901 cells. The results measured by flow cytometry showed GBEP could down-regulate the expression of c-myc gene and up-regulate the expression of c-fos in SGC-7901 cells at the concentrations of 40-160 mg/L. It indicates that inhibition on cell proliferation and inducement on cell differentiation might be involved in the therapeutic mechanism of GBEP on gastric cancer. C-myc and c-fos genes might contribute to the regulation of proliferation and differentiation.

ACKNOWLEDGMENTS

We are very grateful to Drs. Huo-Ying Shi, Li-Ming Yuan

and Wei-Dong Zhou, Center of Electroscope, Yangzhou University, and Mei-Zao Le, Department of Pathology, Bayi Hospital, Nanjing, China for their technical assistance in ultrastructural analysis; Drs. Zhi-Jiang Wu, Lü-Rong Men, Department of Cellular and Molecular Biology, Shanghai Institute of Biochemistry and Cell Biology, Academica Sinica for their technical assistance in flow cytometry.

REFERENCES

1 **Xu AH,** Chen HS, Xiang XR, Gu WR, Zhang HQ. The suppressive effects of ginkgo biloba exocarp polysaccharides (GBEP) on tumor in mice. *Zhongyao Iaoli yu Linchuang* 1996; **12**: 24-26
2 **Chen HS**, Xu AH, Wang Y, Wang Q, Wang XL. Influence of ginkgo biloba exocarp polysaccharides (GBEP) on interleukin-2 (IL-2) activity and solubility interleukin-2 receptor (sIL-2R) level in mice under lower immune function. *Zhongyao Yaoli yu Linchuang* 2001; **17:** 17-19
3 **Zhai F,** Chen HS. Clinical observation on effects of ginkgo biloba exocarp polysaccharides (GBEP) in Treatment of 84 Cases in cancer of middle-late stage. *Liaoning Zhongyi Zazhi* 2002; **29:** 564
4 **Xu A,** Chen H, Wang L, Wang Q. Influence of Ginkgo biloba L. exocarp polysaccharides on serum superoxide dismutase activity and malondialdehyde level in mice under different states. *Zhongguo Zhongyao Zazhi* 1998; **23:** 746-747
5 **Mosmann T.** Rapid colorimetric assay for cellular growth and survival: appli- cation to proliferation and cytotoxicity assays. *J Immunol Methods* 1983; **65:** 55-63
6 **Wu Q,** Chen Z, Su W. Mechanism of inhibition on activator protein-1 activity by all-trans retinoic acid in gastric cancer cells. *Chin Med J* 2000; **113:** 972-976
7 **Liu C,** Gao P, Qian J, Yan W. Immunological study on the antitumor effects of fungus polysaccharides compounds. *Wei Sheng Yan Jiu* 2000; **29:** 178-180
8 **Wang Z,** Wang Y, Huang Z, Zhong S, Wu Y, Yu L. Study on antitumor effect and mechanism of aloe polysaccharides. *Zhong Yao Cai* 2001; **24:** 350-353
9 **Kodama N,** Komuta K, Sakai N, Nanba H. Effects of D-Fraction, a polysaccharide from Grifola frondosa on tumor growth involve activation of NK cells. *Biol Pharm Bull* 2002; **25:** 1647-1650
10 **Lu X,** Su M, Li Y, Zeng L, Liu X, Li J, Zheng B, Wang S. Effect of Acanthopanax giraldii Harms Var. Hispidus Hoo polysaccharides on the human gastric cancer cell line SGC-7901 and its possible mechanism. *Chin Med J* 2002; **115:** 716-721
11 **Yan J,** Xu YH. Tributyrin inhibits human gastric cancer SGC-7901 cell growth by inducing apoptosis and DNA synthesis arrest. *World J Gastroenterol* 2003; **9:** 660-664
12 **Su M,** Dai M, Lu X, Li H, Liu J. Effect of traditional Chinese medicine compounds aining on the expression of apoptosis inducing genes of human gastric cancer cell. *Zhong Yao Cai* 2002; **25:** 563-566
13 **Gao F,** Yi J, Shi GY, Li H, Shi XG, Tang XM. The sensitivity of digestive tract tumor cells to As2O3 is associated with the inherent cellular level of reactive oxygen species. *World J Gastroenterol* 2002; **8:** 36-39
14 **Kimura H,** Konishi K, Kaji M, Maeda K, Yabushita K, Tsuji M, Ogino H, Satomura Y, Unoura M, Miwa A. Apoptosis, cell proliferation and expression of oncogenes in gastric carcinomas induced by preoperative administration of 5-fluorouracil. *Oncol Rep* 2000; **7:** 971-976
15 **Sugamura K,** Makino M, Shirai H, Kimura O, Maeta M, Itoh H, Kaibara N. Enhanced induction of apoptosis of human gastric carcinoma cells after preoperative treatment with 5-fluorouracil. *Cancer* 1997; **79:** 12-17
16 **Masutani M,** Suzuki J, Matsuda T, Dochin A, Sadaoka K, Nomura A, Ohira K, Takahashi K, Yamazaki K, Dosaka-Akita H, Nishimura M, Kawakami Y. Increased apoptosis associated with depressed type of early intestinal gastric cancer. *Jpn J Cancer Res* 2001; **92:** 1214-1219
17 **Zhao AG,** Zhao HL, Jin XJ, Yang JK, Tang LD. Effects of Chinese jianpi herbs on cell apoptosis and related gene expression in human gastric cancer grafted onto nude mice. *World J Gastroenterol* 2002; **8:** 792-796
18 **Cao J,** Qiao Y, Min J. Bcl-2 anti-sense oligonucleotide sensitizes Fas-mediated apoptosis of gastric cancer cells. *Zhonghua Zhongliu Zazhi* 2000; **22:** 466-468
19 **Zhou HB,** Zhu JR. Paclitaxel induces apoptosis in human gastric carcinoma cells. *World J Gastroenterol* 2003; **9:** 442-445
20 **Wu YL,** Sun B, Zhang XJ, Wang SN, He HY, Qiao MM, Zhong J, Xu JY. Growth inhibition and apoptosis induction of Sulindac on Human gastric cancer cells. *World J Gastroenterol* 2001; **7:** 796-800
21 **Hofler H,** Becker KF. Molecular mechanisms of carcinogenesis in gastric cancer. *Recent Results Cancer Res* 2003; **162:** 65-72
22 **Dixon D,** Flake GP, Moore AB, He H, Haseman JK, Risinger JI, Lancaster JM, Berchuck A, Barrett JC, Robboy SJ. Cell proliferation and apoptosis in human uterine leiomyomas and myometria. *Virchows Arch* 2002; **441:** 53-62
23 **Wang NS,** Unkila MT, Reineks EZ, Distelhorst CW. Transient expression of wild-type or mitochondrially targeted Bcl-2 induces apoptosis, whereas transient expression of endoplasmic eticulum-targeted Bcl-2 is protective against Bax-induced cell death. *Biol Chem* 2001; **276:** 44117-44128
24 **Li JQ,** Chen RC, Cai KX, Ye ZY. Apoptosis of human gastric cancer cell induced by photochemical riboflavin. *Ai Zheng* 2003; **22:** 253-256
25 **Liu S,** Wu Q, Ye XF, Cai JH, Huang ZW, Su WJ. Induction of apoptosis by TPA and VP-16 is through translocation of TR3. *World J Gastroenterol* 2002; **8:** 446-450
26 **Chen JP,** Lin C, Xu CP, Zhang XY, Fu M, Deng YP, Wei Y, Wu M. Molecular therapy with recombinant antisense c-myc adenovirus for human gastric carcinoma cells *in vitro* and *in vivo*. *J Gastroenterol Hepatol* 2001; **16:** 22-28
27 **Liu HL,** Lo CR, Jones BE, Pradhan Z, Srinivasan A, Valentino KL, Stockert RJ, Czaja MJ. Inhibition of c-Myc expression sensitizes hepatocytes to tumor necrosis factor-induced apoptosis and Necrosis. *Biol Chem* 2000; **275:** 40155-40162
28 **Zhu GH,** Wong BC, Eggo MC, Ching CK, Yuen ST, Chan EY, Lai KC, Lam SK. Non-steroidal anti-inflammatory drug-induced apoptosis in gastric cancer cells is blocked by protein kinase C activation through inhibition of c-myc. *Br J Cancer* 1999; **79:** 393-400
29 **Ishii HH,** Gobe GC, Pan W, Yoneyama J, Ebihara Y. Apoptosis and cell proliferation in the development of gastric carcinomas: associations with c-myc and p53 protein expression. *J Gastroenterol Hepatol* 2002; **17:** 966-972
30 **Tsuji M,** Funahashi S, Takigawa M, Seiki M, Fujii K, Yoshida T. Expression of c-fos gene inhibits proteoglycan synthesis in transfected chondrocyte. *FEBS Lett* 1996; **381:** 222-226
31 **Ito N,** Hirose M, Takahashi S. Cell proliferation and forestomach carcinogenesis. *Environ Health Perspect* 1993; **101**(Suppl 5): 107-110
32 **Kane S**, Prentice MA, Mariano JM, Cuttitta F, Jakowlew SB. Differential induction of early response genes by adrenomedullin and transforming growth factor-beta1 in human lung cancer cells. *Anticancer Res* 2002; **22:** 1433-1444

Edited by Zhang JZ and Wang XL

P.O.Box 2345, Beijing 100023,China
Fax: +86-10-85381893
E-mail: wjg@wjgnet.com www.wjgnet.com

World J Gastroenterol 2003;9(11):2428-2432
World Journal of Gastroenterology
 ISSN 1007-9327

• LIVER CANCER •

Segregation analysis of hepatocellular carcinoma in a moderately high-incidence area of East China

Ru-Lin Cai, Wei Meng, Hong-Yan Lu, Wen-Yao Lin, Feng Jiang, Fu-Min Shen

Ru-Lin Cai, Wei Meng, Feng Jiang, Fu-Min Shen, Department of Epidemiology, School of Public Health, Fudan University, Shanghai 200032, China
Hong-Yan Lu, Wen-Yao Lin, Haimen City Anti-epidemic Station, Haimen 226100, Jiangsu Province, China
Supported by the National Natural Science Foundation of China, No. 39930160
Correspondence to: Dr. Wei Meng, Department of Epidemiology, School of Public Health, Fudan University, Shanghai 200032, China. wmeng@shmu.edu.cn
Telephone: +86-21-54237767 or 7710
Received: 2002-12-28 **Accepted:** 2003-02-19

Abstract

AIM: To explore the mode of inheritance of hepatocellular carcinoma (HCC) in a moderately high-incidence area of East China.

METHODS: A pedigree survey was conducted in 210 families (3315 individuals) ascertained through 210 HCC probands in Haimen, Jiangsu Province. Simple segregation analysis was conducted using SEGRANB software. The probability of ascertainment (p), segregation ratio (p), and the proportion of sporadic cases (x) were estimated. Complex segregation analysis was performed using the REGTL program of S.A.G.E. Models were fitted on the data of 3212 individuals that allowed for personal HBsAg status and variable age of onset in REGTL program.

RESULTS: The estimate of segregation ratio was 0.191 by SEGRANB. The probability of ascertainment was 0.0266, and the proportion of sporadic cases was 0.465. The results of complex segregation analysis showed that Mendelian autosomal recessive inheritance of a major gene that influenced the age of onset distribution of HCC, provided the best fit to the data. In the best-fitting recessive model, the frequency of the disease allele was 0.11138. HBsAg seropositive status would significantly increase the risk of developing HCC.

CONCLUSION: These results suggest that at least one major gene is involved in the genetic predisposition to develop HCC at an earlier age of onset. The seropositive HBsAg status can significantly increase the risk of developing HCC, which provides strong support for the interaction between genetic and environmental risk factors.

Cai RL, Meng W, Lu HY, Lin WY, Jiang F, Shen FM. Segregation analysis of hepatocellular carcinoma in a moderately high-incidence area of East China. *World J Gastroenterol* 2003; 9 (11): 2428-2432
http://www.wjgnet.com/1007-9327/9/2428.asp

INTRODUCTION

Hepatocellular carcinoma (HCC) is one of the most common types of malignant tumor in the world, the estimated number of new cases worldwide annually is over 500 000[1], ranking third in cause of cancer deaths in China. An estimated 26 000 deaths are from HCC annually worldwide, among which about 40 % are in China[2]. Classical epidemiological studies have shown that certain risk factors are associated with HCC, though the odds ratios (ORs) vary considerably from study to study[3-5]. On a worldwide basis, chronic infection with hepatitis B virus (HBV) appears to be the most important risk factor for HCC. About 80 % of the patients of HCC in China are seropositive for hepatitis B surface antigen (HBsAg)[6]. An IARC working group in 1993 found that the evidence for a causal association of HBV with HCC was pretty strong. HCC is common in cirrhotic patients when cirrhosis is secondary to chronic viral hepatitis[1]. In addition to viral factors, environmental exposures and genetic susceptibility are clearly involved. Dietary aflatoxin exposure is an important codeterminant of HCC risk in Africa and parts of Asia[7]. Aflatoxins together with chronic hepatitis B virus (HBV) infection contribute to the high incidence of hepatocellular carcinoma in developing countries[8-10]. Contaminated drinking water and chemical carcinogens are also associated with the development of HCC[3].

Many familial clusterings of HCC have been reported[11,12]. The prevalence of HCC among the first-degree relatives is significantly higher than that among the second-degree and third-degree relatives, which suggests that genetic mechanisms may be responsible for familial HCC. Haimen city is a HCC high-incidence area of East China, however, only a few studies have been performed to explore the genetic mode of HCC in this area. Consequently, in this study, data of 210 pedigrees ascertained through HCC probands were collected and segregation analysis of HCC was performed.

MATERIALS AND METHODS

Materials and data collection

Probands were 210 HCC patients from an eight-year follow-up of a 90 000-person Haimen City cohort. All the patients were pathologically diagnosed in hospitals of counties and cities. Information on four-generation pedigrees was obtained for 210 families. Data on 3 315 individuals in the 210 families were collected primarily by face-to-face interviews or by checking the medical records and according to the recall of their relatives if the proband patients were dead. Data on 3 212 individuals (97 %) were used to fit models in the REGTL program of S.A.G.E. The remaining individuals were excluded because of little information available.

Family history interview and data management

A family history of HCC was collected as part of an interview to gather information on the medical history of probands and their relatives. The questionnaire included questions on age, occupation, tobacco use, drinking water source by decades (60 s, 70 s, 80 s, 90 s), staple food consumption by decades, result of HBsAg test, history of chronic hepatitis B, history of other chronic diseases, family history of HCC and relationship of family member with HCC to proband cases.

All the questionnaires were reviewed and checked for quality control. Pedigree information database was developed using Epi-Info v5.0.

Statistical methods

Simple segregation analysis by SEGRANB program In SEGRANB, models were fitted to the data and maximum likelihood scores of parameters were estimated. Hypothesis tests were performed to determine which set of parameter was most consistent with the observed data. The involved parameters were probability of ascertainment (p) (the probability for a patient to be identified as a proband), segregation ratio (p), and the proportion of sporadic cases (x). S is the sibship size, r is the total number of the affected siblings and a is the total number of the probands. The function for the probability of ascertainment is:

$$P(a \mid a>0;\ r, \pi) = \frac{\binom{r}{a} p^{a}(1-p)^{r-a}}{\left[1-(1-p)^{r}\right]}$$

The function for the estimate of the segregation ratio in the pedigrees with more than one patient is:

$$P(r>1) = \frac{\binom{s}{r} p^{r} q^{s-r}\left[1-(1-p)^{r}\right]}{1-(1-pp)^{s}-psq^{s-1}}$$

The functions for estimate of p and x are:

$$P(r=1) = \frac{spp\left[x+(1+x)\ q^{s-1}\right]}{xspp+(1+x)\left[1-(1-pp)^{s}\right]}$$

$$P(r>1) = \frac{(1-x)\binom{s}{r} p^{r}(1-p)^{s-r}\left[1-(1-p)^{r}\right]}{sppx+(1-x)\left[1-(1-pp)^{s}\right]}$$

U_{π},U_{p}, and U_{x} are the maximum likelihood scores for p, p and x, respectively. If the value of U was negative, the initial estimated value of the parameter should be reduced to fit the observed data, and vice versa.

Complex segregation analysis using REGTL program of S.A.G.E. (Statistical analysis for genetic epidemiology, v3.1. Case Western Reserve University, Cleveland, OH) The REGTL program of S.A.G.E. (1997) (release 3.1) under a Window' s 9x operating system was used to perform complex segregation analysis. This program uses maximum-likelihood methods to estimate parameters of mathematical models of disease occurrence in families. It assumes that under a class A regressive model, a censored trait, such as age of onset to a disease or of the disease susceptibilities, follows a logistic distribution. Sibs are dependent on one another only because of common parentage. Mendelian inheritance, if present, is presumed to be through a single autosomal locus with two alleles, A and B, A being associated with the affected state. The "type" was used to describe the discrete factors that affect a person' s phenotype. The same concept was denoted as "ousiotype". Genotypes are the special case of types, or ousiotypes, that transmit to offspring in Mendelian fashion. Thus we should use the term "type" to allow for any kind of discrete transmission, whether Mendelian or not. Two general models can be assumed. In model 1, the segregation of a possible major locus is allowed for by letting the baseline and age coefficient parameters of the age of onset distribution, but not the susceptibility, depends on an unobserved qualitative factor u=AA, AB, BB. Susceptibility depends solely on randomly distributed environmental characteristics of the population studied. In model 2, type is presumed to influence susceptibility to the affected state, but not the parameters of the age-at-onset distribution, and groups of individuals of different types have the same mean age at onset. Analysis was performed under the model 1 in this study. HCC was represented by a dichotomous variable y, in which y=1 for affected and 0 for unaffected. The following parameters were estimated: type frequencies Ψ_{u} (u=AA, AB, BB. If the type frequencies are in Hardy-Weinberg equilibrium proportions, then they are defined in terms of q_{A}=frequency of allele A), transmission probabilities τ_{u} (the probability that a parent of type u transmits allele A to an offspring, under Mendelian transmission, τ_{AA}=1, τ_{AB}=0.5, τ_{BB}=0), baseline parameter β which can be sex-dependent and/or type-dependent, covariate coefficient ζ_{HbsAg} which is coded 1 if the individual is HBsAg positive and is coded 0 if negative or 9 if unknown. Thus, the coefficient ζ_{HBsAg} is the change in the logit (the risk of HCC) according to the HBsAg status, age adjustment coefficient α, and susceptibility parameter γ which can be sex-dependent. Susceptibility is the probability that an individual is susceptible.

To correct for ascertainment bias, the likelihood of each pedigree is conditioned on the proband' s HCC status by age at exam or death and his or her actual age of onset. This assumes single ascertainment, which is a reasonable approximation since only 1 (0.5 %) of 210 families has more than one patient eligible to be a proband. Under single ascertainment, the probability that any one family will be ascertained is small and proportional to the number of affected children in the family.

As the process of parameter estimate is complex and time consuming when complex models are fitted, a program written in Perl program was used to facilitate the estimate of the initial value of parameters. This program was used to generate random values for the initial estimate of parameters and to call modules in the REGTL program of the S.A.G.E. package to perform segregation analysis. For each model, thirty converged results were saved, among which the best-fitted result of each model was chosen.

Under the model 1, six hypotheses were tested against the likelihood of a general (unrestricted) model, in which all parameters were unrestricted and allowed to fit the empirical data. Thus this general model would give the best fit to the data. The six hypotheses of transmission are as follows: major gene type, Mendelian dominant, Mendelian recessive, Mendelian additive, purely environmental effect and no transmission. Twice the differences between the natural log likelihood (InL) for the data under the hypothesis of interest and that under the unrestricted model is in accordance with χ^{2} distribution, thus it is used to assess the degree of departure from expectation statistically. The degree of freedom (df) for the χ^{2} statistic is given by the differences in the number of estimated parameters between the hypothesis and the unrestricted model. If one or more parameters are fixed at a bound at the end of the estimation process, a range of the df and P values are given when appropriate. A non-significant χ^{2} indicates that the hypothetical model cannot be rejected. When covariates and major gene effects are considered simultaneously, the number of potential hypothesis tests is large and the natural hierarchy of the models may not be clear. In this case, models can also be compared with use of Akaike' s (1974) information criterion (AIC), which is defined as AIC= -2lnL+2×(Number of parameters estimated). A lower value of AIC represents a better fitting model.

RESULTS

Distribution of HCC and HBsAg status among relatives

Of 3 315 individuals in the 210 extended pedigrees, 330 (10.0 %)

including probands were affected with HCC. The distribution of HCC and HBsAg status among the relatives is summarized in Table 1. Among the first-degree relatives, the prevalence of HCC was 6.6 % (100/1511). Among the second-degree relatives, it was 2.1 % (20/945). The prevalence of HCC was 23.1 % (30/130) among the HBsAg positive first-degree relatives, it was 19.2 (5/26) among the HBsAg positive second-degree relative. As shown in Table 2, among the fathers of the probands, the

Table 1 HBsAg status of HCC cases among first-degree and second-degree relatives

HBsAg status	First-degree relatives		Second-degree relatives	
	No. of relatives	No. (%) of HCC	No. of relatives	No. (%) of HCC
+	130	30 (23.1 %)	26	5 (19.2 %)
-	1104	47 (4.3 %)	711	4 (0.6 %)
Unknown	277	23 (8.3 %)	208	11 (5.3 %)
Total	1511	100 (6.6 %)	945	20 (2.1 %)

Table 2 Distribution of HCC among the relatives of 210 probands

Characteristic	Relatives						
	Father	Mother	Brother	Sister	Son	Daughter	Spouse
No. (%) of HCC	11 (5.5 %)	14 (7.0 %)	59 (16.1 %)	15 (5.0 %)	1 (0.5 %)	0 (0 %)	2 (1.0 %)
Total	200	199	366	298	221	227	202

Table 3 Distribution of probands and affected siblings among families

Number of affected siblings	1	2	3	4	4	5
Number of probands in family	1	1	1	1	2	1
Number of families	162	32	7	7	1	1

Table 4 Maximum likelihood estimates of parameters of segregation models for HCC by SEGRANB

π	p	x	U_π	U_p	U_x	χ^2_π	χ^2_p	χ^2_x	$\bar{\pi}$	$\bar{p}$	$\bar{x}$	P value
0.026 556	0.50	0.00	116.922	-929.338	2482.747	1 069.75	1 074.303	1 712.618	9.176	-0.655 98	0.689 81	<0.05
0.026 556	0.25	0.00	50.272	-530.853	230.405	134.657	134.794	144.777	2.705	-0.003 92	0.628 36	<0.05
0.026 556	0.20	0.60	-7.363	50.253	-34.966	4.140	4.069	4.090	-0.536	0.280 97	0.483 03	<0.05
0.026 556	0.280 97	0.483	8.856	-41.824	36.699	3.566	3.806	3.817	0.429	0.189 96	0.587 05	<0.05
0.026 556	0.189 96	0.483	-0.055	0.200	0.464	0.097	0.098	0.09	-0.055	0.200 11	0.463 91	>0.05
0.026 556	0.189 96	0.464	-0.054	0.559	0.007	1.976E-04	3.118E-04	2.146E-07	0.029	0.190 52	0.463 94	>0.05
0.026 556	0.190 52	0.464	0.013	-0.003	0.276	1.097E-05	8.709E-09	3.252E-04	0.027	0.190 52	0.465 08	>0.05
0.026 6	0.190 52	0.465	-0.054	0.529	0.016	1.909E-04	2.822E-04	1.064E-06	0.030	0.191 06	0.465 07	>0.05
0.026 6	0.191	0.465	0.005	0.059	0.244	1.517E-06	3.486E-06	2.505E-04	0.027	0.191 06	0.466 03	>0.05

π, p and x: initially estimated values for π, p and x, respectively. U_π, U_p and U_x: maximum likelihood scores for π, p and x, respectively. χ^2_π, χ^2_p and χ^2_x: χ^2 of the estimated π, p and x, respectively. $\bar{\pi}$, $\bar{p}$, and $\bar{x}$: corrected value for π, p and x, respectively.

Table 5 Complex segregation analysis on HCC among the 210 extended pedigrees (SAGE-REGTL, model 1)

Parameter[a]	Hypothesis						
	Mendelian						
	Dominant	Recessive	Additive	Major gene	Environmental	No transmission	General
qA	0.003 04	0.111 38	0.114 51	0.879 64	0.022 29	0[b]	0.008 61
τAA	1.0[b]	1.0[b]	1.0[b]	1.0[b]	1.0[c]	0[b]	1.0[c]
τAB	0.5[b]	0.5[b]	0.5[b]	0.5[b]	1.0[c]	0[b]	0.0[c]
τBB	0[b]	0[b]	0[b]	0[b]	1.0[c]	0[b]	1.0[c]
βAA	-5.748 96	-6.862 19	-7.300 81	-13.664 08	-7.274 45	-6.744 03	-9.222 95
βAB	-5.748 96[d]	-14.229 74	-14.452 92	-22.641 40	-4.142 30	-6.744 03[d]	-6.194 60
βBB	-11.625 77	-14.229 74[d]	-21.605 02	-6.835 46	-9.940 49	-6.744 03[d]	-20.472 73
α	0.100 39	0.123 35	0.128 67	0.123 85	0.074 99	0.057 10	0.084 64
γ	0.721 25	1.000[c]	0.869 15	1.000[c]	0.899 22	1.000[c]	1.000[c]
ζHBsAg	0.931 55	1.363 80	1.840 08	1.202 00	2.723 39	2.708 74	1.475 35
-2lnL	831.079 18	799.687 16	805.170 10	798.206 61	822.204 67	842.795 94	803.246 35
AIC	843.079 18	811.687 16	817.170 10	812.206 61	838.204 67	850.795 94	825.246 35
χ^2	27.832 83	3.559 19	1.923 75	5.039 74	18.958 32	39.549 59	-
df[e]	1-5	2-5	1-5	1-4	2-3	4-7	-
P value	P<0.001	P>0.1	P>0.1	0.01<P<0.03	P<0.001	P<0.001	-

a: See Materials and Methods for definitions of the parameters. b: Parameter was fixed at this value and estimation was not carried out. c: Parameter estimate reached its bound. d: Parameter was constrained to equal the preceding one and was not estimated. e: Range in degrees of freedom was given since parameters in models reached their bounds.

prevalence of HCC was 5.5 % (11/200). Among siblings, it was 11.1 % (74/664) (16.1 % for brothers, 5.0 % for sisters). Among offsprings, it was 0.2 % (1/448), and among spouses of the probands, it was 1.0 % (2/202).

Parameter estimate in simple segregation analysis by SEGRANB software

The distribution of probands and their affected siblings among the 210 families is shown in Table 3. There was one family with two patients eligible to be a proband. The best fitted probability of ascertainment p was 0.026556, U_p was 6.500244×10^{-3}, χ^2 was 2.848217×10^{-8}. The estimated sets of parameters are shown in Table 4. The best fitted probability of ascertainment p was 0.0266, the segregation ratio p was 0.191, and the proportion of sporadic cases x was 0.465.

Results of complex segregation analysis by REGTL program of S.A.G.E.

Of the 210 families, 48 (22.9 %) had two or more HCC patients. The mean age at onset was 50 (range 21-83). Complex segregation analyses were performed by REGTL under model 1 that did not include regressive familial effects in the models and in which age at onset and susceptibility were not sex-dependent. One environmental covariate, HBsAg status, as a dichotomous variable was included in the models.

In Table 5, the best fitted parameter estimates for general and hypothetical models were reported. As a result, the Mendelian recessive and additive (codominant) hypotheses were not rejected (P>0.1) and the major gene model was marginally not rejected (0.01<P<0.03). All other models were rejected at a 0.001 significance level. According to AIC, Mendelian recessive inheritance was the best-fitted hypothesis, but the AICs for recessive (811.68716) and major gene (812.20661) models were very close. The recessive model suggested that approximately 11.1 % of the population could be expected to carry the candidate gene (or gene pattern). The coefficient of the covariate HBsAg was positive. If its standard deviation is to do the Wald' s test, we got $|\beta_{HBsAg}|/|S_{HBsAg}|=1.36380/0.40661=3.354>1.96$, P<0.05, which suggested that HBsAg seropositive status would increase the risk of developing HCC.

DISCUSSION

In this study, we explored the inheritance mode of HCC in the 210 extended pedigrees in Haimen City by simple and complex segregation analyses. This study used SEGRANB software and REGTL program of S.A.G.E. analyzing a population-based family data set to investigate the presence of a major gene effect for HCC. In simple segregation analysis procedure, as the estimate of segregation ratio p could be substantially affected by the estimated value of the probability of ascertainment p [13,14], especially on complex traits, therefore p was calculated using maximum likelihood method by SEGRANB program in this study. The estimated value of p was 0.0266, which suggested a single ascertainment for this study. Then the segregation ratio and the proportion of sporadic cases were also estimated by maximum likelihood method using SEGRANB. The best-fitted parameter set is shown in Table 4. The segregation ratio was 0.191 and the proportion of sporadic cases was 0.465 for this data, which suggested that HCC did not follow a mono-gene inheritance pattern in this population and environmental factors appeared to influence the development of HCC since 46.5 % of the cases were sporadic.

Due to the modest sample size and relatively high proportion of missed information for the elder generations of the probands in the studied pedigrees, gender and familial residual effects were not estimated simultaneously with other parameters of the corresponding models in complex segregation analysis. The results showed that although both the recessive and additive (codominant) hypotheses could not be rejected, Mendelian autosomal recessive inheritance of a major gene that influenced baseline and age of onset of HCC provided the best fit to the data. The estimated gene frequency under the recessive hypothesis was 0.11138. The result in this study was consistent with the result of an earlier complex segregation analysis by Shen *et al*. (1991) using the POINTER program in which an autosomal recessive major gene yielding lifetime risk of PHC (primary hepatocellular carcinoma) was suggested. In this study, the information of serum HBsAg status for relatives was obtained through the questionnaire and sometimes the report of laboratory test was unavailable. Although this situation could cause miss of information for many individuals in analysis, which might ruin the statistical power, the significance of seropositive HBsAg effect could still be observed. It strongly suggested that chronic HBV infection was a risk factor in developing HCC in this population.

The ultimate test of the utility of segregation analysis is whether the resulting models can be used in linkage analysis to identify disease-susceptibility loci. Although the recessive hypothesis provided the best fit to the data, segregation analysis had its limitation that it could not distinguish the effect of a single locus that underlied a trait from the effects of two or more independently acting loci with similar transmission patterns[15]. Thus, more than one gene, with different penetrances and modes of inheritance, may be involved. Even under oligogenic inheritance, the parameters derived from a single locus segregation analysis can provide power for detecting the susceptibility loci. Many studies have been performed to search for susceptibility genes for HCC[16-29], and several novel genes have been suggested to play a role in HCC development[30-32]. The HCC mortality differs in different areas in China and there are some environmental factors (e.g. local economic status, geographical factors, habit of food consumption and viral infection) that might differ in different areas. With the same environmental exposures, HCC occurrence differs a great deal from family to family, which is typified by the existence of highly aggregated "cancer families". It is hard to say which factor (environmental or genetic) is more important. All can play important roles in the etiology of HCC. The mutation of HCC gene (s) may act as a trigger for HCC onset, or people with the gene (s) may tend to be more susceptible to HCC under the influence of certain environmental risk factors.

In conclusion, our study showed that a Mendelian autosomal recessive major gene might play an important role in the etiology of HCC in a moderately high-incidence area of East China. This study provides some modeling parameters of HCC (in this area) for further linkage studies. The identification of the putative gene detected by the study is warranted.

ACKNOWLEDGEMENTS

This work was supported in part by the National Natural Science Foundation of China (No: 39930160). Some of the results in this paper were obtained by using the program package S.A.G.E., which was supported by a U.S. Public Health Service Resource Grant (1 P41 RR03655) from the National Center for Research Resources. Prof. Fu-Min Shen donated the version of the program package S.A.G.E. used in this study. We thank Dr. Yin Hu of the NCI Center for Bio-informatics for his help on compiling Perl script and on tackling some technical problems.

REFERENCES

1 **Montalto G,** Cervello M, Giannitrapani L, Dantona F, Terranova A, Castagnetta LA. Epidemiology, risk factors, and natural history of hepatocellular carcinoma. *Ann N Y Acad Sci* 2002; **963**: 13-20

2 **Zhao ZT,** Jia CX. Epidemiology of liver cancer. In: Liu Q, Wang WQ, eds. Cancer. *Beijing: People's Health Press* 2000: 221-239

3 **Evans AA,** Chen G, Ross EA, Shen FM, Lin WY, London WT. Eight-year follow-up of the 90000-person Haimen City cohort: I. Hepatocellular carcinoma mortality, risk factors, and gender differences. *Cancer Epidemiol Biomarkers Prev 2002*; **11**: 369-376

4 **Yoshizawa H.** Hepatocellular carcinoma associated with hepatitis C virus infection in Japan: projection to other countries in the foreseeable future. *Oncology* 2002; **62**(Suppl 1): 8-17

5 **Donato MF,** Arosio E, Del Ninno E, Ronchi G, Lampertico P, Morabito A, Balestrieri MR, Colombo M. High rates of hepatocellular carcinoma in cirrhotic patients with high liver cell proliferative activity. *Hepatology* 2001; **34**: 523-528

6 **Wang YL,** Zhou HG, Gu GW. Advances in liver cancer research. *Shanghai: Shanghai Science and Technology Literature Press* 1999: 13-27

7 **Ming L,** Thorgeirsson SS, Gail MH, Lu P, Harris CC, Wang N, Shao Y, Wu Z, Liu G, Wang X, Sun Z. Dominant role of hepatitis B virus and cofactor role of aflatoxin in hepatocarcinogenesis in Qidong, China. *Hepatology* 2002; **36**: 1214-1220

8 **Wild CP,** Yin F, Turner PC, Chemin I, Chapot B, Mendy M, Whittle H, Kirk GD, Hall AJ. Environmental and genetic determinants of aflatoxin-albumin adducts in the Gambia. *Int J Cancer* 2000; **86**: 1-7

9 **Chen SY,** Chen CJ, Tsai WY, Ahsan H, Liu TY, Lin JT, Santella RM. Associations of plasma aflatoxin B1-albumin adduct level with plasma selenium level and genetic polymorphisms of glutathione S-transferase M1 and T1. *Nutr Cancer* 2000; **38**: 179-185

10 **Wang JS,** Huang T, Su J, Liang F, Wei Z, Liang Y, Luo H, Kuang SY, Qian GS, Sun G, He X, Kensler TW, Groopman JD. Hepatocellular carcinoma and aflatoxin exposure in Zhuqing Village, Fusui County, People's Republic of China. *Cancer Epidemiol Biomarkers Prev* 2001; **10**: 143-146

11 **Tai DI,** Changchien CS, Hung CS, Chen CJ. Replication of hepatitis B virus in first-degree relatives of patients with hepatocellular carcinoma. *Am J Trop Med Hyg* 1999; **61**: 716-719

12 **Yu MW,** Chang HC, Liaw YF, Lin SM, Lee SD, Liu CJ, Chen PJ, Hsiao TJ, Lee PH, Chen CJ. Familial risk of hepatocellular carcinoma among chronic hepatitis B carriers and their relatives. *J National Cancer Institute* 2000; **92**: 1159-1164

13 **Tai JJ,** Hsiao CK. Effects of implicit parameters in segregation analysis. *Hum Hered* 2001; **51**: 192-198

14 **Haghighi F,** Hodge SE. Likelihood formulation of parent-of–origin effects on segregation analysis, including ascertainment. *Am J Hum Genet* 2002; **70**: 142-156

15 **Jarvik GP.** Complex segregation analyses: Uses and limitations. *Am J Hum Genet* 1998; **63**: 942-946

16 **Tufan NL,** Lian Z, Liu J, Pan J, Arbuthnot P, Kew M, Clayton MM, Zhu M, Feitelson MA. Hepatitis Bx antigen stimulates expression of a novel cellular gene, URG4, that promotes hepatocellular growth and survival. *Neoplasia* 2002; **4**: 355-368

17 **Yu MW,** Yang YC, Yang SY, Chang HC, Liaw YF, Lin SM, Liu CJ, Lee SD, Lin CL, Chen PJ, Lin SC, Chen CJ. Androgen receptor exon 1 CAG repeat length and risk of hepatocellular carcinoma in women. *Hepatology* 2002; **36**: 156-163

18 **Kinoshita M,** Miyata M. Underexpression of mRNA in human hepatocellular carcinoma focusing on eight loci. *Hepatology* 2002; **36**: 433-438

19 **Fu XY,** Wang HY, Tan L, Liu SQ, Cao HF, Wu MC. Overexpression of *p*28 / gankyrin in human hepatocellular carcinoma and its clinical significance. *World J Gastroenterol* 2002; **8**: 638-643

20 **Ito Y,** Miyoshi E, Takeda T, Nagano H, Sakon M, Noda K, Tsujimoto M, Monden M, Matsuura N. Linkage of elevated ets-2 expression to hepatocarcinogenesis. *Anticancer Res* 2002; **22**: 2385-2389

21 **Nakau M,** Miyoshi H, Seldin MF, Imamura M, Oshima M, Taketo MM. Hepatocellular carcinoma caused by loss of heterozygosity in Lkb1 gene knockout mice. *Cancer Res* 2002; **62**: 4549-4553

22 **Wei Y,** Van Nhieu JT, Prigent S, Srivatanakul P, Tiollais P, Buendia MA. Altered expression of E-cadherin in hepatocellular carcinoma: correlations with genetic alterations, beta-catenin expression, and clinical features. *Hepatology* 2002; **36**: 692-701

23 **Chiao PJ,** Na R, Niu J, Sclabas GM, Dong Q, Curley SA. Role of Rel / NF-kappaB transcription factors in apoptosis of human hepatocellular carcinoma cells. *Cancer* 2002; **95**: 1696-1705

24 **Jiang Y,** Zhou XD, Liu YK, Wu X, Huang XW. Association of hTcf-4 gene expression and mutation with clinicopathological characteristics of hepatocellular carcinoma. *World J Gastroenterol* 2002; **8**: 804-807

25 **Ikeguchi M,** Hirooka Y, Kaibara N. Quantitative analysis of apoptosis-related gene expression in hepatocellular carcinoma. *Cancer* 2002; **95**: 1938-1945

26 **Gao CJ,** Guo LL, Guo Y, Cao CA. Relationship between hepatitis C virus infection and expression of apoptosis-related gene bcl-2, bax and ICH-1 in hepatocellular carcinoma tissues. *Diyi Junyi Daxue Xuebao* 2002; **22**: 797-799

27 **Levy L,** Renard CA, Wei Y, Buendia MA. Genetic alterations and oncogenic pathways in hepatocellular carcinoma. *Ann N Y Acad Sci* 2002; **963**: 21-36

28 **Wang Y,** Wu MC, Sham JS, Tai LS, Fang Y, Wu WQ, Xie D, Guan XY. Different expression of hepatitis B surface antigen between hepatocellular carcinoma and its surrounding liver tissue, studied using a tissue microarray. *J Pathol* 2002; **197**: 610-616

29 **Joo M,** Kang YK, Kim MR, Lee HK, Jang JJ. Cyclin D1 overexpression in hepatocellular carcinoma. *Liver* 2001; **21**: 89-95

30 **Kohno H,** Nagasue N, Rahman MA. COX-2 - a target for preventing hepatic carcinoma? *Expert Opin Ther Targets* 2002; **6**: 483-490

31 **Zeng JZ,** Wang HY, Chen ZJ, Ullrich A, Wu MC. Molecular cloning and characterization of a novel gene which is highly expressed in hepatocellular carcinoma. *Oncogene* 2002; **21**: 4932-4943

32 **Harada H,** Nagai H, Ezura Y, Yokota T, Ohsawa I, Yamaguchi K, Ohue C, Tsuneizumi M, Mikami I, Terada Y, Yabe A, Emi M. Down-regulation of a novel gene, DRLM, in human liver malignancy from 4q22 that encodes a NAP-like protein. *Gene* 2002; **296**: 171

Edited by Wu XN and Wang XL

P.O.Box 2345, Beijing 100023,China
Fax: +86-10-85381893
E-mail: wjg@wjgnet.com www.wjgnet.com

World J Gastroenterol 2003;9(11):2433-2440
World Journal of Gastroenterology
 ISSN 1007-9327

• LIVER CANCER •

Expression of TNF-related apoptosis-inducing Ligand receptors and antitumor tumor effects of TNF-related apoptosis-inducing Ligand in human hepatocellular carcinoma

Xiao-Ping Chen, Song-Qing He, Hai-Ping Wang, Yong-Zhong Zhao, Wan-Guang Zhang

Xiao-Ping Chen, Song-Qing He, Hai-Ping Wang, Yong-Zhong Zhao, Wan-Guang Zhang, Hepatic Surgery Center, Affiliated Tongji Hospital, Tongji Medical College,Huazhong University of Science and Technology,Wuhan,430030, China
Supported by the major Foundation of Ministry of Public Health, No.2001-2003
Correspondence to: Xiao-Ping Chen, MD, Professor & Director, Hepatic Surgery Center, Tongji Hospital, Tongji Medical College, Huazhong University of Science and Technology, Wuhan 430030, Hubei Province, China. chenxp_53@sina.com
Telephone: +86-27-83662599 **Fax:** +86-27-83646605
Received: 2002-10-21 **Accepted:** 2002-11-20

Abstract

AIM: To investigate the expression of TNF-related apoptosis -inducing Ligand (TRAIL) receptors and antitumor effects of TRAIL in hepatocellular carcinoma (HCC).

METHODS: Expression of TRAIL receptors was determined in 60 HCC tissues, 20 normal liver samples and two HCC cell lines (HepG2 and SMMC-7721). The effects of TRAIL on promoting apoptosis in HCC cell lines were analyzed after the cells were exposed to the recombinant TRAIL protein, as well as transfected with TRAIL-expression construct. *In vivo* effects of TRAIL on tumor growth were investigated by using nude mice HCC model of hepG2.

RESULTS: Both death receptors were expressed in all HCC tissues and normal hepatic samples. In contrast, 54 HCC tissues did not express DcR1 and 25 did not express DcR2. But both DcR were detectable in all of the normal liver tissues. The expression patterns of DR and DcR in HCC samples (higher DR expression level and lower DcR expression level) were quite different from those in normal tissue. DR5, DR4, and DcR2 expressed in both cell lines, while no DcR1 expression was detected. Recombinant TRAIL alone was found to have a slight activity as it killed a maximum of 15 % of HCC cells within 24 h. Transfection of the TRAIL cDNA failed to induce extensive apoptosis in HCC lines. *In vivo* administration of TRAIL gene could not inhibit tumor growth in nude mice HCC model. However, chemotherapeutic agents or anticancer cytokines dramatically augmented TRAIL-induced apoptosis in HCC cell lines.

CONCLUSION: Loss of DcR (especially DcR1) in HCC may contribute to antitumor effects of TRAIL to HCC.HCC is insensitive towards TRAIL-mediated apoptosis, suggesting that the presence of mediators can inhibit the TRAIL cell-death-inducing pathway in HCC. TRAIL and chemotherapeutic agents or anticancer cytokines combination may be a novel strategy for the treatment of HCC.

Chen XP, He SQ, Wang HP, Zhao YZ, Zhang WG. Expression of TNF-related apoptosis-inducing Ligand receptors and antitumor tumor effects of TNF-related apoptosis-inducing Ligand in human hepatocellular carcinoma. *World J Gastroenterol* 2003; 9(11): 2433-2440
http://www.wjgnet.com/1007-9327/9/2433.asp

INTRODUCTION

Apoptosis, the process of programmed cell death, is a fundamental mechanism in developmental and homeostatic maintenance of complex biological systems. Maladjustment or disturbance in apoptotic process will result in transformation and provide a growth advantage to transformed cells. Members of the tumor necrosis factor (TNF) superfamily contribute to a variety of cell biological functions, including cellular activation, proliferation and death, by interaction with their corresponding receptors[1-3]. TNF and fasL have been focused on because of they can induce tumor cells apoptosis, whereas TNF and fas ligand were unlikely to provide useful target neoplastic elimination of tumors cells for two reasons. One is that many tumor cells are resistant to FasL or TNF-mediated cell death, as shown in the present studies, the other is that systemical administeration of TNF and FasL is limited by their acute cytotoxic effects on normal tissues *in vivo*, thereby limiting their widespread use in the treatment of cancer[4-7].

TNF-related apoptosis-inducing ligand (TRAIL), another TNF superfamily member, is a promising cancer therapeutic agent[8]. TRAIL appears to specifically kill transformed cells, and spare most normal cells[9]. TRAIL induces apoptotic death on binding to either of two proapoptosic TRAIL receptors, DR5 or DR4.Normal cells are believed to be resistant to TRAIL because of expressing higher levels of TRAIL decoy receptors DcR1 or DcR2 on their cell surface.

A recent study reported that chemotherapeutic agents could augment TRAIL-induced apoptosis in human hepatocellular carcinoma cell lines, indicating that TRAIL may have therapeutic potential in the treatment of human HCC[28]. In the present study, we investigated the expression of TRAIL receptors and antitumor effects of TRAIL in human HCC, in order to find an effective treatment of HCC.

MATERIALS AND METHODS

HCC and control liver Tissues

Sixty surgically resected specimens employed in this study were obtained from patients with HCC who had undergone potentially curative tumor resection at the Hepatic Surgery Center, Tongji Hospital during January, 2000-December, 2000. All HCC tissues were pathologically confirmed. Tweenty normal liver samples obtained from patients with benign tumor were used as control at the same time. We obtained informed consent from all patients. Resected tissues were frozen immediately at -70 ℃. All cases were selected on the basis of availability of frozen materials for study and in the absence of extensive tumor necrosis. Materials were composed of 5 cases of grade I, 23 cases of grade II, 27 cases of grade III and 5 cases of grade IV according to TNM system (1987). The tumor

lesions analyzed here including 35 poor differentiations, 15 moderate differentiations and 10 well differentiations. There were 53 males and 7 females, and the age was from 18 to 75 years with an average of 45.8 years (s, 13.5 years), HBsAg positive 55 and negative 5. Routinely processed 4 % paraformaldehyde-fixed, paraffin-embedded blocks containing principal tumor were selected. Serial sections of 5 μm thickness were prepared from the cut surface of blocks at the maximum cross-section of tumor.

Cell lines and cell culture

Human HCC cell lines (HepG2, SMMC-7721), Jurkat T-cell line and human colangiocarcinma cell line QBC939 were purchased from ATCC. Cells were cultured in DMEM supplemented with 1 % penicillin/streptomycin and 10 % heat-inactivated fetal calf serum in a 5 % CO_2 incubator at 37 ℃.

Detection of TRAIL-R

The expression of TRAILR1, TRAILR2, TRAILR3 and TRAILR4 in HCC cell lines and human HCC tissues was detected by *in situ* hybridization. Digoxigenin-labeled antisense and sense TRAILR probes were purchased from Boster Biotechnology Inc. *In situ* mRNA expressions were performed according to the manufacturer' s protocol. Deparaffinized, rehydrated tissue sections (5 μM) on silane-coated slides were permeabilized by incubation in proteinase 75 (20 μg/ml) for 30 min at 37 ℃ and acetylated in PBS containing 0.25 % acetic anhydride and 0.1 M triethanolamine for 10 min at room temperature. Prehybridization was carried out in 50 % formamide, 4×SSC, 1×Denhardt' s solution, 125 μg/ml tRNA, and 100 μg/ml freshly denatured salmon sperm DNA for 2-4 h at 42 ℃. Hybridization was performed using prehybridization solution containing denatured TRAILR antisense or sense probes (50 ng/slide) for 36 h at 42 ℃ and followed by washes at 52 ℃ with different solutions (2×SSC and 50 % formamide, 30 min; 1×SSC and 50 % formamide, 30 min; 0.5×SSC and 50 % formamide, 30 min). After that, the sections were incubated in turn in buffer 1 [150 mM NaCl and 100 mM Tris-HCl (pH 7.5)] containing 5 % BSA and 0.3 % Triton X-100 for 30 min and in horseradish peroxidase-conjugated antidigoxigenin antibody diluted 1:500 with buffer 1 containing 5 % BSA and 0.3 % Triton X-100 for 2 h at room temperature. After washed in buffer 1, the sections were immersed briefly in buffer 2 [100 mM NaCl, 50 mM $MgCl_2$, and 100 mM Tris-HCl (pH 9.5)] and incubated in buffer 2 containing 0.025 % diaminobenzidine and 0.02 % H_2O_2 for 15 min at 4 ℃. Finally, the sections were immersed in 10 mM Tris-HCl, 1 mM EDTA buffer (pH 8.0), rinsed in water, and mounted with glycerol mountant.

In vitro effects of TRAIL on cellular apoptosis of HCC

HCC cells were seeded into 96-well microtiter plates with 5×10^3 cells per well and cultured in DMEM supplemented with 10 % fetal calf serum at 37 ℃ under a humidified atmosphere of 5 % CO_2 for 24 h when the cells were in the exponential phase of growth. After treated with TRAIL at the indicated concentration (1, 10, 100, 1 000 ng/ml), the cell viability was assessed with MTT method and the absorbance was measured at 490 nm with a microtiter plate reader. Cell death was estimated with the following formula.

% specific death=A(untreated cells)-A(treated cells)/A (untreated cells)×100.

Results were derived form 3 individual experiments. Each experimental condition was repeated at least in sextuplicate wells for each experiment. We used the same method to detect the effects of TRAIL on Jurkat T-cell line and human colangiocarcinma cell line QBC939.

Construction of TRAIL expression plasmids

The sequence corresponding to the C-terminus extracellular region of 114-281 amino acid (aa) of TRAIL was amplified by PCR, and subcloned into the EcoRV/EcoRI site of expression vector pIRES-EGFP. Following DNA plasmid transfection with superfect reagent for 72 hours, cells were evaluated for apoptosis. The expression of cellular TRAIL protein was verified with Western blot. Briefly, cells were collected by centrifugation at 2 000 g for 10 minutes, cells lysed with lyse cell solution (50 mmol/L Tris-cl, 150 mmol/L NaCl, 0.02 % sodium azide, 0.1 % SDS, 100 ug/ml PMSF, 1 μg/ml aprotinin, 1 % NP-40, 0.5 % deoxysodium cholate), protein in the supernants was separated by 12 % SDS-PAGE and transferred by electroblotting to nitrocellulose membranes. The membranes were blocked by TBST (TBS-Tween) with 5 % non-fat milk, and then incubated with primary antibody (anti-hTRAILmAb) in TBST with 5 % non-fat milk overnight. Proteins were detected with horseradish peroxidase-conjucated secondary antibody and performed chemiluminscence according to the manufacturer' s instructions. MTT assay was used to measure cell viability. The tumor cells were infected with pIRES-EGFP-null as a control.

Flow cytometry

Collected cells were washed with PBS, fixed in 70 % ethanol, digested with RNase A (10 mg/L) in PBS for 30 min and then stained with propidium iodide (PI), and analyzed on a FACScan.

Gene therapy of experimental nude mice subcutaneous hepatocellular carcinoma by direct intratumoral injection of TRAIL gene

5×10^6 HepG2 cells were inoculated subcutaneously into the back of nude mice. One cm tumors were formed in nude mice about ten days after inoculation. Plasmid carrying TRAIL gene was delivered into the tumor by intra-tumor injection (n=10). pIRES-EGFP-null injection as a control (n=10). RT-PCR was adopted to examine the expression of TRAIL gene in tumor. The expression of TRAIL protein was detected by Western blotting. The anti-tumor effect of gene therapy was evaluated according to the sizes of tumors for 4 weeks. Therapeutic effects of TRAIL gene on experimental cholangiocarcinoma induced in nude mice were detected using the same method.

Treatment of HCC cell lines in combination with TRAIL and IFN-γ, IL-2 or chemotherapy drug

HCC cells exposed to IL-2 (different concentrations) combined with recombinant TRAIL protein (50 ng/ml) for 72 h were compared with treatment of TRAIL alone. In the same time, the effect of TRAIL in combination with IFN-γ or chemotherapy drugs (such as mitomycin, 5-fluorouracil) was investigated. Cell viability was examined by MTT assay.

Statistical analysis of data

Quantitative comparisons were performed by Student t test or the chi-square and Fisher exact tests. All statistical analyses were performed using SAS software. Statistical significance was set at 0.05.

RESULTS

Expression of TRAIL-R in HCC cell lines and tissues

DR5 and DR4 were present in all HCC tissue as well as normal hepatic tissues. In contrast, 54 tumors did not express DcR1 and 25 tumors did not express DcR2, but DcR1 and DcR2 were detected in all of the normal liver tissues. The expression patterns of DR and DcR in HCC samples (higher DR expression

level and lower DcR expression level) were quite different from those in normal tissue. DR5, DR4, and DcR2 were expressed, but DcR1 did not express in both cell lines. Expression of TRAIL-R was located mainly in the cytoplasm (Figure 1).

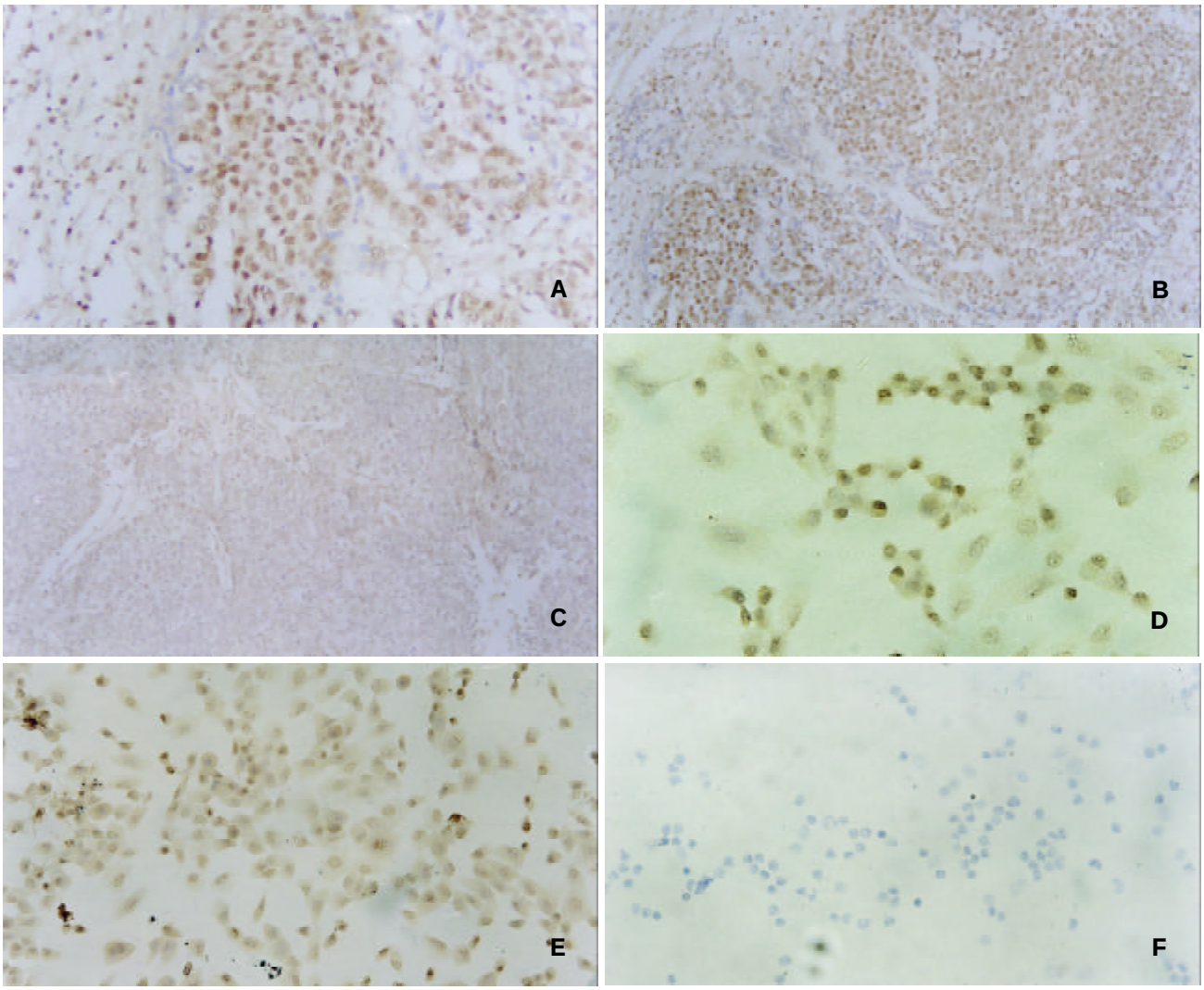

Figure 1 Expression of TRAILR in human HCC tissues and HCC cell lines by *in situ* hybridization. Stronger expression of DR5 (A and D) and DR4 (B and E) as well as negative expression of DcR1 C and F) in both human HCC tissues and HCC cell lines. Note that TRAIL-R staining was found mainly in the cytoplasm and membrane.

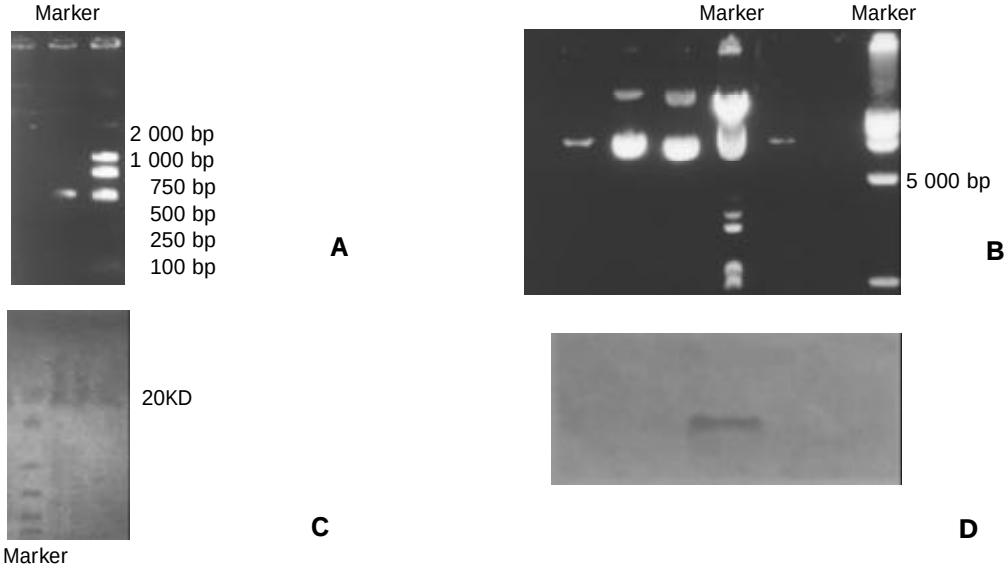

Figure 2 Construction of pIRES-EGFP-TRAIL. A: the C-terminus extracellular region of 114-281 amino acid (aa) was amplified by PCR, including EcoRV / EcoRI at two end, 523 bp. B: TRAIL expression plasmids pIRES-EGFP-TRAIL. C: The cellular proteins were separated by SDS-PAGE. D: Western blot identified expression of TRAIL, negative expression of TRAIL in control.

Production of TRAIL protein

TRAIL expression was assayed by Western blotting as shown, a 19.6 KD band sTRAIL monomers. In contrast, no corresponding bands were present in the negative control. These results demonstrated that the transfection of pIRES-EGFP-TRAIL resulted in transgene expression in human liver cancer cell lines (Figure 2).

Resistance of human HCC cells to both TRAIL and pIRES-EGFP-TRAIL transfection

TRAIL protein alone failed to induce significant apoptosis in both HCC cell lines, even at a dose up to 100 ng/ml, it killed only about 10 % of HCC cells within 24 h, compared with 70 % of Jurkat cells and about 50 % of cholangiocarcinoma cell line QBC939. Production of TRAIL following pIRES-EGFP-TRAIL transfection also failed to lead to tumor cell death. HCC cell lines were adequately transfected with pIRES-EGFP-TRAIL. Minimal cell death of HepG2 cells was observed upon infection with pIRES-EGFP-TRAIL. Analysis of TRAIL protein production by Western blot revealed detectable levels in HepG2 cell lysed by 6h post infection, with levels increasing over the entire time course. These results demonstrated that tumor cells infected with pIRES-EGFP-TRAIL could produce TRAIL protein, however failed to lead to their extensive death (Figure 3).

Effects of gene therapy on experimental hepatocellular caricinoma

Direct intra-tumor injection of pIRES-EGFP carrying TRAIL gene was performed on experimental hepatocellular caricinoma induced in nude mice. RT-PCR was adopted to examine the expression of TRAIL gene in nude mice tumor,the anti-tumoral

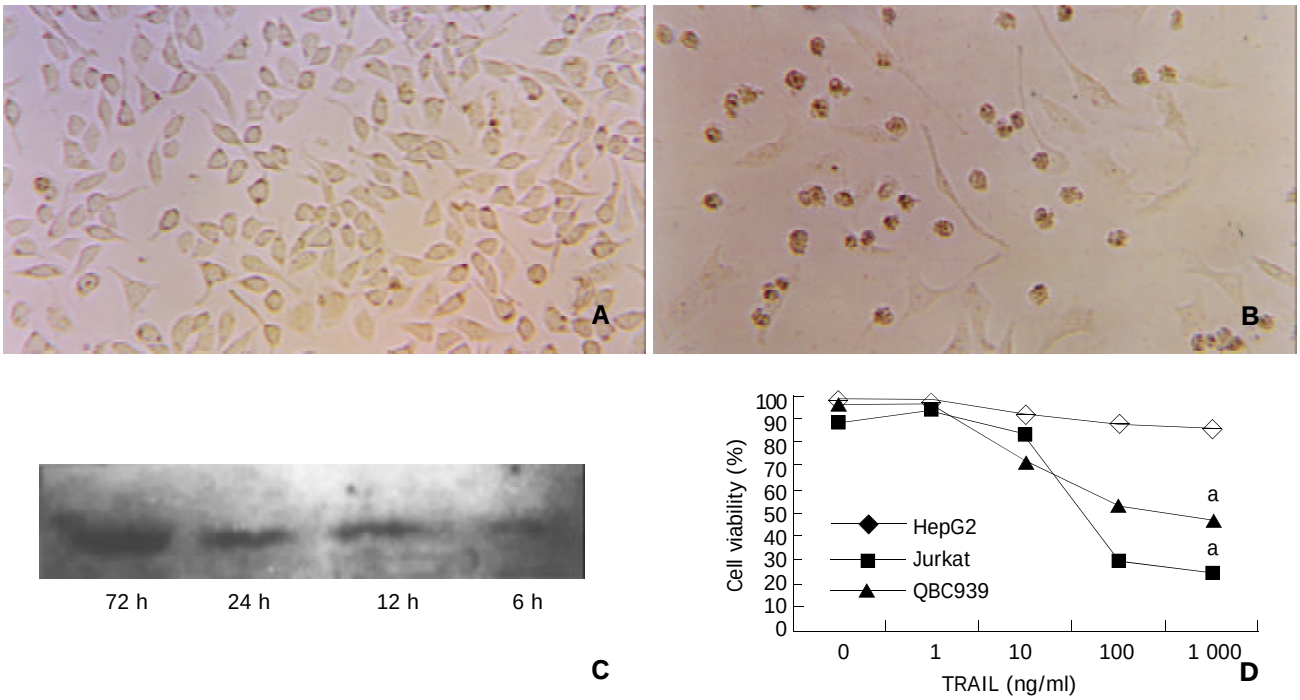

Figure 3 Determination of the percentage of cell viability by *in vitro* administration of recombinant TRAIL.A: Normal HepG2 shapes. B: HepG2 shaped treatment with TRAIL (100 ng / ml, 24 h). C: Western blot analyzed expression of TRAIL protein transfected with pIRES-EGFP-TRAIL (6 h, 12 h, 24 h 72 h). D:Survival of tumor cells treatment with TRAIL, detected by MTT. Each value represents the mean of the three wells. For clarity, SD bars are omitted from the graph, but are less than 5 % for all data points. Experiments were performed at least three separate times with similar results. [a]: Compared with hepG2, statistical significant (P<0.05). The results similar to HepG2 were obtained in SMMC-7721.

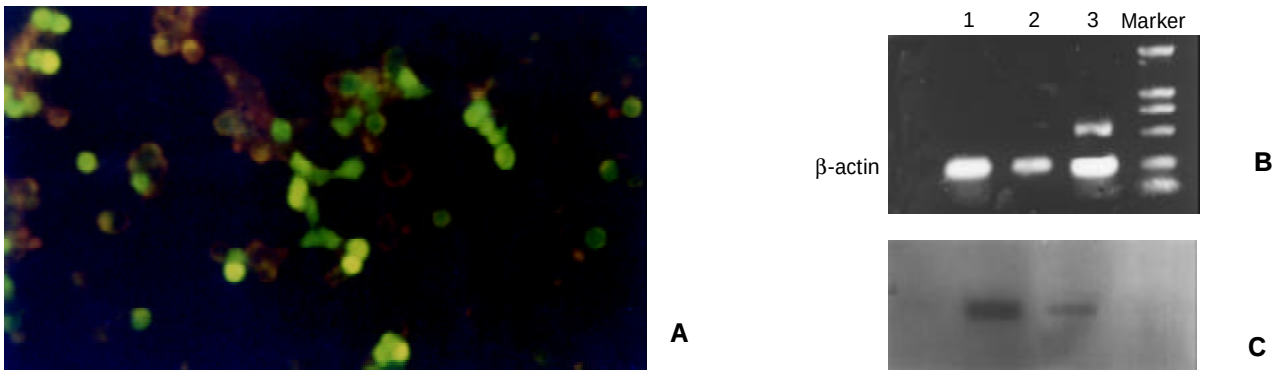

Figure 4 Transfection of pIRES-EGFP-TRAIL *in vitro* and *in vivo*. A: Transfected efficiency observed with fluorescence microscope (*in vitro*). B: The expression of TRAIL gene in nude mice tumor was all relatively strong (*in vivo*). (1), the expression of TRAIL gene in tissue near the tumor was weak (2) and that in normal liver tissue was negative after transfection of TRAIL gene (3). C: TRAIL protein production was determined by Western blot analysis. (a) Nude mice HCC tissue, (b) Adjacent tissue and (c) Normal tissue.

effect of gene therapy was evaluated according to the sizes of the tumors (as shown by Figure 4). Ten days after transfection of TRAIL gene, the expression of TRAIL gene in nude mice tumor was relatively strong, the expression of TRAIL transgene in tissue near the tumor was weaker and that in normal liver tissue was negative.

However, the tumor sizes were slightly less than those in control group (as shown in Table 1). TRAIL gene intra-tumor injection could lead to effective gene delivery and gene expression but had limited effect on experimental HCC in nude mice.

Table 1 Antitumor effects of pIRES-EGFP-TRAIL transfection on tumor growth in nude mice (tumor size $\bar{x}\pm s$, cm)

Target cell	pIRES-EGFP-TRAIL (n=10)	pIRES-EGFP-null (n=10)	P
HepG2	1.05±0.39	1.30±0.27	0.174
QBC939	0.85±0.23	0.32±0.15	0.023

Synergistic induction of apoptosis by combination of TRAIL and chemotherapeutic drugs

We incubated HCC cells with mitomycin (0.001 mg/ml) or 5-fluorouracil (5-Fu) (0.025 mg/ml) in combination with TRAIL (50 ng/ml). Cell viability was examined after 24-72 h. Cytoxicity of the combination of TRAIL and chemotherapeutic agents was compared with either agent alone (Figure 5). Sensitization of HCC cells to TRAIL-inducing apoptosis was independent of p53 status because both HepG2 and SMMC-7721 were similarly sensitized to TRAIL in combination with chemotherapeutic agents, and transfection of p53 could not enhance the sensitivity of SMMC-7721 to TRAIL-inducing apoptosis. The results demonstrated TRAIL could decrease the threshold of some chemotherapeutic drugs 50-100 folds.

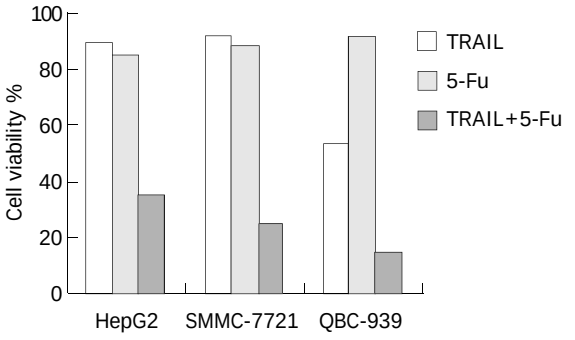

Figure 5 Cell viability of tumor cells incubated with TRAIL in combination with 5-Fu. Cell viability is shown as the percentage of viable cells relative to control cell after 24 h of incubation with TRAIL (50 ng/ml), 5-Fu (0.025 mg/ml) or both. SD bars are less than 5 % for all data points and omitted.

Low dose of interleukin-2 enhanced TRAIL-inducing apoptosis in HCC cells

HCC cells were cultured in the presence of TRAIL or TRAIL plus IL-2 or IFN-γ. Cultures were examined by phase contrast light microscopy at 6, 12, 24, 48, and 72 h. A rounded cytopathic effect was detectable in HCC cell cultures in the presence of TRAIL plus low dose IL-2 after 12 h, but was more prominent after 24 h. Extensive cell death was apparent in HCC cell cultures treated with TRAIL plus IL-2 at 48-72 h. To quantitate the extent of cell death, we measured cell viability treated with IL-2, TRAIL, or IL-2 and TRAIL using MTT. In contrast, HCC cultures treated with IL-2 alone appeared healthy throughout the experiment. Importantly, the death-inducing synergistic effects of TRAIL in combination with IL-2 were not specific to HCC cells, but also induced other tumor cells death (such as cholangiocarcinoma cell line QBC939, data not shown). These data indicated that TRAIL in combination with low dose IL-2 could induce cell death in HCC cells cultures *in vitro*. To our surprise, Low dose of IL-2 significantly enhanced TRAIL-inducing apoptosis in HCC cells after 48-72 h, but high dose of IL-2 only had a weaker role.

To delineate that TRAIL and IL-2 specifically killed HCC cells and spared normal liver cells, we cultured primary normal liver cells and normal fetal liver cell line L02 in the presence of TRAIL and IL-2 for 48 or 72 h. We subsequently determined whether they were undergoing apoptosis. By contrast to HCC cells, normal cells cultured in the presence of TRAIL and IL-2 exhibited no signs of apoptosis. These data indicated that TRAIL in combination with IL-2 could selectively induce apoptosis of HCC cells but not normal liver cells. Furthermore, we obtained similar synergistic results with combination of TRAIL and IFN-γ.

Apoptosis detection by FACScan

Cell death might occue through apoptosis or necrosis. Here, we found that TRAIL could kill HCC cells through apoptosis by FACScan (Figure 6).

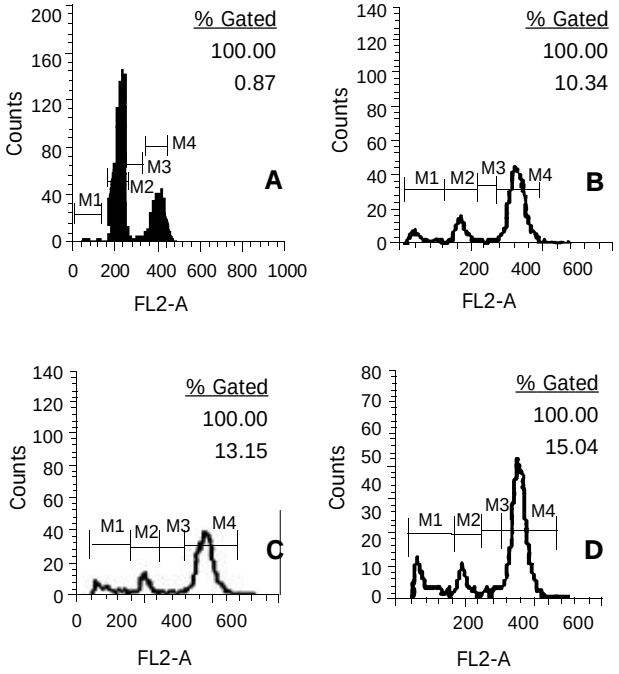

Figure 6 Apoptosis of HepG2 after treatment with TRAIL.A: HepG2 without treatment. B, C, D: HepG2 treatment with TRAIL for 24 h (B, 10 ng/ml. C, 100 ng/ml. D, 1 000 ng/ml). Compared to A P<0.05.

DISCUSSION

To selectively kill target tumor cells and spare normal tissues are one of the ultimate goals of cancer research. TRAIL, a type II transmembrane protein, was initially identified based on the homology of its extracellular domain with FasL, TNF and lymphotoxin-α[8]. TRAIL transcripts have been detected in the adult spleen, thymus, lung, prostate, ovary, small intestine, peripheral blood lymphocytes, colon, heart, placenta, skeletal muscle, and kidney, but not in the adult liver, brain, and testis. Receptors that bind to TRAIL include death receptor (DR) 4/TRAILR1[10], DR5/KILLER/TRAILR2/TRICK2[11-16], decoy receptor (DcR) 1/TRAILR3/TRID (TRAIL without an extracellular domain)/LIT (Lymphocyte Inhibitor of TRAIL)[12-15,19], DcR2/TRAILR4/TRUDD (TRAIL receptor

with a truncated death domain)[19-21] and a soluble receptor called osteoprotegerin (OPG)[22]. DR4, DR5, DcR1, and DcR2 have been shown to bind TRAIL with similar affinities. However, only two of the TRAIL receptors, DR4 and DR5, contain functional death domains and are capable of inducing apoptosis. DcR1, DcR2 are highly expressed in normal tissues, but have substantially lower expression in malignant cells, indicating a low cytotoxic effect in normal tissues. In contrast, DR4 and DR5 are expressed in malignant cells as well as in normal tissues. Despite having multiple receptors, TRAIL can selectively target tumor cells to undergo apoptosis while leaving normal cells unaffected. The selectivity of TRAIL-induced apoptosis has been demonstrated by systemic administration of TRAIL, which reduces tumor growth *in vivo*, without the severe toxic effects often seen in TNF or FasL treated mice. A relatively large number of tumor cell lines, such as leukemia, lymphoma, myeloma, melanoma, breast cancer, colon carcinoma, cholangiocarcinoma or thyroid carcinoma, are sensitive to cytotoxic effects of TRAIL, indicating that TRAIL may be a powerful selective cancer therapeutic [8,21-31].

However, the potential utility and safety of systemic administration of TRAIL have been recently questioned because results showed sensitivity of human but not monkey or mouse hepatocytes to a polyhisidine-tagged recombinant soluble form of TRAIL (amino acids 114-281,114-281TRAIL. his)[32]. Fortunately, another study showed that the toxicity of histidine-tagged TRAIL to human hepatocytes *in vitro* had aberrant biochemical properties, i.e., loss of zinc with the formation of intersubunit disulfide bonds. When this reagent was replaced by a nontagged soluble TRAIL zinc-replete TRAIL (114-281.TRAIL.rs), normal liver cell cytotoxicity was not observed[33-35].

Another potential drawback of TRAIL therapy was that not all cancer cells were sensitive to TRAIL. The regulation of TRAIL signaling is extremely complex, the mechanisms of TRAIL-resistance remain unclear. It has been suggested that the reason why some cells are susceptible to TRAIL while others appear to be resistant lies in the endogenous presence of the non-death-signaling TRAILR[35]. However, examination of various tumor cell types has shown that basal expression of TRAILR did not correlate with susceptibility to TRAIL[36,37]. Alternatively, the presence or absence of intracellular inhibitors of apoptosis such as the cellular inhibitor of caspase 8/FLICE-inhibitory protein (cFLIP) might be important[38-44], and in some circumstances, cFLIP expression did correlate with the susceptibility of tumor cells to TRAIL[37]. It has been found that NF-κB activation also protected cells against TRAIL-induced apoptosis[19]. Taken together, previous studies indicated that TRAIL resistance to apoptosis might be cell-type specific requiring up-regulation or down-regulation of one of the TRAIL receptors, assembly of different receptors, involvement of decoy receptors, and functions of intracellular inhibitors or intracellular anti-apoptotic/survival pathways working in concert. There is long way to clarify TRAIL-resistance mechanisms. How to reverse TRAIL-resistance is also an important topic before TRAIL is developed into an effective anticancer drug. Therefore, as the first step we detected the assembly of different receptors in HCC.

In the present study, both DR were present in all HCC tissue as well as in normal hepatic tissues derived from surgically resected margins of benign tumor. In contrast, 54 HCC tumors did not express DcR1 and 25 HCC tumors did not express DcR2. Both DcR were detectable in all of the normal liver tissues. High expression of DR and low or no expression of DcR in HCC tissue differed from low expression of DR and high expression of DcR in normal hepatic tissues. DR5, DR4, and DcR2 were expressed in both cell lines examined, but DcR1 did not express in both cell lines. Although expressed detectable TRAIL-R1 and -R2, both HCC cell lines showed strong resistance to TRAIL-induced apoptosis. Recombinant TRAIL (100 ng/ml) alone was found to have a slight activity as it killed about 10 % of HCC cells within 24 h compared with over 70 % of Jurkat cells and about 50 % of human cholangiocarcinoma cell line QBC939. Transfection of TRAIL cDNA also failed to induce extensive apoptosis in HCC lines. *In vivo* administration of TRAIL gene could not inhibit tumor growth in nude mice HCC model. These results suggest that some possibly endogenous suppressors of TRAIL-mediated apoptosis might exist in HCC cells. Certainly, components for TRAIL-induced apoptosis existed in these cell lines, and resistance to apoptosis in HCC was more likely mediated by intracellular signaling events than by alternations in receptor expression or the presence of decoy receptors. The mechanisms of TRAIL resistance in HCC should be identified in order to reverse TRAIL resistance.

The pharmacokinetic profile of soluble TRAIL indicated that after iv injection the majority of protein was cleared within 5 hours. Increasing in *vivo* t1/2 of soluble TRAIL or developing an alternative means of delivery may increase the relative tumoricidal activity of TRAIL. Identification of alternate methods to deliver TRAIL to the tumor site is also critical for further developing and testing anti-tumor activity of TRAIL *in vivo*. The results in our work described the production of an expression vector engineered to carry the gene for TRAIL. Shortly after cell tranfection, TRAIL protein was detected, rapidly leading to the induction of apoptosis in TRAIL-sensitive tumor cells (such as cholangiocarcinoma cell line QBC939, data not shown) *in vitro*, indicating the potential of using TRAIL gene and local expression of TRAIL to destroy TRAIL-sensitive tumor cells *in vivo*. As for TRAIL resistant tumor cells, effective treatment would be attached by new therapy strategies such as combining gene therapy.

How to reverse TRAIL-resistance is an important topic before TRAIL is developed into an effective anticancer drug. Consistent with several previous reports, our results showed that chemotherapeutic agents significantly sensitized HCC cell lines to TRAIL-induced apoptosis. TRAIL could decrease the threshold of some chemotherapeutic drugs 50-100 flods. The mechanism of overcoming tumor resistance to TRAIL-induced apoptosis by chemotherapeutic agents must be reserved for further investigation. Therefore, our results also showed that cytokines that compose part of the arsenal of the immune system against tumors might alter HCC sensitivities to TRAIL, For example, a subtoxic level of interlukin-2 could overcome the resistance of HCC cells. No significant apoptosis was induced in cells pretreated with IL-2 alone even at 10 000 unit/ml, and TRAIL (50 ng/ml) induced 10 % cell death after 24 h treatment. However, HCC cells treated with IL-2 (50 unit/ml) in combination with TRAIL (50 ng/ml) were killed about 50 % at 48 h, indicating that IL-2 could sensitize HCC cells to TRAIL-induced apoptosis. The effect of IL-2 which enhanced TRAIL-mediated apoptosis was not dose-depent, low dose IL-2 had a stronger sensitizing effect while high dose IL-2 had a weaker role. HCC cells could become sensitive to TRAIL-mediated cell death after treatment IFN-γ, too. The possible explanations for these effects are that IFN-γ could induce TRAIL expression, up-regulate DR and Caspase 8, significantly decrease NF-κB-activation, and prevent IAP2[45-48]. These findings have therapeutic implications because resistance to apoptosis in HCC cells may be dramatically overcome by agents used in combination.

In summary, TRAILR expression is prevalent in HCC and there is a different expression of receptor types in HCC cells compared with normal hepatic tissue. HCC cells are insensitive

to TRAIL-mediated apoptosis, suggesting the presence of mediators can inhibit the TRAIL-inducing apoptosis pathway in HCC and has a limited therapeutic role for TRAIL as a single agent in HCC. However, TRAIL-based tumor therapy in combination with chemotherapeutic agents or anticancer cytokines might be a powerful treatment for HCC.

REFERENCES

1 **Ashkenazi A**, Dixit VM. Apoptosis control by death and decoy receptors. *Curr Opin Cell Biol* 1999; **11**: 255-260
2 **Cosman D**. A family of ligands for the TNF receptor superfamily. *Stem Cells* 1994; **12**: 440-455
3 **Smith CA**, Farrah T, Goodwin RG. The TNF receptor superfamily of cellular and viral proteins: activation, costimulation, and death. *Cell* 1994; **76**: 959-962
4 **Havell EA**, Fiers W, North RJ. The antitumor function of tumor necrosis factor (TNF). I.Therapeutic action of TNF against an established murine sarcoma is indirect, immunologically dependent and limited by severe toxicity. *J Exp Med* 1988; **167**: 1067-1085
5 **Bird GL**, Sheron N, Goka AK, Alexander GL, Williams RS. Increased plasma tumor necrosis factor in severe alcoholic hepatitis. *Ann Intern Med* 1990; **112**: 917-920
6 **Schilling PJ**, Murray JL, Markowitz AB. Novel tumor necrosis factor toxic effects. Pulmonary hemorrhage and severe hepatic dysfunction. *Cancer* 1992; **69**: 256-260
7 **Ogasawara J**, Watanabe-Fukunaga R, Adachi M, Matsuzawa A, Kasugai T, Kitamura Y, Itoh N, Suda T, Nagata S. Lethal effect of the anti-Fas antibody in mice. *Nature* 1993; **364**: 806-809
8 **Wiley SR**, Schooley K, Smolak PJ, Din WS, Huang CP, Nicholl JK, Sutherland GR, Smith TD, Rauch C, Smith CA. Identification and characterization of a new member of the TNF family that induces apoptosis. *Immunity* 1995; **3**: 673-682
9 **Sheridan JP**, Marsters SA, Pitti RM, Gurney A, Skubatch M, Baldwin D, Ramakrishnan L, Gray CL, Baker K, Wood WI, Goddard AD, Godowski P, Ashkenazi A. Control of TRAIL-induced apoptosis by a family of signaling and decoy receptors. *Science* 1997; **277**: 818-821
10 **Pan G**, O'Rourke K, Chinnaiyan AM, Gentz R, Ebner R, Ni J, Dixit VM. The receptor for the cytotoxic ligand TRAIL. *Science* 1997; **276**: 111-113
11 **Walczak H**, Degli-Esposti MA, Johnson RS, Smolak PJ, Waugh JY, Boiani N, Timour MS, Gerhart MJ, Schooley KA, Smith CA, Goodwin RG, Rauch CT. TRAIL-R2: a novel apoptosis-mediating receptor for TRAIL. *EMBO J* 1997; **16**: 5386-5397
12 **Pan G**, Ni J, Wei YF, Yu G, Gentz R, Dixit VW. An antagonist decoy receptor and a death domain-containing receptor for TRAIL. *Science* 1997; **277**: 815-818
13 **Screaton GR**, Monkolsapaya J, Xu XN, Cowper AE, McMichael A, Bell JI. TRICK2, a new alternatively spliced receptor that transduces the cytotoxic signal from TRAIL. *Curr Biol* 1997; **7**: 693-696
14 **Schneider P**, Bodmer JL, Thome M, Hofmann K, Holler N, Tschopp J. Characterization of two receptors for TRAIL. *FEBS Lett* 1997; **416**: 329-334
15 **MacFarlane M**, Ahmad M, Srinivasula SM, Fernandes-Alnemri T, Cohen GM, Alnemri ES. Dentification and molecular cloning of two novel receptors for the cytotoxic ligand TRAIL. *J Biol Chem* 1997; **272**: 25417-25420
16 **Sheridan JP**, Marsters SA, Pitti RM, Gurney A, Skubatch M, Baldwin D, Ramakrishnan L, Gray CL, Baker K, Wood WI, Goddard AD, Godowski P, Ashkenazi A. Control of TRAIL-induced apoptosis by a family of signaling and decoy receptors. *Science* 1997; **277**: 818-821
17 **Miller LK**. The role of caspase family of cysteine proteases in apoptosis. Semin. *Immunol* 1997; **9**: 35
18 **Degli-Esposti MA**, Smolak PJ, Walczak H, Waugh J, Huang CP, DuBose RF, Goodwin RG, Smith CA. Cloning and characterization of TRAIL-R3, a novel member of the emerging TRAIL receptor family. *J Exp Med* 1997; **186**: 1165-1170
19 **Degli-Esposti MA**, Dougall WC, Smolak PJ, Waugh JY, Smith CA, Goodwin RG. The novel receptor TRAIL-R4 induces NF-κB and protects against TRAIL-mediated apoptosis, yet retains an incomplete death domain. *Immunity* 1997; **7**: 813-820
20 **Marsters SA,** Sheridan JP, Pitti RM, Huang A, Skubatch M, Baldwin D, Yuan J, Gurney A, Goddard AD, Godowski P, Ashkenazi A. A novel receptor for Apo2L/TRAIL contains a truncated death domain. *Curr Biol* 1997; **7**: 1003-1006
21 **Pan G**, Ni J, Yu G, Wei YF, Dixit VM. TRUNDD, a new member of the TRAIL receptor family that antagonizes TRAIL signaling. *FEBS Lett* 1998; **424**: 41-45
22 **Emery JG**, McDonnell P, Burke MB, Deen KC, Lyn S, Silverman C, Dul E, Appelbaum ER, Eichman C, DiPrinzio R, Dodds RA, James IE, Rosenberg M, Lee JC, Young PR. Ostroprotegerin is a receptor for the cytotoxic ligand TRAIL. *J Biol Chem* 1998; **273**: 14363-14367
23 **Keane MM**, Ettenberg SA, Nau MM, Russell EK, Lipkowitz S. Chemotherapy augments TRAIL-induced apoptosis in breast cell lines. *Cancer Res* 1999; **59**: 734-741
24 **Gibson SB**, Oyer R, Spalding AC, Anderson SM, Johnson GL. Increased expression of death receptors 4 and 5 synergizes the apoptosis response to combined treatment with eptoposide and TRAIL. *Mol Cell Biol* 2000; **20**: 205-212
25 **Gliniak B**, Le T. Tumor necrosis factor-related apoptosis-inducing ligand's antitumor activity *in vivo* is enhanced by the chemotherapeutic agent CPT-11. *Cancer Res* 1999; **59**: 6153-6158
26 **Gong B**, Almasan A. Apo2 ligand/TNF-related apoptosis-inducing ligand and death receptor 5 mediate the apoptotic signaling induced by ionizing radiation in leukemic cells. *Cancer Res* 2000; **60**: 5754-5760
27 **Tanaka S**, Sugimachi K, Shirabe K, Shimada M, Wands JR. Expression and antitumor effects of TRAIL in human cholangiocarcinoma. *Hepatology* 2000; **32**: 523-527
28 **Yamanaka T**, Shiraki K, Sugimoto K, Ito T, Fujikawa K, Ito M, Takase K, Moriyama M, Nakano T, Suzuki A. Chemotherapeutic agents augment TRAIL-induced apoptosis in human hepatocellular carcinoma cell lines. *Hepatology* 2000; **32**: 482-490
29 **Ahmad M**, Shi Y. TRAIL-induced apoptosis of thyroid cancer cells: potential for therapeutic intervention. *Oncogene* 2000; **19**: 3363-3371
30 **Mitsiades N**, Poulaki V, Tseleni-Balafouta S, Koutras DA, Stamenkovic I. Thyroid carcinoma cells are resistant to FAS-mediated apoptosis but sensitive tumor necrosis factor-related apoptosis-inducing ligand. *Cancer Res* 2000; **60**: 4122-4129
31 **Walczak H**, Miller RE, Ariail K, Gliniak B, Griffith TS, Kubin M, Chin W, Jones J, Woodward A, Le T, Smith C, Smolak P, Goodwin RG, Rauch CT, Schuh JC, Lynch DH. Tumoricidal activity of tumor necrosis factor–related apoptosis-inducing ligand *in vivo. Nat Med* 1999; **5**: 157-163
32 **Jo M**, Kim TH, Seol DW, Esplen JE, Dorko K, Billiar TR, Strom SC. Apoptosis induced in normal human hepatocytes by tumor necrosis factor-related apoptosis-inducing ligand. *Nat Med* 2000; **6**: 564-567
33 **Nicholson DW**. From bench to clinic with apoptosis-based therapeutic agents. *Nature* 2000; **407**: 810-816
34 **Lawrence D**, Shahrokh Z, Marsters S, Achilles K, Shih D, Mounho B, Hillan K, Totpal K, DeForge L, Schow P, Hooley J, Sherwood S, Pai R, Leung S, Khan L, Gliniak B, Bussiere J, Smith CA, Strom SS, Kelley S, Fox JA, Thomas D, Ashkenazi A. Differential hepatocyte toxicity of recombinant Apo2L/TRAIL versions. *Nat Med* 2001; **7**: 383-385
35 **Gura T,** How TR. AIL kills cancer cells, but not normal cells. *Science* 1997; **277**: 768
36 **Griffith TS**, Rauch CT, Smolak PJ, Waugh JY, Boiani N, Lynch DH, Smith CA, Goodwin RG, Kubin MZ. Functional analysis of TRAIL receptors using monoclonal antibodies. *J Immunol* 1999; **162**: 2597-2605
37 **Griffith TS**, Chin WA, Jackson GC, Lynch DH, Kubin MZ. Intracellular regulation of TRAIL-induced apoptosis in human melanoma cells. *J Immunol* 1998; **161**: 2833-2840
38 **Irmler M**, Thome M, Hahne M, Schneider P, Hofmann K, Steiner V, Bodmer JL, Schroter M, Burns K, Mattmann C. Inhibition of death receptor signals by cellular FLIP. *Nature* 1997; **388**: 190-195
39 **Kischkel FC**, Lawrence DA, Chuntharapai A, Schow P, Kim KJ, Ashkenazi A. Apo2L/TRAIL-dependent recruitment of endogenous FADD and caspase-8 to death receptors 4 and 5. *Immunity* 2000; **12**: 611-620

40 **Sprick MR**, Weigand MA, Rieser E, Rauch CT, Juo P, Blenis J, Krammer PH, Walczak H. FADD/MORT1 and caspase-8 are recruited to TRAIL receptors 1 and 2 and are essential for apoptosis mediated by TRAIL receptor 2. *Immunity* 2000; **12**: 599-609

41 **Kim IK**, Chung CW, Woo HN, Hong GS, Nagata S, Jung YK. Reconstitution of caspase-8 sensitizes JB6 cells to TRAIL. *Biochem Biophys Res Commun* 2000; **277**: 311-316

42 **Grotzer MA**, Eggert A, Zuzak TJ, Janss AJ, Marwaha S, Wiewrodt BR, Ikegaki N, Brodeur GM, Phillips PC. Resistance to TRAIL-induced apoptosis in primitive neuroectodermal brain tumor cells correlates with a loss of caspase-8 expression. *Oncogene* 2000; **19**: 4604-4610

43 **Peter ME**. The TRAIL DISCussion: It is FADD and caspase-8. *Cell Death Differ* 2000; **7**: 759-760

44 **Hopkins-Donaldson S**, Bodmer JL, Bourloud KB, Brognara CB, Tschopp J, Gross N. Loss of caspase-8 expression in highly malignant human neuroblastoma cells correlates with resistance to tumor necrosis factor-related apoptosis-inducing ligand-induced apoptosis. *Cancer Res* 2000; **60**: 4315-4319

45 **Shin EC**, Ahn JM, Kim CH, Choi Y, Ahn YS, Kim H, Kim SJ, Park JH. IFN-gamma induces cell death in human hepatoma cells through a RAIL/death receptor-mediated apoptotic pathway. *Int J Cancer* 2001; **93**: 262-268

46 **Langaas V**, Shahzidi S, Johnsen JI, Smedsrod B, Sveinbjornsson B. Interferon-gamma modulates TRAIL-mediated apoptosis in human colon carcinoma cells. *Anticancer Res* 2001; **21**: 3733-3738

47 **Park SY**, Billiar TR, Seol DW. IFN-gamma inhibition of TRAIL-induced IAP-2 upregulation, a possible mechanism of IFN-gamma-enhanced TRAIL-induced apoptosis. *Biochem Biophys Res Commun* 2002; **291**: 233-236

48 **Qin JZ**, Bacon P, Chaturvedi V, Nickoloff BJ. Role of NF-kappaB activity in apoptotic response of keratinocytes mediated by interferon-gamma, tumor necrosis factor-alpha, and tumor-necrosis-factor-related apoptosis-inducing ligand. *J Invest Dermatol* 2001; **117**: 898-907

Edited by Zhu L and Wang XL

P.O.Box 2345, Beijing 100023,China
Fax: +86-10-85381893
E-mail: wjg@wjgnet.com www.wjgnet.com

World J Gastroenterol 2003;9(11):2441-2444
World Journal of Gastroenterology
 ISSN 1007-9327

• LIVER CANCER •

Serum from rabbit orally administered cobra venom inhibits growth of implanted hepatocellular carcinoma cells in mice

Peng Sun, Xian-Da Ren, Hai-Wei Zhang, Xiao-Hong Li, Shao-Hui Cai, Kai-He Ye, Xiao-Kun Li

Peng Sun, Xian-Da Ren, Xiao-Hong Li, Shao-Hui Cai, Department of Clinical Pharmacology, Pharmacy College, Jinan University, Guangzhou 510632, Guangdong Province, China
Hai-Wei Zhang, Department of Pathology, Medical College, Jinan University, Guangzhou 510632, Guangdong Province, China
Kai-He Ye, Department of Pharmacology, Pharmacy College, Jinan University, Guangzhou 510632, Guangdong Province, China
Xiao-Kun Li, Biopharmaceutical R&D Center of Jinan University, Guangzhou 510632, Guangdong Province, China
Supported by the Overseas Chinese Affairs Office of the State Council Foundation, No. 98-33
Correspondence to: Xiao-Kun Li, Biopharmaceutical R&D Center of Jinan University, Guangzhou 510632, Guangdong Province, China. xiaokunli@163.net
Telephone: +86-20-8556-5109
Received: 2003-03-19 **Accepted:** 2003-06-07

Abstract

AIM: To investigate the inhibitory effect of serum preparation from rabbits orally administered cobra venom (SRCV) on implanted hepatocellular carcinoma (HCC) cells in mice.

METHODS: An HCC cell line, HepA, was injected into mice to prepare implanted tumors. The animals (n=30) were divided randomly into SRCV, 5-fluorouracil (5-FU), and distilled water (control) groups. From the second day after transplantation, 20 mg/kg 5-FU was administered intraperitoneally once a day for 9 days. SRCV (1 000 mg/kg) or distilled water (0.2 mL) was given by gastrogavage. Tumor growth inhibition was described by the inhibitory rate (IR). Apoptosis was detected by transmission electron microscopy (TEM), flow cytometry (FCM), and terminal deoxynucleotidyl transferase-mediated dUTP-biotin nick end labeling (TUNEL). Student's t-test was performed for statistical analysis.

RESULTS: The tumor growth was inhibited markedly by SRCV treatment compared to that in the control group (P<0.01). The treatment resulted in a significant increase in the apoptotic rate of cancer cells by the factors of 10.5±2.4 % and 20.65±3.2 % as demonstrated through TUNEL and FCM assays, respectively (P<0.01). The apoptotic cells were also identified by characteristic ultrastructural features.

CONCLUSION: SRCV can inhibit the growth of implanted HepA cells in mice, and the apoptosis rate appears to elevate during the process.

Sun P, Ren XD, Zhang HW, Li XH, Cai SH, Ye KH, Li XK. Serum from rabbit orally administered cobra venom inhibits growth of implanted hepatocellular carcinoma cells in mice. *World J Gastroenterol* 2003; 9(11): 2441-2444
http://www.wjgnet.com/1007-9327/9/2441.asp

INTRODUCTION

Snake venoms are complex mixtures of pharmacologically active polypeptides, some are of potential therapeutic value for embolism, cancer and other severe human disorders. Several snake venoms and their components have been demonstrated to be able to inhibit tumor growth and to induce apoptosis of neoplastic cells *in vitro* and *in vivo*[1-7]. We prepared a serum preparation from rabbits administered cobra venom (SRCV)[8]. Our *in vitro* studies have shown its growth-inhibitory and apoptosis-inducing effects of SRCV on cancer cells[9]. In the present study, we observed its effects *in vivo* using implanted hepatocellular carcinoma (HCC) cell line HepA in mice.

MATERIALS AND METHODS

Drugs and reagents

5-FU was purchased from Nantong Pharmaceutical Co (Cat. No. 001121; Nantong, Jiangsu, China). SRCV was prepared as described previously[8]. Briefly, the rabbits were given oral Chinese cobra (*Naja naja atra*) venom 45 mg/kg (Guangzhou Research Institute of Snake Venom, Guangzhou, Guangdong, China) once a day for 3 days. Serum was collected from the rabbits at 4 h after the last administration, then heated in a water bath for 30 min at 56 ℃, frozen at -20 ℃, lyophilized using a vacuum drier and stored at 4 ℃.

Animals

Female Kunming mice (18-22 g, No. 26-2002A002) were supplied from the Medical Animal Center of Guangdong Province. All animals were fed on basic diet and water. The cell line HepA was provided by the Cancer Institute of Sun Yet-Sen University.

Experimental schedule

As described previously[10,11], HepA cells, 2×10^7/mL, were injected subcutaneously into mice, 200 μL for each. Thirty Kunming mice with implanted HepA tumor were divided randomly into SRCV-, 5-FU-treated groups and control group. From the second day after the implantation, 20 mg/kg 5-FU was administered intraperitoneally once a day for 9 days. SRCV (1 000 mg/kg) or distilled water (0.2 mL, control group) was given by gastrogavage. The mice were sacrificed at 24 h after the last administration. The tumors were isolated and weighed immediately in order to calculate the inhibitory rate (IR) according to the formula: IR of tumor (%)=(1-tumor weight in test groups/mean tumor weight in control group)×100 %. Then, the tumors were fixed and used for transmission electron microscopy (TEM), flow cytometry (FCM) and terminal deoxynucleotidyl transferase-mediated dUTP-biotin nick end labeling (TUNEL). All of the tests were repeated twice.

Morphological analysis of apoptosis

Dissected tumor samples were fixed with 2.5 % glutaraldehyde for 1 h. After washed three times in a buffer, the samples were post-fixed in 1 % OsO_4 in a cacodylate buffer for 1 h, then dehydrated in graded ethanol and embedded in epoxy resin (Agar 100). Thin sections (70 nm) were stained with uranyl acetate and reynolds lead citrate and examined at 75 kV in an electron microscope (JEM-100CX 11/T). Morphological changes in the nuclear chromatin of cells undergoing apoptosis were detected by TEM.

Flow cytometry analysis

Cell apoptotic rate was quantitatively determined by flow cytometry. The percentage of cells with a sub-G1 DNA content was taken as the fraction of apoptotic cell population[12,13]. According to the procedure described previously[14-16], tumor tissues were sliced at a thickness of 400-500 μm, then the slices were gently pulverized using a mortar and pestle in phosphate-buffered saline (PBS) (pH7.2). The cell suspension was infiltrated through 200 and 350 μm meshes to remove residues. The cells were collected by centrifugation at 2 000 rpm for 10 min. The cell suspension was fixed in 70 % ice-cold ethanol in PBS, and stored at -20 ℃. Prior to analysis, the cells were washed and resuspended in PBS, then incubated with 10 mg/mL RNase A for 3-5 min and 50 μg/mL propidium iodide (PI) at 4 ℃ for 30 min in a dark chamber. The apoptotic cells having DNA strand breaks that had been labeled were detected by a flow cytometer (FACSCan, Becton Dickinson, San Jose, California, USA).

TUNEL reaction

An ApopTag plus peroxidase *in situ* apoptosis detection kit (Intergen Co Ltd., Burlington, Massachusetts, USA) was used to visualize the cells with DNA fragmentation. The procedure was performed following instructions of the manufacturer and in reference of the previous observations[17-19]. Briefly, 4-μm thick sections were dewaxed and hydrated, treated with 20 μg/mL proteinase K for 15 min at 37 ℃, equilibrated in a buffer for 5 min at room temperature, and incubated in a buffer containing terminal deoxynucleotidyl transferase (TdT) enzyme for 1 h in a humidified chamber at 37 ℃. The reaction was demonstrated by incubation with anti-digoxigenin-peroxidase for 30 min in a humidified chamber at room temperature and visualized in a buffer containing diaminobenzidine (DAB).

The positive cells were identified, counted and analyzed based on morphological characteristics of apoptotic cells as previously described[17]. Under the light microscope, apoptotic cells manifested as brownish staining in the nuclei. Non-necrotic zone was selected in the tissue section and images were randomly selected. At least 1000 tumor cells were counted, and the percentage of TUNEL-positive cells was determined.

Statistical analysis

The data shown were mean values of 8-10 samples and expressed as mean ± standard deviations. Student' s *t*-test was performed for statistical analysis. A *P* value less than 0.05 was considered statistically significant.

RESULTS

Anti-tumor effect of SRCV on implanted HepA tumor

In two separate experiments, the IRs were 30.4 % and 35.8 % after treatment with SRCV. The data, listed in Table 1, demonstrated the inhibitory effect of SRCV treatment on implanted HepA tumor growth, though it was not as strong as that of 5-FU.

Apoptosis - inducing effect of SRCV in mice with implanted HepA tumor

The apoptosis-inducing effect of SRCV was confirmed by electron microscopy. Compared with control group (Figure 1A), morphological changes indicative of apoptosis included cell shrinkage, nuclear chromatin condensation and peripheral shift of condensed chromatin to nuclear membrane or formation of crescent. In addition, the nuclear membrane was intact and there was little or no swelling of mitochondria or other organelles (Figure 1B).

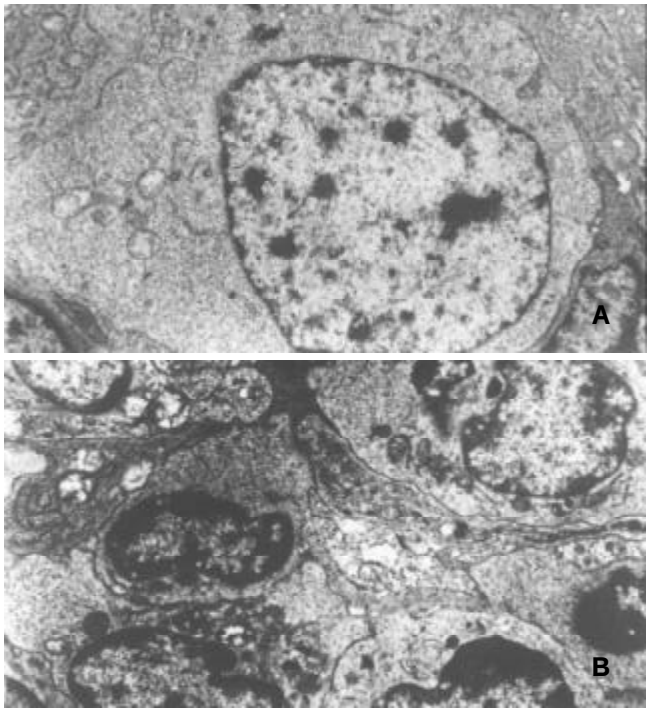

Figure 1 Morphological changes characteristic of apoptotic cells under transmission electron microscope in implanted tumors after treatment with SRCV. A: The normal tumor cells in distilled water control group (×5000). B: The apoptotic cells in SRCV group (×5000).

Table 2 Apoptotic rates (AR) of implanted tumor in SRCV treated mice determined by TUNEL and FCM methods (n=8, $\bar{x}\pm s$)

Groups	Mean apoptotic rate ± SEM (%)	
	TUNEL	FCM
SRCV	10.50±2.42[b]	20.65±3.2[b]
Control group	1.67±1.3	2.28±1.54

[b]P<0.01 *vs* control group.

The apoptosis-inducing effect of SRCV was further confirmed by FCM and TUNEL. After treatment with SRCV, the apoptotic rate was significantly increased in the SRCV group compared with the control group (Table 2). In TUNEL

Table 1 Anti-tumor effect of CVSR on implanted HepA tumors in mice (n=10, $\bar{x}\pm s$)

Group	Dose	Tumor weight/(g)		Inhibition rate (%)	
		First	Twice	First	Twice
SRCV	1 000 mg/kg	1.14±0.28[a]	1.14±0.13[a]	30.35±17.07	35.83±7.11
5-FU	20 mg/kg	0.78±0.14[a]	0.99±0.22[a]	52.57±8.56	44.39±10.5
Control	0.2 ml	1.63±0.26	1.78±0.47		

[a]P<0.01 *vs* control group.

assay, induction of apoptosis was represented by an increase in DNA fragments detected by a peroxidase reaction (Figure 2A), and the apoptotic cells in control tumors were scarcely scattered (Figure 2B).

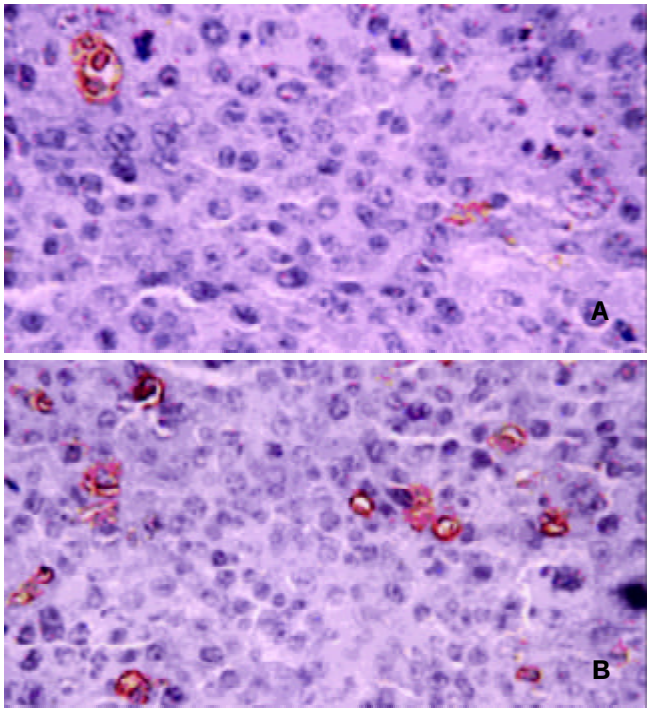

Figure 2 Apoptotic cells of implanted HepA tumors in SRCV treated mice detected by TUNEL assay. A: control group (× 400), B: SRCV 1 000 mg / kg group (×400).

DISCUSSION

Snake venoms have inhibitory effects on the growth of a variety of tumors *in vitro* and *in vivo*[20,21]. Markland *et al*. found that contortrostatin (CN), a homodimeric disintegrin from southern copperhead venom, inhibited dissemination ovarian cancer in a nude mouse model[22]. According to Da Silva *et al*., *Bothrops jararaca* venom (BjV) had anti-tumor effects on Ehrlich ascites tumor (EAT) cells in *vivo* and *in vitro*[23].

Snake venom was also shown to induce apoptosis in tumors. Apoptosis, in contrast to necrosis, was an active process of gene-directed cellular suicide[24]. It has been clear that apoptosis is often upregulated in tumor by many anticancer drugs[25-32].

Since Araki *et al*. first described that hemorrhagic snake venoms induced apoptosis in vascular endothelial cells (VEC)[33], data have been accumulated rapidly about apoptosis-inducing action of various snake venoms and their active components. In 1994, Strizhkov *et al*. reported that both neurotoxin II (NT II) from venom of *Naja naja oxiana* and 20-30 kDa proteins partially purified from pig brain (NTlm) cross-reacting with antibodies to NT II were cytotoxic to L929 and K562 tumor cells at concentrations of 10^{-6}-10^{-8} M, and induced apoptosis in L929 and K562 cells *in vitro*[34]. After that, L-amino acid oxidase (LAO) was found to induce apoptosis in human embryonic kidney cell line 293T[35] and human monocyte line MM6[36]. Recently, Araki *et al*.[37] and Masuda *et al*[38] associated integrins with vascular apoptosis-inducing protein 1 (VAP1)-induced apoptosis. Data from Zhao *et al*. indicated that snake venom secreted phospholipase A_2 ($sPLA_2$) induced apoptosis in Mv1Lu cells in a dose- and time-dependent manner, and was associated with a rapid increase in intracellular ceramide level[39].

The clinical trial using snake venom and their active components have succeeded in cancer therapies, but its application was confined to the auxiliary treatment of patients in the late stage[40,41]. Its toxic and side effects were unavoidable. Great efforts have been made[42-45], but the problem remains unresolved. So a long-standing goal in snake venom therapy of cancer is to find a stable, low toxic, highly effective chemotherapeutic agent that selectively targets tumor cells. Based on this idea, we prepared the SRCV agent[8].

In our previous studies, the anti-tumor activity and apoptosis-inducing effect of SRCV were shown *in vitro* using HepG-2, HL-60 and human lung adenocarcinoma cell line, and no cytotoxicity was observed on human fetal lung fibroblast cells[46-48]. The results presented herein demonstrate that SRCV has inhibitory and apoptosis-inducing effects on implanted HepA tumors. Further studies are needed to identify the active components of SRCV and to elucidate their underlying mechanism.

REFERENCES

1 **Souza DH**, Eugenio LM, Fletcher JE, Jiang MS, Garratt RC, Oliva G, Selistre-de-Araujo HS. Isolation and structural characterization of a cytotoxic L-amino acid oxidase from Agkistrodon contortrix laticinctus snake venom: preliminary crystallographic data. *Arch Biochem Biophys* 1999; **368**: 285-290
2 **Du XY**, Clemetson KJ. Snake venom L-amino acid oxidases. *Toxicon* 2002; **40**: 659-665
3 **Correa MC Jr**, Maria DA, Moura-da-Silva AM, Pizzocaro KF, Ruiz IR. Inhibition of melanoma cells tumorigenicity by the snake venom toxin jararhagin. *Toxicon* 2002; **40**: 739-748
4 **Della Morte R**, Squillacioti C, Garbi C, Derkinderen P, Belisario MA, Girault JA, Di Natale P, Nitsch L, Staiano N. Echistatin inhibits pp125FAK autophosphorylation, paxillin phosphorylation and pp125FAK-paxillin interaction in fibronectin-adherent melanoma cells. *Eur J Biochem* 2000; **267**: 5047-5054
5 **Zhou Q**, Nakada MT, Brooks PC, Swenson SD, Ritter MR, Argounova S, Arnold C, Markland FS. Contortrostatin, a homodimeric disintegrin, binds to integrin alphavbeta 5. *Biochem Biophys Res Commun* 2000; **267**: 350-355
6 **Kang IC,** Lee YD, Kim DS. A novel disintegrin salmosin inhibits tumor angiogenesis. *Cancer Res* 1999; **59**: 3754-3760
7 **Abe Y**, Shimoyama Y, Munakata H, Ito J, Nagata N, Ohtsuki K. Characterization of an apoptosis-inducing factor in Habu snake venom as a glycyrrhizin (GL)-binding protein potently inhibited by GL *in vitro*. *Biol Pharm Bull* 1998; **21**: 924-927
8 **Sun P,** Xu C, Ren XD, Liu JJ, Li XH. Acute toxicity test of three Cobra Venom preparation and their inhibitory effect on transplanted hepatoma in mice. *Jinan Daxue Xuebao* 2002; **23**: 1-4
9 **Luo YR**, Ye CL, Ren XD, Li HL, Zhong L. Inhibition of proliferation and apoptosis in HL60 cells induced by cobra venom serum. *Zhongguo Yaolixue Tongbao* 2002; **18**: 291-293
10 **Wang W**, Qin SK, Chen BA, Chen HY. Experimental study on antitumor effect of arsenic trioxide in combination with cisplatin or doxorubicin on hepatocellular carcinoma. *World J Gastroenterol* 2001; **7**: 702-705
11 **Bi WX**, Xu SD, Zhang PH, Kong F. Antitumoral activity of low density lipoprotein-aclacinomycin complex in mice bearing H (22) tumor. *World J Gastroenterol* 2000; **6**: 140-142
12 **Ryan KM**, Ernst MK, Rice NR, Vousden KH. Role of NF-kappaB in p53-mediated programmed cell death. *Nature* 2000; **404**: 892-897
13 **Chun YJ**, Park IC, Park MJ, Woo SH, Hong SI, Chung HY, Kim TH, Lee YS, Rhee CH, Lee SJ. Enhancement of radiation response in human cervical cancer cells *in vitro* and *in vivo* by arsenic trioxide (As2O3). *FEBS Lett* 2002; **519**: 195-200
14 **Lin SB**, Wu LC, Huang SL, Hsu HL, Hsieh SH, Chi CW, Au LC. *In vitro* and *in vivo* suppression of growth of rat liver epithelial tumor cells by antisense oligonucleotide against protein kinase C-alpha. *J Hepatol* 2000; **33**: 601-608
15 **Hou L**, Li Y, Jia YH, Wang B, Xin Y, Ling MY, Lu S. Molecular mechanism about lymphogenous metastasis of hepatocarcinoma cells in mice. *World J Gastroenterol* 2001; **7**: 532-536
16 **Tian G**, Yu JP, Luo HS, Yu BP, Yue H, Li JY, Mei Q. Effect of nimesulide on proliferation and apoptosis of human hepatoma

SMMC-7721 cells. *World J Gastroenterol* 2002; **8**: 483-487
17 **Cui RT**, Cai G, Yin ZB, Cheng Y, Yang QH, Tian T. Transretinoic acid inhibits rats gastric epithelial dysplasia induced by N-methyl-N-nitro-N-nitrosoguanidine: influences on cell apoptosis and expression of its regulatory genes. *World J Gastroenterol* 2001; **7**: 394-398
18 **Barnett KT**, Fokum FD, Malafa MP. Vitamin E succinate inhibits colon cancer liver metastases. *J Surg Res* 2002; **106**: 292-298
19 **Zhang XL**, Liu L, Jiang HQ. Salvia miltiorrhiza monomer IH764-3 induces hepatic stellate cell apoptosis via caspase-3 activation. *World J Gastroenterol* 2002; **8**: 515-519
20 **Zhou Q**, Sherwin RP, Parrish C, Richters V, Groshen SG, Tsao-Wei D, Markland FS. Contortrostatin, a dimeric disintegrin from Agkistrodon contortrix, inhibits breast cancer progression. *Breast Cancer Res Treat* 2000; **61**: 249-260
21 **Yeh CH**, Peng HC, Yang RS, Huang TF. Rhodostomin, a snake venom disintegrin, inhibits angiogenesis elicited by basic fibroblast growth factor and suppresses tumor growth by a selective alpha(v)beta(3) blockade of endothelial cells. *Mol Pharmacol* 2001; **59**: 1333-1342
22 **Markland FS**, Shieh K, Zhou Q, Golubkov V, Sherwin RP, Richters V, Sposto R. A novel snake venom disintegrin that inhibits human ovarian cancer dissemination and angiogenesis in an orthotopic nude mouse model. *Haemostasis* 2001; **31**: 183-191
23 **Da Silva RJ,** da Silva MG, Vilela LC, Fecchio D. Antitumor effect of Bothrops jararaca venom. *Mediators Inflamm* 2002; **11**: 99-104
24 **Yu CL**, Tsai MH. Fetal fetuin selectively induces apoptosis in cancer cell lines and shows anti-cancer activity in tumor animal models. *Cancer Lett* 2001; **166**: 173-184
25 **Wu K**, Zhao Y, Liu BH, Li Y, Liu F, Guo J, Yu WP. RRR-alpha-tocopheryl succinate inhibits human gastric cancer SGC-7901 cell growth by inducing apoptosis and DNA synthesis arrest. *World J Gastroenterol* 2002; **8**: 26-30
26 **Panichakul T**, Wanun T, Reutrakul V, Sirisinha S. Synergistic cytotoxicity and apoptosis induced in human cholangiocarcinoma cell lines by a combined treatment with tumor necrosis factor-alpha (TNF-alpha) and triptolide. *Asian Pac J Allergy Immunol* 2002; **20**: 167-173
27 **Zhang XL**, Liu L, Jiang HQ. Salvia miltiorrhiza monomer IH764-3 induces hepatic stellate cell apoptosis via caspase-3 activation. *World J Gastroenterol* 2002; **8**: 515-519
28 **Sun ZX**, Ma QW, Zhao TD, Wei YL, Wang GS, Li JS. Apoptosis induced by norcantharidin in human tumor cells. *World J Gastroenterol* 2000; **6**: 263-265
29 **Zhang C**, Gong Y, Ma H, An C, Chen D, Chen ZL. Reactive oxygen species involved in trichosanthin-induced apoptosis of human choriocarcinoma cells. *Biochem J* 2001; **355**(Pt3): 653-661
30 **Wang ZM**, Hu J, Zhou D, Xu ZY, Panasci LC, Chen ZP. Trichostatin A inhibits proliferation and induces expressin of p21WAF and p27 in human brain tumor cell lines. *Ai Zheng* 2002; **21**: 1100-1105
31 **Zhao AG**, Zhao HL, Jin XJ, Yang JK, Tang LD. Effects of Chinese Jianpi herbs on cell apoptosis and related gene expression in human gastric cancer grafted onto nude mice. *World J Gastroenterol* 2002; **8**: 792-796
32 **Tu SP**, Zhong J, Tan JH, Jiang XH, Qiao MM, Wu YX, Jiang SH. Induction of apoptosis by arsenic trioxide and hydroxy camptothecin in gastriccancer cells *in vitro*. *World J Gastroenterol* 2000; **6**: 532-539
33 **Du XY**, Clemetson KJ. Snake venom L-amino acid oxidases. *Toxicon* 2002; **40**: 659-665
34 **Strizhkov BN,** Blishchenko EY, Satpaev DK, Karelin AA. Both neurotoxin II from venom of naja naja oxiana and its endogenous analogue induce apoptosis in tumor cells. *FEBS Lett* 1994; **340**: 22-24
35 **Torii S**, Yamane K, Mashima T, Haga N, Yamamoto K, Fox JW, Naito M, Tsuruo T. Molecular cloning and functional analysis of apoxin I, a snake venom-derived apoptosis-inducing factor with L-amino acid oxidase activity. *Biochemistry* 2000; **39**: 3197-3205
36 **Ali SA**, Stoeva S, Abbasi A, Alam JM, Kayed R, Faigle M, Neumeister B, Voelter W. Isolation, structural, and functional characterization of an apoptosis-inducing L-amino acid oxidase from leaf-nosed viper (Eristocophis macmahoni) snake venom. *Arch Biochem Biophys* 2000; **384**: 216-226
37 **Araki S,** Masuda S, Maeda H, Ying MJ, Hayashi H. Involvement of specific integrins in apoptosis induced by vascular apoptosis-inducing protein 1. *Toxicon* 2002; **40**: 535-542
38 **Masuda S**, Ohta T, Kaji K, Fox JW, Hayashi H, Araki S. cDNA cloning and characterization of vascular apoptosis-inducing protein 1. *Biochem Biophys Res Commun* 2000; **278**: 197-204
39 **Zhao S**, Du XY, Chai MQ, Chen JS, Zhou YC, Song JG. Secretory phospholipase A(2) induces apoptosis via a mechanism involving ceramide generation. *Biochim Biophys Acta* 2002; **1581**: 75-88
40 **Cura JE**, Blanzaco DP, Brisson C, Cura MA, Cabrol R, Larrateguy L, Mendez C, Sechi JC, Silveira JS, Theiller E, de Roodt AR, Vidal JC. Phase I and pharmacokinetics study of crotoxin (cytotoxic PLA(2), NSC-624244) in patients with advanced cancer. *Clin Cancer Res* 2002; **8**: 1033-1041
41 **Costa LA**, Miles HA, Diez RA, Araujo CE, Coni Molina CM, Cervellino JC. Phase I study of VRCTC-310, a purified phospholipase A2 purified from snake venom, in patients with refractory cancer: safety and pharmacokinetic data. *Anticancer Drugs* 1997; **8**: 829-834
42 **Fu Q**, Gowda DC. Carbohydrate-directed conjugation of cobra venom factor to antibody by selective derivatization of the terminal galactose residues. *Bioconjug Chem* 2001; **12**: 271-279
43 **Wang XM**, Huang SJ. The selective cytotoxicity of cobra venom factor immunoconjugate on cultured human nasopharyngeal carcinoma cell line. *Hum Exp Toxicol* 1999; **18**: 71-76
44 **Schmitmeier S**, Markland FS, Chen TC. Anti-invasive effect of contortrostatin, a snake venom disintegrin, and TNF-alpha on malignant glioma cells. *Anticancer Res* 2000; **20**: 4227-4233
45 **Juhl H,** Petrella EC, Cheung NK, Bredehorst R, Vogel CW. Additive cytotoxicity of different monoclonal antibody-cobra venom factor conjugates for human neuroblastoma cells. *Immunobiology* 1997; **197**: 444-459
46 **Li HL**, Ren XD, Luo YR, Ye CL, Zhang HW. Effect of serum preparation derived from rabbits after the gastrolavage with Naja naja atra venom on human lung adenocarcinoma cell line. *Jinan Daxue Xuebao* 2001; **22**: 1-5
47 **Li HL**, Ren XD, Luo YR, Ye CL, Zhang HW. Effect of the oral administration with serum preparation of Naja naja atra venom on apoptosis in HepG2 cells. *Zhongguo Binglishengli Zazhi* 2002; **18**: 199-200
48 **Li HL**, Sun P, Ren XD, Luo YR, Ye CL, Zhang HW. A antihepatocarcinoma activity of the oral serum preparation of Naja naja atra venom. *Health Science J Macao* 2002; **2**: 59-61

Edited by Su Q and Wang XL

P.O.Box 2345, Beijing 100023,China
Fax: +86-10-85381893
E-mail: wjg@wjgnet.com www.wjgnet.com

World J Gastroenterol 2003;9(11):2445-2449
World Journal of Gastroenterology
 ISSN 1007-9327

• LIVER CANCER •

Influence of transarterial chemoembolization on angiogenesis and expression of vascular endothelial growth factor and basic fibroblast growth factor in rat with Walker-256 transplanted hepatoma: An experimental study

Xin Li, Gan-Sheng Feng, Chuan-Sheng Zheng, Chen-Kai Zhuo, Xi Liu

Xin Li, Gan-Sheng Feng, Chuan-Sheng Zheng, Chen-Kai Zhuo, Xi Liu, Department of Interventional Radiology, Union Hospital, Tongji Medical College, Huazhong University of Science and Technology, Wuhan 430022, Hubei Province, China
Supported by the National Natural Science Foundation of China, No.39770839
Correspondence to: Dr. Xin Li, Department of Radiology, Union Hospital, Tongji Medical College, Huazhong University of Science and Technology, Wuhan 430022, Hubei Province, China. wxyao2001@yahoo.com.cn
Telephone: +86-27-85726432
Received: 2003-03-02 **Accepted:** 2003-05-11

Abstract

AIM: After transarterial chemoembolization (TACE), the residual cancer cells are under extensive hypoxic or even anoxic environment. Hypoxia can lead to adaptive responses. For example, angiogenesis will help these cells survive. In this study, we examined the effect of TACE on angiogenesis and expression of vascular endothelial growth factor (VEGF) and basic fibroblast growth factor (b-FGF) and to assess their relevance to Walker-256 transplanted hepatoma.

METHODS: Male Wistar rats were inoculated with Walker-256 tumor in the left lobe of liver. Angiography and transarterial chemoembolization were performed at d14 after transplantation. Sixty rats bearing walker-256 transplanted hepatoma were randomly divided into control group, arterial infusion group and TACE group. Each group consisted of twenty rats. Normal saline, 5-Fu, 5-Fu and lipiodol were infused through hepatic artery respectively. Two weeks after the infusion, staining of factor VIII, VEGF and b-FGF was performed by immunohistochemistry method in routine paraffin-embeded sections. Microvessel density (MVD) was counted in endothelial cells with positive factor VIII. Their expression levels were analyzed in conjunction with the pathologic features.

RESULTS: While a smaller tumor volume was found in TACE group (F=37.818, P<0.001), no statistical differences between MVD and expression of VEGF and b-FGF were found among the 3 groups. MVD of the control group, chemotherapy group and chemoemoblization group was 80.84±24.24, 83.05±20.29 and 85.20±23.91 (F=0.193, P=0.873), respectively. The positive expression of VEGF and b-FGF was 75 %, 75 %, 85 % (χ^2=0.449, P=0.799) and 30 %, 25 %, 30 % (χ^2=0.141, P=0.922), respectively. Statistical analysis revealed a positive correlation between the expression of VEGF and MVD (r=0.552, P<0.001).

CONCLUSION: There has been little influence of lipiodol chemoembolization on the formation of tumor angiogenesis, but the development of neovascularization and expression of VEGF play important roles in establishment of collateral circulation and reconstruction of blood supply of residual cancer tissue.

Li X, Feng GS, Zheng CS, Zhuo CK, Liu X. Influence of transarterial chemoembolization on angiogenesis and expression of vascular endothelial growth factor and basic fibroblast growth factor in rat with Walker-256 transplanted hepatoma: An experimental study. *World J Gastroenterol* 2003; 9(11): 2445-2449
http://www.wjgnet.com/1007-9327/9/2445.asp

INTRODUCTION

Transarterial chemoembolization (TACE) has been widely practiced in the treatment of unresectable hepatocellular carcinoma (HCC)[1-5], but long-term TACE therapy was as yet unsatisfactory[6-8]. Histopathologic examination showed although TACE could induce significant necrosis, yet complete tumor necrosis was rare, the residual tumor cells remained viable in the peripheral region, which may play an important role in local recurrence or as a source of metastasis affecting the long-term efficacy of TACE[9-11].

Tissue in hypoxic environment is common in both experimental and human solid tumor[12]. Hypoxia cells have reduced metabolic rate, reduced transcription and translation, even cell cycle arrest. Hypoxia can inhibit cell division or even lead to cell death[13]. But body compensatory reaction can also lead to a wide range of responses including angiogenesis, anti-apoptosis gene expression and changes in metabolic rate at both systemic and cellular levels[14,15]. After TACE, the tumor cells are under extremely hypoxic or even anoxic environment. It is possible that some adaptive responses to hypoxia will help these cells survive, but to our knowledge, studies regarding these are very few.

Recent studies revealed that TACE might enhance the expression of VEGF in meningiomas[16,17]. In the study of hepatoma, TACE could enhance the expression of VEGF[18-21], but not the MVD level[22] or expression of b-FGF[19,22]. All these studies were retrospective.

Walker-256 transplanted hepatoma is a useful model for the study of cancer therapy[20,23,24]. In hepatic arteriography, the tumor is usually hypervascular and receives its blood supply almost exclusively from hepatic artery just as that seen in human HCC[23]. Our study was designed to observe the influence of TACE on the *expression of angiogenesis, VEGF and b-FGF and to assess their relevance to Walker-256 transplanted hepatoma.

MATERIALS AND METHODS

Walker-256 tumor inoculation into the rat livers

Walker-256 carcinoma cells (Cell Preserve Center, Wuhan University, Wuhan, P.R.China) were inoculated subcutaneously

in intact rats. Male Wistar rats (200-250 g) were anesthetized with pentobarbital sodium (30 mg/kg ip), then the tumor was inoculated as described in our previous study[23]. Walker-256 carcinoma cells were inoculated into the subcapsular parenchyma of the left lobe of liver.

Experimental methods

Fourteen days after transplantion, a second laparotomy was performed. A 0.6 mm polyethylene catheter was inserted into the gastroduodenal artery and fixed by a suture. The common hepatic artery and right hepatic artery were temporarily ligated during injection of the drugs. In this study, sixty rats were randomly divided into three groups, twenty rats each group (Table 1).

Table 1 Drug administration in the three groups

Group	Drug administration
Control	0.3 ml normal saline
Arterial infusion (AI group)	5-fluorouracil (5-FU) 20mg/kg
Transarterial chemoembolization (TACE group)	lipiodol ultra-fluis (Andre Guerbet Laboratories, Aulnay-Sous-Bios, France) 0.5ml/kg and 5-Fu 20mg/kg

Tumor volume and degree of tumor necrosis

MR images were performed on 1.5-Tesla system (Siemens Vision, Siemens, Germany) supplemented with a cervical coil. T1-weighted (TR/TE, 450/12 msec) and T2-weighted (TR/TE, 2 800/96 msec) transverse SE images (slice thickness 2 mm) were obtained by acquisition times of 7:25 min and 6:16 min, respectively.

The tumor volume was determined by MR measurements of the largest and smallest diameters and calculated according to the following formula: Tumor volume (mm^3)=largest diameter (mm)×[smallest diameter (mm)]^2/2.

Fourteen days after TACE, hepatoma specimens were obtained and fixed in 10 % formalin for 12 hours, then embedded in paraffin according to routine procedures. The histological sections were stained with hematoxylin-eosin (HE) for observation under light microscopy and measurement of the extent of tumor necrosis.

Immunohistochemistry

Immunohistochemistry was performed in sections from a selected block of each specimen. 5-μm thick sections mounted on 3-aminopropyltrietoxysilane-coated slides were dewaxed in xylene and rehydrated at graded concentrations of alcohol. Endogenous peroxide was blocked with 0.6 %H_2O_2 for 20 min. Then the sections were pretreated in a microwave oven in citrate buffer for 15 min at 95 ℃. Thereafter, the slides were processed according to the standard methods with ABC kit. The primary antibody used was polyclonal antibody of von-Willebrand factor at dilution of 1:100, polyclonal antibodies to VEGF and b-FGF at dilution of 1:50. All these antibodies were from Santa Cruz Biotechnology; Santa Cruz, Calif USA. Diaminobenzine was used for the coloration development. Negative controls were generated by substituting the primary antibody with distilled water.

Determination of MVD

The tumors were frequently inhomogeneous in their microvessel density. For determination of MVD, the five most vascular areas within a section were chosen and counted under a light microscope with a 200-fold magnification as described by Weidner[25]. A brownstain structure clearly separated from the adjacent microvessels was regarded as a single countable microvessel. The average count was recorded as MVD for each case.

Determination of VEGF and b-FGF expression

The counting of VEGF and b-FGF immunoreactive cells was made by scanning and scoring of five high-power fields using ×400 magnification. Positive VEGF and b-FGF were recognized as intensely stained in tumor cell cytoplasm.

The expression of VEGF was semi-quantitatively evaluated as follows. Those having positive staining less than 5 % were regarded as -, between 5 % and 15 % as +, between 15 % and 50 % as 2+, and greater than 50 % as 3+. The b-FGF immunostaining was evaluated by a qualitative method as follows. Positive staining less than 10 % was regarded as negative, greater than 10 % as positive.

Statistical analysis

Statistical analysis was carried out by SPSS packed program. Variance tests, chi-square tests, Mann-Whitney test and linear regression test were used. P value <0.05 based on a two-tailed test was considered statistically significant.

RESULTS

Histopathology findings in tumor

Hematoxylin-eosin (H&E) stained sections of the liver specimens showed poorly-differentiated carcinomas, which were apparently spherical or ovoid in shape. The tumor cells were arranged irregularly with hyperchromatosis, polymorphism and numerous mitoses. The mass was sharply demarcated from the surrounding normal parenchyma, its capsule was thin and composed of collagen fibers caused by tumor compression. The tumor showed inhomogeneous hypervascularization consisting mainly of small arteries and capillaries. Satellite nodules or portal vein tumor thrombus could be seen in some rats.

In TACE group, examination of the sections showed extensive central necrosis of the tumor in all cases. The central necrosis enlarged to moderate (16/20) or severe degree (4/20). Intra-tumoral hemorrhage or bile stases were seen in some, but the tumor cells tended to remain viable at the periphery of the nodules 2 weeks after embolization therapy. We also found thick fibrous capsules with chronic inflammatory and cells infiltration. Various degrees of degeneration and necrosis were seen in normal hepatic parenchyma adjacent to the tumor. In the control and AI groups, the interior of the tumor had many viable tumor cells with spotty and scattered necrosis, the capsules were thin and composed of collagen fibers. Tumor volume and tumor growth rate before and after therapy are listed in Table 2.

Table 2 Tumor volumes and tumor growth rate before and after therapy ($\bar{x}\pm s$)

Group	Tumor volume (mm^3)		Tumor growth rate(%)
	Before therapy	2 weeks after therapy	
Control	195.6±65.9	963.6±214.8	459.2±52.7
AI	218.9±48.7	868.9±179.8	412.2±18.9
TACE	210.2±59.2	356.5±78.4	173.4±20.4
F value	0.272	37.818	197.932
P value	0.764	<0.001	<0.001

Microvessel counts

The von Willebrand Factor (Factor-VIII) antibody gave an intense staining of the vascular endothelial cells (Figure 1). A substantial inhomogeneity in microvessel counts was found

Table 3 MVD counts, expression of VEGF and b-FGF in each group

Group	*n*	MVD ($\bar{x}$±*s*)	VEGF					b-FGF	
			0	+	++	+++	Mean	0	
Control	20	80.80±20.94	5	8	5	2	1.2	14	6
AI	20	83.55±18.26	5	7	6	2	1.25	15	5
TACE	20	85.20±23.91	3	9	5	3	1.4	14	6
Statistic value		*F*=0.193			χ^2=0.449			χ^2=0.141	
P value		*P*=0.873			*P*=0.799			*P*=0.922	

in different areas in the same section. In TACE group, the positive factor VIII cells were found focusing in the newly formed tumor. The MVD of each group is shown in Table 3.

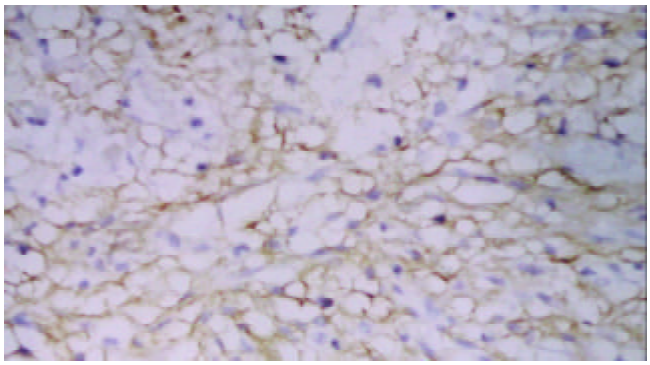

Figure 1 Positive factor-VIII endothelial cells in tumor nest (SABC ×100).

VEGF protein expression and its correlation with MVD

Immunohistochemical staining of VEGF showed strong immunoreactivity in tumor cells and vascular endothelial cells within the tumor tissues (Figure 2). In contrast, non-neoplastic hepatocytes showed weak staining. The staining of VEGF was inhomogeneous. In the sections after TACE, at the tumor nests, boundary of necrotic and non-necrotic area and pericapsular area, VEGF positive tumor cells were relatively easy seen. The expression of VEGF in each group is shown in Table 3.

Linear regression analysis showed a clear correlation between tumor MVD and VEGF protein expression (r=0.452, P<0.01). The MVD counts in negative and positive VEGF groups were 67.86±11.66 and 87.36±22.97 (per high power field), respectively (Table 4).

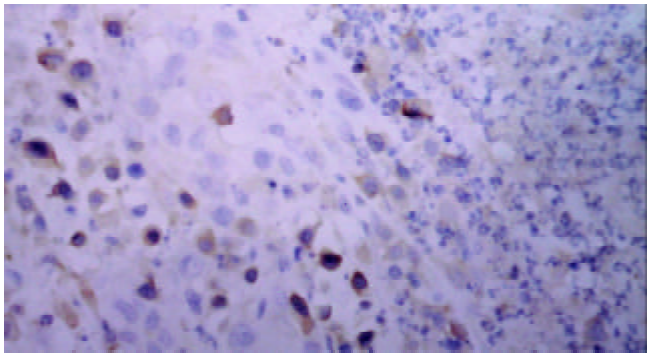

Figure 2 Positive VEGF cells in newly formed tumor nest after TACE (SABC ×200).

b-FGF protein expression and its correlation with MVD

b-FGF protein was identified sporadically in tumor tissues. No statistical differences were found between these groups (P=0.922) (Table 3). There was no correlation between b-FGF and MVD counts (r=0.036, P=0.786).

Table 4 MVD count in negative and positive VEGF groups after TACE

Expression of VEGF	*n*	MVD (per high power field) ($\bar{x}$±*s*)
Negative group	13	67.86±11.66
Positive group	47	87.36±22.97
T value		2.543
P value		0.014

DISCUSSION

Angiogenesis is an inherent property of tumor. It is important in its development and progression. Among many solid tumors, the degree of tumor angiogenesis was closely related to its biological behaviors, which reflect its ability for infiltration, recurrence and metastasis[26-30]. Intratumoral microvessel density (MVD) is commonly used to assess angiogenic activity. Defining and measuring MVD in the residual tumor cells after TACE might help judge the blood supply of residual tumor tissue and prognosticate the activity of these cells to a certain extent indirectly[31].

TACE could hardly abolish tumor blood supply. The possible causes included: incomplete embolization or partial recanalization of the artery, presence of intrahepatic porto-arterial shunt, formation of collateral circulation, and opening of potential communicating vessels[9,32,33]. The present study suggested that neovascularization and expression of VEGF might be another important factor. At the newly formed tumor nests, abundant factor VIII and positive VEGF cells could be found, and slight necrosis was seen in regions that had abundant neovasculature. These suggest that neovascularization plays an important role in the formation of collateral circulation, and relatively abundant blood supply will help tumor cells escape from the damage by TACE and increase the opportunity of survival.

Some authors considered that TACE might increase the chance of tumor recurrence or metastasis[20,34,35], which might be related to hypoxia caused by TACE and increased level of angiogenesis due to hypoxia[36-38]. The present study showed that MVD of TACE group was slightly higher than that of the control group and AI group, but no statistical difference was found, suggesting that TACE would not increase the level of tumor angiogenesis. Although the exact mechanism is currently unclear, we consider the possible explanation would be that the tumor cells were in an extreme hypoxia or even anoxia environment for a longer duration after TACE, which resulted in extensive necrosis and apoptosis of timorous and endothelial cells and decrease of secretion of angiogenic factor and weakening of the paracrine effect.

The intratumoral distribution of tumor neovasculature was inhomogeneous after embolization therapy. The newly formed blood vessels were less in the center of tumor but much more in the periphery and subcapsular area. This phenomenon might be related to the characteristics of tumor blood supply. Although blood supply of the tumor mainly came from hepatic artery, the peripheral area also received portal blood. There

were potential collateral circulations both between the artery-portal veins and between the lobular arteries. After TACE, the portal blood supply increased with opening of collateral circulation, the blood supply of the peripheral region of the tumor restored more easily.

A balance between angiogenic and angiostatic factors regulates the angiogenesis. These factors may be produced either by tumor cells or host cells. The most commonly studied angiogenic factors were VEGF and b-FGF. VEGF could stimulate endothelia cells to proliferate, migrate, and alter their patterns of gene expression, increase microvascular hyperpermeability, extravasate plasma proteins into extravascular space and induce plasma-derived matrix[39,40]. VEGF played a key role in tumoral angiogenesis, it could induce neovascularization and was considered to be crucial in tumor biology[41,42]. b-FGF had synergistic effects with VEGF[43].

In the present study, the expression of VEGF was slightly higher in TACE group than in the control and AI groups, but no statistical difference was found. There was a significant correlation between MVD and VEGF expression. MVD counts in positive VEGF group were much higher than in negative VEGF group. At the newly formed tumor nests, the boundary of necrotic and non-necrotic area and the subcapsular area, positive VEGF tumor cells were more abundant and this was consistent with the distribution of neovasculature. Taken together, the results in the current study strongly suggested that VEGF played a key role in the formation of tumor neovasculature after TACE.

In conclusion, the influence of lipiodol chemoembolization on formation of tumor angiogenesis is relatively limited, but the development of neovascularization and expression of VEGF play important roles in establishing collateral circulation and reconstructing blood supply of residual cancer tissue.

REFERENCES

1 **Rose DM**, Chapman WC, Brockenbrough AT, Wright JK, Rose AT, Meranze S, Mazer M, Blair T, Blanke CD, Debelak JP, Pinson CW. Transcatheter arterial chemoembolization as primary treatment for hepatocellular carcinoma. *Am J Surg* 1999; **177**: 405-410

2 **Zhang Z**, Liu Q, He J, Yang J, Yang G, Wu M. The effect of preoperative transcatheter hepatic arterial chemoembolization on disease-free survival after hepatectomy for hepatocellular carcinoma. *Cancer* 2000; **89**: 2606-2612

3 **Poyanli A**, Rozanes I, Acunas B, Sencer S. Palliative treatment of hepatocellular carcinoma by chemoembolization. *Acta Radio* 2001; **42**: 602-607

4 **Chen MS**, Li JQ, Zhang YQ, Lu LX, Zhang WZ, Yuan YF, Guo YP, Lin XJ, Li GH. High-dose iodized oil transcatheter arterial chemoembolization for patients with large hepatocellular carcinoma. *World J Gastroenterol* 2002; **8**: 74-78

5 **Saccheri S**, Lovaria A, Sangiovanni A, Nicolini A, De Fazio C, Ronchi G, Fasani P, Del Ninno E, Colombo M. Segmental transcatheter arterial chemoembolization treatment in patients with cirrhosis and inoperable hepatocellular carcinomas. *J Vasc Interv Radiol* 2002; **13**: 995-999

6 **Llad inverted question marko L,** Virgili J, Figueras J, Valls C, Dominguez J, Rafecas A, Torras J, Fabregat J, Guardiola J, Jaurrieta E. A prognostic index of the survival of patients with unresectable hepatocellular carcinoma after transcatheter arterial chemoembolization. *Cancer* 2000; **88**: 50-57

7 **Ueno K**, Miyazono N, Inoue H, Nishida H, Kanetsuki I, Nakajo M. Transcatheter arterial chemoembolization therapy using iodized oil for patients with unresectable hepatocellular carcinoma: evaluation of three kinds of regimens and analysis of prognostic factors. *Cancer* 2000; **88**: 1574-1581

8 **Chan AO**, Yuen MF, Hui CK, Tso WK, Lai CL. A prospective study regarding the complications of transcatheter intraarterial lipiodol chemoembolization in patients with hepatocellular carcinoma. *Cancer* 2002; **94**: 1747-1752

9 **Higuchi T**, Kikuchi M, Okazaki M. Hepatocellular carcinoma after transcatheter hepatic arterial embolization. *Cance* 1994; **73**: 2260-2267

10 **Lin Z**, Ren Z, Xia J. Appraisal of postoperative transcatheter arterial chemoembolization (TACE) for prevention and treatment of hepatocellular carcinoma recurrence. *Zhonghua Zhongliu Zazhi* 2000; **22**: 315-317

11 **Lee JK**, Chung YH, Song BC, Shin JW, Choi WB, Yang SH, Yoon HK, Sung KB, Lee YS, Suh DJ. Recurrences of hepatocellular carcinoma following initial remission by transcatheter arterial chemoembolization. *J Gastroenterol Hepatol* 2002; **17**: 52-58

12 **Harrington EA**, Fanidi A, Evan GI. Oncogenes and cell death. *Curr Opin Genet Dev* 1994; **4**: 120-129

13 **Schmaltz C**, Hardenbergh PH, Wells A, Fisher DE. Regulation of proliferation-survival decisions during tumor cell hypoxic. *Mol Cell Biol* 1998; **18**: 2845-2854

14 **Semenza GL**, Roth PH, Fang HM, Wang GL. Transcriptional regulation of genes encoding glycolytic enzymes by hypoxia-inducible factor 1. *J Biol Chem* 1994; **269**: 23757-23763

15 **Hockel M**, Schlenger K, Aral B, Mitze M, Schaffer U, Vaupel P. Association between tumor hypoxic and malignant progression in advanced cancer of the uterine cervix. *Cancer Res* 1996; **56**: 4509-4515

16 **Jensen RL**, Soleau S, Bhayani MK, Christiansen D. Expression of hypoxic inducible factor-1 alpha and correlation with preoperative embolization of meningiomas. *J Neurosurg* 2002; **97**: 658-667

17 **Park K**, Kim JH, Nam DH, Lee JI, Kim JS, Hong SC, Shin HJ, Eoh W, Park K. Vascular endothelial growth factor expression under ischemic stress in human meningiomas. *Neurosci Lett* 2000; **283**: 45-48

18 **An FQ**, Matsuda M, Fujii H, Matsumoto Y. Expression of vascular endothelial growth factor in surgical specimens of hepatocellular carcinoma. *J Cancer Res Clin Oncol* 2000; **126**: 153-160

19 **Shao G**, Wang J, Zhou K, Yan Z. Intratumoral microvessel density and expression of vascular endothelial growth factor in hepatocellular carcinoma after chemoembolization. *Zhonghua Ganzangbing Zazhi* 2002; **10**: 170-173

20 **Guo WJ**, Li J, Ling WL, Bai YR, Zhang WZ, Cheng YF, Gu WH, Zhuang JY. Influence of hepatic arterial blockage on blood perfusion and VEGF, MMP-1 expression of implanted liver cancer in rats. *World J Gastroenterol* 2002; **8**: 476-479

21 **Miyazaki M**, Shimoda T, Itoh H. Enhancement of cytotoxicity of doxorubicin by verapamil in the hepatic artery infusion for liver tumors in rats. *Cancer* 1993; **72**: 349-354

22 **Shao G**, Wang J, Zhou K, Yan Z. Intratumoral microvessel density and expression of vascular endothelial growth factor in hepatocellular carcinoma after chemoembolization. *Zhonghua Ganzangbing Zazh* 2002; **10**: 170-173

23 **Li X**, Zheng CS, Feng GS, Zhuo CK, Zhao JG, Liu X. An implantable rat liver tumor model for experimental transarterial chemoembolization therapy and its imaging features. *World J Gastroenterol* 2002; **8**: 1035-1039

24 **Yang R**, Rescorla FJ, Reilly CR, Faught PR, Sanghvi NT, Lumeng L, Franklin TD, Grosfeld JL. A reproducible rat liver cancer model for experimental therapy: introducing a technique of intrahepatic tumor implantation. *J Surg Res* 1992; **52**: 193-198

25 **Weidner N**, Carroll PR, Flax J, Blumenfeld W, Folkman J. Tumor angiogenesis correlates with metastasis in invasive prostate carcinoma. *Am J Pathol* 1993; **143**: 401-409

26 **Folkman J**. Role of angiogenesis in tumor growth and metastasis. *Semin Oncol* 2002; **29**: 15-18

27 **Takeda A**, Stoeltzing O, Ahmad SA, Reinmuth N, Liu W, Parikh A, Fan F, Akagi M, Ellis LM. Role of angiogenesis in the development and growth of liver metastasis. *Ann Surg Oncol* 2002; **9**: 610-616

28 **Koide N**, Nishio A, Hiraguri M, Shimada K, Shimozawa N, Hanazaki K, Kajikawa S, Adachi W, Amano J. Cell proliferation, apoptosis and angiogenesis in gastric cancer and its hepatic metastases. *Hepatogastroenterology* 2002; **49**: 869-873

29 **Qin LX**, Tang ZY. The prognostic molecular markers in hepatocellular carcinoma. *World J Gastroenterol* 2002; **8**: 385-392

30 **Skobe M**, Rockwell P, Goldstein N, Vosseler S, Fusenig NE. Halting angiogenesis suppresses carcinoma cell invasion. *Nature Med* 1997; **11**: 1222-1227

31 **Hasan J**, Byers R, Jayson GC. Intra-tumoral microvessel density

in human solid tumours. *Br J Cancer* 2002; **86**: 1566-1577
32 **Matsui O**, Kawamura I, Takashima T. Occurrence of an intrahepatic porto-arterial shunt after hepatic artery embolization with Gelfoam powder in rats and rabbits. *Acta Radiol Diagn* 1986; 27: 119-122
33 **Demachi H**, Matsui O, Takashima T. Scanning electron microscopy of intrahepatic microvasculature casts following experimental hepatic artery embolization. *Cardiovasc Intervent Radiol* 1991; **14**: 158-162
34 **Liou TC**, Shih SC, Kao CR, Chou SY, Lin SC, Wang HY. Pulmonary metastasis of hepatocellular carcinoma associated with transarterial chemoembolization. *J Hepatol* 1995; **23**: 563-568
35 **Hanazaki K**, Kajikawa S, Shimozawa N, Mihara M, Shimada K, Hiraguri M, Koide N, Adachi W, Amano J. Survival and recurrence after hepatic resection of 386 consecutive patients with hepatocellular carcinoma. *J Am Coll Surg* 2000; **191**: 381-388
36 **Shweiki D**, Itin A, Soffer D, Keshet E. Vascular endothelial growth factor induced by hypoxic may mediate hypoxic-initiated angiogenesis. *Nature* 1992; **359**: 843-845
37 **Hockel M**, Vaupel P. Biological consequences of tumor hypoxic. *Semin Oncol* 2001; **28**: 36-41
38 **Giatromanolaki A**, Harris AL. Tumor hypoxic, hypoxic signaling pathways and hypoxic inducible factor expression in human cancer. *Anticancer Res* 2001; **21**: 4317-4324
39 **Dvorak HF**, Brown L, Detmar M, Dvorak AM. Vascular permeability factor/vascular endothelial growth factor, microvascular hyperpermeability, and angiogenesis. *Am J Pathol* 1995; **146**: 1029-1039
40 **Dvorak HF**. Vascular permeability factor/vascular endothelial growth factor: a critical cytokine in tumor angiogenesis and a potential target for diagnosis and therapy. *J Clin Oncol* 2002; **20**: 4368-4380
41 **Park YN**, Boros P, Zhang DY, Sheiner P, Kim-Schluger L, Thung SN. Increased expression of vascular endothelial growth factor and angiogenesis in the early stage of multistep hepatoarcinogenesis. *Arch Pathol Lab Med* 2000; **124**: 1061-1065
42 **O'Byrne KJ**, Dalgleish AG, Browning MJ, Steward WP, Harris AL. The relationship between angiogenesis and the immune responses in carcinogenesis and the progression of malignant disease. *Eur J Cancer* 2000; **36**: 151-169
43 **Asahara T**, Bauters C, Zheng LP, Takeshita S, Bunting S, Ferrara N, Symes JF, Isner JM. Synergistic effect of vascular endothelial growth factor and basic fibroblast growth factor on angiogenesis *in vivo*. *Circulation* 1995; **92**: II365-371

Edited by Wu XN and WangXL

P.O.Box 2345, Beijing 100023,China
Fax: +86-10-85381893
E-mail: wjg@wjgnet.com www.wjgnet.com

World J Gastroenterol 2003;9(11):2450-2454
World Journal of Gastroenterology
 ISSN 1007-9327

• LIVER CANCER •

Expression of p27, cyclin E and cyclin A in hepatocellular carcinoma and its clinical significance

Qi Zhou, Qiang He, Li-Jian Liang

Qi Zhou, Qiang He, Li-Jian Liang, Department of Hepatobilliary Surgery, the First Affiliated Hospital of Sun Yat-Sen University, Guangzhou 510080, Guandong Province, China
Correspondence to: Professor Li-Jian Liang, Department of Hepatobilliary Surgery, the First Affiliated Hospital of Sun Yat-Sen University, Guangzhou 510080, Guandong Province, China. lianglj@medmail.com.cn
Telephone: +86-20-87755766-8096 **Fax:** +86-20-87755766-8663
Received: 2003-05-13 **Accepted:** 2003-06-02

Abstract

AIM: To investigate the expression of p*27*, cyclin E and cyclin A in hepatocellular carcinoma (HCC) and its potential clinical significance.

METHODS: Expression of p27, cyclin E and cyclin A in 45 HCC specimens and 30 adjacent noncancerous lesions obtained from 45 patients during surgery was examined by immunohistochemical SABC assay. The diameter of tumor ranged from 1 cm to 19 cm (d≤5 cm, 9 samples; 5 cm<d≤ 10 cm, 19 samples; d>10 cm, 17 samples). The tumors were graded according to the criteria described by Edmondson-Steiner: well-differentiated HCC group (Grade I+II), 26 samples; poorly-differentiated HCC group (Grade III+IV), 19 samples. According to the clinical-pathologic features, 19 samples were poorly encapsulated, 15 samples had portal invasion of cancer, 11 samples had extrahepatic metastasis, and 12 samples had intrahepatic metastasis. All of the samples were classified as the invasive and metastatic group, while the remaining was classified as the non-invasive and non- metastatic group.

RESULTS: The average labeling index (LI) of p27 in HCC lesions was significantly higher than that in adjacent noncancerous lesions (45.87±14.21 *vs* 33.77±12.92, t=3.745, P<0.001). The LI of p27 was associated with differentiation, invasiveness and metastasis of the tumors (34.46±12.29 *vs* 52.80±11.36, t=5.17; 41.42±12.86 *vs* 51.44±14.10, t=2.48; P<0.05). Cyclin E was overexpressed in 16 cases (35.6 %) while cyclin A was overexpressed in 21 cases (46.7 %) in HCC lesions. No overexpression of cyclin E or cyclin A could be observed in adjacent non-carcinoma lesions and normal liver tissues. The overexpressions of cyclin E and cyclin A were correlated with differentiation, tumor thrombus, invasiveness and metastasis (P<0.05). Expression of cyclin E was significantly correlated with expression of cyclin A (r=0.329, P<0.05). The LI of p27 was significantly decreased in cyclin E, cyclin A positive groups (40.33±11.91 *vs* 49.50±13.76, t=3.05; 38.86±11.19 *vs* 52.57±12.62, t=3.89; P<0.05).

CONCLUSION: p27, cyclin E, cyclin A play cooperative roles in HCC tumorigenesis, differentiation, invasiveness and metastasis. Detection of their expression may be helpful in prediction of tumor progression.

Zhou Q, He Q, Liang LJ. Expression of p27, cyclin E and cyclin A in hepatocellular carcinoma and its clinical significance. *World J Gastroenterol* 2003; 9(11): 2450-2454
http://www.wjgnet.com/1007-9327/9/2450.asp

INTRODUCTION

Hepatocellular carcinoma is one of the most common malignant tumors in China and has poor prognosis due to its high incidence of recurrence and metastasis. Recent studies on HCC have been focused on tumorigenesis, progression, invasiveness as well as novel strategy of therapeutics.

It has been implicated that the activity of cell proliferation is directly associated with tumorigenesis, progression and invasiveness. Therefore estimation of cell proliferative activity is important in prediction of the biological aggressiveness of tumor cells. The regulatory molecules of cell cycle are parameters for the prediction of cell proliferative activity[1]. Cell cycle progression is controlled by protein complexes such as cyclins, cyclin dependent kinases (CDKs) and cyclin dependent kinase inhibitors (CDKIs). The sequential activation and subsequent inactivation of cyclin-CDK complexes govern the progression of eukaryatic cells throughout cell cycle[2]. In cell cycle, the period from the late G1 to S phase is the most important restriction point for cell proliferation. Whether cells pass the G1/S restriction point determines the continuity of cell proliferation[3]. The most direct protein at G1/S point is retinoblastoma protein (pRb)[4]. Phosphorylated pRb can bind to transcription factor (E2F) that regulates cell cycle by activation of DNA synthesis. Both cyclin E and cyclin A play important roles in G1/S restriction point[5,6]. Cyclin E dramatically increases from the late G1 phase to the early S phase[5] which binds to CDK2 and phosphorylates pRb. When cell enters S phase, cyclin E and cyclin A-CDK2 complex cooperate continuously for the phosphorylation of pRb until the end of M phase[6]. As one of CDKIs, p27 can prevent pRb from phosphorylation and arrest the cell cycle at G1 phase[7]. Cyclin E and cyclin A are direct substrates of p27. Recent researches have shown that the activity of p27 protein can be up-regulated by multiple tumorigenesis related factors such as transforming growth factor β[8], interferon[9] and cAMP[10]. The expression of p27 has been implicated in the tumorigenesis of many kinds of tumors[11-15]. However, little is known about the association between cyclins and hepatocellular carcinoma. In the present study, we detected the expression of p27, cyclin E and cyclin A in 45 HCC samples and 30 adjacent noncancerous lesions by immunohistochemical assay to elucidate their correlation with tumorigenesis, progression and metastasis of HCC.

MATERIALS AND METHODS

Data of patients

From 1998 to 1999, 45 HCC specimens and 30 adjacent noncancerous lesions were obtained from 45 patients with HCC during surgery in our hospital. A senior pathologist made the final diagnosis on the basis of histological examination. No patient had received radioactive therapy, chemotherapy,

transcatheter arterial chemoembolization or immunotherapy before operation. There were 36 (80 %) males and 9 (20 %) females, aged from 30 to 65 with an average age of 45±11. A total of 30 (66.67 %) patients had AFP levels over 400 ng/ml, 32 (71.1 %) patients were HbsAg positive. The diameter of tumor in this group ranged from 1 cm to 19 cm (less than 5 cm in 9 samples, 5 cm to 10 cm in 19 samples, more than 10 cm in 17 samples). These tumors were graded based on the criteria of Edmondson-Steiner (Grade I+II in 26 samples, grade III+IV in 19 samples). According to the clinical-pathologic features, 19 specimens had no or little capsule, 12 samples had portal vein invasion of the tumors, 11 samples had extrahepatic metastasis and 12 samples had intrahepatic metastasis. The criteria for invasiveness or metastasis of tumor were the tumor tissue with no or poor capsule, or portal vein invasion, or intrahepatic or extrahepatic metastasis[16]. Twenty-five cases (55.56 %) were defined as invasive/metastatic group.

Tissue sampling

Fresh surgical tissue samples were fixed immediately in formaldehyde solution for 12-24 h and paraffin-embedded for immunohistochemical assay.

Immunohistochemical assay

Immunohistochemical study was performed using avidin-biotin-complex method. Briefly, 4 μm slices of tissue section were deparaffinized and rehydrated. Endogenous peroxidase activity was blocked with 0.3 % hydrogen peroxide for 10 min. Sections were then incubated with 0.03 mol/L citrate buffer (pH=6.0) and heated in microwave oven for 10 min. After three times of rinsing with phosphate-buffered saline (PBS) (pH=7.4), the slides were incubated with 10 % normal goat serum at room temperature for 20 min to block the nonspecific reaction, and incubated overnight with primary antibody (p27 monoclonal antibody 1:50, cyclin E polyclonal antibody 1:50 and cyclin A polyclonal antibody 1:100) at 4 ℃. After rinsed in PBS, they were incubated with second antibody (1:100) for 30 min at room temperature, and reacted with the avidin-biotin peroxidase complex at a concentration of 1:100 for 30 min after washed in PBS. The peroxidase reaction was visualized by incubating the section with 0.01 % 3,3'-diaminobenzidine tetrahydrochloride and hydrogen peroxide mixture. The slides were counterstained with hematoxylin. In negative control, primary antibody was replaced by normal mouse serum.

Immunohistochemical evaluation

The protein reaction (p27, cyclin E or cyclin A) was considered as positive when nuclei showed staining signals. At least 500 *p*27 positive cells from at least 5 randomly selected fields (×400) were counted[17]. When the positive rate for each protein of carcinoma cells was over 5 %, overexpression of cyclin E and cyclin A was defined according to the report[18,19].

Statistical analyses

The correlation of *p*27, cyclin E or cyclin A with carcinogenesis, differentiation, invasion and metastasis of HCC was analyzed with SPSS8.0 software. The χ^2 test and Student *t* test were employed for analyses, *P* value less than 0.05 was regarded as statistically significant.

RESULTS

*p*27 was expressed both in HCC and in adjacent noncancerous lesions (Figures 1,2). The average LI of p27 in HCC lesions was significantly higher than that in adjacent noncancerous lesions (45.87±14.21 *vs* 33.77±12.92, *P*<0.001). The LI of p27 was associated with differentiation, tumor size, invasiveness and metastasis of HCC (*P*<0.05). No correlation was found between the LI of p27 and the number of cancer foci (Table 1).

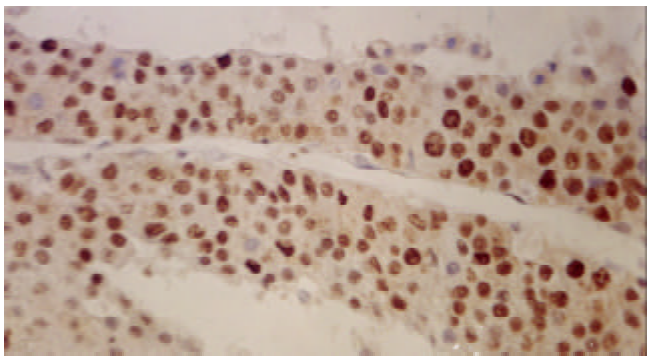

Figure 1 Nuclear staining of p27 protein in HCC (SABC, 400×).

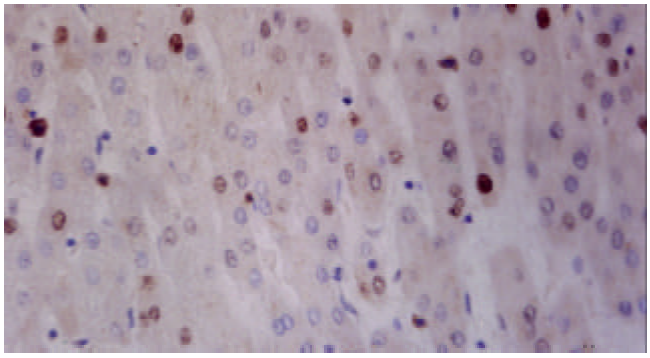

Figure 2 Nuclear staining of p27 protein in adjacent noncancerous lesions (SABC, 400×).

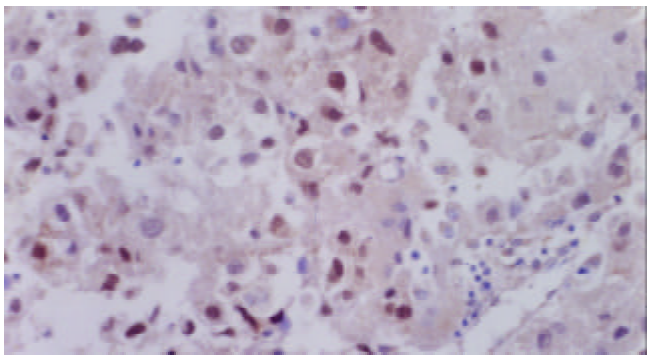

Figure 3 Nuclear staining of cyclin E protein in HCC (SABC, 400×).

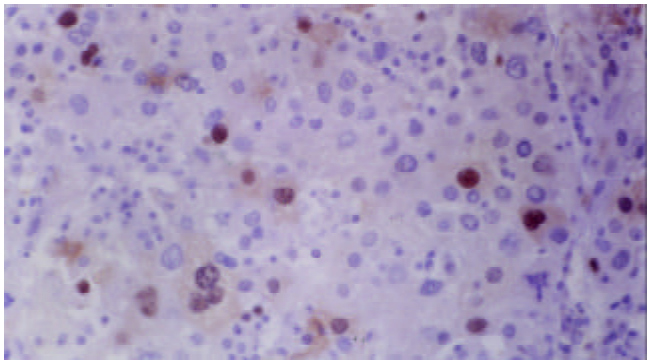

Figure 4 Nuclear staining of cyclin A protein in HCC (SABC, 400×).

Table 1 Expression of p27 and pathological features ($\bar{x}\pm s$)

Groups		*n*	p27 LI($\bar{x}\pm s$)		*P*
Histological grade	I+II	26	52.80±11.36	*t*=5.17	<0.001
	III+IV	19	34.46±12.29		
Tumor size (d)	≤5 cm	9	53.28±15.17	*F*=5.934	<0.005
	5 cm<d≤10 cm	19	49.50±10.96		
	>10 cm	17	37.59±13.12		
Envelope	Full	26	48.82±13.35	*t*=1.76	>0.05
	Rupture	19	41.54±14.15		
Tumor thrombi	+	13	36.83±12.74	*t*=2.77	<0.01
	-	32	49.16±13.41		
Metastasis	Positive	11	35.52±11.70	*t*=3.02	<0.05
	Negative	34	49.22±13.43		
Number	<2	33	47.65±15.08	*t*=1.41	>0.05
	≥2	12	40.98±10.52		
Non-invasive and non- metastatic group		20	51.44±14.10	*t*=2.48	<0.02
Invasive and metastatic group		25	41.42±12.86		

Table 2 Expression of cyclin E, cyclin A and pathological features

Group		*n*	Cyclin E		Cyclin A	
			+	χ^2 / *P*	+	χ^2 / *P*
Histological grade	I+II	26	5 (19.23 %)	7.16 / <0.05	8 (30.77 %)	6.25 / <0.05
	III+IV	19	11 (57.89 %)		13 (68.42 %)	
Tumor size (d)	≤5 cm	9	1 (11.11 %)	1.58 / >0.05	5 (55.56 %)	1.29 / >0.05
	5<d≤10 cm	19	7 (36.84 %)		7 (36.84 %)	
	>10 cm	17	8 (47.06 %)		9 (52.94 %)	
Envelope	Full	26	7 (26.92 %)	2.00 / >0.05	10(38.46 %)	1.67 / >0.05
	Rupture	19	9 (47.37 %)		11 (57.89 %)	
Tumor thrombi	+	13	8 (61.54 %)	5.38 / <0.01	10 (76.92 %)	6.72 / <0.01
	-	32	8 (25.00 %)		11 (34.38 %)	
Metastasis	Positive	11	6 (54.55 %)	1.32 / >0.05	9 (81.82 %)	7.23 / <0.01
	Negative	34	10 (29.41 %)		12 (35.29 %)	
Number	<2	33	9 (27.28 %)	2.47 / >0.05	12 (36.36 %)	5.76 / <0.05
	≥2	12	7 (58.33 %)		9 (75.00 %)	
Non-invasive and non- metastatic group			4 (20.00 %)	3.86 / <0.05	4 (20.00 %)	9.95 / <0.01
Invasive and metastatic group			12 (48.00 %)		17 (68.00 %)	

The overexpression of cyclin E and cyclin A could be exclusively seen in HCC (Figures 3,4), the overexpression rate was 35.6 %(16/45) for cyclin E and 46.7 %(21/45) for cyclin A. The overexpression of cyclin E and cyclin A was associated with differentiation, invasiveness and metastasis of HCC (P<0.05). No correlation could be found between the LI of p27 and the tumor size (P>0.05)(Table 2).

The LI of p27 decreased significantly both in cyclin E and in cyclin A overexpressed tissues (40.33±11.91 *vs* 49.50±13.76, 38.86±11.19 *vs* 52.57±12.62, P<0.05). The overexpression of cyclin E was significantly correlated with that of cyclin A (P<0.05, r=0.329), (Table 3).

Table 3 Relationship between expressions of cyclin E and cyclin A

		Cyclin A		*P*
		+	-	
cyclin E	+	11	5	<0.05
	-	10	19	

DISCUSSION

Uncontrollable proliferation is the property of tumor cells. Cell proliferation activity involves in tumorigenesis and progression, and is one of the prominent parameters in evaluating the biological aggressiveness of carcinoma.

As one of the major CDK inhibitors, p27 can arrest cell cycle by blocking phosphorylation of pRB. Its substrate is G1 cyclins such as cyclin E and cyclin A. Low p27 protein levels were found in aggressive stomach[11], lung[12], prostate[13], breast[14] and pituitary[15] cancers, suggesting that p27 might suppress the progression of tumor[20].

Our data showed that the LI of p27 was higher in HCC than in adjacent noncancerous tissues, and the expression of p27 was mainly localized in nuclei. This might suggest that p27 works as a positive regulator in tumorigenesis of HCC. Two possible mechanisms could be involved. First, p27 might be regulated by self-stabilization. It has been demonstrated[21] that expression of p27 was regulated primarily at the posttranscriptional level and its mRNA level was stable throughout the cell cycle. When cells are stimulated by

mitogen, p27 protein undergoes rapid degradation via the ubiquitin-proteasome pathway. However, this proteolysis was dramatically reduced in resting cells[22]. Thus, increased expression of p27 in some tumors may be resulted from self-stable regulating mechanism by which increased expression of cyclins attenuates the activity of the proteasome pathway for p27, and then causes an increased expression of free p27 protein that can counteract the increased cyclins in tumorigenesis. Second, gene mutation may also be responsible for this situation. Recent studies have revealed a gene deletion and polymorphism in primary breast cancer and leukemia[23,24]. Whether increased expression of p27 in HCC is caused by mutant protein remains to be elucidated.

In the present study, the expression of p27 was decreased in cases with biologically aggressive phenotypes such as poor differentiation, metastasis and invasiveness. It has been reported that cultured tumor cells expressed more p27 as they grew from single layer to tri-dimension and cell contact inhibition could be suppressed by p27 antisense oligonucleotide[25]. All these suggested that decreased expression of p27 was related with tumor progression and could be used as a potential prediction factor for HCC.

Although many researchers focused on the role of cyclin E and cyclin A in cell cycle in tumor cells[26,27], few studies have ever addressed on the aspect of HCC. Our data showed that cyclin E and cyclin A proteins were exclusively expressed in HCC but not in adjacent noncarcinous lesions. The expression of cyclin E and cyclin A was mainly localized in nuclei, suggesting that overexpression of cyclin E and cyclin A could promote cell cycle and cell proliferation, and therefore was associated with tumorigenesis. Cyclin E expressed in cytoplasm of tumor cell may be caused by increased synthesis, decreased degradation and failure to transportation. Our data also showed that overexpression rate of cyclin E and cyclin A was associated with low histological grade of tumors with high expression rate in poorly differentiated tumors, suggesting the overexpression of cyclin E and cyclin A was associated with poor differentiation. Overexpression of cyclin E was correlated with formation of tumor thrombi, while overexpression of cyclin A was associated with tumor thrombi, metastasis and satellite lesions. Thus overexpression of cyclin E and cyclin A is linked to tumor invasiveness and metastasis potency, suggesting a poor prognosis for patients with overexpression of cyclin E and cyclin A. Patients with cyclin E overexpression had a four-year survival rate[28] and overexpression of cyclin A had a positive relationship with the amount of cells at S-phase and a reverse correlation with the four-year survival rate[18]. Our data were partially similar to these findings. Unfortunately, we were unable to evaluate the correlation of overexpression of cyclin E and cyclin A with the prognosis due to incomplete follow-up data of the patients.

p27 suppresses cyclin/CDK complexes mainly by binding itself to cyclins. It has been reported that p27 could bind to CDK2 and played an inhibitory role in regenerating liver[29]. Zerfass-Thome[30] reported that p27 arrested cell cycle by blocking transactivation of cyclin-A gene which is dependent on cyclin-E gene expression, suggesting a mechanism of interaction among p27, cyclin E and cyclin A. The lower p27 LI in positive cyclin E and cyclin A group in our study might be resulted from the interaction of cyclin-CDK complexes that can suppress its expression. And expression of cyclin E had a positive relationship with expression of cyclin A. These suggest that p27, cyclin E and cyclin A play cooperatively important roles in tumorigenesis, differentiation, aggressiveness and metastasis of HCC.

Although a lot of studies on cyclins/CDKI have been done, many questions remain to be answered. It has been reported that proliferative tumor cells *in vitro* could be arrested in G1 phase by using antibody IgM against cyclin E and cyclin A in culture[31]. Other studies *in vivo* showed that invasiveness of tumor could be dramatically suppressed by down-regulation of G1 and S phase proteins[32]. It seems that cyclins may become potential targets for tumor therapy in the near future. Further studies are needed to elucidate the mechanism of interaction among cyclins and the pathway of regulation before they can finally be used as a novel strategy for prediction of prognosis and therapeutics of HCC.

REFERENCES

1 **Sheer CJ**. Cancer cell cycles. *Science* 1996; **274**: 1672-1678
2 **Draetta GF**, Mammalian G. Cyclins. *Curr Opin Cell Biol* 1994; **6:** 842-846
3 **Hartwell LA**, Weinnert TA. Checkpoints: control that ensure the order of cell cycle events. *Science* 1989; **246**: 629-634
4 **Toyoshima H,** Hunter T. p27, a novel inhibitor of G1 Cyclin dependent kinase protein kinase activity is related to p21. *Cell* 1994; **78**: 67-71
5 **Wimmel A,** Lucibello FC, Sewing A, Adolph S, Muller R. Wimmel A. Inducible acceleration of G1 Progression through tetra cycline-regulated expression of human cyclin E. *Oncogene* 1994; **9**: 995-997
6 **Pagano M,** Pepperkok R, Verde F, Ansorge W, Draetta G. Pagano M. Cyclin A is required at two points in the human cell cycle. *EMBO J* 1992; **11**: 961-967
7 **Hengst T**, Reed SI. Translational control of p27kip1 accumulation during the cell cycle. *Science* 1996; **271**: 1861-1864
8 **Polyak K,** Kato JY, Solomon MJ, Sherr CJ, Massague J, Roberts JM, Koff A. p27kipl, a Cyclin dependent kinase inhibitor, links transforming growth factor-β and contact inhibition to cell cycle arrest. *Genes Dev* 1994; **8**: 9-17
9 **Harvat BL**, Seth P, Jetten AM. The role of p27kip1 in gamma interferon mediated growth arrest of mammary epithelial cells and related defects in mammary carcinoma cell. *Oncogene* 1997; **372**: 570-573
10 **Kato JY,** Matsuoka M, Polyak K, Massague J, Sherr CJ. Cyclin AMP induce G1 phase arrest mediated by an inhibitor (p27kip1) of Cyclin dependent kinase 4 activation. *Cell* 1994; **79**: 487-495
11 **Ohtani M,** Isozaki H, Fujii K, Nomura E, Niki M, Mabuchi H, Nishiguchi K, Toyoda M, Ishibashi T, Tanigawa N. Impact of the expression of Cyclin dependent kinase inhibitor p27kip1 and apoptosis in tumor cells on the overall survival of the patients with non-early stage of gastric carcinomas. *Cancer* 1999; **85**: 1711-1718
12 **Esposito V,** Baldi A, De Luca A, Groger AM, Loda M, Giordano GG, Caputi M, Baldi F, Pagano M, Giordano A. Prognostic role of Cyclin dependent kinase inhibitor p27 in non-small cell lung cancer. *Cancer Res* 1997; **57**: 3381-3385
13 **Tsihlias J,** Kapusta LR, DeBoer G, Morava-Protzner I, Zbieranowski I, Bhattacharya N, Catzavelos GC, Klotz LH, Slingerland JM. Loss of Cyclin dependent kinase inhibitor p27kip1 is a novel prognostic factor in located human prostate adenocarcinoma. *Cancer Res* 1998; **58**: 542-548
14 **Tan P,** Cady B, Wanner M, Worland P, Cukor B, Magi-Galluzzi C, Lavin P, Draetta G, Pagano M, Loda M. The cell cycle inhibitor p27 is an independent prognostic marker in small (Ta, Tb) invasive breast carcinomas. *Cancer Res* 1997; **57**: 1259-1268
15 **Takeuchi S,** Koeffler HP, Hinton DR, Miyoshi I, Melmed S, Shimon I. Mutation and expression analysis of the Cyclin dependent kinase inhibitor gene p27kip1 in pituitary tumors. *J Endocrinol* 1998; **157**: 337-342
16 **Yao M**, Zhou XD, Liu YK,Tang ZY. E-cadherin expression in invasive hepatocellular carcinoma. *Zhonghua Xiaohua Zazhi* 1998; **18**: 31-33
17 **Ito Y,** Matsuura N, Sakon M, Miyoshi E, Noda K, Takeda T, Umeshita K, Nagano H, Nakamori S, Dono K, Tsujimoto M, Nakahara M, Nakao K, Taniguchi N, Monden M. Expression and prognostic roles of the G1-Smodulators in hepatocellular carcinoma: p27 independently predicts the recurrence. *Hepatology* 1999; **30:** 90-99
18 **Volm M,** Koomagi R, Mattern J, Stammler G. Cyclin A is associated with an unfavourable outcome in patient with non-small-cell lung carcinomas. *Br J Cancer* 1997; **75**: 1774-1778

19 **Peng SY,** Chou SP, Hsu HC. Association of down-regulation of Cyclin D and of overexpression of cyclin E with p53 mutation, high tumor grade and poor prognosis in hepatocellular carcinoma. *J Hepatol* 1998; **29**: 281-289
20 **Sgambato A**, Cittadini A, Faraglia B, Weinstein IB. Multiple functions of p27kip1 and its alterations in tumor cell: A review. *J Cell Physio* 2000; **183**: 18-27
21 **Asessandrini A**, Chiaur OS, Pagano M. Regulation of the Cyclin dependent kinase inhibitor p27kip1 by degradation and phosphrylation. *Leukemia* 1997; **11:** 342-345
22 **Pagano M,** Tam SW, Theodoras AM, Beer-Romero P, Del Sal G, Chau V, Yew PR, Draetta GF, Rolfe M. Role of the ubiquitin – proteasome pathway in regulating abundance of the Cyclin dependent kinase inhibitor p27. *Science* 1995; **269**: 682-691
23 **Ferrando AA,** Balbin M, Pendas AM, Vizoso F, Velasco G, Lopez-Otin C. Mutational analysis of the human Cyclin dependent kinase inhibitor p27kip1 in primary breast carcinomas. *Hum Genet* 1996; **97**: 91-94
24 **Morosetti R**, Kawamata N, Gombart AF. Alternation of the p27kip1 gene in non-Hodgkin's lymphomas and adult T-cell leukemia lymphoma. *Blood* 1995; **86**: 1924-1930
25 **Levenberg S,** Yarden A, Kam Z, Geiger B. p27 is involved in N-cadherin mediated contact inhibition of cell growth and S-phase entry. *Oncogene* 1999; **18**: 869-876
26 **Donnellan R**, Chetty R. Cyclin E in human cancers. *FASEB J* 1999; **13**: 773-780
27 **Huntunem RL**, Blomquist CP, Bohling TO. Expression of cyclin A in soft tissue sarcomas correlates with tumor aggressiveness. *Cancer Res* 1999; **59**: 2885-2892
28 **Ohashi R,** Gao C, Miyazaki M, Hamazaki K, Tsuji T, Inoue Y, Uemura T, Hirai R, Shimizu N, Namba M. Enhanced expression of cyclin E and cyclin A in human hepatocellular carcinomas. *Anticancer Res* 2001; **21**: 657-662
29 **Fero ML,** Randel E, Gurley KE, Roberts JM, Kemp CJ. The murine gene p27 is haplo-inufficent for tumor suppression. *Nature* 1998; **396**: 177-180
30 **Zerfass-Thome K,** Schulze A, Zwerschke W, Vogt B, Helin K, Bartek J, Henglein B, Jansen-Durr P. p27kip1 blocks Cyclin-E dependent transactivation of Cyclin-A gene expression. *Mol Cell Biol* 1997; **17**: 407-415
31 **Marches R,** Schenermann RH, Uhr TW. Cancer dormancy: role of Cyclin-dependent kinase inhibitors in induction of cell cycle arrest mediated via memberane IgM. *Cancer Res* 1998; **58**: 691-697
32 **Pascale RM,** Simile MM, De Miglio MR, Muroni MR, Calvisi DF, Asara G, Casabona D, Frau M, Seddaiu MA, Feo F. Cell cycle deregulation in liver lesions of rats with and without genetic predisposition to hepatocarcinogenesis. *Hepatology* 2002; **35**: 1341-1350

Edited by Ren SY and Wang XL

P.O.Box 2345, Beijing 100023,China
Fax: +86-10-85381893
E-mail: wjg@wjgnet.com www.wjgnet.com

World J Gastroenterol 2003;9(11):2455-2459
World Journal of Gastroenterology
 ISSN 1007-9327

• LIVER CANCER •

Study on hepatocelluar carcinoma-associated hepatic arteriovenous shunt using multidetector CT

Ming-Yue Luo, Hong Shan, Zai-Bo Jiang, Lu-Fang Li, Hui-Qing Huang

Ming-Yue Luo, Hong Shan, Zai-Bo Jiang, Lu-Fang Li, Hui-Qing Huang, Department of Radiology, the Third Affiliated Hospital, Sun Yat-Sen University, Guangzhou 510630, Guangdong Province, China
Correspondence to: Dr. Ming-Yue Luo, Department of Radiology, the Third Affiliated Hospital, Sun Yat-Sen University, Guangzhou 510630, Guangdong Province, China. myluo@yahoo.com.cn
Telephone: +86-20-85516867 Ext 3108 **Fax:** +86-20-87536401
Received: 2003-05-10 **Accepted:** 2003-06-02

Abstract

AIM: To investigate multidetector CT (MDCT) findings of hepatocelluar carcinoma (HCC)- associated hepatic arteriovenous shunt (HAVS) and to evaluate their clinical significance.

METHODS: Thin-slice and dynamic enhancement MDCT of HAVS was performed on 56 patients with HCC. MDCT findings, including those of portal veins, hepatic veins, superior mesenteric veins, splenic veins, HCC foci, liver parenchyma without HCC foci, spleens, and thromboses in portal veins and hepatic veins, were all confirmed by digital subtract angiography and analyzed.

RESULTS: MDCT demonstrated earlier enhancement of main portal trunks and/or the first order branches than that of superior mesenteric veins or splenic veins (n=31). One patient had strong early enhancement of left hepatic vein with thromboses in left hepatic vein and upper part of inferior vena cava and 1 patient had transient patchy enhancement peripheral to HCC foci in late hepatic arterial phase among them. It demonstrated stronger opacification of main portal trunks and/or the first order branches than that of superior mesenteric veins or splenic veins (n=18), and earlier enhancement of the second order and smaller branches of portal veins than that of main portal trunks (n=4), stronger opacification of the second order and smaller branches of portal veins than that of main portal trunks (n=3), with transient patchy enhancement (n=3) or wedge-shaped enhancement (n=4) peripheral to HCC foci in late hepatic arterial phase. Enhancement degree of HCC foci was all decreased. As for 49 patients with severe or moderate shunts, enhancement degree of liver parenchyma without HCC foci was increased with heterogeneous density, but enhancement degree of spleens was decreased. There were thromboses in main portal trunks and/or the first order branches in 32 patients.

CONCLUSION: The main MDCT findings of HCC-associated HAVS are earlier enhancement and stronger opacification of portal veins and/or hepatic veins. Understanding of these findings will contribute to the diagnosis and prognosis of the disease and improve therapy for the patients.

Luo MY, Shan H, Jiang ZB, Li LF, Huang HQ. Study on hepatocelluar carcinoma-associated hepatic arteriovenous shunt using multidetector CT. *World J Gastroenterol* 2003; 9(11): 2455-2459
http://www.wjgnet.com/1007-9327/9/2455.asp

INTRODUCTION

Hepatic arteriovenous shunt (HAVS) is the communication between hepatic artery or its branches and portal vein or hepatic vein, forming hepatic artery portal venous shunt (HAPVS) or hepatic artery hepatic venous shunt (HAHVS) respectively. Hepatocelluar carcinoma (HCC) is the most common condition associated with HAVS because of its easy invasion of portal vein and hepatic vein. HAVS could result in direct blood flow between hepatic artery and portal vein or hepatic vein, which may cause severe portal hypertension and consequently, splenomegaly, ascites, and esophagogastric varices and bleeding, accelerating intrahepatic dissemination and extrahepatic metastasis of carcinoma cells[1,2]. Understanding of CT findings of HCC-associated HAVS is of significant clinical implications. Multidetector CT (MDCT) could contribute to the diagnosis of HAVS associated with HCC due to its fast scanning and improved image resolution and quality[3]. The purpose of this study was to examine MDCT findings of HCC-associated HAVS and to evaluate their clinical significance.

MATERIALS AND METHODS

Clinical data

Fifty-six patients (49 men and 7 women, range 29-73 years, mean age 49.8 years) with HCC-associated HAVS were included in the present study. The diagnosis of HCC was based on the results of percutaneous needle biopsy (n=5) or laboratory testings, including elevated serum alpha-fetoprotein level, in combination with imaging appearance and follow-up images (n=51) according to the diagnostic criteria for HCC formulated by Chinese National Association of Anticancer Committee.

MDCT

MDCT scanning was performed with a LightSpeed QX/i MDCT scanner (General Electronic Medical System, Milwaukee, USA). Multidetector row helical technique was applied to the scanning in cranial to caudal direction. Plain scanning of the liver was carried out first. This was followed by enhancement scanning of 2.5 mm axial section performed at 15 seconds, 25 seconds and 65 seconds after injection of contrast media for early hepatic arterial phase, late hepatic arterial phase and portal venous phase image acquisition respectively. A total of 100 ml contrast medium (Ultravist 300, Schering Pharmacy, Guangzhou, China; or Iopamiro 300, Bracco S.P.A., Milano, Italy) was administered to each patient, with a power injector at a rate of 3.5 ml.sec^{-1} through a catheter placed in the peripheral vein of the antecubital fossa.

Digital subtract angiography (DSA)

DSA was performed using a TOSHIBA Digital 1000 MAX (Toshiba Corporation, Tokyo, Japan) within 2 weeks of MDCT examination. A catheter was introduced via the right femoral artery by the Seldinger technique. The celiac (6 patients) or selective hepatic (50 patients) DSA was carried out with a catheter placed in the celiac trunk or in the proper hepatic artery and 40 ml Ultravist 300 (Schering Pharmacy, Guangzhou, China)

or Iopamiro 300 (Bracco S.P.A., Milano, Italy) was injected with a power injector at a rate of 5.0 ml.sec^{-1}. Serial anterior-posterior images were obtained at 1 every 2 seconds for the first 8 seconds and a slower rate thereafter.

Diagnostic criterion for HAVS

Diagnostic criteria for HAPVS[4] were the earlier enhancement of main portal trunk and/or its first order branches than that of superior mesenteric vein or splenic vein, or stronger opacification of main portal trunk and/or its first order branches than that of superior mesenteric vein or splenic vein; or earlier enhancement of the second order and smaller branches of portal veins than that of main portal trunk, or stronger opacification of the second order and smaller branches of portal veins than that of main portal trunk. Diagnostic criteria for HAHVS were the earlier enhancement and stronger opacification of hepatic vein, approaching the density of enhanced aorta. The diagnosis of HAVS based on MDCT was confirmed by DSA.

Determination of shunting types and degrees of HAVS

According to the location of shunting, HAVS was divided into three types. The central HAVS was the shunting located in porta hepatis with earlier enhancement of main portal trunk and/or the first order branches, or hepatic veins at early hepatic arterial phase. The peripheral HAVS was the shunting located in peripheral liver parenchyma with earlier enhancement of the second order and smaller branches of portal vein, and transient patchy or wedge-shaped enhancement peripheral to HCC foci at late hepatic arterial phase. The mixed HAVS showed both central and peripheral HAVS.

According to the time of appearance of HAVS on images, HAVS was divided into three degrees. The severe HAVS showed opacification of main portal trunk and/or the first order branches, or hepatic veins, with enhancement of hepatic arterial and its branches at early hepatic arterial phase, without enhancement or with early enhancement of HCC foci. The moderate HAVS showed opacification of main portal trunk and/or the first order branches, or hepatic veins, with middle or late enhancement of HCC foci at late hepatic arterial phase. The mild HAVS showed opacification of the second order and smaller branches of portal veins at late hepatic arterial phase, with transient patchy or wedge-shaped enhancement peripheral to HCC foci.

Image analysis

Image analysis included examination of the shunting types and degrees of HAVS with or without thromboses in portal veins and/or hepatic veins; locations, gross pathologic patterns and enhancement of HCC; enhancement of liver parenchyma without HCC foci, spleens, superior mesenteric veins and splenic veins.

RESULTS

Earlier enhancement and stronger opacification of portal veins and hepatic veins

Earlier enhancement and stronger opacification of portal veins and hepatic veins were the major MDCT findings of HAVS. Their relations with shunting types and degrees of HAVS are shown in Table 1.

There was transient patchy (n=3, Figure 1) or wedge-shaped (n=4, Figure 2) enhancement peripheral to HCC foci at late hepatic arterial phase in patients with mild and peripheral HAVS, in addition to earlier enhancement of the second order and smaller branches of portal veins than that of main portal trunks, or stronger opacification of the second order and smaller branches of portal veins than that of main portal trunks.

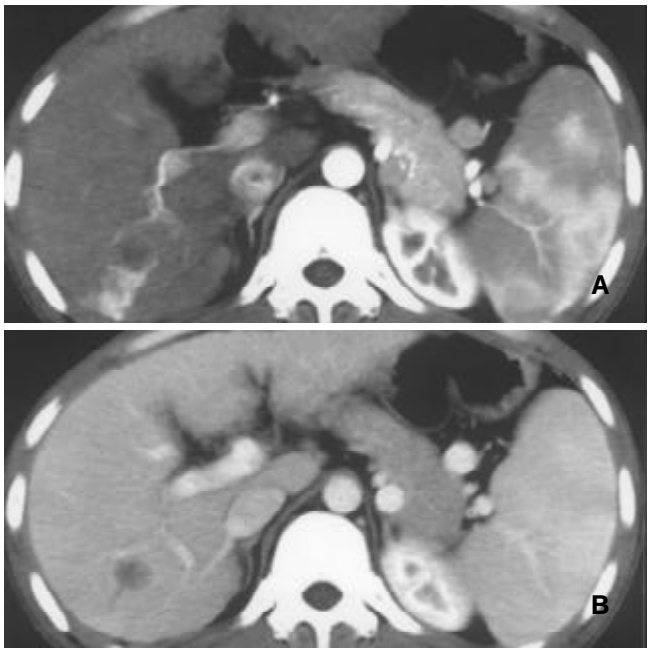

Figure 1 Nodular pattern of HCC with mild and peripheral HAVS. Transient patchy enhancement lateral to HCC foci at late hepatic arterial phase (A), becoming isoattenuation at portal vein phase (B).

Table 1 MDCT findings of earlier enhancement and stronger opacification of portal veins and hepatic veins and their relations with shunting types and degrees of HAVS

MDCT findings	Shunting patterns			Shunting degrees		
	Central	Peripheral	Mixed	Severe	Moderate	Mild
Earlier enhancement of MPT and / or the first order branches than that of SMV or SV	30	0	1[a]	31	0	0
Stronger opacification of MPT and / or the first order branches than that of SMV or SV	18	0	0	11	7	0
Earlier enhancement of the second order and smaller branches of PV than that of MPT	0	4	0	0	0	4
Stronger opacification of the second order and smaller branches of PV than that of MPT	0	3	0	0	0	3
Earlier enhancement and stronger opacification of HV, approaching density of enhanced aorta	1[b]	0	0	1[b]	0	0

a: mixed HAPVS, with transient patchy enhancement peripheral to HCC foci at late hepatic arterial phase at the same time. b: HAHVS+HAPVS, combined with earlier enhancement of main portal trunk and the first order branches than that of superior mesenteric vein. MPT=main portal trunk, SMV=superior mesenteric vein, SV=splenic vein, HV=hepatic vein.

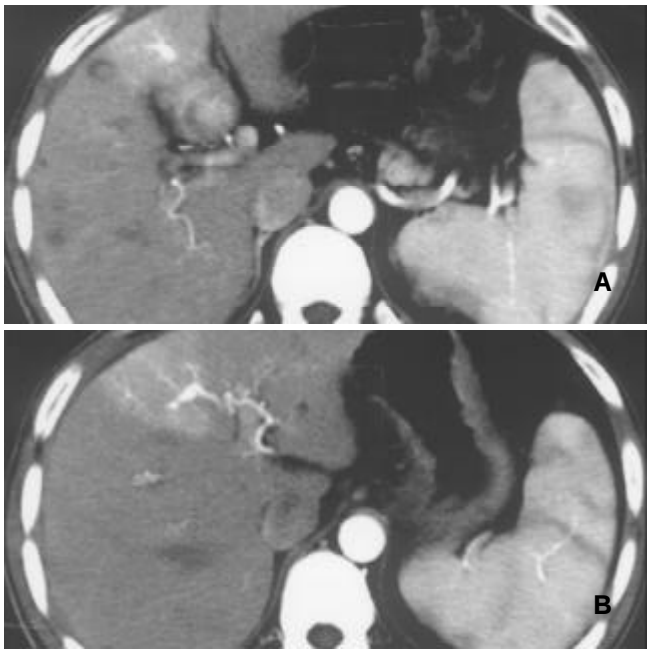

Figure 2 Nodular pattern of HCC accompanied by mild and peripheral HAVS. Stronger opacification of the third order portal vein branches than that of main portal trunk at late hepatic arterial phase with transient wedge-shaped enhancement lateral to HCC foci (A, B).

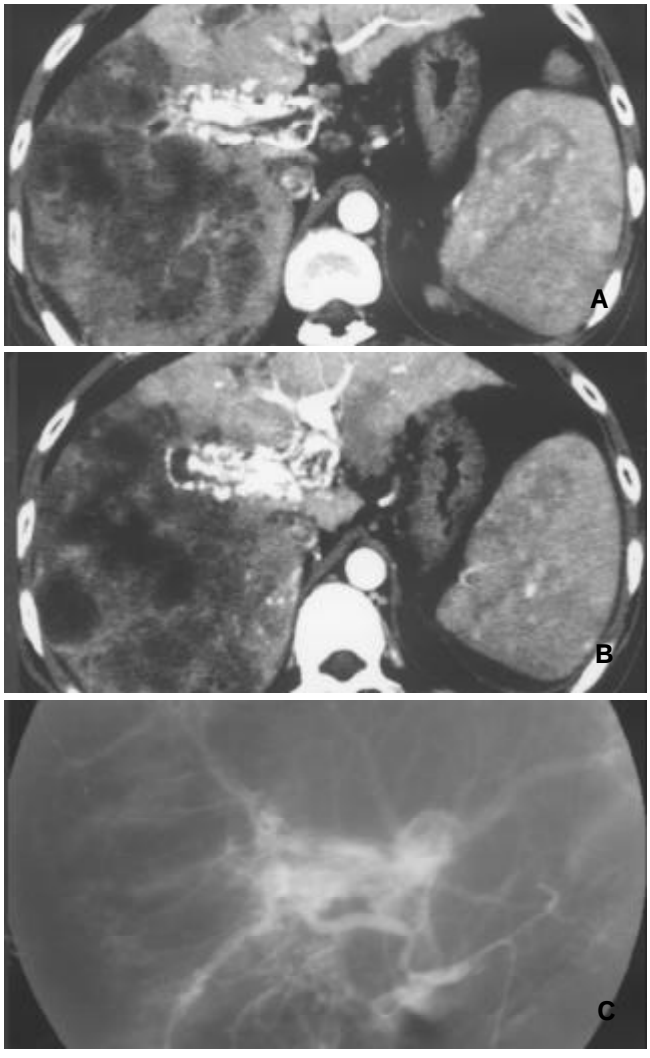

Figure 3 Massive and nodular pattern of HCC associated with severe and central HAVS. Earlier enhancement and stronger opacification of main portal trunk and the left and right first order branches with thromboses in them were shown. Enhancement degree of HCC foci was decreased, and enhancement degree of liver parenchyma without HCC foci was increased with heterogeneous density (A and B). DSA finding of the same patient (C).

Thromboses in portal veins and hepatic veins

Thromboses in portal veins and hepatic veins were seen in all cases of central HAVS. Thirty-two patients had thromboses in portal veins, including 18 patients with thromboses in main portal trunks and the first order branches (Figure 3), 11 patients with thromboses in the right first order branches and 3 patients with thromboses in the left first order branches. One patient with mixed HAVS had thromboses in the left hepatic vein and upper part of inferior vena cava.

Location, gross pathologic pattern and enhancement of HCC

HCC was located in different parts of liver parenchyma. Of the 49 patients with severe or moderate HAVS, 40 had foci adjacent to porta hepatis and 1 patient had foci nearby the secondary porta hepatis. Gross pathologic patterns included massive pattern (n=17), nodular pattern (n=11), massive and nodular pattern (n=23) and diffuse pattern (n=5). The enhancement of HCC foci was all decreased.

Enhancement of liver parenchyma without HCC foci and spleens

Liver parenchyma without HCC foci showed transient patchy (n=3) or wedge-shaped (n=4) enhancement peripheral to HCC foci at late hepatic arterial phase in 7 patients with mild and peripheral HAVS. In the 49 patients with severe or moderate and central HAVS, the enhancement degree of liver parenchyma without HCC foci was increased and heterogeneous, and enhancement degree of the spleen was all decreased (Figure 4).

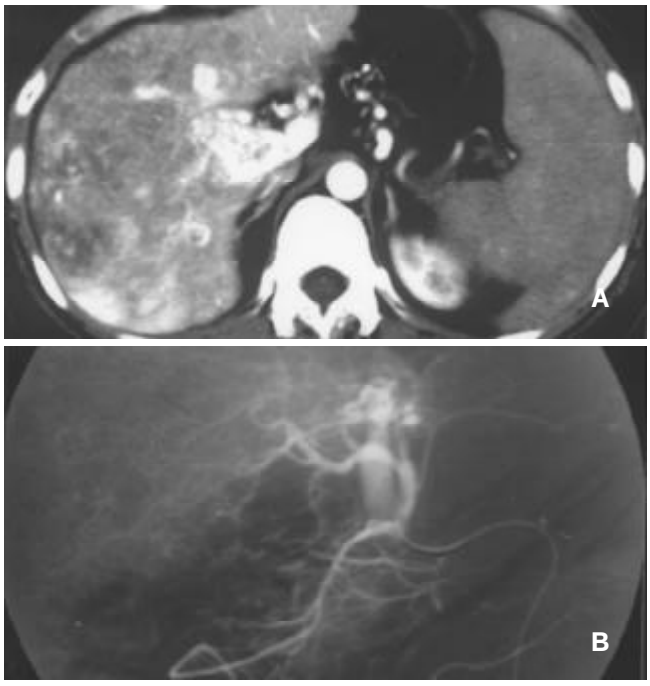

Figure 4 Massive pattern of HCC complicated with severe, central and slight, peripheral HAVS. Earlier enhancement and stronger opacification of main portal trunk with small thromboses in it were seen, with patchy enhancement internal and lateral to HCC foci. Enhancement degrees of HCC foci and spleen were decreased, enhancement degree of liver parenchyma without HCC foci was increased with heterogeneous density (A). DSA finding of the same patient (B).

DISCUSSION

Mechanism of formation of HAVS associated with HCC and MDCT findings

The formation of HAVS might be attributed to complex anatomy and various pathological conditions. Anatomically, hepatic artery and portal vein respectively branch and converge into hepatic sinuses, followed by entering into central vein and hepatic veins before into system circulation. Hence, there were abundant anastomoses between hepatic artery and portal vein[5, 6]. The pathological conditions may include followings. With continued progression of HCC adjacent to porta hepatis, it might directly invade and destroy portal veins and/or hepatic veins, forming tumor thromboses in them or growing along the venous wall. The tumor thromboses are vascularized by arterial network nourished by hepatic artery branches around the vein and are growing up. The enlarged and dilated hepatic artery branches might become the main supplying arteries of the tumor thromboses and their blood flow might enter directly into portal veins and/or hepatic veins which act as the efferent vessels, resulting in transvasal HAVS. In our serial, HCC foci of 40 patients were adjacent to porta hepatis and 1 patient adjacent to the secondary porta hepatis with apparent invasion of main portal trunks and/or the first order branches or hepatic veins. Irregular, tortuous and dilated arterial networks were seen around the porta hepatis or the secondary porta hepatis, which were confirmed by DSA as the supplying arteries of HAVS. The direct invasion and destruction of main portal trunks and/or the first order branches, or hepatic veins, were the main causes of transvasal HAVS. It was specially the case for HCC in internal left hepatic lobe where HAVS might occur even if HCC focus was small. The transvasal HAVS had severe shunts shown as an earlier enhancement of main portal trunks and/or the first order branches, or hepatic veins than that of superior mesenteric veins or splenic veins at early hepatic arterial phase (n=31), or as stronger opacification of main portal trunks and/or the first order branches than that of superior mesenteric veins or splenic veins (n=11), but livers and spleens were ischemia due to "stolen blood" by HAVS. HCC might thus show no or little enhancement, and enhancement of the spleen decreased.

Blood flow of portal veins might be obstructed due to compression of the first order branches of portal vein by HCC or carcinoma thromboses in the first order branches of portal vein. The compensative hyperplasia of vessel plexus around larger biliary ducts in the central part of liver might result in opening of hepatopetal collateral vessels and formation of transplexal HAPVS. In our study, 7 patients with moderate shunts manifested as stronger opacification of main portal trunks and/or the first order branches than that of superior mesenteric veins or splenic veins at late hepatic arterial phase with MDCT.

Compression and invasion of branches of hepatic veins by HCC might obstruct hepatic veins and cause hypertension of hepatic sinuses. The portal veins might thus become their efferent vessels and receive blood supply of hepatic arteries directly when pressure of hepatic sinuses was higher than that of portal veins, resulting in transsinusoidal HAPVS. Subsequently, functional blood flow of portal veins in this area decreased and blood flow of hepatic arteries increased as a compensation, aggravating transsinusoidal HAPVS[6]. In addition, because tumor vessel had no muscular layer and its capability of regulating blood flow by systolic function of vessel wall was poor, the normal branches of hepatic arteries around HCC would preferably take in compensatively increased hepatic arterial blood due to obstruct of hepatic veins, resulting in further intensifying of transsinusoidal HAPVS. On MDCT, it had mild shunts shown as an earlier enhancement of the second order and smaller branches of portal veins than that of main portal trunks (n=4), or stronger opacification of the second order and smaller branches of portal veins than that of main portal trunks (n=3) at late hepatic arterial phase, with transient patchy or wedge-shaped enhancement peripheral to HCC foci. In our series, 7 cases of peripheral HAPVS and 1 case of mixed HAPVS showed these findings.

Diagnosis and differential diagnosis of HCC- associated HAVS

It could be seen from above analyses that there seemed no much difficulty in diagnosis of severe or moderate and central HAVS associated with HCC. However, mild HAVS and peripheral HAVS should be differentiated from hepatic perfusion abnormalities of physiological conditions and other pathological causes[7-14].

Hepatic perfusion abnormalities caused by physiological conditions such as origin variety of segment or subsegment hepatic artery, aberrant biliary bladder vein or gastric vein were only shown as local transient hepatic parenchyma hyperattenuation at hepatic arterial phase with no abnormality at portal vein phase and no HCC foci[15]. HAPVS in hepatic hemangioma manifested as a wedge-shaped or irregular homogenous hyperattenuation in the liver parenchyma adjacent to the tumor at hepatic arterial phase, becoming isoattenuation or slight hyperattenuation, and hemangioma itself tending to show rapid enhancement at portal vein phase, specially for hemangioma of 2-3 cm in diameter or less[16-18]. Hepatic adenoma and focal nodular hyperplasia appeared as homogenous enhancement at hepatic arterial phase, being hypoattenuation at delayed time phase. Abnormal perfusion in cirrhotic liver had the typical wedge-shaped and homogeneous appearance with or without internal linear branching structures at hepatic arterial phase, returning to isoattenuation or slight hyperattenuation at portal vein phase[5]. The site of abnormal perfusion associated with thrombosis in portal vein was conformed to respective portal vein distribution. Hepatic metastasis with abundant blood supply, liver infection, Budd-Chiari syndrome, changes after transjugular intrahepatic portosystemic shunt (TIPS), HAVS following liver biopsy, abnormal perfusion resulted from acute biliary bladder inflammation and acute pancreas inflammation all had their own MDCT features. With the help of clinical materials, they could be differentiated from mild and peripheral HAVS[5,19-26].

Clinical significance of diagnosis of HCC- associated HAVS by MDCT

Diagnosis of HAVS was mainly based on transcatheter hepatic angiography (including DSA) in the past. However, a proportion of patients could not undergo transcatheter hepatic angiography due to restriction of equipment conditions and technology, cost and invasive examination etc., resulting in missed diagnosis of HAVS and loss of treatment opportunity[24, 27].

MDCT is a breakthrough in medical imaging examination technology. Equipped with a multidetector array, MDCT can perform multislice data acquisition simultaneously, which greatly reduces the time of volume scanning. In addition, image quality is improved due to increased image resolution and clarity. MDCT could therefore offer thin-slice and dynamic enhancement scanning of liver at early hepatic arterial phase, late hepatic arterial phase and portal venous phase and provide a convenient, fast and noninvasive new technology for examination of HAVS associated with HCC[3, 28].

Clinically, correct interpretation of MDCT findings of HCC-associated HAVS could assist in making right diagnosis and prognosis and working out effective therapeutic strategy. Forty-nine patients with severe or moderate and central HAVS in our series underwent transcatheter supplying artery embolism of HAVS under the guidance of MDCT information and their esophagogastric varix bleeding, ascites and stubborn diarrhea were all brought under control timely. Moreover, MDCT

provides a new technology for the study of mechanism of HAVS formation. With MDCT, shunting locations, types and degrees of HAVS can be determined, and mechanism of HAVS formation can be estimated. These may form the basis for comprehensive therapy of HCC and embolism of HAVS. Our study suggested that transvasal, transplexal and transsinusoidal HAVS might be the causes of severe, moderate and mild HAVS respectively, and enlarged and dilated nourishing artery manifested as irregular arterial network, originating from proximal proper hepatic artery, might be the main supplying artery of severe and central HAVS. Therefore, in embolism of HAVS, superselective embolism of nourishing artery rather than hepatic artery trunk was performed. If HAVS was supplied by many arteries, they should be embolized respectively. In addition, embolism agent should arrive at the end of nourishing artery to achieve permanent embolism and reduce the possibility of recanalization and recurrence of HAVS[29-33]. Our above-mentioned forty-nine patients with severe or moderate and central HAVS were all completely embolized by absolute ethanol combined with spring steel coil via 4.0F catheter or 3.0F microcatheter superselective embolism without recanalization and recurrence of HAVS by follow-up MDCT examinations.

In conclusion, our study investigated the complex MDCT findings of HAVS associated with HCC. The classification of shunting degrees into severe, moderate and mild shunts according to appearing time of HAVS at early or late hepatic arterial phase can contribute to the diagnosis and treatment of patients. It is also noted that transvasal, transplexal, transsinusoidal HAVS may be behind the formation of severe, moderate and mild HAVS respectively.

REFERENCES

1 **Tang ZY**. Hepatocellular carcinoma-cause, treatment and metastasis. *World J Gastroenterol* 2001; **7**: 445-454
2 **Guo WP**, Zhang HX, Wang ZM, Wang YQ, Ni DH, Li WX, Guan Y. DSA analysis of hepatic arteriovenous fistula concurrent with hepatic cancer and its clinical significance. *World J Gastroenterol* 2000; **6**: 872-876
3 **Mortele KJ**, McTavish J, Ros PR. Current techniques of computed tomography. Helical CT, multidetector CT, and 3D reconstruction. *Clin Liver Dis* 2002; **6**: 29-52
4 **Chen JH**, Chai JW, Huang CL, Hung HC, Shen WC, Lee SK. Proximal arterioportal shunting associated with hepatocellular carcinoma: features revealed by dynamic helical CT. *Am J Roentgenol* 1999; **172**: 403-407
5 **Kim TK**, Choi BI, Han JK, Chung JW, Park JH, Han MC. Nontumorous arterioportal shunt mimicking hypervascular tumor in cirrhotic liver: two-phase spiral CT findings. *Radiology* 1998; **208**: 597-603
6 **Nagino M**, Nimura Y, Kamiya J, Kanai M, Hayakawa N, Yamamoto H. Immediate increase in arterial blood flow in embolized hepatic segments after portal vein embolization: CT demonstration. *Am J Roentgenol* 1998; **171**: 1037-1039
7 **Luo TY**, Shi B, Li YM, Lu FJ, Yuan SW, Yan M, Wu JQ. A study on the transient hepatic abnormal enhancement in the hepatic arterial phase during dynamic contrast-enhanced spiral CT. *Zhonghua Fangshexue Zazhi* 2003; **37**: 258-263
8 **Quiroga S**, Sebastia C, Pallisa E, Castella E, Perez-Lafuente M, Alvarez-Castells A. Improved diagnosis of hepatic perfusion disorders: value of hepatic arterial phase imaging during helical CT. *Radiographics* 2001; **21**: 65-81
9 **Gryspeerdt S**, Van Hoe L, Marchal G, Baert AL. Evaluation of hepatic perfusion disorders with double-phase spiral CT. *Radiographics* 1997; **17**: 337-348
10 **Choi BI**, Lee KH, Han JK, Lee JM. Hepatic arterioportal shunts: dynamic CT and MR features. *Korean J Radiol* 2002; **3**: 1-15
11 **Park CM**, Cha SH, Kim DH, Choi JA, Cha IH, Kim YH, Chung KB, Suh WH. Hepatic arterioportal shunts not directly related to hepatocellular carcinoma: findings on CT during hepatic arteriography, CT arterial portography and dual phase spiral CT. *Clin Radiol* 2000; **55**: 465-470
12 **Chen WP,** Chen JH, Hwang JI, Tsai JW, Chen JS, Hung SW, Su YG, Lee SK. Spectrum of transient hepatic attenuation differences in biphasic helical CT. *Am J Roentgenol* 1999; **172:** 419-424
13 **Li L**, Wu PH, Mo YX, Lin HG, Zheng L, Li JQ, Lu LX, Ruan CM, Chen L. CT arterial portography and CT hepatic arteriography in detection of micro liver cancer. *World J Gastroenterol* 1999; **5**: 225-227
14 **Li L**, Wu PH, Lin HG, Li JQ, Mo YX, Zheng L, Lu LX, Ruan CM, Chen L. Findings of non-pathologic perfusion defects by CT arterial portography and non-pathologic enhancement of CT hepatic arteriography. *World J Gastroenterol* 1998; **4**: 513-515
15 **Yoon KH**, Matsui O, Kadoya M, Yoshigawa J, Gabata T, Arai K. Pseudolesion in segments II and III of the liver on CT during arterial portography caused by aberrant right gastric venous drainage. *J Comput Assist Tomogr* 1999; **23:** 306-309
16 **Kim KW**, Kim TK, Han JK, Kim AY, Lee HJ, Choi BI. Hepatic hemangiomas with arterioportal shunt: findings at two-phase CT. *Radiology* 2001; **219**: 707-711
17 **Vilgrain V**, Boulos L, Vullierme MP, Denys A, Terris B, Menu Y. Imaging of atypical hemangiomas of the liver with pathologic correlation. *Radiographics* 2000; **20**: 379-397
18 **Naganuma H**, Ishida H, Konno K, Hamashima Y, Komatsuda T, Ishida J, Masamune O. Hepatic hemangioma with arterioportal shunts. *Abdom Imaging* 1999; **24**: 42-46
19 **Yamasaki M,** Furukawa A, Murata K, Morita R. Transient hepatic attenuation difference (THAD) in patients without neoplasm: frequency, shape, distribution, and causes. *Radiat Med* 1999; **17**: 91-96
20 **Lee WK**, Stuckey S. Arterioportal fistula following liver biopsy demonstrated by lipiodol computed tomography. *Clin Radiol* 2000; **55**: 489-491
21 **Sato M**, Ishida H, Konno K, Komatsuda T, Hamashima Y, Naganuma H, Ohyama Y. Longstanding arterioportal fistula after laparoscopic liver biopsy. *Abdom Imaging* 1999; **24**: 383-385
22 **Lim JH**, Lee SJ, Lee WJ, Lim HK, Choo SW, Choo IW. Iodized oil retention due to postbiopsy arterioportal shunt: a false positive lesion in the investigation of hepatocellular carcinoma. *Abdom Imaging* 1999; **24**: 165-170
23 **Thampanitchawong P**, Piratvisuth T. Liver biopsy: complications and risk factors. *World J Gastroenterol* 1999; **5**: 301-304
24 **Chen JH**, Chen WP, Huang CL, Shen WC. Dynamic helical CT as a novel technique for diagnosing hepatic perfusion disorders. *Hepatogastroenterology* 1999; **46**: 303-307
25 **Quiroga S**, Sebastia MC, Moreiras M, Pallisa E, Rius JM, Alvarez-Castells A. Intrahepatic arterioportal shunt: helical CT findings. *Eur Radiol* 1999; **9**: 1126-1130
26 **Arita T**, Matsunaga N, Takano K, Hara A, Fujita T, Honjo K. Hepatic perfusion abnormalities in acute pancreatitis: CT appearance and clinical importance. *Abdom Imaging* 1999; **24**: 157-162
27 **Chen JH**, Huang CL, Hwang JI, Lee SK, Shen WC. Dynamic helical biphasic CT emerges as a potential tool for the diagnosis of proximal arterioportal shunting. *Hepatogastroenterology* 1999; **46**: 1791-1797
28 **Takahashi S**, Murakami T, Takamura M, Kim T, Hori M, Narumi Y, Nakamura H, Kudo M. Multi-detector row helical CT angiography of hepatic vessels: depiction with dual-arterial phase acquisition during single breath hold. *Radiology* 2002; **222**: 81-88
29 **Guan SH**, Dan H, Jiang ZB, Huang MS, Zhu KS, Li ZR, Meng XC. Transmicrocatheter local injection of ethanol to treat hepatocellular carcinoma with high flow arteriovenous shunts. *Zhonghua Fangshexue Zazhi* 2002; **36**: 997-1000
30 **Luo PF**, Chen XM, Zhang LM, Zhou ZJ, Fu L, Wei ZH. The management of arteriovenous shunting in hepatocellular carcinoma. *Zhonghua Fangshexue Zazhi* 2002; **36**: 114-117
31 **Fan J**, Wu ZQ, Tang ZY, Zhou J, Qiu SJ, Ma ZC, Zhou XD, Ye SL. Multimodality treatment in hepatocellular carcinoma patients with tumor thrombi in portal vein. *World J Gastroenterol* 2001; **7**: 28-32
32 **Li L**, Wu PH, Li JQ, Zhang WZ, Lin HG, Zhang YQ. Segmental transcatheter arterial embolization for primary hepatocellular carcinoma. *World J Gastroenterol* 1998; **4**: 511-512
33 **Fan J**, Ten GJ, He SC, Guo JH, Yang DP, Wang GY. Arterial chemoembolization for hepatocellular carcinoma. *World J Gastroenterol* 1998; **4**: 33-37

Edited by Liu HX and Wang XL

P.O.Box 2345, Beijing 100023,China
Fax: +86-10-85381893
E-mail: wjg@wjgnet.com www.wjgnet.com

World J Gastroenterol 2003;9(11):2464-2468
World Journal of Gastroenterology
 ISSN 1007-9327

• COLORECTAL CANCER •

Investigation of Epstein-barr virus in Chinese colorectal tumors

Huan-Xin Liu, Yan-Qing Ding, Xin Li, Kai-Tai Yao

Huan-Xin Liu, Yan-Qing Ding, Xin Li, Kai-Tai Yao, Department of Pathology, the First Military Medical University, Guangzhou 510515, Guangdong Province, China
Correspondence to: Dr. Yan-Qing Ding, Department of Pathology, the First Military Medical University, Guangzhou 510515 Guangdong Province, China. dyq@fimmu.edu.cn
Telephone: +86-20-61642148 **Fax:** +86-20-61642148
Received: 2002-10-09 **Accepted:** 2002-11-09

Abstract

AIM: To elucidate the association of Epstein-Barr virus (EBV) with colorectal tumors and to demonstrate whether infection of EBV existed in different stages of colorectal tumors involves in the carcinogenesis.

METHODS: One hundred and thirty paraffin-embedded tissues of colorectal tumors were classified into 5 groups: 26 adenomas, 23 adenomas complicated with dysplasia, 22 adenomas complicated with carcinomatous, 36 colon carcinoma and 23 HNPCC, were examined by PCR, IHC and ISH, respectively.

RESULTS: EBV DNA was detected by PCR in 26 cases out of the 130 specimens, including 5 cases of adenomas, 5 adenomas complicated with dysplasia, 5 adenomas complicated with carcinomatous, 7 colorectal carcinoma and 4 HNPCC. IHC detection showed the expression of LMP1 in 7 cases, including 1 adenoma, 1 adenoma with dysplasia, 1 HNPPC, 2 adenomas complicated with carcinomatous, and 2 colorectal carcinomas. The expression of EBER1 detected by ISH was positive in 6 cases, including 1 adenoma with dysplasia, 2 adenomas complicated with carcinomatous and 3 colorectal carcinomas. There were no significant differences among the results of PCR, IHC and ISH in the 5 groups. In all cases of HNPCC, none of the tumor cells showed positive signals of EBER1, but some EBV-positive tumor infiltrating lymphocytes were found in 2 of 23 cases.

CONCLUSION: Our results showed that infection of EBV exists in human colorectal tumors, which indicates that EBV may be involved in the carcinogenesis of colorectal tumors but does not play an important role. The mechanisms need to be clarified further.

Liu HX, Ding YQ, Li X, Yao KT. Investigation of Epstein-barr virus in Chinese colorectal tumors. *World J Gastroenterol* 2003; 9(11): 2464-2468
http://www.wjgnet.com/1007-9327/9/2464.asp

INTRODUCTION

Epstein-Barr virus (EBV) is a ubiquitous herpes virus that infects and establishes a persistent infection in the host. Clinically, its primary infection ranges from a mild self-limited illness in children to infectious mononucleosis in adolescents and adults[1,2]. EBV is associated with a number of human malignancies,including Burkitt lymphoma and nasopharyngeal carcinoma,etc. Recently, involvement of EBV has been demonstrated in gastric carcinoma. Detection rates of EBV in gastric carcinomas varied in different studies from 4 % to 18 %[5-15]. Although there are many similar features in histology and pathogenesis between gastric and colorectal carcinoma, there have been few papers about the relationship of EBV with colorectal cancers. However, a great deal of evidences support an etiologic role of EBV in carconogenesis in patients with EBV-positive gastric carcinomas[16,17,20]. In this study, we investigated the presence of EBV in 130 cases of colorectal tumors, including colorectal adenomas, adenomas complicated with dysplasia, adenomas complicated with carcinomatous, colorectal cancer and hereditary non-polyposis colorectal cancer (HNPCC) using immunohistochemical demonstration (IHC), polymerase chain reaction (PCR) and *in situ* hybridization (ISH).

MATERIALS AND METHODS

Tissue specimens

Surgical specimens for EBV detection were collected from 129 patients with colorectal tumors from February, 1998 to February, 2002. All cases were diagnosed by the Department of Pathology, NanFang Hospital, First Military Medical University. All specimens were formalin-fixed and paraffin-embedded. The age and sex of the patients among the five groups were similar (ANOVA analysis, $P>0.05$). As positive controls, Hodgkin' s disease and nasopharyngeal carcinoma specimens confirmed as EBV positive were used in every staining batch.

Immunohistochemitry

The monoclonal antibody LMP1 (DAKO) was used. Immunohistochemitry was performed on paraffin sections. Four-micrometer-thick specimens sectioned from a paraffin-embedded block were dewaxed in xylene and rehydrated in serially graded ethanol (100 %, 95 %), then treated with 0.28 % iodic acid for 60 sec,horse serum and first antibody for 10 minutes at 37 ℃, S-P-second antibody for 10 minutes at 37 ℃, S-P-third antibody for 10 minutes at 37 ℃, then detection was performed using the avidin-biotin-peroxidase complex technique and DAB (diaminobenzidine). A section of Hodgkin' s disease lymph node was used as an external positive control, while negative controls were obtained by replacing the primary antibody with nomal mouse serum.

Polymerase chain reaction

DNA was extracted from formalin-fixed and paraffin-embedded tissues. Two 5 μm thick rections were cut from each block, the samples were suspended in 50-150 μl of extraction buffer containing 100-300 μg/ml of proteinase K(Sigma, Missouri,USA), 50 mM tris-hydrochloric acid (ph8.5), 1 mM EDTA (PH8.0), and 0.5 % Tween20. After incubation for 36 h at 55 ℃, the samples were heated at 100 ℃ for 10 min. The primers corresponding to the 409 base pair region of the EBV BamHI W fragment, were synthesized based on the DNA sequences of GenBank (from www.icnet.uk/bmm) (primer: 1,5' -TCGCGTTGCTAGGCCACCTT-3' ; 2, 5' -CTTGGATGGCGGAGTCAGCG-3'), the PCR reaction mixture contained 1 μl model-DNA, 2.5 μl of 10×PCR buffer (mg^{2+}free), 1.5 μl of 25 mM$MgCl_2$, 2 μl of 2.5M dNTP mixture, 1 μl of 10 pmol/μl primer, and 1 μl of 1 Unit/ μl Taq polymerase

(HuaMei Biotech,China) in a final volume of 25 μl. After an initial incubation for 5 min at 94 ℃, the samples were subjected to 34 amplification cycles (at 94 ℃ for 45 s, at 55 ℃ for 45s and at 72 ℃ for 45 s). After the last cycle, the samples were held at 72 ℃ for 5 min.

In situ hybridization

Oligonucleotide probes used to detect EBER-1 were designed by our reseach group using Primer5.0 software, then synthesized and labeled with Dig by Bioasia Biotech, ShangHai. Each probe was labeled with 2 Dig. The method of *in situ* hybridization was described in the manual of BOSD Biotech. Four-micrometer-thick specimens sectioned from a paraffin-embedded block were dewaxed in xylene and rehydrated in serially graded ethanol (100 %, 95 %), then digested with pepsin (3 %) for 5-10 min at 30 ℃ and hybridized for 14 hours at 40 ℃. The slides were washed with 2×SSC for 5 min×2, 0.5×SSC for 15 min,0.2×SSC for 15 min at 37 ℃, then blocked with BSA at 37 ℃ for 30 min after trickled with biotin-rabbit antibodies to Dig at 37 ℃ for 60 min, slides were washed with 0.5M PBS for 5 min×4, then added SABC at 37 ℃ for 20 min and biotin- peroxidase at 37 ℃ for 20 min. At last, the slides were wished with 0.5M PBS for 5 min×4, stained with DAB for 10 min and counter-stained with hematein for 8 min. Two cases of nasopharyngeal carcinoma known to contain EBV were routinely used as positive controls, two slides treated without probe were used as negative controls.

Statistical analysis

Difference in proportions among the groups was calculated by Pearson χ^2 test using the spss 8.0 statistical software program (SPSS inc, Chicago, il). *P* values <0.5 were considered statistically significant.

RESULTS

The results of LMP1 immunohistochemistry (IHC) are shown in Table1. The positive-signals were localized over the cytoplasm of tumor cells. The cases which exhibited LMP1 staining in more than 10 % of the tumor cell cytoplasm were considered to be LMP1-positive (Figures1-4). A section of Hodgkin' s disease lymph node was used as an external positive control, while negative controls were obtained by replacing the primary antibody with normal mouse serum.IHC revealed that 7 of the 130 cases of colorectal tumors showed LMP1 signals, whereas non-carcinomatous colorectal mucosa was negative for LMP1.

Table 1 Results of immunohistochemistry

Group	*n*	EBV-positive	Positive rate (%)
Adenoma	26	1	3.8
Adenoma with dysplasia	23	1	4.3
Carcinomatous adenoma	22	2	9.1
Colorectal carcinoma	36	3	8.3
HNPCC	23	0	0
Total	130	7	5.4

χ^2 test, $\chi^2=0.0403<\chi^2_{0.05,4}=9.49$, $P>0.05$.

EBV DNA was amplified by PCR using the primers flanking the site of BamHI W fragment in 26 of 130 colorectal tumor tissues,including 5 cases of adenoma-group, 5 cases of adenomas complicated with dysplasia group, 5 cases of carcinomatous adenoma group, 7 cases of colorectal cancer and 4 cases of hereditary non-polyposis colorectal cancer (HNPCC) (Table 2 and Figue 5).

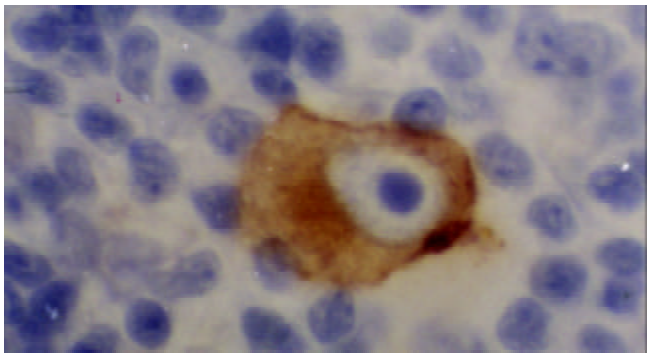

Figure 1 Positive-control of LMP1 from lymphoma of Hodgkin' disease. The cytoplasm of R-S cell showed clear positive signal.

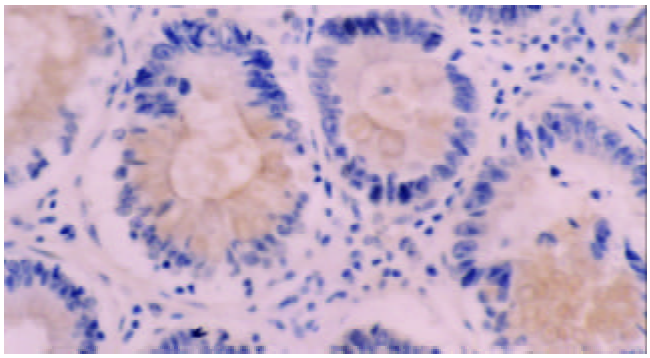

Figure 2 Immunohistochemical staining with anti-LMP1 antibody of adenoma specimen with dysplasia. The positive signals were localized at cytoplasm and membranes.

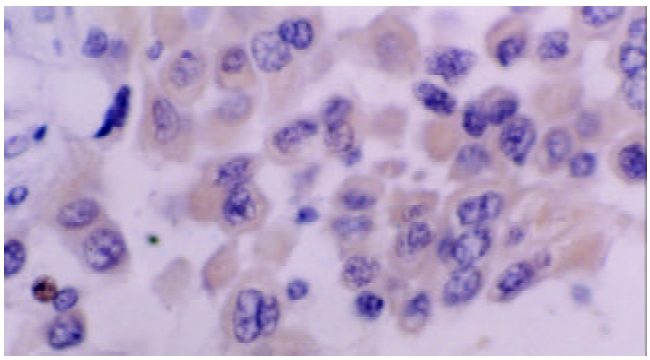

Figure 3 Immunohistochemical staining with anti-LMP1 antibody of colorectal carcinoma cells. The positive signals were localized at cytoplasm. But no clear positive signals localized at membranes.

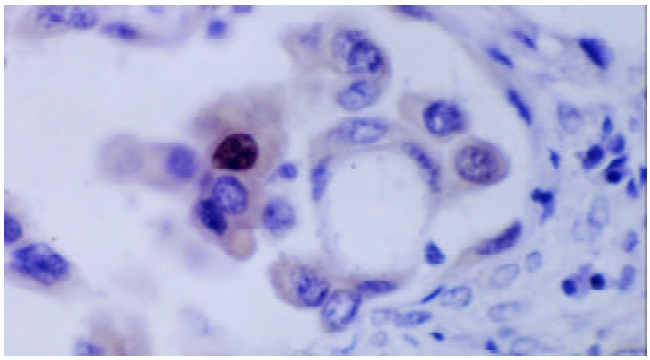

Figure 4 Metastatic colorectal carcinoma cells in lymphatic. The cytoplasm of neoplasm cells showed LMP1 positive, the nucleic showed positive signals too.

Table 2 Results of PCR

Group	*n*	EBV-positive	Positive rate (%)
Adenoma	26	5	19.2
Adenomas with dysplasia	23	5	21.7
Carcinomatous adenoma	22	5	22.7
Colorectal carcinoma	36	7	19.4
HNPCC	23	4	17.4
Total	130	26	20.0

χ^2 test, $\chi^2=2.725<\chi^2_{0.05,4}=9.49$, $P>0.05$.

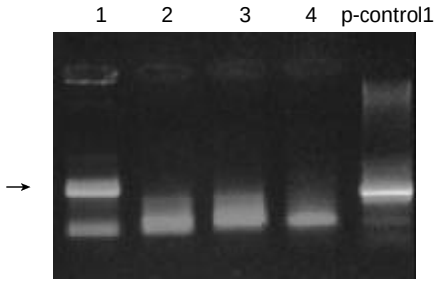

Figure 5 The electrophoresis photo of PCR. Arrow points to the positive lane.

The result of EBER *in situ* hybridization was similar to that of IHC, the signals of EBER were localized over the nuclei of most tumor cells (Figures 6-9), only the signal of EBER within the tumor nuclei was considered as a positive case. 6 of 130 cases showed EBER signals, and 5 cases that showed LMP1 signals were EBER positive (Table3). All cases with LMP1-positive and all cases with EBER-positive were PCR positive.

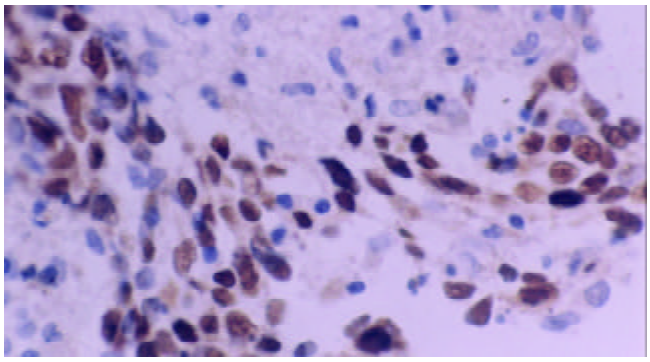

Figure 6 Positive control of EBER1 from a NPC specimen. Clear and strong hybridization signals (yellow nuclear grains) were shown in nuclei of the tumor cells. DAB and hematoxylin counterstaining,×200.

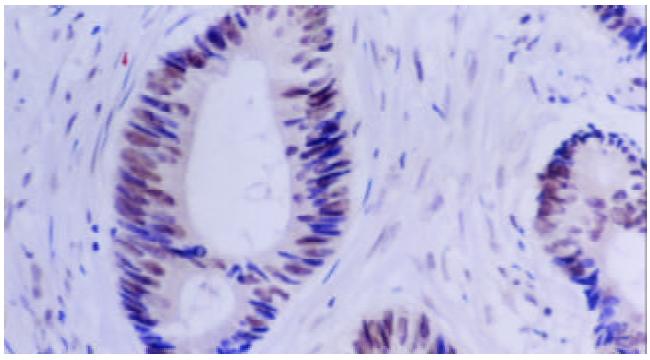

Figure 7 *In situ* hybridization with EBER1 (from an carcinomatous adenoma). Positive signals were shown in nuclei of the tumor cells. DAB and hematoxylin counterstaining, ×200.

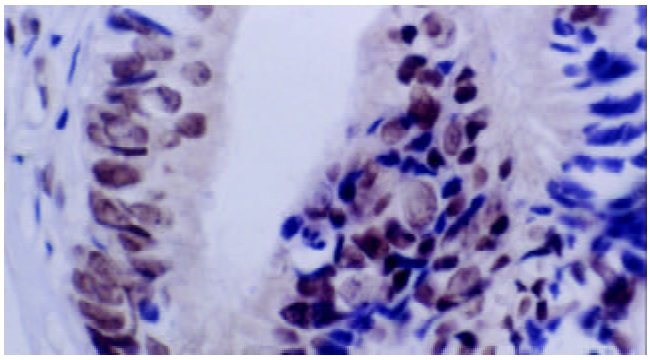

Figure 8 *In situ* hybridization with EBER1 (from a colorectal carcinoma). Clear and strong hybridization signals were shown in nuclei of the tumor cells. DAB and hematoxylin counterstaining, ×400

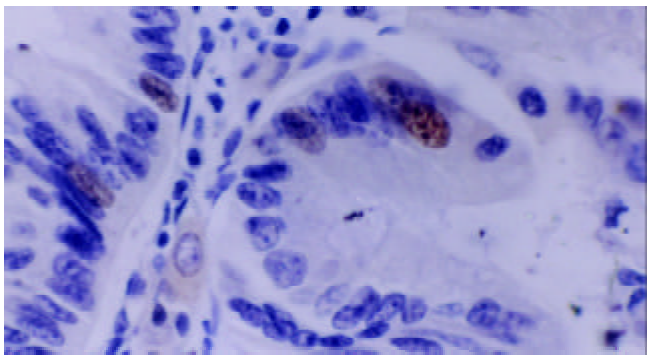

Figure 9 *In situ* hybridization with EBER1 (from a colorectal carcinoma, too). Interspersed positive signals were shown in neoplasm cells. DAB and hematoxylin counterstaining, ×400.

Table 3 Results of EBER-ISH

Group	*n*	EBV-positive	Positive rate (%)
Adenoma	26	0	0
Adenomas with dysplasia	23	1	4.3
Carcinomatous adenoma	22	2	9.1
Colorectal carcinoma	36	3	8.3
HNPCC	23	0	0
Total	130	6	4.6

χ^2 test, $\chi^2=5.39$, $P>0.05$.

DISCUSSION

The relationship between EBV and gastric carcinoma has been testified by Shibata, Tokunaga, Oda and Cho[13-15,19,24]. Throughout the world, EBV is detected in the tissues of about 10 % of gastric carcinoma cases[4]. Though colorectal epithelium is similar to that of gastric, and colorectal carcinoma is similar to gastric carcinoma, too, the association of EBV and colorectal tumors remains controversial. Yuen *et al*[22] investigated for the presence of EBV in 74 cases of gastric adenocarcinoma and 36 cases of colorectal adenocarcinoma from Chinese patients by *in situ* hybridization (ISH) using an antisense EBER probe, but none of the colorectal carcinomas showed a positive signal. Kijima *et al*[21] demonstrated the association of Epstein-Barr virus (EBV) with primary epithelial neoplasm in the south part of Kyushu, Japan, they found that there were no positive signals in 102 cases of colorectal cancer using EBER *in situ* hybridization. Cho *et al*[24] reported the same result that EBV was not associated with colorectal tumors. However, Yanai *et al*[23] found that EBV was detected in 63.6 % of Crohn's disease cases and 60 % of ulcerative colitis

cases using *in situ* hybridization for EBV-encoded small RNA1 (EBER-1), indicating that EBV infection may be related to IBD colonic diseases. Ioachim *et al*[26] studied 15 cases of primary anorectal lymphoma in AIDS patients and compared them with 4 cases of anorectal lymphoma unrelated to AIDS. In the AIDS-associated anorectal lymphomas, the presence of Epstein-Barr virus (EBV) in a latent form was demonstrated by an abundance of Epstein-Barr-encoded RNA (EBER) in 14 of 15 cases and latent membrane protein (LMP) in 4 cases, suggesting EBV may be associated to this kind of anorectal lymphomas. Samaha *et al*[25]and Kon *et al*[29] reported that lymphoepithelioma-like carcinoma of rectum was probably related to EBV, Ruschoff *et al*[27] used polymerase chain reaction test to examine the EBV DNA in 3 cases out of 20 differentiated colorectal adenocarcinomas. Though the positive signals restricted to the peritumor lymphoid infiltrate as shown by *in situ* hybridization, all of these findings suggest that EBV may associate to colorectal tumors. Moreover, Kim *et al*[30] investigated for the presence of EBV in 20 cases of colorectal adenocarcinomas and found 2 cases were EBER-positive. As a similarity, Grinstein *et al*[28] results suggested that EBV was not restricted to lymphoepithelioma-like carcinomas but might play an oncogenic role in frequent epithelial cancers, including colorectal cancers, and possibly also in hyperplasias and certain dysplasias preceding carcinomas.

In the current study, we analyzed 130 cases of colorectal tumors for the presence of EBV using immunohistochemistry, polymerase chain reaction and *in situ* hybridization. EBV was detected by each method, but the positive rates were different with different methods. Among the three methods, *in situ* hybridization was considered as the golden standard[3], nevertheless, we found 6 cases of colorectal tumors were EBER-positive. In our study, 1 case of adenoma complicated with dysplasia showed positive signals for EBER. This finding was different from the observation of Kijima *et al*, Yuen *et al* and Cho *et al*[21,22,24]. Moreover, detection of EBV in 1 case of dysplastic adenoma suggested that EBV infection occurred in the dysplastic phase before the occurrence of colorectal carcinoma, further indicating that EBV may play a role in tumor progression.

In all the EBV-assciated carcinomas,the virus was detected in the neoplasm cells but not in the nomal colorectal epithelium using ISH and IHC. However, we found much more positive-cases using PCR technique. In our study, 19 cases of PCR-positive colorectal tumors showed IHC negative and 20 cases showed EBER-negative. This could be interpreted as colorectal tumors with lymphoid stroma because the possibility of false positives using the PCR technique should be included[17]. Furthermore, reactive lymphocytes might possibly be contaminated during the micro dissection of a tumor portion and might become PCR-positive for EBV[16]. This supports the hypothesis that EBER *in situ* hybridization without further PCR method is enough to facilitate the detection of EBV within cancer cells. But Glaser *et al*[32] found that EBV EBER-1 transcript was not commonly expressed in breast cancer, based on a broadly representative case series. Therefore, in order to clarify the infection of EBV, more than one kind of methods should be used. Gulley *et al*[3] thought that new molecular tests combined with traditional serological or histochemical assays were helpful for diagnosis and monitoring of EBV-related diseases, PCR and IHC test were indispensable to the diagnosis of EBV associated diseases.

Our findings showed that in all EBV-positive colorectal tumors, male was preponderance. Other researchers, such as Chang *et al*[9], Oda *et al*[14] and Tokunaga *et al*[16] found the same results in the study of relationship between EBV and gastric carcinoma, the mechanism needs to be clarified further. Human cancer tissues are infiltrated by tumor-infiltrating lymphocytes (TILs), which have been considered a manifestation of a host immune response to cancer cells[22], the role of EBV-positive TILs in carcinoma remains unclear. Our data suggest that regardless of the site, the chances for epithelial cells to be exposed to EBV are similar in the gastrointestinal tract, because it is believed that EBV-carrying lymphocytes are a reservoir of EBV and may transfer EBV to the epithelial cells. Therefore, whether EBV plays an etiologic role in the carcinigenesis of this tissues is probably dependent on the infectability of epithelial cell interaction after infection.

Our data showed no significant differences in the frequency of EBV using PCR, IHC or ISH among adenoma, adenomas complicated with dysplasia, carcinomatous adenomas, colorectal cancer and hereditary non-polyposis colorectal cancer (HNPCC). The low frequency of EBV in HNPCC might be explained by different histological types of carcinoma, and the susceptibility to EBV of HNPCC might be lower than the other four groups. Our findings suggest that EBV does exist in colorectal tumor tissues in South China population, and the frequency of EBV positive colorectal tumors in Guangzhou, South China, where NPC is the most common in the world, may be higher than that in other parts of China. These findings agree with Hao *et al*[11] and Qiu *et al*[12]. Corvalan *et al*[18] thought that Epstein-Barr virus associated gastric carcinoma(EBVaGC) was linked to regional, ethnic, location of carcinoma in the organism and the histology type of tumors.

In conclusion, the present study has shown that EBV may play an etiologic role in the carcinogenesis of these tissues. But our data showed a very low frequency of EBV in these colorectal tumors, indicating that EBV does not play a major role in the etiology of colorectal carcinoma, and the carcinogenesis mechanism needs to be further elucidated.

REFERENCES

1 **Chow VT**. Cancer and viruses. *Ann Acad Med Singapore* 1993; **22**: 163-169

2 **Liebowitz D**. Pathogenesis of Epstein-Barr virus in McCance DJ (ed): Human Tumor Viruses. Washington, DC. *ASM Press* 1998; **24**: 175-179

3 **Gulley ML**. Molecular diagnosis of Epstein-Barr virus-related diseases. *J Mol Diagn* 2001; **3**: 1-10

4 **Takada K**. Epstein-Barr virus and gastric carcinoma. *Mol Pathol* 2000; **53**: 255-261

5 **Hsieh LL**, Lin PJ, Chen TC, Ou JT. Frequency of Epstein-Barr virus-associated gastric adenocarcinoma in Taiwan. *Cancer Lett* 1998; **129**: 125-129

6 **Gurtsevich VE**, Galetskii SA, Nered SN, Novikova EV, Iakovleva LS, Land ChE, Davydov MI, Klimenkov AA, Petrovichev NN, Tokunaga M. Detection and characterization of gastric carcinoma associated with epstein-barr herpes virus. *Vestn Ross Akad Med Nauk* 1999; **3**: 56-59

7 **Galetsky SA**, Tsvetnov VV, Land CE, Afanasieva TA, Petrovichev NN, Gurtsevitch VE, Tokunaga M.Epstein-Barr-virus-associated gastric cancer in Russia. *Int J Cancer* 1997; **73**: 786-789

8 **Chang MS**, Lee HS, Kim CW, Kim YI, Kim WH. Clinicopathologic characteristics of Epstein-Barr virus-incorporated gastric cancers in Korea. *Pathol Res Pract* 2001; **197**: 395-400

9 **Chang MS**, Kim WH, Kim CW, Kim YI. Epstein-Barr virus in gastric carcinomas with lymphoid stroma**.** *Histopathology* 2000; **37**: 309-315

10 **Koriyama C,** Akiba S, Iriya K, Yamaguti T, Hamada GS, Itoh T, Eizuru Y, Aikou T, Watanabe S, Tsugane S, Tokunaga M. Epstein-Barr virus-associated gastric carcinoma in Japanese Brazilians and non-Japanese Brazilians in Sao Paulo. *Jpn J Cancer Res* 2001; **92**: 911-917

11 **Hao Z,** Koriyama C, Akiba S, Li J, Luo X, Itoh T, Eizuru Y, Zou J. The Epstein-Barr virus-associated gastric carcinoma in Southern and Northern China. *Oncol Rep* 2002; **9**: 1293-1298

12 **Qiu K,** Tomita Y, Hashimoto M, Ohsawa M, Kawano K, Wu DM, Aozasa K. Epstein-Barr virus in gastric carcinoma in Suzhou,

China and Osaka, Japan: association with clinico-pathologic factors and HLA-subtype. *Int J Cancer* 1997; **71**: 155-158

13 **Shibata D,** Hawes D, Stemmermann GN, Weiss LM. Epstein-Barr virus-associated gastric adenocarcinoma among Japanese Americans in Hawaii. *Cancer Epidemiol Biomarkers Prev* 1993; **2**: 213-217

14 **Oda K,** Tamaru J, Takenouchi T, Mikata A, Nunomura M, Saitoh N, Sarashina H, Nakajima N. Association of Epstein-Barr virus with gastric carcinoma with lymphoid stroma. *Am J Pathol* 1993; **143**: 1063-1071

15 **Shibata D,** Weiss LM. Epstein-Barr virus-associated gastric adenocarcinoma. *Am J Pathol* 1992; **140**: 769-774

16 **Tokunaga M,** Land CE, Uemura Y, Tokudome T, Tanaka S, Sato E. Epstein-Barr virus in gastriccarcinoma. *Am J Pathol* 1993; **143**: 1250-1255

17 **Nakamura S,** Ueki T, Yao T, Ueyama T, Tsuneyoshi M. Epstein-Barr virus in gastric carcinoma with lymphoid stroma. Special reference to its detection by the polymerase chain reaction and in situ hybridization in 99 tumors, including a morphologic analysis. *Cancer* 1994; **73**: 2239-2249

18 **Corvalan A,** Koriyama C, Akiba S, Eizuru Y, Backhouse C, Palma M, Argandona J, Tokunaga M. Epstein-Barr virus in gastric carcinoma is associated with location in the cardia and with a diffuse histology: a study in one area of Chile. *Int J Cancer* 2001; **94**: 527-530

19 **Tokunaga M,** Uemura Y, Tokudome T, Ishidate T, Masuda H, Okazaki E, Kaneko K, Naoe S, Ito M, Okamura A. Epstein-Barr virus related gastric cancer in Japan: a molecular patho-epidemiological study. *Acta Pathol Jpn* 1993; **43**: 574-581

20 **Takano Y,** Kato Y, Saegusa M, Mori S, Shiota M, Masuda M, Mikami T, Okayasu I. The role of the Epstein-Barr virus in the oncogenesis of EBV(+) gastric carcinomas. *Virchows Arch* 1999; **434**: 17-22

21 **Kijima Y,** Hokita S, Takao S, Baba M, Natsugoe S, Yoshinaka H, Aridome K, Otsuji T, Itoh T, Tokunaga M, Eizuru Y, Aikou T. Epstein-Barr virus involvement is mainly restricted to lymphoepithelial type of gastric carcinoma among various epithelial neoplasms. *J Med Virol* 2001; **64**: 513-518

22 **Yuen ST,** Chung LP, Leung SY, Luk IS, Chan SY, Ho J. *In situ* detection of Epstein-Barr virus in gastric and colorectal adenocarcinomas. *Am J surg Pathol* 1994; **18**: 1158-1163

23 **Yanai H,** Shimizu N, Nagasaki S, Mitani N, Okita K. Epstein-Barr virus infection of the colon with inflammatory bowel disease. *Am J Gastroenterol* 1999; **94**: 1582-1586

24 **Cho YJ,** Chang MS, Park SH, Kim HS, Kim WH. *In situ* hybridization of Epstein-Barr virus in tumor cells and tumor-infiltrating lymphocytes of the gastrointestinal tract. *Hum Pathol* 2001; **32**: 297-301

25 **Samaha S,** Tawfik O, Horvat R, Bhatia P. Lymphoepithelioma-like carcinoma of the colon: report of a case with histologic, immunohistochemical, and molecular studies for Epstein-Barr virus. *Dis Colon Rectum* 1998; **41**: 925-928

26 **Ioachim HL,** Antonescu C, Giancotti F, Dorsett B, Weinstein MA. EBV-associated anorectal lymphomas in patients with acquired immune deficiency syndrome. *Am J Surg Pathol* 1997; **21**: 997-1006

27 **Ruschoff J,** Dietmaier W, Luttges J, Seitz G, Bocker T, Zirngibl H, Schlegel J, Schackert HK, Jauch KW, Hofstaedter F. Poorly differentiated colonic adenocarcinoma, medullary type: clinical, phenotypic, and molecular characteristics. *Am J Pathol* 1997; **150**: 1815-1825

28 **Grinstein S,** Preciado MV, Gattuso P, Chabay PA, Warren WH, De Matteo E, Gould VE. Demonstration of Epstein-Barr virus in carcinomas of various sites. *Cancer Res* 2002; **62**: 4876-4878

29 **Kon S,** Kasai K, Tsuzuki N, Nishibe M, Kitagawa T, Nishibe T, Sato N. Lymphoepithelioma-like carcinoma of rectum: possible relation with EBV. *Pathol Res Pract* 2001; **197**: 577-582

30 **Kim YS,** Paik SR, Kim HK, Yeom BW, Kim I, Lee D. Epstein-Barr virus and CD21 expression in gastrointestinal tumors. *Pathol Res Pract* 1998; **194**: 705-711

31 **Vilor M,** Tsutsumi Y. Localization of Epstein-Barr virus genome in lymphoid cells in poorly differentiated adenocarcinoma with lymphoid stroma of the colon. *Pathol Int* 1995; **45**: 695-697

32 **Glaser SL,** Ambinder RF, DiGiuseppe JA, Horn-Ross PL, Hsu JL. Absence of Epstein-Barr virus EBER-1 transcripts in an epidemiologically diverse group of breast cancers. *Int J Cancer* 1998; **75**: 555-558

Edited by Zhao M and Wang XL

P.O.Box 2345, Beijing 100023,China
Fax: +86-10-85381893
E-mail: wjg@wjgnet.com www.wjgnet.com

World J Gastroenterol 2003;9(11):2469-2473
World Journal of Gastroenterology
 ISSN 1007-9327

• COLORECTAL CANCER •

Lack of inhibitory effects of Lactic acid bacteria on 1,2-dimethylhydrazine-induced colon tumors in rats

Wei Li, Chong-Bi Li

Wei Li, Department of Obstetrics and Gynecology, First People's Hospital of Hangzhou, Hangzhou 310006, Zhejiang Province, China
Chong-Bi Li, Department of Biology, College of Zhaoqing, Duanzhou-Qu, Zhaoqing 526000, Guangdong Province, China
Correspondence to: Dr. Wei Li, Department of Obstetrics and Gynecology, First People's Hospital of Hangzhou, 261 Wansha-lu, Shangcheng-Qu, Hangzhou 310006, Zhejiang Province, China. lwmyj@hotmail.com
Telephone: +86-571-87065701-4331 **Fax**: +86-571-87914773
Received: 2003-03-05 **Accepted:** 2003-04-01

Abstract

AIM: A myriad of healthful effects has been attributed to the probiotic lactic acid bacteria, perhaps the most controversial issue remains that of anticancer activity. This study was aimed at investigating the putative anti-cancer effects of lactic acid bacteria strains on the progression of colon tumor in 1,2-dimethylhydrazine (DMH)-treated animals.

METHODS: The strain of lactic acid bacteria used in this study was lactic acid bacteria NZ9000 that conformed to the characteristics of plasmid free. Sixty male Wistar rats were given subcutaneous injections of DMH at a dose of 40 mg/kg body wt or saline once a week for 10 weeks. The rats were divided into 6 experimental groups. After the last DMH injection, animals in groups 1 and 4 were gavaged with 1 ml of lactic acid bacteria at a dose of 5×10^9 per day or vehicle until sacrifice at the end of week 22 or week 52. Animals in groups 1-3 were killed at the end of week 22 for histopathological examination. The whole period of experimental observation was 52 weeks.

RESULTS: By the end of 22nd week, final average body weights of the rats treated with DMH alone and all animals receiving lactic acid bacteria were significantly decreased compared with the vehicle control ($P<0.05$). No differences in tumor incidence, multiplicity, dimensions and stage in the colonic mucosa were observed among the groups. At week 52, the survival rate of the rats administered lactic acid bacteria was lower than that of the rats treated with DMH that were fed on control fluids of non-*lactococcus lactis*. The mean survival time of lactic acid bacteria-treated animals was 39 weeks.

CONCLUSION: These results indicate that lactic acid bacteria lacks inhibitory effects on the progression of colon tumor in DMH-treated animals, and does not support the hypothesis that alteration of colonic flora may exert an influence on the progression of colon tumor.

Li W, Li CB. Lack of inhibitory effects of Lactic acid bacteria on 1,2-dimethylhydrazine-induced colon tumors in rats. *World J Gastroenterol* 2003; 9(11): 2469-2473
http://www.wjgnet.com/1007-9327/9/2469.asp

INTRODUCTION

Epidemiological studies have provided evidences that the morbidity of colon cancer is influenced by diet. Several studies of humans and experimental animals suggested that the influence of diet was mediated by altering the metabolic activity of intestinal bacterial flora[1,2]. Some of these enteric bacteria are beneficial to the host and have been shown to exert antimutagenic and anticarcinogenic properties[3-5]. By definition, probiotic bacteria can beneficially affect the host by improving its intestinal microbial balance. Bacterial flora that ferment the dairy products (e.g. lactic acid bacteria) might be used for cancer chemoprevention[4].

Lactobacilli are one of the dominant species in the small intestine, and these micro-organisms presumably affect metabolic reactions occurring in this part of the gastrointestinal tract. Some metabolites of lactic bacteria, such as lactic acid and enzymes, have been reported to have some chemotherapeutic value[6]. Furthermore, several studies have also shown that consumption of *bifidobacteria* reduces colon cancer risk in carcinogen-treated animals, suggesting that consumption of certain bacteria has a beneficial effect on the balance of colon *bacteria*[7,8]. Although a myriad of healthful effects have been attributed to the probiotic lactic acid *bacteria*, perhaps the most controversial issue is its anticancer activity. How dietary components, including lactic acid *bacteria*, interact with genes contributes to tumor development?

An autochthonous colon cancer model is useful to evaluate the clinical therapeutic efficacy of drugs for colorectal cancer[9,10]. The experimental carcinogen DMH has been used in the study of the effect of diet in experimental animals[1,11]. As the DMH model is known to closely parallel the human disease in term of disease presentation, gross and microscopic pathology[12], it is anticipated that DMH-induced colon tumor in rats would respond to chemotherapeutic drugs used in man[13]. Although clinical use of 5-fluorouracil (5-FU) derivatives was tested in the DMH model, few studies on the effect of lactic acid bacteria on chemically induced colon tumor progression have been reported.

Supplementation of diet with components possessing antimutagenic and anticarcinogenic properties might result in a significant decrease of tumor frequency. A number of studies indicate that administration of *bifidobacteria* or lactobacilli alone or in combination with fermentable carbohydrate(defined as a prebiotic) can alter colonic microflora populations and decrease the development of early preneoplastic lesions and tumors. This study was aimed at investigating the putative anti-cancer effects of lactic acid bacteria strains on the progression of colon tumor in DMH-treated animals.

MATERIALS AND METHODS

Materials

Animals and chemicals Male Wistar rats at 5 weeks of age were obtained (Department of Animals, Chinese Academy of Medical Sciences, Beijing, China) and housed in plastic cages with wood chips for bedding in an animal room with a 12 h light/dark cycle at 22±2 ℃ and 44 %±5 % relative humidity. The rats were fed on the basal diet. Water was available *ad libitum*, and body weight and food consumption were measured weekly

during the experiments. DMH was purchased from Tokyo Kasei Co. (Tokyo, Japan).

Methods

Treatment protocol The experimental design is shown in Figure 1. One week after acclimatization, sixty rats of 6-week-old were randomly divided into six groups (10 rats/group). Animals in Groups 1 and 4 were given subcutaneous injections of DMH dissolved in normal saline solution (40 mg/kg body wt) once a week for 10 weeks. Rats in groups 2 and 5 were injected 0.9 % normal saline (vehicle) at the same time. After the last DMH treatment, the animals in groups 1 and 4 were additionally gavaged with 1 ml of lactic acid bacteria at a dose of 5×10^9 per day for 12 weeks or until they were dead. Groups 2 and 5 were gavaged with 1 ml of protective reagents per day (the vehicle control). Groups 3 and 6 served as a carcinogen control. The course of treatments differed slightly from each experiment. All surviving animals were sacrificed under ether anesthesia at week 22 (Groups 1-3) and at the end of experiment (Groups 4-6), respectively. The whole period of experimental observation was 52 weeks.

Tissue processing All animals were autopsied. The colons were removed, flushed with saline, opened along the longitudinal median axis. Macroscopically, the number of tumors in each colon was counted. Tumor width (*W*) and length (*L*) were measured with calipers. Tumor volume (*TV*) was determined according to the following formula: $TV=(L\times W^2)/2$[14]. After the gross pathologic changes (number, dimensions and distribution of the tumors) were recorded, the colons were fixed flat between pieces of filter paper in 10 % phosphate-buffered formalin. The liver and kidneys were removed and weighed. Other major organs (stomach, small intestine, spleen, lungs and lymph nodes) were also excised and fixed in 10 % phosphate-buffered formalin solution. Afterward, all tissues were embedded in paraffin and used for sectioning. After the sections were stained with routine hematoxylin and eosin, the colons were divided into proximal, intermediate, and distal segments and examined for histopathological analysis.

Tumor staging Animals with DMH-induced colon cancer characteristically developed multiple tumors and each tumor was at a different histological stage[15]. Consequently, for the purpose of this experiment, animals were staged (Duke's stage) with reference to a single index tumor, defined as the largest macroscopically and histologically identifiable colon tumor.

Preparation of lactococcus lactis The strain of *L. lactis* used in this study was lactic acid bacteria NZ9000 that conformed to the characteristics of plasmid free. The strain was obtained from French Academy of Agricultural Sciences. All cloning steps were done with *E.coli* Top10. *E. coli* was grown on Luria-Bertani (LB) medium and incubated at 37 ℃ under aeration. *L.lactis* was grown without shaking on M17 medium in which 1 %(wt/vol.) glucose was added (M17-Glu) and incubated at 30 ℃. When appropriate, antibiotics was added to the culture medium. For lactic acid bacteria strains, chloramphenicol was used at a final concentration of 10 ug/ml. Ampicillin was supplied at a concentration of 100 ug/ml in the case of *E.coli*. In the experiments, the lactic acid bacteria was induced with nisin as follows. An overnight culture of lactic acid bacteria was transferred into a fresh medium at a dilution of 1:50. After 3-4 h of incubation, 1 ng/ml of nisin (Sigma) was added to the culture, which was incubated for 3-4 h. For *L.lactis*, nisin induction was performed as described previously[16].

After incubation, lactic acid bacteria was concentrated to 5×10^9 cells/ml in PBS buffer (pH 7.0). This concentration would be used as an oral dosage for a rat. PBS buffer (pH 7.0) was used as a liquid protecting solution for lactic acid bacteria. The preparations were preserved at 4 ℃ for a week.

Statistical analysis

Statistical analyses were completed with SPSS 9.0 (Statistical Package for the Social Science). The significance of differences between the average values of the groups was analyzed using Cochran's two-tailed Student's *t*-test. The significance of differences in lesion incidences between the groups was assessed by chi-square test. Rat mortality was analysed by the Log Rank method of Peto *et al*[17].

RESULTS

All rats in groups1-3 and 5 survived to the final termination and maintained a relatively healthy appearance throughout the experiment. No signs of severe toxicity or diarrhea were observed in all animals given lactic acid bacteria. No tumors were found in vehicle-treated animals fed on the protective reagents. By the end of 22nd week, final average body weights of the rats treated with DMH alone and all animals receiving lactic acid bacteria were significantly decreased compared with the vehicle control ($P<0.05$). Relative liver and kidney weights

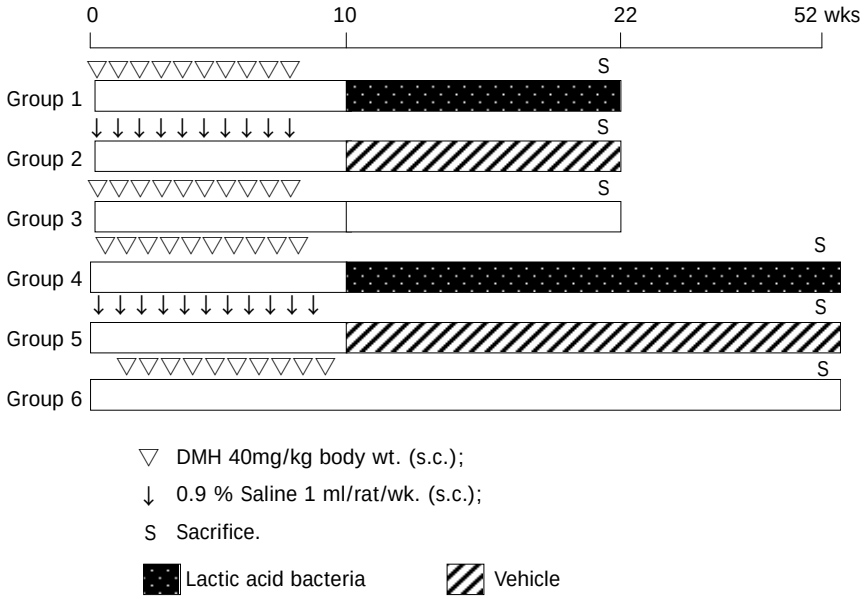

Figure 1 Experimental design.

Table 1 Average final body weight, relative liver and kidney weights, and food consumption data (22wk)

Group	Treatment	No. of rats	Final body Wt, (g)	Relative liver Wt, (g)	Relative kidney Wt, (g)	Average food consumption (g/rat/day)
1	DMH+ lactic acid	10	389.6±44.1[e]	2.92±0.24	0.54±0.06	19.45
2	Saline+ vehicle	10	439.5±39.3	3.09±0.35	0.56±0.12	20.07
3	DMH	10	383.5±19.2[e]	3.10±0.40	0.55±0.07	18.48

a: Values are means ±SD, DMH, 1, 2-dimethylhydrazine, b: Statistical significance: [e]$P<0.05$, Student's *t*-test, *vs* Group 2. c: Kidney weight values are totals for both kidneys.

Table 2 Colon tumor incidence, classification, multiplicity, tumor volume and stage in rats treated with DMH followed or not by lactic acid bacteria (22wk)[a]

Treatment	Incidence *n*(%)	Total no. tumors	Adenoma No (%)	Carcinoma *in situ* No (%)	Carcinoma No (%)	Multiplicity[b] No.	Tumor volume mm^3	Duke's stage[c] A	B	C
DMH+ lactic acid	9 (90)	28	12 (43)	8 (28.5)	8 (28.5)	3.11±2.00	1.64±1.92	0	2	1
DMH	10 (100)	40	27 (67.5)	3 (7.5)	10 (25)	4.00±2.96	4.31±4.56	0	0	3

a: Values are means ±SD. b: No. of tumors/tumor-bearing rat. c: No. of rats with carcinoma were allocated to one of three tumor stages.

and food consumption were not significantly differ among the groups (shown in Table 1). Macroscopically, the distribution of colon tumors was predominantly observed in the proximal and middle colon at the end of 22nd week, there were no significant differences among the groups (data not shown). Histo-pathological examinations of adenocarcinomas in the proximal and middle colon showed that all were invasive through the *muscularis mucosa* and moderately differentiated.

Histo-pathological findings are summarized in Table 2. Colon epithelial lesions were divided into adenoma, carcinoma *in situ* and carcinoma. At the end of 22nd week, the incidence of colon tumor was not significantly affected by lactic acid bacteria. The mean tumor incidence per tumor-bearing rat was 3.11 in group 1 and 4.00 in group 3. Tumor volume was decreased in rats receiving lactic acid bacteria, however, the differences were also not significant compared with DMH- treated group. On the other hand, there was no significant difference in the incidence of metastasis (Duke's stage) between the animals treated with DMH alone and those received lactic acid bacteria.

At the termination, the survival rate of rats in groups 4-6 is shown in Figure 2. None of the rats received *L. lactis* survived the full duration of the experiment, while the DMH-treated rats had a 20 % survival rate. However, the survival rats were sacrificed and macroscopically visible metastases were found in their lungs and livers. There was no significant differene in the survival rate between the lactic acid bacteria treated rats and DMH treated rats. All rats in Group 5 (the vehicle control) survived. The mean survival in lactic acid bacteria-treated animals was 39 weeks.

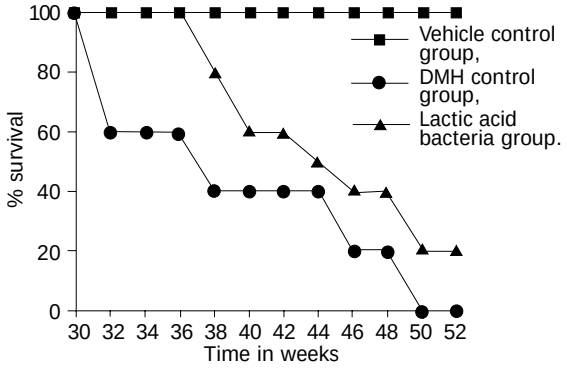

Figure 2 Survival rate of rats injected DMH followed or not by lactic acid bacteria and normal saline.

DISCUSSION

Oral administration of lactic acid bacteria has been shown to effectively reduce DNA damage in animals induced by chemical carcinogens, especially the damage of gastric and colonic mucosa in rats[7]. Certain strains of lactic acid bacteria have also been found to be able to prevent putative preneoplastic lesions induced by carcinogens and have antitumor activity[18,19]. However, findings of in current study do not support the suggestion that addition of lactic acid bacteria may protect against the progression of DMH-induced colon tumor in rats.

The exact change in tumor size or survival of the animals may be crucial for sensitivity determination of anticancer drugs. In this regard, our experimental results seem to be not ideal. The present data did not show any inhibitory effect of lactic acid bacteria on the dimension, multiplicity and invasion of colon tumors. By the end of 22nd week, although there was a reduction in colon tumor volume in animals received lactic acid bacteria, this difference was not statistically significant. The Duke's staging system for human colorectal cancer provides accurate prognostic information. In other words, animals with less advanced diseases (stage A) can survive significantly longer than those with more advanced diseases (stage B and C), irrespective of treatment. In the present study, there was no significant difference in the incidence of metastases at necropsy in lactic acid bacteria-treated and untreated animals. Moreover, the survival rate of rats received lactic acid bacteria was lower than that of rats treated with DMH that were fed on non-lactic acid bacteria. The lower survival rate of rats administered *L. lactis* suggested that lactic acid bacteria had no protective role in decreasing DMH-induced mortality. Whether lactic acid bacteria has some promoting role in the progression of colon tumor is not clear.

In fact, the data from experimental studies indicated that ingestion of certain lactic cultures or their fermented dairy products could reduce the risk of certain types of cancer and inhibit tumor growth[20-22]. The animal experiments did indicate that feeding certain lactic cultures or fermented milk not only suppressed the incidence of DMH-induced colon carcinogenesis but also increased the survival rate of rats with chemically induced colon cancer[23]. These lactic cultures have been shown to possess antimutagenic properties[24], and the probiotic was given during the initiation and promotion phases. However, the antimutagenic activity of lactic acid-producing bacteria was suspected to reside in cell wall[25], as lactic acid itself had no antimutagenic effects[26]. In a previous study, the findings failed

to demonstrate that *bifidobacteria* or *lactobacilli* administration alter colonic microflora had effects on the host[27], and no significant effect was observed when probiotic was given after the promotion phase. In the present study, the lower survival rate of the lactic acid bacteria group (Figure 2) suggested that lactic acid bacteria had no protective role in decreasing DMH-induced mortality. The observed results in survival rats might be due to the fact that lactic acid bacteria can not decrease faecal enzymes involved in formation of carcinogenesis. In addition, our studies failed to show a significant reduction in total number of colon tumors in rats. We believe that this indicates lactic acid bacteria lacks effects on colon cancer in rats. At present, the results from epidemiological studies do not appear to support the results from experimental studies of lactobacilli or lactic acid bacteria on colon cancer prevention or treatment. The reason for this is unclear but might be explained by differences in bacterial strains. The precise mechanisms by which lactic acid *bacteria* may inhibit colon cancer are presently unknown. However, many antitumor activities attributed to lactic cultures have been suggested to involve an enhanced immune response. Therefore, more work needs to be done to identify the specific strains and their antitumor effects and the mechanisms underlying these effects.

Human cancer-nude mice subcutaneous xenograft system as a sensitivity test for chemotherapeutic drugs was studied[28], but it has not been established that the system is a predictive model for screening anticancer drugs. Recently, investigators have been giving greater attention to more rigorous experimental endpoints, such as tumor regression[29-31]. In this respect, autochthonous colon cancer in rats may be suitable to disease oriented *in vivo* screening. DMH-induced rat colon tumor model might be a valuable for new therapeutic agents[9,10]. The fact that clinically used drugs such as 5FU could inhibit the growth of DMH-induced colon tumors and prolong the survival of their rodent hosts suggested a parallel in tumor sensitivity[13]. Therefore, colon tumors induced by DMH at present were the most popular models used in experimental oncology to study various aspects of the morphology, pathogenesis, prevention and treatment of colorectal cancer[9-13]. The animal model described in this study was a truly adjuvant model since the rats developed primary colon tumors *in situ*, which resembled the histopathologic features of human colon tumors. Moreover, DMH decreased animal body weight at the end of week 22, but had no effect on food intake, probably due to its aggressive effect on the mucosa and carcinogenicity.

In the present study, two possible reasons for the failure to alter rat colon tumor were put forward. One was that *L. lactis* lacked inhibitory effects because the initiation of DMH was too strong in our study. The other was that the dose of *L. lactis* might be inadequate to significantly alter colonic flora. It is clear that an optimal condition must be met for each inhibitor to be used for animal and possibly for human cancer prevention and treatment. Otherwise, the same substance, it might enhance the processes of growth of tumor instead of inhibiting. Therefore, it will be extremely difficult, to devise an optimal diet because of the wide variety of cancer inhibitors and enhancers present in human diet.

In conclusion, this study did not find any inhibitory effect in experimental colon tumor progression by addition of lactic acid bacteria after the promotion stage of carcinogenesis and thus does not support the hypothesis that alteration of colonic flora may exert an influence on the progression of DMH-induced colon tumor.

ACKNOWLEDGMENTS

Authors are very grateful to Prof. Shoji Fukushima, Department of Pathology, Osaka City Medical School (Japan) for valuable discussion and comments, and Prof. Yanfeng Zhong, Department of Pathology, Beijing University Medical School for histopathological examination.

REFERENCES

1 **Balansky R**, Gyosheva B, Ganchev G, Mircheva Z, Minakova S, Georgiev G. Inhibitory effects of freeze-dried milk fermented by selected Lactobacillus bulgaricus strains on carcinogenesis induced by 1,2-dimethylhydrazine in rats and by diethylnitrosamine in hamsters. *Cancer lett* 1999; **147**: 125-137

2 **Femia AP,** Luceri C, Dolara P, Giannini A, Biggeri A, Salvadori M, Clune Y, Collins KJ, Paglierani M, Caderni G. Antitumorigenic activity of the prebiotic inulin enriched with oligofructose in combination with the probiotics Lactobacillus rhamnosus and Bifidobacterium lactis on azoxymethane-induced colon carcinogenesis in rats. *Carcinogenesis* 2002; **23**: 1953-1960

3 **Renner HW**, Munzner R. The possible role of probiotics as dietary antimutagen. *Mutat Res* 1991; **262**: 239-245

4 **Lidbeck A,** Nord CE, Gustafsson JA, Refter J. Lactobacilli, anticarcinogenic activities and human intestinal microflora. *Eur J Cancer Prev* 1992; **1**: 341-353

5 **Vorob'eva LI,** Abilev SK. Antimutagenic properties of bacteria: a review. *Prikl Biokhim Mikrobiol* 2002; **38**: 115-127

6 **Shahani KM**, Chandan RC. Nutritional and healthful aspects of cultured and culture-containing dairy foods. *J Dairy Sci* 1979; **62**: 1685-1694

7 **Pool-Zobel BL**, Neudecker C, Domizlaff I, Ji S, Schillinger U, Rumney C, Moretti M, Vilarini I, Scassellati-Sforzolini R, Rowland I. Lactobacillus- and Bifidobacterium-mediated antigenotoxicity in the colon of rats. *Nutr Cancer* 1996; **26**: 365-380

8 **Singh J**, Rivenson A, Tomita M, Shimamura S, Ishibashi N, Reddy BS. Bifidobacterium longum, a lactic acid-producing intestinal bacterium inhibits colon cancer and modulates the intermediate biomarkers of colon carcinogenesis. *Carcinogenesis* 1997; **18**: 833-841

9 **Tsunoda A**, Shibusawa M, Tsunoda Y, Nakao K, Yasuda N, Kusano M. A model for sensitivity determination of anticancer agents against chemically-induced colon cancer in rats. *Anticancer Res* 1994; **14**: 2637-2642

10 **Tsunoda A**, Shibusawa M, Tsunoda Y, Yokoyama N, Nakao K, Kusano M, Nomura N, Nagayama S, Takechi T. Antitumor effect of S-1 on DMH induced colon cancer in rats. *Anticancer Res* 1998; **18**: 1137-1141

11 **Li W**, Wanibuchi H, Salim EI, Wei M, Yamamoto S, Nishino H, Fukushima S. Inhibition by ginseng of 1,2- dimethylhydrazine induction of aberrant crypt foci in the rat colon. *Nutr Cancer* 2000; **36**: 66-73

12 **LaMont JT**, O'Gorman TA. Experimental colon cancer. *Gastroenterology* 1978; **75**: 1157-1169

13 **Danzi M,** Lewin MR, Cruse JP, Clark CG. Combination chemotherapy with 5-fluorouracil (5FU) and 1,3-bis (2-chloro-ethyl)-1-nitrosourea (BCNU) prolongs survival of rats with dimethylhydrazine-induced colon cancer. *Gut* 1983; **24**: 1041-1047

14 **Yoon SS,** Eto H, Lin CM, Nakamura H, Pawlik TM, Song SU, Tanabe KK. Mouse endostatin inhibits the formation of lung and liver metastases. *Cancer Res* 1999; **59**: 6251-6256

15 **Pozharisski KM**. Morphology and morphogenesis of experimental epithelial tumours of the intestine. *J Natl Cancer Inst* 1975; **54**: 1115-1135

16 **De Ruyter PG,** Kuipers OP, Beerthuyzen MM, van Alen-Boerrigter I, de Vos WM. Functional analysis of promoters in the nisin gene cluster of Lactoccus lactis. *J Bacteriol* 1996; **178**: 3434-3439

17 **Peto R**, Pike MC, Armitage P, Breslow NE, Cox DR, Howard SV, Mantel N, McPherson K, Peto J, Smith PG. Design and analysis of randomized clinical trials requiring prolonged observation of each patient II analysis and examples. *Br J Cancer* 1977; **35**: 1-39

18 **Kelkar SM**, Shenoy MA, Kaklij GS. Antitumor activity of lactic acid bacteria on a solid fibrosarcoma, sarcoma-180 and Ehrlich ascites carcinoma. *Cancer Lett* 1988; **42**: 73-77

19 **Goldin BR**, Gualtieri LJ, Moore RP. The effect of Lactobacillus GG on the initiation and promotion of DMH-induced intestinal tumors in the rat. *Nutr Cancer* 1996; **25**: 197-204

20 **Bolognani F,** Rumney CJ, Pool-Zobel BL, Rowland IR. Effect of lactobacilli, bifidobacteria and inulin on the formation of aberrant crypt foci in rats. *Eur J Nutr* 2001; **40**: 293-300
21 **Gallaher DD,** Khil J. The effect of synbiotics on colon carcinogenesis in rats. *J Nutr* 1999; **129**(7Suppl): 1483S-1487S
22 **Reddy BS.** Possible mechanisms by which pro- and prebiotics influence colon carcinogenesis and tumor growth. *J Nutr* 1999; **129**(7Suppl): 1478S-1482S
23 **Shackelford LA**, Rao DR, Chawan CB, Pulusani SR. Effect of feeding fermented milk on the incidence of chemically-induced colon tumors in rats. *Nutr Cancer* 1983; **5**: 159-164
24 **Renner HW**, Munzner R. The possible role of probiotics as dietary antimutagen. *Mutat Res* 1991; **262**: 239-245
25 **Tejada-Simon MV,** Pestka JJ. Proinflammatory cytokine and nitric oxide induction in murine macrophages by cell wall and cytoplasmic extracts of lactic acid bacteria. *J Food Prot* 1999; **62**: 1435-1444
26 **Morita T**, Takeda K, Okumura K. Evaluation of clastogenicity of formic acid, acetic acid and lactic acid on cultured mammalian cells. *Mutat Res* 1990; **240**: 195-202
27 **Nielsen OH**, Jorgensen S, Pedersen K, Justesen T. Microbiological evaluation of jejunal aspirates and fecal samples after oral administration of bifidobacteria and lactic acid bacteria. *J Appl Bacteriol* 1994; **76**; 469-474
28 **Boven E**, Winograd B, Berger DP, Dumont MP, Braakhuis BJ, Fodstad O, Langdon S, Fiebig HH. Phase II preclinical drug screening in human tumor xenografts: a first European multicenter collaborative study. *Cancer Res* 1992; **52**: 5940-5947
29 **Gadducci A,** Viacava P, Cosio S, Fanelli G, Fanucchi A, Cecchetti D, Cristofani R, Genazzani AR. Intratumoral microvessel density, response to chemotherapy and clinical outcome of patients with advanced ovarian carcinoma. *Anticancer Res* 2003; **23:** 549-556
30 **Snyder C,** Harlan L, Knopf K, Potosky A, Kaplan R. Patterns of Care for the Treatment of Bladder Cancer. *J Urol* 2003; **169:** 1697-1701
31 **Raghavan D.** Progress in the chemotherapy of metastatic cancer of the urinary tract. *Cancer* 2003; **97**(8 Suppl): 2050-2055

Edited by Zhao M and Wang XL

P.O.Box 2345, Beijing 100023,China
Fax: +86-10-85381893
E-mail: wjg@wjgnet.com www.wjgnet.com

World J Gastroenterol 2003;9(11):2474-2479
World Journal of Gastroenterology
 ISSN 1007-9327

• VIRAL HEPATITIS •

Establishment of a cell-based assay system for hepatitis C virus serine protease and its primary applications

Hong-Xia Mao, Shui-Yun Lan, Yun-Wen Hu, Li Xiang, Zheng-Hong Yuan

Hong-Xia Mao, Shui-Yun Lan, Yun-Wen Hu, Li Xiang, Zheng-Hong Yuan, Key Laboratory of Medical Molecular Virology, Shanghai Medical College, Fudan University, Shanghai 200032, China
Supported by the National Natural Science Foundation of China, No. 39870010, No. 39825501, the Shanghai Scientific Development Foundation, No. 00QMH1404 and the State 973 Program of China, No. G1999054105
Correspondence to: Zheng-Hong Yuan, Key Laboratory of Medical Molecular Virology, Shanghai Medical College, Fudan University, 138 Yi Xue Yuan Road, Shanghai 200032, China. zhyuan@shmu.edu.cn
Telephone: +86-21-64161928 **Fax:** +86-21-64227201
Received: 2003-03-10 **Accepted:** 2003-06-12

Abstract

AIM: To establish an efficient, sensitive, cell-based assay system for NS3 serine protease in an effort to study further the property of hepatitis C virus (HCV) and develop new antiviral agents.

METHODS: We constructed pCI-neo-NS3/4A-SEAP chimeric plasmid, in which the secreted alkaline phosphatase (SEAP) was fused in-frame to the downstream of NS4A/4B cleavage site. The protease activity of NS3 was reflected by the activity of SEAP in the culture media of transient or stable expression cells. Stably expressing cell lines were obtained by G418 selection. Pefabloc SC, a potent irreversible serine protease inhibitor, was used to treat the stably expressing cell lines to assess the system for screening NS3 inhibitors. To compare the activity of serine proteases from 1b and 1a, two chimeric clones were constructed and introduced into both transient and stable expression systems.

RESULTS: The SEAP activity in the culture media could be detected in both transient and stable expression systems, and was apparently decreased after Pefabloc SC treatment. In both transient and stable systems, NS3/4A-SEAP chimeric gene from HCV genotype 1b produced higher SEAP activity in the culture media than that from 1a.

CONCLUSION: The cell-based system is efficient and sensitive enough for detection and comparison of NS3 protease activity, and screening of anti-NS3 inhibitors. The functional difference between NS3/4A from 1a and 1b subtypes revealed by this system provides a clue for further investigations.

Mao HX, Lan SY, Hu YW, Xiang L, Yuan ZH. Establishment of a cell-based assay system for hepatitis C virus serine protease and its primary applications. *World J Gastroenterol* 2003; 9 (11): 2474-2479

http://www.wjgnet.com/1007-9327/9/2474.asp

INTRODUCTION

The infection of hepatitis C virus (HCV) is associated with a high frequency of chronic hepatitis (up to 80 %), which often progresses to liver cirrhosis and hepatocellular carcinoma (up to 20 %)[1]. Until now, there has been no vaccine against HCV and the most efficacious pharmacological treatment, a combined therapy of interferon alpha and ribavirin, which could lead to sustained remission only in a minority of cases[2,3]. Considerable efforts have been therefore undertaken to develop specific antiviral agents.

HCV is a positive-sense, single-stranded RNA virus and belongs to the flaviviridae family. Its genome is about 9.6 kb in length and encodes the structural proteins C, E1, E2, and the non-structural proteins NS2, NS3, NS4A, NS4B, NS5A and NS5B, which are released by action of both host cell and virally encoded proteases[4,5]. The N-terminal domain of the NS3 protein contains a serine protease, belonging to the chymotrypsin family[6], which is responsible for the proteolytic cleavage at the NS3/4A, NS4A/NS4B, NS4B/NS5A and NS5A/5B junctions of the viral polyprotein[4]. The NS3 thus plays a pivotal role in the viral maturation and replication. It is also known to affect normal cellular functions, such as cell proliferation and cell death, suggesting its involvement either direct or indirect in HCV hepatocarcinogenesis[7-9]. Therefore, the NS3 protease has become one of the most attractive targets for the development of HCV specific antiviral agent.

To establish an efficient, sensitive, cell-based assay system for NS3 serine protease in an effort to study further the property of HCV and develop new antiviral agents, we first constructed the pCI-neo-NS3/4A-SEAP chimeric plasmid, in which the secreted alkaline phosphatase (SEAP) gene was fused in-frame to the downstream of NS4A/4B cleavage site. The protease activity of NS3 was reflected by the activity of SEAP in the culture media of transient or stably expressing cells. Stably expressing cell lines were obtained by G418 selection. To explore the possibility of applying this system to the screening of NS3 inhibitors, Pefabloc SC, a potent irreversible serine protease inhibitor, was then used to treat the stably expressing cell lines. After that, we investigated the difference of serine protease activity between HCV genotype 1b and 1a by constructing two pCI-neo-NS3/4A-SEAP chimeric clones and studying them in both transient and stable expression systems.

MATERIALS AND METHODS

Cloning of HCV NS3/4A and SEAP genes

To amplify NS3/4A region (HCV 1b) using PCR from a near-full length HCV cDNA (from a patient with 1b genotype), two pairs of primers were used: NS3/4A5' , 5' -CCG GAA TTC ATG GCC CCC ATC ACA GCC TAT-3' (nucleotides [nt] 3 420-3 437), and NS3/4A3' , 5' -CAGT CTC GAG GAG GTG TGA GGC GCA-3' (nucleotides [nt] 5 472-5 486); NS3/4A (TGA)3' , 5' - CCG CTC GAG *TCA* GCA CTC CTC CAT CTC ATC-3' (nucleotides [nt] 5 457-5 474, with stop codon, as negative control). RNS3/4A (HCV 1a) was amplified with primer RNS3/4A5' , 5' -AT GAA TTC ATG GCG CCC ATC ACG GCG TAC-3' (nucleotides [nt] 3 420-3 437) and primer RNS3/4A3' , 5' -GCC AAG CTT TAA GTG CTG AGA GCA-3' (nucleotides [nt] 5 472-5 486) from p90/HCV FL-long pU (AF009606) (a generous gift from Professor Charle M Rice from the Center for the Study of Hepatitis C, Rockefellor

University). SEAP fragment was obtained by PCR with two pairs of primers: SEAP(XhoI)5' , 5' -AT CTC GAG ATG CTG CTG CTG CTG CTG CTG-3' (nucleotides [nt] 54-74), SEAP (HindIII)5' , 5' -AT AAG CTT ATG CTG CTG CTG CTG CTG CTG CTG-3' (nucleotides [nt] 54-77), and SEAP3' , 5' -AT GCGGCCGC TCA GGG AGC AGT GGC CGT C-3' (nucleotides [nt] 1 628-1 647) from pCMV-SEAP (generously provided by Professor Byan R.Cullen of the Medical Center, Duke University).

Construction of pCI-neo-NS3/4A-SEAP

The NS3/4A fragment from HCV 1b genotype and digested with *Eco*RI and *Xho*I, was ligated into *Eco*RI/*Not*I site of pCI-neo vector (Stratagene) with the SEAP fragment digested with *Xho*I and *Not*I to generate pCI-neo-NS3/4A-SEAP. The HCV 1a RNS3/4A fragment digested with *Eco*RI and *Hind* III and the SEAP fragment digested with *Hind* III and *Not* I were ligated into *Eco*RI/*Not* I site of pCI-neo vector to generate pCI-neo-RNS3/4A-SEAP. The schematic diagram is shown in Figure 1. The *Eco*RI/*Xho* I fragment from the pET28a-NS3/4A(TGA) was ligated into *Eco*RI/*Sal* I site of pCI-neo vector and the clone was named as pCI-neo-NS3/4A(TGA).

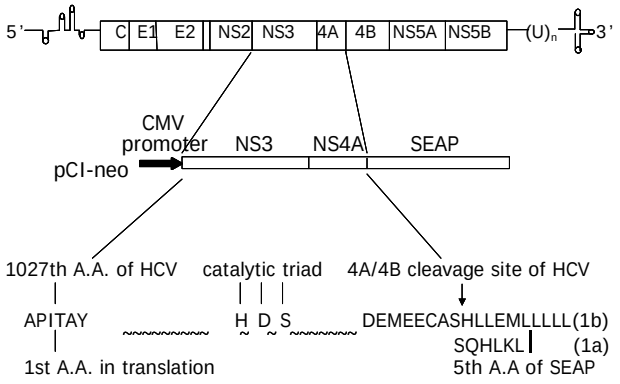

Figure 1 Schematic diagram of the pCI-neo-NS3/4A-SEAP and pCI-neo-RNS3/4A-SEAP expression vectors. The SEAP gene, which has N-terminal signal sequence, was fused in-frame to the HCV sequence encoding the full-length NS3 proteins followed by the NS4A cofactor. Amino acid sequences of (R)NS3/4A and SEAP in the fusion regions are shown by capitalized, bold characters. The cleavage site between NS4A and NS4B is indicated by arrow. HDS is the catalytic triad of NS3 protease.

Cell culture and transfection

HepG2 cells or Cos7 cells were cultured in Dulbecco's modified Eagle's medium (DMEM) with penicillin (100 U/ml) and streptomycin (100 μg/ml), supplemented with 10 % fetal calf serum. Recombinant plasmid DNA used for transfection was extracted and purified with the Qiagen Midiprep kits. DNA (5 μg) was used to transfect HepG2 or Cos7 cells in 6-well NUNC multidish by the calcium phosphate precipitation method as reported previously[10]. Duplicate dishes were used for all samples, and 3 μg of reporter plasmid pcDNA3.1-CAT expressing chloramphenicol acetyltransferase (CAT) was cotransfected as an internal control to normalize the transfection efficiency among dishes. Forty-eight hours after transfection, culture media and cells were collected separately to monitor the secretion of SEAP in the supernatant and NS3 protease expression in transfected cells. pCI-neo-NS3/4A (TGA) was used as a mock transfection control. Transfection experiments were repeated twice on separate days.

Colorimetric assay for SEAP

The SEAP activity of the culture media was measured at 48 h after transfection by performing a colorimetric assay according to the author's recommendation[11]. Briefly, 20 μl heat-treated (at 65 ℃ for 5 min) medium was adjusted to 1×SEAP assay buffer (1.0 M diethanolamine pH9.8, 0.5 mM $MgCl_2$, 10 mM L-homoarginine) in a final volume of 200 μl and prewarmed to 37 ℃ for 10 min in a 96-well flat-bottom culture dish. Twenty μl of prewarmed 120 mM *p*-nitrophenylphosphate dissolved in SEAP assay buffer was then added with mixing. The A_{405} of the reaction mixture was read in a BIO-RAD (Benchmark) microplate reader at 5-min intervals. The change in absorbance was plotted and the maximum linear reaction rate determined. The SEAP activity was expressed in milliunits (mU) per ml. One mu equals an increase of 0.04 A_{405} units per min. Each SEAP assay was performed in triplicate.

Establishment of NS3/4A-SEAP stable expression system

Two different cell lines of Cos7 and HepG2 cells were transfected with the plasmid pCI-neo-NS3/4A-SEAP, pCI-neo-RNS3/4A-SEAP or pCI-neo-NS3/4A (TGA), respectively by calcium phosphate precipitation method mentioned above. At 48 h after transfection, the cells were subcultured and selected with the 600 mg/l of G418. After 3 weeks of selection, the colonies were picked up and amplified in the presence of 200 mg/l G418.

Inhibition of HCV protease activity by Pefabloc SC

Cos7 cell lines (1b and 1a type) were seeded into a 6-well NUNC multidish at a density of 10^5 cells/ml in 3 ml medium and cultured overnight at 37 ℃ in a 50 ml· L^{-1} CO_2 incubator. The overnight culture media were changed with fresh one containing Pefabloc SC at the concentration of 0.1 mM, 0.2 mM, 0.4 mM, 0.5 mM, or 0.6 mM. The cells without Pefabloc SC treatment were set as control. After 24 hours, the media were collected for the colorimetric assay for SEAP activity. Effect of Pefabloc SC on the viability of Cos7 stable cells was evaluated by the alamarBlue™ assay (Biosource International Corp.)[12]. Alamar Blue was added in an amount equal to 10 % of the culture volume and after 2 hours of incubation at 37 ℃, the panels were read spectrofluorometrically (excitation, 544 nm; emission, 590 nm) by Ascent FL. The experiment was performed twice and each sample was detected in duplicate.

Northern blot analysis of NS3/4A expression in transfected cells

Total RNA was extracted using GIBCO-BRL TRIZOL Reagent (Cat No. 15596 Gibco Life Tech) according to the instructions of manufacturers. It was digested with RNase free DNase (Promega) to wipe off the transfected plasmid DNA. After electrophoresis in a 1 % agarose gel, 10 μg total RNA was blotted onto a positively charged Nylon membrane (Roche). HCV NS3/4A (100 ng of PCR products, 1a and 1b respectively) and random primers were used to prepare the [^{32}P] dCTP labled probes for hybridization. The signals were detected by autoradiography and scanned with densitometry for semiquantification of the intensity of signals. The corresponding intensity of β-actin signals was used as controls.

Western blot analysis of NS3/4A expression in transfected cells

To assess the expression levels of the HCV NS3/4A of two HCV genotypes in the transfected HepG2 or Cos7, Western blot analysis was conducted as described[13] with some modifications. Briefly, cells were lysed in 200 μl TSA buffer (50 mM Tris-HCl, 140 mM NaCl, 5 ml· L^{-1} NP40, 1 mM PMSF, 1 mM DTT). Ten μl aliquot was subjected to 7.5 % SDS-PAGE eletrophoresis. The separated proteins were transferred to nitrocellulose membrane in transfer buffer (20 mM Tris-HCl, 190 mM Glycine, 200 ml· L^{-1} methanol, pH 8.3) using Mini Trans-blot transfer system (Bio-Rad) at 100V for 1 h. The membrane was blocked with 50 mg· L^{-1} nonfat dried milk in

PBST (Tris-buffered saline containing 0.5 ml· L^{-1} Tween-20) and then incubated with mouse anti-NS3 multiclonal antibody. After three washes in PBST, the membrane was incubated with peroxidase-conjugated goat anti-mouse second antibody (A90-131P, BETHYL Co.). The blot was incubated with TMB substrate to reveal the antigen bands. Cellular protein La (a phosphoprotein, 47 KD, present at proximately 2×10^7 molecules per cell) was used as a quantificational control. The expression levels of the NS3 of two HCV isolates were compared by the semi-quantification of scanned intensity of antigen bands.

RESULTS

Transient expression of NS3/4A-SEAP

The plasmids pCI-neo-NS3/4A-SEAP, pCI-neo-NS3/4A (TGA) and pCMV-SEAP were transfected into HepG2 or Cos7 cells by calcium phosphate method and the SEAP activity of the culture media was measured at 48 h after transfection. As expected, in HepG2 cells, the pCMV-SEAP produced SEAP activity about 30.16±3.46 mu/ml, while pCI-neo-NS3/4A (TGA) produced 0.34±0.48 mu/ml, which is almost the background level (Figure 2). The culture media from cells transfected with pCI-neo-NS3/4A-SEAP showed a SEAP activity of about 12.05±1.25 mu/ml. Similar results were obtained in Cos7 cells (data not shown). The processing of fusion proteins expressed in transfected cells was examined by immunoblotting with anti-HCV human sera and mouse derived multiple-clonal sera. Processed NS3 protein of 70KD was detected (Figure 6). The results indicate that, depending on the cleavage activity of the NS3 protease, the SEAP could be cleaved and secreted into the extracellular media.

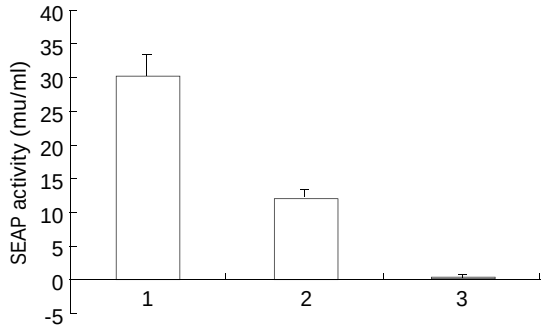

Figure 2 SEAP activity in the media of the transfected HepG2 cells. Lane 1: pCMV-SEAP, Lane 2: pCI-neo-NS3/4A-SEAP, Lane 3: pCI-neo-NS3/4A(TGA)(as negative control).

Stable expression of NS3/4A-SEAP

To establish the NS3/4A-SEAP assay system in stable expression cells, HepG2 and Cos7 cells transfected with the pCI-neo-NS3/4A-SEAP were selected for stable expression ones. During 600 mg/l G418 selection, most transfected HepG2 or Cos7 cells died out after 4 changes of media and the selected colonies were picked up and amplified in the presence of 200 mg/l G418. Results of SEAP assay showed that all selected stably expressing cell lines produced SEAP in their supernatant. However, the media from Cos7-derived stably expressing cell lines showed higher SEAP activity than those from HepG2-derived cell lines. Initially, the two kinds of stably expressing cell lines did not show any significant differences. Then, the HepG2-derived cell lines appeared to lose supernatant SEAP activity, depending on the passages and showed finally, very low SEAP activity (data not shown) while selected cell lines derived from Cos7 appeared to express high levels of SEAP during continuous passages over 4 months.

Comparison of protease activity of NS3/4A from HCV 1a and 1b two subtypes in both transient and stable expression systems

To compare the activity of serine proteases from HCV subtype 1b and 1a, two chimeric clones were constructed and studied in both transient and stable expression systems. Results of SEAP assay showed that, in transient expression system, the Cos7 cells transfected with the pCI-neo-NS3/4A(1b)-SEAP produced higher supernatant SEAP activity (37.49±3.06 mu/ml) than those transfected with pCI-neo-RNS3/4A(1a)-SEAP (3.48±0.15 mu/ml). The overall assay results were similar in HepG2 cells with pCI-neo-NS3/4A(1b)-SEAP at 11.82±0.92 mu/ml and pCI-neo-RNS3/4A(1a)-SEAP at 2.49±0.67 mu/ml. The above results indicated that cells transfected with pCI-neo-NS3/4A-SEAP from HCV 1b isolate produced 5-10 folds higher supernatant SEAP activity than those transfected with pCI-neo-RNS3/4A-SEAP from HCV 1a isolate (Figure 3). Consistently, the 1b derived stable cell lines also produced higher SEAP activity in media (39.11±2.97 mu/ml, 25.36±1.41 mu/ml) than those derived from 1a (6.92±0.56 mu/ml, 7.85±0.57 mu/ml, Figure 4).

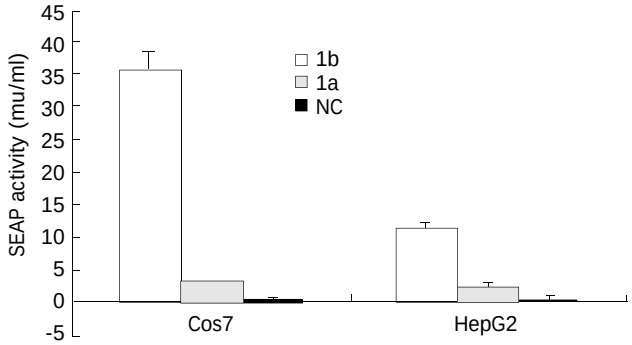

Figure 3 SEAP activity in the media of the transfected HepG2 and Cos7 cells. 1b: pCI-neo-NS3/4A-SEAP; 1a: pCI-neo-RNS3/4A-SEAP; NC: pCI-neo-NS3/4A(TGA)(as negative control).

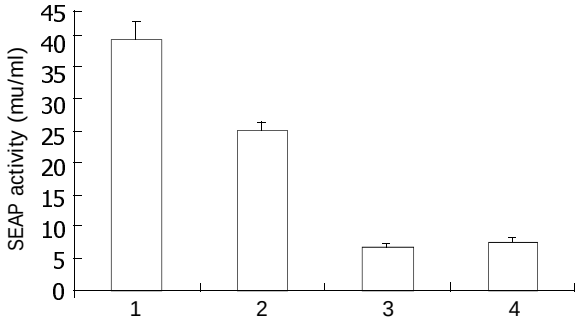

Figure 4 SEAP activity in the media of Cos7-derived stably expressing cell lines. Lane 1, 2: 1b type stable expression cell lines; Lane 3, 4: 1a type stable expression cell lines.

Northern blot analysis of NS3/4A mRNA level in transfected cells

To compare the amounts of NS3/4A mRNAs in transfected HepG2 and Cos7 cells, Northern blotting was carried out using the isotope-labeled DNA probes corresponding to NS3/4A regions of 1b and 1a. The NS3/4A specific signals could be detected in both HepG2 and Cos7 cells transfected with pCI-neo-NS3/4A-SEAP(1b), pCI-neo-NS3/4A(TGA), or pCI-neo-RNS3/4A-SEAP(1a) respectively. The hybridization signals of NS3/4A mRNA were similar between conspecific cells transfected with 1b or 1a constructs as the ratio of signal densities of NS3/4A to β-actin in pCI-neo-NS3/4A-SEAP(1b),

pCI-neo-NS3/4A(TGA) and pCI-neo-RNS3/4A-SEAP(1a) transfected cells were similar (2 066/2 360/2 400 in transfected Cos7 cells and 0.8/0.6/0.7 in transfected HepG2 cells) (Figure 5).

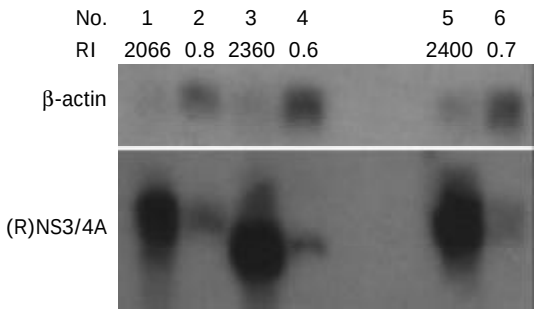

Figure 5 Northern blot analysis of NS3/4A mRNA level in transfected Cos7 cells (Lane 1, 3, 5) and HepG2 cells (Lane 2, 4, 6). Lane 1, 2 pCI-neo-NS3/4A-SEAP (1b type); Lane 3, 4 pCI-neo-NS3/4A (TGA) (control); Lane 5, 6 pCI-neo-RNS3/4A-SEAP (1a type); Intensity of hybridization signal was measured by densitometry, and the relative intensities of NS3/4A signal to β-actin are indicated below the lane No.

Western blot analysis of NS3 protein level in transfected cells

To compare the levels of NS3 proteins in transfected cells, Western blotting was carried out to detect the HCV protease expression with mouse anti-NS3 antibody. The expression levels of the NS3 were compared by the semiquantification of bands detected by immunoblotting. The relative intensities (RI) of NS3 to cellular protein La are indicated in Figure 6. The results showed that NS3 level expressed by pCI-neo-NS3/4A-SEAP (1b) was similar to the one expressed by pCI-neo-RNS3/4A-SEAP (1a) (3/3 in transfected Cos7 cells and 1/1 in transfected HepG2 cells) in transfected cells (Figure 6).

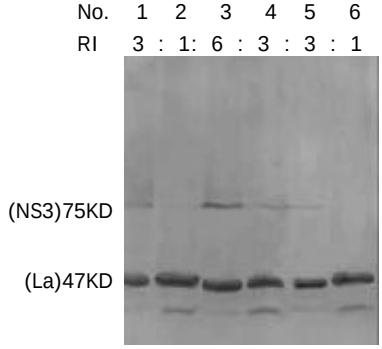

Figure 6 Western blot analysis of NS3 protein level in transfected Cos7 cells (Lane1, 3, 5) and HepG2 cells (Lane 2, 4, 6). Lane 1, 2 pCI-neo-NS3/4A-SEAP (1b type), Lane 3, 4 pCI-neo-NS3/4A(TGA) (control), Lane 5, 6 pCI-neo-RNS3/4A-SEAP (1a type). Intensity of hybridization signal was measured by densitometry, and the relative intensities (RI) of NS3 to cellular protein La in samples are indicated.

Inhibition of protease activity of NS3/4A by Pefabloc SC

Pefabloc SC, a serine protease inhibitor was added into the media of Cos7-derived stable expression cells at the concentration of 0.1 mM, 0.2 mM, 0.4 mM, 0.5 mM, or 0.6 mM. After 24 hours, the media were collected for the colorimetric assay of SEAP activity. The effect of Pefabloc SC on the viability of stable expression cells was evaluated by the alamarBlue™ assay. Results showed that, although the Pefabloc SC was relatively toxic to cells, it had some specific inhibitory effect on the protease activity of NS3/4A as the secretion of SEAP, which was dependent on the active HCV protease, was decreased more than the metabolic activity of the cells after treatment, and it was 60-70 % when the treated cells still kept almost 100 % metabolic activity (Figure 7).

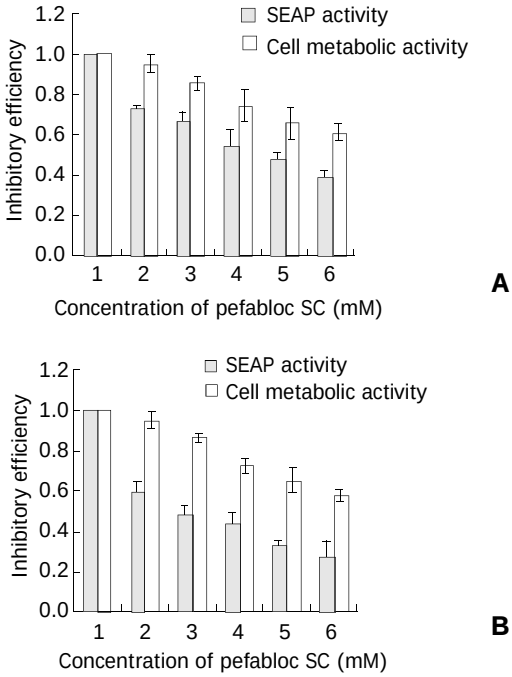

Figure 7 SEAP activity and viability of Cos7 stable cells treated with Pefabloc SC. The SEAP activity and viability of cells were measured with colorimetric and alamar Blue™ assay according to manufactures' recommendations. Each assay was performed in triplicate. A: 1b type stable expression cell lines, B: 1a type stable expression cell lines. 1: no treatment, 2: 0.1 mM, 3: 0.2 mM, 4: 0.4 mM, 5: 0.5 mM, 6: 0.6 mM.

DISCUSSION

It has been reported that the cleavage activity of NS3 could be detected by *in vitro* transcription/translation and transient expression experiments[14-16], or using purified active NS3 protease[17,18]. But they are known to be difficult to apply for screening specific NS3 inhibitors at large scale. Another problem has to be considered referring to the rather featureless substrate binding pocket of NS3[19], which may make the development of specific inhibitors rather difficult. Alternative *in vivo* assay systems for NS3 protease, which can differentiate the inhibitors' effects on NS3 protease and cellular metabolic activity (including cellular serine-type protease), will accelerate the screening of specific inhibitors. Several chimeric viral replication systems had been developed to screen HCV inhibitors in tissue culture[20,21]. These systems have some disadvantages regarding instability of chimeric viruses and difficulty in evaluating the inhibition quantitatively. Comparably, our cell-based NS3/4A-SEAP expression system is safe, easy to handle and the report gene of SEAP can be sensitively and quantitatively measured continuously without killing cells[11].

In the scheme of pCI-neo-NS3/4A-SEAP constructs, the NS4A/SEAP junction has the sequence DEMEEC ↓ ASHL (HCV 1b subtype)[22] or DEMEEC ↓ SQHL (HCV 1a subtype) which contains NS4A/4B cleavage site. The rationale for this system was based on the assumption that the secretion of SEAP protein into the culture media depends on the cleavage between NS4A protein and SEAP protein by HCV NS3 protease. The unusual substrate specificity, which is quite distinct from cellular serine-type proteases, makes it possible for the system to generate inhibitors with a high degree of selectivity[23,24]. To make the system more suitable for the screening of NS3

inhibitors, we also established the stably expressing cell lines. During the screening, the inhibitor could be introduced into the stable cells by transfection or simply adding in culture media[25] according to their own characteristics.

In the process of establishing both transient and stable expression systems, we found that Cos7-derived cells always showed higher SEAP activity in media than HepG2-derived ones. It is consistent with the previous report that Cos7 cells and other cell lines expressing the SV40 large T-antigen, have been of great benefit to the transfection studies using transient expression vectors containing the SV40 origin of replication, as these cells yield plasmid replication to a high copy number[26]. In addition, we also observed that the two kinds of cell lines initially did not show any significant differences in cell growth and morphology, but depending on the passages, the HepG2-derived cell lines appeared to lose SEAP activity and finally showed very low SEAP activity (data not shown). However, the Cos7-derived cell lines appeared to express high levels of SEAP activity during continuous passages even after 4 months. It is likely that the expression of active protease is relatively toxic in some cells, leading to selection of cells with low protease activity in the process of G418 selection and passage[22].

When this assay system was used to compare the activity of HCV serine proteases from different genotypes (1b and 1a), the cells transfected with 1b type plasmid DNA showed 5-10 folds higher SEAP activity in culture media than those with 1a type one in transient system. And there were no significant differences in protein and mRNA levels of NS3/4A between them in either transiently transfected Cos7 or HepG2 cells. The results indicated that the cleavage efficiency of 1b type NS3 protease was 5-10 folds higher than that of 1a type. Consistently, we observed similar results in the stable expression system. Since the NS3 serine protease activity is required for cleavages at the downstream 3/4A, 4A/4B, 4B/5A, 5A/5B sites, its cleavage efficiency will affect the assembly of functional HCV RNA replication complex, viral particle maturation and host-virus interaction. It has been reported that the success in establishing efficient HCV replication depended on the particular genotype 1b consensus cDNA clone studied[27]. Whether the higher protease activity of 1b subtype NS3 contributes to the above phenomenon is worthy of further investigations. The availability of replication system[27-29] will promote such studies.

In this study, the cell-based system was also successfully used to evaluate the inhibition effect of Pefabloc SC on the NS3 protease *in vivo*. Pefabloc SC[30] is one of the most potent inhibitors of the class of sulfonyl fluorides like phenylmethylsulfonylfluoride (PMSF). It has been widely used to inhibit all kinds of serine proteases (including HCV NS3)[31,32]. It was reported that 8mM of Pefabloc SC showed strong effects on NS3-4A junction in a trans-cleavage assay system[33]. Due to its toxicity to cells, the concentrations of Pefabloc SC used in our system were only from 0.1 mM to 0.6 mM. However, results here still showed that it had some specific inhibitory effect on the protease activity of the HCVNS3/4A as the secretion of SEAP, which depended on the active HCV protease, was decreased more than the metabolic activity of the cells after treatment (Figure 6). As shown in Figure 6, when the cells treated with 0.1 mM Pefabloc SC still kept near 100 % metabolic activity, the SEAP activity in culture media had decreased to 60-70 %. These data reflected the sensitivity of our system and its practicability for the detection and comparison of NS3 protease activity and the screening anti-NS3 inhibitors.

In summary, we reported the establishment of the cell-based NS3/4A-SEAP expression system in both transiently transfected and stable cell lines. It was further applied to the evaluation of Pefabolc SC, a known protease inhibitor and the comparison of activities of NS3 protease from 1a, 1b genotypes. It could be concluded that this cell-based system is efficient and sensitive enough for the detection and comparison of NS3 protease activity and the screening of anti-NS3 inhibitors. The functional difference between NS3/4A from 1a and 1b subtypes revealed by this system provides a clue for further investigations.

REFERENCES

1 **Saito I**, Miyamura T, Ohbayashi A, Harada H, Katayama T, Kikuchi S, Watanabe Y, Koi S, Onji M, Ohta Y. Hepatitis C virus infection is associated with the development of hepatocellular carcinoma. *Proc Natl Acad Sci U S A* 1990; **87**: 6547-6549

2 **Saracco G**, Ciancio A, Olivero A, Smedile A, Roffi L, Croce G, Colletta C, Cariti G, Andreoni M, Biglino A, Calleri G, Maggi G, Tappero GF, Orsi PG, Terreni N, Macor A, Di Napoli A, Rinaldi E, Ciccone G, Rizzetto M. A randomized 4-arm multicenter study of interferon alfa-2b plus ribavirin in the treatment of patients with chronic hepatitis C not responding to interferon alone. *Hepatology* 2001; **34**: 133-138

3 **Kronenberger B**, Ruster B, Elez R, Weber S, Piiper A, Lee JH, Roth WK, Zeuzem S. Interferon alfa down-regulates CD81 in patients with chronic hepatitis C. *Hepatology* 2001; **33**: 1518-1526

4 **Neddermann P**, Tomei L, Steinkuhler C, Gallinari P, Tramontano A, De Francesco R. The nonstructural proteins of the hepatitis C virus: structure and functions. *Biol Chem* 1997; **378**: 469-476

5 **Bartenschlager R**. The NS3/4A proteinase of the hepatitis C virus: unravelling structure and function of an unusual enzyme and a prime target for antiviral therapy. *J Viral Hepat* 1999; **6**: 165-181

6 **Lesk AM**, Fordham WD. Conservation and variability in the structures of serine proteinases of the chymotrypsin family. *J Mol Biol* 1996; **258**: 501-537

7 **Sakamuro D**, Furukawa T, Takegami T. Hepatitis C virus nonstructural protein NS3 transforms NIH 3T3 cells. *J Virol* 1995; **69**: 3893-3896

8 **Zemel R**, Gerechet S, Greif H, Bachmatove L, Birk Y, Golan-Goldhirsh A, Kunin M, Berdichevsky Y, Benhar I, Tur-Kaspa R. Cell transformation induced by hepatitis C virus NS3 serine protease. *J Viral Hepat* 2001; **8**: 96-102

9 **Fujita T**, Ishido S, Muramatsu S, Itoh M, Hotta H. Suppression of actinomycin D-induced apoptosis by the NS3 protein of hepatitis C virus. *Biochem Biophys Res Commun* 1996; **229**: 825-831

10 **Lin X,** Yuan ZH, Wu L, Ding JP, Wen YM. A single amino acid in the reverse transcriptase domain of hepatitis B virus affects virus replication efficiency. *J Virol* 2001; **75**: 11827-11833

11 **Berger J**, Hauber J, Hauber R, Geiger R, Cullen BR. Secreted placental alkaline phosphatase: a powerful new quantitative indicator of gene expression in eukaryotic cells. *Gene* 1988; **66**: 1-10

12 **Nakayama GR**, Caton MC, Nova MP, Parandoosh Z. Assessment of the Alamar Blue assay for cellular growth and viability *in vitro*. *J Immunol Methods* 1997; **204**: 205-208

13 **Kong WH**, Zheng G, Lu JN, Tso JK. Temperature dependent expression of cdc2 and cyclin B1 spermatogenic cells during spermatogenesis. *Cell Res* 2000; **10**: 289-302

14 **Du GX**, Hou LH, Guan RB, Tong YG, Wang HT. Establishment of a simple assay *in vitro* for hepatitis C virus NS3 serine protease based on recombinant substrate and single-chain protease. *World J Gastroenterol* 2002; **8**: 1088-1093

15 **Kolykhalov AA**, Agapov EV, Rice CM. Specificity of the hepatitis C virus NS3 serine protease: effects of substitutions at the 3/4A, 4A/4B, 4B/5A, and 5A/5B cleavage sites on polyprotein processing. *J Virol* 1994; **68**: 7525-7533

16 **Bartenschlager R**, Ahlborn-Laake L, Yasargil K, Mous J, Jacobsen H. Substrate determinants for cleavage in cis and in trans by the hepatitis C virus NS3 proteinase. *J Virol* 1995; **69**: 198-205

17 **Bianchi E**, Steinkuhler C, Taliani M, Urbani A, Francesco RD, Pessi A. Synthetic depsipeptide substrates for the assay of human hepatitis C virus protease. *Anal Biochem* 1996; **237**: 239-244

18 **Steinkuhler C**, Urbani A, Tomei L, Biasiol G, Sardana M, Bianchi E, Pessi A, De Francesco R. Activity of purified hepatitis C virus protease NS3 on peptide substrates. *J Virol* 1996; **70**: 6694-6700

19 **Pizzi E**, Tramontano A, Tomei L, La Monica N, Failla C, Sardana

M, Wood T, De Francesco R. Molecular model of the specificity pocket of the hepatitis C virus protease: Implications for substrate recognition. *Proc Natl Acad Sci U S A* 1994; **91**: 888-892

20 **Hahm B**, Back SH, Lee TG, Wimmer E, Jang SK. Generation of a novel poliovirus with a requirement of the hepatitis C virus protease NS3 activity. *Virology* 1996; **226**: 318-326

21 **Cho YG**, Moon HS, Sung YC. Construction of hepatitis C-SIN virus recombinants with replicative dependency on hepatitis C virus serine protease activity. *J Virol Methods* 1997; **65**: 201-207

22 **Cho YG,** Yang SH, Sung YC. *In vivo* assay for hepatitis C viral serine protease activity using a secreted protein. *J Virol Methods* 1998; **72**: 109-115

23 **Grakoui A**, McCourt DW, Wychowski C, Feinstone SM, Rice CM. Characterization of the hepatitis C virus-encoded serine proteinase: Determination of proteinase-dependent polyprotein cleavage sites. *J Virol* 1993; **67**: 2832-2843

24 **Komoda Y**, Hijikata M, Sato S, Asabe S, Kimura K, Shimotohno K. Substrate requirements of hepatitis C virus serine proteinase for intermolecular polypeptide cleavage in Echerichia coli. *J Virol* 1994; **68**: 7351-7357

25 **Heintges** T, Encke J, zu Putlitz J, Wands JR. Inhibition of hepatitis C virus NS3 function by antisense oligodeoxynucleotides and protease inhibitor. *J Med Virol* 2001; **65**: 671-680

26 **Harvey TJ**, Macnaughton TB, Gowans EJ. The development and characterisation of a SV40 T-antigen positive cell line of human hepatic origin. *J Virol Methods* 1997; **65**: 67-74

27 **Lohmann V**, Korner F, Koch J, Herian U, Theilmann L, Bartenschlager R. Replication of subgenomic hepatitis C virus RNAs in a hepatoma cell line. *Science* 1999; **285**: 110-113

28 **Blight KJ**, Kolykhalov AA, Rice CM. Efficient initiation of HCV RNA replication in cell culture. *Science* 2000; **290**: 1972-1974

29 **Guo JT**, Bichko VV, Seeger C. Effect of alpha interferon on the hepatitis C virus replicon. *J Virol* 2001; **75**: 8516-8523

30 **Dentan C**, Tselepis AD, Chapman MJ, Ninio E. Pefabloc, 4-[2-aminoethyl]benzenesulfonyl fluoride, is a new, potent nontoxic and irreversible inhibitor of PAF-degrading acetylhydrolase. *Biochim Biophys Acta* 1996; **1299**: 353-357

31 **Angelloz-Nicoud P**, Harel L, Binoux M. Recombinant human insulin-like growth factor (IGF) binding protein-3 stimulates prostate carcinoma cell proliferation via an IGF-dependent mechanism. Role of serine proteases. *Growth Regul* 1996; **6**: 130-136

32 **Hiramatsu N**, Ichikawa N, Fukada H, Fujita T, Sullivan CV, Hara A. Identification and characterization of proteases involved in specific proteolysis of vitellogenin and yolk proteins in salmonids. *J Exp Zool* 2002; **292**: 11-25

33 **Hahm B**, Han DS, Back SH, Song OK, Cho MJ, Kim CJ, Shimotohno K, Jang SK. NS3-4A of hepatitis C virus is a chymotrypsin-like protease. *J Virol* 1995; **69**: 2534-2539

Edited by Ma JY

P.O.Box 2345, Beijing 100023,China
Fax: +86-10-85381893
E-mail: wjg@wjgnet.com www.wjgnet.com

World J Gastroenterol 2003;9(11):2480-2483
World Journal of Gastroenterology
 ISSN 1007-9327

Oxymatrine therapy for chronic hepatitis B: A randomized double-blind and placebo-controlled multi-center trial

Lun-Gen Lu, Min-De Zeng, Yi-Min Mao, Ji-Qiang Li, Mo-Bin Wan, Cheng-Zhong Li, Cheng-Wei Chen, Qing-Chun Fu, Ji-Yao Wang, Wei-Min She, Xiong Cai, Jun Ye, Xia-Qiu Zhou, Hui Wang, Shan-Ming Wu, Mei-Fang Tang, Jin-Shui Zhu, Wei-Xiong Chen, Hui-Quan Zhang

Lun-Gen Lu, Min-De Zeng, Yi-Min Mao, Ji-Qiang Li, Shanghai Institute of Digestive Disease, Renji Hospital,Shanghai Second Medical University, Shanghai 200001, China
Mo-Bin Wan, Cheng-Zhong Li, Changhai Hospital, Second Military Medical University, Shanghai 200433, China
Cheng-Wei Chen, Qing-Chun Fu, Liver Disease Research Center, Nanjing Military Command, Shanghai 200233, China
Ji-Yao Wang, Wei-Min She, Zhongshan Hospital,Fudan University, Shanghai 200032, China
Xiong Cai, Changzheng Hospital, Second Military Medical University, Shanghai 200003, China
Jun Ye, Shanghai Putuo District Central Hospital, Shanghai 200062, China
Xia-Qiu Zhou, Hui Wang, Ruijin Hospital,Shanghai Second Medical University, Shanghai 200025, China
Shan-Ming Wu, Mei-Fang Tang, Shanghai General Hospital of Infectious Diseases, Shanghai 200083, China
Jin-Shui Zhu, Wei-Xiong Chen, Shanghai No.6 People' s Hospital, Shanghai 200230, China
Hui-Quan Zhang, Shanghai Shibei Hospital, Shanghai 200073, China
Supported by the Key Project of Shanghai Medical Development Foundation (NO: 99ZDI001) and grants from 1999 Foundation of Chinese Liver Diseases Association for Yong Scholars
Correspondence to: Lun-Gen Lu, MD, Shanghai Institute of Digestive Disease, Renji Hospital, Shanghai Second Medical University, Shanghai 200001, China. lulungen@online.sh.cn
Telephone: +86-21-33070834 **Fax:** +86-21-63364118
Received: 2003-05-13 **Accepted:** 2003-06-19

Abstract

AIM: To evaluate the efficacy and safety of capsule oxymatrine in the treatment of chronic hepatitis B.

METHODS: A randomised double-blind and placebo-controlled multicenter trial was conducted. Injection of oxymatrine was used as positive-control drug. A total of 216 patients with chronic hepatitis B entered the study for 24 weeks, of them 108 received capsule oxymatrine, 36 received injection of oxymatrine, and 72 received placebo. After and before the treatment, clinical symptoms, liver function, serum hepatitis B virus markers, and adverse drug reaction were observed.

RESULTS: Among the 216 patients, six were dropped off, and 11 inconsistent with the standard were excluded. Therefore, the efficacy and safety of oxymatrine in patients were analysed. In the capsule treated patients, 76.47 % became normal in ALT level, 38.61 % and 31.91 % became negative both in HBV DNA and in HBeAg. In the injection treated patients, 83.33 % became normal in ALT level, 43.33 % and 39.29 % became negative both in HBV DNA and in HBeAg. In the placebo treated patients, 40.00 % became normal in ALT level, 7.46 % and 6.45 % became negative both in HBV DNA and in HBeAg. The rates of complete response and partial response were 24.51 % and 57.84 % in the capsule treated patients, and 33.33 % and 50.00 % in the injection treated patients, and 2.99 % and 41.79 % in the placebo treated patients, respectively. There was no significance between the two groups of patients, but both were significantly higher than the placebo. The adverse drug reaction rates of the capsule, injection and placebo were 7.77 %, 6.67 % and 8.82 %, respectively. There was no statistically significant difference among them.

CONCLUSION: Oxymatrine is an effective and safe agent for the treatment of chronic hepatitis B.

Lu LG, Zeng MD, Mao YM, Li JQ, Wan MB, Li CZ, Chen CW, Fu QC, Wang JY, She WM, Cai X, Ye J, Zhou XQ, Wang H, Wu SM, Tang MF, Zhu JS, Chen WX, Zhang HQ. Oxymatrine therapy for chronic hepatitis B: A randomized double-blind and placebo-controlled multi- center trial. *World J Gastroenterol* 2003; 9 (11): 2480-2483

http://www.wjgnet.com/1007-9327/9/2480.asp

INTRODUCTION

Oxymatrine is a kind of alkaloid extracted from a Chinese herb *Sophora alopecuraides L.*[1]. Basic and clinical researches suggested that oxymatrine had the following pharmacological effects such as anti-virus, protecting hepatocytes, anti-hepatic fibrosis, immune regulation, etc[2-7]. In particular, wide attention was paid to its inhibitory effect on hepatitis B virus (HBV) in recent years. Oxymatrine has been proved to have distinct anti-virus effect in the treatment of chronic hepatitis B (CHB)[8-11]. But no information is available about the therapeutic efficacy and safety of oxymatrine capsule treated CHB. In this paper, we evaluated the therapeutic efficacy and safety of oxymatrine (kurorinone) capsule in the treatment of CHB based on a randomized multi-centre, double-blind and placebo-controlled clinical trial.

MATERIALS AND METHODS

Research design

This study was a clinical trial characterized by multi-centre, randomization, double blinding and placebo-control, which was fulfilled by Renji Hospital of Shanghai Second Medical University, Zhongshan Hospital of Fudan University, Changhai Hospital of Second Military Medical University.

Selection of subjects

Enrolled criteria: Age: 18-65 years old, regardless of sex, positiveness of serum HBsAg and HBV DNA for at least 6 months before enrolling, positiveness of serum HBeAg for at least 6 months before enrolling, abnormal serum value of alanine transaminase (ALT) twice or more with a value 1.2 times greater than normal upper limit and a duration more than 8 weeks between two tests within 6 months before enrolling, the serum

level of ALT was more than normal upper limit when screening, total serum bilirubin (TB) level less than or equal to 85.5 μmol/L, non-history of administrating antiviral and immunoregulating drugs, signing in the informed consent form, promising not to receive other drugs in clinical trial and systemic anti-viral agents, cytotoxic agents, hormone, immunoregulators, drugs capable of reducing serum enzyme activity and bilirubin level and Chinese traditional medicines, etc.

Exclusion criteria Patients with positive laboratory test of HIV, positiveness of serum anti-HCV and/or HCV RNA, uncompensable liver diseases, suggestive of autoimmune diseases with antinuclear antibody (ANA) titer greater than a 1:160 dilution, abnormality of serum creatinine with a value of 1.5 times greater than normal, concurrence of other associated severe diseases which might affect the present treatment, hypersensitive to oxymatrine capsule, women with pregnancy and during breast-feeding period.

Treatment procedures and drugs

A total of 216 selected patients were randomly divided into 3 groups: 108 in capsule oxymatrine group, 36 in injection oxymatrine group and 72 in placebo group. Both capsule oxymatrine and injection oxymatrine were provided by Ningxia Pharmaceutic Institute, Ningxia, China (Batch numbers 990426 and 990325, respectively). The magnitude, colour, shape and taste of the vacant placebo capsule were consistent with capsule oxymatrine. Capsule oxymatrine group: 300 mg oxymatrine capsules orally 3 times a day. Injection oxymatrine group: 400 mg intramuscularly once a day. Placebo group: 3 tablets, three times a day. Treatment course of the 3 groups was 24 weeks. After completion of selection and assessment, qualified subjects were allocated randomly into capsule oxymatrine group, injection oxymatrine group and placebo group for a treatment course of 24 weeks according to the treatment code based on stratified randomization.

Observing indexes and assessment

Clinical manifestations Weakness, pain in hepatic region, jaundice, hepatomegaly, splenomegaly, etc.

Liver function indexes Serum levels of total protein, albumin, ratio of albumin and globulin, ALT, aspartate aminotransferase (AST), γ-glutamyl transpeptidase (GGT), total bilirubin (TB), direct bilirubin (DB) and alkaline phosphatase (ALP).

Detection of serum markers of HBV HBV DNA was measured by dot blotting assay. HBsAg, anti-HBsAg, anti-HBc, HBeAg and anti-HBe were measured by Abbott kit before the treatment, 12 and 24 weeks after the treatment.

Analysis of blood and urine All parameters including electrolytes and renal function were measured before the treatment, 12 and 24 weeks after the treatment.

Assessment criteria of therapeutic effect and safety

Mainly evaluated indexes were negatively converting rate of serum HBV DNA and HbeAg, and the normalization rate of serum ALT. The assessment criteria of therapeutic effect were as follow. Complete response: negative conversion of HBeAg and HBV DNA, and normalization of serum ALT. Partial response: negative conversion of HBeAg and HBV DNA or normalization of serum ALT. Nonresponse: the effect didn' t reach the above criteria. Any abnormal clinical manifestations and laboratory tests occurred during the treatment were recorded and filled in a report form of side effects in time whether they were associated with drugs for trial or not.

Statistical analysis

Statistical analysis of the data was performed with SAS 6.12 software kit.

RESULTS

Number of subjects

A total of 216 patients were enrolled in the study, of them 108 in capsule oxymatrine group, 36 in injection oxymatrine group, and 72 in placebo control group. Twelve cases withdrew, and the withdrawal rate was 2.78 %. Eleven cases were excluded for not conforming selection criteria, and the excluding rate was 5.09 %. One hundred and ninety-nine cases entered statistical analysis of therapeutic effect included 102 cases in capsule oxymatrine group, 30 cases in injection oxymatrine group, and 67 cases in placebo control group.

General state of patients in three groups before treatment

Before treatment, the following data were similar among three groups (P>0.05, respectively), including sex, age, duration of hepatitis, abnormality of serum ALT and AST 2-fold higher than normal elevation, etc. There were no significant differences among three groups in symptoms and signs before treatment (P>0.05).

Negative conversion of serum virus markers

Negative conversion rate of serum HBsAg in capsule oxymatrine group, injection oxymatrine group and placebo group was 1.98 %, 3.33 %, and 0.00 %, respectively (Table 1). There were no obvious differences among 3 groups (P=0.269). The negative conversion rate of HBV DNA was 38.61 %, 43.33 % and 7.46 % respectively in the above groups. There were obvious differences between capsule oxymatrine group and placebo group or between injection oxymatrine group and placebo group (P=0.001), but there were no significant difference between capsule oxymatrine group and injection oxymatrine group (P=0.643). The negative conversion rate of serum HBeAg was 31.91 %, 39.29 % and 6.45 % respectively in the above groups. There was an obvious difference between capsule oxymatrine group and placebo group or between injection oxymatrine group and placebo group (P=0.001), but no significant difference between capsule oxymatrine group and injection oxymatrine group (P=0.469).

Normalization rate of serum ALT

The normalization rate of serum ALT in capsule oxymatrine group, injection oxymatrine group and placebo group was 76.47 %, 83.33 % and 40.00 %, respectively. There was an obvious difference between capsule oxymatrine group and placebo group or between injection oxymatrine group and placebo group (P=0.001, Table 2), but no significant difference between capsule oxymatrine group and injection oxymatrine group (P=0.425).

Comparison of therapeutic effect among 3 groups of chronic hepatitis B

The complete and partial response rates were 24.51 % and 57.84 % in capsule oxymatrine group, 33.33 % and 50.00 % in injection oxymatrine group, 2.99 % and 41.79 % in placebo group. There was an with obvious difference between capsule oxymatrine group and placebo group or between injection oxymatrine group and placebo group (P=0.001, Table 3), but no significant difference between capsule oxymatrine group and injection oxymatrine group (P=0.4589).

Adverse effects

In this study, 8 patients had adverse effects in capsule oxymatrine group with an incidence of 7.77 %, 2 patients in injection oxymatrine group with an incidence of 6.67 %, and 6 patients in placebo group with an incidence of 8.82 %. The difference among 3 groups had no statistical significance

Table 1 Negative conversion rates of serum HBsAg and comparison among capsule oxymatrine group, injection oxymatrine group and placebo group

Index	Group	Positive number	Number of negative conversion	Negative conversion rate (%)	Comparison among 3 groups	
					χ^2	*P* value
HBsAg	Capsule	101	2	1.98		
	Injection	30	1	3.33		0.269
	Placebo	67	0	0.00		
HBV DNA	Capsule	101	39	38.61		
	Injection	30	13	43.33	22.716	0.001
	Placebo	67	5	7.46		
HBeAg	Capsule	94	30	31.91		
	Injection	28	11	39.29	17.042	0.001
	Placebo	62	4	6.45		

The comparison of negative conversion rates of serum HBsAg, HBV DNA and HBeAg was performed with chi-square test, statistic was χ^2.

Table 2 Normalization rate of serum ALT and comparison among capsule oxymatrine group, injection oxymatrine group and placebo group

Group	Number of ALT abnormality before treatment	Number of ALT normalization after treatment	Normalization rate (%)	Comparison among 3 groups	
				χ^2	*P* value
Capsule	102	78	76.47		
Injection	30	25	83.33	28.352	0.001
Placebo	65	26	40.00		

The comparison of ALT normalization rate was performed with chi-square test, statistic was χ^2.

Table 3 Comparison of therapeutic effect among 3 groups with chronic hepatitis B

Group	Complete response	Partial response	Non-response	Comparison among 3 groups	
				χ^2	*P* value
Capusle (*n*=102)	25 (24.51 %)	59 (57.84 %)	18 (17.65 %)		
Injection (*n*=30)	10 (33.33 %)	15 (50.00 %)	5 (16.67 %)	35.957	0.0001
Placebo (*n*=67)	2 (2.99 %)	28 (41.79 %)	37(55.22 %)		

The comparison of therapeutic effect among 3 groups was performed with K-W test, statistic was χ^2.

(*P*=0.931). The adverse effects were mild or moderate and mainly manifested as symptoms of upper alimentary tract, rash, bad taste. No severe adverse effect occurred. The statistical analysis of adverse effects included 2 cases withdrawn because of side effects.

DISCUSSION

Hepatitis B virus is a DNA virus that produces both acute and chronic infections of the liver in humans. It has been estimated that over 300 million people worldwide are chronically infected with HBV and that over 250 000 people would die each year due to HBV-associated complications of cirrhosis and primary hepatocellular carcinoma[12-18]. For many years, alpha interferon has been the only approved therapy for chronic HBV infection in most countries. Interferon was effective in 30-40 % of patients, and it must be given by injection and was frequently associated with fever and influenza-like symptoms[19-23]. Recently, lamivudine was approved for the treatment of chronic HBV infection in many regions of the world. Although convenient and well-tolerated, lamivudine' s efficacy rate was similar to interferon and prolonged administration of lamivudine was associated with development of resistance[24-30]. New agents, such as adefovir dipivoxil, offered a promise either alone or in combination with lamivudine in the treatment of individuals who were ' treatment naï ve' have developed lamivudine resistance[31-33]. Up to date, no specific therapy is available for chronic hepatitis B. The following factors may be associated with its pathogenesis such as virulence of HBV strains, number of infected hepatocytes and host immune response, antiviral agents, immunomodulators and drugs might be capable of improving liver function[12-15,34-41].

Traditional Chinese medicine has been widely used for the treatment of liver disease in China[11]. Oxymatrine extracted from *Sophora alopecuraides L.* has been shown to have a remarkable HBV suppressing effect with 40 % serum conversion rate for HBeAg and HBV DNA, similar to that of alpha interferon[8,9,11]. Experiment *in vitro* indicated that oxymatrine had an inhibitory role in the secretion of HBsAg and HBeAg by 2.2.15 cell line transfected with HBV DNA and the inhibitory rates increased gradually following increased oxymatrine concentration and the extension of effect time within a definite range[42]. *In vivo* study of HBV transgenic mouse showed that when mice were injected intraperitoneally oxymatrine at 100 mg/kg, 200 mg/kg and 300 mg/kg once a day for 30 days, the quantity of HBsAg and HBeAg in the liver decreased obviously compared with control group, and there was no significant difference among 3 doses[10]. Clinical research suggested that the normalization rates of serum ALT and TB, and the negative conversion rates of serum HBsAg and HBV DNA were similar to alpha interferon when oxymatrine was applied to treatment of chronic hepatitis B. The results in

present study were similar to the therapeutic effect of interferon in the treatment of chronic hepatitis B at home and abroad[9,11,17,43], indicating that capsule oxymatrine is an effective and safe agent for treatment of chronic hepatitis B.

REFERENCES

1 **Lai JP**, He XW, Jiang Y, Chen F. Preparative separation and determination of matrine from the Chinese medicinal plant Sophora flavescens Ait by molecularly imprinted solid-phase extraction. *Anal Bioanal Chem* 2003; **375**: 264-269
2 **Liu J**, Manheimer E, Tsutani K, Gluud C. Medicinal herbs for hepatitis C virus infection: a Cochrane hepatobiliary systematic review of randomized trials. *Am J Gastroenterol* 2003; **98**: 538-544
3 **Dong Y**, Xi H, Yu Y, Wang Q, Jiang K, Li L. Effects of oxymatrine on the serum levels of T helper cell 1 and 2 cytokines and the expression of the S gene in hepatitis B virus S gene transgenic mice: a study on the anti-hepatitis B virus mechanism of oxymatrine. *J Gastroenterol Hepatol* 2002; **17**: 1299-1306
4 **Xiang X**, Wang G, Cai X, Li Y. Effect of oxymatrine on murine fulminant hepatitis and hepatocyte apoptosis. *Chin Med J* 2002; **115**: 593-596
5 **Yang W**, Zeng M, Fan Z, Mao Y, Song Y, Jia Y, Lu L, Chen CW, Peng YS, Zhu HY. Prophylactic and therapeutic effect of oxymatrine on D-galactosamine-induced rat liver fibrosis. *Zhonghua Ganzangbing Zazhi* 2002; **10**: 193-196
6 **Chen Y**, Li J, Zeng M, Lu L, Qu D, Mao Y, Fan Z, Hua J. The inhibitory effect of oxymatrine on hepatitis C virus *in vitro*. *Zhonghua Ganzangbing Zazhi* 2001; **9**(Suppl):12-14
7 **Li J**, Li C, Zeng M. Preliminary study on therapeutic effect of oxymatrine in treating patients with chronic hepatitis C. *Zhongguo Zhongxiyi Jiehe Zazhi* 1998; **18**: 227-229
8 **Chen YX**, Mao BY, Jiang JH. Relationship between serum load of HBV-DNA and therapeutic effect of oxymatrine in patients with chronic hepatitis B. *Zhongguo Zhongxiyi Jiehe Zazhi* 2002; **22**: 335-336
9 **Yu YY**, Wang QH, Zhu LM, Zhang QB, Xu DZ, Guo YB, Wang CQ, Guo SH, Zhou XQ, Zhang LX. A clinical research on oxymatrine for the treatment of chronic hepatitis B. *Zhonghua Ganzangbing Zazhi* 2002; **10**: 280-281
10 **Chen XS**, Wang GJ, Cai X, Yu HY, Hu YP. Inhibition of hepatitis B virus by oxymatrine *in vivo*. *World J Gastroenterol* 2001; **7**: 49-52
11 **Wang BE**. Treatment of chronic liver diseases with traditional Chinese medicine. *J Gastroenterol Hepatol* 2000; **15**(Suppl): E67-70
12 **Lok AS**, Heathcote EJ, Hoofnagle JH. Management of hepatitis B: 2000-summary of a workshop. *Gastroenterology* 2001; **120**: 1828-1853
13 **Gow PJ**, Mutimer D. Treatment of chronic hepatitis. *BMJ* 2001; **323**: 1164-1167
14 **Arguedas MR**, Fallon MB. Prevention in liver disease. *Am J Med Sci* 2001; **321**: 145-151
15 **Maddrey WC**. Update in hepatology. *Ann Intern Med* 2001; **134**: 216-223
16 **Ryder SD**, Beckingham IJ. ABC of diseases of liver, pancreas, and biliary system: Chronic viral hepatitis. *BMJ* 2001; **322**: 219-221
17 **Pramoolsinsup C**. Management of viral hepatitis B. *J Gastroenterol Hepatol* 2002; **17**(Suppl): S125-145
18 **Yuen MF**, Lai CL. Treatment of chronic hepatitis B. *Lancet Infect Dis* 2001; **1**: 232-241
19 **Feld J**, Locarnini S. Antiviral therapy for hepatitis B virus infections: new targets and technical challenges. *J Clin Virol* 2002; **25**: 267-283
20 **Rivkina A**, Rybalov S. Chronic hepatitis B: current and future treatment options. *Pharmacotherapy* 2002; **22**: 721-737
21 **Wai CT**, Lok AS. Treatment of hepatitis B. *J Gastroenterol* 2002; **37**: 771-778
22 **Schalm S**, De Man R, Janssen H. Combination and newer therapies for chronic hepatitis B. *J Gastroenterol Hepatol* 2002; **17** (Suppl 3): S338-S341
23 **Karayiannis P**. Hepatitis B virus: old, new and future approaches to antiviral treatment. *J Antimicrob Chemother* 2003; **51**: 761-785
24 **Marcellin P**. Advances in therapy for chronic hepatitis B. *Semin Liver Dis* 2002; **22**(Suppl 1): 33-36
25 **Zoulim F**. Assessing hepatitis B virus resistance *in vitro* and molecular mechanisms of nucleoside resistance. *Semin Liver Dis* 2002; **22**(Suppl 1): 23-31
26 **Papatheodoridis GV**, Dimou E, Papadimitropoulos V. Nucleoside analogues for chronic hepatitis B: antiviral efficacy and viral resistance. *Am J Gastroenterol* 2002; **97**: 1618-1628
27 **Bozdayi AM**, Uzunalimoglu O, Turkyilmaz AR, Aslan N, Sezgin O, Sahin T, Bozdayi G, Cinar K, Pai SB, Pai R, Bozkaya H, Karayalcin S, Yurdaydin C, Schinazi RF. YSDD: a novel mutation in HBV DNA polymerase confers clinical resistance to lamivudine. *J Viral Hepat* 2003; **10**: 256-265
28 **Torresi J**, Locarnini S. Antiviral chemotherapy for the treatment of hepatitis B virus infections. *Gastroenterology* 2000; **118**(2 Suppl 1): S83-103
29 **Doo E**, Liang TJ. Molecular anatomy and pathophysiologic implications of drug resistance in hepatitis B virus infection. *Gastroenterology* 2001; **120**: 1000-1008
30 **Zollner B**, Petersen J, Schroter M, Laufs R, Schoder V, Feucht HH. 20-fold increase in risk of lamivudine resistance in hepatitis B virus subtype adw. *Lancet* 2001; **357**: 934-935
31 **Pessoa MG**, Wright TL. Update on clinical trials in the treatment of hepatitis B. *J Gastroenterol Hepatol* 1999; **14**(Suppl): S6-11
32 **Galan MV**, Boyce D, Gordon SC. Current pharmacotherapy for hepatitis B infection. *Expert Opin Pharmacother* 2001; **2**: 1289-1298
33 **Marcellin P**, Chang TT, Lim SG, Tong MJ, Sievert W, Shiffman ML, Jeffers L, Goodman Z, Wulfsohn MS, Xiong S, Fry J, Brosgart CL. Adefovir dipivoxil for the treatment of hepatitis B e antigen-positive chronic hepatitis B. *N Engl J Med* 2003; **348**: 808-816
34 **Rich JD**, Ching CG, Lally MA, Gaitanis MM, Schwartzapfel B, Charuvastra A, Beckwith CG, Flanigan TP. A review of the case for hepatitis B vaccination of high-risk adults. *Am J Med* 2003; **114**: 316-318
35 **Shaw T**, Bowden S, Locarnini S. Chemotherapy for hepatitis B: new treatment options necessitate reappraisal of traditional endpoints. *Gastroenterology* 2002; **123**: 2135-2140
36 **Yao N**, Hong Z, Lau JY. Application of structural biology tools in the study of viral hepatitis and the design of antiviral therapy. *Gastroenterology* 2002; **123**: 1350-1363
37 **Chin R**, Locarnini S. Treatment of chronic hepatitis B: current challenges and future directions. *Rev Med Virol* 2003; **13**: 255-272
38 **Liaw YF**. Therapy of chronic hepatitis B: current challenges and opportunities. *J Viral Hepat* 2002; **9**: 393-399
39 **Lau GK**, Carman WF, Locarnini SA, Okuda K, Lu ZM, Williams R, Lam SK. Treatment of chronic hepatitis B virus infection: an Asia-Pacific perspective. *J Gastroenterol Hepatol* 1999; **14**: 3-12
40 **Farrell GC**. Clinical potential of emerging new agents in hepatitis B. *Drugs* 2000; **60**: 701-710
41 **Zoulim F**, Trepo C. New antiviral agents for the therapy of chronic hepatitis B virus infection. *Intervirology* 1999; **42**: 125-144
42 **Zeng Z**, Wang GJ, Si CW. Basic and clinical study of oxymatrime on HBV infection. *J Gastroenterol Hepatol* 1999; **14**(Suppl): A295-297
43 **Chen C**, Guo SM, Liu B. A randomized controlled trial of kurorinone versus interferon-alpha2a treatment in patients with chronic hepatitis B. *J Viral Hepat* 2000; **7**: 225-229

Edited by Zhang JZ and Wang XL

P.O.Box 2345, Beijing 100023,China
Fax: +86-10-85381893
E-mail: wjg@wjgnet.com www.wjgnet.com

World J Gastroenterol 2003;9(11):2484-2489
World Journal of Gastroenterology
 ISSN 1007-9327

• VIRAL HEPATITIS •

Liver fibrosis in chronic viral hepatitis: An ultrasonographic study

Rong-Qin Zheng, Qing-Hui Wang, Ming-De Lu, Shi-Bin Xie, Jie Ren, Zhong-Zhen Su, Yin-Ke Cai, Ji-Lu Yao

Rong-Qin Zheng, Qing-Hui Wang, Jie Ren, Department of Ultrasound, Third Affiliated Hospital, Sun Yat-Sen University, Guangzhou 510630, Guangdong Province, China
Ming-De Lu, Department of Ultrasound, First Affiliated Hospital, Sun Yat-Sen University, Guangzhou 510089, Guangdong Province, China
Shi-Bin Xie, Jie Ren, Zhong-Zhen Su, Yin-Ke Cai, Ji-Lu Yao, Department of Infectious Diseases, Third Affiliated Hospital, Sun Yat-Sen University, Guangzhou 510630, Guangdong Province, China
Supported by the Medical Science Foundation of Guangdong Province, No. A1999198
Correspondence to: Rong-Qin Zheng, Ph.D., Department of Ultrasound, Third Affiliated Hospital, Sun Yat-Sen University, Guangzhou 510630, Guangdong Province, China. zhengrongqin@hotmail.com
Telephone: +86-20-85516867-3030 **Fax:** +86-20-87536401
Received: 2002-08-03 **Accepted:** 2002-08-31

Abstract

AIM: To select valuable ultrasonographic predictors for the evaluation of hepatic inflammation and fibrosis degree in chronic hepatitis, and to study the value of ultrasonography in the evaluation of liver fibrosis and compensated liver cirrhosis in comparison with serology and histology.

METHODS: Forty-four ultrasonographic variables were analyzed and screened using color Doppler ultrasound system in 225 patients with chronic viral hepatitis and compensated liver cirrhosis. The valuable ultrasonographic predictors were selected on the basis of a comparison with histopathological findings. The value of ultrasonography and serology in the evaluation of liver fibrosis degree and the diagnosis of compensated liver cirrhosis was also studied and compared. Meanwhile, the influencing factors on ultrasonographic diagnosis of compensated liver cirrhosis were also analyzed.

RESULTS: By statistical analysis, the maximum velocity of portal vein and the degree of gall-bladder wall smoothness were selected as the valuable predictors for the inflammation grade (G), while liver surface, hepatic parenchymal echo pattern, and the wall thickness of gall-bladder were selected as the valuable predictors for the fibrosis stage (S). Three S-related independent ultrasonographyic predictors and three routine serum fibrosis markers (HA, HPCIII and CIV) were used to discriminate variables for the comparison of ultrasonography with serology. The diagnostic accuracy of ultrasonography in moderate fibrosis was higher than that of serology ($P<0.01$), while there were no significant differences in the general diagnostic accuracy of fibrosis as well as between mild and severe fibrosis ($P<0.05$). There were no significant differences between ultrasonography and serology in the diagnosis of compensated liver cirrhosis. However, the diagnostic accuracy of ultrasonography was higher in inactive liver cirrhosis and lower in active cirrhosis than that of serology (both $P<0.05$). False positive and false negative results where found when the diagnosis of compensated liver cirrhosis was made by ultrasonography.

CONCLUSION: There are different ultrasonographic predictors for the evaluation of hepatic inflammation grade and fibrosis stage of chronic hepatitis. Both ultrasonography and serology have their own advantages and disadvantages in the evaluation of liver fibrosis and compensated liver cirrhosis. Combined application of the two methods is hopeful to improve the diagnostic accuracy.

Zheng RQ, Wang QH, Lu MD, Xie SB, Ren J, Su ZZ, Cai YK, Yao JL. Liver fibrosis in chronic viral hepatitis: An ultrasonographic study. *World J Gastroenterol* 2003; 9(11): 2484-2489
http://www.wjgnet.com/1007-9327/9/2484.asp

INTRODUCTION

Viral hepatitis is one of the most common and prevalent infectious diseases in China. It was found that 25-40 % of the patients with chronic viral hepatitis would become liver cirrhosis or even hepatocellular carcinoma[1,2]. Prompt and effective treatment could postpone or interrupt the development of chronic hepatitis into liver cirrhosis. Accurate estimation of the disease severity is helpful for the evaluation of the therapeutic effect and the prognosis of the disease. At present, there are three ways for this purpose, namely histology, serology and imaging. Liver histological diagnosis based on needle biopsy is the gold standard to evaluate the degree of hepatic inflammation and fibrosis. However, liver biopsy can not be performed routinely at clinical settings becouse of its invasiveness. In addition, it is well known that liver parenchymal damage in chronic hepatitis and cirrhosis is not uniform. Sample errors were commonly encountered[3-5]. Serological examination is a non-invasive routine method. However, serological markers of fibrosis with high specificity have not been available yet in addition to the lack of organ specificity of these markers[6-8]. Imging technologies such as ultrasonography, computed tomography, magnetic resonance imaging could provide useful information on the morphological changes of the liver, and are important in the evaluation of chronic liver diseases[9-15]. Among them, ultrasonography has become the most common and valuable method because of its low cost, easy performance and high acceptability by the patient. It could provide not only valuable information on the morphological changes of the liver but also liver hemodynamics by color Doppler flow imaging[16-19].

It was reported that evaluating liver morphology and hemodynamics in patients with cirrhosis and portal hypertension had an important value for the estimation of the disease severity and prognosis[17-21]. As the disease progresses from chronic hepatitis to cirrhosis, a variety of intra- and extrahepatic abnormalities would occur. Using multiple ultrasonographic variables to evaluate morphological and hemodynamic changes of the liver, gallbladder and the spleen could be expected to reveal these abnormalites and improve the diagnostic ability of ultrasound[15,22,23].

In this study, 44 ultrasonographyic variables were analyzed and screened using color Doppler ultrasoud system in 225 patients with chronic viral hepatitis and compensated liver cirrhosis. The results were compared with histological findings based on the assessment criteria of the imflammation grade and fibrosis stage for chronic hepatitis, which were proposed

by the academic meeting of Chinese Medical Association on epidemic and parasitosis in 1995 (95-Protocol)[24]. The valuable predictors were selected by statistical analysis. The value of ultrasonography in the evaluation of fibrosis and compensated liver cirrhosis was investigated and compared with serology.

MATERIALS AND METHODS

Patients selected

Two hundred and twenty-five patients with chronic viral hepatitis and compensated liver cirrhosis were treated in our hospital from 1996 to 1999. Among them, 199 were males and 26 were females, their average age was 30.5 years (range from 10 to 57 years). The pathogenic diagnoses were: hepatitis B in 208 patients, hepatitis C in 10 patients, coinfection of hepatitis B and C in 3 patients, coinfection of hepatitis B and E in 2 patients, hepatitis B plus A and hepatitis B plus D in 1 patient, respectively. Clinical diagnoses were mild chronic hepatitis in 78 patients, moderate chronic hepatitis in 114 patients, severe chronic hepatitis in 12 patients, and cirrhosis in 21 patients. No clinical manifestations of decompensated liver cirrhosis were found in all the patients.

Fifty-one healthy volunteers were examined as a control group. There were 26 males and 25 females, their average age was 27.8 years (range from 18 to 76 years). Serological and biochemical tests were normal.

Ultrasonographic examination

Using Esaote AU4 color Doppler system with 3.5-5.0 MHz curved probe, ultrasonographic examination was performed for the patients fasted for about 8 hours 12-24 hours after liver biopsy. First, sonographic findings of the liver, spleen and gallbladder, such as size, form, surface, internal echo, and diameter of vessels were observed and measured. Second, blood flow parameters of the hepatic and splenic vessels were measured by color Doppler flow imaging with the patient holding his/her breath at the end of a quiet breathing. Sample volume was adjusted slightly smaller than the diameter of vessels, and the sample angle was less than 60 degrees. Doppler spectrum with 3-5 stable heart cycles was selected for the measurement, which was performed at least two times and the average value was used.

Forty-four ultrasonographyic variables were analyzed, including the largest oblige diameter (RL_{OD}) and anterior-posterior diameter (RL_{AP}) of the right liver lobe, longitudinal diameter and anterior-posterior diameter of the left liver lobe (LL_L, LL_{AP}), the caudate liver lobe (CL_L, CL_{AP}), the ratio of CL_L/LL_L, transverse diameter (SP_T) and longitudinal diameter (SP_L) of the spleen, liver surface (L_{sur}) and hepatic parenchymal echo pattern (L_E), size (GB_{siz}) and wall thickness (GB_T) of the gall-bladder, degree of gall-bladder wall smoothness (GB_{sm}), complication of gall-bladder stone (GB_{st}) and gall-bladder pulypus (GB_P), umbilical vein patent (U); diameter of the main portal vein trunk (PV_D), right portal vein (RPV_D) and left portal vein (LPV_D); maximum and mean blood flow velocity of the main portal vein trunk (PV_{max},PV_{mea}), right portal vein (RPV_D, RPV_{max}) and left portal vein (LPV_{max}, LPV_{mea}), blood flow volume of the main portal vein trunk (PV_F), right portal vein (RPV_F) and left portal vein (LPV_F); congestive index of the portal vein (CI); diameter (HV_D) and Doppler waveform (HV_W) of the hepatic vein; diameter (HA_D), peak systolic blood flow velocity (HA_S), blood flow volume (HA_F) and resistant index (HARI) of the hepatic artery; diameter (SPA_D), peak systolic blood flow velocity (SPA_S), blood flow volume (SPA_F), and resistant index (SPARI) of the splenic artery; diameter (SPV_D) and maximum blood flow velocity (SPV_{max}) of the splenic vein, and the ratio of SPV_F/PV_F.

The measurements and evaluation of the parameters referred to the methods described in the literature[1,4-6]. Liver surface and the degree of gall-bladder wall smoothness were classified into 3 grades, namely smooth, less smooth and rough. Hepatic parenchymal echo patterns were classified into 5 grades according to the distribution and echogenicity of the parenchymal echo texture as the renal parenchymal echo was used as the contrast.

Examination of serum fibrosis markers

One hundred and ninety-seven cases underwent ultrasonographic and serologic examinations successively. Among them, 48 had compensated cirrhosis, and the rest had chronic hepatitis. The serum fibrosis markers including hyalurionic acid (HA), human procollagen III(HPCIII) and collagen type IV(CIV) were tested using radioimmunological method. The normal ranges were HA(57±27 ng/L), HPCIII($\leqslant$120 μg/L)and CIV (38.22±11.88 μg/L)

Histological study

All the patients underwent liver biopsy. The tissue sections were stained with HE and reticular fibers respectively. Histological study was performed according to the 95-Protocol[24], in which inflammation grade (G) and fibrosis stage (S) were classified from G1 to G4, and S0 to S4, respectively, based on the various degrees of inflammation or fibrosis. Furthermore, G1-2, G3 and G4 were defined as mild, moderate and severe inflammation, respectively, while S0-2, S3 and S4 were defined as mild, moderate and severe fibrosis, respectively. S4 also meant early or definite cirrhosis.

Quantitative assessment of liver fibrosis

Quantitative assessment of liver fibrosis was performed in 107 liver specimens with reticular fiber stain using an imagine analysis system (KONTRON IBAS2.5, German). The images were amplified by 400 times. Fibrosis degree was expressed as the ratio of fibrous area to the section area. Three to five fields of vision were selected randomly at the peripheral and center of the section for the average value of the ratio.

Statistical analysis

SPSS 9.0 software was used for this study. Numerical variables were described as mean ±standard deviation. For the comparison of means in different groups, univariate analysis and Student-Newman-Keuls test were used. While for the categorical variables, non-parameter analysis and χ^2 test were used for the comparison. A P value less than 0.05 was considered statistically significant. Spearman' s rank correlation coefficient was used for the correlation analysis. As for the selection of useful variables from categorical and numerical data, stepwise discriminant analysis and multiple linear regression analysis were used, respectively.

RESULTS

Screening for valuable ultrasonographic predictors

Histological diagnosis of the case group is shown in Table 1.

Table 1 Histological results in case group

Inflammation grade (G)	No. subjects	Fibrosis stage (S)	No. subjects
0	0	0	7
1	31	1	54
2	85	2	66
3	85	3	52
4	24	4	46
Total	225		225

According to univariate analysis, there were 21 variables with significant difference (P<0.05) among groups classified by the inflammation grade. While there were 19 variables with significant difference (P<0.05) among groups classified by the fibrosis stage (Tables 2 and 3). When stepwise correlation analysis was used, 20 variables were correlated with G (P<0.01), and 18 variables were correlated with S (P<0.01).

Table 2 Univariate analysis of quantitative variables

Variables	Grouped by G		Grouped by S	
	F value	*P* value	F value	*P* value
PV_{max}	29.17	<0 .001	19.38	<0.001
GB_T	24.03	<0.001	14.60	<0.001
PV_D	20.43	<0.001	18.07	<0.001
PV_{mea}	18.69	<0.001	11.28	<0.001
HV_D	16.88	<0.001	20.21	<0.001
RPV_{max}	14.24	<0.001	7.18	<0.001
SP_L	11.57	<0.001	14.87	<0.001
SPV_D	9.47	<0.001	12.76	<0.001
SP_T	9.28	<0.001	11.18	<0.001
CI	5.22	<0.01	3.96	<0.01
RPV_D	5.30	<0.01	3.43	<0.01
LL_L	2.99	<0.05	3.41	<0.05
SPV_F	2.72	<0.05	4.97	<0.01
SPA_D	4.20	<0.01	2.29	>0.05

Table 3 Non-parametric analysis of categorical variables

Variables	Grouped by G		Grouped by S	
	χ^2 value	*P* value	χ^2 value	*P* value
L_E	50.17	<0.001	91.34	<0.001
GB_{siz}	22.18	<0.001	21.00	<0.001
HV_W	22.14	<0.001	33.34	<0.001
GB_{sm}	20.07	<0.001	78.99	<0.001
L_{sur}	18.31	<0.001	66.92	<0.001
U	13.66	<0.01	32.07	<0.001
GB_{st}	8.45	<0.05	6.06	>0.05

The correlation coefficient between the quantitative analysis results of liver fibrosis and S was 0.76 (P<0.001). The correlation coefficient between G and S was 0.75 (P<0.001).

Twenty-two ultrasonographic variables associated with G and 19 variables associated with S were selected on the basis of univariate and correlation analysis results (Table 4), and used as the preliminary valuable variables for further analysis. When compared between case group and control group, there were significant differences in these selected variables (P<0.05).

Table 4 Ultrasonographic variables with significant correlation with G and S

	Ultrasonographic variables
Associated with G (22 items)	GB_{sm}, PV_{max}, GB_T, L_E, PV_D, HV_D, PV_{mea}, RPV_{max}, SP_L, SP_T, SPV_D, HV_W, GB_{siz}, L_{sur}, CI, RPV_D, RPV_{mea}, U, LL_L, GB_{st}, SPV_F and SPA_D
Associated with S (19 items)	GB_T, $L_{E,,}$, GB_{sm}, PV_D, PV_{max}, L_{sur}, HV_D, PV_{mea}, RPV_{max}, SP_L, SP_T, SPV_D, HV_W, GB_{siz}, CI, U, LL_L, SPV_F and RPV_D

Stepwise discriminant analysis was used for further selection of valuable predictors. GB_{sm}, PV_{max} were finally selected as independent predictors which were significantly correlated to G, while the independent predictors of L_E, GB_T and L_{sur} were significantly correlated to S.

Comparison of ultrasonography and serology in evaluation of fibrosis degree and diagnosis of compensated cirrhosis

Evaluation of fibrosis degree Liver fibrosis was divided into mild, moderate and severe fibrosis on the basis of fibrosis stage according to the 95-Protocol. The case distribution was mild fibrosis in 127 patients, moderate fibrosis in 52 patients, and severe fibrosis in 46 patients.

Three independent ultrasonographyic predictors associated with S (L_E, GB_T, L_{sur}) and three serum fibrosis markers (HA, HPCIII and CIV) were taken as discriminating variables for the comparison.

The correlation coefficients of L_E, GB_T and L_{sur} were 0.63, 0.58 and 0.5, respectively (P<0.001). While the correlation coefficients of HA, HPCIII and CIV were 0.60, 0.46 and 0.50, respectively (P<0.001).

The comparison between ultrasonographic variables and serologic fibrosis markers for the evaluation of fibrosis degree is shown in Table 5.

Table 5 Diagnostic accuracy of ultrasonography and serology for the evaluation of fibrosis degrees (%)

	Mild fibrosis	Moderate fibrosis	Severe fibrosis
Serology	79.5	19.1[b]	66.7
Ultrasonography	74.5	46.8[b]	62.5

[b]P<0.01 serology *vs* ultrasonography.

The diagnostic accuracy of ultrasonography and serology was higher in mild liver fibrosis than in severe and moderate liver fibrosis. There were no significant differences between ultrasonography and serology in the general diagnostic accuracy of fibrosis and diagnostic accuracy of mild and severe fibrosis (P>0.05). However, the diagnostic accuracy of ultrasonography in moderate fibrosis was higher than that of serology (P<0.01).

Diagnosis of compensated cirrhosis

Among the 48 patients with compensated cirrhosis, 46 patients had hepatitis-related cirrhosis, and 2 patients had cholestatic cirrhosis. The fibrosis stage of all these patients was S4. All of them had no symptoms of decompensated cirrhosis.

The diagnostic accuracy of ultrasonography for compensated cirrhosis was 80.7 %, while that of serology was 79.7 %. There was no significant difference between them. However, ultrasonography had a lower sensitivity (62.5 % *vs* 72.9 %) and a higher specificity (86.6 % *vs* 81.9 %) compared with serology (P<0.05).

According to the 95-Protocol, it would be regarded as active cirrhosis when G>2 and S=4, while it was regarded as inactive cirrhosis when G⩽2 and S=4. In our patient group, there were 41 patients with active cirrhosis and 7 patients with inactive cirrhosis. Among the 7 patients with inactive cirrhosis, the clinical diagnoses were mild chronic hepatitis in 3 patients, moderate chronic hepatitis in 2 patients, and liver cirrhosis in 2 patients.

For the evaluation of inactive liver cirrhosis, the diagnostic accuracy of ultrasonography was higher than that of serology (100 % *vs* 42.9 %, P<0.05). However, the diagnostic accuracy of ultrasonography was lower than that of serology in active cirrhosis (56.1 % *vs* 78.0 %, P<0.05).

Ultrasonographic, histological and clinical figures of compensated cirrhosis with false positive and false negative results on ultrasonography

False negative results of cirrhosis on ultrasonography Eighteen patients who were predicted as mild or moderate

fibrosis by ultrasonography were finally diagnosed as cirrhosis by histology. Among them, 9 patients were diagnosed as moderate chronic hepatitis, 5 patients as severe chronic hepatitis and 4 patients as liver cirrhosis according to their clinical manifestations.

The ultrasonographic features were coarse and homogenous hepatic parenchymal echo patterns (Figure 1). All of these patients had active liver cirrhosis with fine and sparse fibrotic septa (Figure 2) or small and uniform pseudolobular nodules on histology. Serologic tests showed that liver dysfunction was evident. The serum level of fibrosis markers in these patients increased obviously (HA: 408.06±219.26, HPC3: 217.78±84.96, and IVC: 210.28±181.88).

Figure 1 Active cirrhosis. Ultrasonography showed that the hepatic parenchymal echo became coarse and dot-shaped, and the distribution was still homogenous.

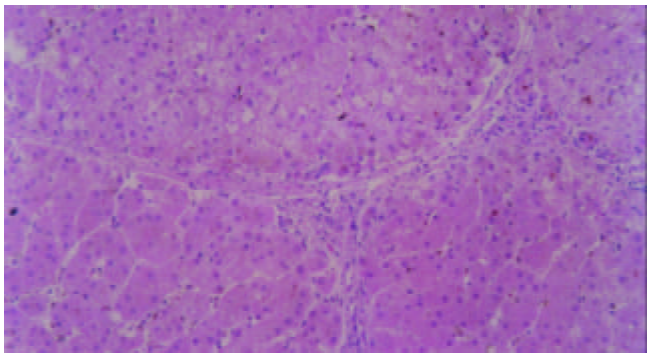

Figure 2 Active cirrhosis. Small and sparse fibroitc septa were shown on histology. (HE stain ×100).

Figure 3 Chronic viral hepatitis. On ultrasonography, the hepatic parenchymal echo became coarse and heterogeneous with speckled hyper- and hypoechoic areas.

False positive results of cirrhosis on ultrasonography Twenty patients who were predicted as liver cirrhosis by ultrsonography were finally diagnosed as mild (n=6) and moderate (n=14) fibrosis by histology. Among them, 3 patients were diagnosed as mild chronic hepatitis, 12 patients as moderate chronic hepatitis, 1 patient as severe chronic hepatitis and 4 patients as liver cirrhosis according to their clinical manifestations.

The ultrasonographic and histological features were as follows. Hepatic parenchymal echo patterns became coarse and heterogeneous with speckled hyper- and hypoechoic areas (Figure 3), the correspondent histological findings were fatty degeneration foci heterogeneously distributed within the sections in addition to the inflammation and fibrosis changes (Figure 4), and changes of liver cirrhosis were not found. Hepatic parenchymal echoes were strip-shaped and coarse (Figure 5), the correspondent histology showed wide and compact fibrotic septa (Figure 6), lobular generation was not evident.

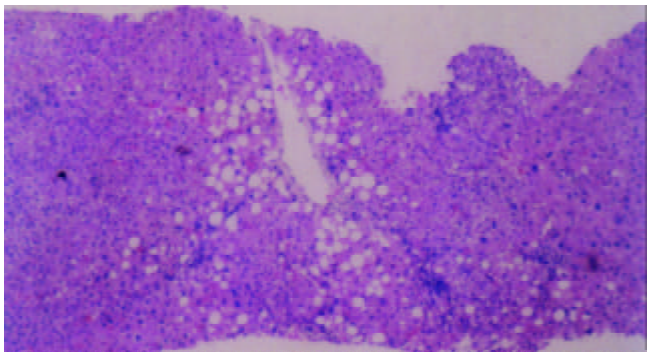

Figure 4 Chronic viral hepatitis. On histology, focal fatty degeneration foci were shown. (HE stain, ×40).

Figure 5 Chronic viral hepatitis. Ultrasonography showed the hepatic parenchymal echo to be strip-shaped and coarse.

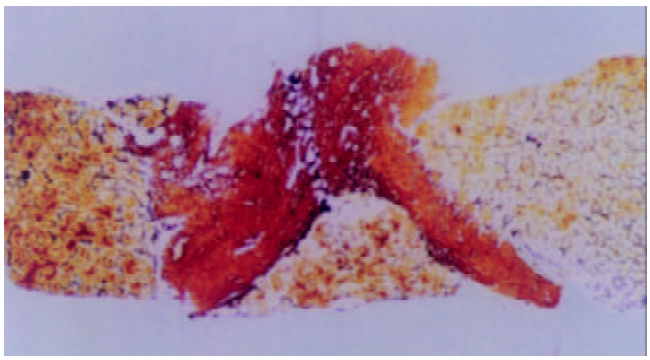

Figure 6 Chronic viral hepatitis. Wide and compact fibrotic septum was shown histologically. (Reticular fiber stain, ×40).

DISCUSSION

Among the multiple ultrasonographic parameters, PV_{max} and

GB_{sm} were selected as the independent predictors for the evaluation of fibrosis stage, while L_E, L_{sur} and GB_T were the independent predictors for the evaluation of inflammation grade. The results of this study showed that the portal venous velocity decreased and the wall of gallbladder became rough with the progress of fibrosis stage. While as the aggravation of inflammation grade, the liver parenchymal echo became coarse and heterogeneous, liver surface was rough and irregular, and the gallbladder wall became thick.

The decrease of portal venous velocity might relate to the increase of portal venous resistance. It was reported that patients with acute hepatitis and fulminant hepatitis developed portal hypertension with the aggravation of hepatic inflammation degrees[25,26].

There have been only a few reports about the relationship between the hemodynamic changes of portal vein and the histological changes in chronic hepatitis[22,27]. Aube *et al*[22] considered that the decrease of portal venous velocity was closely correlated with the histological degree of fibrosis. Our investigation showed that the decrease of portal venous velocity was significantly correlated not only with fibrosis stage but also with inflammation grade. The difference in the histological evaluating protocol used, and the difference in the sample size might partially account for the discrepancy.

The development of liver fibrosis into cirrhosis is a gradient course. There are non-specific findings on imaging. However, as the progresses of liver fibrosis reached to a certain degree, the liver pathological changes would become obvious. The acoustic interfaces would increase and the acoustic impedance between fibrotic tissue and other hepatic tissues would become large. On ultrasonography, the echo pattern of liver parenchymal would become coarse and echogenic, and the liver surface would become irregular. In this sense, the ultrasonographic features of liver parenchymal echo and liver surface would directly reflect the fibrotic changes in chronic hepatitis and liver cirrhosis, and thus playing an important role in the evaluation of fibrosis degree.

There is a close relationship between biliary system and the liver in histogenesis, anatomy and function. Viral hepatitis is often associated with biliary disorders. It was reported that abnormal ultrasonographic findings of the gallbladder such as wall thickening and double-edge sign, and abnormal size of the gallbladder and gallbladder stones were frequent in patients with hepatitis and liver cirrhosis[28-31]. The mechanism underlying the gallbladder disorders in viral hepatitis is still unclear. Some factors have been considered to be related with it[31,32] such as direct invasiveness of hepatitis virus, secondary infections, immunity injury, and edema of the gallbladder wall due to portal hypertension, circumfluence obstruction of the gallbladder vein, ete.

Ultrasonography and serology are both non-invasive methods in the evaluation of liver fibrosis and cirrhosis. However, their viewing aspects are different. The former is given priority to the reflection of morphological changes, while the latter reflects the function and metabolic changes. The knowledge about what are the similarities and differences between them in evaluating the liver fibrosis degree and diagnosis of cirrhosis is rarely known at present.

In our investigation, three independent ultrasonographic predictors correlated with fibrosis stage were chosen and compared with three serologic variables. Results showed that the correlation coefficients of ultrasonographic variables were similar to those of serological variables. There was the same tendency that the diagnostic accuracy of mild liver fibrosis was higher than that of moderate and severe fibrosis in both ultrasonography and serology, and the diagnostic accuracy of moderate liver cirrhosis was higher in ultrasonography. There were no significant differences between ultrasonography and serology in evaluating mild and severe liver fibrosis.

Referring to the diagnosis of compensated liver cirrhosis, there was no significant difference between ultrasonography and serology. However, the diagnostic sensitivity of ultrasonography was lower than that of serology, but its diagnostic specificity was higher than that of serology. It suggested that serological results should be mainly consulted for the early detection of pathological changes, while for the sake of exceptional diagnosis of cirrhosis, doctors had better to consult the results of ultrasonography in clinical practice.

Although the general diagnostic accuracy of compensated liver cirrhosis by ultrasonography and serology was similar, they were different in evaluating active and inactive stage cirrhosis. Results in our study showed that the diagnostic accuracy of ultrasonography for evaluating active stage cirrhosis was lower than that of serology with a high possibility of false-positive results, while the diagnostic accuracy for evaluating inactive stage cirrhosis was higher by ultrasonography than by serology. This difference might reflect the different features of the two modalities.

The serum fibrosis markers might reflect the activity of liver fibrosis and cirrhosis. When there was extensive inflammation in the liver, the level of serum fibrosis markers would raise with the active aggradation and degradation of the extracellular stroma. However, even if there was extensive fibrosis in the inactive stage cirrhosis, the level of serum fibrosis markers would be normal without active aggradation of the extracellular stroma[7]. Our results also illuminated that the level of serum fibrosis variables was distinctly higher in active stage cirrhosis than in inactive stage cirrhosis. Ultrasonography reflected the morphological changes of liver fibrosis and cirrhosis. When the accumulation of tissue morphological changes reached a certain degree, ultrasonography could depict these changes to a certain extent even if it was in the inactive fibrosis stage. Nevertheless, for the active fibrosis course at the level of cell and molecule, ultrasonography might fail to detect these fine morphological changes, and thus could not accurately evaluate the state of the disease.

It was inferred from our investigation that it was important to combine the two modalities for the evaluation of liver fibrosis and cirrhosis in clinical practice. When the level of serum fibrosis markers was normal, and the liver function damage was mild, liver cirrhosis should not be easily excluded with the distinct findings of cirrhosis showed by ultrasonography. The inactive stage cirrhosis might be possible at this situation. While the level of serum fibrosis markers rose obviously, and the liver function damage was severe, diagnosis of active stage cirrhosis should be considered with a long history of hepatitis viral infection even if there were no typical findings of cirrhosis on ultrasonography.

These results indicated that ultrasonography and serology both had their own advantages and disadvantages in the evaluation of liver fibrosis and liver cirrhosis.

The limitation of our investigation was that the case number of inactive stage cirrhosis was small. It was only a preliminary study and should be conducted more profoundly with a large sample size.

Ultrasonography is valuable in the evaluation of liver cirrhosis because of its low cost, easy performance, and high acceptability by the patients. However it is not a specific method and the diagnostic accuracy is still to be improved. Several factors could affect the diagnostic accuracy such as extra- and intraobserver variability, technical level of the operator, interference of obesity, ascites and intestinal gas, and modulation of the apparatus.

False positive and negative results might appear when diagnosis of compensated liver cirrhosis was made by ultrasonography. In patients with active stage liver cirrhosis,

ultrasonography could not depict the abnormalities caused by histological changes such as fine and sparse fibrotic septa or small and uniform pseudolobular nodules, thus false negative diagnosis might be made. However, high level of serum fibrotic markers might be valuable for the accurate diagnosis.

In some patients with a relative long history of chronic hepatitis, liver active inflammation and inactive phase occurred by turns, which made the pathological changes of the liver more complicated. The changes such as focal fatty degeneration or wide and compact fibrotic septa might cause coarse and heterogeneous parenchyma echo patterns in the liver, leading to a false positive diagnosis of liver cirrhosis on ultrasonography. The possible mechanisms might be assumed as follows. The acoustic interfaces between different liver tissues changed and the scatters increased because of focal fatty degeneration of the liver cells, thus causing focal echo attenuation and heterogeneous parenchyma echo patterns in the liver. When the fibrotic septa became wide and compact, the acoustic interfaces also became large and the acoustic impedance increased, causing coarse parenchyma echo patterns in the liver.

Hepatic pathological changes are often heterogeneous in patients with chronic hepatitis and liver cirrhosis. Sampling errors are liable. Gaiani *et al*[23] reported that thirty-two patients considered as liver cirrhosis by ultrasonography were identified as chronic hepatitis by histology. However, eight of these patients showed clinical manifestations of decompensated cirrhosis in the follow-up for half a year later. It indicated that ultrasonography could make up the deficiency of histology in the diagnosis of liver cirrhosis in certain situations.

In summary, there are different ultrasonographic predictors for the evaluation of hepatic inflammation grade and fibrosis stage of chronic hepatitis. Both ultrasonography and serology have their own advantages and disadvantages in the evaluation of liver fibrosis and compensated liver cirrhosis. False positive and negative results may occur in the diagnosis of compensated liver cirrhosis by ultrasonography. Combined application of ultrasonography and serology can contribute to the improvement in their diagnostic accuracy.

REFERENCES

1 **Wang BE**. Liver fibrosis: diagnosis and evaluation of disease severity. *Zhonghua Ganzangbing Zazhi* 1998; **6**: 193-194
2 **Yang XB**, Huang ZM, Wang JH. The drug therapy of liver fibrosis. *Shijie Huaren Xiaohua Zazhi* 2002; **10**: 956-957
3 **Cui DL**, Yao XX. Serum test of liver fibrosis. *Shijie Huaren Xiaohua Zazhi* 2000; **8**: 683-684
4 **Yao SK**, Yin F. The early diagnosis of liver fibrosis. *Shijie Huaren Xiaohua Zazhi* 2000; **8**: 681-683
5 **Maharaj B**, Maharaj RJ, Leary WP, Cooppan RM, Naran AD, Pirie D, Pudifin DJ. Sampling variability and its influence on the diagnostic yield of percutaneous needle biopsy of the liver. *Lancet* 1986; **1**: 523-525
6 **Bai WY**, Yao XX, Feng LY. Researching of liver fibrosis: status in quo. *Shijie Huaren Xiaohua Zazhi* 2000; **8**: 1267-1268
7 **Luo KX**. Serodiagnosis of liver fibrosis. *Linchuang Gandanbing Zazhi* 1996; **12**: 1-2
8 **Jing B**, Li YB. Diagnostic strategy for liver fibrosis. *Zhonghua Xiaohua Zazhi* 1997; **17**: 170-172
9 **Harisinghani MG**, Hahn PF. Computed tomography and magnetic resonance imaging evaluation of liver cancer. *Gastroenterol Clin North Am* 2002; **31**: 759-776
10 **Martin DR**. Magnetic resonance imaging of diffuse liver diseases. *Top Magn Reson Imaging* 2002; **13**: 151-163
11 **Kim MJ**, Mitchell DG, Ito K, Kim JH, Pasqualin D, Rubin R. Hepatic iron deposition on magnetic resonance imaging: correlation with inflammatory activity. *J Comput Assist Tomogr* 2002; **26**: 988-993
12 **Hung CH**, Lu SN, Wang JH, Lee CM, Chen TM, Tung HD, Chen CH, Huang WS, Changchien CS. Correlation between ultrasonographic and pathologic diagnoses of hepatitis B and C virus-related cirrhosis. *J Gastroenterol* 2003; **38**: 153-157
13 **Colli A**, Fraquelli M, Andreoletti M, Marino B, Zuccoli E, Conte D. Severe liver fibrosis or cirrhosis: accuracy of US for detection-analysis of 300 cases. *Radiology* 2003; **227**: 89-94
14 **Filly RA**, Reddy SG, Nalbandian AB, Lu Y, Callen PW. Sonographic evaluation of liver nodularity: Inspection of deep versus superficial surfaces of the liver. *J Clin Ultrasound* 2002; **30**: 399-407
15 **Xu Y**, Wang B, Cao H. An ultrasound scoring system for the diagnosis of liver fibrosis and cirrhosis. *Chin Med J* 1999; **112**: 1125-1128
16 **Tchelepi H**, Ralls PW, Radin R, Grant E. Sonography of diffuse liver disease. *J Ultrasound Med* 2002; **21**: 1023-1032
17 **Martinez-Noguera A**, Montserrat E, Torrubia S, Villalba J. Doppler in hepatic cirrhosis and chronic hepatitis. *Semin Ultrasound CT MR* 2002; **23**: 19-36
18 **Arda K**, Ofelli M, Calikoglu U, Olcer T, Cumhur T. Hepatic vein Doppler waveform changes in early stage (Child-Pugh A) chronic parenchymal liver disease. *J Clin Ultrasound* 1997; **25**: 15-19
19 **Gorka W**, al Mulla A, al Sebayel M, Altraif I, Gorka TS. Qualitative hepatic venous Doppler sonography versus portal flowmetry in predicting the severity of esophageal varices in hepatitis C cirrhosis. *Am J Roentgenol* 1997; **169**: 511-515
20 **Li XH**, Wang L, Fang YW, Lu YK. Color Doppler evaluation for the hemodynamics of portal hypertension in liver cirrhosis. *Shijie Huaren Xiaohua Zazhi* 1999; **7**: 453-454
21 **Ohta M**, Hashizume M, Kawanaka H, Akazawa K, Tomikawa M, Higashi H, Kishihara F, Tanoue K, Sugimachi K. Prognostic significance of hepatic vein waveform by Doppler ultrasonography in cirrhotic patients with portal hypertension. *Am J Gastroenterol* 1995; **90**: 1853-1857
22 **Aube C**, Oberti F, Korali N, Namour MA, Loisel D, Tanguy JY, Valsesia E, Pilette C, Rousselet MC, Bedossa P, Rifflet H, Maiga MY, Penneau-Fontbonne D, Caron C, Cales P. Ultrasonographic diagnosis of hepatic fibrosis or cirrhosis. *J Hepatol* 1999; **30**: 472-478
23 **Gaiani S**, Gramantieri L, Venturoli N, Piscaglia F, Siringo S, D'Errico A, Zironi G, Grigioni W, Bolondi L. What is the criterion for differentiating chronic hepatitis from compensated cirrhosis? A prospective study comparing ultrasonography and percutaneous liver biopsy. *J Hepatol* 1997; **27**: 979-985
24 **The academic meeting of Chinese Medical Association on Epidemic and Parasitosis in Beijing**. The protocol for the prevention and treatment of viral hepatitis. *Zhonghua Chuanranbing Zazhi* 1995; **13**: 241-247
25 **Yang SS**, Wu CH, Chen TK, Lee CL, Lai YC, Chen DS. Portal blood flow in acute hepatitis with and without ascites: a non-invasive measurement using an ultrasonic Doppler. *J Gastroenterol Hepatol* 1995; **10**: 36-41
26 **Tai DI**, Changchien CS, Chen CJ, Huang CS, Lo SK, Kuo CH. Changes in portal venous hemodynamics in patients with severe acute hepatitis over one year. *J Clin Ultrasound* 2000; **28**: 83-88
27 **Koda M**, Murawaki Y, Kawasaki H, Ikawa S. Portal velocity and portal blood flow in patients with chronic viral hepatitis: relation to histological liver fibrosis. *Hepatogastroenterology* 1996; **43**: 199-202
28 **Wang TF**, Hwang SJ, Lee EY, Tsai YT, Lin HC, Li CP, Cheng HM, Liu HJ, Wang SS, Lee SD. Gall-bladder wall thickening in patients with liver cirrhosis. *J Gastroenterol Hepatol* 1997; **12**: 445-449
29 **Dogra R**, Singh J, Sharma MP. Enterically transmitted non-A, non-B hepatitis mimicking acute cholecystitis. *Am J Gastroenterol* 1995; **90**: 764-766
30 **Portincasa P**, Moschetta A, Di Ciaula A, Palmieri VO, Milella M, Pastore G, Palasciano G. Changes of gallbladder and gastric dynamics in patients with acute hepatitis A. *Eur J Clin Invest* 2001; **31**: 617-622
31 **Xiao SS**. Ultrasonigraphic abnormalities of gallbladder in patients with viral hepatitis and liver cirrhosis: clinical significance. *Weichangbingxue He Ganbingxue Zazhi* 1996; **5**: 77-79
32 **Yan FM**, Chen AS, Hao F, Zhao XP, Gu CH, Zhao LB, Yang DL, Hao LJ. Hepatitis C virus may infect extrahepatic tissues in patients with hepatitis C. *World J Gastroenterol* 2000; **6**: 805-811

Edited by Zhang JZ and Wang XL

P.O.Box 2345, Beijing 100023,China
Fax: +86-10-85381893
E-mail: wjg@wjgnet.com www.wjgnet.com

World J Gastroenterol 2003;9(11):2490-2496
World Journal of Gastroenterology
 ISSN 1007-9327

• VIRAL HEPATITIS •

Diagnostic value of platelet derived growth factor-BB, transforming growth factor-b_1, matrix metalloproteinase-1, and tissue inhibitor of matrix metalloproteinase-1 in serum and peripheral blood mononuclear cells for hepatic fibrosis

Bin-Bin Zhang, Wei-Min Cai, Hong-Lei Weng, Zhong-Rong Hu, Jun Lu, Min Zheng, Rong-Hua Liu

Bin-Bin Zhang, Wei-Min Cai, Hong-Lei Weng, Zhong-Rong Hu, Jun Lu, Min Zheng, Rong-Hua Liu, Institute of Infectious Diseases, First Affiliated Hospital, School of Medicine, Zhejiang University, Hangzhou 310003, Zhejiang Province, China
Correspondence to: Professor Wei-Min Cai, Institute of Infectious Diseases, First Affiliated Hospital, School of Medicine, Zhejiang University, Hangzhou 310003, Zhejiang Province, China. zbb-2051@163.com
Telephone: +86-571-87236580
Received: 2003-03-20 **Accepted:** 2003-04-14

Abstract

AIM: Noninvasive diagnosis of hepatic fibrosis has become the focus because of the limited biopsy, especially in the surveillance of treatment and in screening hepatic fibrosis. Recently, regulatory elements involved in liver fibrosis, such as platelet derived growth factor-BB (PDGF-BB), transforming growth factor-β_1 (TGF-β_1), matrix metalloproteinase-1 (MMP-1), and tissue inhibitor of matrix metalloproteinase-1 (TIMP-1), have been studied extensively. To determine whether these factors or enzymes could be used as the indices for the diagnosis of hepatic fibrosis, we investigated them by means of receiver operating characteristic (ROC) curve.

METHODS: Serum samples from sixty patients with chronic viral hepatitis B and twenty healthy blood donors were assayed to determine the level of PDGF-BB, TGF-β_1, MMP-1, and TIMP-1 with ELISA, and HA, PCIII, C-IV, and LN level with RIA. The message RNA (mRNA) expression of TIMP-1 and MMP-1 in peripheral blood mononuclear cells (PBMCs) was detected by RT-PCR and Northern blot hybridization. Liver biopsy was performed in all patients. The biopsy samples were histopathologically examined. The trial was double-blind controlled.

RESULTS: The serum level of PDGF-BB, TIMP-1, the ratio of TIMP-1 and MMP-1 (TIMP-1/MMP-1), mRNA expression of TIMP-1 (TIMP-1mRNA), and the ratio of TIMP-1mRNA and MMP-1mRNA (TIMP-1mRNA/MMP-1mRNA) in patients was significantly higher than those in the healthy blood donors (t=2.514-11.435, P=0.000-0.016). The serum level of PDGF-BB, TIMP-1, TIMP-1/MMP-1, and TIMP-1mRNA was positively correlated with fibrosis stage and inflammation grade (r=0.239-0.565, P=0.000-0.033), while the serum level of MMP-1 was negatively correlated with fibrosis stage and inflammation grade, and TIMP-1mRNA/MMP-1mRNA was positively correlated with inflammation grade. Through the analysis by ROC curve, serum PDGF-BB was the most valuable marker, and its sensitivity was the highest among the nine indices. The markers with the highest specificity were TIMP-1mRNA and TIMP-1mRNA/MMP-1mRNA in PBMCs. The area under the curve (AUC) of PDGF-BB, TIMP-1mRNA, TIMP-1mRNA/MMP-1mRNA, TIMP-1/MMP-1, HA, PCIII, TIMP-1, C-IV, and LN was 0.985, 0.876, 0.792, 0.748, 0.728, 0.727, 0.726, 0.583, and 0.463, respectively. The sensitivity and the specificity in the parallel test was 99.0 % and 95.0 % when serum PDGF-BB, TIMP-1mRNA and TIMP-1mRNA/MMP-1mRNA was detected simultaneously.

CONCLUSION: Serum level of PDGF-BB, TIMP-1mRNA, TIMP-1mRNA/MMP-1mRNA in PBMCs, and serum level of TIMP-1 and TIMP-1/MMP-1 can be used as the indices for the diagnosis of hepatic fibrosis, but the former three are more useful. The combination of serum PDGF-BB, TIMP-1mRNA and TIMP-1mRNA/MMP-1mRNA in PBMCs is even more efficient in screening liver fibrosis.

Zhang BB, Cai WM, Weng HL, Hu ZR, Lu J, Zheng M, Liu RH. Diagnostic value of platelet derived growth factor-BB, transforming growth factor-β_1, matrix metalloproteinase-1, and tissue inhibitor of matrix metalloproteinase-1 in serum and peripheral blood mononuclear cells for hepatic fibrosis. *World J Gastroenterol* 2003; 9(11): 2490-2496
http://www.wjgnet.com/1007-9327/9/2490.asp

INTRODUCTION

Fibrosis is the leading cause of morbidity and mortality in hepatic diseases. More attention has been paid to its mechanism, diagnosis and treatment. The proper and rapid treatment depends on the accurate and simple diagnosis. Noninvasive diagnosis of hepatic fibrosis has become the focus because of the limited biopsy, especially in the surveillance of treatment and in screening hepatic fibrosis. Recently, regulatory factors involved in the mechanism of liver fibrosis such as PDGF-BB, TGF-β_1, interstitial enzyme, MMP-1 and its inhibitor, TIMP-1, have been studied extensively[1-14]. To find out whether these factors or enzymes could be used as the indices for diagnosis of liver fibrosis, protein level and mRNA expression were studied in sixty patients with chronic viral hepatitis B and twenty healthy blood donors. At the same time, these markers were compared with liver biopsy results and the routine serum markers (HA, PCIII, C-IV and LN) to identify their values in clinical practice via ROC curve and the combination test.

MATERIALS AND METHODS

Subjects

During the Sixth National Conference on Infectious and Parasitic Diseases in 2000, the Protocol of Prevention and Treatment for Viral Hepatitis (abbreviated as "2000 Criteria")[15] was modified. According to the "2000 Criteria", 60 patients with typical presentations of chronic hepatitis were included. Among them, 54 were men with an average age of 34.9±8.1 years, 6 were women with an average age of 36.6±1.0 years. Twenty-eight and thirty-two patients showed moderate and severe

degree of the disease, respectively. The patients' histories were mainly collected from the First Affiliated Hospital, School of Medicine, Zhejiang University and several other hospitals in Zhejiang Province between July 1998 and September 1999. All were positive in HBV markers without other viral infections or disorders except liver disease. The diagnosis was made by liver biopsy according to the "2000 Criteria". The normal control group included 20 healthy blood donors selected according to the random number table.

Histology

Biopsy samples of the liver >1 cm in length were fixed in 10 % neutralized formaldehyde, embedded in paraffin and stained with hematoxylin and eosin. The reticulin and Masson trichrome techniques were used specially for staining fibrous tissue components. Histological assessment of the liver for the division of fibrosis stage and inflammation grade, expressed as S1 to S4 and G1 to G4, was performed according to the "2000 Criteria".

Determination of serum level of PDGF-BB, TGFb_1, TIMP-1, MMP-1, HA, PCIII, C-IV, and LN

Serum specimens were stored at -20 ℃. The serum level of PDGF-BB, TGF-β_1, TIMP-1 and MMP-1 was assayed by ELISA. The kits of PDGF-BB and TGF-β_1 were provided by the American Genzyme Corporation, the American AND Corporation, respectively. The kits of TIMP-1 and MMP-1 were provided by the American ChemCon Corporation. The serum level of HA, PCIII, C-IV and LN was determined by RIA. The kits of HA, C-IV and LN were provided by Shanghai Navy Medical Institute. The PCIII kit was provided by Chongqing Tumor Institute. Assays were done following the manufacturers' manual.

Determiantion of TIMP-1mRNA and MMP-1mRNA in PBMCs

Total RNA extraction PBMCs were separated by Ficoll (GiBco. Life Technologies Inc) and the total RNA was extracted by Trizol reagent (GiBco. Life Technologies Inc).

Northern blot hybridization Total RNA 20 μg was denatured and undergone electrophoresis with 1 % agarose containing 2.2 mol/L formaldehyde and was transferred onto nitrocellulose membrane, which was dried at 80 ℃ for two hours. The filters were prehybridized at 68 ℃ for 1 hour in the solution containing 6×standard saline citrate (SSC), 5×Denhardt' s solution, 0.5×sodium dodecyl sulfate (SDS), and 100 mg/L salmon sperm DNA. The denatured probes were added into the solution for hybridization at 68 ℃ overnight. The filters were washed for three times, and then autoradiographed at -70 ℃.

RT-PCR Total RNA 1 μg and primer Oligo (dT) were used for reverse transcription (Promega). 5 μl reverse transcription template was used for amplification through PCR. The primers are MMP-1: 5' CTTCAGTGGTGATGTTCAGC3', 5' CATCGATATGCTTCAACGTTC3', 412 bp, TIMP-1: 5' GGAGTCCAGCAGACCACCTTA3', 5' -TGGGACACAG GTGCATGCCCTGCT-3', 110 bp. The amplified sequence length of β-actin is 224 bp. The PCR products were through 1.5 % (w/v) agarose gel electrophoresis and analyzed by gel imaging system.

Statistical analysis

Results were expressed as mean ± standard deviation ($\bar{x}\pm s$). *t* test and Spearman rank-correlation test were used. The results were considered statistically significant at $P<0.05$. Evaluation of the diagnostic test was made via ROC curve.

RESULTS

Comparison of serum level of PDGF-BB, TGF-b_1, TIMP-1, MMP-1 and TIMP-1/MMP-1 between patients and healthy blood donors

The serum level of PDGF-BB, TIMP-1 and TIMP-1/MMP-1 in 60 patients was significantly higher than that in the normal control group with an increase of 2.52, 0.5 and 1.67 fold, respectively. However, there was no difference in the serum level of MMP-1 and TGF-β_1 between patients and normal controls (Table 1). The serum level of MMP-1 was further studied. A declining tendency along the increase of fibrosis stage, inflammation grade and severity of the hepatic disease was observed while a significant difference appeared only between the patients in S4, G4 or with severe diseases and blood donors (Table 2). Moreover, it was also different between patients in S4 and those in S2 (Table 2). As to the serum level of TGF-β_1, there was no difference between patients and normal controls, even no significant difference among patients with the increase of fibrosis stage, inflammation grade and severity of the disease (Table 2).

Table 2 Comparison of the serum level of MMP-1 and TGF-β_1 between patients at different fibrosis stages, inflammation grades, and with different severities of the disease and the healthy controls ($\bar{x}\pm s$)

Group (*n*)	MMP-1(μg/L)	TGF-β_1(μg/L)
Controls (20)	7.98±3.13	26.28±16.69
S2(16)	6.34±2.96	31.66±18.01
S3(31)	6.80±5.34	34.19±26.23
S4(13)	3.93±2.93[ac]	25.16±20.90
G2(2)	7.66±0.36	18.25±6.01
G3(28)	6.41±4.91	31.89±21.61
G4(30)	5.61±4.15[a]	32.14±25.25
Mild disease (28)	6.56±3.66	34.39±24.43
Severe disease (32)	5.61±5.05	29.08±21.97

There was a statistically significant difference as compared with the control group [a]$P<0.05$, and a statistically significant difference as compared with S2 group [c]$P<0.05$.

Comparison of TIMP-1mRNA, MMP-1mRNA and TIMP-1mRNA/MMP-1mRNA in PBMCs between patients and healthy controls

As shown in Table 3, TIMP-1mRNA and TIMP-1mRNA/MMP-1mRNA were significantly elevated in patients than those in healthy controls with an increase of 1.6 and 1.79 fold, respectively. However, no difference was found in MMP-1mRNA expression between patients and healthy controls.

Table 1 Comparison of the serum level of PDGF-BB, TGF-β1, TIMP-1, MMP-1 and TIMP-1/MMP-1 between patients and healthy blood donors ($\bar{x}\pm s$)

Group (*n*)	PDGF-BB (ng/L)	TGF-β_1(μg/L)	TIMP-1(μg/L)	MMP-1(μg/L)	TIMP-1/MMP-1
Patients	67.75±30.08[b]	31.41±23.22	258.87±77.75[a]	6.05±4.44	83.66±100.36[b]
Controls	19.85±10.28	26.28±16.69	205.80±35.66	7.98±3.13	31.95±20.03
t	11.435	0.912	2.646	-1.79	3.176
P	0.000	0.365	0.01	0.077	0.002

There was a statistically significant difference as compared with the control group [a]$P<0.05$, [b]$P<0.01$.

Table 3 Comparison of TIMP-1mRNA, MMP-1mRNA and TIMP-1mRNA / MMP-1mRNA in PBMCs between patients and healthy controls ($\bar{x}\pm s$)

Group (n)	TIMP-1mRNA	MMP-1mRNA	TIMP-1mRNA / MMP-1mRNA
Patients (60)	1.05±0.69[b]	0.39±0.36	4.77±3.78[a]
Controls (20)	0.40±0.19	0.24±0.11	1.71±0.89
t	2.934	0.741	2.514
P	0.005	0.462	0.016

There was a statistically significant difference compared with the control group [a]P<0.05, [b]P<0.01.

Table 4 Relationship between serum level of PDGF-BB, TGF-β1, TIMP-1, MMP-1 and TIMP-1 / MMP-1, TIMP-1mRNA, MMP-1mRNA and TIMP-1mRNA / MMP-1mRNA and fibrosis stage and inflammation grade

Index	Fibrosis stage r	P	Inflammation grade r	P
TIMP-1	0.239[a]	0.033	0.261[a]	0.019
MMP-1	-0.333[b]	0.003	-0.266[a]	0.017
TIMP-1 / MMP-1	0.405[b]	0.000	0.340[b]	0.002
PDGF-BB	0.565[b]	0.000	0.534[b]	0.000
TGF-β1	-0.041	0.718	0.039	0.733
TIMP-1mRNA	0.366[b]	0.009	0.391[a]	0.015
TIMP-1mRNA / MMP-1mRNA	0.340	0.071	0.497[b]	0.006
MMP-1mRNA	0.091	0.582	0.001	0.995

[a]P<0.05, [b]P<0.01, compared with r_s threshold value.

Table 5 ROC curve analysis of nine indices

Index	AUC	P	Cut-off point	Sensitivity (%)	Specificity (%)	YI
PDGF-BB	0.985	0.000	≥40.50 ng / L	90.0	95.0	0.850
TIMP-1mRNA	0.876	0.000	≥0.79	73.7	100	0.737
TIMP-1mRNA / MMP-1mRNA	0.792	0.005	≥3.20	65.8	100	0.658
TIMP-1 / MMP-1	0.748	0.001	≥34.69	70.0	75.0	0.450
HA	0.728	0.003	≥145.20 μg / L	62.0	87.5	0.497
PCIII	0.727	0.004	≥137.40 mg / L	59.2	81.2	0.404
TIMP-1	0.726	0.003	≥254.00 μg / L	46.7	95.0	0.417
CIV	0.583	0.287	≥74.20 mg / L	55.1	68.7	0.238
LN	0.463	0.636	≥156.65 μg / L	37.8	75.0	0.128

YI (Youden Index)=sensitivity+specificity-1.

Table 6 Parameters of the combined diagnosis in the parallel test

Combined indices	Sensitivity (%)	Specificity (%)
TIMP-1mRNA+TIMP-1mRNA / MMP-1mRNA+PDGF-BB	99.0	95.0
PDGF-BB+TIMP-1mRNA+HA	99.0	83.1
TIMP-1mRNA+TIMP-1mRNA / MMP-1mRNA+PDGF-BB+HA	99.6	83.1
PDGF-BB+TIMP-1mRNA / MMP-1mRNA+HA	98.7	83.1
PDGF-BB+TIMP-1mRNA	97.4	95.0
TIMP-1mRNA+TIMP-1mRNA / MMP-1mRNA+HA	97.0	87.5
PDGF-BB+TIMP-1mRNA / MMP-1mRNA	96.6	95.0
PDGF-BB+HA	96.0	83.1
TIMP-1mRNA+TIMP-1mRNA / MMP-1mRNA	91.0	100
TIMP-1mRNA+HA	90.0	87.5
TIMP-1mRNA / MMP-1mRNA+HA	87.0	87.5

Table 7 Parameters of the combined diagnosis in the serial test

Combined indices	Sensitivity (%)	Specificity (%)
PDGF-BB+TIMP-1mRNA	66.3	100
PDGF-BB+TIMP-1mRNA / MMP-1mRNA	59.2	100
PDGF-BB+HA	56.0	99.4
TIMP-1mRNA+TIMP-1mRNA / MMP-1mRNA	48.5	100
TIMP-1mRNA+HA	45.7	100
PDGF-BB+TIMP-1mRNA+HA	41.1	100
TIMP-1mRNA / MMP-1mRNA+HA	40.8	100
TIMP-1mRNA+TIMP-1mRNA / MMP-1mRNA+PDGF-BB	40.4	100
PDGF-BB+TIMP-1mRNA / MMP-1mRNA+HA	36.7	100
TIMP-1mRNA+TIMP-1mRNA / MMP-1mRNA+HA	30.1	100
TIMP-1mRNA+TIMP-1mRNA / MMP-1mRNA+PDGF-BB+HA	27.1	100

Relationship between serum level of PDGF-BB, TGF-b_1,TIMP-1, MMP-1 and TIMP-1/MMP-1, TIMP-1mRNA, MMP-1mRNA and TIMP-1mRNA/MMP-1mRNA in PBMCs and fibrosis stage and inflammation grade

The serum level of PDGF-BB, TIMP-1, TIMP-1/MMP-1 and TIMP-1mRNA in PBMCs was positively correlated with fibrosis stage and inflammation grade, while the serum level of PDGF-BB had a stronger correlation than the other three indices. The serum level of MMP-1 was negatively correlated with fibrosis stage and inflammation grade. TIMP-1mRNA/MMP-1mRNA was positively correlated with inflammation grade. However, the serum level of TGF-β_1 and MMP-1mRNA was correlated with neither fibrosis stage nor inflammation grade.

Diagnostic value of serum level of PDGF-BB, TIMP-1, TIMP-1/MMP-1, MMP-1, HA, PCIII, CIV, LN and TIMP-1mRNA and TIMP-1mRNA/MMP-1mRNA in PBMCs

Table 5 shows that serum level of PDGF-BB, TIMP-1, TIMP-1/MMP-1, HA and PCIII, and TIMP-1mRNA and TIMP-1mRNA/MMP-1mRNA in PBMCs could be used to diagnose hepatic fibrosis. Among them, the serum level of PDGF-BB was most useful for its AUC and YI were close to 1, followed by TIMP-1mRNA and TIMP-1mRNA/MMP-1mRNA in PBMCs. Furthermore, the serum level of PDGF-BB was most sensitive, and the next was TIMP-1mRNA and TIMP-1mRNA/MMP-1mRNA in PBMCs. TIMP-1mRNA and TIMP-1mRNA/MMP-1mRNA in PBMCs were most specific, followed by the serum level of PDGF-BB and TIMP-1. When both the sensitivity and the specificity were taken into consideration, serum PDGF-BB, serum HA, TIMP-1mRNA and TIMP-1mRNA/MMP-1mRNA were the relatively efficient indices.

Diagnostic value of the single index combination

When both the sensitivity and the specificity needed to be taken into account, we could combine the following four indices, namely serum PDGF-BB, serum HA, TIMP-1mRNA/MMP-1mRNA and TIMP-1mRNA in PBMCs. Table 6 indicates that the combination of serum level of PDGF-BB, TIMP-1mRNA and TIMP-1mRNA/MMP-1mRNA in PBMCs was more useful in the parallel test. However, no efficient combination in the serial test was observed (Table 7).

DISCUSSION

Hepatic fibrosis is characterized by imbalanced deposition and degradation of extracellular matrix (ECM). Many factors are involved in the process. Thus, it is difficult to evaluate the fibroproliferative activity. Liver biopsy is still regarded as the gold standard for the diagnosis of fibrosis, but even elaborated scores of histological activity are limited to evaluate the prognosis in the individual case. Moreover, it is not convenient, to some degree, to use it as a routine method for the diagnosis, evaluation and supervision of the disease in clinical practice. Unfortunately, there have been no established noninvasive markers or tests for the diagnosis of hepatic fibrosis. Therefore, it is essential to explore the noninvasive and reliable indices for assessing the progress of liver fibrosis. Previously, we revealed the diagnostic value of ultrasonography on assessing liver fibrosis resulted from Schistosomiasis japonica[16], but sometimes we could not distinguish benign fatty infiltration from fibrosis, because both of their echogenicities appeared increased or diffuse. Detection of the biochemical indices in serum has been the focus in the filed of hepatic fibrosis. At present, the serum indices revealing the progress of hepatic fibrosis mainly include two kinds, reflecting deposition and degradation. Previously, more attention was paid to the factors reflecting the deposition or metabolism of ECM, and the serum level of HA, PCIII, PIIIP, CIVand LNwas studied. Zheng *et al*[17,18] confirmed the clinical value of the serum fibrosis indices (HA, PCIII, CIVand LN) through comparing them with the histological reports performed on liver fibrosis patients resulted from chronic hepatitis B. Furthermore, the serum level of HA was considered to be the most sensitive among the four indices, this result was also reported by others[19,20]. However, the four indices did not fully reflect the histological changes and were often influenced by other factors, moreover, in some chronic hepatitis B cases, they did not correspond to the biopsy results[21]. Thus, it is important and necessary to explore new and more reliable indices. With the mechanism of hepatic fibrosis elucidated further, the focus has been the elements involved in the degradation of ECM such as MMP-1[14,22,23] and TIMP-1[24-27] and the regulatory factors such as PDGF-BB and TGF-β_1 whose vital roles in hepatic fibrosis have been confirmed.

To establish the noninvasive index, the first step was to observe whether it demonstrated a difference between patients and normal controls. In our study, we compared the serum level of PDGF-BB, TIMP-1, MMP-1, TIMP-1/MMP-1 and TGF-β_1 between 60 fibrosis patients and 20 healthy blood donors. The serum level of PDGF-BB, TIMP-1 and TIMP-1/MMP-1 in patients was significantly elevated than that in healthy controls. However, the serum level of MMP-1 demonstrated a declining tendency with the severity of liver fibrosis, inflammation and the disease condition although the difference between two groups existed only when the patients were in S4, G4 or with severe hepatitis. This result indicted that the abnormal serum MMP-1 did not appear until the patients were in the advanced fibrosis. With regard to TGF-β_1 serum level, it was not different from that of the control group with the progress of liver fibrosis, inflammation and the severity of the disease, showing that serum TGF-β_1 may not be sensitive as a diagnostic index. Similar results were also reported. Daniluk *et al*[28] found that serum level of TGF-β_1 in alcohol-related liver cirrhosis was similar to that in controls. Oberti *et al*[29] detected several indices of chronic hepatitis patients, including HA, PT, GGT, alph2 macroglobulin, PIIIP, LN and TGF-β_1. They found that HA and PT were significant in cirrhosis. In fact, TGF-β_1 is secreted from cells in the manner of the complex formed by TGF-β_1 and its binding protein. However, pre TGF-β_1 can be activated to its active form only after its binding protein is released. This does not mean that TGF-β_1 may play a role freely once it is released into blood, for its corresponding receptors still block it. There are a lot of studies about the correlation of plasma TGF-β_1 with chronic hepatitis, liver fibrosis or cirrhosis[30,31]. But, in general, analysis of plasma level is fraught with difficulties related to contamination of the sample by TGF-β from platelets. Moreover, the plasmin in the plasma may increase the amount of TGF-β_1 through opening the LAP-TGF-β_1 complex. Clearance of TGF-β is also complicated. It binds locally at sites of injury to ECM and generally to vascular endothelium, it may be sequestered by soluble proteins, and can also undergo renal excretion or be taken up by hepatocytes. These modes of sequestration or clearance may vary at different circumstances. Thus, increase in plasma TGF-β may not reflect pericellular concentrations at the injury site, and due to this reason, plasma TGF-β is unlikely to be diagnostically useful[32,35]. But Kobayashi *et al*[36] found that serum TGF-β_1 could be used as an accurate indicator of progressive fibrogenesis in postoperative biliary atresia patients. The reason for the disagreement may be the different criteria for the division of liver fibrosis.

Correlation analysis was carried out to elucidate the cause leading to the difference in some indices between patients and normal controls. We found that the serum level of PDGF-BB,

TIMP-1 and TIMP-1/MMP-1 was positively correlated with fibrosis stage and inflammation grade while the serum level of MMP-1 was inversely correlated with fibrosis stage and inflammation grade. The data indicated that histological changes could directly result in the higher level of serum PDGF-BB, serum TIMP-1 and TIMP-1/MMP-1 in patients and could explain the declining tendency appearing in the comparison between each group of patients and the controls as well. Serum level of TGF-β_1 was not correlated with fibrosis stage or inflammation grade. This may confirm that detection of serum TGF-β_1 was not reliable in clinical practice.

It has been reported that mRNA levels of TIMP and MMP and corresponding proteins were related to liver fibrosis or cirrhosis. Chen *et al*[37] studied the collagen metabolism of liver fibrosis at transcription level in rabbits infected by Schistosomiasis japonica, and found that mRNA levels of MMP-1 and MMP-9 declined almost to the normal level at the later stage of fibrosis. Yata *et al*[38] found that mRNA expression of hepatic TIMP-1 increased in hepatic fibrosis. Lichtinghagen *et al*[27] investigated the mRNA levels of hepatic TIMP-1, 2, 3 and MMP-2, 7, 9 in 29 chronic active hepatitis C patients (CAH) and 7 cirrhosis patients resulted from hepatitis C virus, and found that none of mRNA levels was significantly different between CAH patients with and without fibrosis, while MMP-2, MMP-7, and TIMP-1 provided the best discrimination between cirrhosis and pre-cirrhotic stages. Lichtinghagen *et al*[39] found that mRNA expression of MMP-2, MMP-9 and TIMP in peripheral blood cells had no correlation with the circulating concentrations of these proteins, which indicated that detection of MMP mRNA and TIMP mRNA in peripheral blood cells may also give us important information about liver fibrosis. Boker *et al*[40] reported that TIMP-1 could be detected in lymphocytes and granulocytes. To determine whether TIMP-1mRNA and MMP-1mRNA in PBMCs could be used as the diagnostic markers, we detected them and TIMP-1mRNA/MMP-1mRNA, and compared these indices between patients and the healthy blood donators. The results demonstrated that TIMP-1mRNA, TIMP-1mRNA/MMP-1mRNA significantly increased while no change in mRNA expression of MMP-1 was observed. Correlation analysis revealed that TIMP-1mRNA was positively correlated with fibrosis stage and inflammation grade, while TIMP-1mRNA/MMP-1mRNA was only positively correlated with inflammation grade. No relationship was found between MMP-1mRNA and fibrosis stage or inflammation grade. With regard to MMP-1mRNA in PBMCs, no statistical difference may attribute to the higher standard deviation among individual values. Other factors influencing mRNA expression may also involve. Therefore, it could be more useful to detect TIMP-1mRNA in PBMCs for evaluating liver fibrosis.

As there was a difference in the serum level of PDGF-BB, TIMP-1, TIMP-1/MMP-1, MMP-1, TIMP-1mRNA and TIMP-1mRNA/MMP-1mRNA in PBMCs between patients and the normal controls, we wanted to know whether these indices could be used for diagnosis, and if they could, the following problem was whether they were more valuable than those four routine serum markers (HA, PCIII, CIV, LN). AUC and YI of the serum level of PDGF-BB were the closest to 1 through ROC curve. This revealed that the diagnostic value of serum level of PDGF-BB was the highest among nine indices (Table 5). Although TGF-β_1 as the main fibrogenic mediator mediates HSC activation and transformation, additional growth factors like PDGF become important in the later stage of HSC transformation. That means PDGF is vital in the progress of liver fibrosis. PDGF has been proved to be the main stimulator of HSC proliferation, migration and the strong mitogen for HSCs. Among the three subunits-AA, AB and BB, PDGF-BB is the vital cytokine for the signaling pathway in HSC and other cells[41-44]. In recent years, studies have not been adequately performed on the serum level of PDGF-BB for assessing liver fibrosis. Our results indicated that detection of the serum level of PDGF-BB had profound significance. TIMP-1mRNA and TIMP-1mRNA/MMP-1mRNA in PBMCs was inferior to serum PDGF-BB. The diagnostic value of serum level of HA, PCIII, TIMP-1 and TIMP-1/MMP-1 is similar, for their AUC are closer, but detection of serum level of HA and TIMP-1/MMP-1 was more applicable if we evaluated them according to YI. Researchers have studied TIMPs from hepatic tissues, serum level to mRNA expression, revealing the important relationship of TIMPs with fibrosis stage or inflammation grade. But it is still unclear whether the serum level of TIMP-1 and TIMP-1mRNA in PBMCs can be used as the markers for the diagnosis of liver fibrosis. If they can, are they superior or inferior to other established markers[45-47]? Our results demonstrated that TIMP-1mRNA was more sensitive than TIMP-1. Some studies[26,39] have revealed the role of the ratio of MMPs and TIMPs such as MMP-1/TIMP-1, MMP-2/TIMP-1, but did not report whether the ratio could be used for the diagnosis of liver fibrosis. We observed that both TIMP-1mRNA/MMP-1mRNA in PBMCs and TIMP-1/MMP-1 in serum could be used for the diagnosis of hepatic fibrosis. However, the former was superior to the latter. The data suggested that we should take both the protein level and mRNA expression into account to explore the noninvasive markers. The value of the serum level of CIV and LN was relatively low. In fact, their AUC values were 0.5 for their *P* values were above 0.05. The roles of serum MMPs in liver fibrosis had been studied[22,47]. Murawaki *et al*[22] found that the serum MMP-1 test was superior to the serum PIIINP test in assessing liver necroinflammation, and thought that the serum MMP-1 test might be useful clinically to differentiate active from inactive types of hepatitis in patients with chronic viral hepatitis, but they did not elucidate whether serum MMP-1 could be more efficient than other indices for assessing liver fibrosis. We evaluated the diagnostic value of MMP-1 for pre-cirrhosis and severe inflammation as there was a difference between patients in S4 or G4 and the normal controls. But the results revealed that the serum level of MMP-1 was of no use for assessing liver fibrosis and evaluating the severity of inflammation. However, our results revealed the declining tendency of the serum MMP-1 with the progress of hepatic fibrosis. The problem is worth further investigating.

The diagnostic value, the sensitivity and the specificity should be taken together, when an index is evaluated for the diagnosis of liver fibrosis. ROC curve analysis revealed that the sensitivity and the specificity of one index were not desirable. Thus, to overcome the limitation of the single index, combination test should be used. There are two kinds of combination test in clinical practice. One is the parallel test and the other is the serial test. The former is often used to screening diseases because it focuses on improving the sensitivity and decreasing the missing incidence. The latter is used to confirm the diagnosis. Table 6 showed that indices in the parallel test were more sensitive than one index. Furthermore, its specificity was also improved. These results revealed that the parallel test was beneficial to screening hepatic fibrosis because hepatic fibrosis continue to progress even though the pathogen have been eliminated. Table 7 showed that the specificity was improved, while the sensitivity was evidently decreased. The data demonstrated that the combination of serum PDGF-BB, HA, TIMP-1mRNA, and TIMP-1mRNA/MMP-1mRNA in PBMCs was clinically limited. However, the specificity of each kind of the combination in the serial test reached close to 100 %, indicating that the diagnostic value of any kind of combination was important and could provide the key information for doctors once some abnormal

results appeared.

In conclusion, we think that serum PDGF-BB, TIMP-1, TIMP-1/MMP-1, TIMP-1mRNA and TIMP-1mRNA/MMP-1mRNA in PBMCs may be used to diagnose hepatic fibrosis. Among them, serum PDGF-BB, TIMP-1mRNA and TIMP-1mRNA/MMP-1mRNA are more sensitive and could be used in clinical practice. The combination of serum PDGF-BB, TIMP-1mRNA and TIMP-1mRNA/MMP-1mRNA in PBMCs is more efficient in screening liver fibrosis. However, the ideal combination for confirming the diagnosis need to be further explored.

REFERENCES

1 **Yuan N**, Wang P, Wang X, Wang Z. Expression and significance of platelet derived growth factor and its receptor in liver tissues of patients with liver fibrosis. *Zhonghua Ganzangbing Zazhi* 2002; **10**: 58-60

2 **Weiner JA**, Chen A, Davis BH. Platelet-derived growth factor is a principal inductive factormodulating mannose 6-phosphate / insulin-like growth factor-II receptorgene expression via a distal E-box in activated hepatic stellate cells. *Biochem J* 2000; **345**(Pt2): 225-231

3 **Kinnman N**, Hultcrantz R, Barbu V, Rey C, Wendum D, Poupon R, Housset C. PDGF-mediated chemoattraction of hepatic stellate cells by bile duct segments in cholestatic liver injury. *Lab Invest* 2000; **80**: 697-707

4 **Benedetti A**, Di Sario A, Casini A, Ridolfi F, Bendia E, Pigini P, Tonnini C, D'Ambrosio L, Feliciangeli G, Macarri G, Svegliati-Baroni G. Inhibition of the NA(+) / H(+)exchanger reduces rat hepatic stellate cell activity and liver fibrosis: an *in vitro* and *in vivo* study. *Gastroenterology* 2001; **120**: 545-556

5 **Issa R,** Williams E, Trim N, Kendall T, Arthur MJ, Reichen J, Benyon RC, Iredale JP. Apoptosis of hepatic stellate cells: involvement in resolution of biliary fibrosis and regulation by soluble growth factors. *Gut* 2001; **48**: 548-557

6 **Huang YX**, Zhang GX, Lu MS, Fan GR, Chen NL, Wu GH. Increased expression of transforming growth factor-β1 in hepatocellular carcinoma. *Shijie Huaren Xiaohua Zazhi* 1999; **7**: 150-152

7 **Wang GY**, Cai WM, Weng HL, Chen F. Changes and significance of TGF-beta1 and IFN- gamma in experimental liver fibrosis. *Zhejiang Yixue Zazhi* 1999; **21**: 469-471

8 **Liu F**, Wang XM, Liu JX, Wei MX. Relationship between serum TGF-β1 of chronic hepatitis B and hepatic tissue pathology and hepatic fibrosis quantity. *ShijieHuaren Xiaohua Zazhi* 2000; **8**: 528-531

9 **Yan JC**, Chen WB, Ma Y, Tian RX, Ding TL, Xu CJ. Relationship between transforming growth factor beta-1 and vascular diseases in hepatitis B. *Shijie Huaren Xiaohua Zazhi* 2001; **9**: 751-754

10 **Dudas J**, Kovalszky I, Gallai M, Nagy JO, Schaff Z, Knittel T, Mehde M, Neubauer K, Szalay F, Ramadori G. Expression of decorin, transforming growth factor-beta1, tissue inhibitor metalloproteinase 1 and 2, and type IV collagenases in chronic hepatitis. *Am J Clin Pathol* 2001; **115**: 725-735

11 **Knittel T**, Mehde M, Grundmann A, Saile B, Scharf JG, Ramadori G. Expression of matrix metalloproteinases and their inhibitors during hepatic tissue repair in the rat. *Histochem Cell Biol* 2000; **113**: 443-453

12 **Mitsuda A**, Suou T, Ikuta Y, Kawasaki H. Changes in serum tissue inhibitor of matrix metalloproteinase-1 after interferon alpha treatment in chronic hepatitis C. *J Hepatol* 2000; **32**: 666-672

13 **Watanabe T,** Niioka M, Hozawa S, Kameyama K, Hayashi T, Arai M, Ishikawa A, Maruyama K, Okazaki I. Gene expression of interstitial collagenase in both progressive and recovery phase of rat liver fibrosis induced by carbon tetrachloride. *J Hepatol* 2000; **33**: 224-235

14 **Yang C**, Hu G, Tan D. Effects of MMP-1 expressing plasmid on rat liver fibrosis. *Zhonghua Ganzangbing Zazhi* 1999; **7**: 230-232

15 **Society of Infectious Disease and Parasitic Disease, CMA.** Criteria on the prevention and treatment for virus hepatitis. *Zhonghua Neike Zazhi* 2001; **40**: 62-68

16 **Cai WM**, Chen F, Zhao JK, Liu RH. The practical value of ultrasound examination in schistosomiasis japonica. *Chin Med J* 2000; **113**

17 **Zheng M**, Cai W, Weng H, Liu R. Determination of serum fibrosis indexes in patients with chronic hepatitis and its significance. *Chin Med J* 2003; **116**: 346-349

18 **Zheng M**, Cai WM, Weng HL, Liu RH. ROC curves in evaluation of serum fibrosis indices for hepatic fibrosis. *World J Gastroenterol* 2002; **8**: 1073-1076

19 **Li C**, Wan M, Zeng M, Su B, He Q, Lu L, Mao Y. A preliminary study of the combination of noninvasive parameters in the diagnosis of liver fibrosis. *Zhonghua Ganzangbing Zazhi* 2001; **9**: 261-263

20 **Tran A**, Hastier P, Barjoan EM, Demuth N, Pradier C, Saint-Paul MC, Guzman-Granier E, Chevallier P, Tran C, Longo F, Schneider S, Piche T, Hebuterne X, Benzaken S, Rampal P. Non invasive prediction of severe fibrosis in patients with alcoholic liver disease. *Gastroenterol Clin Biol* 2000; **24**: 626-630

21 **Cai WM**, Tao J, Weng HL, Liu RH. Study on the influence factors of the serum fibrosis markers. *Zhonghua Ganzangbing Zazhi* 2003; **11**: 23-25

22 **Murawaki Y**, Ikuta Y, Idobe Y, Kawasaki H. Serum matrix metalloproteinase-1 in patients with chronic viral hepatitis. *J Gastroenterol Hepatol* 1999; **14**: 138-145

23 **Okazaki I**, WatanabeT, Hozawa S, Niioka M, Arai M, Maruyama K. Reversibility of hepatic fibrosis: from the first report of collagenase in the liver to the possibility of gene therapy for recovery. *Keio J Med* 2001; **50**: 58-65

24 **Yoshiji H,** Kuriyama S, Miyamoto Y, Thorgeirsson UP, Gomez DE, Kawata M, Yoshii J Ikenaka Y, Noguchi R, Tsujinoue H, Nakatani T, Thorgeirsson SS, Fukui H. Tissue inhibitor of metalloproteinases-1 promotes liver fibrosis development in a transgenic mouse model. *Hepatology* 2000; **32**: 1248-1254

25 **Vaillant B,** Chiaramonte MG, Cheever AW, Soloway PD, Wynn TA. Regulation of hepatic fibrosis and extracellular matrix genes by the th response: new insight into the role of tissue inhibitors of matrix metalloproteinases. *J Immunol* 2001; **167**: 7017-7026

26 **Ninomiya T**, Yoon S, Nagano H, Kumon Y, Seo Y, Kasuga M, Yano Y, Nakaji M, Hayashi Y. Significance of serum matrix metalloproteinases and their inhibitors on the antifibrogenetic effect of interferon –alfa in chronic hepatitis C patients. *Intervirology* 2001; **44**: 227-231

27 **Lichtinghagen R**, Michels D, Haberkorn CI, Arndt B, Bahr M, Flemming P, Manns MP, Boeker KH. Matrix metalloproteinase (MMP)-2, MMP-7, and tissue inhibitor of metalloproteinase-1 are closely related to the fibroproliferative process in the liver during chronic hepatitis C. *J Hepatol* 2001; **34**: 239-247

28 **Daniluk J**, Szuster-Ciesielska A, Drabko J, Kandefer-Szerszen M. Serum cytokine levels in alcohol-related liver cirrhosis. *Alcohol* 2001; **23**: 29-34

29 **Oberti F**, Valsesia E, Pilette C, Rousselet MC, Bedossa P, Aube C, Gallois Y, Rifflet H, Maiga MY, Penneau-Fontbonne D, Cales P. Noninvasive diagnosis of hepatic fibrosis or cirrhosis. *Gastroenterology* 1997; **113**: 1609-1616

30 **Tsushima H**, Kawata S, Tamura S, Ito N, Shirai Y, Kiso S, Doi Y, Yamada A, Oshikawa O, Matsuzawa Y. Reduced plasma transforming growth factor-beta1 levels in patients with chronic hepatitis C after interferon-alpha therapy: association with regression of hepatic fibrosis. *J Hepatol* 1999; **30**: 1-7

31 **Flisiak R**, Pytel-Krolczuk B, Prokopowicz D. Circulating transforming growth factor beta (1) as an indicator of hepatic function impairment in liver cirrhosis. *Cytokine* 2000; **12**: 677-681

32 **Matsuzaki K**, Date M, Furukawa F, Tahashi Y, Matsushita M, Sakitani K, Yamashiki N, Seki T, Saito H, Nishizawa M, Fujisawa J, Inoue K. Autocrine stimulatory mechanism by transforming growth factor beta in human hepatocellular carcinoma. *Cancer Res* 2000; **60**: 1394-1402

33 **Shah M**, Revis D, Herrick S, Baillie R, Thorgeirson S, Ferguson M, Roberts A. Role of elevated plasma transforming growth facotor-beta1 levels in wound healing. *Am J Pathol* 1999; **154**: 1115-1124

34 **Okuno M**, Akita K, Moriwaki H, Kawada N, Ikeda K, Kaneda K, Suzuki Y, Kojima S. Prevention of rat hepatic fibrosis by the protease inhibitor, camostat mesilate, via reduced generation of active TGF-beta. *Gastroenterology* 2001; **120**: 1784-1800

35 **Breitkopf K**, Lahme B, Tag CG, Gressner AM. Expression and matrix deposition of latent transforming growth factor beta binding proteins in normal and fibrotic rat liver and transdifferentiating hepatic stellate cells in culture. *Hepatology* 2001; **33**: 387-396

36 **Kobayashi H**, Horikoshi K, Yamataka A, Lane GJ, Furuhata A, Sueyoshi N, Miyano T. Are stable postoperative biliary atresia patients really stable? *Pediatr Surg Int* 2001; **17**: 104-107
37 **Chen F,** Cai W, Chen Z, Chen X, Liu R. Dynamic changes in the collagen metabolism of liver fibrosis at the transcription level in rabbits with Schistosomiasis japonica. *Chin Med J* 2002; **115**: 1637-1640
38 **Yata Y**, Takahara T, Furui K, Zhang LP, Jin B, Watanabe A. Spatial distribution of tissue inhibitor of metalloproteinase-1 mRNA in chronic liver disease. *J Hepatol* 1999; **30**: 425-432
39 **Lichtinghagen R**, Huegel O, Seifert T, Haberkorn CI, Michels D, Flemming P, Bahr M, Boeker KH. Expression of matrix metalloproteinase-2 and -9 and their inhibitors in peripheral blood cells of patients with chronic hepatitis C. *Clin Chem* 2000; **46**: 183-192
40 **Boker KH,** Pehle B, Steinmetz C, Breitenstein K, Bahr M, Lichtinghagen R. Tissue inhibitors of metalloproteinases in liver and serum / plasma in chronic active hepatitis C and HCV-induced cirrhosis. *Hepatogastroenterology* 2000; **47**: 812-819
41 **Ikeda K**, Wakahara T, Wang YQ, Kadoya H, Kawada N, Kaneda K. *In vitro* migratory potential of rat quiescent hepatic stellate cells and its augmentation by cell activation. *Hepatology* 1999; **29**: 1760-1767
42 **Powell DW**, Mifflin RC, Valentich JD, Crowe SE, Saada JI, West AB. Myofibroblasts. II. Intestinal subepithelial myofibroblasts. *Am J Physiol* 1999; **277**(2 Pt1): C183-201
43 **Wang SN**, Hirschberg R. Growth factor ultrafiltration in experimental diabetic nephropathy contributes to interstitial fibrosis. *Am J Physiol Renal Physiol* 2000; **278**: F554-560
44 **Lohmann CH**, Schwartz Z, Niederauer GG, Carnes DL Jr, Dean DD, Boyan BD. Pretreatment with platelet derived growth factor-BB modulates the ability of costochondral resting zone chondrocytes incorporated into PLA / PGA scaffolds to form new cartilage *in vivo*. *Biomaterials* 2000; **21**: 49-61
45 **Murawaki Y,** Ikuta Y, Kawasaki H. Clinical usefulness of serum tissue inhibitor of metalloproteinases (TIMP)-2 assay in patients with chronic liver disease in comparison with serum TIMP-1. *Clin Chim Acta* 1999; **281**: 109-120
46 **Walsh KM,** Timms P, Campbell S, MacSween RN, Morris AJ. Plasma levels of matrix metalloproteinase-2 (MMP-2) and tissue inhibitors of metalloproteinases-1 and -2 (TIMP-1 and TIMP-2) as noninvasive markers of liver disease in chronic hepatitis C: comparison using ROC analysis. *Dig Dis Sci* 1999; **44**: 624-630
47 **Nie QH,** Cheng YQ, Xie YM, Zhou YX, Bai XG, Cao YZ. Methodologic research on TIMP-1, TIMP-2 detection as a new diagnostic index for hepatic fibrosis and its significance. *World J Gastroenterol* 2002; **8**: 282-287

Edited by Ma JY and Wang XL

P.O.Box 2345, Beijing 100023,China
Fax: +86-10-85381893
E-mail: wjg@wjgnet.com www.wjgnet.com

World J Gastroenterol 2003;9(11):2497-2500
World Journal of Gastroenterology
 ISSN 1007-9327

Influence factors of serum fibrosis markers in liver fibrosis

Jun Tao, Hui-Qin Peng, Wei-Min Cai, Feng-Qin Dong, Hong-Lei Weng, Rong-Hua Liu

Jun Tao, Hui-Qin Peng, Wei-Min Cai, Feng-Qin Dong, Hong-Lei Weng, Rong-Hua Liu, Institute of Infectious Diseases, First Affiliated Hospital, School of Medicine, Zhejiang University, Hangzhou 310003 Zhejiang Province, China
Correspondence to: Dr. Jun Tao, Institute of Infectious Diseases, First Affiliated Hospital, School of Medicine, Zhejiang University, Hangzhou 310003 Zhejiang Province, China. taojun20001@163.com
Telephone: +86-571-87236580 **Fax:** +86-571-87068731
Received: 2003-05-12 **Accepted:** 2003-06-02

Abstract

AIM: To analyze the factors which influence the serum levels of hyaluronic acid (HA), type III pro-collagen (PCIII), laminin (LN) and type IV collagen (C-IV) in liver fibrosis.

METHODS: The serum specimens from 141 chronic hepatitis patients were assayed for fibrosis indexes including HA, PCIII, LN and C-IV with radioimmunoassay (RIA) and liver function indexes by an automatic biochemistry analyzer. The patients were then divided into consistent group and inconsistent group. The patients' clinical manifestations were recorded, routine blood pictures were done by a blood counter and analyzer (AC-900). Liver biopsy specimens were examined path-morphologically. The inner diameters of portal vein, splenic vein and thickness of spleen were all measured by ultrasonography.

RESULTS: Sixteen patients (14.16 %) had serum fibrosis indexes inconsistent with histological stage of their hepatic fibrosis. Their serum fibrosis indexes did not correlate with the stage of hepatic fibrosis ($P>0.05$), but were positively correlated with the grade of inflammation ($\chi^2=12.07$, $P<0.05$). At the same time, serum albumin (ALB) and the ratio of albumin and globulin (A/G) were significantly increased ($t=3.06$, $P<0.01$), ($t=3.70$, $P<0.01$). Serum levels of glutamic-pyruvic transaminase (ALT), glutamic-oxaloacetic transaminase (AST), γ-glutamyl transferase (GGT) and globulin (GLB) were all significantly decreased ($t=2.45$, $P<0.05$), ($t=2.33$, $P<0.05$), ($t=2.08$, $P<0.05$), ($t=3.03$, $P<0.01$). Weary degree also decreased more obviously ($\chi^2=7.52$, $P<0.05$), but other clinical manifestations, routine blood indexes, serum levels of alkaline phosphatase (AKP), total bilirubin (TBIL), total protein (TP), width of main portal vein, width of splenic vein and thickness of spleen had no significant change ($P>0.05$).

CONCLUSION: Serum fibrosis indexes can be influenced by the grade of inflammation, some liver function indexes and clinical manifestations. Comprehensive analysis is necessary for its proper interpretation.

Tao J, Peng HQ, Cai WM, Dong FQ, Weng HL, Liu RH. Influence factors of serum fibrosis markers in liver fibrosis. *World J Gastroenterol* 2003; 9(11): 2497-2500
http://www.wjgnet.com/1007-9327/9/2497.asp

INTRODUCTION

Many chronic injuries can lead to fibrosis of liver[1-11]. Hepatic fibrosis is resulted from the loss of normal liver cell function due to disorganized over-accumulation of extra-cellular matrix (ECM) components in the liver[12-17]. It is clear that the increased production and degradation of ECM components are responsible for the altered ECM metabolism. Liver biopsy has traditionally been the standard method for assessing hepatic fibrosis, but the procedure is invasive in nature and has complications though with a low incidence. So its popularity is somewhat hindered. Reports showed that serum fibrosis indexes, including HA, PCIII, LN, C-IV and others, could reflect the activity of hepatic fibrosis to some extent[18-27]. Mean ± SD has always been used to express the standard for hepatic fibrosis. We have explored the clinical significance of the four serum fibrosis indexes by detecting them in 2 600 patients with chronic hepatitis including 280 patients undertaken biopsy[28,29]. At same time, patients whose four serum fibrosis indexes were not consistent with the degree of hepatic fibrosis were found, so we selected these patients to analyze what factors might influence the four serum fibrosis indexes (HA, PCIII, LN and C-IV) in diagnosing liver fibrosis.

MATERIALS AND METHODS

Subjects

During the Sixth National Conference for Infectious and Parasitic Diseases, the protocol of prevention and treatment for virus hepatitis was modified in 2000 (abbreviated as "2000 criteria")[30]. One hundred and forty-one patients had typical presentations of chronic hepatitis, 121 were males and 20 females. There were mild, moderate and severe degrees of the disease in the group. Case histories were mainly collected from the First Affiliated Hospital, School of Medicine, Zhejiang University. Some were from other hospitals in Zhejiang Province between July, 1998 and May, 2000. The age ranged from 18 to 62 years, the average age was 38.75±14.53. Weary Degree: 0: did not feel weary; 1: could join routine activities, but felt weary; 2: could join light work, but felt weary; 3: could not work, felt weary while moving. The disease course was from one to 30 years.

Clinical manifestations

Total volume of food taken by the patient every day, length of liver and spleen under costal margin were recorded. The criteria of clinical manifestations were as following: (1). Weary degree: as stated above. (2). Degree of abdominal distension: 0: did not feel abdominal distension; 1: felt abdominal distension while taking food or abdominal distension usually; 2: felt abdominal distension while taking a little food, but can endure; 3: felt abdominal distension, did not want to take food, felt abdominal distension while taking food, can not endure. (3). Secret anguish degree: 0: did not feel secret anguish; 1: felt secret anguish, but could take food; 2: felt secret anguish, could endure; 3: felt secret anguish, could not endure, needed medication.

Histology

The needles (18G) were purchased from Angiomed Corporation in German. The length of liver biopsy specimen exceeded 1 cm. Biopsy fragments of the livers were fixed in 10 % neutralized formaldehyde, embedded in paraffin, and then stained with hematoxylin and eosin. Reticulum fibrosis

stain and Sirius red method were used specially for staining fibrous tissue components. Histological assessment of the liver was done according to Wang' s report[31], and staging of fibrosis was divided into four, expressed as S1 to S4 according to the "2000 criteria"[30]. S0 showed no fibrosis. S1 showed expansion in portal tract areas with fibrosis. S2 showed fibrosis around portal tract areas with formation of fibrosis segregation while maintain lobular structure. S3 showed formation of fibrosis segregation and disorder of lobular structure without hepatic cirrhosis, and S4 showed early stage or confirmed cirrhosis.

Determination of serum fibrosis tests and liver function indexes

The serum specimens from 141 chronic hepatitis patients were stored at -20 ℃. Assay of the levels of serum HA, PCIII, C-IV and LN was done by RIA. The kits of HA, C-IV and LN were provided by the Shanghai Navy Medical Institute. The kit of PCIII was supplied by the Chongqing Tumor Institute. The procedures were performed according to the user' s manual. The assay of liver function indexes was measured by an automatic biochemistry analyzer, these indexes included total bilirubin (TBIL), gliutamic-pyruvic transaminase (ALT), glutamic-oxaloacetic transaminase (AST), γ glutamyl-transferase (GGT), alkaline phosphatase (AKP), total protein (TP), albumin (ALB), globulin (GLB) and the ratio of albumin and globulin (A/G).

Determination of routine blood indexes

Blood samples were drawn from the veins and treated with EDTA-K_2 (the concentration was 1.5 mg/ml). WBC, RBC and platelet were determined by a blood cell counter and analyzer (AC-900).

Ultrasonic examination

All patients were forbidden to take water and food for eight hours before examination. Inner diameters of the portal vein, splenic vein and thickness of the spleen were measured, all the procedures were performed by the same physician.

Definition of patients whose serum fibrosis indexes were inconsistent with histologic staging of their hepatic fibrosis

All patients were divided into two groups. If in S≥2 group, all four serum fibrosis indexes were less than or equal to the mean value of that in S1 group, these patients would then be classified as inconsistent group. On the contrary, they would be classified as the consistent group. There was also inconsistency in a single index, that meant staging belonged to S≥2, but the index was less than or equal to the mean of that in S1 group.

Statistical analysis

Results were expressed as mean ± standard deviation ($\bar{x}\pm s$) and *t* test was done when necessary, nonparametric one-way ANOVA was used for nonparametric data, all tests were done by SPSS 10.0 statistical program and considered statistically significant at $P<0.05$.

RESULTS

Inconsistency between each serum fibrosis index and stage of hepatic fibrosis

When hepatic fibrosis was in stage 1, the mean of HA was 187.23 ng/ml, LN was 144.68 ng/ml, PCIII was 151.42 μg/L, and C-IV was 74.26 μg/L. One hundred and thirteen patients were found in hepatic fibrosis stage II or more than that, 33 cases were inconsistent with staging of hepatic fibrosis for HA. More cases were inconsistent for C-IV, 43 cases were inconsistent with staging of hepatic fibrosis for LN (Table 1).

Table 1 Inconsistency between each serum fibrosis index and stage of hepatic fibrosis

Stage (S)	*n*	HA	C-IV	PCIII	LN
S2	30	13	14	16	17
S3	31	9	10	10	11
S4	52	11	12	13	15
Total	113	33 (29.20%)	36(31.86%)	39(34.51%)	43 (38.05%)

Distribution of patients whose four serum fibrosis indexes were inconsistent with stage of hepatic fibrosis

Among 113 patients, 16 (14.16 %) were in inconsistent group and 97(85.84 %) in consistent group, no significant difference was found in staging of hepatic fibrosis between two groups ($P>0.05$), (Table 2).

Table 2 Staging comparison between two groups

Groups	Stage of hepatic fibrosis		
	S2	S3	S4
Consistent group	24	27	46
Inconsistent group	6	4	6

$\chi^2=1.18$, $P>0.05$.

Inflammation grading of patients in inconsistent group

Table 3 shows that inflammation grade was mainly G2 in inconsistent group, while mainly G3 and G4 in consistent group. The difference was significant between two groups ($P<0.05$).

Table 3 Comparison of inflammation grade between two groups

Groups	Inflammation grade			
	G1	G2	G3	G4
Consistent group	5	17	49	26
Inconsistent group	1	9	4	2

$\chi^2=12.07$, $P<0.05$.

Clinical manifestations in inconsistent group

Table 4 and table 5 show no patient whose degree of weary, abdominal distension and secret anguish exceeded 2 in consistent group. There was no patient whose degree of weary, abdominal distension and secret anguish exceeded 1 in inconsistent group. The daily food volume of the patients increased slightly, the palpable length of liver and spleen decreased slightly. The difference was not significant between two groups ($P>0.05$) except weary degree ($P<0.05$).

Table 4 Comparison of clinical manifestations between two groups

Groups	Weary degree			Abdominal distension degree			Secret anguish degree		
	0	1	2	0	1	2	0	1	2
Consistent group	39	41	17	72	24	1	86	8	3
Inconsistent group	12[a]	4	0	14	2	0	16	0	0

$\chi^2=7.52$, $P<0.05$.

Table 5 Comparison of clinical manifestations between two groups ($\bar{x}\pm s$)

Groups	*n*	Volume of food(g)	Length of liver (cm)	Length of spleen(cm)
Consistent group	97	427.11±194.15	0.31±0.63	0.53±0.85
Inconsistent group	16	456.25±160.08	0.28±0.55	0.34±0.60

Change of routine blood indexes in inconsistent group

No significant difference was found in WBC, RBC and PLT between two groups (P>0.05), (Table 6).

Table 6 Comparison of routine blood tests between two groups ($\bar{x}\pm s$)

Groups	*n*	WBC	RBC	PLT
Consistent group	97	5.07±1.12	4.61±0.52	116.52±34.14
Inconsistent group	16	4.90±1.24	4.64±0.57	117.00±26.38

Change of liver function tests in inconsistent group

Serum ALT, AST, GGT and GLB decreased obviously in inconsistent group (P<0.05) or (P<0.01), ALB and A/G increased evidently (P<0.01), but AKP, TBIL and TP did not change significantly (P>0.05), (Table 7).

Table 7 Comparison of liver function tests between two groups ($\bar{x}\pm s$)

Groups	*n*	TBIL (μmol/L)	TP (g/L)	ALB (g/L)	GLB (g/L)	A/G
Consistent group	97	18.19±8.51	74.60±6.75	42.34±4.81	32.13±5.18	1.35±0.28
Inconsistent group	16	16.35±6.41	74.31±4.36	46.19±3.61[b]	28.05±3.47[b]	1.63±0.26[b]

[b]P<0.01 *vs* consistent group

Groups	*n*	ALT(U/L)	AST(U/L)	GGT(U/L)	AKP(U/L)
Consistent group	97	89.28±64.25	66.10±42.30	86.26±70.36	91.65±34.95
Inconsistent group	16	49.31±26.75[a]	40.83±22.40[a]	48.99±29.96[a]	85.25±30.60

[a]P<0.05 *vs* consistent group.

Results of ultrasonic examination in inconsistent group

Table 8 shows no significant difference in width of main portal vein, splenic vein and thickness of spleen between two groups (P>0.05).

Table 8 Comparison of ultrasonic examination between two groups (cm, $\bar{x}\pm s$)

Groups	*n*	Width of main portal vein	Width of splenic vein	Thickness of spleen
Consistent group	97	1.20±0.13	0.74±0.12	4.02±0.64
Inconsistent group	16	1.23±0.12	0.77±0.13	4.09±0.62

DISCUSSION

The basic pathological changes of chronic liver disease are inflammation and fibrosis, so they were analysed respectively in pathological diagnosis in recent year. Many semi quantitative score systems, such as Chevallier's criterion, Scheuer's criterion were developed[31-33], so chronic liver disease has been recognized more accurately and profoundly. Staging of liver fibrosis can help us to recognize the development of chronic liver disease. Serum indexes such as HA, PCIII, LN and C-IV which reflect the stage of liver fibrosis have been paid much attention to by many scholars[34-36] HA, PCIII, LN and C-IV were mainly produced by hepatic stellate cells[35,36]. HA and PCIII were absorbed and degraded by endothelial cells of hepatic sinusoids[37,38]. When liver fibrosis takes place, the phenotypes of the membrane of endothelial cells of hepatic sinusoids change, their absorption is blocked, the contents of serum HA, PCIII increase to some degree. LN and C-IV reflected basement membrane transformation and had some relation to portal hypertension[39,40]. Many scholars agreed the four serum fibrosis indexes had values in the serodiagnosis of hepatic fibrosis, including the diagnostic value of each serum fibrosis index and combination of several indexes[20,29]. When these indexes were applied to clinical diagnosis, we found some of them were inconsistent with pathological diagnosis. Even with a high stage of hepatic fibrosis, the four serum fibrosis indexes could still be around normal range. So we think it is necessary to find the influencing factors of this phenomenon.

Our results showed the rate of inconsistency between the four serum fibrosis indexes and stage of hepatic fibrosis was 14.16 % in the patients with chronic hepatitis. Table 1 shows the rate of inconsistency of serum HA was 29.21 %, C-IV 31.86 %, PCIII 34.51 % and LN 38.05 %. The rate of consistency between serum HA and stage of hepatic fibrosis was highest, followed by C-IV. This suggests that among the four serum fibrosis indexes, HA is the most ideal index for diagnosing hepatic fibrosis. This was consistent with the results of our previous study on the relationship between serum fibrosis indexes and liver histological changes[41], and was also consistent with other reports in the literature[42]. Stage distribution of hepatic fibrosis in inconsistent patients had no significant difference from that of consistent group. This indicates that inconsistency between the four serum fibrosis indexes and stage of hepatic fibrosis has no relationship with the staging. By further study we found inflammation grade of inconsistent patients was lower than that of consistent group. This suggests that the four serum fibrosis indexes are influenced by inflammation grade. In the patients with chronic hepatitis when their stage of hepatic fibrosis is at high level, such as S3 or S4, and inflammation grade is at low level, it is possible that the four serum fibrosis indexes can be inconsistent with stage of hepatic fibrosis. This could be found in patients with advanced stage of schistosomiasis japonica having severe liver fibrosis, but almost no inflammation or decompensation of hepatic function. In addition, it was also suggested that these four serum fibrosis indexes could be lowered by anti-inflammation treatment in patients with chronic hepatitis. As to clinical manifestations, weary degree of inconsistent patients decreased more obviously than that in consistent group. Other profiles had no obvious change. In liver function tests, we found serum ALT, AST, GGT and GLB of inconsistent patients were decreased more obviously, while serum ALB and A/G increased more evidently, serum AKP, TP and TBIL had no significant change. All these suggest that changes of weary degree, serum ALT, AST, GGT, GLB, ALB and A/G were affected by inflammation grade. So they should be taken into account when we assess the diagnostic value of the four serum fibrosis indexes for stage of hepatic fibrosis. At the same time, change of liver function indexes is more sensitive than clinical manifestations. So even without any clinical symptoms, patients should be checked regularly by liver function tests. In clinical practice, width of main portal vein, splenic vein and thickness of the spleen are usually used to determine whether the pressure of main portal vein is increased or not. Table 7 shows they had no significant change, indicating that these patients' condition did not reach the stage of liver cirrhosis.

We conclude that serum fibrosis indexes can only reflect abnormal metabolism of ECM. They are non-specific biochemical markers, when they are used in the diagnosis of hepatic fibrosis, other diseases should be ruled out. They should not be called hepatic fibrosis markers, serum fibrosis indexes should be the appropriate term. Our study indicates the influencing factors include hepatic inflammatory activity, weary degree and some liver function tests. The activity of inflammation is determined by pathological diagnosis of liver biopsy. So in clinical practice, we should put liver function, case history and clinical manifestations all into consideration in assessment of the diagnostic value of these four fibrosis indexes in the staging of hepatic fibrosis. While assessing therapeutic efficacy of anti-fibrosis drugs, we can also not

depend only on these four fibrosis indexes, a comprehensive analysis is necessary. Further studies on new indexes are needed to better understand the pathological changes of liver.

REFERENCES

1 **Friedman SL**. Molecular mechanisms of hepatic fibrosis and principles of therapy. *J Gastroenterol* 1997; **32**: 424-430
2 **Du LJ**, Tang WX, Dan ZL, Zhang WY, Li SB. Protective effect of Ganyanping on CCl-4 induced liver fibrosis in rats. *Huaren Xiaohua Zazhi* 1998; **6**: 21-22
3 **Yan JC**, Ma Y, Chen WB, Shen XH. Dynamic observation on liver fibrosis and cirrhosis of hepatitis B. *Huaren Xiaohua Zazhi* 1998; **6**: 699-702
4 **Peng YZ**, Huang QT, Yan SN, Deng B, Hu JJ. Effect of RNA against hepatic fibrosis in rabbits infected with Schistosomiasis japonica. *Zhongguo Jishengchongxue Yu Jishengchongbing Zazhi* 1998; **16**: 214-218
5 **Piscaglia F**, Gaiani S, Gramantieri L, Zironi G, Siringo S, Bolondi L. Superior mesenteric artery impedance in chronic liver disease: relationship with disease severity and portal circulation. *Am J Gastroenterol* 1998; **93**: 1925-1930
6 **Assy N**, Paizi M, Gaitini D,Baruch Y, Spira G. Clinical implication of VEGF serum levels in cirrhotic patients with or without portal hypertension. *World J Gastroenterol* 1999; **5**: 296-300
7 **Liu F**, Liu JX, Cao ZC, Li BS, Zhao CY, Kong L, Zhen Z. Relationship between TGF-β1, serum indexes of liver fibrosis and hepatic tissue pathology in patients with chronic liver diseases. *Shijie Huaren Xiaohua Zazhi* 1999; **7**: 519-521
8 **Yao SK**, Yin F. Diagnosis and treatment of hepatic fibrosis. *Shijie Huaren Xiaohua Zazhi* 2000; **8**: 681-683
9 **Bai WY**, Yao XX, Feng LY. The situation of hepatic fibrosis research. *Shijie Huaren Xiaohua Zazhi* 2000; **8**: 1267-1268
10 **Lin H**, Lü M, Zhang YX, Wang BY, Fu BY. Induction of a rat model of alcoholic liver diseases. *Shijie Huaren Xiaohua Zazhi* 2001; **9**: 24-28
11 **Chen WX**, Li YM, Yu CH, Cai WM, Zheng M, Chen F. Quantitatively analysis of transforming growth factor beta 1 mRNA in patients with alcoholic liver disease. *World J Gastroenterol* 2002; **8**: 379-381
12 **Cai WM**, Chen Z, Chen F, Zhou C, Liu RH, Wang JX. Changes of ultrasonography and two serum biochemical indices for hepatic fibrosis in schistosomiasis japonica patients one year after praziquantel treatment. *Chin Med J (Engl)* 1997; **110**: 797-800
13 **Bissell DM**. Hepatic fibrosis as wound repair: a progress report. *J Gastroenterol* 1998; **33**: 295-302
14 **Sun DL**, Sun SQ, Li TZ, Lu XL. Serologic study on extracellular matrix metabolism in patients with viral liver cirrhosis. *Shijie Huaren Xiaohua Zazhi* 1999; **7**: 55-56
15 **Apte MV**, Haber PS, Darby SJ, Rodgers SC, McCaughan GW, Korsten MA, Pirola RC, Wilson JS. Pancreatic stellate cells are activated by proinflammatory cytokines: implications for pancreatic fibrogenesis. *Gut* 1999; **44**: 534-541
16 **Ueki N**, Taguchi T, Takahashi M, Adachi M, Ohkawa T, Amuro Y, Hada T, Higashino K. Inhibition of hyaluronan synthesis by vesnarinone in cultured human myofibroblasts. *Biochim Biophys Acta* 2000; **1495**: 160-167
17 **Li C**, Wan M, Zeng M, Su B, He Q, Lu L, Mao Y. A preliminary study of the combination of noninvasive parameters in the diagnosis of liver fibrosis. *Zhonghua Ganzangbing Zazhi* 2001; **9**: 261-263
18 **Wang X**, Chen YX, Xu CF, Zhao GN, Huang YX, Wang QL. Relationship between tumor necrosis factor-α and liver fibrosis. *World J Gastroenterol* 1998; **4**: 18
19 **Guechot J**, Serfaty L, Bonnand AM, Chazouilleres O, Poupon RE, Poupon R. Prognostic value of serum hyaluronan in patients with compensated HCV cirrhosis. *J Hepatol* 2000; **32**: 447-452
20 **Luo R**, Yang S, Xie J, Zhao Z, He Y, Yao J. Diagnostic value of five serum markers for liver fibrosis. *Zhonghua Ganzangbing Zazhi* 2001; **9**: 148-150
21 **Lu X**, Liu CH, Xu GF, Chen WH, Liu P. Successive observation of laminin and collagen IV hepatic sinusoid during the formation of the liver fibrosis in rats. *Shijie Huaren Xiaohua Zazhi* 2001; **9**: 260-262
22 **Shen M**, Qiu DK, Chen Y, Xiong WJ. Effects of recombinant augmenter of liver regeneration protein, danshen and oxymatrine on rat fibroblasts. *Shijie Huaren Xiaohua Zazhi* 2001; **9**: 1129-1133
23 **He Y**, Wang JB, Wang YM. The diagnosis development of hepatic fibrosis with chronic hepatitis. *Shijie Huaren Xiaohua Zazhi* 2001; **9**: 1305-1309
24 **Leroy V**, De Traversay C, Barnoud R, Hartmann JD, Baud M, Ouzan D, Zarski JP. Changes in histological lesions and serum fibrogenesis markers in chronic hepatitis C patients non-responders to interferon alpha. *J Hepatol* 2001; **35**: 120-126
25 **Xie S**, Zheng R, Peng X, Gao Z. Accurate diagnosis of stage of hepatic fibrosis by measuring levels of serum hyaluronic acid, procollagen type III, and collagen type IV. *Zhonghua Ganzangbing Zazhi* 2001; **9**: 334-336
26 **Cai WM**, Chen F, Zhao JK, Liu RH. The practical value of ultrasomel examination in schistosomiasis japonica. *Zhonghua Yixue Zazhi* 2000: **113**
27 **Zhang BB**, Cai WM, Weng HL, Hu ZR, Lu J, Zheng M, Liu RH. Diagnostic value of platelet derived growth factor-BB, transforming growth factor-β1, matrix metalloproteinase-1 and tissue inhibitor of matrix metalloproteinase-1 in serum and peripheral blood mononucleocytes for hepatic fibrosis. *World J Gastroenterol* 2003; **9**: (in press)
28 **Zheng M**, Cai W, Weng H, Liu R. Determination of serum fibrosis indexes in patients with chronic hepatitis and its significance. *Chin Med J (Engl)* 2003; **116**: 346-349
29 **Zheng M**, Cai WM, Weng HL, Liu RH. ROC curves in evaluation of serum fibrosis indices for hepatic fibrosis. *World J Gastroenterol* 2002; **8**: 1073-1076
30 Chinese Society of Infectious disease and Parasitology and Chinese Society of Hepatology of Chinese medical association. The programme of prevention and cure for viral hepatitis. *Zhonghua Ganzangbing Zazhi* 2000; **8**: 324-329
31 **Wang TL**, Liu X, Zhou YP, He JW, Zhang J, Li NZ, Duan ZP, Wang BE. A semiquantitative scoring system for evaluation of hepatic inflammation and fibrosis in chronic viral hepatitis. *Zhonghua Ganzangbing Zazhi* 1998; **6**: 195-197
32 **Scheuer PJ**. Classification of chronic viral hepatitis: a need for reassessment. *J Hepatol* 1991; **13**: 372-374
33 **Chevallier M**, Guerret S, Chossegros P, Gerard F, Grimaud JA. A histological semiquantitative scoring system for evaluation of hepatic fibrosis in needle liver biopsy specimens: comparison with morphometric studies. *Hepatology* 1994; **20**: 349-355
34 **Li BS**, Wang J, Zhen YJ, Liu JX, Wei MX, Sun SQ, Wang SQ. Experimental study on serum fibrosis markers and liver tissue pathology and hepatic fibrosis in immuno-damaged rats. *Shijie Huaren Xiaohua Zazhi* 1999; **7**: 1031-1034
35 **Oberti F**, Valsesia E, Pilette C, Rousselet MC, Bedossa P, Aube C, Gallois Y, Rifflet H, Maiga MY, Peaneau-Fontbonne D, Cales P. Noninvasive diagnosis of hepatic fibrosis or cirrhosis. *Gastroenterology* 1997; **113**: 1609-1616
36 **Xie S**, Yao J, Zheng S, Yao C, Zheng R. The relationship between the levels of serum fibrosis marks and morphometric quantitative measurement of hepatic histological fibrosis. *Zhonghua Ganzangbing Zazhi* 2000; **8**: 203-205
37 **Tamaki S**, Ueno T, Torimura T, Sata M, Tanikawa K. Evaluation of hyaluronic acid binding ability of hepatic sinusoidal endothelial cells in rats with liver cirrhosis. *Gastroenterology* 1996; **111**: 1049-1057
38 **Nanji AA**, Tahan SR, Khwaja S, Yacoub LK, Sadrzadeh SM. Elevated plasma levels of hyaluronic acid indicate endothelial cell dysfunction in the initial stages of alcoholic liver disease in the rat. *J Hepatol* 1996; **24**: 368-374
39 **Li L**, Yao ZM, Yu T. Influence of BOL on hyaluronic acid, laminin and hyperplasia in hepatofibrotic rats. *World J Gastroenterol* 2001; **7**: 872-875
40 **Cui DL**, Yao XX. Serum diagnosis of hepatic fibrosis. *Shijie Huaren Xiaohua Zazhi* 2000; **8**: 683-684
41 **Cai W**, Zheng M, Weng H, Liu RH. Determination and significance of serum markers for fibrosis in patients with chronic hepatitis. *Zhonghua Neike Zazhi* 2001; **40**: 448-451
42 **Gu S**, Zhang H, Zhang L. Relationship between serum fibrosis markers and fibrosis quantitative analysis of liver tissue. *Zhonghua Ganzangbing Zazhi* 1999; **7**: 199-200

Edited by Xu JY and Wang XL

P.O.Box 2345, Beijing 100023,China
Fax: +86-10-85381893
E-mail: wjg@wjgnet.com www.wjgnet.com

World J Gastroenterol 2003;9(11):2501-2504
World Journal of Gastroenterology
 ISSN 1007-9327

Detection of serum anti-*Helicobacter pylori* immunoglobulin G in patients with different digestive malignant tumors

Ke-Xia Wang, Xue-Feng Wang, Jiang-Long Peng, Yu-Bao Cui, Jian Wang, Chao-Pin Li

Ke-Xia Wang, Xue-Feng Wang, Jiang-Long Peng, Yu-Bao Cui, Jian Wang, Chao-Pin Li, School of Medicine, Anhui University of Science and Technology, Huainan, 232001, Anhui Province, China
Supported by Natural Science Foundation of the Education Department of Anhui Province, China, No.2003kj111
Correspondence to: Dr. Chao-Pin Li, Department of Etiology and Immunology, School of Medicine, Anhui University of Science and Technology,Huainan, 232001, Anhui Province, China. cpli@aust.edu.cn
Telephone: +86-554-6658770 **Fax:** +86-554-6662469
Received: 2003-03-02 **Accepted:** 2003-06-04

Abstract

AIM: To investigate the seroprevalence of *Helicobacter pylori* infection in patients with different digestive malignant tumors.

METHODS: Enzyme linked immunosorbent assay (ELISA) was used to detect serum anti-*Helicobacter pylori* IgG antibody in 374 patients with different digestive malignant tumors and 310 healthy subjects (normal control group).

RESULTS: The seroprevalence of *Helicobacter pylori* infection was 61.50 %(230/374) and 46.77 % (145/310), respectively, in patients with digestive tumors and normal controls ($P<0.05$). The seroprevalence was 52.38 % (33/63), 86.60 % (84/97), 83.14 % (84/101), 45.24 (19/42), 51.13 % (18/35) and 44.44 % (16/36), respectively in patients with carcinomas of esophagus, stomach, duodenum, rectum, colon and liver ($P<0.01$). In patients with intestinal and diffuse type gastric cancers, the seroprevalence was 93.75 % (60/64) and 72.73 % (24/33), respectively ($P<0.05$). In patients with gastric antral and cardiac cancers, the seroprevalence was 96.43 % (54/56) and 73.17 % (30/41), respectively ($P<0.05$). In patients with ulcerous and proliferous type duodenal cancers, the seroprevalence of *H pylori* infection was 91.04 % (61/67) and 52.27 % (23/44), respectively ($P<0.05$). In patients with duodenal bulb and descending cancers, the seroprevalence was 94.20 % (65/69) and 45.20 % (19/42), respectively ($P<0.05$).

CONCLUSION: *H pylori* infection is associated with occurrence and development of gastric and duodenal carcinomas. Furthermore, it is also associated with histological type and locations of gastric and duodenal carcinomas.

Wang KX, Wang XF, Peng JL, Cui YB, Wang J, Li CP. Detection of serum anti-*Helicobacter pylori* immunoglobulin G in patients with different digestive malignant tumors. *World J Gastroenterol* 2003; 9(11): 2501-2504
http://www.wjgnet.com/1007-9327/9/2501.asp

INTRODUCTION

Helicobacter pylori is a gram-negative, spiral-shaped, microaerophilic bacterium that colonizes gastric epithelium of humans[1-4]. Clinical and epidemiological studies have shown a close association between *H pylori* and gastric cancer[5-10]. However, the relationship between *H pylori* and other digestive tumors has not been clarified. In order to investigate the relationship between *H pylori* infection and different digestive cancers, we detected serum anti-*H pylori* IgG in 374 patients with different digestive cancers and 310 healthy subjects, using an enzyme linked immunosorbent assay -(ELISA).

MATERIALS AND METHODS

Materials

Populations A total of 374 patients with different digestive cancers were involved in this study, including 63 esophagus carcinomas, 97 gastric cancers (64 of intestinal type and 33 of diffuse type, and 56 in gastric antrum and 41 in the cardia as displayed under gastroscopy), 101 duodenal carcinomas (67 of ulcerous type and 44 of proliferous type, and 65 in the bulb and 42 in the descending part of duodenum as manifested under gastroscopy), 42 rectal cancers, 35 carcinomas of colon, 36 liver cancers. There were 240 males and 134 females, aged from 23 to 71 years old. At the same time, 310 healthy subjects were recruited as a control group. There was no difference in age and gender between the two groups.

Reagents and instruments The test kit for *H pylori*-IgG was provided by Bioseed Company (USA, batch Hillbough CA 94010). The enzyme-labeling meter was SLT-Spectra-I type (Bio-rad, USA).

Methods

Blood samples were collected from all patients and the control group for the detection of anti-*H pylori* IgG.

Detection of anti-*H pylori* IgG In order to eliminate possibly disrupted other proteins, each sample was diluted at 1:100 and detected in duplicate according to the manufacturer's instructions. A series of standard samples with concentrations of 0, 5, 10, 20, 35 and 70 units/ml were added in corresponding reactive wells. When the reaction was stopped, the optical density (OD) values were tested within 10 min at light wavelength 450nm. To measure the concentrations of anti-*H pylori*-IgG in the serum samples, a standardized curve of each board was mapped with the concentrations of standard samples as the abscissa, and OD values of the two correspondent parallel wells as the ordinate. The average OD value of each sample in the two parallel wells above 12 units/ml was regarded to be positive, otherwise to be negative.

Statistical analysis Data analysis was conducted with χ^2 test.

RESULTS

Detection of serum anti-H pylori IgG in patients with different digestive cancers

The positive rates of anti-*H pylori* IgG in patients with digestive cancers and healthy subjects were 61.50 % (230/374) and 46.77 % (145/310), respectively, which were significantly different ($P<0.01$). The positive rates were 52.38 % (33/63), 86.60 % (84/97), 83.14 % (84/101), 45.24 % (19/42), 51.13 % (18/35) and 44.44 % (16/36), respectively, in patients with esophageal carcinoma, gastric cancer, duodenal carcinoma,

rectal cancer, colon carcinoma and liver cancer. There was a significant difference (P<0.01). The detailed results are shown in Table 1.

Table 1 Positive rates of *H pylori*-IgG in patients with different peptic cancers

	n	Anti-*H pylori* IgG	
		-	+ (%)
Normal group	310	165	145 (46.77)[a]
Cancer group	374	144	230 (61.50)[a]
Esophagus carcinoma	63	30	33 (52.38)[b]
Gastric cancer	97	13	84 (86.60)[b]
duodenal Carcinoma	101	17	84 (83.17)[b]
Rectal cancer	42	23	19 (45.24)[b]
Carcinoma of colon	35	17	18 (51.43)[b]
Liver cancer	36	20	16 (44.44)[b]

[a]P<0.01, χ^2=14.8; [b]P<0.01, χ^2=58.69.

Serum anti-H pylori IgG in patients with gastric cancer

The positive rates of anti-*H pylori* IgG in intestinal and diffuse type gastric cancer were 93.75 % (60/64) and 72.73 % (24/33), respectively (P<0.05).In addition, the positive rates in gastric antrum and cardia were 96.43% (54/56) and 73.17% (30/41) (P<0.05). The detailed results are shown in Table 2.

Table 2 Positive rates of anti-*H pylori* IgG in patients with gastric cancer of different types and at different locations

Group	*n*	*H pylori*-IgG	
		Positive	Positive rates (%)
Gastric cancer	97	84	86.60
Intestinal type	64	60	93.75[c]
Diffuse type	33	24	72.73[c]
Gastric antrum	56	54	96.43[d]
Gastric cardiac	41	30	73.17[d]

[c]P<0.05, χ^2=8.29; [d]P<0.05, χ^2=11.03.

Serum anti-H pylori IgG in patients with duodenal carcinoma

The positive rates of anti-*H pylori* IgG in patients with ulcerous and proliferous type duodenal carcinoma were 91.04 % (61/67) and 52.27 % (23/44) (P<0.05). In addition, the positive rates of *H pylori*-IgG in the bulb and descending part of duodenum were 94.20 % (65/69) and 45.20 % (19/42), (P<0.05). The detailed results are shown in Table 3.

Table 3 Positive rates of *H pylori*-IgG in patients with duodenal carcinoma of different types and at different locations

Group	*n*	*H pylori*-IgG	
		Positive	Positive rates (%)
Duodenal carcinoma	101	84	83.17
Ulcerous type	67	61	91.04[e]
Proliferous type	44	23	52.27[e]
Bulb of duodenum	69	65	94.20[f]
Descending part	42	19	45.20[f]

[e]P<0.05, χ^2=19.74; [f]P<0.05, χ^2=28.97.

DISCUSSION

H pylori is one of the common bacteria causing chronic infection, infects more than 50 % of the human population, causes chronic gastritis and plays an important role in the pathogenesis of gastroduodenal ulceration. *H pylori* has also been suggested to be involved in the genesis of adenocarcinoma and MALT lymphoma of the stomach[11-13]. It is believed that *H pylori* infection might result in the release of various bacterial and host dependent cytotoxic substances including ammonia, platelet activating factor, cytotoxins and lipopolysaccharide as well as cytokines such as interleukins (IL)-1-12, tumor necrosis factor alpha (TNF-alpha) and reactive oxygen species[14-20], tissue damage and gastro-duodenal disease[21-25]. In 1994, the World Health Organization and International Agency for Research on Cancer (IARC) classified it as a class I carcinogen[26-28]. In this study sera from 374 patients with digestive cancers and 310 healthy controls were tested for *H pylori* using a specific IgG ELISA. The results showed that the positive rate of anti-*H pylori* IgG was 61.50 % in the patients, which was significantly greater than that (46.77 %) in the control group (P<0.01). This finding indicated that patients with digestive cancers were more susceptible to infection by *H pylori* than healthy subjects, which might be related to a lower immunity in these patients. Furthermore, there was a significant difference in the positive rate among patients with cancers of esophageal, stomach, duodenum, rectum, colon and liver. This observation indicated that the prevalence of *H pylori* infection in patients with different digestive cancers was different, which was significantly higher in gastric and duodenal carcinomas than in other digestive cancers. All of these results were concordant with those previously reported[29-34].

In this study, the infection rate was 86.60 % (84/97) in patients with gastric cancer, with a rate of 96.43 % in antral cancer and 93.75 % in intestinal type cancer. We postulate that *H pylori* infection plays an important role in carcinomatous changes in gastric antrum, and is an important pathogenic factor causing intestinal type gastric cancer. This notion is consistent with previous literatures[35-39]. The histological process of intestinal type gastric cancer has been described as normal gastric mucosa→superficial chronic gastritis→atrophic gastritis→intestinal metaplasia→atypical hyperplasia→gastric cancer[40]. After long-term infection of *H pylori* in gastric mucosa, secretion of gastric acid could be reduced, flora in intestinal tract might survive and breed in stomach, and some bacteria recovering nitrate salts might form N-nitroso compounds that are important carcinogens. Moreover, *H pylori* leads to a decrease of vitamin C, which is a strong antioxidant and protective factor in gastric juice, preventing against the occurrence of gastric cancer. As a result, the levels of reactive oxygen and free radicals would increase, and direct DNA damage would incur. Thus, the chances of gene mutation would increase, and further accelerate the development of gastric cancer[41,42].

At present, the definite etiological factors of duodenal carcinoma are not clear, although many studies have suggested that some cholic acids like deoxycholic acid and its degradation products be related to the occurrence and development of duodenal carcinoma. Additionally, ulcerous and genetic factors have been considered to be associated with duodenal carcinoma. Stromberg *et al* found that the levels of several cytokines, such as interleukin-8 (IL-8), transforming growth factor beta (TGF-beta) and gamma interferon (IFN-gamma), were significantly lower in duodenal ulcer (DU) patients than in asymptomatic carriers (AS) and uninfected individuals. Then it was suggested that a number of cytokines might be important for the mucosal host defense against *H pylori* and a down-regulated immune response would play a role in the development of duodenal ulcers[43]. Colonizing in gastric antrum, *H pylori* can destroy the inhibitory feedback adjustment of gastrin release, which results in increased acid load in

duodenum, raises the risk of impairment of duodenal mucous membrane and thus convering of duodenal mucosa to gastric metaplasia. The metaplastic epithelium could provide a site where *H pylori* colonize, and cause duodenitis that was pre-ulcer status of DU and formed ulcer in the end[44]. In addition, some studies have suggested that the development of DU is related to *H pylori* density in patients. There was a tendency of higher *H pylori* density when the degree of deformity of the duodenal bulb increased[45]. The results of our study showed that 83.17 % of the patients with duodenal carcinoma were infected by *H pylori*, with the rate being 91.04 % in ulcerous type and 94.20 % in the bulb carcinoma. Therefore, we conclude that *H pylori* infection is associated with the development of duodenal carcinoma, especially with ulcerous type and in duodenal bulb.

ACKNOWLEDGEMENTS

We thank Department of Pathology, Benbu Medical College, Department of Oncology, Huainan First Miner' s Hospital and Department of Oncology, Huainan Second Miner' s Hospital, as well as Department of Oncology, Huainan Third Miner' s Hospital for sample collection.

REFERENCES

1 **Oyedeji KS,** Smith SI, Arigbabu AO, Coker AO, Ndububa DA, Agbakwuru EA, Atoyebi OA. Use of direct Gram strain of stomach biopsy as a rapid screening method for detection of *Helicobacter pylori* from peptic ulcer and gastritis patients. *J Basic Microbiol* 2002; **42**: 121-125

2 **Nguyen TN**, Barkun AN, Fallone CA. Host determinants of *Helicobacter pylori* infection and its clinical outcome. *Helicobacter* 1999; **4**: 185-197

3 **Brigic E**, Hodzic L, Zildzic M. *Helicobacter pylori* and gastroduodenal disease in our patients: 2-year experience. *Med Arh* 2000; **54**: 313-316

4 **Zawilak A**, Zakrzewska-Czerwinska J. Organization of the *Helicobacter pylori* genome. *Postepy Hig Med Dosw* 2001; **55**: 355-367

5 **Vandeplas Y.** *Helicobacter pylori* infection. *World J Gastroenterol* 2000; **6**: 20-31

6 **McNamara D**, O' Morain C. *Helicobacter pylori* and gastric cancer. *Ital J Gastroenterol Hepatol* 1998; **30**: 294-298

7 **Pineros DM,** Riveros SC, Marin JD**,** Ricardo O, Diaz OO. *Helicobacter pylori* in gastric cancer and peptic ulcer disease in a Colombian population. Strain heterogeneity and antibody profiles. *Helicobacter* 2001; **6:** 199-206

8 **Tanida N,** Sakagami T, Nakamura Y, Kawaua A, Hikasa Y, Shimoyama T. *Helicobacter pylori* and gastric cancer. *Nippon Geka Gakkai Zasshi* 1996; **97**: 257-262

9 **Hirai M,** Azuma T, Ito S, Kato T, Kohli Y, Fujiki N. High prevalence of neutralizing activity to *Helicobacter pylori* cytotoxin in serum of gastric-carcinoma patients. *Int J Cancer* 1994; **56**: 56-60

10 **Queiroz DM,** Mendes EN, Rocha GA, Oliveira AM, Oliveira CA, Cabral MM, Nogueira AM, Souza AF. Serological and direct diagnosis of *Helicobacter pylori* in gastric carcinoma: a case-control study. *J Med Microbiol* 1999; **48**: 501-506

11 **Nakajima N,** Kuwayama H, Ito Y, Iwasaki A, Arakawa Y. *Helicobacter pylori*, neutrophils, interleukins, and gastric epithelial proliferation. *J Clin Gastroenterol* 1997; **25**: 198-202

12 **Satoh K,** Sugano K. Causal relationship between *Helicobacter pylori* infection and upper gastroduodenal diseases. *Nippon Rinsho* 2001; **59**: 239-245

13 **Muller S,** Seifert E, Stolte M. Simultaneous MALT-type lymphoma and early adenocarcinoma of the stomach associated with *Helicobacter pylori* gastritis. *Z Gastroenterol* 1999; **37**: 153-157

14 **Ramirez Ramos AA.** *Helicobacter pylori*. *Rev Gastroenterol Peru* 2001; **21**: 99-101

15 **Yoshimura N**, Suzuki Y, Saito Y. Suppression of *Helicobacter pylori*-induced interleukin-8 production in gastric cancer cell lines by an anti-ulcer drug, geranylgeranylacetone. *J Gastroenterol Hepatol* 2002; **17**: 1153-1160

16 **Stassi G,** Arena A, Speranza A, Iannello D, Mastroeni P. Different modulation by live or killed *Helicobacter pylori* on cytokine production from peripheral blood mononuclear cells. *New Microbiol* 2002; **25**: 247-252

17 **Ji KY,** Hu FL. Progress on *Helicobacter pylori* and cytokine. *Shijie Huaren Xiaohua Zazhi* 2002; **10**: 503-508

18 **Walker MM.** Cyclooxygenase-2 expression in early gastric cancer, intestinal metaplasia and *Helicobacter pylori* infection. *Eur J Gastroenterol Hepatol* 2002; **14**: 347-349

19 **Konturek PC,** Konturek SJ, Bielanski W, Karczewska E, Pierzchalski P, Duda A, Starzynska T, Marlicz K, Popiela T, Hartwich A, Hahn EG. Role of gastrin in gastric cancerogenesis in *Helicobacter pylori* infected humans. *J Physiol Pharmacol* 1999; **50**: 857-873

20 **Han FC**, Yan XJ, Su CZ. Expression of the CagA gene of *H pylori* and application of its product. *World J Gastroenterol* 2000; **6**: 122-124

21 **Recavarren Ascencios R**, Recavarren Arce S. Chronic atrophic gastritis: pathogenic mechanisms due to cellular hypersensitivity. *Rev Gastroenterol Peru* 2002; **22**: 199-205

22 **Al- Muhtaseb MH,** Abu-Khalaf AM, Aughsteen AA. Ultrastructural study of the gastric mucosa and *Helicobacer pylori* in duodenal ulcer patients. *Saudi Med J* 2000; **21**: 569-573

23 **Zhang ZW**, Farthing MJ. Molecular mechanisms of *H pylori* associated gastric carcinogenesis. *World J Gastroenterol* 1999; **5**: 369-374

24 **Naito Y,** Yoshikawa T. Molecular and celluar mechanisms involved in *Helicobacter pylori*-induced inflammation and oxidative stress (1,2). *Free Radic Biol Med* 2002; **33**: 323-326

25 **Allen LA.** Intracellular niches for extracellular bacteria: lessons from *Helicobacter pylori*. *J Leukoc Biol* 1999; **66**: 753-756

26 **Xue FB,** Xu YY, Wan Y, Pan BR, Ren J, Fan DM. Association of *H pylori* infection with gastric carcinoma: a Meta analysis. *World J Gastroenterol* 2001; **7**: 801-804

27 **Palatka K,** Altorjay I, Szakall S, Gyorffy A, Udvardy M. Detection of *Helicobacter pylori* in tissue samples of stomach cancer. *Orv Hetil* 1999; **140**: 1985-1989

28 **Miehlke S,** Kirsch C, Dragosics B, Gschwantler M, Oberhuber G, Antos D, Dite P, Lauter J, Labenz J, Leodolter A, Malfertheiner P, Neubauer A, Ehninger G, Stolte M, Bayerdorffer E. *Helicobacter pylori* and gastric cancer: current status of the Austrain Czech German gastric cancer prevention trial (PRISMA Study). *World J Gastroenterol* 2001; **7**: 243-247

29 **Lan J,** Xiong YY, Lin YX, Wang BC, Gong LL, Xu HS, Guo GS. *Helicobacter pylori* infection generated gastric cancer through p53-Rb tumor-suppressor system mutation and telomerase reactivation. *World J Gastroenterol* 2003; **9**: 54-58

30 **Wu AH,** Crabtree JE, Bernstein L, Hawtin P, Cockburn M, Tseng CC, Forman D. Role of *Helicobacter pylori* CagA+ strains and risk of adenocarcinoma of the stomach and esophagus. *Int J Cancer* 2003; **103**: 815-821

31 **Kuniyasu H,** Yasui W, Yokozaki H, Tahara E. *Helicobacter pylori* infection and carcinogenesis of the stomach. *Langebecks Arch Surg* 2000; **385**: 69-74

32 **Meining A,** Bayerdorffer E, Muller P, Miehlke S, Lehn N, Holzel D, Hatz R, Stolte M. Gastric carcinoma risk index in patients infected with *Helicobacter pylori*. *Virchows Arch* 1998; **432**: 311-314

33 **Kuipers EJ**, Gracia-Casanova M, Pena AS, Pals G, Van Kamp G, Kok A, Kurz-pohlmann E, Pels NF, Meuwissen SG. *Helicobacter pylori* serology in patients with gastric carcinoma. *Scand J Gastroenterol* 1993; **28**: 433-437

34 **Rudelli A**, Vialette G, Brazier F, Seurat PL, Capron D, Dupas JL. *Helicobacter pylori* and gastroduodenal lesions in 547 symptomatic young adults. *Gastroenterol Clin Biol* 1996; **20**: 367-373

35 **Farinati F**, Valiante F, Germana B, Della Libera G, Baffa R, Rugge M, Plebani M, Vianello F, Di Mario F, Naccarato R. Prevalence of *Helicobacter pylori* infection in patients with precancerous changes and gastric cancer. *Eur J Cancer Prev* 1993; **2**: 321-326

36 **Meining AG**, Bayerdorffer E, Stolte M. *Helicobacter pylori* gastritis of the gastric cancer phenotype in relative of gastric carcinoma patients. *Eur J Gastroenterol Hepatol* 1999; **11**: 712-720

37 **El-Zimaity HM,** Ota H, Graham DY, Akamatsu T, Katsuyama T.

Patterns of gastric atrophy in intestinal type gastric carcinoma. *Cancer* 2002; **94**: 1428-1436

38 **Vasilenko IV**, Surgai NN, Sidorova ID. Modifications of gastric mucosa in diffuse and intestinal cancer. *Arkh Patol* 2001; **63**: 26-30

39 **Xia HH,** Kalantar JS, Talley NJ, Wyatt JM, Adams S, Chueng K, Mitchell HM. Antral-type mucosa in the gastric incisura, body, and fundus (antralization): a link between *Helicobacter pylori* infection and intestinal metaplasia. *Am J Gastroenterol* 2000; **95**: 114-121

40 **Meining A,** Morgner A, Miehlke S, Bayerdorffer E, Stolte M. Atrophy-metaplasia-dysplasia-carcinoma sequence in the stomach: a reality or merely an hypothesis? *Best Pract Res Clin Gastroeterol* 2001; **15**: 983-998

41 **Xia HH**, Talley NJ. Apoptosis in gastric epithelium induced by *Helicobacter pylori* infection: implications in gastric carcinogenesis. *Am J Gastroenterol* 2001; **96**: 16-26

42 **Pignatelli B,** Bancel B, Esteve J, Malaveille C, Calmels S, Correa P, Patricot LM, Laval M, Lyandrat N, Ohshima H. Inducible nitric oxide synthase, anti-oxidant enzymes and *Helicobacter pylori* infection in gastritis and gastric precancerous lesion in humans. *Eur J Cancer Prev* 1998; **7**: 439-447

43 **Kuipers EJ**, Thijs JC, Feston HP. The prevalence of *Helicobacter pylori* in peptic ulcer disease. *Aliment Pharmacol Ther* 1995; **9**: 59-69

44 **Olbe L,** Hamlet A, Dalenback J, Fandriks L. A mechanism by which *Helicobacter pylori* infection of the antrum contributes to the development of duodenal ulcer. *Gastroenterology* 1996; **110**: 1386-1394

45 **Lai YC,** Wang TH, Liao CC, Huang SH, Wu CH, Yang SS, Lee CL, Chen TK. Correlation between the degree of duodenal bulbar deformity and the density of *Helicobacter pylori* infection in patients with active duodenal ulcers. *J Formos Med Assoc* 2002; **101**: 263-267

Edited by Xia HHX and Wang XL

P.O.Box 2345, Beijing 100023,China
Fax: +86-10-85381893
E-mail: wjg@wjgnet.com www.wjgnet.com

World J Gastroenterol 2003;9(11):2505-2508
World Journal of Gastroenterology
 ISSN 1007-9327

• BASIC RESEARCH •

Effect of tetramethylpyrazine on exocrine pancreatic and bile secretion

Wen-Chao Zhao, Jin-Xia Zhu, Ning Tang, Yu-Lin Gou, Dewi Kenneth Rowlands, Yiu-Wa Chung, Ying Xing, Hsiao-Chang Chan

Yu-Lin Gou, Dewi Kenneth Rowlands, Yiu-Wa Chung, Hsiao-Chang Chan, Epithelial Cell Biology Research Center, Department of Physiology, Faculty of Medicine, The Chinese University of Hong Kong, Shatin, Hong Kong
Wen-Chao Zhao, Jin-Xia Zhu, Ning Tang, Ying Xing, Department of Physiology, Medical School, Zhengzhou University, Zhengzhou 450052, Henan, Province China
Supported by Innovation and Technology Funds of Hong Kong and strategic Program of the Chinese University of Hong Kong
Correspondence to: Professor Hsiao-Chang Chan, Epithelial Cell Biology Research Center, The Department of Physiology, Faculty of Medicine, The Chinese University of Hong Kong, Shatin, NT, Hong Kong, SAR, China. hsiaochan@cuhk.edu.hk
Telephone: +852-2609-6839 **Fax**: +852-2603-5022
Received: 2003-05-11 **Accepted:** 2003-08-19

Abstract

AIM: To investigate the effect of tetramethylpyrazine (ligustrazine, TMP) on the secretion of exocrine pancreas (and biliary).

METHODS: In *in vivo* study, we investigated the effect of TMP on the secretion of pancreatic-bile juice (PBJ) in rats. Using human pancreatic duct cell line, CAPAN-1, combined with the short-circuit current (I_{SC}) technique we further studied the effect of TMP on the pancreatic anion secretion.

RESULTS: Administration of TMP (80 mg/kg, ip) significantly increased the secretion of PBJ ($P<0.05$), but the pH of PBJ and the secretion of pancreatic protein were not significantly affected. Basolateral addition of TMP produced a dose-dependent increase in I_{SC} (EC_{50}=1.56 mmol/L), which contained a fast transient I_{SC} response followed by a slow decay. Apical application of Cl^- channel blockers, DPC (1 mmol/L), decreased the response by about 67.1 % ($P<0.001$), whereas amiloride (100 μmol/L), a epithelial sodium channel blockers, had no effect. Removal of extracellular HCO_3^- abolished TMP-induced increase in I_{SC} by about 74.4 % ($P<0.001$), but the removal of external Cl^- did not. Pretreatment with phosphodiesterase inhibitor, IBMX(0.5 mmol/L), decreased the TMP-induced I_{SC} by 91 % ($P<0.001$).

CONCLUSION: TMP could stimulate the secretion of PBJ, especially pancreatic ductal HCO_3^- secretion via cAMP or cGMP-dependent pathway. It need further study to investigate the roles of cAMP or cGMP in the effect of TMP on the secretion of exocrine pancreas.

Zhao WC, Zhu JX, Tang N, Gou YL, Rowlands DK, Chung YW, Xing Y, Chan HC. Effect of tetramethylpyrazine on exocrine pancreatic and bile secretion. *World J Gastroenterol* 2003; 9 (11): 2505-2508
http://www.wjgnet.com/1007-9327/9/2505.asp

INTRODUCTION

Tetramethylpyrazine (TMP, $C_8H_{12}N_2$, molecular mass 136.20 u, also known as ligustrazine) is an active alkaloid contained in the rhizome of *Chuanxiong*[1]. TMP has been widely used for the treatment of patients with cardiovascular and cerebrovascular diseases[1-5]. Its proposed pharmacological actions include antagonizing calcium mobilization[6], inhibiting platelet aggregation[7] and increasing intracellular cAMP level by inhibiting phosphodiesterase activity[8]. Recently it has been reported that TMP has antioxidant effect, reducing free radical generation[9,10] and decreasing nitric oxide production[11,12]. However, the effect of TMP on the pancreatic exocrine secretion are unknown. Since TMP is known to activate cAMP, it may act similarly to secretin, a physiological regulator of pancreatic secretion by elevating intracellular cAMP to act on pancreatic epithelial CFTR, which is a cAMP/cGMP-regulated Cl^- channel[13,14] and involved in pancreatic HCO_3^- secretion. In the present study, we investigated the effect of TMP on the secretion of pancreatic-bile juice (PBJ), which includes both pancreatic protein and HCO_3^-. We also undertook the present study using the short-circuit current (I_{SC}) technique to investigate TMP effect on HCO_3^- secretion by human pancreatic duct cell line, CAPAN-1, which retains most of the properties of pancreatic duct cells[15,16].

MATERIALS AND METHODS

Materials

Hydrochloride tetramethylpyrazine was purchased from the First Chengdu pharmaceutical Factory (Chengdu, China). RPMI 1640 medium and fetal bovine serum, trypsin-EDTA were supplied by Gibco Laboratories (New York). Hanks' balanced salt solution (HBSS), diphenylamine-2, 2'-dicarboxylic acid (DPC), glucose, calcium gluconate, N-2-hydroxethypiperazine-N'-2-ethanessulfonic acid (HEPES), sodium bicarbonate, DMEG, penicillin-streptomycin (P/S) and Bradford reagent were supplied by Sigma Chemical (St.Louis, MO). Calcium chloride, magnesium sulfate, potassium chloride, sodium chloride, were obtained from Merck (Darmstadt, Germany). Potassium gluconate and sodium gluconate were from BDH Chemicals (Poole, England). Tris was from Amersham Biosciences (Stockholm, Sweden).

Methods

Animal preparation Animal experimentation was conducted according to institutional guidelines. Adult male Sprague-Dawley rats, weighing 220-280 g, were housed under controlled temperature (23 ℃) and fasted for 12 h with free access to water before surgery. Midline abdominal incisions were made under xylazine and ketamine anesthesia (13 and 87 mg /kg body weight, respectively, im), followed by insertion of a polyethylene tube into the proximal duodenum for diversion of PBJ to the duodenum. A pancreatic duct cannula was made by inserting a polyethylene tube at the junction between the pancreatic duct and the duodenal wall for collection of PBJ[17-19].

Collection and measurement of exocrine pancreatic-bile secretions The animals were divided into two groups randomly: TMP group (TMP 80 mg/kg, ip. pH 2.3) and control

group (9 g/L NaCl solution, ip. pH 2.3). After a 30-minute stabilization period, pancreatic-bile secretions were collected every 15 minutes for 90 minutes. The volume was measured by a 1mL syringe and the pH value of PBJ was determined by a pH analyzer. 10 μL of PBJ was taken and diluted for pancreatic protein determination using spectra MAX 250 and Brandford reagent. The remaining undiluted PBJ was pumped into the duodenum via the duodenal cannula during the next collection period. Administrations were given after 2-time collections (30 minutes) and the second 15-minute-secretion was the basal PBJ secretion.

Cell culture Experiments were performed on the human pancreatic duct cell line, CAPAN-1 at a passage of 50-58. Cells were grown in RPMI 1640 medium with 200 mL/L fetal bovine serum and 10 g/L penicillin-streptomycin (P/S) as described previously[20,21]. Briefly, a volume of 0.2 mL of the cell suspension (1.5×10^9/L) was plated onto each permeable support, which was made of a millipore filter and a silicon ring with a confined area of 0.45 cm^2, floating on culture medium and incubated at 37 ℃ with 50 mL/L CO_2 and 950 mL/L O_2 for 7-8 days. The cells were used for I_{SC} once the monolayers reached confluence.

Short-circuit current measurement The basic principles of the short-circuit current experiments performed in the present study were the same as previously described[20,21]. Monolayers grown on permeable supports were clamped vertically between two halves of the Ussing chamber and bathed in Krebs-Henseleit (K-H) solutions with following compositions (mmol/L): NaCl, 117; KCl, 4.7; $MgSO_4$, 1.2; KH_2PO_4, 1.2; $NaHCO_3$, 24.8; $CaCl_2$, 2.56; Glucose, 11.1; with an osmalarity of 285 gassed with 950 mL/L O_2 and 50 mL/L CO_2. In some experiments, gluconate was used to replace Cl^-. For HCO_3^--free solution, HEPES and Tris were used and the solution was gassed in air. All the electrodes were connected to the voltage-current clamp amplifier. The signal output from the amplifier was the I_{SC} measured and recorded online by chart recorders. A 0.1 mV voltage pulse was applied intermittently across the epithelium and the transepithelial resistance was calculated from the corresponding current changes.

Statistical analysis

The data were collected and analyzed by SPSS statistical package 10.0. The results were expressed as $\bar{x}\pm S_{\bar{x}}$. Comparisons between groups of data were carried out using Student' s paired or unpaired *t*-test. Comparisons in one group of data were carried out using One-way ANOVA. A *P*-value less than 0.05 was considered to be statistically significant. EC_{50} values were determined by non-linear regression by GraphPad Prism software.

RESULTS

Effect of TMP on secretion of PBJ

Table 1 shows the volume of pancreatic-bile juice (PBJ) collected at different time points before and after intraperitoneal administration of TMP or 9 mL/L NaCl (control). Compared with the basal secretion, the PBJ secretion in TMP treated rats was increased by 7.0 % ($P<0.05$), 22.3 % ($P<0.001$), 14.3 % ($P<0.01$), 18.2 % ($P<0.01$) and 14.2 % ($P<0.01$) at 15, 30, 45, 60 and 75minutes, respectively ($n=13$) (Figure 1). However, the same treatment with of 9 mL/L NaCl solution did not produce significant effect ($n=12$) (Figure1). Protein content in PBJ and pH of PBJ were shown to have no differences between TMP-treated and control groups (data not shown).

Effect of TMP on CAPAN-1 cell line

The CAPAN-1 monolayer clamped in Ussing chambers bathing with normal K-HS (Cl^-/HCO_3^--containing) exhibited a potential difference of 0.52±0.04 mV, basal I_{SC} of 5.70±0.53 μA/cm^2 and transmembrane resistance of 93.6±4.5 Ωcm^2 ($n=77$). In Cl^--free ($n=9$) and HCO_3^--free ($n=9$) K-H solution, the transepithelial potential difference was 0.62±0.15 mV and 0.86±0.28 mV and the basal I_{SC} was 1.90±0.50 μA/cm^2 and 3.98±1.32 μA/cm^2, respectively, and the resistance of the monolayers were 208.6±33.6 Ωcm^2 and 161.8±25.6 Ωcm^2.

Table 1 Volume of secretion of pancreatic bile juice ($\bar{x}\pm S_{\bar{x}}$, μL)

	Groups	TMP $n=13$	Control $n=12$
After administration	Basal	372.3±22.2	342.5±15.8
	15 min	398.5±23.3	326.7±1.74
	30 min	455.4±18. 8	344.2±14.5
	45 min	425.4±19.8	331.7±17.5
	60 min	440.0±25.8	357.5±18.8
	75 min	425.0±25.2	342.5±18.2

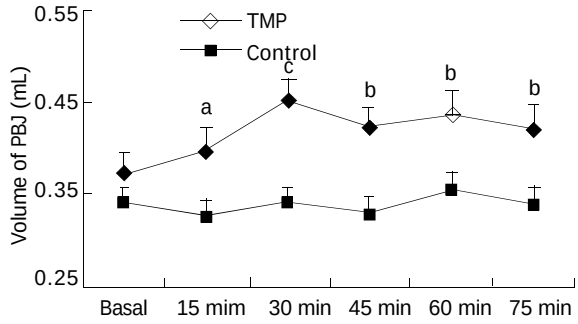

Figure 1 Effect of TMP on Volume of pancreatic-bile juice secretion. The volume of pancreatic-bile juice secretion collected before (basal) and 15, 30, 45, 60 and 75 minutes after intraperitoneal administration of TMP (80 mg/kg) and 9 mL/L NaCl in rats. The results were expressed as $\bar{x}\pm S_{\bar{x}}$. $^aP<0.05$, $^bP<0.01$, $^cP<0.001$, as compared to basal values.

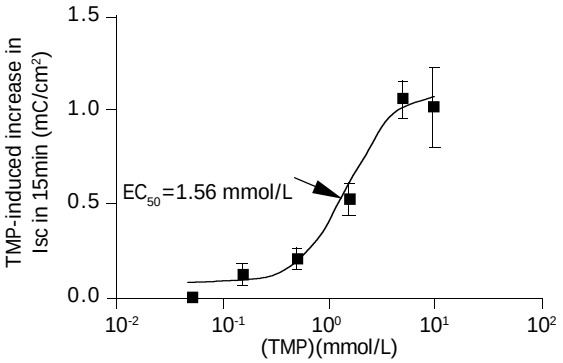

Figure 2 Concentration-response curve for TMP-induced I_{SC} in CAPAN-1 cells. Different concentrations of TMP were added to basalateral side. Each data point was obtained from at least 4 individual experiments. Arrow shows EC_{50}.

Basolateral addition of TMP (0.05, 0.15, 0.5, 1.5, 5 and 10 mmol/L) produced a dose-dependent increase in I_{SC}. EC_{50} was about 1.56 mmol/L (Figure 2). TMP (5 mmol/L)-induced I_{SC} increase was biphasic: a fast transient peak followed by a slow decay. The total transported charges for 15 minutes (the area under the curve of the TMP-induced I_{SC} response) were about 1.06±0.99 mC/cm^2 ($n=27$, Figure 3.A and C). TMP-induced current increase was inhibited by 67.1 % after apical pretreatment of 1 mmol/L DPC, a non-specific Cl^- channel blockers ($n=8$, $P<0.001$) (Figure 3.B and C). However apical application of epithelial sodium channel blockers, amiloride

(100 μmol/L) did not affect the TMP-produced response (n=3, Figure 3.C). After the removal of external HCO_3^-, TMP-induced I_{SC} was blocked by 74.4 % (n=9, P<0.001) (Figure 3. D), but the removal of external Cl^- did not reduce but increase the TMP-induced I_{SC} (n=8, P<0.05) (Figure 3.D). Pretreatment of phosphodiesterase inhibitor, IBMX (0.5 mmol/L) for 15 minutes decreased the TMP-induced I_{SC} by 91 % (n=4, P<0.001) (Figure 4.A and B).

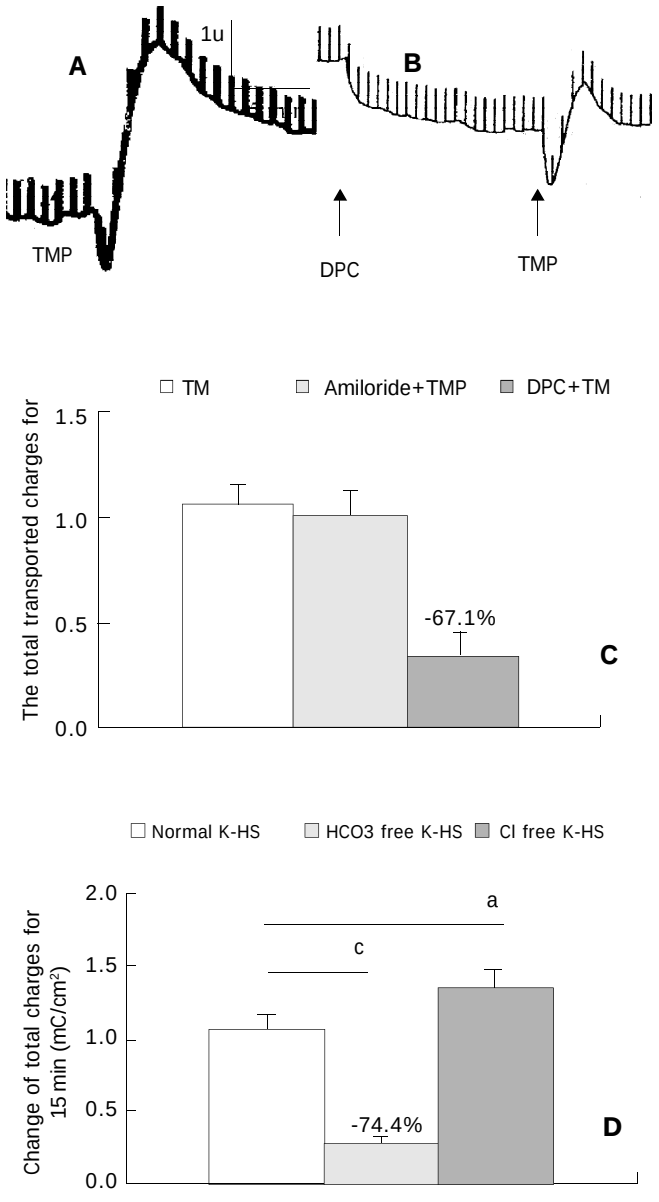

Figure 3 TMP-induced HCO_3^- secretion in CAPAN-1 cells. Comparison of TMP (5 mmoL/L)-induced I_{SC} (mC/cm²) obtained in control (A, C), pretreatment with DPC (1 mmoL/L) (B, C), Amiloride 100 umoL/L (C), HCO_3^--free solution (D), Cl^--free solution (D), Values are $\bar{x}\pm S_{\bar{x}}$, ^aP<0.05, ^cP<0.001.

DISCUSSION

While TMP has been widely used clinically for treating cardiovascular disorders and cerebrovascular diseases[1-5], little is known about its effect on pancreatic secretion. In the present study, intraperitoneal application of TMP increased secretion of pancreatic-bile juice (PBJ), but the protein content and pH value were not affected. It is known that PBJ consists of both bile and pancreatic juice, the volume of the basal secretion (or agonist induced) of pancreatic juice is normally very low, only about 9-18 μL in 15 minutes in rat[17,18], as compared to that of

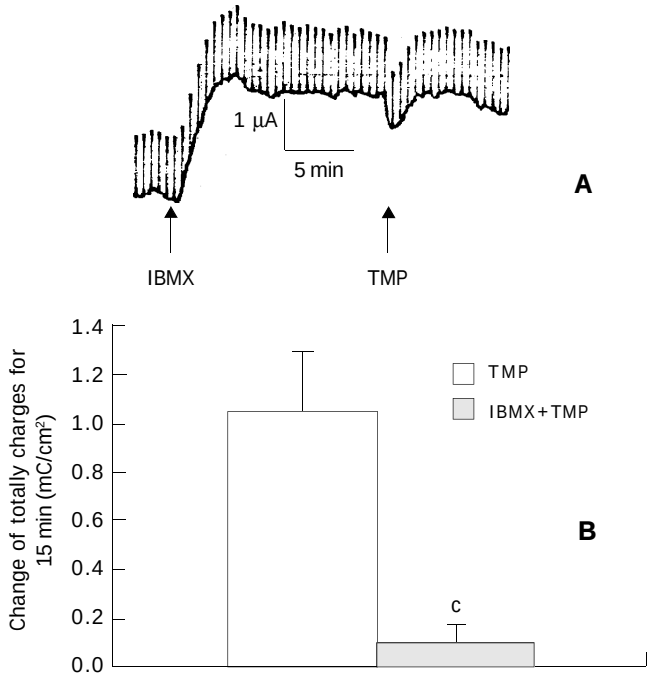

Figure 4 Pretreatment with IBMX decreased TMP–induced I_{SC} by 91 %. Values are $\bar{x}\pm s$, ^cP<0.001.

the liver. Although TMP increased the secretion of PBJ by 26-83 μL in 15 minutes, it was difficult to assess the contribution to exocrine pancreatic secretion from our experiments *in vivo*. Therefore, CAPAN-1 cell line was used to further demonstrate the effect of TMP on the pancreatic secretion. Our data suggested that TMP could directly stimulate HCO_3^- secretion in human pancreatic duct cells.

According to the HCO_3^- secretory model[22], the intracellular HCO_3^- was accumulated from the tissue fluid via the basolateral membrane[23-25] and mainly secreted by a Cl^-/HCO_3^- exchanger[26,27] and/or directly via cAMP/cGMP-dependent Cl^- channel (CFTR)[13,26,28]. Recently, it was reported that CFTR could also secrete HCO_3^- as Cl^-/HCO_3^- exchanger[29,30]. The TMP- increased I_{SC} in CAPAN-1 could be blocked by Cl^- channel blockers, as well as phosphodiesterase inhibitors, which were known to increase cAMP and cGMP, and abolished by removal of extracellular HCO_3^-, suggesting that TMP can stimulate pancreatic HCO_3^- secretion via CFTR since it has been shown to be activated by both cAMP and cGMP. The TMP-induced increase in the volume of PBJ observed in the rats could be due to an increase in pancreatic HCO_3^- secretion, as well as bile secretion, leading to enhanced water secretion. However, the inability of TMP to increase the pH of PBJ appeared to contradict to its observed effect on the increase in HCO_3^- secretion. This could be explained by two possible reasons. One is that the mechanism of HCO_3^- secretion in human pancreatic duct cells was different from that in rats since the HCO_3^- concentration of pancreatic juice in rats was only 70 mmol/L while in human was 145 mmol/L[22]. The other is that the HCO_3^- secreted by the pancreas might be diluted by bile juice and thus having less prominent effect on pH. It is interesting to note that TMP could stimulate HCO_3^- secretion that could be inhibited by extracellular Cl^- as evidenced by the increase in the TMP-induced I_{SC} observed in the absence of extracellular Cl^-. However, the mechanism for the observed inhibition of HCO_3^- secretion by extracellular Cl^- remains to be elucidated.

In conclusion, the present *in vivo* and *in vitro* results suggest that TMP can promote the secretion of PBJ in rats and HCO_3^- secretion in human pancreatic duct cells, which may be beneficial to improving digestive function.

REFERENCES

1 **Zheng HZ**, Dong ZH, Yu J. Chuanxiong in: Zhongyao XiandaiYanjiu Yu Yingyong. 1st Ed. *Beijing: Xueyuan Publisher* 1997: 629-682

2 **Liu LS,** Chen MQ, Zeng GY, Zhou BF. A forty-year study on hypertension. *Zhongguo Yixue Kexue Yuan Xuebao* 2002; **24**: 401-408

3 **Cai Y,** Ren M, Yang R. Observation on curative effect of acute ischemic cerebrovascular disease treated with different dosage of ligustrazine. *Zhongguo Zhongxiyi Jiehe Zazhi* 2000; **20**: 747-749

4 **Liao F**. Herbs of activating blood circulation to remove blood stasis. *Clin Hemorheol Microcirc* 2000; **23**: 127-131

5 **Huang RJ**, Liao CX, Chen DZ. Effect of tetramethylpyrazine on endothelin, von Willebrand factor and thromboxane A2 during cardiopulmonary bypass in patients of congenital heart disease with pulmonary hypertension. *Zhongguo Zhongxiyi Jiehe Zazhi* 2003; **23**: 268-271

6 **Zou LY**, Hao XM, Zhang GQ, Zhang M, Guo JH, Liu TF. Effect of tetramethyl pyrazine on L-type calcium channel in rat ventricular myocytes. *Can J Physiol Pharmacol* 2001; **79**: 621-626

7 **Sheu JR**, Kan YC, Hung WC, Lin CH, Yen MH. The antiplatelet activity of tetramethylpyrazine is mediated through activation of NO synthase. *Life Sci* 2000; **67**: 937-947

8 **Lin CI**, Wu SL, Tao PL, Chen HM, Wei J. The role of cyclic AMP and phosphodiesterase activity in the mechanism of action of tetramethylpyrazine on human and dog cardiac and dog coronary arterial tissues. *J Pharm Pharmacol* 1993; **45**: 963-966

9 **Pei L**, Wang J. Protective effect of tetramethylpyrazine on red blood cells during autotransfusion. *Zhonghua Yixue Zazhi* 2002; **82**: 322-324

10 **Shih YH**, Wu SL, Chiou WF, Ku HH, Ko TL, Fu YS. Protective effects of tetramethylpyrazine on kainate-induced excitotoxicity in hippocampal culture. *Neuroreport* 2002; **13**: 515-519

11 **Zhang Z**, Wei T, Hou J, Li G, Yu S, Xin W. Tetramethylpyrazine scavenges superoxide anion and decreases nitric oxide production in human polymorphonuclear leukocytes. *Life Sci* 2003; **72**: 2465-2472

12 **Wu CC**, Liao MH, Chen SJ, Yen MH. Tetramethylpyradizine prevents inducible NO synthase expression and improves survival in rodent models of endotoxic shock. *Naunyn Schmiedebergs Arch Pharmacol* 1999; **360**: 435-444

13 **Kulaksiz H**, Schmid A, Honscheid M, Eissele R, Klempnauer J, Cetin Y. Guanylin in the human pancreas: a novel luminocrine regulatory pathway of electrolyte secretion via cGMP and CFTR in the ductal system. *Histochem Cell Biol* 2001; **115**: 131-145

14 **Gray M**, O'Reilly C, Winpenny J, Argent B. Anion interactions with CFTR and consequences for HCO3- transport in secretory epithelia. *J Korean Med Sci* 2000; **15**(Suppl): S12-15

15 **Shumaker H**, Amlal H, Frizzell R, Ulrich CD 2nd, Soleimani M. CFTR drives Na+-nHCO-3 cotransport in pancreatic duct cells: a basis for defective HCO-3 secretion in CF. *Am J Physiol* 1999; **276**(1Pt1): C16-25

16 **Lohi H**, Kujala M, Kerkela E, Saarialho-Kere U, Kestila M, Kere J. Mapping of five new putative anion transporter genes in human and characterization of SLC26A6, a candidate gene for pancreatic anion exchanger. *Genomics* 2000; **70**: 102-112

17 **Li JP**, Chang TM, Chey WY. Roles of 5-HT receptors in the release and action of secretin on pancreatic secretion in rats. *Am J Physiol Gastrointest Liver Physiol* 2001; **280**: G595-602

18 **Li JP**, Lee KY, Chang TM, Chey WY. MEK inhibits secretin release and pancreatic secretion: roles of secretin-releasing peptide and somatostatin. *Am J Physiol Gastrointest Liver Physiol* 2001; **280**: G890-896

19 **Li Y**, Wu XY, Zhu JX, Owyang C. Intestinal serotonin acts as paracrine substance to mediate pancreatic secretion stimulated by luminal factors. *Am J Physiol Gastrointest Liver Physiol* 2001; **281**: G916-923

20 **Zhu JX**, Lo PS, Zhao WC, Tang N, Zhou Q, Rowlands DK, Gou YL, Chung YW, Chan HC. Bak Foong Pills stimulate anion secretion across normal and cystic fibrosis pancreatic duct epithelia. *Cell Biol Int* 2002; **26**: 1011-1018

21 **Cheng HS,** Wong WS, Chan KT, Wang XF, Wang ZD, Chan HC. Modulation of Ca2+-dependent anion secretion by protein kinase C in normal and cystic fibrosis pancreatic duct cells. *Biochim Biophys Acta* 1999; **1418**: 31-38

22 **Sohma Y**, Gray MA, Imai Y, Argent BE. HCO3- transport in a mathematical model of the pancreatic ductal epithelium. *J Membr Biol* 2000; **176**: 77-100

23 **Satoh H**, Moriyama N, Hara C, Yamada H, Horita S, Kunimi M, Tsukamoto K, Iso-O N, Inatomi J, Kawakami H, Kudo A, Endou H, Igarashi T, Goto A, Fujita T, Seki G. Localization of Na+-HCO-3 cotransporter (NBC-1) variants in rat and human pancreas. *Am J Physiol Cell Physiol* 2003; **284**: C729-737

24 **Marino CR**, Jeanes V, Boron WF, Schmitt BM. Expression and distribution of the Na^+-HCO_3^- cotransporter in human pancreas. *Am J Physiol* 1999; **277**(2 Pt1): G487-494

25 **Ishiguro H**, Naruse S, San Roman JI, Case M, Steward MC. Pancreatic Ductal Bicarbonate Secretion: Past, Present and future. *JOP* 2001; **2**(4 Suppl): 192-197

26 **Sohma Y**, Gray MA, Imai Y, Argent BE. 150 mM HCO3(-)-how does the pancreas do it? Clues from computer modelling of the duct cell. *JOP* 2001; **2**(4 Suppl): 198-202

27 **Novak I**. Keeping up with bicarbonate. *J Physiol* 2000; **528** (Pt2): 235

28 **Ishiguro H**, Naruse S, Kitagawa M, Mabuchi T, Kondo T, Hayakawa T, Case RM, Steward MC. Chloride transport in microperfused interlobular ducts isolated from guinea-pig pancreas. *J Physiol* 2002; **539**(Pt1): 175-189

29 **Choi JY**, Muallem D, Kiselyov K, Lee MG, Thomas PJ, Muallem S. Aberrant CFTR-dependent HCO3- transport in mutations associated with cystic fibrosis. *Nature* 2001; **410**: 94-97

30 **Choi JY**, Lee MG, Ko S, Muallem S. Cl(-)-dependent HCO3- transport by cystic fibrosis transmembrane conductance regulator. *JOP* 2001; **2**(4 Suppl): 243-246

Edited by Wang XL

P.O.Box 2345, Beijing 100023,China
Fax: +86-10-85381893
E-mail: wjg@wjgnet.com www.wjgnet.com

World J Gastroenterol 2003;9(11):2509-2512
World Journal of Gastroenterology
 ISSN 1007-9327

• BASIC RESEARCH •

Interleukin-10 modified dendritic cells induce allo-hyporesponsiveness and prolong small intestine allograft survival

Min Zhu, Ming-Fa Wei, Fang Liu, Hui-Fen Shi, Guo Wang

Min Zhu, Ming-Fa Wei, Hui-Fen Shi, Guo Wang, Department of Pediatric Surgery, Tongji Hospital, Tongji Medical College, Huazhong University of Science and Technology, Wuhan 430030, Hubei Province, China
Fang Liu, Department of Burns, Wuhan Third People' s Hospital, Wuhan 430060, Hubei Province, China
Correspondence to: Min Zhu, Institute of Organ Transplantation, Tongji Hospital, Tongji Medical College, Huazhong University of Science and Technology, Wuhan 430030, Hubei Province, China. eming43@hotmail.com
Telephone: +86-27-83663152 **Fax:** +86-27-83662892
Received: 2003-04-04 **Accepted:** 2003-05-19

Abstract

AIM: To investigate whether IL-10-transduced dendritic cells (DCs) could induce tolerogenicity and prolong allograft survival in rat intestinal transplantation.

METHODS: Spleen-derived DCs were prepared and genetically modified by hIL-10 gene. The level of IL-10 expression was quantitated by ELISA. DC function was assessed by MTT in mixed leukocyte reaction. Allogeneic T-cell apoptosis was examined by flow cytometric analysis. Seven days before heterotopic intestinal transplantation, 2×10^6 donor-derived IL-10-DC were injected intravenously, then transplantation was performed between SD donor and Wistar recipient.

RESULTS: Compared with untransduced DC, IL-10-DC could suppress allogeneic mixed leukocyte reaction (MLR). The inhibitory effect was the most striking with the stimulator/effector (S/E) ratio of 1:10. The inhibition rate was 33.25 %, 41.19 % ($P<0.01$) and 22.92 % with the S/E ratio of 1:1, 1:10 and 1:50 respectively. At 48 hours and 72 hours by flow cytometry counting, apoptotic T cells responded to IL-10-DC in MLR were 13.8 % and 30.1 %, while untransduced group did not undergo significant apoptosis ($P<0.05$). IL-10-DC pretreated recipients had a moderate survival prolongation with a mean allograft survival of 19.8 days ($P<0.01$), compared with 7.3±2.4 days in control group and 8.3±2.9 days in untransduced DC group. Rejection occurred in the control group within three days. The difference between untreated DC group and control group was not significant.

CONCLUSION: IL-10-DC can induce allogenic T-cell hyporesponsiveness *in vitro* and apoptosis may be involved in it. IL-10-DC pretreatment can prolong intestinal allograft survival in the recipient.

Zhu M, Wei MF, Liu F, Shi HF, Wang G. Interleukin-10 modified dendritic cells induce allo-hyporesponsiveness and prolong small intestine allograft survival. *World J Gastroenterol* 2003; 9(11): 2509-2512
http://www.wjgnet.com/1007-9327/9/2509.asp

INTRODUCTION

Dendritic cells (DCs) play critical roles in the initiation and modulation of immune responses and may determine the balance between tolerance and immunity[1-3]. Evidence has demonstrated that immunosuppressive cytokines modified DCs favour the induction of alloantigen-specific T cells anergy and prolong allograft survival. To date, there have been only a few reports of genetic manipulation of DCs for therapeutic application in organ transplantation. Retroviral and adenoviral gene transfer methods, for example, have been used to express immunosuppressive molecules such as vIL-10, TGF-β by DC[4,5]. In the present study, we demonstrated the feasibility of liposome transduction of DC to express hIL-10. In addition, we tested the *in vivo* ability of IL-10-DC to prevent small bowel graft rejection in rat intestinal transplantation model.

MATERIALS AND METHODS

Animals

Healthy adult Sprague-Dawley (SD) and Wistar-Furth rats, weighing 200-250 g, were used as donors and recipients, respectively. They were obtained from the Experimental Animal Center of Tongji Medical College, Huazhong University of Science and Technology.

DC propagation and transfection

Splenocyte suspensions from SD rats were prepared in RPMI1640 complete medium (Gibco/BRL), supplemented with 10 % v/v heat-inactivated fetal calf serum (Hyclone) in the presence of granulocyte-macrophage colony-stimulating factor (GM-CSF, 10 ng/ml, R&D) and IL-4 (10 ng/ml, R&D). Cultures were fed every 3 days by complete medium exchange including cytokines. After 6-8 days of culturing, when the adherent cells presented with primitive dendrites observed under electronic microscope, DC was propagated successfully. pcDNA3/hIL-10 vector encoding human IL-10 cDNA sequence was transfected to DC by the liposome method using the Lipofectamin 2000 kit (Gibco/BRL) according to the manufacturer' s instructions and the vector without insert was also transduced as a control. After 10-14 days in selective medium, DCs were then selected for geneticin-resistant colonies.

ELISA

The supernatant from transfected DCs was assayed for IL-10 expression by ELISA kit(Genzyme). The clone that gave the maximum ELISA reading was chosen for use in *in vivo* and *in vitro* experiments.

Mixed leukocyte reaction (MLR)

The ability of transduced DC to stimulate naive allogeneic T cells, assayed by using MTT (Sigma) method, was determined by MLR. Various numbers (2×10^3-2×10^5/well) of DC and IL-10-DC, pretreated with mitomycin C (25 μg/ml, Amresco), were cocultured with allogenic T-cells from Wistar rats as responders (2×10^5/well) at a ratio of 1:1, 1:10 and 1:50 for 72 hours in 0.2 ml RPMI-1640 complete medium in a 96-well U-bottomed microtiter plate. The results monitored by a microtiter plate reader (Bio-Rad, Tokyo, Japan) at 570 nm, were expressed as inhibition rate and calculated according to

the following equation: inhibition rate=1-(mean OD_{570nm} value of experiment group/mean OD_{570nm} value of control group)×100.

Flow cytometric analysis

At the indicated time point, supernatant cells were washed twice in cold PBS and then resuspended in 1×binding buffer at a concentration of 1×10^6 cells/ml. One hundred μl of the solution (1×10^5cells) was transferred to a 5 ml culture tube, then 5 μl of FITC-Annexin V and 10 μl of propidium iodide (Gibco/BRL) were added. The cells were gently vortexed and incubated for 15 min at room temperature in the dark and subjected to FACS. Those cells with negative propidium iodide staining and positive annexin V staining were considered as the proportion of cells actively undergoing apoptosis.

Experimental group and intestinal transplantation

All rats were randomized into three groups and each group had six pairs of rats. These groups were treated with a single intravenous injection of IL-10-DCs (2×10^6), untransduced DCs (2×10^6) or empty plasmid through tail vein seven days before intestinal transplantation. Operation procedures were performed under ether anesthesia. The small intestine was transplanted according to the modified procedure described by Monchik *et al*[6]. In brief, after an overnight fast, a 10-cm segment of proximal jejunum or distal ileum, including the superior mysenteric artery and vein, was removed from the donor after ligation of small mysenteric vessel branches and intravascular irrigation with cold heparinized saline solution. The graft was kept in 4 ℃ cold Ringer's solution until transplantation. The recipient abdomen was opened and the graft was reperfused by end-to-side anastomosis of the superior mesenteric artery and vein to the recipient's abdominal aorta and inferior vena cava under operative microscope, respectively. Both ends of the graft were then exteriorized through the right abdominal wall as stomas, isolating the segment from the recipient's native gastrointestinal tract. Death due to technical failure that occurred within 72 hours of operation was excluded from the study.

Histological examination

The rats were sacrificed and used for histological examination when recipients showed clinical signs of rejection[7,8]. After fixed in 10 % buffered formalin, embedded in paraffin, samples were stained with hematoxylin and eosin and examined by light microscope. Three samples were obtained at the time of donor operation and used as normal group for histological study.

Statistical analysis

All data were expressed as mean ± standard deviation. Statistical analyses were performed using Student's *t* test. Probability values of less than 0.05 were considered significant.

RESULTS

IL-10-DCs induced allospecific T cell hyporesponsiveness

We examined the responses of naï ve allospecific T cells to IL-10-DCs. As shown in Figure 1, IL-10-DCs could suppress allogeneic MLR compared with that of untransduced DCs. The latter were potent stimulators of allogeneic T-cell proliferation. The inhibitory effect was most striking with the stimulator / effector (S/E) ratio of 1:10. The inhibition rates were 33.25 %, 41.19 % and 22.92 % with the S/E ratio of 1:1, 1:10 and 1:50 respectively (Figure 1).

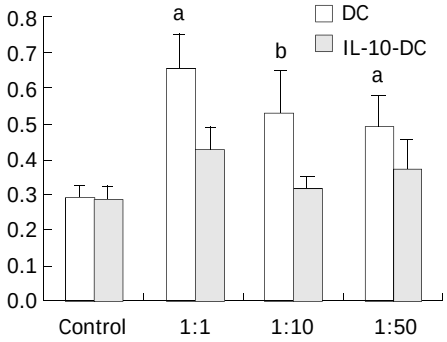

Figure 1 Inhibitory effect of IL-10-DC on allogenic T cell proliferation. [a]$P<0.05$, [b]$P<0.01$, *vs* DC group.

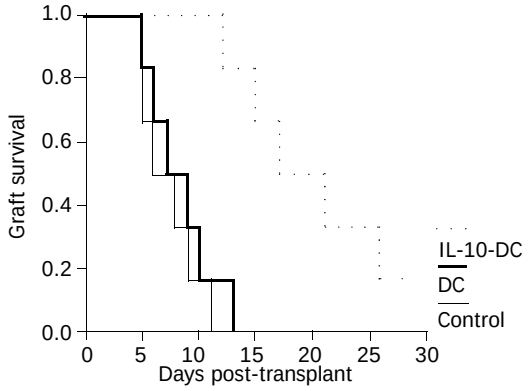

Figure 3 Survival (%) of recipient small intestines from control group (n=6), untransduced DC group (n=6) and IL-10-DC group (n=6).

Apoptosis assay by flow cytometric analysis

Supernatant T cells cocultured with IL-10-DCs in MLR underwent apoptosis. At 48 hours and 72 hours by flow cytometry counting apoptotic T cells were 13.8 % and 30.1 % with the S/E ratio of 1:10, but control group did not undergo significant apoptosis ($P<0.05$) (Figure 2).

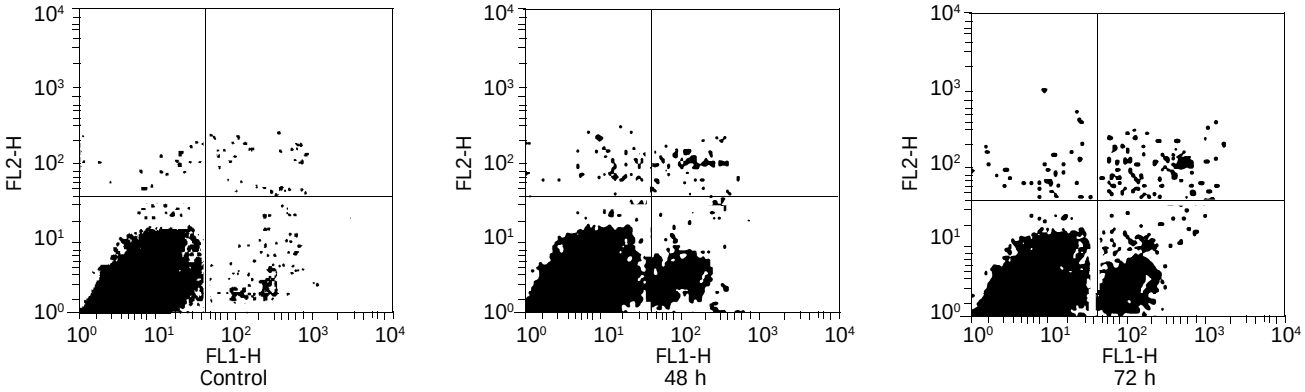

Figure 2 Flow cytometric analysis for apoptotic T cells induced by IL-10-DC.

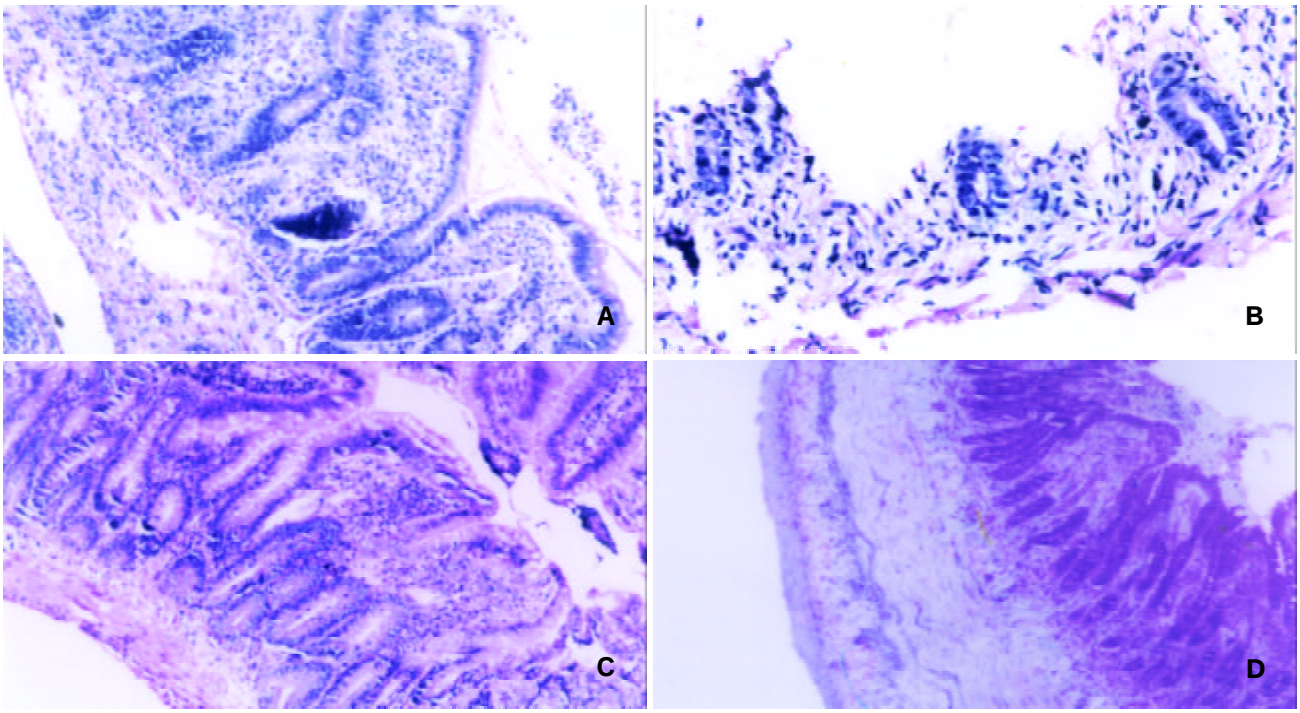

Figure 4 Histological comparison of allografts between control group rats and IL-10-DC pretreated rats. Control group showed acute rejection sign on POD 3 (A) and mucosal sloughing and necrosis and destruction of normal glandular architecture on POD 7(B). IL-10-DC group demonstrated mild lymphocyte infiltration and blunting of villi with edema on POD 7 (C) and fibroblastic proliferation extending from the submucosa to the lamina muscularis (D). (hematoxylin-erosin staining, ×200).

Allograft survival and histological evaluation

Untransduced DCs pretreatment did not affect allograft survival and the recipients pretreated with IL-10-DCs had a moderate allograft prolongation. Mean allograft survival in IL-10-DCs group was 19.8±6.3 days (P<0.01), compared with 7.3±2.4 days in control group and 8.3±2.9 days in untransduced DCs group (Figure 3). Although untreated recipient on postoperative day (POD) 3 showed acute rejection with blunted villi, the number of goblet cells was decreased and a large amount of inflammatory cell infiltration occurred in lamina propria mucosa, the grafts treated with IL-10-DCs demonstrated normal intestinal mucosa negative for rejection on POD 5 and mild lymphocyte infiltration and blunting of villi with edema on POD 7(Figure 4).

DISCUSSION

Despite improvements in the posttransplantation immunosuppressive therapeutic regimens, the management of allograft rejection has been still dependent on the use of nonspecific immunosuppressive agents[9], which could prevent the host from complications, such as infections and lymphoproliferative disorders[10,11]. In this regard, the successful induction of donor-specific immune tolerance remains a major challenge in organ transplantation. However, the lymphoid-rich small intestinal allograft might differ from such lymphoid-poor organs as the heart and kidney, making tolerance induction a particularly troublesome approach specific to this organ[12-14]. An approach to modify donor-derived DC in order to induce an immunological hyporesponsive state in the recipient has been attractive as a potential strategy in transplantation as it would theoretically let the possibility of donor-specific tolerance come true[15,16].

IL-10 has been regarded as an immunosuppressive cytokine because of its ability to down-regulate the synthesis of a broad spectrum of proinflammatory cytokines by DCs, monocytes or macrophages, and to inhibit allogeneic proliferative responses *in vitro*[17-19]. It is for these reasons that IL-10 has been considered as a potential means in the induction of tolerance. In the immature state, DC could express low levels of CD80, CD86 and co-stimulatory molecules that are essential for the amplification of immune response to foreign peptides[16,20-22]. IL-10 has been shown to block DC maturation *in vitro*[23,24]. Our approach was therefore to investigate strategies that might delay maturation of DC to prolong their immature phenotype. In our studies we found that these IL-10-DCs were less stimulatory in the MLR compared with untransduced DCs. One of the major mechanisms by which IL-10 inhibited DC antigen presenting function was to down-regulate MHC class II and costimulatory molecule expression on DC[25].

Our data confirmed that IL-10-DC could inhibit the proliferation of allogeneic T cells and induce these cell apoptosis, which may be related to the prolonged survival of graft. It has been accepted that the initiation of T-cell responses to grafted tissues requires two distinct signals[26-28]. The essential signal is the engagement of T cell receptors (TCR) to antigen peptide in the content of major histocompatibility complex molecules on antigen presenting cells. Other costimulatory receptor-ligand interactions between T cell and APC are needed. Signals through the TCR alone could lead to allospecific T-cell anergy or apoptosis[29]. Schartz[30] has demonstrated that lack of second signal would result in increased amounts of a negative regulatory factor, Nil-2a, in anergic human T cells. This factor has been shown to suppress IL-2 nuclear transcription factors of AP-1 and NF-κB. NF-κB could inhibit apoptosis by induction or up-regulation expression of anti-apoptotic gene such as Bcl-2. Therefore, the suppression of NF-κB activation could give rise to decreased IL-2 expression and T cell apoptosis[31,32].

Our studies were consistent with previous studies, perhaps not surprisingly, showing that IL-10-DC could exert tolerogenic effects on organ transplantation[25, 33]. In IL-10-DC group, median intestine allograft survival time was 19.8±6.3 days. Compared with control group (7.3±2.4 days) and untransduced DC group (8.3±2.9 days), the survival time was 2.5-fold longer. There are two possible explanations for the lack of long- term

survival in our study. One is that IL-10-DC might not survive long enough to induce a permanent state of tolerance. Long-term survival of IL-10-DC *in vivo* would be particularly important if apoptosis induction of allogeneic T cells was a major mechanism of allograft survival. The other, as far as long-term tolerance is concerned, is that the level of expression of IL-10 by IL-10-DC was still not high enough to affect the recipient immune modulation for all alloreactive T cells, though the level of IL-10 expression was higher than that in normal condition. For intestine, considering its high immunogenicity, it would be necessary to enhance gene transfer efficiency and transgene expression level[34].

In conclusion, these studies demonstrate the feasibility of immunosuppressive gene delivery system. We believe that this highly targeted method of inducing tolerogenicity of donor derived DC may reduce the need for recipient nonspecific immunosuppression and play an important role in clinical strategies of tolerance induction.

REFERENCES

1 **Steinman RM**. The dendritic cell system and its role in immunogenicity. *Annu Rev Immunol* 1991; **9**: 271-296
2 **Thomson AW**, Lu L. Dendritic cells as regulators of immune reactivity: implications for transplantation. *Transplantation* 1999; **68**: 1-8
3 **Brocker T**, Riedinger M, Karjalainen K. Targeted expression of major histocompatibility complex [MHC] class II molecules demonstrates that dendritic cells can induce negative but not positive selection of thymocytes *in vivo*. *J Exp Med* 1997; **185**: 541-550
4 **Takayama T**, Kaneko K, Morelli AE, Li W, Tahara H, Thomson AW. Retroviral delivery of transforming growth factor-beta1 to myeloid dendritic cells: inhibition of T-cell priming ability and influence on allograft survival. *Transplantation* 2002; **74**: 112-119
5 **Takayama T**, Nishioka Y, Lu L, Lotze MT, Tahara H, Thomson AW. Retroviral delivery of viral interleukin-10 into myeloid dendritic cells markedly inhibits their allostimulatory activity and promotes the induction of T-cell hyporesponsiveness. *Transplantation* 1998; **66**: 1567-1574
6 **Monchik GJ**, Russell PS. Transplantation of small bowel in the rat: technical and immunological considerations. *Surgery* 1971; **70**: 693-702
7 **Grover R**, Lear PA, Ingham Clark CL, Pockley AG, Wood RF. Method for diagnosing rejection in small bowel transplantation. *Br J Surg* 1993; **80**: 1024-1026
8 **Tzakis AG**, Thompson JF. Current status of diagnosis of small bowel rejection. *Pediatr Transplant* 1998; **2**: 87-88
9 **Sher LS**. Immunosuppression. *Curr Opin Organ Transplant* 2001; **6**: 311
10 **Ghanekar A**, Grant D. Small bowel transplantation. *Curr Opin Crit Care* 2001; **7**: 133-137
11 **De Bruin RW**, Heineman E, Marquet RL. Small bowel transplantation: an overview. *Transpl Int* 1994; **7**: 47-61
12 **Tam PKH**, Guo WH. Intestinal transplantation: Current Status. *Asian J Surg* 1999; **22**: 146-151
13 **Abu-Elmagd K**, Bond G. The current status and future outlook of intestinal transplantation. *Minerva Chir* 2002; **57**: 543-560
14 **Adams DH**. Immunologic aspects of small bowel transplantation. *Transplant Proc* 1998; **30**: 2557-2559
15 **Luke PP**, Thomson AW. Blockade of costimulatory molecules on dendritic cells: implications for tolerance induction. *Transplant Proc* 2001; **33**: 507-508
16 **Banchereau J**, Steinman RM. Dendritic cells and the control of immunity. *Nature* 1998; **392**: 245-252
17 **Akdis CA**, Blaser K. Mechanisms of interleukin-10-mediated immune suppression. *Immunology* 2001; **103**: 131-136
18 **De Fazio SR**, Gozzo JJ. Role of graft interleukin-10 expression in the tolerogenicity of neonatal skin allografts. *Transplantation* 2000; **70**: 1371-1377
19 **Moore KW**, de Waal Malefyt R, Coffman RL, O'Garra A. Interleukin-10 and the interleukin-10 receptor. *Annu Rev Immunol* 2001; **19**: 683-765
20 **Ni K**, O'Neill HC. The role of dendritic cells in T cell activation. *Immunol Cell Biol* 1997; **75**: 223-230
21 **Lee WC**, Jeng LB, Chiang YJ, Wang HC, Huang CC. Dendritic cell progenitors prolong allograft survival through T-helper 2 deviation of the Th1/Th2 paradigm. *Transplant Proc* 2000; **32**: 2076-2077
22 **DePaz HA**, Oluwole OO, Adeyeri AO, Witkowski P, Jin MX, Hardy MA, Oluwole SF. Immature rat myeloid dendritic cells generated in low-dose granulocyte macrophage-colony stimulating factor prolong donor-specific rat cardiac allograft survival. *Transplantation* 2003; **75**: 521-528
23 **Steinbrink K**, Wolfl M, Jonuleit H, Knop J, Enk AH. Induction of tolerance by IL-10-treated dendritic cells. *J Immunol* 1997; **159**: 4772-4780
24 **De Smedt T**, Van Mechelen M, De Becker G, Urbain J, Leo O, Moser M. Effect of interleukin-10 on dendritic cell maturation and function. *Eur J Immunol* 1997**; 27**: 1229-1235
25 **Coates PT**, Krishnan R, Kireta S, Johnston J, Russ GR. Human myeloid dendritic cells transduced with an adenoviral interleukin-10 gene construct inhibit human skin graft rejection in humanized NOD-scid chimeric mice. *Gene Ther* 2001; **8**: 1224-1233
26 **McCoy KD**, Le Gros G. The role of CTLA-4 in the regulation of T cell immune responses. *Immunol Cell Biol* 1999; **77**: 1-10
27 **Greenfield EA**, Nguyen KA, Kuchroo VK. CD28/B7 costimulation: a review. *Crit Rev Immunol* 1998; **18**: 389-418
28 **Kishimoto K**. The role of CD154-CD40 versus CD28-B7 costimulatory pathways in regulationg allogeneic Th1 and Th2 responses *in vivo*. *J Clin Inve* 2000; **106**: 63-72
29 **Jenkins MK**, Chen CA, Jung G, Mueller DL, Schwartz RH. Inhibition of antigen-specific proliferation of type 1 murine T cell clones after stimulation with immobilized anti-CD3 monoclonal antibody. *J Immunol* 1990; **144**: 16-22
30 **Schwartz RH**. Models of T cell anergy: Is there a common molecular mechanism? *J Exp Med* 1996; **184**: 1-5
31 **Ballard DW**. Molecular mechanisms in lymphocyte activation and growth. *Immunol Res* 2001; **23**: 157-166
32 **Prasad AS**, Bao B, Beck FW, Sarkar FH. Zinc enhances the expression of interleukin-2 and interleukin-2 receptors in HUT-78 cells by way of NF-kappaB activation. *J Lab Clin Med* 2002; **140**: 272-289
33 **Hong YS**, Laks H, Cui G, Chong T, Sen L. Localized immunosuppression in the cardiac allograft induced by a new liposome-mediated IL-10 gene therapy. *J Heart Lung Transplant* 2002; **21**: 1188-1200
34 **Gojo S**, Yamamoto S, Patience C, LeGuern C, Cooper DK. Gene therapy-its potential in surgery. *Ann R Coll Surg Engl* 2002; **84**: 297-301

Edited by Zhu LH and Wang XL

P.O.Box 2345, Beijing 100023,China
Fax: +86-10-85381893
E-mail: wjg@wjgnet.com www.wjgnet.com

World J Gastroenterol 2003;9(11):2513-2518
World Journal of Gastroenterology
 ISSN 1007-9327

• BASIC RESEARCH •

Effect of NF-κB and p38 MAPK in activated monocytes/macrophages on pro-inflammatory cytokines of rats with acute pancreatitis

Hong-Shan Liu, Cheng-En Pan, Qing-Guang Liu, Wei Yang, Xue-Min Liu

Hong-Shan Liu, Cheng-En Pan, Qing-Guang Liu, Wei Yang, Xue-Min Liu, Department of Hepatobiliary Surgery, First Affiliated Hospital, Xi' an Jiaotong University, Xi' an 710061, Shaanxi Province, China

Correspondence to: Dr. Hong-Shan Liu, Department of Hepatobiliary Surgery, First Affiliated Hospital, Xi' an Jiaotong University, Xi' an 710061, Shaanxi Province, China. doctorliuqi@yahoo.com.cn
Telephone: +86-29-5324009 **Fax:** +86-29-5324009
Received: 2003-04-05 **Accepted:** 2003-05-11

Abstract

AIM: Proinflammatory cytokines TNF-α and IL-6 play a main role in acute pancreatitis (AP). Cytokine biosynthesis runs through two major signaling pathways at the level of proteins: nuclear transcription factor-κB (NF-κB) and p38 mitogen-activated protein kinase (p38 MAPK). The aim of the study was to investigate the effect of NF-κB and p38 MAPK in activated monocytes/macrophages on cytokines of rats with acute pancreastitis.

METHODS: Taurocholate (3 % and 5 %) at doses of 1 mL/kg was administered into the biliopancreatic duct of male Sprague-Dawley (SD) rats to reduce acute edematous pancreariris (AEP) and acute necrotizing pancreatitis (ANP). Pancreatic tissues were prepared immediately after death. At this point, blood was obtained for determination of serum amylase and pro-inflammatory TNF-α and IL-6. Activated monocytes/macrophages were captured from blood and so were ascites. NF-κB and p38 MAPK in activated monocytes/macrophages were measured by immunohistochemistry method. Pancreatic tissue samples were prepared for routine light microscopy, using hematoxylin and eosin (HE) staining.

RESULTS: The serum levels of amylase were 3 056.00±1 232.35 IU/L and 4 865.12±890.34 IU/L at 3 and 6 hours in ANP group, which were significantly higher than those (3 056.00±1 232.35 IU/L and 3 187.17±821.16 IU/L) ($P<0.05$, respectively) in AEP group. In ascites the levels were 3.32±1.01 g and 3.76±1.12 g at 3 and 6 hours in ANP group, which were significantly higher than those (1.43±1.02 g and 2.56±1.21 g) ($P<0.05$, respectively) in AEP group. The serum levels of TNF-α were 54.27±23.48 pg/ml and 67.83±22.02 pg/ml in AEP group and 64.28±20.79 pg/ml and 106.59±43.71 pg/ml in ANP group, and the serum levels of IL-6 were 428.12±140.30 pg/ml and 420.13±139.40 pg/ml in AEP group and 1 600.32±309.78 pg/ml and 2 203.76±640.85 pg/ml in ANP group, which were far significantly higher than those in sham group ($P<0.001$, respectively). The serum level of TNF-α 6 hours after establishment of the studied model and that of IL-6 at 3 and 6 hours in ANP group were significantly higher than those in AEP ($P<0.05$, $P<0.001$, $P<0.05$). In ANP group, the levels of serum TNF-α and IL-6 6 hours after establishment of the studied model were significantly higher than those 3 hours after establishment of studied model ($P<0.05$, $P<0.05$, respectively). Three and 6 hours after establishment of the model, typical pathological changes of AEP and ANP were found, such as large numbers of inflammatory cells, edema, hemorrhage, necrosis, large amount of ascites. In AEP, NF-κB and p38 MAPK in activated monocytes/macrophages were moderately found at 3 and 6 hours after introduction of the model. However, in ANP, the expression of NF-κB and p38 MAPK in activated monocytes/macrophages was upregulated evidently at 3 and 6 hours after introduction of the model, reaching their highest levels at 6 hours after introduction of the model, which were consistent with the levels of TNF-α and IL-6.

CONCLUSION: Cytokine TNF-α and IL-6 play a main role in acute pancreatitis, expression of NF-κB and p38 MAPK in activated monocytes/macrophages might play a major role in cytokine transcription and biosynthesis.

Liu HS, Pan CE, Liu QG, Yang W, Liu XM. Effect of NF-κB and p38 MAPK in activated monocytes/macrophages on pro-inflammatory cytokines of rats with acute pancreatitis. *World J Gastroenterol* 2003; 9(11): 2513-2518
http://www.wjgnet.com/1007-9327/9/2513.asp

INTRODUCTION

The etiology of acute pancreatitis (AP) is mostly alcoholic or gallstone. Whatever the etiologic factors are, once the disease is initiated by an early molecular mechanism (which is still controversial) in or around acinar cells, a host inflammatory response is evoked in the pancreas. This locally limited inflammation is then manifested and amplified by the actions of diverse inflammatory mediators, such as cytokines (tumor necrosis factor-α (TNF-α), interleukin-1(IL-1) and interleukin-6(IL-6)), reactive oxygen species, proteolytic enzymes, lipids, as well as gaseous mediators, resulting in the induction of systemic inflammatory response syndrome (SIRS)[1-3]. Although SIRS is principally considered to be the normal host response to the insults, sustained or exaggerated SIRS, followed by the development of multiple organ dysfunction syndrome (MODS), is ultimately responsible for most pancreatitis- associated mortality and morbidity. Thus, the most distinctive feature of AP could be defined as its propensity to propagate locally limited inflammation into SIRS, and subsequently into MODS[4,5].

In AP, the very early phenomena that appear to occur are monocytes and neutrophils in the circulation migrating into the pancreatic interstitial space, mainly mediated by adhesion molecules on leukocytes[6,7]. These infiltrating cells accelerate further production and secretion of cytokines, as well as other inflammatory mediators. As a result, leukocytes in the circulation, as well as endothelial cells, in the pancreas and specific distant organs such as the lung, liver and spleen, are activated, eliciting further microcirculatory derangements, such as increased vascular permeability and accelerated leukocyte transmigration. The contribution of cytokines during this cascade of events has been increasingly apparent in the past decade, as indicated by several clinical and experimental studies exhibiting increased levels of cytokines in plasma, lymph, and ascites,as well as enhanced activitity of circulating leukocytes. Of the

various kinds of inflammatory mediators, TNF-α and IL-1 are regarded as most prominent "first-line" cytokines[8-10]. IL-6 is well known to be the primary inducer of acute-phase response. Therefore, IL-6 was recently reported to be the best prognostic parameter of pulmonary failure[11]. IL-6, IL-8 and TNF-α can be synthesized by monocytes/macrophages, neutrophils, endothelial cells, and even pancreatic duct cells.

Recent experimental studies appeared to have shed some light on the intracellular signaling pathway in the inflammatory cascade in AP. For example, recent evidence strongly suggested the crucial role of NF-κB in the initiation of AP, not only in pancreatic acinar cells and monocytes/macrophages but also in specific distant organs, such as the lung. NF-κB is able to mediate a variety of inflammatory mediators involved in AP, including cytokines and adhesion molecules, as well as specific inducible isoform of nitric oxide synthase enzymes[12-21]. Additionally, recent evidence has also shown the contribution of p38 MAP kinase to the mechanism underlying cytokine expression in pancreatic acinar cells and monocytes/ macrophages. An *in-vitro* experiment showed that cytokine expression of acinar cells was mediated by two separate signal pathways, i.e, NF-κB and p38 MAP kinase. of which p38 MAP kinase is now suggested to play a major role[22-27]. The definitive role of these intracellular signaling cascades may lead to new designs for cytokine modulation therapy.

This study was to investigate the effect of NF-κB and p38 MAPK in activated monocytes/macrophages on pro-inflammatory cytokines of mice with acute pancreatitis and to explore the biosynthesis mechanism of pro-inflammatory cytokines TNF-α and IL-6.

MATERIALS AND METHODS

Materials

Sixty pathogen-free male Sprague-Dawley (SD) rats (Animal Center, Xi' an Jiaotong University), weighing 250-300 g, were used in this experiment. The animals were kept at a constant room temperature of 25 ℃ with a 12-hour light-dark cycle, and were allowed free access to water. The animals were housed in the animal facility for at least seven days prior to use in order to stabilize their intestinal flora. All procedures including the rats receiving a very small amount of methoxyflurane for induction and pentobarbital intra-peritoneal injection (50 mg/kg) for anesthesia were performed under sterile conditions. SD rats were divided into subgroups of pancreatitis and controls. Taurocholate (3 % and 5 %, Sigma) at doses of 1 mL/kg was administered into the biliopancreatic duct of the rats to establish acute edematous pancreatitis (AEP) and acute necrotizing pancreatitis (ANP). In the sham group, the mice were only operated but not infused anything. All values reported were from animals killed at defined time points. During experiments the rats were closely observed, and pancreas tissues were prepared immediately after death. At this point, blood was obtained for determination of serum amylase and TNF-α and IL-6. The activated monocytes/ macrophages were captured from blood and ascites respectively.

Macroscopic assessment of the pancreas

Necrosis, hemorrhage and edema of the pancreas were each graded from 0 to 3 as follows: (a) necrosis: no necrosis =0, isolated necrotic lesion (<5 % of the pancreas)=1, necrotic areas 5-25 %=2, necrotic areas >25 % and partial destruction of the organ=3; (b) hemorrhage: not evident=0, single focal hemorrhage=1, multiple disseminated hemorrhagic dots=2, massive confluent hemorrhage=3; (c) edema: normal size=0, enlargement of the pancreas=1, recognizable accumulated fluid in the tissue=2, massive swelling and fluid accumulation=3. The scores of these parameters were summed, and the highest possible total score for an individual rat was 9[28].

Microscopic assessment of the pancreas

Pancreas tissue samples were prepared for routine light microscopy, using hematoxylin and eosin (HE) staining and examined by a pathologist who was unaware of the source of specimens. HE-stained pancreas sections were observed with a standard light microscope to evaluate morphologic alterations following AP.

Pancreatic water contents

The wet weight-dry weight ratio of the pancreas was obtained after about 200 mg of freshly prepared pancreatic tissue was dried for 20 h at 105 ℃.

Amylase assay

Amylase activity in plasma was determined using the a-amylase EPS assay purchased from Roche (Sigma) at 37 ℃.

Serum of TNF-α and IL-6

Blood was collected and centrifuged (3 000 rpm/min, for 5 min). The serum was captured and stored at -30 ℃. The pro-inflammatory TNF-α and IL-6 were measured by enzyme-linked immunosorbent assay (ELISA).

NF-κB and p38 MAPK in activated monocytes/macrophages

The activated monocytes/macrophages were captured from blood and ascites, respectively. They were separated and pasted for 12 hours in 10 % calf serum of 1640. NF-κB and p38 MAPK in activated monocyte/macrophage were measured by immunohistochemistry method (S-ABC). In brief, endogenous peroxidases were blocked for 15 min with methanol-H_2O_2, and after several washes unspecific-binding sites were blocked for 2 h with 3 % normal horse serum. Samples were then incubated overnight in a humidified chamber at 4 ℃ with the primary antibody against NF-κB and p38 MAPK(Sigma) diluted 1:200. This was followed by biotinylated goat anti-mouse antibody diluted 1:200 for 1 h, and the avidin-biotin complex (ABC kit, Vector Laboratories) (1:100) for 1 h. The reaction was developed with 0.05 % diaminobenzidine and 0.03 % H_2O_2. Negative controls were carried out by omission of the primary antibody in the overnight incubation. Several sections were counterstained with hematoxylin.

Statistical analysis

The values were expressed as the mean ±standard error (SEM). The data were analyzed for statistical significance using Student' s *t* test. There were six animals in each group at each time point. As the values in some data sets were not normally distributed or exhibited unequal standard deviations, the nonparametric Wilcoxon rank sum test was used to test for statistical differences between groups. In all instances $P<0.05$ was considered to be significant.

RESULTS

Amylase assay and ascites

The serum levels of AMS and ascites in AEP and ANP groups were significantly higher than those in sham group ($P<0.01$). The serum levels of AMS and ascites at 3 and 6 hours after the establishment of the studied model in ANP group were significantly higher than that in AEP ($P<0.05$). In ANP group, the levels of serum AMS and ascites 6 hours after the establishment of the studied model were not significantly higher than those 3 hours after the establishment of the studied model ($P>0.05$) (Table 1).

Table 1 Levels of AMS and ascites of AEP and ANP($\bar{x}\pm s$)

Group	AMS (IU/L)		Ascites (g)	
	3 h	6 h	3 h	6 h
Sham	792.80±265.08	793.8 0±265.08	0	0
AEP	3 056.00±1232.35[b]	3 187.17±821.16[b]	1.43±1.02[b]	2.56±1.21[b]
ANP	4 345.30±1005.77[ab]	4 865.12±890.34[ab]	3.32±1.01[ab]	3.76±1.12[ab]

[b]$P<0.01$ *vs* sham, [a]$P<0.05$ *vs* AEP.

Pancreatic water contents

The extent of pancreatic edema was determined as the wet weight/dry weight ratio of the tissue, and the macroscopic appearance of the pancreas was evaluated by a score (Table 2). In pancreatitis both parameters were significantly increased compared to the control ($P<0.05$).

Table 2 Macrocopic appearance and edema of pancreas in AEP and ANP (at 6 hours after of model)

	n	Sham	AEP	ANP
Score	0.2	1.1	6.9[a]	6.3[ac]
ww/dw	4.3	5.3	7.1[a]	8.2[ac]

The macroscopic appearance of the pancreas was scored. For an individual rat the highest possible score was 9. Pancreatic water content was estimated as the wet weight/dry weight ratio (ww/dw) of the tissue. N: untreated animals, anesthesia omitted; S: sham operations. [a]$P<0.05$ compared to the untreated group; [c]$P<0.05$ compared to the control group at 6 hours after induction of model.

Serum levels of TNF-α and IL-6

The serum levels of TNF-α and IL-6 in AEP and ANP groups were far significantly higher than those in sham group ($P<0.001$). The serum levels of TNF-α and IL-6 6 hours after establishment of the model in ANP group were significantly higher than those in AEP ($P<0.05$, $P<0.001$, $P<0.05$). In ANP group, the levels of serum TNF-α and IL-6 6 hours after establishment of the studied model were significantly higher than those 3 hours after establishment of the studied model ($P<0.05$) (Table 3).

Table 3 Serum levels of TNF-α and IL-6 in AEP and ANP ($\bar{x}\pm s$)

Group	TNF-α (pg/ml)		IL-6 (pg/ml)	
	3 h	6 h	3 h	6 h
Sham	4.13±2.5	55.87±3.79	100.79±53.89	151.04±91.79
AEP	54.27±23.48[b]	67.83±22.02[b]	428.12±140.30[b]	420.13±139.40[b]
ANP	64.28±20.79[b]	106.59±43.71[abc]	1 600.32±309.78[ab]	2 203.76±640.85[abc]

[b]$P<0.001$ *vs* sham group; [a]$P<0.05$ or 0.001 *vs* AEP group; [c]$P<0.05$ *vs* 3 h group.

Morphological examination

After induction of the AEP and ANP models, the pancreas showed mild edema and congestion. Three and 6 hours after introduction of the model, typical pathological changes of AEP and ANP were found, such as large numbers of inflammatory cells, edema, hemorrhage, necrosis, large amount of ascites (Table 1).

NF-κB and p38 MAPK in activated monocytes/macrophages

The expression of NF-κB and p38 MAPK in activated monocytes/macrophages at 3 and 6 hours was assessed by immunohistochemistry. In AEP, mild expression of NF-κB and p38 MAPK in activated monocytes/macrophages was found 3 and 6 hours after introduction of the model. However, in ANP, the expression of NF-κB and p38 MAPK in activated monocytes/macrophages was upregulated evidently 3 and 6 hours after introduction of the model, reaching their highest levels at 6 hours after introduction of the model (Figures 1,2,3 and 4).

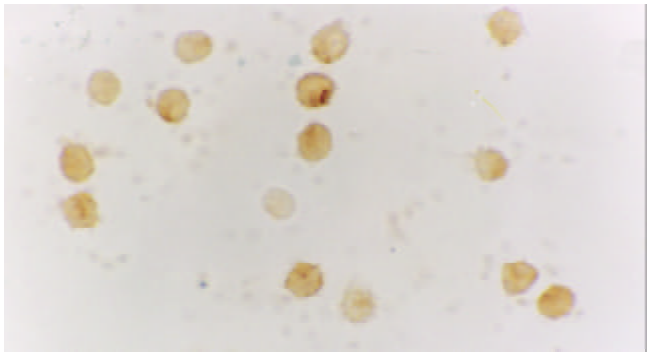

Figure 1 Moderate expression of NF-κB in the cytoplasm/nucleolus of monocytes in AEP (6 hours) 10×100.

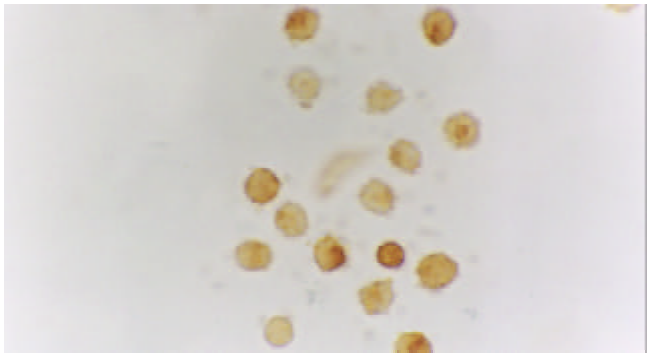

Figure 2 Strong expression of NF-κB in the cytoplasm/nucleolus of monocytes in ANP (6 hours) 10×100.

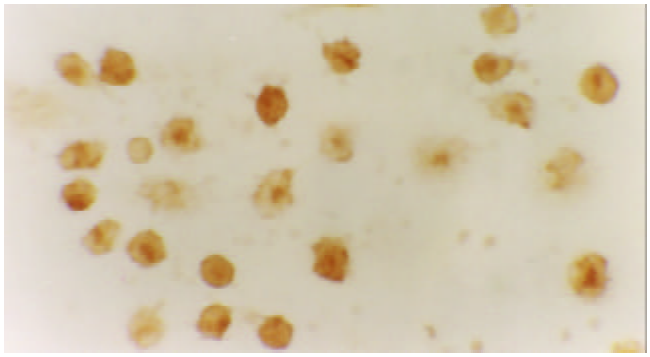

Figure 3 Moderate expression of p38MAPK in the cytoplasm/nucleolus of monocytes in AEP (6 hours) 10×100.

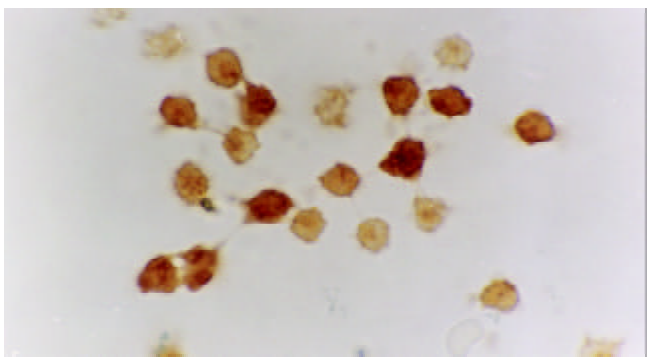

Figure 4 Strong expression of p38MAPK in the cytoplasm/nucleolus of monocytes in ANP (6 hours) 10×100.

DISCUSSION

The clinical manifestations of AP vary significantly from mild to lethal, severity of the disease is largely determined by the actions of various kinds of inflammatory mediators, including cytokines, reactive oxygen species, proteolytic enzymes, and lipids, as well as gaseous mediators. Despite increasing knowledge implicating the involvement of cytokines in the progression of AP, no clinical trials pertaining to cytokine modulation have been performed so far. Progress in intensive care technologies has contributed to the improvement of mortality and morbidity rates in severe AP in the past decade. However, it appears to be reasonable for clinicians to "line up their sights" on the modulation of cytokines as a direct treatment.

Pro-inflammatory cytokines played a main role in acute pancreatitis and complications due to acute pancreatitis[29,30]. Failure of different organ systems is a frequent problem in severe acute pancreatitis. The majority of fatalities in patients with severe acute pancreatitis are associated with the failure of at least one or more organ systems. Organ failure in severe acute pancreatitis has to be regarded as part of the inflammatory response following the liberation of activated enzymes from the pancreas. The mediators involved in this process include IL-1, TNF-α, IL-6, platelet activating factor, and IL-8. Of the various kinds of inflammatory mediators, TNF-α and IL-1 are regarded as the most prominent "first-line" cytokines. The primary involvement of TNF-α was demonstrated by elevation of TNF-α levels in rat severe AP models. This was confirmed by subsequent TNF-α antagonism experiments, using anti-TNF-α antibodies or a recombinant dimeric form of p55 TNF receptor. Similarly, the concurrent blockade of cytokines showed no additional benefit in the amelioration of pancreatic injury, however, it attenuated the systemic response, as indicated by reduced IL-6 levels and decreased mortality rates. With few exceptions, most studies carried out with the purpose of blocking proximal cytokines, such as TNF-α, IL-1 or IL-6, during the progression of AP showed favorable results in experimental settings. However, neither TNF-α nor IL-1 has a causative role in the initiation of AP. For example, exposure of isolated acinar cells to TNF-α and IL-1 *in vitro* did not induce either intracellular zymogen activation or release of enzymes. In addition, these cytokines were not able to induce either biological or histological evidence of pancreatitis by *in-situ* perfusion of isolated human pancreas[31].

As to the primary site of cytokine production, infiltrating macrophages in the pancreas and ascites are suggested to be the initial cellular origins of TNF-α. In a mouse cerulein AP model, the expression of TNF-α messenger RNA within the inflamed pancreas was observed as early as 30 min after the induction of AP, and was followed by elevation of intrapancreatic and serum TNF-α levels. In addition, neutrophils that have migrated into the inflamed pancreas appear to be equally involved in the production of TNF-α, IL-6 and IL-1. The production of these cytokines was subsequently observed in specific distant organs, such as the lungs, liver, and spleen. In particular, production of TNF-α and IL-1 in the lung was known to be closely associated with the development of adult respiratory distress syndrome (ARDS), which was the major cause of early death in patients with SAP[32].

IL-6 is well known to be the primary inducer of acute-phase response, while its level in circulation during AP reaches the maximum value 24-48 h before the maximal C-reactive protein level is reached. Therefore, IL-6 has been recently reported to be the best prognostic parameter of pulmonary failure. IL-6 is synthesized by monocytes/macrophages, neutrophils, endothelial cells, and even pancreatic duct cells. It is able to stimulate neutrophil chemotaxis and release of enzymes, thereby leading to tissue destruction when overproduced. In clinical settings, some authors have reported elevated IL-6 levels in AP patients, particularly in those with complications. This observation has been supported by *in-vitro* studies, using isolated blood monocytes from patients with AP, in which systemic complications were found to be closely associated with enhanced secretion of IL-6 and IL-8 from the cells. Based on an increasing body of evidence, both IL-6 and IL-8 are now considered to be early and excellent predictors of patient outcome, and are widely used as secondary end points in clinical trails[33].

Recent experimental studies have shed some light on the intracellular signaling pathway in the inflammatory cascade in AP. For example, recent evidence strongly suggested the crucial role of NF-κB in the initiation of AP, not only in pancreatic acinar cells, monocytes/macrophages and neutrophils, but also in specific distant organs such as the lung. NF-κB is able to mediate a variety of inflammatory mediators involved in AP, including cytokines and adhesion molecules, as well as specific enzymes. NF-κB plays a key role in the transcriptional regulation of adhesion molecules, enzymes and cytokines involved in acute inflammatory diseases. NF-κB is a key transcription factor for the expression of various proinflammatory molecules such as chemokines, cytokines, and adhesion molecules. This notion has recently been verified by adenoviral-mediated gene transfer of an active subunit, RelA/p65, into acinar cells delivered through an injection into the rat pancreatic duct. The overexpressed RelA/p65 protein trans-activated NF-κB and induced pancreatic inflammation, a pathological state very similar to acute pancreatitis. In addition to the importance of NF-κB in the pathogenesis of acute pancreatitis, it was also reported that NF-κB activation in macrophages was a key event both in the development of generalized complications during severe acute pancreatitis and as a cause of the high mortality in this condition. Studies also showed that glucocorticoids were one of the most potent inhibitors of NF-κB, which might be attributable to the inhibition of this key transcription factor both in acinar cells and in inflammatory cells such as monocytes/macrophages. It is known that the mechanism of the inhibition of NF-κB by corticosteroids is multifactorial. One is via the induction of IκBa, the inhibitor molecule of NF-κB, which can form a complex with NF-κB in the cytoplasm, inhibiting the translocation of NF-κB into the nucleus, where it enhances the transcriptional activation of various proinflammatory genes. The other is a cross-coupling mechanism of inhibition between activated glucocorticoid receptors and activated NF-κB. Because the activation of NF-κB is an early event in the pathogenetic mechanism of acute pancreatitis, it is reasonable that in most studies corticosteroids showed beneficial effects on acute pancreatitis[34].

Moreover, inflammatory mediators released during acute diseases activate multiple intracellular signalling cascades including the MAPK signal transduction pathway, which plays a significant role in the recruitment of leukocytes to sites of inflammation. Stimulation of leukocytes by pro-inflammatory cytokines is known to result in activation of MAPK isoform p38. However, the functional consequences of p38 MAPK activation during leukocyte recruitment, including adhesion, migration and effector functions such as oxidative burst and degranulation, are only just beginning to be elucidated. Recently, p38 MAPK has been implicated in the activation of NF-κB. Several groups have demonstrated that p38 MAPK-specific inhibitor SB203580 potently attenuated NF-κB-dependent transcription. However, phosphorylation of NF-κB subunits, nuclear translocation and DNA binding to NF-κB were not affected by this p38 inhibitor. This suggests that NF-κB and p38 MAPK are activated by separate effector pathways, which might converge further downstream in the cell nucleus.

So recent experimental studies have shed some light on the intracellular signaling pathway in the inflammatory cascade. Cytokine transcription and biosynthesis bifurcate into two major signaling pathways at the level of proteins. One runs through the NF-κB inducing kinase route, which regulates phosphorylation of inhibitory-kb (IκB) protein, the cytosolic inhibitor of NF-κB which allows NF-κB complex to translocate to the nucleus and promotes gene expression. The other is mediated through p38MAPK pathway and makes p38MAPK phosphorylated and activated[35].

So in recent years, much effort has been focused on delineating intracellular signaling cascades in inflammatory pathways. The intracellular signaling pathways used by leukocytes in response to pro-inflammatory stimuli have only begun to be unravelled. Much attention has been given to MAPK superfamily owing to their activation by pro-inflammatory cytokines IL-6 and TNF-α, which play a central role during inflammatory responses and in inflammatory diseases.

In this study, it showed that retrograde infusion of sodium taurocholate into the pancreatic duct resulted in an increase of amylase activity and ascites 3 and 6 hours after pancreatitis. The levels of serum AMS and ascites in AEP and ANP groups were far significantly higher than those in sham group (P<0.01). The serum levels of TNF-α and IL-6 in AEP and ANP groups were far significantly higher than those in sham group (P<0.001). The serum level of TNF-α of the studied model and the serum level of IL-6 3 and 6 hours in ANP group were significantly higher than that in AEP (P<0.05, P<0.001, P<0.05). In ANP group, the levels of serum TNF-α and IL-6 6 hours after establishment of the studied model were significantly higher than those 3 hours after establishment of the studied model (P<0.05, P<0.05).

After induction of AEP and ANP models, pancreas showed mild edema and congestion. Three and 6 hours after introduction of the model, typical pathological changes of AEP and ANP were found, such as large numbers of inflammatory cell, edema, hemorrhage, necrosis, large amount of ascites.

The expression of NF-κB and p38 MAPK in activated monocytes/macrophages at 3 and 6 hours after pancreatitis was assessed by immunohistochemistry. In AEP, moderate expression of NF-κB in activated monocytes/macrophages was found 3 and 6 hours after introduction of the model. However, in ANP, the expression of NF-κB and p38 MAPK in activated monocytes/macrophages were upregulated evidently 3 and 6 hours after introduction of the model, reaching their highest levels 6 hours after introduction of the model. So the expression of NF-κB and p38 MAPK in activated monocytes/macrophages at 3 and 6 hours assessed by immunohistochemistry was consistent with the increase of pro-inflammatory cytokines TNF-α and IL-6.

Thus, increased understanding of the signal transduction pathways involved in the regulation of cytokine production and cytokine signaling in inflammatory cells has opened the door for the discovery of novel therapeutics for treating a variety of inflammatory diseases in which cytokine production or signaling is implicated. The availability of potent and selective inhibitors of such signaling pathways also provides a means to further dissect the pathways to increase our understanding about the complex events underlying a particular immune mediated event at the cellular and molecular level. NF-κB and p38 MAPK are the most studied signaling molecules in this regard and their relevance to such disease states has been established primarily through the use of inhibitors. Indeed, selective inhibition of NF-κB and p38 MAP kinase inhibitors has demonstrated efficacy in a variety of animal models[36-40]. Specific p38 inhibitors and selective inhibition of NF-κB aimed at reducing the production of inflammatory mediators are now being developed, and might in the future provide more effective treatment for inflammatory diseases. At present, it may be too early to take an optimistic view of therapeutic cytokine modulation in AP. There are many obstacles to overcome. However, direct therapy by cytokine modulation sounds very attractive to clinicians.

REFERENCES

1 **Morrison CP,** Teague BD, Court FG, Wemyss-Holden SA, Metcalfe MS, Dennison AR, Maddern GJ. Experimental studies of serum cytokine concentration following pancreatic electrolytic ablation. *Med Sci Monit* 2003; **9**: 43-46

2 **Zhang Q,** Ni Q, Cai D, Zhang Y, Zhang N, Hou L.Mechanisms of multiple organ damages in acute necrotizing pancreatitis. *Chin Med J (Engl)* 2001; **114:** 738-742

3 **Makhija R,** Kingsnorth AN. Cytokine storm in acute pancreatitis. *J Hepatobiliary Pancreat Surg* 2002; **9:** 401-410

4 **Bhatia M,** Neoptolemos JP, Slavin J. Inflammatory mediators as therapeutic targets in acute pancreatitis. *Curr Opin Investig Drugs* 2001; **2:** 496-501

5 **Wereszczynska-Siemiatkowska U,** Dabrowski A, Siemiatkowski A, Mroczko B, Laszewicz W, Gabryelewicz A. Serum profiles of E-selectin, interleukin-10, and interleukin-6 and oxidative stress parameters in patients with acute pancreatitis and nonpancreatic acute abdominal pain. *Pancreas* 2003; **26:** 144-152

6 **Lundberg AH,** Granger N, Russell J, Callicutt S, Gaber LW, Kotb M, Sabek O, Gaber AO. Quantitative measurement of P-and E-selectin adhesion molecules in acute pancreatitis: correlation with distant organ injury. *Ann Surg* 2000; **231:** 213–222

7 **Qin RY,** Zou SQ,Wu ZD. Experimental research on production and uptake sites of TNF-α in rat with acute hemorrhagic necrotic pancreatitis. *World J Gastroenterol* 1998; **4:** 144-146

8 **Shimada M,** Andoh A, Hata K, Tasaki K, Araki Y, Fujiyama Y, Bamba T. IL-6 secretion by human pancreatic periacinar myofibroblasts in response to inflammatory mediators. *J Immunol* 2002; **168:** 861-868

9 **Riche FC,** Cholley BP, Laisne MJ, Vicaut E, Panis YH, Lajeunie EJ, Boudiaf M, Valleur PD. Inflammatory cytokines, C reactive protein, and procalcitonin as early predictors of necrosis infection in acute necrotizing pancreatitis. *Surgery* 2003; **133:** 257-262

10 **Coelho AM,** Machado MC, Cunha JE, Sampietre SN, Abdo EE. Influence of pancreatic enzyme content on experimental acute pancreatitis. *Pancreas* 2003; **26:** 230-234

11 **Mayer J,** Rau B, Gansauge F, Beger HG. Inflammatory mediators in human acute pancreatitis: clinical and pathophysiological implications. *Gut* 2000; **47:** 546–552

12 **Jaffray C,** Yang J, Carter G, Mendez C, Norman J. Pancreatic elastase activates pulmonary nuclear factor kappa B and inhibitory kappa B, mimicking pancreatitis-associated adult respiratory distress syndrome. *Surgery* 2000; **128:** 225-231

13 **Kim H,** Seo JY, Kim KH. NF-kappaB and cytokines in pancreatic acinar cells. *J Korean Med Sci* 2000; **15**(Suppl): S53-S54

14 **Blanchard JA,** Barve S, Joshi-Barve S, Talwalker R, Gates LK Jr. Cytokine production by CAPAN-1 and CAPAN-2 cell lines. *Dig Dis Sci* 2000; **45:** 927-932

15 **Frossard JL,** Pastor CM, Hadengue A. Effect of hyperthermia on NF-kappaB binding activity in cerulein-induced acute pancreatitis. *J Physiol Gastrointest Liver Physiol* 2001; **280:** G1157-1162

16 **Blanchard JA,** Barve S, Joshi-Barve S, Talwalker R, Gates LK Jr. Antioxidants inhibit cytokine production and suppress NF-kappaB activation in CAPAN-1 and CAPAN-2 cell lines. *Dig Dis Sci* 2001; **46:** 2768-2772

17 **Tando Y,** Algul H, Schneider G, Weber CK, Weidenbach H, Adler G, Schmid RM. Induction of IkappaB-kinase by cholecystokinin is mediated by trypsinogen activation in rat pancreatic lobules. *Digestion* 2002; **66:** 237-245

18 **Algul H,** Tando Y, Schneider G, Weidenbach H, Adler G, Schmid RM. Acute Experimental Pancreatitis and NF-kappaB/Rel Activation. *Pancreatology* 2002; **2:** 503-509

19 **Murr MM,** Yang J, Fier A, Kaylor P, Mastorides S, Norman JG. Pancreatic elastase induces liver injury by activating cytokine production within Kupffer cells via nuclear factor-Kappa B. *J Gastrointest Surg* 2002; **6:** 474-480

20 **Rakonczay Z,** Jarmay K, Kaszaki J, Mandi Y, Duda E, Hegyi P,

Boros I, Lonovics J, Takacs T. NF-kappaB activation is detrimental in arginine-induced acute pancreatitis. *Free Radic Biol Med* 2003; **34:** 696-709

21 **Altavilla D,** Famulari C, Passaniti M, Campo GM, Macri A, Seminara P, Marini H, Calo M, Santamaria LB, Bono D, Venuti FS, Mioni C, Leone S, Guarini S, Squadrito F. Lipid peroxidation inhibition reduces NF-kappaB activation and attenuates cerulein-induced pancreatitis. *Free Radic Res* 2003; **37:** 425-435

22 **Blinman TA,** Gukovsky I, Mouria M, Zaninovic V, Livingston E, Pandol SJ, Gukovskaya AS. Activation of pancreatic acinar cells on isolation from tissue: cytokine upregulation via p38 MAP kinase. *Am J Physiol Cell Physiol* 2000; **279:** 1993-2003

23 **Chen X,** Ji B, Han B, Ernst SA, Simeone D, Logsdon CD. NF-kappaB activation in pancreas induces pancreatic and systemic inflammatory response. *Gastroenterology* 2002; **122:** 448-457

24 **Murr MM,** Yang J, Fier A, Gallagher SF, Carter G, Gower WR Jr, Norman JG. Regulation of Kupffer cell TNF gene expression during experimental acute pancreatitis: the role of p38-MAPK, ERK1/2, SAPK/JNK, and NF-kappaB. *J Gastrointest Surg* 2003; **7:** 20-25

25 **Masamune A,** Kikuta K, Satoh M, Satoh A, Shimosegawa T. Alcohol activates activator protein-1 and mitogen-activated protein kinases in rat pancreatic stellate cells. *J Pharmacol Exp Ther* 2002; **302:** 36-42

26 **Fleischer F,** Dabew R, Goke B, Wagner AC. Stress kinase inhibition modulates acute experimental pancreatitis. *World J Gastroenterol* 2001; **7:** 259-265

27 **Dabrowski A,** Boguslowicz C, Dabrowska M, Tribillo I, Gabryelewicz A. Reactive oxygen species activate mitogen-activated protein kinases in pancreatic acinar cells. *Pancreas* 2000; **21:** 376-384

28 **Gilgenast O,** Brandt-Nedelev B, Wiswedel I, Lippert H, Halangk W, Reinheckel T. Differential oxidative injury in extrapancreatic tissues during experimental pancreatitis modification of lung proteins by 4-hydroxynonenal. *Dig Dis Sci* 2001; **46:** 932-937

29 **Osman MO,** Gesser B, Mortensen JT, Matsushima K, Jensen SL, Larsen CG. Profiles of pro-inflammatory cytokines in the serum of rabbits after experimentally induced acute pancreatitis. *Cytokine* 2002; **17:** 53-59

30 **Bidarkundi GK,** Wig JD, Bhatnagar A, Majumdar S. Clinical relevance of intracellular cytokines IL-6 and IL-12 in acute pancreatitis, and correlation with APACHE III score. *Br J Biomed Sci* 2002; **59:** 85-89

31 **Yamauchi J,** Shibuya K, Sunamura M, Arai K, Shimamura H, Motoi F, Takeda K, Matsuno S. Cytokine modulation in acute pancreatitis. *J Hepatobiliary Pancreat Surg* 2001; **8:** 195-203

32 **Denham W,** Yang J, Norman J. Evidence for an unknown component of pancreatic ascites that induces adult respiratory distress syndrome through an interleukin-1 and tumor necrosis factor-dependent mechanism. *Surgery* 1997; **122:** 295–301

33 **Powell JJ,** Murchison JT, Fearon KC, Ross JA, Siriwardena AK. Randomized controlled trial of the effect of early enteral nutrition on markers of the inflammatory response in predicted severe acute pancreatitis. *Br J Surg* 2000; **87:** 1375-1381

34 **Takaoka K,** Kataoka K, Sakagami J. The effect of steroid pulse therapy in the development of acute pancreatitis induced by closed duodenal loop in rats. *J Gastroenterol* 2002; **37:** 537–542

35 **Haddad JJ.** The involvement of L-gamma-glutamyl-L-cysteinyl-glycine (glutathione/GSH) in the mechanism of redox signaling mediating MAPK(p38)-dependent regulation of pro-inflammatory cytokine production. *Biochem Pharmacol* 2002; **63:** 305-320

36 **Ethridge RT,** Hashimoto K, Chung DH, Ehlers RA, Rajaraman S, Evers BM. Selective inhibition of NF-kappaB attenuates the severity of cerulein-induced acute pancreatitis. *J Am Coll Surg* 2002; **195:** 497-505

37 **Legos JJ,** McLaughlin B, Skaper SD, Strijbos PJ, Parsons AA, Aizenman E, Herin GA, Barone FC, Erhardt JA. The selective p38 inhibitor SB-239063 protects primary neurons from mild to moderate excitotoxic injury. *European J Pharmacol* 2002; **447:** 37- 42

38 **Elenitoba-Johnson KS,** Jenson SD, Abbott RT, Palais RA, Bohling SD, Lin Z, Tripp S, Shami PJ, Wang LY, Coupland RW, Buckstein R, Perez-Ordonez B, Perkins SL, Dube ID, Lim MS. Involvement of multiple signaling pathways in follicular lymphoma trans formation: p38-mitogen- activated protein kinase as a target for therapy. *Proc Natl Acad Sci* 2003; **10:** 1073-1082

39 **El Bekay R,** Alvarez M, Alba G, Chacon P, Vega A, Martin-Nieto J, Jimenez J, Monteseirin J, Pintado E, Bedoya FJ, Sobrino F. Oxidative stress is a critical mediator of the angiotensin II signal in human neutrophils: involvement of map kinases, calcineurin, and the transcription factor NF-kappaB. *Blood* 2003; **10:** 1464-1476

40 **Torres M.** Mitogen-activated protein kinase pathways in redox signaling. *Front Biosci* 2003; **8:** 369-391

Edited by Zhu LH and Wang XL

P.O.Box 2345, Beijing 100023,China
Fax: +86-10-85381893
E-mail: wjg@wjgnet.com www.wjgnet.com

World J Gastroenterol 2003;9(11):2519-2522
World Journal of Gastroenterology
 ISSN 1007-9327

• BASIC RESEARCH •

Influence of Kupffer cells on hepatic signal transduction as demonstrated by second messengers and nuclear transcription factors

Hong Ding, Jie-An Huang, Jing Tong, Xin Yu, Jie-Ping Yu

Hong Ding, Jing Tong, Xin Yu, Department of Pharmacology, College of Pharmacy, Wuhan University, Wuhan 430072, Hubei Province, China
Jie-An Huang, Department of Internal Medicine, the First Affiliated Hospital of Guangxi Medical University, Nanning 530021, Guangxi Zhuang Autonomous Region, China
Jie-Ping Yu, Department of Internal Medicine, the First Affiliated Hospital of School of Medicine, Wuhan University, Wuhan 430064, Hubei Province, China
Supported by the Chen Guang Project of Wuhan, No.20005004038, and the Natural Science Foundation of Hubei Province, No. 2001ABB160
Correspondence to: Dr. Hong Ding, Wuhan University College of Pharmacy, Wuhan 430072, Hubei Province, China. dinghong2000@263.net.cn
Telephone: +86-27-87682339 **Fax:** +86-27-87682339
Received: 2003-03-03 **Accepted:** 2003-04-11

Abstract

AIM: To understand the influence of Kupffer cell (KC) on signal transduction pathways in the liver.

METHODS: To decrease selectively the number and function of KC, Kunming mice were ip injected with a single dose of gadolinium chloride ($GdCl_3$, 20 mg·kg^{-1}), the time-effect relationship assessment was performed after 1 d, 3 d and 6 d. sALT, sGST, liver glycogen content, phagocytic index, and expression of CD68 were assessed as the indexes of hepatotoxicity and functions of KC respectively, and morphology of KC was observed with transmission electron microscopy. Furthermore, cAMP, PGE_2 level, nitric oxide(NO) content, and mRNA expression of NFkappaBp65, Erk1, STAT1 were examined.

RESULTS: $GdCl_3$ could selectively cause apoptosis of KC and obvious reduction of KC's activity, but no hepatotoxicity was observed. One day after KC blockade, NO, PGE_2, cAMP contents in the liver were reduced 21.0 %, 6.94-fold, 8.3 %, respectively, and mRNA expression of NFkappaBp65 was decreased 3.0-fold. The change tendency of NO, PGE_2, and cAMP contents and mRNA expression of NFkappaBp65 were concomitant with recovery of the functions of KC. The contents of NO, PEG2, cAMP were increased when the functions of KC was recovered. However, all of the changes could not return to the normal level except NO content after 6 d $Gdcl_3$ treatment. No obvious changes were found in STAT1 and Erk1 mRNA expression in the present study.

CONCLUSION: Hepatic NO, PGE2, cAMP level and mRNA expression of NFkappaBp65 are closely related with the status of KC. It suggests that KC may play an important role in the cell to cell signal transduction in the liver.

Ding H, Huang JA, Tong J, Yu X, Yu JP. Influence of Kupffer cells on hepatic signal transduction as demonstrated by second messengers and nuclear transcription factors. *World J Gastroenterol* 2003; 9(11): 2519-2522
http://www.wjgnet.com/1007-9327/9/2519.asp

INTRODUCTION

Kupffer cells (KCs) account for a major portion of the tissue macrophages and play an important role in the defense mechanisms of the body[1]. KCs are involved in the pathogenesis of chemically mediated liver injury through release of biologically active mediators that promote the pathogenic process[2]. KCs can synthesize and release a variety of immunomodulating and inflammatory mediators such as oxygen-derived free radicals, nitric oxide, lipid mediators, and cytokines, etc. There are certain points to be elucidated that KCs involve in the pathophysiologic response of liver injury[3]. And now, many new functions have been found. KCs can reverse liver fibrosis and are critical for the progression of alcoholic injury[3,4]. Abolishment of KCs sensitization could prevent alcoholic liver injury[5]. KCs are major contributors to cytokine production in hepatic ischemia/reperfusion[6] and play a stimulatory role in liver regeneration[7]. Up to now, few studies about the influence of KCs on signal transduction in the liver have been reported. NO, PGE_2, cAMP are important second messengers transmitting and magnifying messages to modulate gene expression. NFkappaB, STAT, Erk are important nuclear transcription factors, which are involved in the regulation of cell proliferation and differentiation[8,9]. To understand the effect of KCs on the second messengers and nuclear transcription factors is of great importance in studying the mechanism of liver diseases. $Gdcl_3$, as an inhibitor of KCs, is often used as a tool for studying the role of KC[10]. Kupffer cell toxicant $GdCl_3$ prevents stellate cell activation and the development of fibrosis[11]. The present study was designed to clarify the effect of KC on signal transduction pathway in the liver following $GdCl_3$-induced KC blockade.

MATERIALS AND METHODS

Reagents

Gadolinium chloride ($GdCl_3$), collagenase IV, Indian ink were purchased from Sigma, USA. NO, PGE_2 detection kits were obtained from Bangding Biotechnology Co., Ltd. cAMP detection kit was obtained from Shanghai College of Chinese Traditional Medicine. CD68 immunohistochemical kit and NFkappaBp65, STAT1, Erk1 *in situ* hybridization kit were purchased from Wuhan Boster Biological Technology Co., Ltd. Other reagents were all of A.R.

Animal treatment

Kunming ♂ mice (aged 4-6 wk), weighing 22±3 g were obtained from the Experimental Animal Center of School of Medicine, Wuhan University. The animals were fed on a standard diet in pellets, and allowed free access to water. The mice were randomly distributed to control group, $GdCl_3$-1d

Table 1 Influence of $GdCl_3$ on hepatic function and activity of KCs in mice (n=8, $\bar{x}\pm s$)

Group	sALT ($mmol\cdot min^{-1}\cdot L^{-1}$)	sGST ($\mu mol\cdot min^{-1}\cdot L^{-1}$)	Liver glycogen ($\mu mol\cdot mg^{-1}\cdot pro^{-1}$)	Phagocytic activity(α)	Expression of CD68 (relative O.D.)
Control	2.4±0.3	15.2±2.2	4.9±0.9	9.7±0.7	0.131±0.018
$GdCl_3$-1d	2.6±0.9	14.9±1.9	5.4±1.4	5.2±0.4[b]	0.065±0.010[b]
$GdCl_3$-3d	2.6±1.0	16.5±3.1	5.8±1.1	6.0±1.1[a]	0.084±0.015[b]
$GdCl_3$-6d	2.6±1.4	15.7±2.3	5.0±0.2	6.8±1.3[a]	0.108±0.014[b]

[a]P<0.05, [b]P<0.01 *vs* control.

group, $GdCl_3$-3d group, $GdCl_3$-6d group, in which the mice received ip injection of a single dose of 20 $mg\cdot kg^{-1}$ of $GdCl_3$, and were sacrificed after administration of $GdCl_3$ for 1 d, 3 d, 6 d, respectively.

Test for phagocytic function

14 % Indian ink (10 $ml\cdot kg^{-1}$) was injected into the mice tail vein. After 1 min and 5 min, 20 μl blood was obtained from the orbital vein of the mice and added into 2 ml of 0.1 % Na_2CO_3 solution. Absorbance (OD) at 600 nm was read, and the phagocytic activity (α) of KCs was calculated as described[12].

Biochemical assay

Twenty-five percent liver homogenate was prepared, the glycogen content was quantified by an enzymatic reaction as previously described[13]. NO content was measured by Griess reaction[14]. PGE_2 and cAMP concentration were determined by radioimmunoassay, and the radioactivity of the samples was measured with a P△CK△RD CA-2000 liquid scintillation spectrometer[15]. The protein content of liver homogenate was determined by Lowry[16].

In situ hybridization and immunohistochemistry methods

The livers were briefly washed in cold 0.1 M phosphate buffer containing 0.1 % DEPC and then fixed in cold 4 % formaldehyde (in 0.1 M phosphate buffer, pH7.4), paraffin-embedded sections in 5-6 μm thickness were cut and placed onto aminopropyltriethoxysilane-coated glass slides. The expression of CD68 was determined by i*n situ* hybridization with DIG detection system kit. The anti-sense sequence of the probe was 5' -AAGCT TGGCC CAAGC CACCT TGGTT TTAGA-3' for Erk1 (extracellular signal-regulated kinase), 5' -CAGGT TGTCT GTGGT CTGAA GTCTA GAAGG-3' for STAT1 (signal transducers and activators of transcription), 5' -AGTTG ATGTC CGCAA TGGAG GTCTT-3' for NF-kBp65 (nuclear factor kappa B p65).

Image analysis of immunohistochemistry and in situ hybridization

Microscopic images through an interference filter (Nikon, Tokyo, Japan) were transferred to the processor (HPIAS image analysis system, Wuhan Tongji Medical University). Average absorbances in defined areas of the sections were measured, relative optical density(OD) was used to evaluate expression level.

Liver cells isolation and transmission electron-microscopic study

Liver cells were isolated as described[17]. In brief, after washed in D-Hanks, liver tissue was digested with 0.075 % collagenase for 30 min. The resulting suspension was passed through 70 μm gaze and then 1 g of sediment was generated after 10 min. Hepatocytes were fixed in 2.5 % glutaraldehyde in 0.1 $mol\cdot L^{-1}$ phosphate buffer, transmission electron- microscope was used to observe the morphology of KCs.

Statistical analysis

The data were presented as $\bar{x}\pm s$, and statistical analysis was performed with Student's t-test.

RESULTS

Effect of $GdCl_3$ on sALT, sGST, liver glycogen and activity of KCs

After administration of $GdCl_3$, no changes in sALT, sGST level and liver glycogen content were observed. Liver expression of CD68 (specific surface antigen of macrophage) and phagocytic activity (α) obviously reduced 102 %, 86 % respectively after 1 d of $GdCl_3$ treatment, then the function of KCs was gradually recovered. However they could not return to the normal level after 6 d of $GdCl_3$ treatment.

Electron microscopic study

The characteristics of apoptosis (the membrane of KCs was integrate, chromatin in the nucleus presented uneven distribution and was close to nuclear measure) were observed after treatment of $GdCl_3$ (Figure 1).

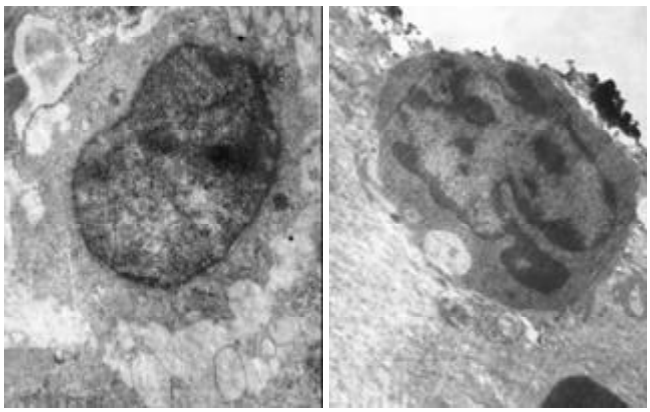

Figure 1 Influence of $GdCl_3$ on morphology of KCs under EM.

Effect on NO, PGE_2, cAMP content

After 1 d of $GdCl_3$ treatment, NO, PGE_2, cAMP contents were reduced 21.0 %, 6.94-fold, 8.3 %, respectively, and then they were gradually recovered. However, PGE_2 and cAMP contents could not return to the normal level after 6 d of treatment.

Table 2 Influence of $GdCl_3$ on NO, PGE_2, cAMP contents in liver (n=8 mice, $\bar{x}\pm s$)

Group	NO content ($pmol\cdot mg^{-1}\cdot pro^{-1}$.)	PGE_2 content ($pg\cdot mg^{-1}\cdot pro^{-1}$.)	cAMP content ($pmol\cdot mg^{-1}\cdot pro^{-1}$.)
Control	2.5±0.4	6.8±1.8	0.157±0.031
$GdCl_3$-1d	2.1±0.3[a]	0.9±0.2[b]	0.145±0.027[a]
$GdCl_3$-3d	2.0±0.3[a]	2.5±1.3[b]	0.131±0.010[a]
$GdCl_3$-6d	2.2±0.3	5.0±2.6[a]	0.133±0.010[a]

[a]P<0.05, [b]P<0.01 *vs* control.

Effect on NFkappaB, STAT1 and Erk1 mRNA expression

The time course of alteration of NFkappaB, STAT1 and Erk1 mRNA expressions after administration of 20 mg· kg^{-1} $GdCl_3$ showed that NFkappaB mRNA expression was decreased (3-fold) after administration of $GdCl_3$ for 1 d, then it was gradually recovered, but did not return to the normal level after 6 d of treament. No obvious influence on STAT1, Erk1 mRNA expressions was observed (Figure 2).

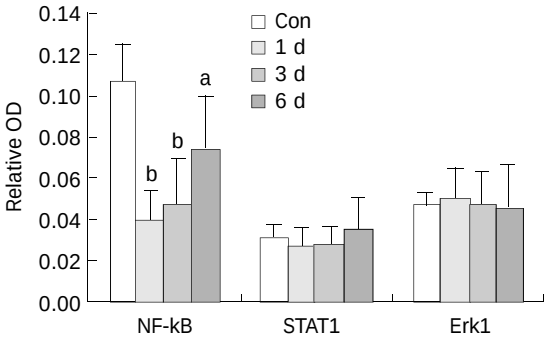

Figure 2 Time course of alteration of NFkappaB, STAT1 and Erk1 mRNA expressions after administration of 20 mg· kg^{-1} $GdCl_3$ (n=6, $\bar{x}\pm s$). $^aP<0.05$, $^bP<0.01$ *vs* control.

DISCUSSION

In the present study, ip injection of a single dose of $GdCl_3$ could selectively cause apoptosis of KCs, but did not induce hepatotoxicity. Therefore, it can be used as a tool for studying the role of KCs.

KCs are the phagocytic macrophages in the liver. NO, PGE_2, and cAMP could transmit and magnify extracellular messages to cells through a cascade system to regulate gene expression and cell proliferation and differentiation[18]. NO, PGE_2, and cAMP had different functions in hepatoprotection and hepatic injury. NO from KCs could induce membrane barrier dysfunction in liver sinusoid[19]. But according to Abou-Elella *et al*, the exacerbation of hepatocyte death by KCs was not related to NO[20]. Hsu *et al*, sproposed that KCs be the major source of induction of inducible NO synthase(iNOS) activity and NO production have a beneficial role in hepatic IR injury and the constitutive isoforms of NOS play a hepatoprotective role in hepatic injury[21-23]. The protective function of NO against hepatic injury might lie in that it could reduce tissue oxygenation[24]. PGE_2 derived from KCs increased cAMP, which caused triglyceride accumulation in the liver and fatty liver[3]. Increase of cAMP levels in KCs occurred during the late stage of polymicrobial sepsis, and might contribute to the depression of macrophage phagocytic function[25]. The current study showed that NO, PGE_2, and cAMP contents in the liver were reduced following KC blockade, and recovered following the functional recovery of KCs. It suggests that Kupffer cells may mediate signaling of second messengers in the liver. Moreover, in the present experiment, the hepatic function did not change following the alterations of NO, PGE_2, and cAMP content, the reasons remain to be researched.

It has widely been accepted that NFkappaB activation plays an important role in the pathophysiology of inflammatory disorders[26]. NFkappaB is an essential component of TNF proliferative pathway and TNF-induced changes in IL-6 mRNA, STAT3, and c-myc mRNA are dependent on NFkappaB activation[27]. NFkappaB activation may be important in "switching off" the cytokine cascade during acute pancreatitis[28]. The current study showed that mRNA expression of NFkappaB in the liver was down-regulated after KC blockade, suggesting that KCs may play an important role in mediating liver diseases and inflammatory disorders via changes of the signal transduction pathway in the liver.

In this experiment, STAT1 and Erk1 mRNA expressions were not affected by $GdCl_3$. STAT1 played a harmful role in Con A-mediated hepatitis, whereas STAT3 protected against liver injury[29]. Inhibition of STAT1 activation without reduction of STAT1 protein level might be one of the factors that are involved in the cAMP-dependent stellate cell growth arrest[30]. In this study, we only examined the expression of STAT1 mRNA, the relationship between STAT1 and hepatic injury needs to be further studied.

REFERENCES

1 **Fukumura D,** Yonei Y, Kurose I, Saito H, Ohishi T, Higuchi H, Miura S, Kato S, Kimura H, Ebinuma H, Ishi H. Role of nitric oxide in Kupffer cell-mediated hepatoma cell cytotoxicity *in vitro* and ex vivo. *Hepatology* 1996; **24**: 141-149

2 **Luckey SW**, Petersen DR. Activation of Kupffer cells during the course of carbon tetrachloride-induced liver injury and fibrosis in rats. *Exp Mol Pathol* 2001; **3**: 226-240

3 **Enomoto N**, Ikejima K, Yamashina S, Enomoto A, Nishiura T, Nishimura T, Brenner DA, Schemmer P, Bradford BU, Rivera CA, Zhong Z, Thurman RG. Kupffer cell-derived prostaglandin E(2) is involved in alcohol-induced fat accumulation in rat liver. *AM J Physiol Gastrointest Liver Physio* 2000; **279**: G100-106

4 **Sakaida I**, Hironaka K, Terai S, Okita K. Gadolinium chloride reverses dimethylnitrosamine (DMN)-induced rat liver fibrosis with increased matrix metalloproteinases (MMPs) of Kupffer cells. *Life Sci* 2003; **8**: 943-959

5 **Enomoto N**, Takei Y, Hirose M, Ikejima K, Miwa H, Kitamura T, Sato N. Thalidomide prevents alcoholic liver injury in rats through suppression of Kupffer cell sensitization and TNF-alpha production. *Gastroenterology* 2002; **1**: 291-300

6 **Mosher B**, Dean R, Harkema J, Remick D, Palma J, Crockett E. Inhibition of Kupffer cells reduced CXC chemokine production and liver injury. *J Surg Res* 2001; **2:** 201-210

7 **Takeishi T**, Hirano K, Kobayashi T, Hasegawa G, Hatakeyama K, Naito M. The role of Kupffer cells in liver regeneration. *Arch Histol Cytol* 1999; **5**: 413-422

8 **Liu DY**, Gorrod JW. Effects of cAMP-dependent protein kinase and ATP on N1oxidation of 9-benzyladenine by animal hepatic microsomes. *Life Sci* 2000; **66**: 77-88

9 **Wheeler MD**, Kono H, Rusyn I, Arteel GE, McCarty D, Jude Samulski R, Thurman RG. Chronic ethanol increases adeno-associated viral transgene expression in rat liver via oxidant and NFkappaB-dependent mechanisms. *Hepatology* 2000; **32**: 1050-1059

10 **Neyrinck A**, Eeckhoudt SL, Meunier CJ, Pampfer S, Taper HS, Brtnrrvl RK. Modulation of paracetamol metabolism by Kupffer cells; A study on rat liver slices. *Lif Sci* 1999; **65**: 2851-2859

11 **Rivera CA**, Bradford BU, Hunt KJ, Adachi Y, Schrum LW, Koop DR, Burchardt ER, Rippe RA, Thurman RG. Attenuation of CCl (4)-induced hepatic fibrosis by GdCl(3) treatment or dietary glycine. *Am J Physiol Gastrointest Liver Physiol* 2001; **1**: G200-207

12 **Joseph B,** Malhi H, Bhargava KK, Palestro CJ, McCuskey RS, Gupta S. Kupffer cells participate in early clearance of syngeneic hepatocytes transplanted in the rat liver. *Gastroenterology* 2002; **5**: 1677-1685

13 **Jaime RP**, Rosa G, Inmaculada A, Jose MS. Prenatal alcohol exposure affects galactosyltransferase activity and glycoconjugates in the Golgi apparatus of fetal rat hepatocytes. *Hepatology* 1997; **25**: 343-350

14 **Bartholomew B**. A rapid method for the assay of nitrate in urine using the nitrate reductase enzyme of Escherichia cilli. *Food Chem Toxicol* 1984; **22**: 543-551

15 **Hahn PY**, Yoo P, Ba ZF, Chaudry IH, Wang P. Upregulation of Kupffer cell beta-adrenoceptors and cAMP levels during the late stage of sepsis. *Biochim Biophys Acta* 1998; **1404**: 377-384

16 **Lowry OH**, Rosebrough NJ, Farr AL, Randall RJ. Protein measurement with the Folin phenol reagent. *J Biol Chem* 1951; **193**: 265-275

17 **Giorgio N**, Federica M, Giuseppe M, Claudio C, Anna C. Action of chronic CCl4 on the retinol and dolichol content of rat liver paren-

chymal and non-parenchymal cells. *Lif Sci* 2000; **67**: 2293-2304
18 **O'Dell TJ**. Test of the roles of two diffusible substances in long-term potentiation, evidence for nitric oxide as a possible early retrograde messenger. *Proc Natl Acad Sci U S A* 1991; **88**: 11285-11289
19 **Fukumura D**, Yonei Y, Kurose I, Saito H, Ohishi T, Higuchi H, Miura S, Kato S, Kimura H, Ebinuma H, Ishi H. Role in nitric oxide in Kupffer cell-mediated hepatoma cell cytotoxicity *in vitro* and *ex vivo*. *Hepatology* 1996; **1**: 141-149
20 **Abou-Elella AM**, Siendones E, Padillo J, Montero JL, De la Mata M, Relat JM. Tumour necrosis factor-alpha and nitric oxide mediate apoptosis by D-galactosamine in a primary culture of rat hepatocytes: exacerbation of cell death by cocultured Kupffer cells. *Can J Gastroenterol* 2002; **11**: 791-799
21 **Hsu CM**, Wang JS, Liu CH, Chen LW. Kupffer cells protect liver from ischemia-reperfusion injury by an inducible nitric oxide synthase-dependent mechanism. *Shock* 2002; **4**: 280-285
22 **Liu TH**, Robinson EK, Helmer KS, West SD, Castaneda AA, Chang L, Mercer DW. Does upregulation of inducible nitric oxide synthase play a role in hepatic injury? *Shock* 2002; **6**: 549-554
23 **Rhee JE**, Jung SE, Shin SD, Suh GJ, Noh DY, Youn YK, Oh SK, Choe KJ. The effects of antioxidants and nitric oxide modulators on hepatic ischemic-reperfusion injury in rats. *J Korean Med Sci* 2002; **4**: 502-506
24 **Koti RS**, Seifalian AM, McBride AG, Yang W, Davidson BR. The relationship of hepatic tissue oxygenation with nitric oxide metabolism in ischemic preconditioning of the liver. *FASEB J* 2002; **12**: 1654-1656
25 **Hahn PY**, Yoo P, Ba ZF, Chaudry IH, Wang P. Upregulation of Kupffer cell beta-adrenoceptors and cAMP levels during the late stage of sepsis. *Biochim Biophys Acta* 1998; **3**: 377-384
26 **Renard P**, Raes M. The proinflammatory transcription factor NFkappaB: a potential target for novel therapeutical strategies. *Cell Biol Toxicol* 1999; **15**: 341-344
27 **Kirillova I**, Chaisson M, Fausto N. Tumor necrosis factor induces DNA replication in hepatic cells through nuclear factor kappaB activation. *Cell Growth Differ* 1999; **12**: 819-828
28 **Murr MM**, Yang J, Fier A, Gallagher SF, Carter G, Gower WR Jr, Norman JG. Regulation of Kupffer cell TNF gene expression during experimental acute pancreatitis: the role of p38-MAPK, ERK1/2, SAPK/JNK, and NF-kappaB. *J Gastrointest Surg* 2003; **1**: 20-25
29 **Hong F**, Jaruga B, Kim WH, Radaeva S, El-Assal ON, Tian Z, Nguyen VA, Gao B. Opposing roles of STAT1 and STAT3 in T cell-mediated hepatitis: regulation by SOCS. *J Clin Invest* 2002; **10**: 1503-1513
30 **Kawada N**, Uoya M, Seki S, Kuroki T, Kobayashi K. Regulation by cAMP of STAT1 activation in hepatic stellate cells. *Biochem Biophys Res Commun* 1997; **2**: 464-469

Edited by Zhu LH and Wang XL

P.O.Box 2345, Beijing 100023,China
Fax: +86-10-85381893
E-mail: wjg@wjgnet.com www.wjgnet.com

World J Gastroenterol 2003;9(11):2523-2527
World Journal of Gastroenterology
 ISSN 1007-9327

• BASIC RESEARCH •

Gene and protein expressions of p28^{GANK} in rat with liver regeneration

Jian-Min Qin, Xiao-Yong Fu, Shen-Jing Li, Shu-Qin Liu, Jin-Zhang Zeng, Xiu-Hua Qiu, Meng-Chao Wu, Hong-Yang Wang

Jian-Min Qin, Xiao-Yong Fu, Shen-Jing Li, Shu-Qin Liu, Jin-Zhang Zeng, Xiu-Hua Qiu, Meng-Chao Wu, Hong-Yang Wang, International Co-operation Laboratory on Signal Transduction, Eastern Hepatobiliary Surgery Institute, Second Military Medical University, Shanghai, 200438, China
Correspondence to: Dr. Hong-Yang Wang, International Co-operation Laboratory on Signal Transduction, Eastern Hepatobiliary Surgery Institute, Second Military Medical University, Shanghai, 200438, China. hywangk@online.sh.cn
Telephone: +86-21-25070846 **Fax:** +86-21-65566851
Received: 2002-12-22 **Accepted:** 2003-02-11

Abstract

AIM: To observe the gene and protein expression changes of p28^{GANK} in regenerating liver tissues, and to reveal the biological function of p28^{GANK} on the regulation of liver regeneration.

METHODS: One hundred and thirty two adult male Sprague-Dawley rats were selected, weighing 200-250 g, and divided randomly into sham operation (SO) group and partial hepatectomy (PH) group. Each group had eleven time points: 0, 2, 6, 12, 24, 30, 48, 72, 120, 168 and 240 h, six rats were in each time point. The rats were undergone 70 % PH under methoxyflurane anesthesia by resection of the anterior and left lateral lobes of the liver. SO was conducted by laparotomy plus slight mobilization of the liver without resection. Liver specimens were collected at the indicated time points after PH or SO. The expression level of p28^{GANK} mRNA was determined by Northern blot as well as at protein level via immunohistochemical staining. The expressions of p28^{GANK} mRNA in these tissues were analyzed by imaging analysis system of FLA-2000 FUJIFILM and one way analysis of variance. The protein expressions of p28^{GANK} in these tissues were analyzed with Fromowitz' method and Rank sum test.

RESULTS: The expression of p28^{GANK} mRNA in the regenerating liver tissues possessed two transcripts, which were 1.5 kb and 1.0 kb. There was a significantly different expression patterns of p28^{GANK} mRNA between SO and PH groups (P<0.01). The expression of p28^{GANK} mRNA increased 2 h after PH, the peak time was 72 h (SO group: 163.83±1.4720; PH group: 510.5±17.0499, P<0.01). There was a significant difference in the 1.5 kb transcript, which decreased gradually after 72 hours. The protein expression of p28^{GANK} was mainly in the cytoplasm of regenerating hepatocytes, and increased near the central region 24 h after PH, and became strongly positive at 48 h (+++, *vs* the other time points P<0.05), but decreased 72 h after PH.

CONCLUSION: The expression of p28^{GANK} mRNA increases in the early stage of rat liver regeneration, the protein expression of p28^{GANK} is mainly in the cytoplasm of regenerating liver cells. It suggests that the gene of p28^{GANK} may be an important regulatory and controlled factor involved in hepatocyte proliferation during liver regeneration.

Qin JM, Fu XY, Li SJ, Liu SQ, Zeng JZ, Qiu XH, Wu MC, Wang HY. Gene and protein expressions of p28^{GANK} in rat with liver regeneration. *World J Gastroenterol* 2003; 9(11): 2523-2527
http://www.wjgnet.com/1007-9327/9/2523.asp

INTRODUCTION

Liver regeneration after 70 % partial hepatectomy in an adult rat involves initiation of proliferation of the remaining parenchymal cells and is a useful model for studying signaling molecules and other factors involved in cell proliferation. Cell proliferation begins very early during liver regeneration, peaking at 24 hours, followed by proliferating biliary epithelium at 48 hours, and kupffer cells and stellate cells at 72 hours. The proliferation of sinusoidal endothelial cells was peaked at 96 hours. Through its regenerative ability, the liver provides a model system for *in vivo* study of cell proliferation events following reentry into the cells cycle from the quiescent G_0 phase. The damage caused by surgical resection or treatment with toxins results in a cascade of growth factors and cytokines to restore the liver mass to its original size[1-6]. The residual hepatic parenchymal cells and nonparenchymal cells can proliferate and differentiate through the action of some cytokines, hormones and growth factors. When liver regeneration is induced by partial hepatectomy or inflammation, the cell cycle can transit from G_0 phase to G_1 phase, enter into the preparing stage of division and proliferation, and then into S phase, G_2 phase and M phase in turn. The late G_1 phase contains a restriction point (R point), which has a selective division function and decides cell entry into S phase or reverse to G_0 phase. The hepatic parenchymal and nonparenchymal cells can reconstitute the hepatic volume when they proliferate to some extent, and the liver regenerating response can be terminated by some factors[1,7,8], but the mechanisms of initiation and termination of liver regeneration have not been eventually clarified and need further study. Recently, a novel gene named *gankyrin* was cloned and identified from human hepatocellular carcinoma[9]. The *gankyrin* gene sequence is identical to one subunit of 26S proteasome named *p28* which was firstly cloned from human cDNA library by comparing a subunit amino acid of purified bovine erythrocyte PA700 complex (also defined as 19S complex) with protein structure of human protein cDNA library databases. The product of *gankyrin* or *p28* gene (p28^{GANK} protein) was an oncoprotein consisting of six conservative ankyrin repeats. The mRNA and protein level of p28^{GANK} increased substantially in hepatocellular carcinomatous tissues, compared with levels in the respective non-cancerous portion of the resected livers, but the increase was not related to the grade or stage of the cancer. The finding that the increase occurred regardless of the staging or grading of cancer indicates that p28^{GANK} may be involved in an early and essential step of liver carcinogenesis. However, the liver regeneration is involved in hepatocyte division, proliferation and termination. It is unclear whether p28^{GANK} can participate in hepatocyte proliferation. This study was intended to disclose the biological function of p28^{GANK} by establishing a liver regeneration rat

model and determining the expression of p28^{GANK} mRNA and protein levels.

MATERIALS AND METHODS

Experimental animal

One hundred and thirty two adult male Sprague-Dawley rats were obtained from the Experimental Animal Center of the Second Military Medical University, weighing from 200-250 g, and were randomly divided into sham operation (SO) group and partial hepatectomy (PH) group. Each group had eleven time points: 0, 2, 6, 12, 24, 30, 48, 72, 120, 168 and 240 h, six rats in each time point. The rats were housed in a room at 21 ℃ under a 12 -hour light/dark cycle and given tap water and commercial rat chow. The animals were acclimatized to the laboratory conditions for 1 week prior to the experiments.

Establishment of liver regenerating model

The rats were undergone 70 % PH under methoxyflurane anesthesia by resection of the anterior and left lateral lobes of the liver[10]. SO was undertaken only by laparotomy plus slight mobilization of the liver without resection. The rats were injected intraabdominally with 0.5-1 ml normal saline for fluid resuscitation after operation. Liver specimens were collected at 0, 2, 6, 12, 24, 30, 48, 72, 120, 168 and 240 h after PH or SO. The liver specimens obtained were snap frozen in liquid nitrogen. Total RNA was extracted using the guanidine isothiocyanate and phenol-chloroform method and aliquots of RNA samples were stored at -85 ℃ until use. The remaining liver was fixed in 4 % formaldehyde polymerisatum, embedded in paraffin and then sectioned for histological examination and analysis of protein expression.

Cloning of rat p28^{GANK} cDNA

The rat p28^{GANK} cDNA was cloned from rat placenta based on the GenBank (Rattus novegicus mRNA for p28^{GANK} homologue: AB022014), sense (11 bp-30 bp, G1): 5' -GTGTGTCTAACCTAATGGTC-3' , anti-sense (643bp-662 bp, G2): 5' -TTGAGTATTAACCCCAGGCC-3' . The segment length was 651 bp. The primers were synthesized by Sangon Company, Shanghai, P.R.China. Briefly, 5 μg of total RNA extracted from rat placenta served as template to synthesize the first strand cDNA. Polymerase chain reaction system was consisted of 1×buffer, 1.5 mM $MgCl_2$, 200 μM dNTPs, 0.5 μM of the oligonucleotide primers specific for rat p28^{GANK} gene, 1 μl of the first strand cDNA synthesized as described above, and 1.25 units of Taq DNA polymerase. Amplification was undertaken by initial denaturation at 94 ℃ for 4 min, followed by 30 reaction cycles (for 50 s at 94 ℃, for 50 s at 53 ℃, and for 60 s at 72 ℃) and a final cycle at 72 ℃ for 10 min. The PCR product with an expected size of 651 bp fractionated on a 2 % agarose gel was purified with QIAQUICK gel extract kit (QIAGEN, Germany) and subcloned into PMD18 vector[11], and then sequenced and compared. The synthetic segment was verified the same sequence as the GenBank.

Northern blot analysis

Rat p28^{GANK} cDNA released from PMD18 vector was labeled with α-^{32}P-dCTP using Promega-gene labeling system (Promega, USA) according to the protocol of the manufacturer[12]. 90 μg of total RNAs was separated on a 1 % formaldehyde/agarose gel by electropherosis, transferred to nitrocellulose and hybridized with α-^{32}P-labeled p28^{GANK} cDNA[13]. The hybridized nitrocellulose filters were exposed to X-ray film at -80 ℃ for 2 weeks. The developed signals were assayed for p28^{GANK} mRNA expression level after normalizion with 18S rRNA as internal standard using FujiFilm image gauge V3.3 analysis software (FujiFilm, Japan).

Immunohistochemistry

Immunohistochemical assay was performed as described by the manufacturer using SP kit (Dako Reagent, Denmark). Briefly, the rat liver sections of four-micrometer were deparaffnized, followed by blockage of endogenous peroxidase activity and restoration of the interested antigens. The sections were then subjected to incubation with purified primary polyclonal antibody (1:50 dilution, obtained from signal transduction laboratory, Shanghai, China) against p28^{GANK} protein at 4 ℃ overnight and with horseradish peroxidase-biotinylated anti-rabbit IgG at 37 ℃ for 30 min. The sections were finally incubated with benzidine and counterstained with hematoxylin for examination. The experiment was performed on control sections with omission of the primary antibody in the same way. The expression of p28^{GANK} was analyzed comprehensively by the staining extent and range referring to Fromowitz standard[14]. 5 visual fields were observed randomly, 100 cells were counted in each visual field. The average number of stained cells in 5 visual fields was regarded as the percent ratio of positively stained cells in each section. Positive range score: 0, 0-5 %; 1, 6-25 %; 2, 26-50 %; 3, 51-75 %; 4, >75 %. Positive extent score: 0, no staining; 1, light yellow; 2, brown; 3, dark brown. Judged by positive range score plus positive extent score: <2, negative (-); 2-3, slight positive (+); 4-5, moderately positive (++); 6-7, strongly positive (+++).

Statistical analysis

The expression level of p28^{GANK} mRNA detected by Northern Blot was presented as mean ± SD. ANOVA software (SPSS 8.0) was used to analyze the difference in mRNA level between the groups and Rank sum test for p28^{GANK} protein assay in immunohistochemical study. *P* values less than 0.05 were considered as having significant difference.

RESULTS

The expression of p28^{GANK} mRNA in regenerating liver tissues possessed two transcripts, which were 1.5 kb and 1.0 kb respectively. There was a significant difference between SO and PH groups ($P<0.01$). The expression of p28^{GANK} mRNA increased 2 h after PH, the peak time was at 72 h (SO group: 163.83±1.4720; PH group: 510.5±17.0499, $P<0.01$). There was a significant difference in the 1.5 kb transcript, which decreased gradually after 72 hours (Figures 1-2).

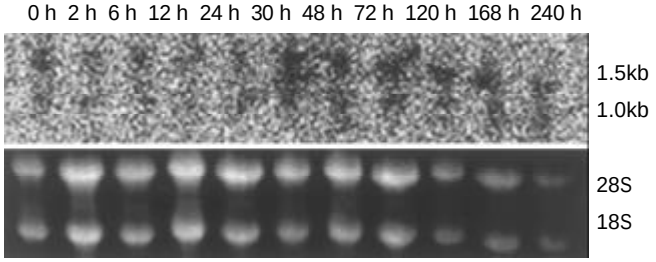

Figure 1 Northern blot of p28^{GANK} mRNA in rat regenerating liver tissues showed two transcripts of 1.5 kb and 1.0 kb. Expression level of p28^{GANK} mRNA increased 2h after PH, and reached the peak level at 72 h. More significant variation was found for 1.5 kb transcript.

The protein expression of p28^{GANK} was mainly in the cytoplasm of regenerating hepatocytes, and became increased near the central region 24 h after PH. The strongly positive expression was observed at 48 h (+++, *vs* the other time points, $P<0.05$), which decreased 72 h after PH (Figure 3).

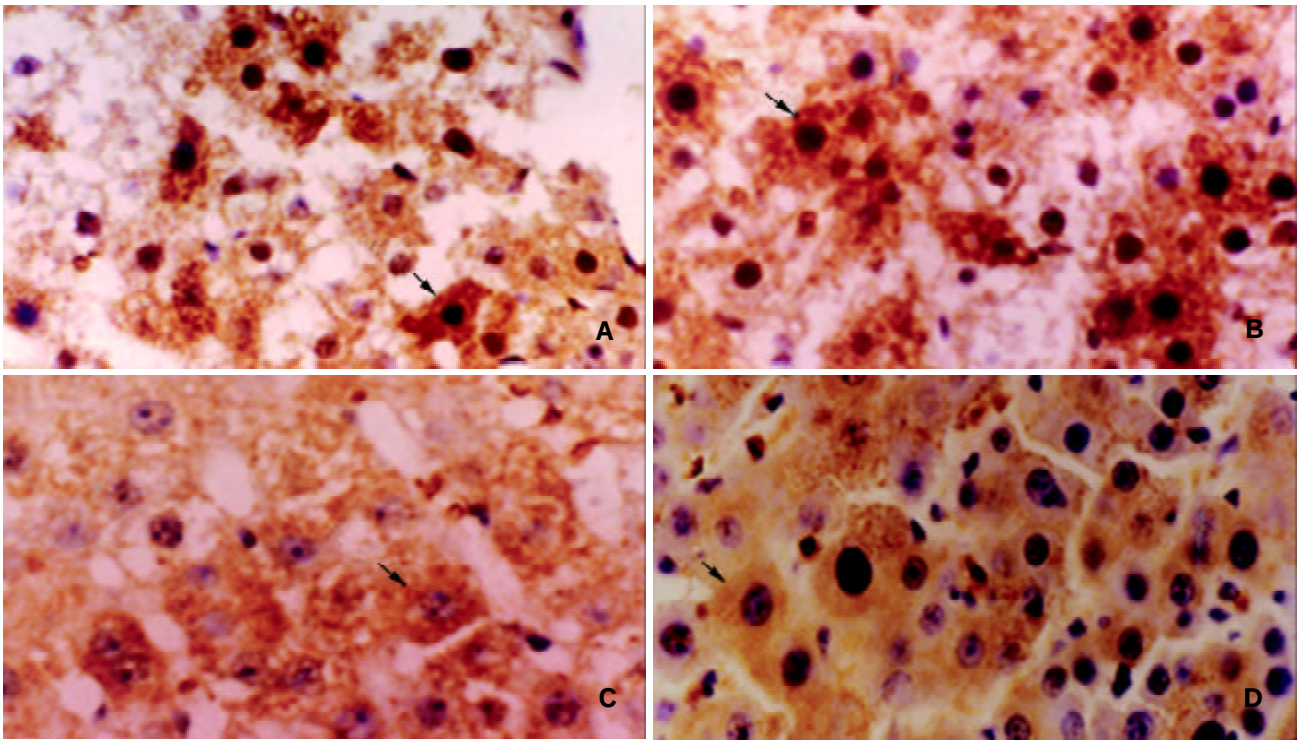

Figure 3 The expression of p28^{GANK} protein in regenerating liver tissues was examined by immunohistochemistry. A: Local brown expression of p28^{GANK} in the cytoplasm and nucleus of regenerating hepatocyte near central region 24 h after PH. IHC×400. B: Diffuse brown expression of p28^{GANK} in the cytoplasm and nucleus of regenerating hepatocyte 48 h after PH. IHC×400. C: Regional light yellow expression of p28^{GANK} in cytoplasm of regenerating hepatocyte 72 h after PH. IHC×400. D: Dispersed light yellow expression of p28^{GANK} in cytoplasm of regenerating hepatocyte 120 h after PH. IHC×400.

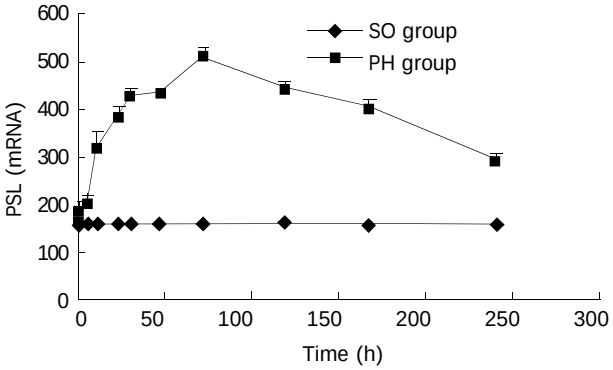

Figure 2 No significant difference of the expression of p28^{GANK} mRNA was seen in the SO group. In the PH group, the expression increased in 1.5 kb transcript 2 h after PH. The peak time was at 72 h, but gradually decreased after 72 hours.

DISCUSSION

Hepatocytes proliferate firstly according to the cascade response induced by growth factors and cytokines after hepatectomy or toxin damage. The first peak of DNA synthesis in hepatocytes occurs at about 24 hours, with a smaller peak between 36 and 48 hours. The restoration of the original number of hepatocytes theoretically requires 1.66 proliferative cycles among the residual hepatocytes. Most of the hepatocytes (95 % in the young and 75 % in very old rats) in the residual lobes participate in one or two proliferative events. The hepatocytes begin to proliferate early, the peak time is at 24 hours. Then biliary epithelial cells proliferate, the peak time is at 48 hours. Then the Kupffer cells and stellate cells proliferate and the proliferative peak is at 72 hours. The proliferative peak of sinusoidal endothelial cells is at 96 hours. Thus these cell proliferations result in restoration of the original volume[3,15]. Hepatocyte proliferation starts in the periportal zone, and then proceeds to the pericentral zone at 36 to 48 hours. The other cells of the liver enter into DNA synthesis about 24 hours after the hepatocytes proliferation, with a peak of DNA synthesis at 48 hours or later. The changes in the extracellular matrix after PH are undetectable until approximately 24 h post-PH. The hepatocytes begin to replicate in the periportal zones without corresponding increases in matrix within 3 days. The periportal areas consist of hepatocyte clusters of 10-14 cells without intervening sinusoids or matrix, as the wave of hepatocyte replication proceeds from periportal to pericentral regions of the lobule. The formation of cell clusters follows, the hepatocyte mitotic activity significantly decreases 4 days post-PH[16-20]. Liver regeneration is a complicated regulatory process, the volume and function of the liver restore after several periods. Many studies focus on the early factors associated with liver regeneration recently and on the important roles of these factors permitting the hepatocytes entering into cell division cycles. Activations of transcription factors (NF-kB and STAT3), immediately early protooncogenes (C-fos, C-myc, C-jun) and proinflammatory factors (TNF-α and IL-6) constitute the early responses to PH congenerically. The early changes play an important role in promoting the hepatocytes into cell cycles induced by hepatocytic reduction. Recruitment of early factors may be a part of ubiquitous response to stress protection and antiapoptosis of the liver, but it is unclear why the late downstream signal dissociates similar to the early response and certain time difference of cell proliferation process and atrophy or maintenance of liver size[21-24].

p28^{GANK} is a novel gene cloned and identified from human hepatocellular carcinoma and is identical to one of the PA700 non-ATPase subunits, a 700 kD multi-subunit regulatory complex of human 26S proteasome. p28^{GANK} contains six conservative ankyrin repeats, which suggests it may contribute to 26S proteasome interaction with other proteins, and its effect in hepatocellular carcinoma may be related to ubiquitin-

proteasome pathway which is often the target of cancer-related deregulation, and is involved in the processes such as oncogenic transformation, tumor progression, escape from immune surveillance and drug resistance[25-29]. The mRNA and protein levels of $p28^{GANK}$ was increased in cancerous tissues of hepatocellular carcinoma, and the increase was more substantial than that of non-cancerous tissues and was not related to the grading or staging of the tumors, indicating that $p28^{GANK}$ plays an early and crucial role in liver carcinogenesis. Moreover, the population doubling times in $p28^{GANK}$-transfected mouse NIH/3T3 cells were 18-20 hours, the control cells were 22-25 hours. All cells transfected with $p28^{GANK}$ formed colonies in soft agar, whereas the control cell did not. In homozygous nude mice, inoculation of all positive clones overexpressing $p28^{GANK}$ produced tumors within 30 days, in contrast, none of nude mice inoculated with control clone developed tumors. These results demonstrated that $p28^{GANK}$ remarkably promoted cell proliferation and was an oncogene. $p28^{GANK}$ had the retinoblastoma (RB_1)-binding motif LxCxE, resulted in an increased amount of the hyperphosphorylated form of RB_1, and accelerated the degradation of RB_1, activated the E2F transcription factors of nuclear partners of RB_1 by increasing the phosphorylation of RB_1, and induced the growth and oncogenity of anchoring independent cells. RB_1 exerts its growth-inhibitory effects in part by binding to and inhibiting essential regulatory proteins, including members of the E_2F family of transcription factors. E_2F is selectively associated with hypophosphorylated RB_1. Inactivation of RB_1 by phosphorylation, mutation or binding to viral oncoprotein seems to release E2F from an inhibitory complex, enabling it to promote the transcription of genes necessary for progression into late G_1 and S phases. $p28^{GANK}$ could bind to S6ATPase of the 26S proteasome and RB_1, increase E_2F activity and destabilize RB_1. It was demonstrated that $p28^{GANK}$ was a cellular protooncogene whose functions were more similar to those of the viral oncoprotein E_7 and related to protein degradation by 26S proteasome. Furthermore, ubiquitin-proteasome pathway played an important role in regulating cell growth and oncogenic transformation[9,30-34].

$p28^{GANK}$, as a positive cell proliferation regulatory factor, could promote cell proliferating process. We found that the expression of $p28^{GANK}$ mRNA was not significantly different at indicated times in control liver tissues during liver regeneration, but the expression of $p28^{GANK}$ mRNA possessed two transcripts in regenerating liver tissues after 70 % PH, about 1.5 kb and 1.0 kb. The mRNA level of $p28^{GANK}$ increased at 2 h, with a peak time at 72 h, but decreased gradually after 72 h, especially in the 1.5 kb transcript. The protein expression of $p28^{GANK}$ was mainly in the cytoplasm of the regenerating hepatocytes, strongly positive local expression of $p28^{GANK}$ in the cytoplasm and nucleus of regenerating hepatocyte near the central region at 24 h after 70 % PH, strongly positive diffuse expression of $p28^{GANK}$ in the cytoplasm and nucleus of regenerating hepatocyte at 48 h, and the expression of $p28^{GANK}$ decreased gradually at 72 h. These demonstrated the mRNA and protein levels of $p28^{GANK}$ occurred a curved changes, because three mitotic replicative waves occurred from 18 to 72 h, the two peak times occurred at 24 h and 36-38 h. Moreover, the two peak times of DNA synthesis occurred at 24 h and 36-48 h. All these suggest that $p28^{GANK}$ might be involved in the whole process of hepatocyte proliferation and the expression of $p28^{GANK}$ restores to its basic level with the termination of liver regeneration. It is necessary to be studied further whether it is the effect of $p28^{GANK}$ on hepatocyte proliferation through S6ATPase-$p28^{GANK}$-Rb-E2F1 pathway or through other pathways during liver regeneration and interaction with positive or negative cytokines, protooncogenes and anti-oncogenes associated with liver regeneration.

REFERENCES

1 **Stolz DB**, Mars WM, Petersen BE, Kim TH, Michalopoulos GK. Growth factor signal transduction immediately after two-thirds partial hepatectomy in the rat. *Cancer Res* 1999; **59**: 3954-3960

2 **Panis Y**, Lomri N, Emond JC. Early gene expression associated with regeneration is intact after massive hepatectomy in rats. *J Surg Res* 1998; **79**: 103-108

3 **Michalopoulos GK**, DeFrances MC. Liver regeneration. *Science* 1997; **276**: 60-66

4 **Widmann JJ**, Fahimi HD. Proliferation of mononuclear phagocytes (kupffer cells) and endothelial cells in regenerating rat liver. Alight and electron microscopic cytochemical study. *Am J Pathol* 1975; **80**: 349-366

5 **Tanaka Y**, Mak KM, Lieber CS. Immunohistochemical detection of proliferating lipocytes in regenerating rat liver. *J Pathol* 1990; **160**: 129-134

6 **Cressman DE**, Greenbaum LE, DeAngelis RA, Ciliberto G, Furth EE, Poli V, Taub R. Liver failure and defective hepatocyte regeneration in interleukin-6 –deficient mice. *Science* 1996; **274**: 1379-1383

7 **Taub R**. Blocking NF-kappa B in the liver:the good and bad news. *Hepatology* 1998; **27**: 1445-1456

8 **Brenner DA**. Signal transduction during liver regeneration. *J Gastroenterol Hepatol* 1998; **13**(Suppl): S93-S95

9 **Higashitsuji H**, Itoh K, Nagao T, Dawson S, Nonoguchi K, Kido T, Mayer RJ, Arii S, Fujita J. Reduced stability of retinoblastoma protein by gankyrin, an oncogenic ankyrin-repeat protein overexpressed in hepatomas. *Nature Med* 2000; **1**: 96-99

10 **Higgins GM**, Anderson RM. Experimental pathology of liver: restoration of liver of the white rat following partial surgical removal. *Arch Patho* 1931; **12**: 186-189

11 **Sambrook J**, Fritsh EF, Maniatis T. Molecular cloning, A Laboratory manual, 2 nd ed, New York, *Cold Spring Harbor Laboratory Press* 1989: 55

12 **Sambrook J**, Fritsh EF, Maniatis T. Molecular cloning, A Laboratory manual, 2 nd ed, New York, *Cold Spring Harbor Laboratory Press* 1989: 502

13 **Sambrook J**, Fritsh EF, Maniatis T. Molecular cloning, A Laboratory manual, 2 nd ed, New York, *Cold Spring Harbor Laboratory Press* 1989: 363

14 **Fromowitz FB**, Voila MV, Chao S, Oravez S, Mishriki Y, Finkel G, Grimson R, Lundy J. Ras P21 expression in the progression of breast cancer. *Hum Pathol* 1987; **18**: 1268-1275

15 **Della Fazia MA**, Pettirossi V, Ayroldi E, Riccardi C, Magni MV, Servillo G. Differential expression of CD44 isoforms during liver regeneration in rats. *J Hepatol* 2001; **34**: 555-561

16 **Gressner AM**. Cytokines and cellular crosstalk involved in the activation of fat-storing cells. *J Hepatol* 1995; **22**: 28-36

17 **Diehl AM**, Rai RM. Regulation of signal transduction during liver regeneration. *FASEB J* 1996; **10**: 215-227

18 **Block GD**, Locker J, Bowen WC, Petersen BE, Katyal S, Strom SC, Riley T, Howard TA, Michalopoulos GK. Population expansion, clonal growth, and specific differentiation patterns in primary cultures of hepatocytes induced by HGF/SF, EGF and TGF alpha in a chemically defined (HGM) medium. *J Cell Biol* 1996; **132**:1133-1149

19 **Sargent LM**, Sanderson ND, Thorgeirsson SS. Ploidy and karyotypic alterations associated with early events in the development of hepatocarcinogenesis in transgenic mice harboring c-myc and transforming growth factor alpha transgenes. *Cancer Res* 1996; **56**: 2137-2142

20 **Rana B**, Mischoulon D, Xie Y, Bucher NL, Farmer SR. Cell-extracellular matrix interactions can regulate the switch between growth and differentiation in rat hepatocytes: reciprocal expression of C/EBPα and immediate-early growth response transcription factors. *Mol Cell Biol* 1994; **14**: 5858-5869

21 **Fausto N**, Laird AD, Webber EM. Role of growth factors and cytokines in hepatic regeneration. *FASEB J* 1995; **9**: 1527-1536

22 **Yamada Y**, Kirillova I, Peschon JJ, Fausto N. Initiation of liver growth by tumor necrosis factor: Deficient liver regeneration in mice lacking type I tumor necrosis factor receptor. *Proc Natl Acad Sci U S A* 1997; **94**: 1441-1446

23 **Plumpe J**, Malek NP, Bock CT, Rakemann T, Manns MP, Trautwein C. NF-κB determines between apoptosis and proliferation in hepatocytes during liver regeneration. *Am J Physiol*

Gastrointest Liver Physiol 2000; **278**: G173-G183
24 **Leu JI**, Crissey MA, Leu JP, Ciliberto G, Taub R. Interleukin-6-induced STAT3 and AP-1 amplify hepatocyte nuclear factor-1 – mediated transactivation of hepatic genes, an adaptive response to liver injury. *Mol Cell Biol* 2001; **21**: 414-424
25 **DeMartino GN**, Moomaw CR, Zagnitko OP, Proske RJ, Chu-Ping M, Afendis SJ, Swaffield JC, Slaughter CA. PA700, an ATP-dependent activator of the 20 S proteasome, is an ATPase containing multiple members of nucleotide-binding protein family. *J Biol Chem* 1994; **269**: 20878-20884
26 **Hori T**, Kato S, Saeki M, DeMartino GN, Slaughter CA, Takeuchi J, Toh-e A, Tanaka K. cDNA cloning and functional analysis of P28-(Nas6p) and P40.5(Nas7p), two novel regulatory subunits of the 26S proteasome. *Gene* 1998; **216**: 113-122
27 **Baumeister W**, Walz J, Zühi F, Seemuller E. The proteasome: paradigm of a self-compartmentalizing protease. *Cell* 1998; **92**:367-380
28 **Venkataramani R**, Swaminathan K, Marmorstein R. Crystal structure of the CDK4/6 inhibitory protein p18INK4c provides insights into ankyrin-like repeat structure/function and tumor-derived p16INK4 mutations. *Nat Struct Biol* 1998; **5**: 74-81
29 **Ciechanover A**, Laszlo A, Bercovich B, Stancovski I, Alkalay I, Ben-Neriah Y, Orian A. The ubiquitin-mediated proteolytic system: involvement of molecular chaperones, degradation of oncoproteins, and activation of transcriptional regulators. *Cold Spring Harb Symp Quant Biol* 1995; **60**: 491-501
30 **Spataro V**, Norbury C, Harris AL. The ubiquitin-proteasome pathway in cancer. *Br J Cance* 1998; **77**: 448-455
31 **Nevins JR**, Leone G, Degregori J, Jakoi L. Role of the Rb/E_2F pathway in cell growth control. *J cell physiol* 1997; **173**: 233-236
32 **Weinberg RA**. The retinoblastoma protein and cell cycle control. *Cell* 1995; **81**: 323-330
33 **Park TJ**, Kim HS, Byun KH, Jang JJ, Lee YS, Lim IK. Sequential changes in hepatocarcinogenesis induced by diethynitrosamine plus thioacetamide in Fischer 344 rats: induction of gankyrin expression on liver fibrosis, pRB degradation in cirrhosis, and methylation of P16(ink4A) exon 1 in hepatocellular carcinoma. *Mol Carcinog* 2001; **30**: 138-150
34 **Fu XY**, Wang HY, Tan L, Liu SQ, Cao HF, Wu MC. Overexpression of p28/gankyrin in human hepatocellular carcinoma and its clinical significance. *World J Gastroenterol* 2002; **8**: 638-643

Edited by Wu XN and Wang XL

P.O.Box 2345, Beijing 100023,China
Fax: +86-10-85381893
E-mail: wjg@wjgnet.com www.wjgnet.com

World J Gastroenterol 2003;9(11):2528-2532
World Journal of Gastroenterology
 ISSN 1007-9327

• BASIC RESEARCH •

Changes of CD8+CD28- T regulatory cells in rat model of colitis induced by 2,4-dinitrofluorobenzene

Wen-Bin Xiao, Yu-Lan Liu

Wen-Bin Xiao, Department of Gastroenterology, Peking University People' s Hospital, Beijing 100044, China
Yu-Lan Liu, Department of Gastroenterology, Peking University People' s Hospital, Beijing 100044, China
Supported by the National Natural Science Foundation of China, No. 30240051
Correspondence to: Dr. Yu-Lan Liu, Department of Gastroenterology, Peking University People' s Hospital, Beijing 100044, China. lanhong@public.bta.net.cn
Telephone: +86-10-68314422 Ext 5448 **Fax:** +86-10-68318386
Received: 2003-03-12 **Accepted:** 2003-06-27

Abstract

AIM: To determine the changes of CD8+ T subsets especially CD8+CD28- T regulatory cells in rat model of experimental colitis induced by 2,4-dinitrofluorobenzene (DNFB).

METHODS: The rat model of experimental colitis was induced by enema with DNFB. Ten days later, colonic intraepithelial and splenic lymphocytes were isolated from colitis animals (n=16) and controls (n=8). The proportion of CD8+ T cells, CD8+CD28+ T cells and CD8+CD28- T regulatory cells were determined by flow cytometry.

RESULTS: The model of experimental colitis was successfully established by DNFB that was demonstrated by bloody diarrhea, weight loss and colonic histopathology. The proportion of CD8+ T cells in either splenic or colonic intraepithelial lymphocytes was not significantly different between colitis animals and controls (spleen: 34.6±7.24 % *vs* 33.5±9.41 %, colon: 14.0±8.93 % *vs* 18.0±4.06 %, P>0.05). But CD8+CD28- T regulatory cells from colitis animals were significantly more than those from controls (spleen: 11.3±2.26 % *vs* 5.64±1.01 %, colon: 6.50±5.37 % *vs* 1.07±0.65 %, P<0.05). In contrast, CD8+CD28+ T cells from colitis animals were less than those from controls (spleen: 23.3±6.14 % *vs* 27.8±9.70 %, P=0.06; colon: 7.52±4.18 % *vs* 16.9±4.07 %, P<0.05). The proportion of CD8+CD28- T regulatory cells in splenic and colon intraepithelial CD8+ T cells from colitis animals was higher than that from controls (spleen: 33.3±5.49 % *vs* 18.4±7.26 %, colon: 46.0±14.3 % *vs* 6.10±3.72 %, P<0.005).

CONCLUSION: Experimental colitis of rats can be induced by DNFB with simplicity and good reproducibility. The proportion of CD8+CD28- T regulatory cells in rats with experimental colitis is increased, which may be associated with the pathogenesis of colitis.

Xiao WB, Liu YL. Changes of CD8+CD28- T regulatory cells in rat model of colitis induced by 2,4-dinitrofluorobenzene. *World J Gastroenterol* 2003; 9(11): 2528-2532
http://www.wjgnet.com/1007-9327/9/2528.asp

INTRODUCTION

It is well known that immune system was involved in the pathogenesis of inflammatory bowel disease(IBD)[1-4]. Several extraintestinal autoimmune phenomena are accompanying IBD and immunosuppressive agents could alleviate the disease. Abnormalities in T-cell mediated immunity have also been noted in these patients[5]. But the exact mechanism remains to be clarified. The changes in T-cell subsets were controversial in the literature and should be deeply explored[6]. Although CD8+ T cells represent a major T-cell subset, there is little information available regarding the role of CD8+ T cells in the pathogenesis of colitis. CD8+ T cells specific for an epithelial cell-derived antigen have been shown to induce intestinal inflammation. It is possible that, like CD4+ T cells, functionally distinct CD8+ T-cell subsets may coexist. Thus we discussed the changes of CD8+ T-cell subsets in experimental colitis.

Another important part of ongoing studies of IBD was to use animal model to replicate some of the clinical features of this disease entity and to explore the mechanisms of IBD[7]. One of the important lessons learned from experimental models has been that recognition of the role of T regulatory cells plays in chronic intestinal inflammation. The ability of T cells to regulate colitis was first shown by studies of Powrie *et al*, who demonstrated that OX-22^{low} T cells could suppress the colitis induced by transfer of CD4+OX22^{high} T cells[8]. In the subsequent studies, several types of regulatory T cells have been identified. The Tr1 cells were initially reported to produce IL-10 and regulate the development of colitis in CD45RB model[9]. The effectiveness of immunosuppressive drugs in IBD may be partly related to the fact that Tr1 cells can be also generated in the presence of dexamethasone and vitamin D3. CD4+CD25+ T regulatory cells also have been demonstrated to prevent colitis in the CD45RB model[10]. A recent human study also showed that CD8+ CD28- T cells activated by the interaction with intestinal epithelial cells through gp-180 possessed a regulatory activity[11], which perhaps played important roles in the pathogenesis of colitis. However, until now there is no study reported about the roles of CD8+CD28- T regulatory cells in colitis.

In previous studies, several models of experimental colitis have been described such as TNBS, DDS, DNCB and CD45RB T-cell infusion. 2,4-dinitrofluorobenzene (DNFB) - inducing experimental colitis in mice was demonstrated to be a suitable cell-immune model[12-14]. Thus we have established the same model in rats to explore the changes in CD8+ T cell subsets especially CD8+CD28- T regulatory cells and their possible roles in the pathogenesis of DNFB-induced experimental colitis.

MATERIALS AND METHODS

Animals

Specific pathogen-free Sprague-Dawley male rats weighing 250-300 g were kept in standard laboratory conditions (room temperature of 22 ℃ with a controlled 12-hour light-dark cycle and free access to animal chow and water). Animal care was in compliance with guidelines from the Peking University Health Science Center Policy on Animal Care and Use. The rats were allowed to adapt to our laboratory environment for

one week before the onset of the experiment.

Reagents

DNFB was purchased from Acros Organics (NJ, USA), olive oil and acetone from Sigma Chemical Co. (St. Louis, Missouri, USA). Mouse anti-rat PE-conjugated-CD8b mAb (clone 341, Mouse IgG1) and FITC-conjugated-CD28 mAb (clone JJ319, Mouse IgG1) were from Serotec (Oxford, UK). Isotype control PE-conjugated mouse IgG1 and FITC-conjugated mouse IgG1 were from BD Pharmingen (San Diego, CA). RPMI 1640 and FCS were obtained from Gibco BRL (Gaithersburg, MD).

Induction of colitis

The animals in the experimental group (n=16) were pretreated with two sensitizing doses of 1 ml of 0.5 % w/v DNFB solution by rubbing the substance on previously shaved abdominal skin, 96 and 72 h before challenge[5]. The DNFB solution was prepared by diluting the original DNFB preparation with 4:1 acetone and olive oil. Freshly prepared solutions were used for each application. All the animals in the experimental group received a rectal enema with 0.4 ml of 0.2 % w/v DNFB solution in acetone and olive oil into the lumen of the colon by means of an 8-cm plastic catheter with an outer diameter of 0.9 mm, attached to a 1-ml syringe. Rectal enemas were administered under light ether anesthesia. The animals in the control group (n=8) received a rectal enema with 0.9 % w/v saline only.

Histology

Animals were killed on day 10 after the challenge enema. The entire colon was dissected, opened longitudinally, washed in ice-cold PBS. The ratio of colon / body weight was calculated, which has been shown to be a marker of colonic inflammation[15].

Macroscopic damage was assessed, according to a previously established score as follows[16]: 0: no ulcer and no inflammation, 1: no ulcer and local hyperemia, 2: ulceration without hyperemia, 3: ulceration and inflammation at one site only, 4: two or more sites of ulceration and inflammation, 5: ulceration extending more than 2 cm, 6-10: increment of 1 for each centimeter of ulceration greater than 2.

Randomized tissue samples from the site of DNFB application were subsequently excised for histology. Paraffin sections were stained with haematoxylin and eosin. Microscopic damage was quantified by image analysis of stained sections in a blinded fashion as follows[17]: 0: No evidence of inflammation. 1: Low level of lymphocyte infiltration seen in $\leqslant$10 % high power field and no structural changes observed. 2: Moderate lymphocyte infiltration seen in 10-25 % high power field and crypt elongation, bowel wall thickening that did not extend beyond the mucosal layer and no evidence of ulceration. 3: High level of lymphocyte infiltration seen in 25-50 % high power field, high vascular density, and thickening of the bowel wall that extended beyond the mucosal layer. 4: Marked degree of lymphocyte infiltration seen in $\geqslant$50 % high power field, high vascular density, crypt elongation with distortion and transmural bowel wall thickening with ulceration.

Isolation of lymphocytes

Splenocytes were isolated by conventional methods. Red blood cells were removed from spleen cell suspensions by using a standard lymphocyte gradient (Chemical Co, Shanghai, China). Intestinal intraepithelial lymphocytes were isolated according to a previously published method[18]. An average of 2-4×10^6 intraepithelial lymphocytes was yielded per colon.

Flow cytometry

A total of 1×10^6 spleen or intraepithelial lymphocytes were prepared in 100 μl and anti-CD8b and anti-CD28 mAb were added to the cell suspension. The cells were incubated at 4 ℃ for 30 min, and then the cells were washed two times with PBS/10 % v/v FCS. The cells were finally resuspended in 250 μl PBS containing 2 % w/v paraformaldehyde and then analyzed using a FACSCalibur with CellQuest software (BD Biosciences, San Jose, CA). 10 000 gated events were acquired for analysis. Isotype control was done according to the manufacturer.

Statistical analysis

Results were expressed as means ± standard deviation (SD). Comparison of results between groups was performed by unpaired t test. A probability (P) value <0.05 was considered as significant.

RESULTS

General findings

One day post-enema, diarrhea, hematochezia and reduced activity were observed in all experimental animals, but not in controls. Ten days later, the body weights of experimental animals were significantly lower than those of controls (P<0.05, as shown in Figure 1). The body weight of experimental animals decreased to the lowest on day 2 (92.8±5.0 % compared with pretreatment *vs* 106.4±1.4 % in controls, P<0.05). One rat died of colonic necrosis on the second day after DNFB enema.

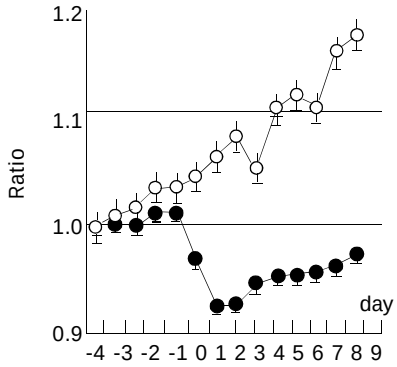

Figure 1 Body weight of experimental animals was significantly lower than that of controls (P<0.01), ○ controls, ● colitis.

Colon inflammation

The ratio of colon/body weight in experimental animals was two times more than that in controls (0.015±0.004 *vs* 0.007±0.002, P<0.05). Oedema, hemorrhage, superficial ulcerations, and necrosis were observed in the colon of experimental animals. Moreover, macroscopical characteritics of chronic phase such as adhesions, thickening of the colonic segments with narrowing of the lumen and prestenotic dilatation, atrophy and even with megacolon formation, were obviously in experimental animals but not in controls. Microscopically, active inflammatory process was characterized by mononuclear infiltration, fibrosis, smooth-muscle hypertrophy and lymphoid hyperplasia (as shown in Figure 2 left). Both the macroscopical and microscopical damage scores in experimental animals were higher than those in controls (macroscopical: 5.2±1.4 *vs* 1.4±0.6, P<0.0001; microscopical: 3.3±0.5 *vs* 1.2±0.5, P<0.0001, Figure 2 right).

Splenic CD8+ T-cell subsets

There was no difference in the proportion of CD8+ T cells between experimental animals and controls. However, CD8+CD28- T regulatory cells of experimental animals were significantly more than controls (as shown in Figure 3). Even

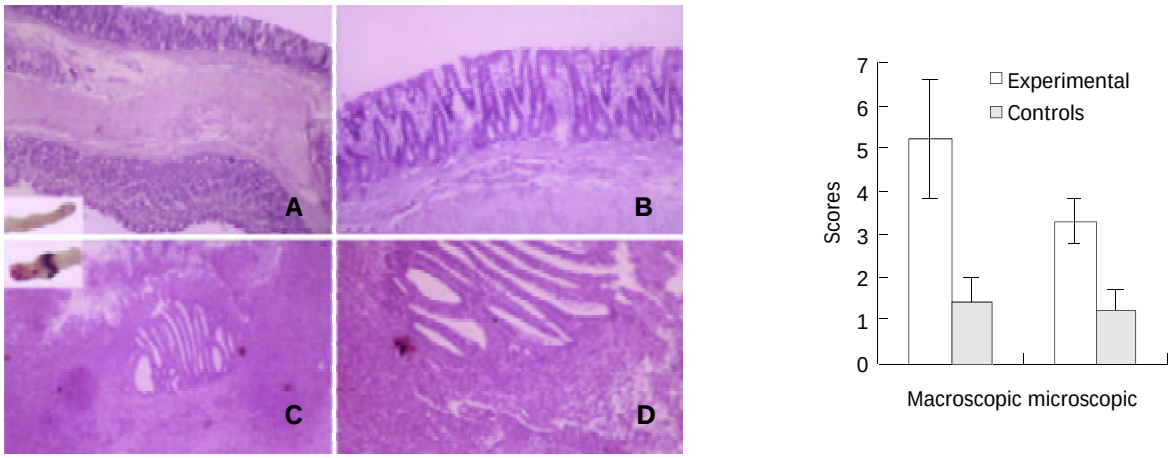

Figure 2 Left: Colon histological manifestation of experimental animals (C: 4×10, upper left is colon; D: 10×10) compared with controls (A: 4×10, lower left is colon; B: 10×10) (haematoxylin and eosin). Right: Macroscopical and microscopical damage scores in experimental animals are higher than those in controls.

Figure 3 Flow cytometry shows the proportion of CD8+CD28- T regulatory cells was 12.4 % in experimental animals (right) and 4.9 % in controls (left).

though it was not significantly, CD8+CD28+ T cells of experimental animals were less than controls. In CD8+ T cells pool, the proportion of CD8+CD28- T regulatory cells of experimental animals was also significantly higher than that of controls (as shown in Table 1).

Table 1 Splenic CD8+ T-cell subsets of experimental animals and controls on day 10 after enema

	Experimental colitis (%, *n*=16)	Control (%, *n*=8)	*P* value
CD8+CD28-T	11.3±2.26	5.64±1.01	0.0001
CD8+CD28+T	23.3±6.14	27.8±9.70	0.41
CD8+T	34.6±7.24	33.5±9.41	0.83
CD8+CD28-T/CD8+T	33.3±5.49	18.4±7.26	0.003

Table 2 Intraepithelial CD8+ T-cell subsets of experimental animals and controls on day 10 after enema

	Experimental colitis (%, *n*=16)	Control (%, *n*=8)	*P* value
CD8+CD28-T	6.50±5.37	1.07±0.65	0.049
CD8+CD28+T	7.52±3.16	16.9±4.07	0.004
CD8+T	14.0±6.83	18.0±4.06	0.38
CD8+CD28-T/CD8+T	46.0±14.3	6.10±3.72	0.0001

Intraepithelial CD8+ T-cell subsets

There was no difference in the proportion of CD8+ T cells between experimental animals and controls. However, CD8+CD28- T regulatory cells of experimental animals were significantly more than those of controls, and CD8+CD28+ T cells of experimental animals were significantly less than those of controls. In CD8+ T cells pool, the proportion of CD8+CD28- T regulatory cells of experimental animals was also significantly higher than that of controls (as shown in Table 2).

DISCUSSION

DNFB, a highly reactive compound with hapten characteristics, could bind to and covalently modify cell surface proteins, changing their antigenic conformation and their immunogenecity. T lymphocytes could recognize and lyse hapten-modified autologous cells quite efficiently in presensitized animals[19]. Thus DNFB was capable of inducing a delay-type hypersensitivity reaction when applied to the skin or to the intestinal mucosa[20]. In addition, DNFB was more reactive in protein modification than DNCB[21,22]. This is a possible explanation for DNFB causing the lesions, more pronounced in both acute phase and chronic phase than in previously described models induced by DNCB. In 1992, Banic *et al.* demonstrated that experimental colitis of mice was induced by DNFB, mimicking inflammatory bowel disease by the intestinal histopathological and extraintestinal manifestations[12-14]. It also responded well to glucorticosteroid and cyclosporine A, resembling TNBS-induced colitis[23,24]. Because of its simplicity and reproducibility this model represents a suitable preparation for investigating pathogenetic mechanisms of IBD especially that involves cellular immunity. We further explored this model in rats as the first time and the results were consistent with Banic *et al*. All morphologic changes in experimental group were similar to the changes characteristically observed in IBD in humans. Thus

experimental colitis model of rats induced by DNFB could be used to study the pathogenesis of IBD.

There is increasing evidence that IBD is a kind of autoimmune diseases. IBD could be envisioned as an imbalance between proinflammatory and anti-inflammatory cytokines[1-4]. It is suspected that changes in certain cytokines could be a result of changes in proportion or function of certain T-cell subsets. In a series study of Jewell *et al*, however, no difference was found in CD4+ and CD8+ T cells of peripheral blood and colonic mucosa between IBD and healthy controls[25-27]. Regretfully, subsets of CD4+ and CD8+ T cells were not further studied. Several studies demonstrated that T cells from IBD patients or experimental colitis model had diminished response to mitogen stimuli[28-30], and it could be recovered partially by exogenous IL-2[5]. The exact mechanism still remains unknown, but the roles of T regulatory cells should be considered[31,32]. Roman *et al*. found that CD4+CD45RO+ T cells were significantly expanded in Crohn' s disease but not in healthy controls[5], and CD4+ T regulatory cells were contained in CD4+CD45RO+ T cells[33]. The role of CD4+ T regulatory cells in pathogenesis of colitis has been studied in detail by Powrie *et al*[8]. To our knowledge, however, few studies have explored the roles of CD8+ T cells especially CD8+CD28- T regulatory cells in pathogenesis of colitis. Our study showed that the proportion of CD8+ T cells of spleen and colonic mucosa in experimental animals was not different from that in controls, which is consistent with previous findings. But we further found that there was increasing population of CD8+CD28- T regulatory cells in experimental animals compared to controls, and decreasing population of CD8+CD28+ T cells at the same time. These results have not been reported before.

CD8+ T cells comprise cells that are in different states of differentiation and under the control of complex homeostatic processes. In a number of situations such as chronic inflammatory conditions, infectious diseases, ageing, immunodeficiency, iron overload, heavy alcohol intake and transplantation, major phenotypic changes, usually associated with an increase in CD8+CD28- T cells, took place[34]. CD8+CD28- T cells are characterized by functional features of suppression. CD8+CD28- T cells could suppress alloreactive immune responses in an antigen-specific, major histocompatibility complex (MHC)-restricted manner[35].

The emergence of expanded CD8+CD28- T-cell clones has been ascribed to extensively continuous or repeated antigenic stimulation leading to immune exhaustion, as suggested by the accumulation of such cells in patients with human immunodeficiency virus (HIV) infection and autoimmune disease. Although the nature of the signals that give origin to this T-cell subset is uncertain, growing evidence argues for the existence of an interplay between epithelial cells, molecules with the MHC-class I fold and CD8+ T cells. By stimulation of antigen especially intestinal epithelial cells, CD8+CD28+ T cells can further differentiate into CD8+CD28- T regulatory cells, which was a kind of ending-stage cell and could suppress the proliferation of lymphocytes[11]. Stimulated by DNFB hapten-antigen, it is possible that CD8+CD28+ T cells differentiate into CD8+CD28- T regulatory cells. Thus the changes of CD8+ T cell pools mentioned above can be explained. We suspect that the increase of CD8+CD28- T regulatory cells is a feedback to autoimmune disease and it could explain diminished response to mitogen stimuli of T cells in IBD. Further study is urgently needed to explore the function of CD8+CD28- T regulatory cells and its exact role in the pathogenesis of IBD.

REFERENCES

1 **Fiocchi C**. Inflammatory bowel disease: etiology and pathogenesis. *Gastroenterology* 1998; **115**: 182-205

2 **Podolsky DK**. Inflammatory bowel disease. *N Engl J Med* 2002; **347**: 417-429

3 **Grimm MC**. Inflammatory bowel disease and inflammatory molecules: chickens, eggs and therapeutic targets. *J Gastroenterol Hepatol* 2002; **17**: 935-937

4 **Plevy S**. The immunology of inflammatory bowel disease. *Gastroenterol Clin North Am* 2002; **31**: 77-92

5 **Roman LI**, Manzano L, De La Hera A, Abreu L, Rossi I, Alvarez-Mon M. Expanded CD4+CD45RO+phenotype and defective proliferative response in T lymphocytes from patients with Crohn's disease. *Gastroenterology* 1996; **110**: 1008-1019

6 **Hoang P**, Senju M, Lowes JR, Jewell DP. Phenotypic characterization of isolated intraepithelial lymphocytes in patients with ulcerative colitis and normal controls. *Dig Dis Sci* 1992; **37**: 1725-1728

7 **Elson CO**, Sartor RB, Tennyson GS, Riddell RH. Experimental models of inflammatory bowel disease. *Gastroenterology* 1995; **109**: 1344-1367

8 **Powrie F**, Mason D. OX-22high CD4+ T cells induce wasting disease with multiple organ pathology: prevention by the OX-22low subset. *J Exp Med* 1990; **172**: 1701-1708

9 **Groux H**, O'Garra A, Bigler M, Rouleau M, Antonenko S, de Vries JE, Roncarolo MG. A CD4+ T cell subset inhibits antigen-specific T-cell responses and prevents colitis. *Nature* 1997; **389**: 737-742

10 **Read S**, Malmstrom V, Powrie F. Cytotoxic T lymphocyteassociated antigen 4 plays an essential role in the function of CD25+CD4+regulatory cells that control intestinal inflammation. *J Exp Med* 2000; **192**: 295–302

11 **Allez M**, Brimnes J, Dotan I, Mayer L. Expansion of CD8+ T cells with regulatory function after interaction with intestinal epithelial cells. *Gastroenterology* 2002; **123**: 1516-1526

12 **Brkic T**, Banic M, Anic B, Grabarevic Z, Rotkvic I, Artukovic B, Duvnjak M, Sikiric P, Troskot B, Hernandez DE. A model of inflammatory bowel disease induced by 2,4-dinitrofluorobenzene in previously sensitized BALB-c mice. *Scand J Gastroenterol* 1992; **27**: 184-188

13 **Anic B**, Brkic T, Banic M, Heinzl R, Dohoczky C, Smud D, Rotkvic I, Buljevac M. Histopathologic features of T-cell mediated colonic injury induced with 2,4-dinitrofluorobenzene in BALB/c mice. *Acta Med Croatica* 1997; **51**: 11-14

14 **Banic M**, Anic B, Brkic T. Animal models of inflammatory bowel disease. *Acta Med Croatica* 1997; **51**: 37-40

15 **Rolandelli RH**, Saul SH, Settle RG, Jacobs DO, Trerotola SO, Rombeau JL. Comparison of parenteral nutrition and enteral feeding with pectin in experimental colitis in the rat. *Am J Clin Nutr* 1988; **47**: 715-721

16 **Wallace JL**, Keenan CM. An orally active inhibitor of leukotriene synthesis accelerates healing in a rat model of colitis. *Am J Physiol* 1990; **258**(4 Pt1): G527-534

17 **Neurath MF**, Fuss I, Kelsall BL, Stuber E, Strober W. Antibodies to interleukin 12 abrogate established experimental colitis in mice. *J Exp Med* 1995; **182**: 1281-1290

18 **Davies MD**, Parrott DM. Preparation and purification of lymphocytes from the epithelium and lamina propria of murine small intestine. *Gut* 1981; **22**: 481-488

19 **Miller SD**. Suppressor T cell circuits in contact sensitivity. II. Induction and characterization of an efferent-acting, antigen-specific, H-2-restricted, monoclonal T cell hybrid-derived suppressor factor specific for DNFB contact hypersensitivity. *J Immunol* 1984; **133**: 3112-3120

20 **Hirashima M**, Sakata K, Tashiro K, Yoshimura T, Hayashi H. Dexamethasone suppresses concanavalin A-induced production of chemotactic lymphokines by releasing a soluble factor from splenic T lymphocytes. *Immunology* 1985; **54**: 533-540

21 **Rabin BS**, Rogers SJ. A cell-mediated immune model of inflammatory bowel disease in the rabbit. *Gastroenterology* 1978; **75**: 29-33

22 **Glick ME**, Falchuk ZM. Dinitrochlorobenzene-induced colitis in the guinea-pig: studies of colonic lamina propria lymphocytes. *Gut* 1981; **22**: 120-125

23 **Banic M**, Brkic T, Anic B, Rotkvic I, Grabarevic Z, Duvnjak M, Troskot B, Mihatov S. Effect of methylprednisolone on small bowel, spleen and liver changes in a murine model of inflammatory bowel disease. *Aliment Pharmacol Ther* 1993; **7**: 201-206

24 **Banic M**, Anic B, Brkic T, Ljubicic N, Plesko S, Dohoczky C, Erceg D, Petrovecki M, Stipancic I, Rotkvic I. Effect of

cyclosporine in a murine model of experimental colitis. *Dig Dis Sci* 2002; **47**: 1362-1368

25 **Selby WS**, Jewell DP. T lymphocyte subsets in inflammatory bowel disease: peripheral blood. *Gut* 1983; **24**: 99-105

26 **Selby WS**, Janossy G, Bofill M, Jewell DP. Intestinal lymphocyte subpopulations in inflammatory bowel disease: an analysis by immunohistological and cell isolation techniques. *Gut* 1984; **25**: 32-40

27 **Senju M**, Wu KC, Mahida YR, Jewell DP. Two-color immunofluorescence and flow cytometric analysis of lamina propria lymphocyte subsets in ulcerative colitis and Crohn's disease. *Dig Dis Sci* 1991; **36**: 1453-1458

28 **Davidsen B**, Kristensen E. Lymphocyte subpopulations, lymphoblast transformation activity, and concanavalin A-induced suppressor activity in patients with ulcerative colitis and Crohn's disease. *Scand J Gastroenterol* 1987; **22**: 785-790

29 **Manzano L**, Alvarez-Mon M, Vargas JA, Giron JA, Abreu L, Fernandez-Corugedo A, Roman LI, Albarran F, Durantez A. Deficient interleukin 2 dependent proliferation pathway in T lymphocytes from active and inactive ulcerative colitis patients. *Gut* 1994; **35**: 955-960

30 **Perez-Machado MA**, Espinosa LM, de la Madrigal EJ, Abreu L, Lorente GM, Alvarez-Mon M. Impaired mitogenic response of peripheral blood T cells in ulcerative colitis is not due to apoptosis. *Dig Dis Sci* 1999; **44**: 2530-2537

31 **Ilan Y**, Weksler-Zangen S, Ben-Horin S, Diment J, Sauter B, Rabbani E, Engelhardt D, Chowdhury NR, Chowdhury JR, Goldin E. Treatment of experimental colitis by oral tolerance induction: a central role for suppressor lymphocytes. *Am J Gastroenterol* 2000; **95**: 966-973

32 **Hoang P**, Dalton HR, Jewell DP. Human colonic intra-epithelial lymphocytes are suppressor cells. *Clin Exp Immunol* 1991; **85**: 498-503

33 **Singh B**, Read S, Asseman C, Malmstrom V, Mottet C, Stephens LA, Stepankova R, Tlaskalova H, Powrie F. Control of intestinal inflammation by regulatory T cells. *Immunol Rev* 2001; **182**: 190-200

34 **Arosa FA**. CD8+CD28- T cells: certainties and uncertainties of a prevalent human T-cell subset. *Immunol Cell Biol* 2002; **80**: 1-13

35 **Chang CC**, Ciubotariu R, Manavalan JS, Yuan J, Colovai AI, Piazza F, Lederman S, Colonna M, Cortesini R, Dalla-Favera R, Suciu-Foca N. Tolerization of dendritic cells by T(S) cells: the crucial role of inhibitory receptors ILT3 and ILT4. *Nat Immunol* 2002; **3**: 237-243

Edited by Zhu L and Wang XL

P.O.Box 2345, Beijing 100023,China
Fax: +86-10-85381893
E-mail: wjg@wjgnet.com www.wjgnet.com

World J Gastroenterol 2003;9(11):2533-2538
World Journal of Gastroenterology
 ISSN 1007-9327

• BASIC RESEARCH •

Ameliorative effects of sodium ferulate on experimental colitis and their mechanisms in rats

Wei-Guo Dong, Shao-Ping Liu, Bao-Ping Yu, Dong-Fang Wu, He-Sheng Luo, Jie-Ping Yu

Wei-Guo Dong, Shao-Ping Liu, Bao-Ping Yu, He-Sheng Luo, Jie-Ping Yu, Department of Gastroenterology, Renmin Hospital of Wuhan University, 238 Jiefang Road, Wuhan 430060, Hubei Province, China
Dong-Fang Wu, Department of Pharmacy, Renmin Hospital of Wuhan University, 238 Jie-fang Road, Wuhan 430060, Hubei Province, China
Supported by key Project in Scientific and Technological Researches of Hubei Province, No. 2001AA308B
Correspondence to: Professor Wei-Guo Dong, Renmin Hospital of Wuhan University, 238 Jiefang Road, Wuhan 430060, Hubei Province, China. dongwg@public.wh.hb.cn
Telephone: +86-27-88054511
Received: 2003-05-13 **Accepted:** 2003-06-02

Abstract

AIM: To investigate the ameliorative effects of sodium ferulate (SF) on acetic acid-induced colitis and their mechanisms in rats.

METHODS: The colitis model of Sprague-Dawley rats was induced by intracolon enema with 8 % (V/V) of acetic acid. The experimental animals were randomly divided into model control, 5-aminosalicylic acid therapy group and three dose of SF therapy groups. The 5 groups were treated intracolonically with normal saline, 5-aminosalicylic acid (100 mg·kg^{-1}), and SF at the doses of 200, 400 and 800 mg·kg^{-1} respectively and daily (8: 00 am) for 7 days 24 h following the induction of colitis. A normal control group of rats clystered with normal saline instead of acetic acid was also included in the study. Pathological changes of the colonic mucosa were evaluated by the colon mucosa damage index (CMDI) and the histopathological score (HS). The insulted colonic mucosa was sampled for a variety of determinations at the end of experiment when the animals were sacrificed by decapitation. Colonic activities of myeloperoxidase (MPO) and superoxide dismutase (SOD), and levels of malondialdehyde (MDA) and nitric oxide (NO) were assayed with ultraviolet spectrophotometry. Colonic contents of prostaglandin E_2 (PGE_2) and thromboxane B_2 (TXB_2) were determined by radioimmunoassay. The expressions of inducible nitric oxide synthase (iNOS), cyclo-oxygenase-2 (COX-2) and nuclear factor kappa B (NF-κB) p65 proteins in the colonic tissue were detected with immunohistochemistry.

RESULTS: Enhanced colonic mucosal injury, inflammatory response and oxidative stress were observed in the animals clystered with acetic acid, which manifested as the significant increase of CMDI, HS, MPO activities, MDA and NO levels, PGE_2 and TXB_2 contents, as well as the expressions of iNOS, COX-2 and NF-κB p65 proteins in the colonic mucosa, although the colonic SOD activity was significantly decreased compared with the normal control (CMDI: 2.9±0.6 *vs* 0.0±0.0; HS: 4.3±0.9 *vs* 0.7±1.1; MPO: 98.1±26.9 *vs* 24.8±11.5; MDA: 57.53±12.36 *vs* 9.21±3.85; NO: 0.331±0.092 *vs* 0.176±0.045; PGE_2: 186.2±96.2 *vs* 42.8±32.8; TXB_2: 34.26±13.51 *vs* 8.83±3.75; iNOS: 0.365±0.026 *vs* 0.053±0.015; COX-2: 0.296±0.028 *vs* 0.034±0.013; NF-κB p65: 0.314±0.026 *vs* 0.039±0.012; SOD: 28.33±1.17 *vs* 36.14±1.91; P<0.01). However, these parameters were found to be significantly ameliorated in rats treated locally with SF at the given dose protocols, especially at 400 mg·kg^{-1}and 800 mg·kg^{-1} doses (CMDI: 1.8±0.8, 1.6±0.9; HS: 3.3±0.9, 3.1±1.0; MPO: 63.8±30.5, 36.2±14.2; MDA: 41.84±10.62, 37.34±8.58; NO: 0.247±0.042; 0.216±0.033; PGE_2: 77.2±26.9, 58.4±23.9;TXB_2: 18.07±14.83; 15.52±8.62; iNOS:0.175±0.018, 0.106±0.019; COX-2: 0.064±0.018, 0.056±0.014; NF-κBp65: 0.215±0.019, 0.189±0.016; SOD: 32.15±4.26, 33.24±3.69; P<0.05-0.01). Moreover, a therapeutic dose protocol of 800 mg·kg^{-1} SF was observed as effective as 100 mg·kg^{-1} of 5-ASA in the amelioration of colonic mucosal injury as evaluated by CMDI and HS.

CONCLUSION: Administration of SF intracolonically may have significant therapeutic effects on the rat model of colitis induced by acetic acid enema, which was probably due to the mechanism of antioxidation, inhibition of arachidonic acid metabolism and NF-κB expression.

Dong WG, Liu SP, Yu BP, Wu DF, Luo HS, Yu JP. Ameliorative effects of sodium ferulate on experimental colitis and their mechanisms in rats. *World J Gastroenterol* 2003; 9(11): 2533-2538
http://www.wjgnet.com/1007-9327/9/2533.asp

INTRODUCTION

Inflammatory bowel disease (IBD) is a collection of chronic idiopathic inflammatory disorders of the intestine and/or colon. Although the pathophysiology of these disorders is not known with certainty, a growing body of experimental and clinical data suggested that this kind of chronic gut inflammation might be resulted from a maladjusted immune response to certain bacterial antigens[1-3]. This uncontrolled immune system activation results in a sustained overproduction of cytokines, eicosanoids, oxygen and nitrogen reactive species, which has been thought to be the major causative factors leading to intestinal and/or colonic injury and dysfunction in inflammatory bowel disease.

Based on this hypothesis, current therapeutic strategy for IBD has therefore focused on the use of anti-inflammatory agents, aminosalicylates and corticosteroids[1,4-9]. However, some notable limitations are found existing in the management of IBD patients and meanwhile some patients are refractory to these therapies. Long term use of glucocorticoids, for example, although effective in suppressing active inflammation, was associated with high rates of relapse and unacceptable toxicity[10-12]. On the other hand, 6-mercaptopurine and its prodrug azathioprine are effective in inducing and maintaining remission, however, a significant number of patients were resistant or intolerant to thiopurines[10]. All these suggest that seeking for more preferable drugs harboring better therapeutic results and less side-effects for the treatment of patients with IBD is urgently necessary.

Sodium ferulate (SF) is one of the effective components of Radix Angelica sinensis. Many researches have revealed that

SF possesses plenty of beneficial pharmacological effects such as inhibiting the production of inflammatory mediators, improving endothelial function, relieving oxidative stress and safe in use[13-18]. We presumed that SF might be a possible candidate to be used for the treatment of IBD, which to our knowledge has not been investigated in previous studies. The present study was therefore conducted to confirm our hypothesis with an effort to demonstrate the therapeutic effects of sodium ferulate on experimental colonitis.

MATERIALS AND METHODS

Animals

Healthy Sprague-Dawley rats of both sexes, weighing 250±30 g, from the Animal Center, Academy of Hubei preventive medical sciences were employed in the present study. The animals were fed on standard rat chow, allowed access to tap water *ad libitum* and acclimatized to the surroundings for one week prior to the experiments. The study protocol was in accordance with the guideline for animal research and was approved by the Ethical and Research Committee of the hospital.

Reagents

Acetic acid was obtained from Wuhan Chemical Corp. SF injection was provided by Pharmaceutical Factory of Zhongnan Hospital, Wuhan University (Lot. 20011219). 5-aminosalicylic acid (5-ASA) was purchased from Guoyi Pharmaceutical Ltd (Lot. 20029477). Polyclonal rabbit anti-rat-iNOS, COX-2 and NF-κB P65 were from Santa Cruz Company. S-P kits were obtained from Beijing Zhongshan Biological Technology CO Ltd. PGE_2 and TXB_2 radioimmunoassay kits were provided by Radioimmunity Institute of PLA General Hospital. MPO, SOD, MDA, NO detection kits were purchased from Nanjing Jiancheng Bioengineering Institute. Other reagents used in the present study were all of analytical grade.

Experimental protocol

The preparation of rat model of colitis was described in the literature[19,20]. Briefly, after rats were anesthetized with ether, a flexible plastic catheter with an outer diameter of 2 mm were inserted rectally into the colon with the aim to place the catheter tip at 8 cm proximal to the anus. Twenty seconds following enema with 2 ml of 8 % (V/V) acetic acid through the catheter, colon lumen was rinsed twice with 5 ml of normal saline. The experimental animals were randomly divided into normal control, model control, 5-aminosalicylic acid therapy and three dose SF therapy groups, and treated intracolonically with normal saline, normal saline, 5-aminosalicylic acid (100 mg· kg^{-1}), and SF 200, 400 and 800 mg· kg^{-1} respectively and daily (8: 00 am) for 7 days 24 h following the induction of colitis. Then the colon mucosa damage index (CMDI) and the histopathological score (HS) were evaluated and the colon mucosa was sampled for a variety of determinations and observations after the animals were sacrificed by decapitation.

Assessment of CMDI and HS

The colon segment taken from 10 cm proximal to anus of the sacrificed rats was excised longitudinally, rinsed by saline buffer and fixed on a wax block. CMDI and HS were assessed respectively by two independent researchers. The scoring formula for assessment of CMDI was reported in previous literature[20]. That is, 0: normal mucosa, no damage on the mucosal surface; 1: mild hyperemia and edema, no erosion or ulcer on the mucosal surface; 2: moderate hyperemia and edema, erosion appearing on the mucosal surface; 3: severe hyperemia and edema, necrosis and ulcer appearing on the mucosal surface with the major ulcerative area extending less than 1 cm; 4: severe hyperemia and edema, necrosis and ulcer appearing on the mucosal surface with the major ulcerative area extending more than 1 cm. For histopathological examination, the colonic samples were fixed in 4 % neutral buffered paraformaldehyde overnight and 4-μm thick sections were routinely prepared and stained with haematoxylin and eosin. The colonic pathological changes were observed and evaluated by two independent researchers with a modified histopathological score formula[19] as: (1) Infiltration of acute inflammatory cells: 0, without; 1, mild; 2, severe. (2) Infiltration of chronic inflammatory cells: 0, without; 1, mild; 2, severe. (3) Fibrin deposition: 0, negative; 1, positive. (4) Submucosal edema: 0, without; 1, focal; 2, diffuse. (5) Necrosis of epithelial cells: 0, without; 1, focal; 2, diffuse. (6) Mucosal ulcer: 0, negative; 1, positive.

Determination of colonic MPO, SOD activities and MDA, NO contents

For determination of colonic MPO activity, the sampled tissues were homogenized (50 g· L^{-1}) in 50 mmol· L^{-1} ice-cold potassium phosphate buffer (pH 6.0) containing 0.5 % of hexadecyltrimethylammoninm bromide. The homogenate was frozen and thawed thrice, then centrifuged at 4 000 rpm for 20 min at 4 ℃. The MPO activity in the supernatant was measured by the assay kit according to its provider' s instructions. The colonic samples for the determination of SOD activity, MDA and NO contents were homogenized in ice-cold PBS (pH 7.4) and centrifuged at 3 000 rpm for 10 min at 4 ℃. The resulting supernatant was stored at 20 ℃ until analysis with corresponding assay kits according to the manufacturer' s guide.

Measurement of colonic PGE_2 and TXB_2 level

Colonic specimens used for the assay of arachidonic acid metabolites were prepared according to the protocol by Raab *et al*[21] and Taniguchi *et al*[22], and their levels of PGE_2 and TXB_2 were measured by using the corresponding radioimmunoassay kits following the manufacturer' s instructions.

Detection of colonic iNOS, COX-2 and NF-κB p65 expression

The immunohistochemical methods for formalin-fixed and paraffin-embedded sections were described previously[23]. The determinations of colonic iNOS, COX-2 and NF-κB p65 expression were all performed with S-P technique following the recommendations of assay kit providers. Briefly, polyclonal rabbit anti-rat-iNOS, COX-2 and NF-κB p65 were diluted with PBS to 1:150, 1:120, 1:200 respectively and used as the primary antibody in the corresponding detections. For each of these determinations, dewaxed sections were incubated first with the primary antibody overnight at 4 ℃ after antigen retrieval. The binding of antibodies to their antigenic sites in the tissue sections was further amplified with biotinylated goat anti-rabbit antibody and followed by reaction with 3, 3' -diaminobenzidine. Sections prepared by substituting PBS for the primary antibody served as the negative control. iNOS, COX-2 or NF-κB p65 negatively expressed cells manifested as blue-stained nuclei while the positive cells as brown or dark brown cytoplasm and/or cell membrane. Expressions of these target proteins were semiquantitated respectively with automatic image analyzer (Nikon, Japan) and HPIAS-2000 image analyzing program, in which the average value of positive cell' s absorbance (A) in ten randomly selected high power fields (400×) for each section was used for the comparison of the target protein expressions.

Statistical analysis

Experimental results were expressed as $\bar{x}$±s. Statistical comparisons between groups were made by ANOVA followed

by Student's *t* test. *P* value less than 0.05 was considered statistically significant.

RESULTS

Inflammatory changes of the colonic mucosa

CMDI, HS and MPO activities were the main parameters for evaluating the degree of colonic inflammation in inflammatory bowel disease. Compared with the normal control, these parameters were all significantly increased in the colonic mucosa of the model control induced by acetic acid ($P<0.01$). After the model rats were treated with SF (400, 800 mg· kg^{-1}) or 5-ASA (100 mg· kg^{-1}) as described in the experimental protocol, these elevated parameters were significantly ameliorated ($P<0.05$ or 0.01) as shown in Table 1, in which a therapeutic dose protocol of 800 mg· kg^{-1} SF was observed as effective as 100 mg· kg^{-1} 5-ASA in the treatment of this rat model of colitis.

Table 1 Effects of sodium ferulate on CMDI, HS and MPO activity in the colon tissue of acetic acid-induced rats colitis (n=8, $\bar{x}\pm s$)

Group	Dose (mg·kg^{-1})	CMDI	HS	MPO (U·g^{-1})
Normal	-	0.0±0.0	0.7±1.1	24.8±11.5
Model	-	2.9±0.6^{d}	4.3±0.9^{d}	98.1±26.9^{d}
5-ASA	100	1.6±0.9^{b}	3.4±0.5^{a}	29.6±10.8^{b}
SF	200	2.0±0.8^{a}	3.6±1.2	79.5±38.4
SF	400	1.8±0.8^{b}	3.3±0.9^{a}	63.8±30.5^{a}
SF	800	1.6±0.9^{b}	3.1±1.0^{a}	36.2±14.2^{b}

$^{a}P<0.05$, $^{b}P<0.01$ *vs* model group; $^{d}P<0.01$ *vs* normal group.

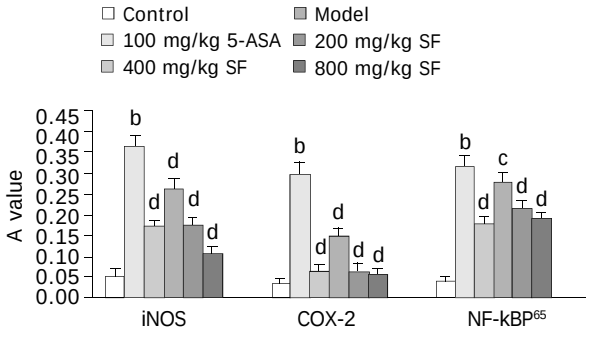

Figure 1 Effects of SF on the expressions of iNOS, COX-2 and NF-κB P65 in the colonic tissue of rats colitis induced by acetic acid (n=8, $\bar{x}\pm s$). $^{b}P<0.01$, *vs* control group; $^{c}P<0.05$, $^{d}P<0.01$, *vs* model group.

Colonic oxidative alterations

Prominent oxidative stress in colonic mucosa was induced by enema of acetic acid in the model controls as shown by the significant elevation of colonic MDA and NO contents and decrease of colonic SOD activities (Table 2). These oxidative abnormalities in colonic mucosa were obviously ameliorated by the treatment with SF at the dose protocols of 200, 400, 800 mg· kg^{-1}, which manifested as the significant reduction of colonic MDA content and the increase of SOD activity compared with the model control rats ($P<0.05$-0.01). Furthermore, a significant improvement for the elevated colonic NO content was also noted in animals treated with SF at the dose protocol of 400 or 800 mg· kg^{-1} ($P<0.05$-0.01) as shown in Table 2.

Effects of SF on the colonic PGE_2, TXB_2 levels

After the rats were insulted by enema of acetic acid, their colonic contents of PGE_2 and TXB_2 were significantly increased compared with the normal control ($P<0.01$). A significant amelioration of PGE_2 contents was observed in animals treated with SF at all dose protocols ($P<0.05$-0.01). However, significant reduction of colonic TXB_2 contents compared with the model control was only seen in rats treated with SF at the dose protocol of 400 and 800 mg· kg^{-1} ($P<0.05$-0.01) as shown in Table 3.

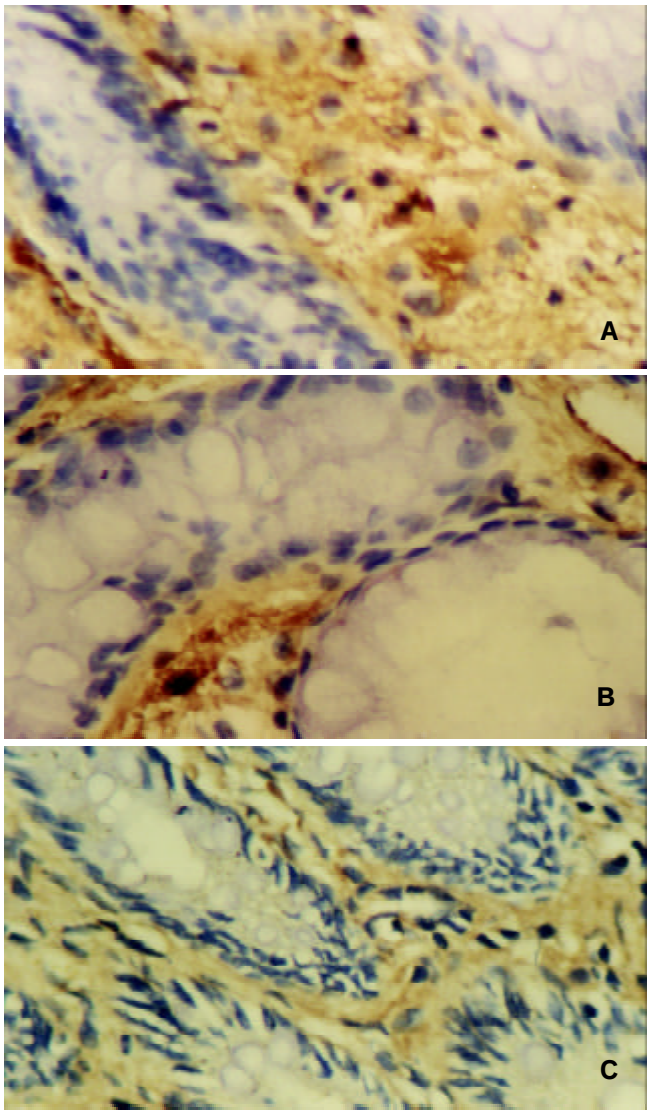

Figure 2 Expressions of iNOS (A), COX-2 (B) and NF-κB p65 (C) in the inflammatory areas of colonic tissue from rats with colitis induced by acetic acid enema, respectively. The strongly positive signal were found. SP stain ×400.

Table 2 Effects of sodium ferulate on SOD activity, MDA and NO contents in the colon tissue of acetic acid-induced rats colitis (n=8, $\bar{x}\pm s$)

Group	Dose (mg·kg^{-1})	SOD (kU·g^{-1})	MDA (nmol·g^{-1})	NO (nmol·g^{-1})
Normal	-	36.14±1.91	9.21±3.85	176±45
Model	-	28.33±1.17^{d}	57.53±12.36^{d}	331±92^{d}
5-ASA	100	32.74±3.52^{b}	31.85±11.72^{b}	244±51^{a}
SF	200	31.63±3.83^{a}	43.25±13.47^{a}	256±54
SF	400	32.15±4.26^{a}	41.84±10.62^{a}	247±42^{a}
SF	800	33.24±3.69^{b}	37.34±8.58^{b}	216±33^{b}

$^{a}P<0.05$, $^{b}P<0.01$, *vs* model group; $^{d}P<0.01$ *vs* normal group.

Table 3 Effects of sodium ferulate on the content of PGE_2 and TXB_2 in the colon tissue of acetic acid-induced rats colitis (n=8, $\bar{x}\pm s$)

Group	Dose ($mg\cdot kg^{-1}$)	PGE_2($ng\cdot g^{-1}$)	TXB_2($ng\cdot g^{-1}$)
Normal	-	42.8±32.8	8.83±3.75
Model	-	186.2±96.2[d]	34.26±13.51[d]
5-ASA	100	67.0±37.7[b]	18.53±14.26[a]
SF	200	90.7±52.3[a]	23.21±12.46
SF	400	77.2±26.9[b]	18.07±14.83[a]
SF	800	58.4±23.9[b]	15.52±8.62[b]

[a] $P < 0.05$, [b] $P < 0.01$ *vs* model group; [d] $P < 0.01$ *vs* normal group.

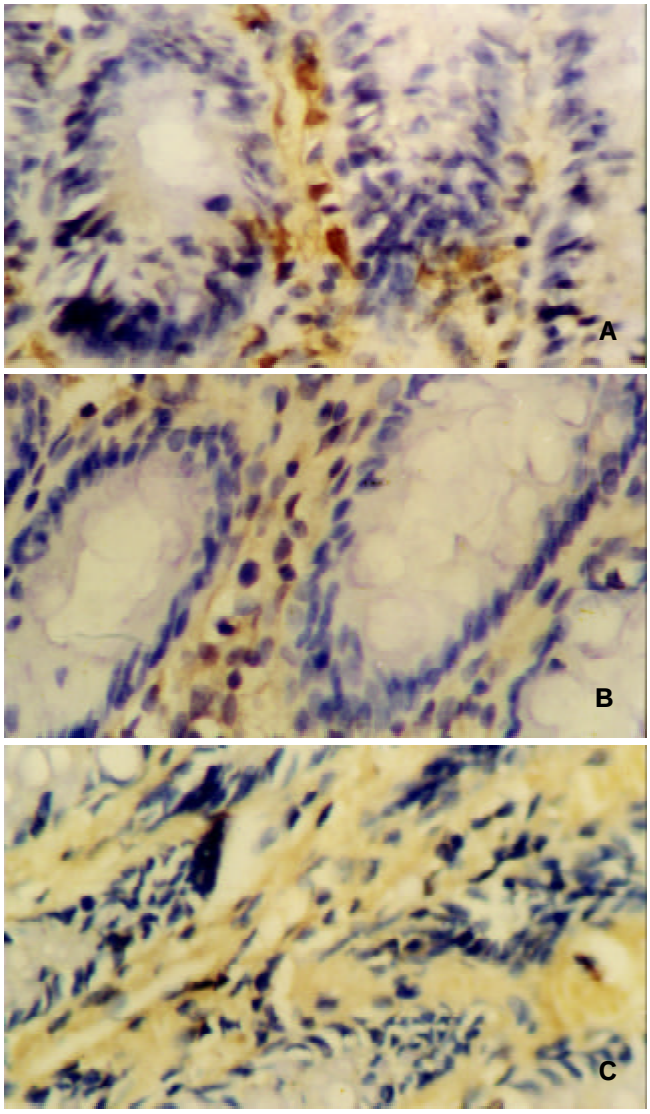

Figure 3 Expressions of iNOS (A), COX-2 (B) and NF-κB p65 (C) were significantly decreaed in the colonic tissue from rats with colitis induced by acetic acid enema after treasted with 800 $mg\cdot kg^{-1}$ ASP, respectively. The weakly positive staining could be found. SP stain ×400.

SF reduces the expression of colonic NOS, COX-2 and NF-κB p65

As shown in Figure 1, 2 and 3, the expressions of colonic NOS, COX-2 and NF-κB p65 proteins were observed to be significantly increased in animals clystered with acetic acid compared with the normal controls (P<0.01), which were ameliorated significantly in a dose-dependent manner as the animals treated with SF at the given doses (P<0.05-0.01).

DISCUSSION

Induction of colitis by acetic acid (AA) in rats is the classical method to produce an experimental model of inflammatory bowel disease (IBD). Several major causative factors in the initiation of human IBD such as exorbitant oxidative stress, enhanced vasopermeability, prolonged neutrophils infiltration and increased production of inflammatory mediators were all involved in the induction of this animal model[19,20,24]. It is therefore acknowledged nowadays that this experimental model is suitable for the investigation of IBD pathogenesis and evaluation the therapeutic agents of this disease.

In the present study, we employed this rat model to make sure whether or not the ameliorative effects of SF on the experimental colitis existed as assessed by CMDI, HS and MPO activities that were usually regarded as the main parameters to evaluate the severity of colonic inflammation in inflammatory bowel disease[19,20]. Compared with the normal control, these parameters were all significantly increased in the colonic mucosa of the model control animals induced by acetic acid (P<0.01). However, these elevated parameters were significantly ameliorated (P<0.05 or 0.01) as shown in Table 1 after the model rats were treated with SF (400, 800 $mg\cdot kg^{-1}$) or 5-ASA (100 $mg\cdot kg^{-1}$) as described in the experimental protocol, in which a therapeutic dose protocol of 800 $mg\cdot kg^{-1}$ SF was observed as effective as 100 $mg\cdot kg^{-1}$ 5-ASA in the treatment of this rat model of colitis. The results confirmed our previous speculation and strongly suggested that SF might serve as an alternative modality for the treatment of inflammatory bowel disease.

Although the pathogenesis is not known with certainty, some hypotheses have been proposed as the major causative factors contributing to inflammatory bowel disease. A large number of studies have revealed that the increase of oxidative stress and iNOS activity was a notable feature of IBD, which resulted in a pathological cascade of free radical reactions and further yielding more oxidative free radicals such as peroxynitrite ($ONOO^-$) to impair the structure and function of cells[2,25-27]. Meanwhile, excessive NO could dilate vasculature and enhance vasopermeability, as well as inactivate the activity of antioxidases such as SOD, CAT, and GSH-Px by means of reacting with hydrosulfide group (-SH) in the enzymes. Some oxidants have been known to modulate the expression of a variety of genes that are involved in the immune and inflammatory responses, which lead to the apoptosis of intestinal epithelial cells, cascades of inflammatory response and the disruption of integrity and function of the intestinal mucosa[28-30].

Abnormal metabolism of arachidonic acid is another vital factor in the IBD pathogenesis. As the crucial synthetase in the arachidonic acid metabolic pathway, COX-2 could be activated to produce excessive PGE_2 and TXB_2, two important inflammatory mediators, in the inflammatory bowel disease, which contribute to the bowel hyperemia, edema and even dysfunction. In addition, TXB_2 could also induce platelet aggregation, vasoconstriction and microthrombosis, aggravating the inflammatory reaction[31-35]. Administration of either COX-2 or thromboxane synthase inhibitors has been shown to be useful for the treatment of IBD[32-34].

Recently, plenty of literatures reported that NF-κB played a critical role in the early transcriptional changes of various immunoregulatory genes[28, 36], whose activation and increased expression have been demonstrated to be involved in the pathogenesis of inflammatory bowel disease[37]. Activated NF-κB could promote the production of various inflammatory factors, chemotaxins, cytokines, and adhesive factors, and the expression of iNOS and COX-2, which interact further with each other and lead to an uncontrollable cascade of inflammatory response[38-41]. NF-κB could also activate anti-apoptotic genes

including TNF receptor related genes (TRAF1, TRAF2), Bcl-2 homologens (A1/Bfl-1, IEX-1L), and repress the apoptosis of some inflammatory cells such as neutrophils and activated macrophages, thereby elongating and worsening tissue inflammatory injury[42-45]. In the NF-κB family, p65 is the major functional subunit, and an antisense oligonucleotide to NF-kappa B p65 has been shown to ameliorate inflammation even after induction of colitis[1].

To elucidate the mechanisms underlying the therapeutic effects of SF on this rat model of colitis, we observed simultaneously the changes of these oxidative and inflammatory variables mentioned above in the colonic tissue after SF therapy. The results revealed that the SOD activity, MDA and NO levels, PGE_2 and TXB_2 contents, as well as the expressions of iNOS, COX-2 and NF-κB p65 proteins in the colonic mucosa were significantly ameliorated in the rats treated locally with SF at the given dose protocols, especially at the 400 mg· kg^{-1} and 800 mg· kg^{-1} doses, compared with that in model control animals (P<0.05-0.01). Taken together, these observations suggest the anti-oxidative stress and anti-inflammatory response are the fundamentals of SF action in the therapy of IBD, although the ameliorating effects of SF might be involved in other multiple mechanisms.

In summary, the results of this study show that intracolonic treatment with SF at 400 mg· kg^{-1} and 800 mg· kg^{-1} dose protocols can ameliorate the pathological changes of experimental colitis in rats, which suggests that SF may serve as an effective therapeutic agent for the treatment of IBD.

REFERENCES

1 **Hibi T,** Inoue N, Ogata H, Naganuma M. Introduction and overview: recent advances in the immunotherapy of inflammatory bowel disease. *J Gastroenterol* 2003; **38**(Suppl 15): 36-42

2 **Pavlick KP,** Laroux FS, Fuseler J, Wolf RE, Gray L, Hoffman J, Grisham MB. Role of reactive metabolites of oxygen and nitrogen in inflammatory bowel disease. *Free Radic Biol Med* 2002; **33:** 311-322

3 **Lakatos L.** Immunology of inflammatory bowel diseases. *Acta Physiol Hung* 2000; **87:** 355-372

4 **Travis S.** Recent advances in immunomodulation in the treatment of inflammatory bowel disease. *Eur J Gastroenterol Hepatol* 2003; **15**: 215-218

5 **Tuvlin JA,** Kane SV. Novel therapies in the treatment of ulcerative colitis. *Expert Opin Investig Drugs* 2003; **12:** 483-490

6 **Goh J,** O'Morain CA. Nutrition and adult inflammatory bowel disease. *Aliment Pharmacol Ther* 2003; **17:** 307-320

7 **Hanauer SB.** Update on medical management of inflammatory bowel disease: ulcerative colitis. *Rev Gastroenterol Disord* 2001; **1:** 169-176

8 **Kane SV.** Novel therapies in the treatment of ulcerative colitis. *Expert Opin Investig Drugs* 2001; **10:** 1223-1229

9 **Das KM,** Farag SA. Current medical therapy of inflammatory bowel disease. *World J Gastroenterol* 2000; **6:** 483-489

10 **Schroder O,** Stein J. Low dose methotrexate in inflammatory bowel disease: current status and future directions. *Am J Gastroenterol* 2003; **98:** 530-537

11 **Holtmann MH,** Galle PR, Neurath MF. Immunotherapeutic approaches to inflammatory bowel diseases. *Expert Opin Biol Ther* 2001; **1:** 455-466

12 **Rampton DS.** Management of difficult inflammatory bowel disease: where are we now? *World J Gastroenterol* 2000; **6:** 315-323

13 **Kikuzaki H,** Hisamoto M, Hirose K, Akiyama K, Taniguchi H. Antioxidant properties of ferulic acid and its related compounds. *J Agric Food Chem* 2002; **50:** 2161-2168

14 **Ogiwara T,** Satoh K, Kadoma Y, Murakami Y, Unten S, Atsumi T, Sakagami H, Fujisawa S. Radical scavenging activity and cytotoxicity of ferulic acid. *Anticancer Res* 2002; **22:** 2711-2717

15 **Zhang ZH,** Yu SZ, Li GS, Zhao BT. Influence of sodium ferulate on human netrophil-derived oxygen metabolites. *Zhongguo Yaolixue Tongbao* 2001; **17:** 515-517

16 **Li YQ,** Zhang JS, Cai HW. Influence of sodium ferulate on MDA, SOD, ET and NO during myocardial ischemia and reperfusion injury. *Zhonghua Mazuixue Zazhi* 1998; **18:** 688-690

17 **Xu LN,** Yu WG, Tian JY, Liu QY. Effect of sodium ferulate on arachidonic acid metabolism. *Yaoxue Xuebao* 1990; **25:** 412-416

18 **Wang Z,** Gao YH, Huang RS, Zhu GQ. Sodium ferulate is an inhibitor of thromboxane A_2 synthetase. *Zhongguo Yaoli Xuebao* 1988; **9:** 430-433

19 **Millar AD,** Rampton DS, Chander CL, Claxson AW, Blades S, Coumbe A, Panetta J, Morris CJ, Blake DR. Evaluating the antioxidant potential of new treatments for inflammatory bowel disease using a rat model of colitis. *Gut* 1996; **39:** 407-415

20 **Deng CH,** Xia B, Chen DJ, Zhou Y, Gong TT, Guao ZQ. The mucosa protective effects of superoxide dismutase on rats colitis induced by acetic acid. *Zhongguo Bingli Shengli Zazhi* 1994; **10:** 23-25

21 **Raab Y,** Sundberg C, Hallgren R, Kuntson L, Gerdin B. Mucosal synthesis and release of prostaglandin E_2 from activated eosinophils and macrophages in ulcerative colitis. *Am J Gastroenterol* 1995; **90:** 614-620

22 **Taniguchi T,** Tsukada H, Nakamura H, Kodama M, Fukuda K, Tominaga M, Seino Y. Effects of a thromboxane A_2, receptor antagonist in an animal model of inflammatory bowel disease. *Digestion* 1997; **58:** 476-478

23 **Linnoila RI,** Jensen SM, Steinberg SM, Mulshine JL, Eggleston JC, Gazdar AF. Peripheral airway cell marker expression in non-small cell lung carcinoma. Association with distinct clinicopathologic features. *Am J Clin Pathol* 1992; **97:** 233-243

24 **Li L,** Wang ZL, Ke JT, Zhang M, Shao JF, Zhong CN. Select animal models for experimental colitis model. *Shijie Huaren Xiaohua Zazhi* 2001; **9:** 584-585

25 **Krieglstein CF,** Cerwinka WH, Laroux FS, Salter JW, Russell JM, Schuermann G, Grisham MB, Ross CR, Granger DN. Regulation of murine intestinal inflammation by reactive metabolites of oxygen and nitrogen: divergent roles of superoxide and nitric oxide. *J Exp Med* 2001; **194:** 1207-1218

26 **Zhou JF,** Cai D, Zhu YG, Yang JL, Peng CH, Yu YH. A study on relationship of nitric oxide, oxidation, peroxidation, lipoperoxidation with chronic chole-cystitis. *World J Gastroenterol* 2000; **6:** 501-507

27 **Wang QG,** He LY, Chen YW, Hu SL. Enzymohistochemical study on burn effect on rat intestinal NOS. *World J Gastroenterol* 2000; **6:** 421-423

28 **Jourd'heuil D,** Morise Z, Conner EM, Grisham MB. Oxidants, transcription factors, and intestinal inflammation. *J Clin Gastroenterol* 1997; **25**(Suppl 1): S61-S72

29 **Banan A,** Fields JZ, Zhang Y, Keshavarzian A. iNOS upregulation mediates oxidant-induced disruption of F-actin and barrier of intestinal monolayers. *Am J Physiol Gastrointest Liver Physiol* 2001; **280:** G1234-G1246

30 **Huycke MM,** Abrams V, Moore DR. Enterococcus faecalis produces extracelluar superoxide and hydrogen peroxide that damages colonic epithelial cell DNA. *Carcinogenesis* 2002; **23:** 529-536

31 **McCowen KC,** Ling PR, Bistrian BR. Arachidonic acid concentrations in patients with Crohn disease. *Am J Clin Nutr* 2000; **71:** 1008

32 **Carty E,** Macey M, McCartney SA, Rampton DS. Ridogrel, a dual thromboxane synthase inhibitor and receptor antagonist: anti-inflammatory profile in inflammatory bowel disease. *Aliment Pharmacol Ther* 2000; **14:** 807-817

33 **Karmeli F,** Cohen P, Rachmilewitz D. Cyclo-oxyenase-2 inhibitors ameliorate the severity of experimental colitis in rats. *Eur J Gastroenterol Hepatol* 2000; **12:** 223-231

34 **Kankuri E,** Vaali K, Korpela R, Paakkari I, Vapaatalo H, Moilanen E. Effects of a COX-2 preferential agent nimesulide on TNBS-induced acute inflammation in the gut. *Inflammation* 2001; **25:** 301-310

35 **Wu JX,** Xu JY, Yuan YZ. Effect of emodin and sandostatin on metabolism of eicosanoids in acute necrotizing pancreatitis. *World J Gastroenterol* 2000; **6:** 293-294

36 **Shi XZ,** Lindholm PF, Sarna SK. NF-kappa B activation by oxi-

dative stress and inflammation suppresses contractility in colonic circular smooth muscle cells. *Gastroenterology* 2003; **124:** 1369-1380

37 **Gan H,** Ouyang Q, Chen Y, Xia Q. Activation of nuclear factor-kappaB and effects of anti-inflammatory treatment thereon in intestinal mucosa of patients with ulcerative colitis. *Zhonghua Yixue Zazhi* 2002; **82:** 384-388

38 **Surh YJ,** Chun KS, Cha HH, Han SS, Keum YS, Park KK, Lee SS. Molecular mechanisms underlying chemopreventive activities of anti-inflammatory phytochemicals: down-regulation of COX-2 and iNOS through suppression of NF- kappa B activation. *Mutat Res* 2001; **480-481:** 243-268

39 **Yamamoto Y,** Gaynor RB. Therapeutic potential of inhibition of the NF-kappaB pathway in the treatment of inflammation and cancer. *J Clin Invest* 2001; **107:** 135-142

40 **Jobin C,** Sartor RB. NF-kappaB signaling proteins as therapeutic targets for inflammatory bowel diseases. *Inflamm Bowel Dis* 2000; **6:** 206-213

41 **Wulczyn FG,** Krappmann D, Scheidereit C. The NF-κB/Rel and IkB gene families: mediators of immune response and inflammation. *J Mol Med* 1996; **74:** 749-769

42 **Sahnoun Z,** Jamoussi K, Zeghal KM. Free radicals and antioxidants: physiology, human pathology and therapeutic aspects (part II). *Therapie* 1998; **53:** 315-339

43 **Petranka J,** Wright G, Forbes RA, Murphy E. Elevated calcium in preneoplastic cells activates NF-kappa B and confers resistance to apoptosis. *J Biol Chem* 2001; **276:** 37102-37108

44 **Potoka DA,** Upperman JS, Nadler EP, Wong CT, Zhou X, Zhang XR, Ford HR. NF-kappa B inhibition enhances peroxynitrite-induced enterocyte apoptosis. *J Surg Res* 2002; **106:** 7-14

45 **Teresa Bengoechea-Alonso M,** Pelacho B, Oses-Prieto JA, Santiago E, Lopez-Moratalla N, Lopez-Zabalza MJ. Regulation of NF-kappa B activation by protein phosphatase 2B and NO, via protein kinase A activity, in human monocytes. *Nitric Oxide* 2003; **8:** 65-74

Edited by Zhu L and Wang XL

P.O.Box 2345, Beijing 100023,China
Fax: +86-10-85381893
E-mail: wjg@wjgnet.com www.wjgnet.com

World J Gastroenterol 2003;9(11):2539-2543
World Journal of Gastroenterology
 ISSN 1007-9327

• BASIC RESEARCH •

Purification and characterization of 33.5 kDa vesicular protein in human bile

Jian-Bin Xiang, Duan Cai, Bao-Jin Ma, Xi-Liang Cha, Li-Ying Wang, Han-Qing Mo, Yan-Ling Zhang

Jian-Bin Xiang, Duan Cai, Bao-Jin Ma, Yan-Ling Zhang, Department of General Surgery, Huashan Hospital, Fudan University, Shanghai 200040, China
Xi-Liang Cha, Li-Ying Wang, Han-Qing Mo, Department of Biochemistry, Fudan University, Shanghai 200032, China
Supported by the National Natural Science Foundation of China, No.30070737
Correspondence to: Jian-Bin Xiang, Department of General Surgery, Huashan Hospital, Fudan University, Shanghai 200040, China. xjbzhw@yahoo.com.cn
Telephone: +86-21-62489999-6484 **Fax:** +86-21-62489743
Received: 2003-05-11 **Accepted:** 2003-06-07

Abstract

AIM: The present study was undertaken to purify and partially characterize the 33.5-kilodalton (33.5 kDa) vesicular protein in human bile and to explore the possible molecular mechanisms of the initial crystal nucleation process.

METHODS: The 33.5 kDa vesicular protein was isolated by ultracentrifugation and further purified by sodium dodecyl sulfate-polyacrylamide gel electrophoresis (SDS-PAGE) under nonreducing conditions. The purified 33.5 kDa vesicular protein was subjected to N-terminal amino acid sequencing and amino acid analysis. Cholesterol crystallization activity was detected by cholesterol crystal growth assay. The sugar chain of the 33.5 kDa vesicular protein was analyzed by dot-immunobinding assay of lectin coupled to a peroxidase (HRP-DSA, HRP-ConA, HRP-WGA) and was deglycosylated using two different enzymatic approaches (*N*-deglycosylation and *O*-deglycosylation) to determine the molecular weight of the protein component, the type of linkage between polypeptide and carbohydrate components.

RESULTS: The 33.5 kDa vesicular protein with complicated glycan was an extensively glycosylated (37.3 %) monomer and these sugar chains strongly bound to DSA, but did not bind to ConA. Amino acid sequencing indicated that the protein was unique. The 33.5 kDa vesicular protein exhibited potent cholesterol crystallization promoting activity *in vitro* with derived crystal growth curve indices It, Ig, Ic presented as 0.57, 1.52, and 1.63 respectively. Both enzymatic proteolysis and *N*-deglycosylation of the protein removed all activity.

CONCLUSION: These data suggest the 33.5 kDa vesicular protein may be responsible for the pathogenesis of cholesterol gallstone disease, and the sugar chains play an important role in pro-nucleating process.

Xiang JB, Cai D, Ma BJ, Cha XL, Wang LY, Mo HQ, Zhang YL. Purification and characterization of 33.5 kDa vesicular protein in human bile. *World J Gastroenterol* 2003; 9(11): 2539-2543
http://www.wjgnet.com/1007-9327/9/2539.asp

INTRODUCTION

Cholesterol nucleation process represents a critical step in the cholesterol gallstone formation. Cholesterol pro-nucleating and anti-nucleating proteins can accelerate or retard the rate of cholesterol crystallization in supersaturated bile, and thus may play important roles in cholesterol crystallization[1-3]. From 1988, both inhibitors and promoters of cholesterol crystallization have been isolated from human bile and characterized[4-7]. The major cholesterol crystallization promoting activity was localized at the concanavalin A-binding fraction of biliary glycoproteins (CABG). These proteins include mucin[8], immunoglobulins[9-11], α_1-acid protein[12], aminopeptidase N[4], low-density protein-lipid complex[5,13], and some unidentified proteins such as 70 kDa[14] and 200 kDa[15] pro-nucleating glycoproteins. Abei *et al*[16] provided comparative data regarding the relative potency of these different glycoprotein promoters and found that α_1-acid protein accounted for the greatest portion (33 %) of the net biliary Con A-bound promoting activity derived from currently defined and well-identified glycoproteins. But still more than 60 % of total Con A-bound promoting activity remains unaccounted for. It was speculated that there was still some other more important proteins involved in cholesterol nucleation process.

Lecithin vesicles are the primary cholesterol carriers in bile supersaturated with cholesterol and have been shown to play an important role in the nucleation of cholesterol. This nucleation takes place after aggregation and fusion of cholesterol-rich biliary vesicles, a process modulated by biliary proteins. Miquel *et al*[17] found a potent cholesterol pro-nucleating activity in purified biliary vesicles. Further study demonstrated that this activity was related with specific vesicular proteins including immunoglobulins IgA, IgG and IgM[18].

In this study, a novel 33.5 kDa vesicular protein obtained from human gallbladder bile of cholesterol gallstone patients was isolated, purified and partially characterized. We attempted to determine whether pro-nucleating activity occurred in the 33.5 kDa vesicular protein and to detect whether the protein was lectin-specific. Our results showed that the 33.5 kDa vesicular protein exhibited potent pro-nucleating activity *in vitro*, which depends on intact structure of peptide and sugar chain, and especially bound DSA lectin.

MATERIALS AND METHODS

Materials

Sodium salts of taurocholic(STC) and taurodeoxycholic (STDC) greater than 99 % purity, cholesterol(CH), egg lecithin and Tween 20 were obtained from Fluka Company. Metrizamide, nitrocellulose sheets, and all the chemicals for SDS-PAGE were obtained from Sigma Chemical Co. Datura stramonium agglutinin (DSA), wheat germ agglutinin (WGA), concanavalin A(Con A), peroxidase(HRP), and Sephadex G150 were also from Sigma Chemical Co. Periodic acid($NaIO_4$) was purchased from Wako Pure Chemical. *N*-glycosidase F, endo-α-N-acetyl-galactosaminidase, neuraminidase, and *Pronase K* were purchased from Boehringer Mannheim Corp., Germany, and 0.22 μm micropore filters were obtained from Millipore Corp., Bedford, MA. USA.

Methods

Patients and bile collection All patients gave written informed consent to participate in the study, which was approved by the ethical committee. Gallbladder bile was obtained from three patients by directly puncturing the gallbladder with a sterile 19G needle at cholecystectomy for cholelithiasis. The bile (20 ml) was immediately transported to the laboratory and stored at -80 ℃ until processed.

Protein purification procedure Pooled bile specimens were separated on a molecular sieving chromatography column (BioGel A-5m, 5×100 cm), eluted with 10 mmol/L Tris-HCl buffer to remove soluble mucin glycoprotein. The main fraction was centrifuged at 10 000 rev/min for 10 minutes at room temperature. The upper fraction was filtered through 0.22 μm micropore filters, and metrizamide (13 % w/v) was directly dissolved in the elution and centrifuged at 45 000 rev/min for 3.5 h at 10 ℃ in a Vti-50 vertical rotor (Beckman Instruments Inc., USA). The top opalescent vesicular fraction was collected by tube puncturing and loaded on SDS-PAGE under nonreducing conditions. The 33.5 kDa vesicular protein lane was resected according to the protein marker position and dialyzed in Tris-HCl buffer and concentrated as Ma *et al*[19] described.

SDS-PAGE SDS-PAGE(5-12 %) was developed in a buffer system described by Laemmli[20]. Aliquots (100 μl) of protein and bile samples were resolubilized with a sample buffer (60 mmol/L Tris-HCl, 2 % SDS, 10 % glycerol, pH 6.8). On completion of the electrophoretic run, gels were fixed in a 50 % methanol, 10 % acidic acid solution for 6 h and stained with Coomassie blue.

Preparation of lectin-HRP conjugate The lectin-HRP conjugate of DSA-HRP, WGA-HRP and Con A-HRP was made according to Guo *et al*[21]. Briefly, 5 mg HRP was dissolved in 0.5 ml distilled water, then added with 0.5 ml 60 mmol/L $NaIO_4$ and kept at 4 ℃ for 30 minutes. Five mg lectin such as DSA, WGA and Con A was mixed with HRP and 0.1 mol/L α-methyl mannose for Con A, and N-acetylglucosamine for DSA and WGA was added to protect the glycan binding site of the lectin. The reaction mixture was dialyzed in 50 mmol/L carbonate buffer (pH 9.5) and centrifuged at 4 000 rev/min for 10 minutes. The supernatant was removed and the pellet was dissolved and dialyzed in sodium phosphate buffer (20 mmol/L, pH 7.4).

Lectin affinity staining Five, 10, 15 μg/ml of purified 33.5 kDa vesicular proteins were blotted to nitrocellulose membrane respectively. The membrane was blocked with 1 % BSA overnight at 37 ℃. Subsequent incubation of the membrane with 1:500 peroxidase-labeled Datura stramonium agglutinin (DSA), wheat germ agglutinin (WGA), concanavalin A(Con A) in the same solution was followed by washing three times in the TTBS buffer (0.05 % Tween 20, 0.1 mol/L Tris-HCl, pH7.5) and chemiluminescent detection.

Amino acid analysis The purified 33.5 kDa vesicular protein was hydrolyzed for 16 hours at 115 ℃ in 6 N HCl/0.2 % phenol containing norleucine as an internal standard. After incubation, samples were dried and redissolved in 100 μl of NaS sample dilution buffer (Beckman Instruments Inc., USA) and run on a Beckman model 7300 Amino Acid Analyzer.

Amino acid sequencing The amino-terminal sequences of the 33.5 kDa vesicular protein were subjected to N-terminal amino acid sequencing with an automated sequencer (model 477A: Protein Sequencer, Applied Biosystems). Determined sequences were compared with those well-identified glycoproteins in the Pub-Med NCBI human gene bank database.

Enzymatic deglycosylation The 33.5 kDa vesicular protein was treated with *N*-glycanase enzyme according to supplier's specifications based on the work of Elder and Plummer *et al*[22,23]. Five hundred μg 33.5 kDa vesicular protein boiled for 5 minutes was diluted with 0.1 mmol/L sodium phosphate buffer, pH 8.6, 10 mmol/L 1, 10-phenanthroline, and then mixed with 10 U *N*-glycanase, and the reaction mixture was incubated for 24 h at 37 ℃. The molecular weight of deglycosylated polypeptide backbone was then detected using SDS-PADE.

In the *O*-deglycosylation study, the vesicular protein was diluted with 10 mmol/L calcium acetate, 20 mmol/L sodium cacodylate buffer (pH 7.0) and was incubated with 10 U/ml of neuraminidase for 12 h at 37 ℃. This was followed by further incubation with 2 U/ml of endo-α-N-acetyl-galactosaminidase for 12 h at 37 ℃. Finally, the mixture was examined using SDS-PAGE.

Proteolysis studies One hundred μg of 33.5 kDa vesicular protein was dissolved in 50 μl ammonium bicarbonate (25 mmol/L, pH 11), and then incubated with 1.5 U *Pronase K* for 24 h at 37 ℃. After incubation, the sample was concentrated and loaded on SDS-PAGE.

Cholesterol crystal growth assay Supersaturated model bile was prepared with a cholesterol saturation index of 1.4, a total lipid concentration of 125 g/L, and a bile acid/phospholipid ratio of 4.4. This model bile was made as Busch *et al*[24,25] described. In brief, this lipid mixture was evaporated to dryness, lyophilized, and then resolubilized with 20 mmol/L Tris-HCl/150 mmol/L NaCl (TBS), pH 7.4 at 55 ℃. After filtration (0.22 μm), 25 μl of this model bile mixed with 50 μg protein or its enzymatic samples was diluted with 475 μl TBS/10 mmol/L STDC solution. After 20 minutes, absorbance at a single wavelength within the visible range (700 nm) was sequentially measured. The cholesterol crystal growth curves of the supersaturated model bile without (control) and with (experimental) protein samples were thus generated for each sample. The three growth curve parameters were derived: growth index Ig=maximal slope of experimental curve/maximal slope of control, crystal index Ic=final crystal concentration of experimental/final crystal concentration of control, time index It=onset time of experimental/onset time of control.

Statistical analysis

The cholesterol crystal growth curves were compared by using analysis of variance (ANOVA) at each time to determine whether difference existed between the study groups. When the ANOVA was statistically significant ($P<0.05$), the Dunnett's multiple comparison procedure was made to compare each of the study groups to the control group.

RESULTS

Purification and identification of novel 33.5 kDa glycoprotein

The bile was divided into three fractions after ultracentrifugation (Figure 1). The top opalescent vesicular fraction was collected by tube puncture and the targeted vesicular protein was further separated by SDS-PAGE. The protein profile from three different gallstone patients with Coomassie blue staining is shown in Figure 2. The protein marker is shown at lane 1 and a single band of 33.5 kDa protein at lanes 2-4 on SDS-PAGE was stained under nonreducing condition. Amino acid analysis of the purified glycoprotein showed that the protein was composed of 153 amino acid residues of which almost one third were the following amino acids: glutamine/glutamic acid and asparagines/aspartic acid (Table 1). N-amino-terminal sequencing of the protein showed H_2N-Asp-Asn-Ser-Gln-His-Arg-Tyr-Val-Phe-Ile, which was different from α_1-acid protein, Ig, aminopeptidase N and phospholipase C. Lectin staining showed higher affinity for *Datura stramonium agglutinin* (DSA) than for wheat germ agglutinin (WGA) and concanavalin A(Con A)(Figure 3). *N*- deglycosylation studies showed disappearance of the original 33.5 kDa protein and the presence of a new 21kDa band on SDS-PAGE (Figure 4), indicating

the protein was heavily glycosylated (37.3 %) and the connection mode between polypeptide and carbohydrate components was *N*-linkage. Proteolysis studies showed the protein was sensitive to *Pronase K* digestion.

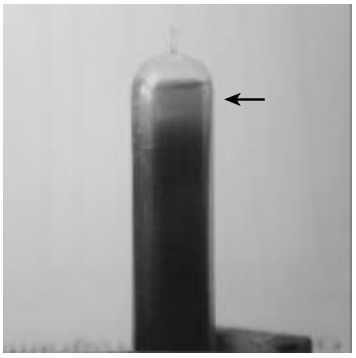

Figure 1 Pretreated bile centrifuged at 45 000 rev/min and divided into three fractions. Horizontal arrows indicate the vesicular phase bile.

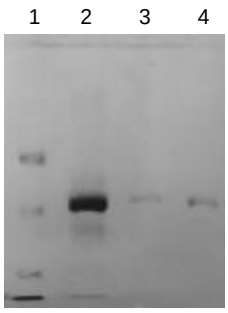

Figure 2 Purified 33.5 kDa vesicular proteins from three different bile samples run on SDS-PAGE. Lane 1: protein marker, Lanes 2-4: the 33.5 kDa vesicular protein.

Table 1 Amino acid composition of 33.5 kDa vesicular protein

Amino acid	nmol/total protein	No. of residues/mol protein
Asp/Asn	6.761	19
Thr	4.488	13
Ser	1.589	5
Glu/Gln	10.434	30
Gly	2.242	6
Ala	2.864	8
Val	2.501	7
Ile	3.226	9
Leu	4.782	14
Tyr	1.937	6
Phe	2.966	8
Lys	4.777	14
His	0.840	2
Arg	2.645	8
Pro	1.411	4
NH_2	11.297	32
Total	64.76	153

Cholesterol crystal growth assay

Figure 5 depicts the promoting effect of 33.5 kDa vesicular protein on cholesterol crystal growth curve at the concentration of 100 μg/ml. The protein strongly promoted cholesterol crystallization, accelerated the onset and increased the total quantity of crystal plates with derived crystal growth curve indices It, Ig, Ic presented as 0.57, 1.52, 1.63 respectively. But no promoting activity was detected in the same supersaturated model bile after incubation with *N*-glycanase enzyme or complete protein degradation (Table 2).

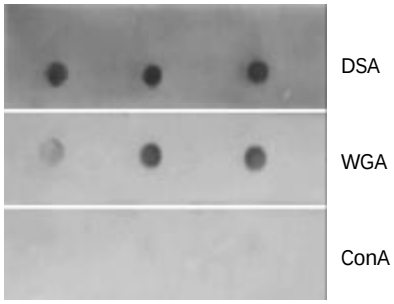

Figure 3 Lectin affinity staining with DSA, WGA, Con A labeled with peroxidase. The 33.5 kDa vesicular protein was strongly connected with DSA, and weakly bound to WGA, but did not react with Con A.

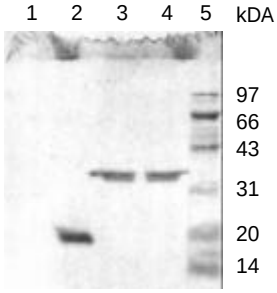

Figure 4 SDS-PAGE (reduced condition) of the 33.5 kDa vesicular protein after *N*-deglycosylation, *O*-deglycosylation and proteolysis. Complete disappearance was observed after incubation with *Pronase K* at lane 1. A single 21 kDa band was stained after treated with *N*-glycanase at lane 2, but no change of the protein after enzymatic *O*-deglycosylation at lane 3. The band of lane 4 and lane 5 represented the 33.5 kDa vesicular protein and protein marker respectively.

Table 2 Effect of 33.5 kDa vesicular protein on activity indices of cholesterol crystallization (100 μg/ml)

	It	Ig	Ic	*P* value
Purified 33.5 kDa protein	0.57	1.52	1.63	<0.05[a]
+ *N*-deglycosylation	1.08	1.01	0.98	<0.05[b]
+ *O*-deglycosylation	0.58	1.61	1.54	<0.05[a]
+ Proteolysis	1.12	0.87	0.99	<0.05[b]

a: compared with control, b: compared with 33.5 kDa vesicular protein group.

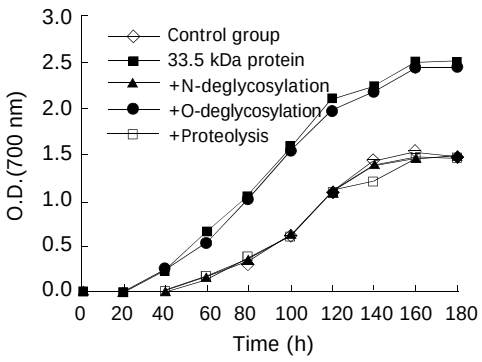

Figure 5 Promoting effect of 33.5 kDa vesicular protein and its enzymatic products on cholesterol crystal growth curves in model bile (TL=125 g/L, BA/PL=4.4, CSI=1.4). All curves are given as the mean ±SD, n=4. P<0.05 *vs* control at each time.

DISCUSSION

Since the first report of the presence of pro-nucleating activity in cholesterol patient' s bile by Burnstein *et al*[26], many groups have tried to purify and identify the active protein-related components[16,17,25,27,28]. Of particular interest are the presence and role of concanavalin A-binding fraction of biliary glycoproteins (CABG), which have a potent cholesterol crystallization-promoting activity. Proteins thought to explain this activity included α_1-acid protein[12], immunoglobulins[9-11], aminopeptidase N[4,6], and a pronase resistant carcinoembryonic antigen-related cell adhesion molecule 1 most recently described by Jirsa *et al*[29], and some unidentified proteins such as 200 kDa pro-nucleating glycoprotein[15]. But still most of the activity has not been identified[30]. In this study we purified and characterized a novel promoting-nucleation glycoprotein with molecular weight of 33.5 kDa in vesicular bile of cholesterol gallstone patients. In 1992, Miquel *et al*[17] isolated and purified human vesicles with potent cholesterol-nucleation-promoting activity, and found that this protein-related activity belonged to immunoglobulins. Although they were from the same vesicular bile, the difference between the immunoglobulin family of glycoprotein and the 33.5 kDa vesicular protein was obvious. We took considerable care to rule out the possibility that the present glycoprotein shared similar features with the immunoglobulins. First, the potent cholesterol-nucleation-promoting vesicular protein had a strong activity of accelerating the onset and increasing the total quantity of crystals appearance and was unique to have a high affinity for *Datura stramonium agglutinin* (DSA), and did not bind to *concanavalin A* (Con A). This was different from the previously described promoting-nucleation glycoprotein. Amino acid sequencing study further demonstrated that the 33.5 kDa vesicular protein with N-amino-terminal sequencing of H_2N-Asp-Asn-Ser-Gln-His-Arg-Tyr-Val-Phe-Ile, was a novel glycoprotein from vesicular bile.

In additional experiments, the 33.5 kDa vesicular protein could not only accelerate onset of nucleation, but also induce rapid cholesterol crystallization growth. We speculate the factor identified in this study may play an important role in the initial stage of the gallstone formation. To study the underlying mechanism and pathophysiological significance of the peptide and carbohydrate moiety, the 33.5 kDa vesicular protein was treated with glycanase enzyme and p*ronase* respectively. Incubation with *N*-glycanase resulted in disappearance of the original 33.5-kilodalton band and presence of a strong 21-kilodalton band on SDS-PAGE, and no cholesterol crystallization promoting activity of 33.5 kDa vesicular protein was detected in supersaturated model bile. It suggested that the sugar chain might be responsible for the promoting-nucleation activity. This striking characteristic of the vesicular protein was very similar to α_1-acid protein. Abei *et al*[12] reported that α_1-acid protein was 37 % glycosylated with mannose, sialic acid content, and some other multiple antennae and the carbohydrate moiety were essential to the promoting activity of glycoprotein. In addition, vesicular glycoprotein was completely degradated and no promoting activity existed after proteolytic digestion.

In conclusion, our results indicate that, the 33.5 kDa vesicular protein with complicated glycan and high affinity for DSA, is a novel and unique pro-nucleating glycoprotein, which exhibits potent cholesterol crystallization promoting activity *in vitro*. However, further studies are needed to evaluate the predictive value, concentration, relative potency and origin of the 33.5 kDa vesicular protein before we can ascertain its specific role in the pathogenesis of cholesterol gallstone disease.

ACKNOWLEDGMENTS

The skillful technical assistance of Dr. Chuan Xin Huang and Dr. Jia Da Li is gratefully acknowledged.

REFERENCES

1 **Miquel JF**, Van Der Putten J, Pimentel F, Mok KS, Groen AK. Increased activity in the biliary Con A-binding fraction accounts for the difference in crystallization behavior in bile from Chilean gallstone patients compared with Dutch gallstone patients. *Hepatology* 2001; **33**: 328-332
2 **Nunes DP**, Afdhal NH, Offner GD. A recombinant bovine gallbladder mucin polypeptide binds biliary lipids and accelerates cholesterol crystal appearance time. *Gastoenterology* 1999; **116**: 936-942
3 **Luk AS**, Kaler EW, Lee SP. Protein lipid interaction in bile: effects of biliary proteins on the stability of cholesterol-lecithin vesicles. *Biochim Biophys Acta* 1998; **1390**: 282-292
4 **Groen AK**, Noordam C, Drapers JA, Egbers P, Jansen PL, Tytgat GN. Isolation of a potent cholesterol nucleation-promoting activity from human gallbladder bile: role in the pathogenesis of gallstone disease. *Hepatology* 1990; **11**: 525-533
5 **Zijlstra AI**, Offner GD, Afdhal NH, van Overveld M, Tytgat GN, Groen AK. The pronase resistance of cholesterol-nucleating glycoproteins in human bile. *Gastroenterology* 1996; **110**: 1926-1935
6 **Nunez L**, Amigo L, Mingrone G, Rigotti A, Puglielli L, Raddatz A, Pimentel F, Greco AV, Gonzalez S, Garrido J, Miquel JF, Nervi F. Biliary aminopeptidase-N and the cholesterol crystalliszation defect in cholelithiasis. *Gut* 1995; **37**: 422-426
7 **Groen AK**, Stout JP, Drapers JA, Hoek FJ, Grijm R, Tytgat GN. Cholesterol nucleation-influencing activity in T-tube bile. *Hepatology* 1988; **8**: 347-352
8 **Gallinger S**, Taylor RD, Harvey PR, Petrunka CN, Strasberg SM. Effect of mucous glycoprotein on nucleation time of human bile. *Gastoenterology* 1985; **89**: 648-658
9 **Harvey PR**, Upadhya GA, Strasberg SM. Immunoglobulins as nucleating proteins in the gallbladder bile of patients with cholesterol gallstones. *J Biol Chem* 1991; **266**: 13996-14003
10 **Upadhya GA**, Harvey PR, Strasberg SM. Effect of human biliary immunoglobulins on the nucleation of cholesterol. *J Biol Chem* 1993; **268**: 5193-5200
11 **Busch N**, Lammert F, Matern S. Biliary secretory immunoglobulin A is a major constituent of the new group of cholesterol crystal-binding proteins. *Gastroenterology* 1998; **115**: 129-138
12 **Abei M**, Kawczak P, Nuutinen H, Langnas A, Svanvik J, Holzbach RT. Isolation and characterization of a cholesterol crystallization promoter from human bile. *Gastroenterology* 1993; **104**: 539-548
13 **De Bruijn MA**, Mok KS, Nibbering CP, Out T, Van Marle J, Stellaard F, Tytgat GN, Groen AK. Characterization of the cholesterol crystallization-promoting low-density particle isolated from human bile. *Gastroenterology* 1996; **110**: 1936-1944
14 **Jiao W**, Zhang YL, Cai D, Wu SQ. Isolation, purification and the characteristics of 70kDa pronucleation glycoprotein in the bile. *Zhonghua Waike Zazhi* 1994; **32**: 271-274
15 **Li F**, Cai D, Mo HQ, Zhang YL. The ELISA for the 200kDa glycoprotein in bile. *Zhonghua Xiaohua Zazhi* 1997; **17**: 333-335
16 **Abei M**, Schwarzendrube J, Nuutinen H, Broughan TA, Kawczak P, Williams C, Holzbach RT. Cholesterol crystallization-promoters in human bile: comparative potencies of immunoglobulins, α_1-acid glycoprotein, phospholipase C, and aminopeptidase N1. *J Lipid Res* 1993; **34**: 1141-1148
17 **Miquel JF**, Rigotti A, Rojas E, Brandan E, Nervi F. Isolation and purification of human biliary vesicles with potent cholesterol-nucleation-promoting activity. *Clin Sci* 1992; **82**: 175-180
18 **Miquel JF**, Nunez L, Rigotti A, Amigo L, Brandan E, Nervi F. Isolation and partial characterization of cholesterol pronucleating hydrophobic glycoproteins associated to native biliary vesicles. *FEBS Lett* 1993; **318**: 45-49
19 **Ma BJ**, Cai D, Zhang QH, Zhang YL. The potent cholesterol-nucleation activity of human biliary vesicles. *Zhonghua Gandan Waike Zazhi* 1998; **4**: 104-106
20 **Laemmli UK**. Cleavage of structural proteins during the assembly of the head of bacteriophage T_4. *Nature* 1970; **227**: 680-685
21 **Guo CX**, Guo XQ. Introducing a simple, rapid, and effective method of labeling antibody with peroxidase using periodic acid. *Shanghai Mianyixue Zazhi* 1983; **2**: 97-100
22 **Elder JH**, Alexander S. Endo-β-N-acetylglucosaminidase F:

endoglycosidase from Flavobacterium meningosepticum that cleaves both high-mannose and complex glycoproteins. *Proc Natl Acad Sci U S A* 1982; **79**: 4540-4544

23 **Plummer TH Jr**, Phelan AW, Tarentino AL. Detection and quantification of peptide-N^4-(N-acetyl-beta-glucosaminyl) asparagine amidases. *Eur J Bioche* 1987; **163**: 167-173

24 **Busch N**, Tokumo H, Holzbach RT. A sensitive method for determination of cholesterol growth using model solutions of supersaturated bile. *J Lipid Res* 1990; **31**: 1903-1909

25 **Busch N**, Matiuck N, Sahlin S, Pillay SP, Holzbach RT. Inhibition and promotion of cholesterol crystallization by protein fractions from normal human gallbladder bile. *J Lipid Res* 1991; **32**: 695-702

26 **Burnstein MJ**, Ilson RG, Petrunka CN, Taylor RD, Strasberg SM. Evidence for a potent nucleating factor in gallbladder bile of patients with cholesterol gallstones. *Gastroenterology* 1983; **85**: 801-807

27 **Chen YQ**, Zhang YL, Cai D, Hua TF, Huang JQ, Zhong CS. The actions of nucleating proteins in vesicle aggregation and fusion: a preliminary study. *Zhonghua Waike Zazhi* 1997; **35**: 181-185

28 **Afdhal NH**, Niu N, Gantz D, Small DM, Smith BF. Bovine gallbladder mucin accelerates cholesterol monohydrate crystal growth in model bile. *Gastroenterology* 1993; **104**: 1515-1523

29 **Jirsa M**, Muchova L, Draberova L, Draber P, Smid F, Kuroki M, Marecek Z, Groen AK. Carcinoembryonic antigen-related cell adhesion molecule 1 is the 85-kilodalton pronase-resistant biliary glycoprotein in the cholesterol crystallization promoting low density protein-lipid complex. *Hepatology* 2001; **34**: 1075-1082

30 **De Bruijn MA**, Mok KS, Out T, Tytgat GN, Groen AK. Immunoglobulins and α_1-acid glycoprotein do not contribute to the cholesterol crystallization-promoting effect of Concanavalin A-binding biliary protein. *Hepatology* 1994; **20**: 626-632

Edited by Zhu LH and Wang XL

P.O.Box 2345, Beijing 100023,China
Fax: +86-10-85381893
E-mail: wjg@wjgnet.com www.wjgnet.com

World J Gastroenterol 2003;9(11):2544-2547
World Journal of Gastroenterology
 ISSN 1007-9327

• BASIC RESEARCH •

Heat shock protein 90 is responsible for hyperdynamic circulation in portal hypertensive rats

Jian-Hua Ai, Zhen Yang, Fa-Zu Qiu, Tong Zhu

Jian-Hua Ai, Zhen Yang, Fa-Zu Qiu, Center for Hepatic Surgery, Tongji Hospital, Tongji Medical College, Huazhong Science and Technological University Wuhan 430030, Hubei Province, China
Tong Zhu, Institute of Organ Transplantation, Tongji Hospital, Tongji Medical College, Huazhong Science and Technological University, Wuhan 430030, Hubei Province, China
Supported by the National Natural Science Foundation of China, No.30170920
Correspondence to: Dr. Jian-Hua Ai, International Cooperation Laboratory on Signal Transduction, Eastern Hepatobiliary Surgery Institute, Second Military Medical University, Shanghai 200438, China. aijh_2000@yahoo.com
Telephone: +86-21-25070846
Received: 2003-05-10 **Accepted:** 2003-06-04

Abstract

AIM: To examine the participation of HSP90 in portal hypertensive rat mesentery *in vitro*.

METHODS: Immunohistochemistry and Western-blot were used to examine the expression of HSP90 in mesenteric vasculature. HSP90 mRNA was detected by RT-PCR, and the role of HSP90 in hyperdynamic circulation was examined by *in vitro* mesenteric perfusion studies.

RESULTS: HSP90 was overexpressed in endothelium of mesentery vasculature in animals with experimental portal hypertension induced by partial portal vein ligation (PVL) compared with normal animals. Geldanamycin (GA), a special inhibitor of HSP90 signaling, attenuated ACh-dependent vasodilation but did not affect vasodilation in response to sodium nitroprusside in normal rats. In PVL animals, the perfused mesentery was hyporesponsive to vasoconstrictor methoxamine. GA significantly potentiated methoxamine-induced vasoconstrictor after PVL.

CONCLUSION: HSP90 plays a key role in NO-dependent hyperdynamic circulation in portal hypertension and provides a novel method for future treatment of portal hypertension.

Ai JH, Yang Z, Qiu FZ, Zhu T. Heat shock protein 90 is responsible for hyperdynamic circulation in portal hypertensive rats. *World J Gastroenterol* 2003; 9(11): 2544-2547
http://www.wjgnet.com/1007-9327/9/2544.asp

INTRODUCTION

Cirrhosis of the liver, which usually develops as a long-term consequence of viral hepatitis or alcohol abuse, is a major cause of morbidity and mortality worldwide. The principal pathophysiologic feature of cirrhosis is an increase in portal pressure initiated by an increase in outflow resistance to the portal circulation. However, advanced cirrhosis was also associated with mesenteric arteriolar vasodilation[1], which contributes to portal hypertension and variceal hemorrhage by increasing portal inflow. It has been well established that portal hypertension was not a purely mechanical phenomenon[2]. There have been a large body of experimental evidences that demonstrated increased synthesis of nitric oxide (NO) in animal models of cirrhosis. Aortic cAMP, a surrogate marker of NO synthesis, was significantly elevated in CCl_4-induced cirrhosis rats compared to controls and the highest levels were observed in those with ascites[3]. Similar evidences also existed for elevated NOS activity in animal models of portal hypertension induced by partial vein ligation[4]. NO and endothelin-1-dependent increases in intrahepatic resistance in conjunction with vasodilation of splanchnic arterioles raised portal pressure and flow, thereby contributing to the vascular component of portal hypertension[5]. Indeed, the importance of splanchnic vasodilation in this process was highlighted by clinical utility of nonselective beta-blockers and octreotide, both of which could reduce splanchnic vasodilation and portal venous inflow[6]. However, cirrhotic vasculature was highly resistant to conventional vasopressors[7], and attempts to correct the hyperdynamic circulation in cirrhosis by antagonism of putative endogenous vasodilator mediators have been unsuccessful so far[8,9]. Pressure and resistance changes in perfused mesenteric vasculature occurred, in part through NO-dependent mechanisms, and in experimental portal hypertension this vascular bed demonstrated a hyporeactivity to vasoconstrictors such as methoxamine (MTX), mainly due to excessive endothelium-derived NO production[10,11].

NO is derived from L-arginine by the enzymatic action of NOS. Two isoforms of NOS have been shown to exist in the vasculature, one is a constitutively expressed and calcium-calmodulin-dependent isoform (eNOS)[12], the other is an inducible and calcium-independent isoform (iNOS)[13]. Indirect evidences for eNOS as the main source of elevated NO from studies showed that endothelial denudation could normalize vascular levels of NO[14] and reverses the hyporeactivity to vasoconstrictors[15,16] in cirrhotic rats. Several studies now suggested that eNOS was the major enzymatic source of NO overproduction[17-20] in vascular endothelium in cirrhosis. However, the molecular mechanism is still unknown. 90 kD heat shock protein (HSP90) has been found to be a molecular chaperon, and a constitutive homodimer, its main intersubunit contacted within COOH-terminal 190 residues[21]. The highly conserved 25 kD NH_2 - terminal domain of HSP90 is the binding site for geldanamycin (GA), a representative of ansamycin drugs, which specially targets HSP90[22]. HSP90 mediates the conformational regulation of a wide range of client proteins involved in signal transduction, cell proliferation and apoptosis. The recently demonstrated importance of HSP90 as an intermediate in the signaling cascades leading to activation of eNOS[23] suggested the possibility of a contributory role of this pathway in NO-dependent mesenteric vascular responses and excessive NO production in experimental portal hypertension.

The goals of this study were to examine HSP90 expression and localization in rat mesenteric microvasculature, to determine whether GA inhibited mesenteric vasodilation, and to test whether GA reversed the hyporeactivity to vasoconstrictors detected in mesenteric vasculature of portal hypertensive animals.

MATERIALS AND METHODS

Animals and reagents

Male Sprague-Dawley rats (Tongji Hospital Laboratories) weighing 250-300 g were used for experiments. Animal experiments and tissue harvesting were performed in accordance with the animal care guidelines of the institution. GA was dissolved in DMSO, and the final concentration of DMSO used in experiments was <0.006 %. MTX, ACh, and sodium nitroprusside (SNP) obtained from Sigma Chemical, were dissolved in distilled water and prepared daily.

Induction of portal hypertension

Prehepatic portal hypertension was provoked by partial portal vein ligation (PVL) as previously described[24]. In brief, rats were anesthetized, and after laparotomy, the portal vein was isolated and a stenosis created by placing a single ligature of 3-0 silk around both the portal vein and a 20-gauge blunt-tipped needle. The needle was then removed from the ligature, creating a calibrated constriction of the portal vein. In sham-operated (SO) rats, the portal vein was isolated but not ligated. Studies were performed in 24 hours fasted rats 21 days after PVL.

Immunohistochemistry

Mesenteric tissue was perfusion fixed *in situ* with 4 % paraformaldehyde, postfixed in sucrose, and embedded in OCT[25]. Frozen tissue sections were incubated overnight with HSP90 MAb, and a secondary incubation was performed with horse anti-mouse IgG for 30 min. Sections were developed with amino ethylcarbazole. Negative controls were incubated with appropriate serum substituted for the primary antibody.

RNA isolation and reverse transcriptase and polymerase chain reaction (RT-PCR)

Mesenteric tissue was harvested by dissecting and removing the highly vascular tissue situated between the mesenteric lymph nodes and small intestine. Mesenteric specimens from SO and PVL rats were immediately frozen in liquid nitrogen, then homogenated with Tripure isolation reagent to isolate total RNA. The RNA concentration in each sample was determined spectrophotometrically, and the quality of each RNA preparation was documented by visualization of 18S and 28S ribosomal bands after electrophoresis through a 1 % agarose gel. Total RNA samples were subjected to reverse transcription with Oligo-dt used as a template-primer. First strand synthesis was carried out for 1 hour at 37 ℃ in 25 μl of a reaction mixture containing 200 U M-MLV, 1 X reaction buffer, 0.5 mmol/L dNTP, 10 mmol/L DTT, 20 U RNAsin ribonuclease inhibitor and 0.25 -μg oligo-dT. The PCR primer sequences were as follow: HSP90 sense 5' GTCTGGGTATCGGAAAGCAAG3', antisense 5' CTGAGGGTTGGGGATGATGTC 3'. PCR assays contained 0.5 U Taq DNA polymerase, 0.5 μmmol/L of each oligonucleotide primer, 0.2 mmol/L dNTP, 1 X reaction buffer, 1.5 mmol/L MgCl in a final volume of 50 μl. 25 cycles were performed at 95 ℃ for 1 min, at 55 ℃ for 1 min, and at 72 ℃ for 2 min. PCR products were analyzed by electrophoresis in TAE buffer with ethidium bromide stained with (0.5 mmol/L) 2 % agarose gel. Each band was selected and used to measure the number of photons emitted.

Western blotting

Mesenteric sections were weighed and homogenized in 10 volumes of ice-cold 1 % NP-40 in 50 mM Tris (pH 8.8) buffer. The homogenates were centrifuged, and the supernatants were transferred into sterile tubes. Fifteen-microgram of protein aliquots of each sample, as determined by the Coomassie blue method, was resolved on 15 % SDS-polyacrylamide gels and transferred onto nitrocellulose membranes. The membranes were blocked with BSA before being incubated with primary antibody overnight at 4 ℃, and rinsed and then incubated for 1 h with peroxidase-conjugated secondary antibody. Immunoreactive proteins were visualized using the enhanced chemiluminescence system.

In vitro mesenteric perfusion

In vitro mesenteric perfusion was performed 14 days after PVL or after sham surgery, using the method described by McGregor and Sieber with some modifications[26]. In brief, the superior mesenteric artery (SMA) was cannulated with a PE-60 catheter and blood was removed by perfusion with 15 ml of warm Krebs solution. The gut was dissected at the mesenteric border, and the SMA with its adjoining mesenteric tissue was placed in a 37 ℃ water-jacketed container. The preparation was continuously perfused in a nonrecirculating system at a fixed rate of 4 ml/min throughout the course of the experiment with Krebs solution. Perfusion pressure was continuously monitored using a strain gauge transducer on a sidearm proximal to the perfusing cannula. The initial preparation was allowed to stabilize for 30 min, after which vehicle was infused for 15 min. Immediately after infusion of vehicle, concentration-response curves were examined in response to MTX infusion (30 and 100 μM). When a stable baseline was maintained in response to 100 μM MTX, responses to ACh boluses (0.1 ml) were examined (1 and 10 μg). All compounds were allowed to wash out over the next 50 min, after which GA was infused (3 μg/ml) for 15 min. Responses to MTX and ACh were repeated as described above. Additional experiments were performed after endothelial denudation. The denudation was achieved by combined treatment with cholic acid and distilled water as previously described[27]. In brief, after cannulation of the SMA and gentle flushing with 10 ml of warmed Krebs solution to eliminate blood, the mesentery was perfused with 1.5 ml of 0.5 % cholic acid for 10 s followed by 15 ml of warmed Krebs solution. The preparation was then transferred to a 37 ℃ water-jacketed container and perfused with warmed, oxygenated Krebs solution for 10 min. After the mesenteric vasculature was relaxed, warmed distilled water was perfused for 10 min. After a 45-min stabilization period, vehicle or alternatively GA was perfused for 15 min. Immediately after pretreatment with vehicle or GA, an infusion of 100 μM MTX was begun. When a stable baseline was maintained in response to 100 μM MTX, concentration-response curves to 0.1-ml SNP boluses (0.001-10 μg) were examined. Additional experiments were also performed in sham and PVL mesenteric vessels in response to GA preinfusion using MTX doses that allowed equivalent levels of constriction in response to preinfusion of vehicle. Equivalent constriction was achieved with 10 and 30 μM MTX in sham and PVL mesentery, respectively.

Statistics

All data were expressed as means ± SE. Statistical analysis was performed using paired and unpaired Student's *t*-tests as well as ANOVA where appropriate.

RESULTS

Expression and localization of HSP90 in mesenteric vasculature

The expression of HSP90 was significantly enhanced in PVL animals compared with SO and normal animals by Western blot and by RT-PCR (Figures 1A and B). The immunohistochemistry showed that HSP90 staining was not only found in vascular endothelium but also in mesenteric smooth cells (Figure 1C).

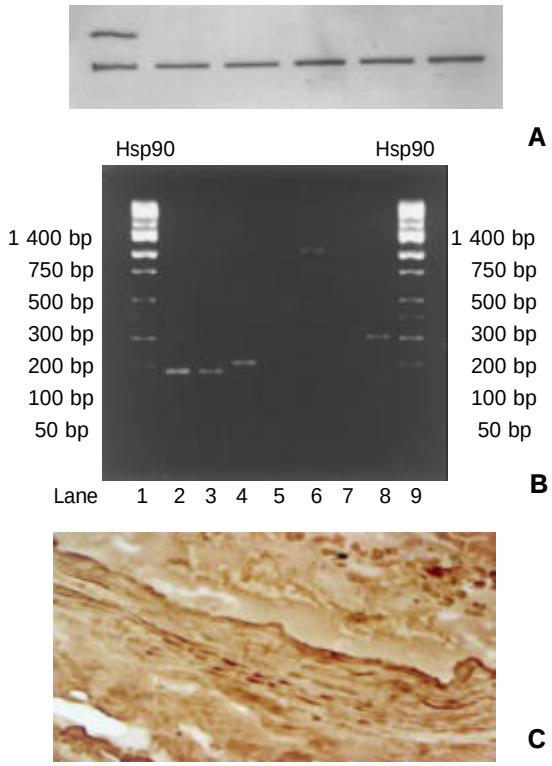

Figure 1 A: Expression of HSP90 by Western blot in PVL anima, B: Expression of HSP90 mRNA in PVL animals, C: Immunohistochemistry showed that HSP90 staining was not only found in vascular endothelium but also in mesenteric smooth cells.

GA potentiated mesenteric vascular responses to MTX in portal hypertensive animals

In response to 100 μM MTX, GA significantly potentiated the increase in perfusion pressure in portal hypertensive animals (Figure 2) (P<0.05, GA vs. vehicle) but not in sham animals. This result suggested that HSP90 was responsible for the hyporesponsness in portal hypertensive rats, thus playing a key role in hemodynamic dysfunction of portal hypertensive animals.

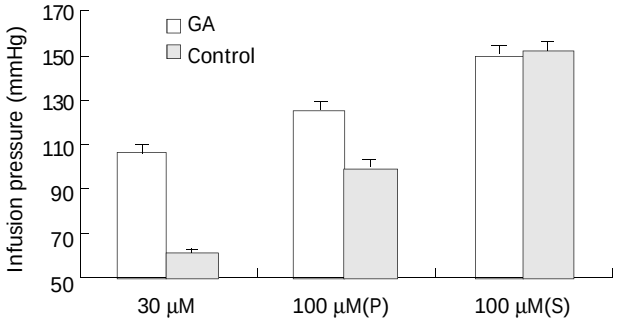

Figure 2 GA potentiates increase of perfusion pressure in portal hypertensive animals.

GA attenuated ACh-dependent vasorelaxation of the normally isolated and perfused rat mesentery but did not affect vasodilation in response to sodium nitroprusside

In this preparation, ACh induced vasorelaxation in a dose-dependent manner after preconstriction of the circulation with MTX. Mesenteric vasorelaxation in response to ACh (1 and 10 μg) was significantly attenuated after preinfusion of GA (3 μg/ml) compared with preinfusion of vehicle (Figure 3) (P<0.05, vehicle vs. GA; n=5). After endothelial denudation, pretreatment with GA did not affect vasodilation in response to SNP (n=6), indicating that the effects of GA were dependent on the endothelium and that GA did not directly affect soluble guanylate cyclase or other smooth muscle cell machinery required for NO-dependent vasodilation. These results showed that HSP90 was an important modulator in vasodilation of mesenteric vasculature.

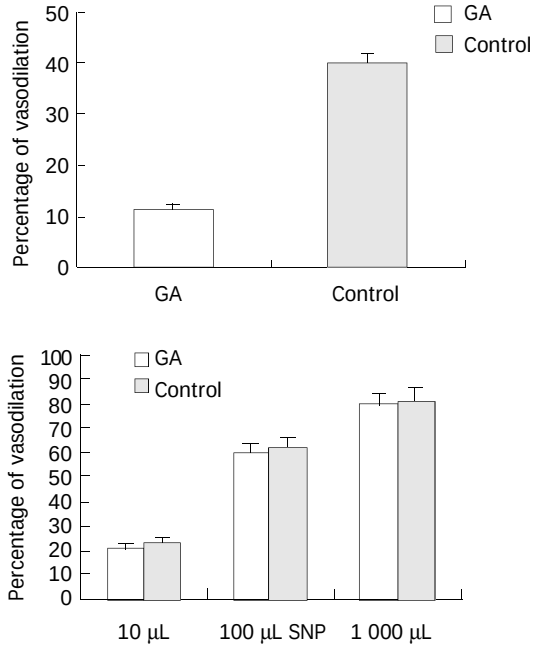

Figure 3 A: GA attenuates Ach dependent vasodilation. B: GA does not affect vasodilation in response to SNP.

DISCUSSION

This study suggested that HSP90 was overexpressed in the endothelium of mesenteric vasculature in PVL induced animals compared with SO and normal animals. Moreover, in PVL animals, the perfused mesentery was hyporesponsive to the vasoconstrictor methoxamine. GA, a special inhibitor of HSP90 signaling, significantly potentiated methoxamine-induced vasoconstrictor after PVL. It thus indicated a mechanism linking protein-protein interactions with vascular manifestations observed in portal hypertension.

HSP90, an ATP-dependent chaperon[28], facilitated the folding and stabilization of cellular proteins, and played a key role in cellular signal transduction networks. The highly conserved 25 kD NH_2-terminal domain of HSP90 was the binding site for ATP and GA[22], and crystallography has shown that GA occupied the nucleotide-binding cleft within the NH_2-terminal domain[28], which thereby has been used as a specific reagent to probe the importance of HSP90 in cellular pathways. An *in vivo* requirement for HSP90 has been established for some steroid hormone receptors[29], several serine/threonine kinases such as pp60/v-src and RAF[30,31] and disparate proteins such as NOS and calcineurin[23,32]. The present study demonstrated that GA also blocked vascular responses mediated by eNOS, without influencing the direct vasodilatory effects of SNP. These data, in conjunction with the above evidences for the specificity of GA, suggested that HSP90 participated in vasodilation of mesentery vasculature as a regulator of endothelial cell signal transduction, leading to eNOS activation and vasorelaxation.

Vessel homeostasis is maintained by a balance of vasoactive substances and hemodynamic forces, including shear stress which mediates vascular responses in part through modulation of eNOS. Two isoforms of NOS have been shown to exist in the vasculature, one is a constitutively expressed and calcium-calmodulin-dependent isoform (eNOS)[12], the other is an

inducible and calcium-independent isoform (iNOS)[13]. Several studies suggested that eNOS was the major enzymatic source of NO overproduction[17-20] in the vascular endothelium in cirrhosis. Our study found that the effects of GA were dependent on the endothelium and that GA did not directly affect soluble guanylate cyclase or other smooth muscle cell machinery required for NO-dependent vasodilation. These studies, in conjunction with the recent demonstration that activation of eNOS was facilitated through HSP90 signaling[23], suggested that eNOS activation in the portal hypertensive vasculature might be linked to a signaling pathway depending on HSP90. Thus we put forward the hypothesis that HSP90 signaling pathway potentiates the activity of eNOS, which results in NO overproduction and thereby induces hyperdynamic circulation in portal hypertension. However, the inability of GA to completely reverse the hyporesponsiveness to MTX in portal hypertensive mesentery suggested that other regulatory pathways for NOS activation in portal hypertension were also involved. In addition, it is possible that a small part of NO derived from iNOS might also contribute to hyperdynamic circulation in portal hypertensive vessels.

In summary, this study suggested that HSP90 played a key role in the NO-dependent hyporeactivity observed in portal hypertension. This interaction likely served to mediate NO-dependent responses in the perfused mesenteric vasculature. Taken together, the present study indicates that HSP90 is responsible for hyperdynamic circulation in portal hypertension, and pharmacological inhibition of the signal system may provide a novel target for future treatment of portal hypertensive complications such as ascites and fatal variceal bleeding.

REFERENCES

1 **Piscaglia F**, Zironi G, Gaiani S, Ferlito M, Rapezzi C, Siringo S, Gaia C, Gramantieri L, Bolondi L. Relationship between splanchnic, peripheral and cardiac haemodynamics in liver cirrhosis of different degrees of severity. *Eur J Gastroenterol Hepatol* 1997; **9:** 799-804

2 **Bhathal PS**, Grossman HJ. Reduction of the increased portal vascular resistance of the isolated perfused cirrhotic rat liver by vasodilators. *J Hepatol* 1985; **1:** 325-337

3 **Niederberger M**, Gines P, Tsai P, Martin PY, Morris K, Weigert A, McMurtry I, Schrier RW. Increased aortic cyclic guanosine monophosphate concentration in experimental cirrhosis in rats: evidence for a role of nitric oxide in the pathogenesis of arterial vasodilation in cirrhosis. *Hepatology* 1995; **21**: 1625-1631

4 **Cahill PA**, Redmond EM, Hodges R, Zhang S, Sitzmann JV. Increased endothelial nitric oxide synthase activity in the hyperemic vessels of portal hypertensive rats. *J Hepatol* 1996; **25**: 370-378

5 **Rockey D**. The cellular pathogenesis of portal hypertension: stellate cell contractility, endothelin, and nitric oxide. *Hepatology* 1997; **25**: 2-5

6 **Rodriguez-Perez F**, Groszmann R. Pharmacologic treatment of portal hypertension. *Gastroenterol Clin North Am* 1992; **21**: 15-40

7 **Wiest R**, Das S, Cadelina G, Garcia-Tsao G, Milstien S, Groszmann RJ. Bacterial translocation in cirrhotic rats stimulates eNOS-derived NO production and impairs mesenteric vascular contractility. *J Clin Invest* 1999; **104**: 1223-1233

8 **Trager K**, Matejovic M, Zulke C, Vlatten A, Vogt J, Wachter U, Altherr J, Brinkmann A, Jauch KW, Georgieff M, Radermacher P. Hepatic O_2 exchange and liver energy metabolism in hyperdynamic porcine endotoxemia: effects of iloprost. *Intensive Care Med* 2000; **26**: 1531-1539

9 **Laffi G**, La Villa G, Pinzani M, Marra F, Gentilini P. Arachidonic acid derivatives and renal function in liver cirrhosis. *Semin Nephrol* 1997; **17**: 530-548

10 **Sieber CC**, Groszmann RJ. *In vitro* hyporeactivity to methoxamine in portal hypertensive rats: reversal by nitric oxide blockade. *Am J Physiol* 1992; **262** (6Pt1): G996-G1001

11 **Sieber CC**, Groszmann RJ. Nitric oxide mediates hyporeactivity to vasopressors in mesenteric vessels of portal hypertensive rats. *Gastroenterology* 1992: **103**: 235-239

12 **Feron O**. Intracellular localization and activation of endothelial nitric oxide synthase. *Curr Opin Nephrol Hypertens* 1999; **8**: 55-59

13 **Kubes P**. Inducible nitric oxide synthase: a little bit of good in all of us. *Gut* 2000; **47**: 6-9

14 **Ros J**, Jimenez W, Lamas S, Claria J, Arroyo V, Rivera F, Rodes J. Nitric oxide production in arterial vessels of cirrhotic rats. *Hepatology* 1995; **21**: 554-560

15 **Castro A**, Jimenez W, Claria J, Ros J, Martinez JM, Bosch M, Arroyo V, Piulats J, Rivera F, Rodes J. Impaired responsiveness to angiotensin II in experimental cirrhosis: role of nitric oxide. *Hepatology* 1993; **18**: 367-372

16 **Weigert AL**, Martin PY, Niederberger M, Higa EM, McMurtry IF, Gines P, Schrier RW. Endothelium-dependent vascular hyporesponsiveness without detection of nitric oxide synthase induction in aortas of cirrhotic rats. *Hepatology* 1995; **22**: 1856-1862

17 **Wiest R**, Shah V, Sessa WC, Groszmann RJ. NO overproduction by eNOS precedes hyperdynamic splanchnic circulation in portal hypertensive rats. *Am J Physiol* 1999; **276**(4 Pt 1): G1043-G1051

18 **Gadano AC**, Sogni P, Yang S, Cailmail S, Moreau R, Nepveux P, Couturier D, Lebrec D. Endothelial calcium-calmodulin dependent nitric oxide synthase in the *in vitro* vascular hyporeactivity of portal hypertensive rats. *J Hepatol* 1997; **26**: 678-686

19 **Martin PY**, Xu DL, Niederberger M, Weigert A, Tsai P, St John J, Gines P, Schrier RW. Upregulation of endothelial constitutive NOS: a major role in the increased NO production in cirrhotic rats. *Am J Physiol* 1996; **270**(3 Pt 2): F494-F499

20 **Hori N**, Wiest R, Groszmann RJ. Enhanced release of nitric oxide in response to changes in flow and shear stress in the superior mesenteric arteries of portal hypertensive rats. *Hepatology* 1998; **28**: 1467-1473

21 **Nemoto T**, Ohara-Nemoto Y, Ota M, Takagi T, Yokoyama K. Mechanism of dimer formation of the 90-kDa heat-shock protein. *Eur J Biochem* 1995; **233**: 1-8

22 **Whitesell L**, Mimnaugh EG, De Costa B, Myers CE, Neckers LM. Inhibition of heat shock protein HSP90-pp60v-src heteroprotein complex formation by benzoquinone ansamycins: essential role for stress proteins in oncogenic transformation. *Proc Natl Acad Sci U S A* 1994; **91**: 8324-8328

23 **Garcia-Cardena** G, Fan R, Shah V, Sorrentino R, Cirino G, Papapetropoulos A, Sessa WC. Dynamic activation of endothelial nitric oxide synthase by Hsp90. *Nature* 1998; **392**: 821-824

24 **Chojkier M**, Groszmann RJ. Measurement of portal-systemic shunting in the rat by using gamma-labelled microspheres. *Am J Physiol* 1981; **240**: G371-G375

25 **Rudic RD**, Shesely EG, Maeda N, Smithies O, Segal SS, Sessa WC. Direct evidence for the importance of endothelium-derived nitric oxide in vascular remodeling. *J Clin Invest* 1998; **101**: 731-736

26 **Sieber CC**, Lopez-Talavera JC, Groszmann RJ. Role of nitric oxide in the *in vitro* splanchnic vascular hyporeactivity in ascitic cirrhotic rats. *Gastroenterology* 1993; **104**: 1750-1754

27 **Atucha NM**, Shah V, Garcia-Cardena G, Sessa WE, Groszmann RJ. Role of endothelium in the abnormal response of mesenteric vessels in rats with portal hypertension and liver cirrhosis. *Gastroenterology* 1996; **111**: 1627-1632

28 **Obermann WM**, Sondermann H, Russo AA, Pavletich NP, Hartl FU. *In vivo* function of HSP90 is dependent on ATP binding and ATP hydrolysis. *J Cell Biol* 1998; **143**: 901-910

29 **Picard D**, Khursheed B, Garabedian MJ, Fortin MG, Lindquist S, Yamamoto KR. Reduced levels of HSP90 compromise steroid receptor action *in vivo*. *Nature* 1990; **348**: 166-168

30 **Whitesell L**, Mimnaugh EG, De Costa B, Myers CE, Neckers LM. Inhibition of heat shock protein HSP90-pp60v-src heteroprotein complex formation by benzoquinone ansamycins: essential role for stress proteins in oncogenic transformation. *Proc Natl Acad Sci U S A* 1994; **91**: 8324-8328

31 **Van der Straten** A, Rommel C, Dickson B, Hafen E. The heat shock protein 83(HSP83) is required for Raf-mediated signaling in *Drosophila*. *EMBO J* 1997; **16**: 1961-1969

32 **Imai J**, Yahara I. Role of HSP90 in salt stress tolerance via stabilization and regulation of calcineurin. *Mol Cell Biol* 2000; **20**: 9262-9270

Edited by Zhang JZ and Wang XL

P.O.Box 2345, Beijing 100023,China
Fax: +86-10-85381893
E-mail: wjg@wjgnet.com www.wjgnet.com

World J Gastroenterol 2003;9(11):2548-2551
World Journal of Gastroenterology
 ISSN 1007-9327

• CLINICAL RESEARCH •

Expression and mutation of c-kit gene in gastrointestinal stromal tumors

Fei Feng, Xiao-Hong Liu, Qiang Xie, Wei-Qiang Liu, Cheng-Guang Bai, Da-Lie Ma

Fei Feng, Xiao-Hong Liu, Qiang Xie, Wei-Qiang Liu, Cheng-Guang Bai, Da-Lie Ma, Department of Pathology, Changhai Hospital, Second Military Medical University, Shanghai 200433, China
Supported by the National Natural Science Foundation of China, No.30070743
Correspondence to: Dr. Da-Lie Ma, Department of Pathology, Changhai Hospital, 174 Changhai Road, Shanghai 200433, China. gzff0524@21cn.com
Telephone: +86-21-25070660-808
Received: 2003-05-10 **Accepted:** 2003-06-07

Abstract

AIM: To investigate the expression and mutation of c-kit gene and its correlation with the clinical pathology and prognosis of gastrointestinal stromal tumors (GISTs).

METHODS: A total of 94 cases of GISTs, 10 leiomyomas and 2 schwannomas were studied for the expression of KIT by immunohistochemistry. The c-kit gene mutations in exon 11 of these specimens were detected by PCR-SSCP technique.

RESULTS: Of the 94 cases of GISTs, 91 (96.8 %) expressed the KIT protein. Leiomyomas and schwannomas were negative for KIT. The c-kit gene mutations of exon 11 were found in 38 out of the 94 cases of GISTs (40.4 %). The mutations involved point mutations (Val560-Asp, Ile563-Met), del 557-559 and 579ins12. No mutations were detectable in benign GISTs, leiomyomas or schwannomas. The patients with mutation-positive GISTs showed more frequent recurrences, invasion and metastasis in adjacent tissues than those with mutation-negative ones.

CONCLUSION: KIT is a useful marker for diagnosis of GISTs. Mutation of the c-kit gene may play a significant role in the pathogenesis of GISTs and may be associated with poor prognosis in patients with GISTs.

Feng F, Liu XH, Xie Q, Liu WQ, Bai CG, Ma DL. Expression and mutation of c-kit gene in gastrointestinal stromal tumors. *World J Gastroenterol* 2003; 9(11): 2548-2551
http://www.wjgnet.com/1007-9327/9/2548.asp

INTRODUCTION

Gastrointestinal stromal tumors (GISTs) are the most common mesenchymal tumors of the human gastrointestinal tract that may occur in the entire gastrointestinal tract[1-4]. In recent years, much attention has focused on GISTs. Studies have shown that GISTs strongly express the KIT protein[1,5,6], a type III tyrosine-kinase receptor encoded by the c-kit proto-oncogene[7,8]. The c-kit gene located in the long arm of chromosome 4, is the cellular homologue of oncogene v-kit of the HZ4 feline sarcoma virus[9]. KIT, which is structurally related to the receptors for platelet-derived growth factor and colony-stimulating factor, consists of an extracellular domain, a transmembrane domain, a juxtamembrane domain and a kinase domain with an insert that splits the kinase domain[10]. KIT and its ligand, stem cell factor (SCF), are known to play crucial roles in the development of germ cells, melanocytes, mast cells and interstitial cells of Cajal[11].

Recently, activated c-kit mutations have been identified in GISTs. Most mutations were detected in the juxtamembrane domain (Lys-550 to Val-560)[1,12-14]. These mutations were related to a poorer prognosis. The purpose of this study was to examine the KIT expression and characterize the range of c-kit mutations in GISTs, and to evaluate the significance between c-kit mutations and prognostic factors.

MATERIALS AND METHODS

Patients

Ninety-four cases of GISTs (62 male, 32 female) diagnosed at Changhai Hospital with a median age of 53 years (ranging from 5-77) were included in the study between January 1991 and December 2002. Forty-six tumors were located in the stomach, thirty-two in the small bowel, ten in the large intestine, three in the esophagus and three in the omentum and mesentery. We used Lewin's determination to separate benign from malignant lesions[15]. Sixty-seven cases of GISTs were malignant and 27 were benign. Of the patients in the malignant group, ten received reoperation due to recurrences, distant metastasis was found in 6 patients at the time of surgery, four to the liver and two to both the liver and peritoneum. The remaining patients were free of distant metastasis. One patient with liver metastasis died after operation. Twelve control tumors were also analyzed, including 10 leiomyomas and 2 schwannomas.

Immunohistochemistry

A rabbit polyclonal antibody against human KIT and an EnVision kit were purchased from DAKO. Immunohistochemistry was performed using the two-step technique. All specimens were fixed in 10 % buffered formalin and embedded in paraffin. Four-μm thick sections were cut from the tissue blocks. The sections were deparaffinized and rehydrated, then treated using a microwave epitope retrieval technique with citrate buffer, pH 6.0 at 85 ℃ for 3 min. After cooled at room temperature, the sections were washed in PBS (0.01M, pH7.2) and incubated with the antibody against c-kit (1:100) at room temperature for 1 hour. After washed in PBS, the sections were incubated with the EnVision compound at room temperature for 30 min. Staining was developed by immersing slides in 0.05 % DAB with 0.33 % hydrogen peroxide. All slides were counterstained with haematoxylin, dehydrated and mounted. PBS substituted for the primary antibody was used as the negative control.

DNA Extraction

DNA was extracted from formalin-fixed, paraffin-embedded tissues using standard methods with proteinase K digested and phenol/chloroform purified.

PCR-SSCP

Exon 11 of the c-kit gene was amplified by PCR using the following oligonucleotide primer pairs: sense primer 5'-

AACTCAGCCTGTTTCTGG-3' and antisense primer 5'-GATCTATTTTTCCCTTTCTC-3'. PCR was carried out with the following conditions: 50 μl total reaction volume, with 5 μl template, 5 μl of each oligonucleotide primer, 10 μl dNTP, 10 μl ddH_2O, 2 μl Taq polymerase, 8 μl Mg^{2+} and 5 μl 10×PCR buffer. Cycling conditions were as follows: an initial penetration at 95 ℃ for 4 min, 38 cycles each at 94 ℃ for 1 min, at 56 ℃ for 1 min, at 72 ℃ for 1 min, followed by one cycle at 72 ℃ for 10 min. PCR products were visualized by gel electrophoresis in 1.7 g/L agarose. Then the PCR products were subjected to 8 % non-denaturation polyacrylamide gel electrophoresis (aer: bis=49:1) with 5 % glycerin and silver nitrate staining.

DNA sequencing

PCR products that showed abnormal gel shift by PCR-SSCP were selected for sequencing after cloned into PMD18-T vector. The sequencing procedures were performed by Sangon Co., Shanghai.

Statistical methods

The data were analyzed with χ^2 test.

RESULTS

Immunohistochemistry

Immunohistochemical analyses revealed strong and diffuse KIT expression in 91 out of the 94 cases of GISTs. The positive signals were localized in cytoplasm and membrane (Figures 1 and 2). Ninety-seven percent of malignant GISTs and ninety-six percent of benign GISTs were KIT positive. Compared with the benign group, some malignant GISTs showed weaker and focal positivity. There was no significant difference in the expression of KIT between benign and malignant GISTs (P>0.05). Leiomyomas and schwannomas were negative for KIT.

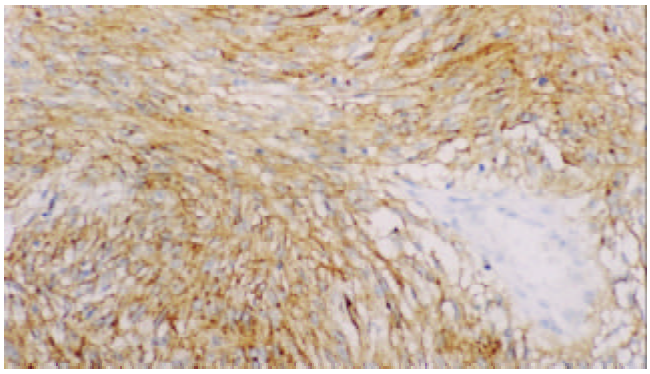

Figure 1 KIT staining in cytoplasm and membrane of GISTs (spindle type)×200.

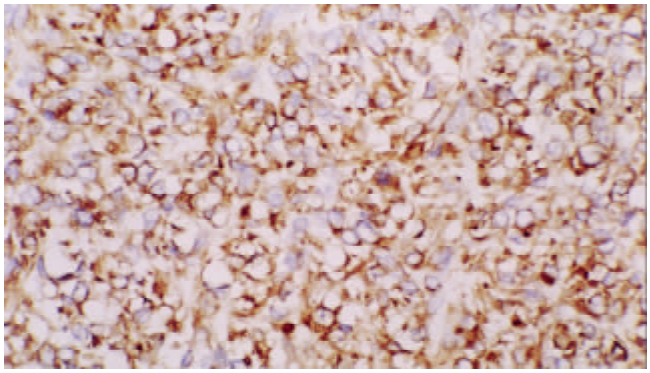

Figure 2 KIT staining in cytoplasm and membrane of GISTs (epithelioid type)×200.

Evaluation of mutations in exon 11 of c-kit gene

Analysis of PCR-SSCP showed abnormal gel shifts in 38 out of the 67 (56.7 %) malignant GISTs. No mutant bands were observed in benign GISTs, as well as in leiomyomas and schwannomas. Sequencing of 6 mutant bands revealed three types of mutations. One case showed point mutations (Val560-Asp and Ile563-Met), one case a 6-bp deletion involving codons 557 to 559, one case a 12-bp insertion at the codon 579 (Figure 3).

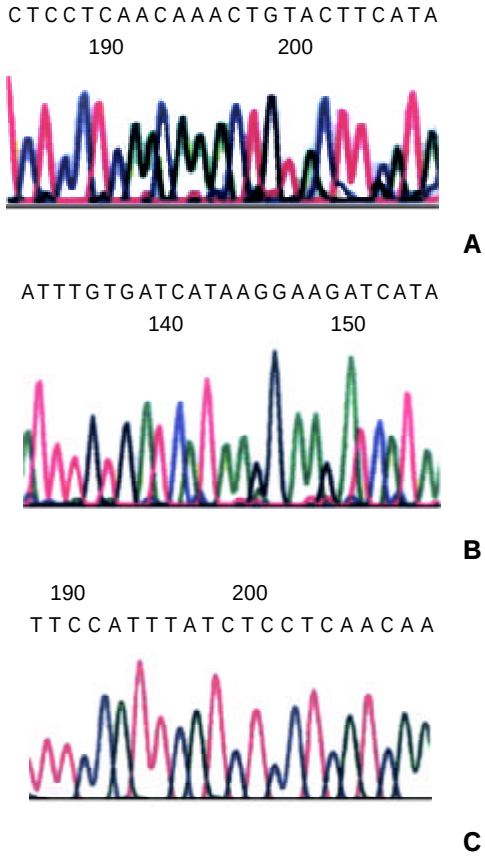

Figure 3 Sequence of the exon 11 of c-kit from the mutant bands obtained from the GISTs. A: 6-bp deletion involving codons 557 and 559 (GGAAGG), B: 12-bp insertion at codon 579 (CTTCCTTATGAT), C: two point mutations (Val 560-Asp, Ile 563-Met).

Correlation of c-kit mutations with clinicopathological parameters

Of the 38 cases of GISTs with c-kit mutations, six developed distant metastasis, eight had local recurrences and one died of liver metastasis. Only two recurrences were found in the remaining 56 cases of GISTs without c-kit mutations.

DISCUSSION

It has been reported that GISTs are strongly and nearly consistent KIT positive and mutations of the c-kit gene were observed in GISTs. In this study, we examined the sequences and expression of c-kit in the spectrum of GISTs, including benign and malignant variants from different sites. The expression and mutations of the c-kit gene were also evaluated in leiomyomas and schwannomas.

As this study has shown, 96.8 % (91/94) GISTs strongly and diffusely expressed KIT irrespective of tumor location, histologic subtype and grade. Neither age nor sex was significantly correlated with the expression levels of KIT. The findings were in agreement with the previous studies[16-18]. No

expression of KIT was found in leiomyomas and schwannomas. These results verified that KIT was a sensitive diagnostic marker for GISTs, but it could not be used as a prognostic index[19,20].

Recently, mutations of the c-kit gene were observed in GISTs. Most mutations were located at the juxtamembrane domain encoded by exon 11, especially between codons 550-560. Mutations of exon 11 were observed in 40.4 % (38/94) of GISTs in our study, and other group observed mutations of exon 11 in 57 %, 42 % and 21 % of GISTs[6,13,21]. The difference in mutation rates appeared to be due to the proportion of malignant GISTs, as suggested by our data and the previous reports. Some studies have shown that the mutant types including insertions or duplications, in addition to deletions and point mutations. These were consistent with our results. DNA sequencing showed that point mutations, deletions and insertions were found in our six GISTs and the range of the c-kit mutations was not only between codons 550-560 but also at codon 579. Although 96.8 % of GISTs expressed KIT, only 40.4 % of GISTs showed mutations in the juxtamembrane region of the c-kit gene. This indicated that some KIT-positive GISTs could occur without mutation of the c-kit gene or with mutations other than exon 11 of the c-kit gene. There was another possibility that some mutations of the NF-1 gene might result in the occurrence of KIT-positive GISTs[1,16,22]. Moreover, the mutations of exons 9, 13, 17, 14 and 15 in GISTs have been identified in recent years[23-25]. But mutations in these exons were found to be few compared with in exon 11[26,27]. These observations demonstrate that multiple mutations of c-kit, irrespective of domain-extracellular, juxtamembrane or kinase, are crucial tumorigenic events in GISTs.

Since c-kit mutations are commonly found in GISTs, how these mutations lead to kinase activation is a field of active investigation. KIT participates in complex networks of signal cascade proteins, and some of these proteins regulate KIT activation in positive or negative manners. Under normal conditions, KIT activation occurs when the receptor is bound to its ligand, a stem cell factor. Ligand-mediated KIT activation triggered various cell-signaling cascades that regulate cell behavior[28,29]. The c-kit mutations of these domains resulted in activation of kinase by allowing ligand-independent receptor dimerization[30-32]. In other words, the mutations in GISTs lead to structural changes of KIT oncoproteins that favor receptor oligomerization and cross-phosphorylation, even in the absence of ligand binding. Because activation of KIT is a ubiquitous oncogenic pathway in most GISTs and important to the growth of GISTs, it has become possible that patients with GISTs can be treated with STI571, a KIT tyrosine kinase inhibitor. STI571 is a 2-phenylaminopyrimidine that selectively inhibits protooncogenic and oncogenic forms of the ABL, PDGFR and c-kit tyrosine kinases[33,34]. STI571 has a potent activity against GIST cells grown *in vitro* and the majority of patients with malignant GIST have shown a benefit to treatment with STI571 in recent clinical trials[35-37].

Finally, we compared clinical outcome between the mutation-positive and negative GISTs, and found more frequent recurrences and poorer prognosis were related with mutation-positive GISTs. In our study, 6 out of the 38 patients with mutation-positive GISTs developed distant metastasis, 8 had local recurrences and 1 died of GIST, whereas only 2 out of the 56 patients with mutation-negative GISTs had recurrences. These findings are consistent with some other previous results[1,6,13,38,39], and indicate that the c-kit mutations seem to be related to poorer prognosis. But there is an opposite opinion recently. The results showed that these mutations occurred very early in the course of GISTs development and were of little prognostic importance in GISTs[40]. And now cytogenetic abnormalities have been detected in GISTs[41-43]. These findings suggest that molecular alterations and c-kit mutations are likely to be involved in determining the biologic behaviors of both benign and malignant GISTs.

Considering these findings, we conclude that most GISTs strongly and diffusely express KIT protein, and KIT is a useful and sensitive marker for diagnosis of GISTs. C-kit mutation is undoubtedly a pivotal event in GISTs and may be associated with poor prognosis. Evaluation of KIT mutation may have both prognostic and therapeutic significances as the new tyrosine kinase inhibitor (STI571) treatments are available. The correlation between c-kit mutations and clinical behaviors is far more complex than initially appreciated, and further studies are needed.

REFERENCES

1 **Hirota S,** Isozaki K, Moriyama Y, Hashimoto K, Nishida T, Ishiguro S, Kawano K, Hanada M, Kurata A, Takeda M, Muhammad Tunio G, Matsuzawa Y, Kanakura Y, Shinomura Y, Kitamura Y. Gain-of-function mutations of c-kit in human gastrointestinal stromal tumors. *Science* 1998; **279:** 577-580

2 **Miettinen M,** Monihan JM, Sarlomo-Rikala M, Kovatich AJ, Carr NJ, Emory TS, Sobin LH. Gastrointestinal stromal tumors / smooth muscle tumors (GISTs) primary in the omentum and mesentery: clinicopathologic and immunohistochemical study of 26 cases. *Am J Surg Pathol* 1999; **23:** 1109-1118

3 **Shibata Y,** Ueda T, Seki H, Yagihashi N. Gastrointestinal stromal tumour of the rectum. *Eur J Gastroenterol Hepatol* 2001; **13:** 283-286

4 **Miettinen M,** Sobin LH. Gastrointestinal stromal tumors in the appendix: a clinicopathologic and immunohistochemical study of four cases. *Am J Surg Pathol* 2001; **25:** 1433-1437

5 **Sarlomo-Rikala M,** Kovatich AJ, Barusevicius A, Miettinen M. CD117: a sensitive marker for gastrointestinal stromal tumors that is more specific than CD34. *Mod Pathol* 1998; **11:** 728-734

6 **Taniguchi M,** Nishida T, Hirota S, Isozaki K, Ito T, Nomura T, Matsuda H, Kitamura Y. Effect of c-kit mutation on prognosis of gastrointestinal stromal tumors. *Cancer Res* 1999; **59:** 4297-4300

7 **Chabot B,** Stephenson DA, Chapman VM, Besmer P, Bernstein A. The proto-oncogene c-kit encoding a transmembrane tyrosine kinase receptor maps to the mouse W locus. *Nature* 1988; **335:** 88-89

8 **Geissler EN,** Ryan MA, Housman DE. The dominant-white spotting (w) locus of the mouse encodes the c-kit proto-oncogene. *Cell* 1988; **55:** 185-192

9 **Majumder S,** Brown K, Qiu FH, Besmer P. C-kit Protein, a transmembrane kinase: identification in tissues and characterization. *Mol Cell Biol* 1988; **8:** 4896- 4903

10 **Hirota S.** Gastrointestinal stromal tumors: their origin and cause. *Int J Clin Oncol* 2001; **6:** 1-5

11 **Huizinga JD,** Thuneberg L, Klusppel M, Malysz J, Mikkelsen HB, Bernstein A. W / kit gene required for interstitial cells of Cajal and for intestinal pacemaker activity. *Nature* 1995; **373:** 347-349

12 **Nakahara M,** Isozaki K, Hirota S, Miyagawa J, Hase-Sawada N, Taniguchi M, Nishida T, Kanayama S, Kitamura Y, Shinomura Y, Matsuzawa Y. A novel gain-of-function mutation of c-kit gene in gastrointestinal stromal tumors. *Gastroenterology* 1998; **115:** 1090-1095

13 **Lasota J,** Jasinski M, Sarlomo-Rikala M, Miettinen M. Mutations in exon 11 of c-Kit occur preferentially in malignant versus benign gastrointestinal stromal tumors and do not occur in leiomyomas or leiomyosarcomas. *Am J Pathol* 1999; **154:** 53-60

14 **Miettinen M,** Lasota J. Gastrointestinal stromal tumors-definition, clinical, histological, immunohistochemical, and molecular genetic features and differential diagnosis. *Virchows Arch* 2001; **438:** 1-12

15 **Lewin KJ,** Riddell RH, Weinstein WM. Gastrointestinal pathology and its clinical implications.1 st ed. *New York: Igaku-shoin* 1992: 284-341

16 **Kindblom LG,** Remotti HE, Aldenborg F, Meis-Kindblom JM. Gastrointestinal pacemaker cell tumor (GIPACT): gastrointestinal stromal tumors show phenotypic characteristics of the interstitial cells of Cajal. *Am J Pathol* 1998; **152:** 1259-1269

17 **Sircar K,** Hewlett BR, Huizinga JD, Chorneyko K, Berezin I, Riddell RH. Interstitial cells of Cajal as precursors for gastrointestinal stromal tumors. *Am J Surg Pathol* 1999; **23:** 377-389

18 **Miettinen M,** Sarlomo-Rikala M, Lasota J. Gastrointestinal stromal tumors: recent advances in understanding of their biology. *Hum Pathol* 1999; **30:** 1213-1220

19 **Hasegawa T,** Matsuno Y, Shimoda T, Hirohashi S. Gastrointestinal stromal tumor: consistent CD117 immunostaining for diagnosis, and prognostic classification based on tumor size and MIB-1 grade. *Hum Pathol* 2002; **33:** 669-676

20 **Fletcher CD,** Berman JJ, Corless C, Gorstein F, Lasota J, Longley BJ, Miettinen M, O'Leary TJ, Remotti H, Rubin BP, Shmookler B, Sobin LH, Weiss SW. Diagnosis of gastrointestinal stromal tumors: A consensus approach. *Hum Pathol* 2002; **33:** 459-465

21 **Moskaluk CA,** Tian Q, Marshall CR, Rumpel CA, Franquemont DW, Frierson HF Jr. Mutations of c-kit JM domain are found in a minority of human gastrointestinal stromal tumors. *Oncogene* 1999; **18:** 1897-1902

22 **Ishida T,** Wada I, Horiuchi H, Oka T, Machinami R. Multiple small intestinal stromal tumors with skeinoid fibers in association with neurofibromatosis 1 (von Recklinghausen's disease). *Pathol Int* 1996; **46:** 689-695

23 **Lux ML,** Rubin BP, Biase TL, Chen CJ, Maclure T, Demetri G, Xiao S, Singer S, Fletcher CD, Fletcher JA. KIT extracellular and kinase domain mutations in gastrointestinal stromal tumors. *Am J Pathol* 2000; **156:** 791-795

24 **Andersson J,** Sjogren H, Meis-Kindblom JM, Stenman G, Aman P, Kindblom LG. The complexity of KIT gene mutations and chromosome rearrangements and their clinical correlation in gastrointestinal stromal (pacemaker cell) tumors. *Am J Pathol* 2002; **160:** 15-22

25 **Rubin BP,** Singer S, Tsao C, Duensing A, Lux ML, Ruiz R, Hibbard MK, Chen CJ, Xiao S, Tuveson DA, Demetri GD, Fletcher CD, Fletcher JA. KIT activation is a ubiquitous feature of gastrointestinal stromal tumors. *Cancer Res* 2001; **61:** 8118-8121

26 **Lasota J,** Wozniak A, Sarlomo-Rikala M, Rys J, Kordek R, Nassar A, Sobin LH, Miettinen M. Mutations in exon 9 and 13 of KIT gene are rare events in gastrointestinal stromal tumors. A study of 200 cases. *Am J Pathol* 2000; **157:** 1091-1095

27 **Hirota S,** Nishida T, Isozaki K, Taniguchi M, Nakamura J, Okazaki T, Kitamura Y. Gain-of-function mutation at the extracellular domain of KIT in gastrointestinal stromal tumors. *J Pathol* 2001; **193:** 505-510

28 **Linnekin D.** Early signaling pathways activated by c-Kit in hematopoietic cells. *Int J Biochem Cell Biol* 1999; **31:** 1053-1074

29 **Taylor ML,** Metcalfe DD. Kit signal transduction. *Hematol Oncol Clin North Am* 2000; **14:** 517-535

30 **Ma Y,** Cunningham ME, Wang X, Ghosh I, Regan L, Longley BJ. Inhibition of spontaneous receptor phosphorylation by residues in a putative alpha-helix in the KIT intracellular juxtamembrane region. *J Biol Chem* 1999; **274:** 13399-13402

31 **Isozaki K,** Terris B, Belghiti J, Schiffmann S, Hirota S, Vanderwinden JM. Germline-activating mutation in the kinase domain of KIT gene in familial gastrointestinal stromal tumors. *Am J Pathol* 2000; **157:** 1581-1585

32 **Heinrich MC,** Rubin BP, Longley BJ, Fletcher JA. Biology and genetic aspects of gastrointestinal stromal tumors: KIT activation and cytogenetic alterations. *Hum Pathol* 2002; **33:** 484-495

33 **Schindler T,** Bornmann W, Pellicena P, Miller WT, Clarkson B, Kuriyan J. Structural mechanism for STI-571 inhibition of abelson tyrosine kinase. *Science* 2000; **289:** 1938-1942

34 **Heinrich MC,** Blanke CD, Druker BJ, Corless CL. Inhibition of KIT tyrosine kinase activity: a novel molecular approach to the treatment of KIT-positive malignancies. *J Clin Oncol* 2002; **20:** 1692-1703

35 **Tuveson DA,** Willis NA, Jacks T, Griffin JD, Singer S, Fletcher CD, Fletcher JA, Demetri GD. STI571 inactivation of the gastrointestinal stromal tumor c-KIT oncoprotein:biological and clinical implications. *Oncogene* 2001; **20:** 5054-5058

36 **Joensuu H,** Roberts PJ, Sarlomo-Rikala M, Andersson LC, Tervahartiala P, Tuveson D, Silberman S, Capdeville R, Dimitrijevic S, Druker B, Demetri GD. Effect of the tyrosine kinase inhibitor STI571 in a patient with a metastatic gastrointestinal stromal tumor. *N Engl J Med* 2001; **344:** 1052-1056

37 **Van Oosterom AT,** Judson I, Verweij J, Stroobants S, Donato di Paola E, Dimitrijevic S, Martens M, Webb A, Sciot R, Van Glabbeke M, Silberman S, Nielsen OS. Safty and efficacy of imatinib (STI571) in metastatic gastrointestinal stromal tumors: a phase I study. *Lancet* 2001; **358:** 1421-1423

38 **Ernst SI,** Hubbs AE, Przygodzki RM, Emory TS, Sobin LH, O'Leary TJ. KIT mutation portends poor prognosis in gastrointestinal stromal/smooth muscle tumors. *Lab Invest* 1998; **78:** 1633-1636

39 **Miettinen M,** El-Rifai W, H L Sobin L, Lasota J. Evaluation of malignancy and prognosis of gastrointestinal stromal tumors: a review. *Hum Pathol* 2002; **33:** 478-483

40 **Corless CL,** McGreevey L, Haley A, Town A, Heinrich MC. KIT mutations are common in incidental gastrointestinal stromal tumors one centimeter or less in size. *Am J Pathol* 2002; **160:** 1567-1572

41 **El-Rifai W,** Sarlomo-Rikala M, Miettinen M, Knuutila S, Andersson LC. DNA copy number losses in chromosome 14: an early change in gastrointestinal stromal tumors. *Cancer Res* 1996; **56:** 3230-3233

42 **O'Leary T,** Ernst S, Przygodzki R, Emory T, Sobin L. Loss of heterozygosity at 1p36 predicts poor prognosis in gastrointestinal stromal/smooth muscle tumors. *Lab Invest* 1999; **79:** 1461-1467

43 **Gunawan B,** Bergmann F, Hoer J, Langer C, Schumpelick V, Becker H, Fuzesi L. Biological and clinical significance of cytogenetic abnormalities in low-risk and high-risk gastrointestinal stromal tumors. *Hum Pathol* 2002; **33:** 316-321

Edited by Zhang JZ and Wang XL

P.O.Box 2345, Beijing 100023,China
Fax: +86-10-85381893
E-mail: wjg@wjgnet.com www.wjgnet.com

World J Gastroenterol 2003;9(11):2552-2556
World Journal of Gastroenterology
 ISSN 1007-9327

• CLINICAL RESEARCH •

Endoscopic patterns of gastric mucosa and its clinicopathological significance

Jian-Min Yang, Lei Chen, Yu-Lin Fan, Xiang-Hong Li, Xin Yu, Dian-Chun Fang

Jian-Min Yang, Lei Chen, Yu-Lin Fan, Xiang-Hong Li, Xin Yu, Dian-Chun Fang, Gastroenterology Research Center, Southwest Hospital, Third Military Medical University, Chongqing 400038, China
Correspondence to: Dr. Jian-Min Yang, Gastroenterology Research Center, Southwest Hospital, Third Military Medical University, Chongqing 400038, China. jianminyang@hotmail.com
Telephone: +86-23-68754678
Received: 2003-04-12 **Accepted:** 2003-05-19

Abstract

AIM: To explore the correlation of magnifying endoscopic patterns and histopathology, *Helicobacter pylori (H pylori)* infection of the gastric mucosa.

METHODS: Gastric mucosal patterns in 140 patients with chronic gastritis were studied using Olympus GIF-Q240Z magnifying endoscope. Histopathological examination, rapid urease test and Warrthin-Starry staining were taken with biopsy samples from the magnified sites of stomach. The magnifying endoscopic patterns were compared with histopathological results and *H pylori* detection.

RESULTS: The pit patterns of gastric mucosa were classified as types A (round spot), B (short rod), C (branched), D (reticular) and E (villus). The detection rate of chronic atrophic gastritis (CAG) by magnifying endoscopy was 94.3 % (33/35), which was significantly higher than that by routine endoscopy (22.9 %, 8/35) ($P<0.01$). The pit patterns of 31 cases of intestinal metaplasia (IM) appeared as type E in 18 cases (58.1 %), type D in 8 cases (25.8 %) and type C in 5 cases (16.1 %). Fourteen out of 18 patients (77.8 %) with complete type (type I) of IM appeared as type E of pit patterns, whereas only 4 of 13 (30.8 %) patients with incomplete type (types II and III) of IM appeared as type E ($P<0.05$). Collecting venules in the anterior of lower part of gastric corpus were subgrouped into types R (regular), I (irregular) and D (disappeared). *H pylori* infection was found in 12.2 %(9/74), 60 %(9/15) and 84.3 %(43/51) cases in these types respectively. *H pylori* infection rate in type R was significantly lower than that in other two types ($P<0.01$).

CONCLUSION: Magnifying endoscopy may have an obvious value in diagnosing chronic atrophic gastritis, intestinal metaplasia and *H pylori* infection.

Yang JM, Chen L, Fan YL, Li XH, Yu X, Fang DC. Endoscopic patterns of gastric mucosa and its clinicopathological significance. *World J Gastroenterol* 2003; 9(11): 2552-2556
http://www.wjgnet.com/1007-9327/9/2552.asp

INTRODUCTION

Recently, magnifying endoscope has been used clinically for its developments in amplifying power, definition and operational capability. Lots of international studies on clinical application of magnifying endoscope especially from Japan have been reported, but most of them were focused on colon and esophagus, only a few of them on gastric mucosa have been published[1-28]. These studies implicate that classification of superficial mucosal appearances defined by magnifying endoscopy can reflect not only histological features but also mucin phenotypes. Magnifying endoscopy is helpful for more correctly distinguishing hyperplastic lesions from adenomatous and cancerous lesions, and for improving detection of early flat and depressed cancer. More interestingly, according to Japanese data, magnifying endoscopy could also be used to predict invasive depth and lymph node metastasis of cancer[6,16]. Up to now only a few studies on the field have been reported in China[29-33]. In this article, we reported our study on correlation of magnifying endoscopic patterns and histopathology, *Helicobacter pylori (H pylori)* infection of gastric mucosa in 140 patients with chronic gastritis to understand the value of magnifying endoscopy in diagnosing the minute lesions of gastric mucosa.

MATERIALS AND METHODS

Subjects

Subjects were 140 out-patients and in-patients (male: 68, female: 72, age range: 18-77 years old, average age: 50.6) with chronic superficial gastritis (CSG, $n=105$) and chronic atrophic gastritis (CAG, $n=35$) during June-August, 2002. All the patients had gastrointestinal symptoms such as abdominal distention, abdominalgia, belch and hyperhydrochloria.

Magnifying endoscope

New model of electronic magnifying endoscope GIF Q-240Z (Olympus Optical Co., Ltd., Tokyo, Japan) was used. It could be used to perform routine endoscopy (observation at standard magnification) as well as to magnify the image 80 times (in 14-inch monitor) as large as the original size through manual adjustment of the focal length.

Endoscopy

Magnifying endoscopy was performed by senior endoscopists and the real time static and successive images were recorded by computer image and text reporting system and video tape recorder. In order to inhibit gastrointestinal peristalsis, 10 mg of anisodaminum (654-2) and 5-10 mg of diazepamum were injected intramuscularly at 10 minutes pre-endoscopy. Routine endoscopy was performed first, and if necessary, dilution of dimethyl silicone oil was used to flush off the foam and mucus, then the appearance of gastric pits in the antrum, angel, corpus and fundus, and collecting venules in the anterior of lower part of gastric corpus were observed so that the patterns of gastric pits and collecting venules could be decided.

Histological examination

One piece of tissue in the greater curvature of gastric antrum was extracted for rapid urease test using RUT kit (Kedi Technology Co., LTD, Zhuhai, China). Two biopsies from the magnified sites in gastric antrum and corpus were performed for hematoxylin-eosin (HE) and Warrthin-Starry staining. Rapid urease test and Warrthin-Starry staining were used for

H pylori detection[34,35]. According to the national standard of China, *H pylori* infection was established after positive results were confirmed by both rapid urease test and Warrthin-Starry staining[35]. HE staining was performed for routine histopathological examination. Inflammatory levels were graded as mild, moderate and severe types according to the infiltration depth of <1/3, 1/3-2/3 and >2/3 of inflammatory cells in the mucous layer and CAG was graded as mild, moderate and severe types according to the decreased levels of <1/3, 1/3-2/3 and >2/3 of the intrinsic glands[35]. At the same time, mucus histochemical stainings of AB/PAS for distinguishing acid mucus from neutral mucus and AF/AB for distinguishing sulphomucins from sialomucins were performed on the samples with IM confirmed by histopathological examination. According to the histological structures and properties of mucus excreted by cells, IM was classified into type I (complete type), type II (incomplete small intestinal type) and type III (incomplete colonic type)[36].

Statistical analysis

Chi-square test was applied and *P* values less than 0.05 were considered significant.

RESULTS

Pit patterns and pathohistological findings

Classification of gastric pits Based on the analysis of recorded static and successive images and refered to Guelrud' s study on mucosal patterns of Barrett' s esophagus with enhanced magnification endoscopy[18], we classified gastric pits into the following five fundamental types: type A, round-spot-like, distributing only in the gastric corpus and fundus with basically normal histology; type B, short-rod-like, with deeper pits, branches and curvatures fewer than those in type C, mainly distributing in the gastric antrum without obvious lesions such as inflammation; type C, with elongated and tortuous pits with obviously increased branches and curvatures, connected to present branch-like form, seen in mucosa with pathological changes as inflammation, edema and IM; type D, with reticular pits, seen in areas with more severe inflammation, edema and IM, also found in mucosa around erosion and ulcers; and type E, with villus-like pits, or with finger-like tubers, similar to enteral villus-like changes, seen only in the areas with IM (Figure 1). Overlappings and crossings of gastric pits might be present except the above five fundamental patterns. For example, a combination of type A and type B of gastric pits was frequently presented in the gastric angle.

In types B, C, D and E, moderate and severe inflammations were seen in 18.6 %(26/140), 85.1 %(40/47), 100 %(13/13) and 88.9 %(16/18) cases respectively. The inflammatory levels in types C, D and E were significantly higher than those in type B ($P<0.01$).

Features of atrophic gastritis under magnifying endoscope Under routine endoscope, changes of rough mucosa, unflat granules, increased white areas, exposure of submucous vessels could be seen in CAG[35]. Generally, theses changes could be

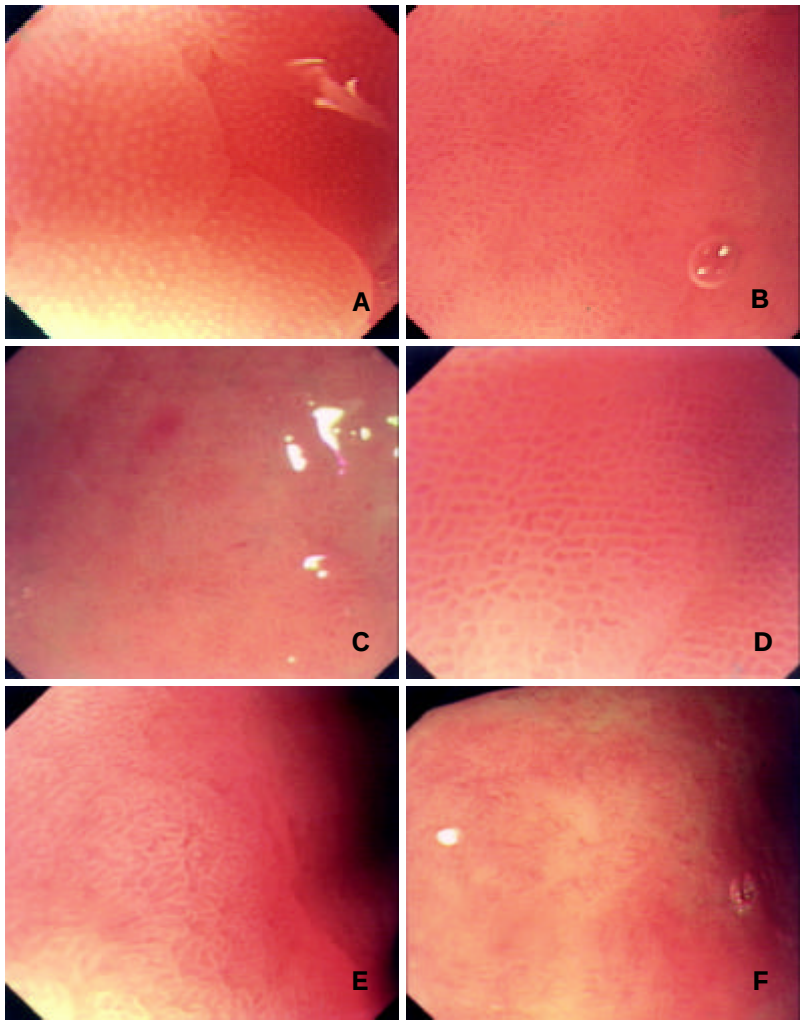

Figure 1 Pit patterns of gastric mucosa under magnifying endoscope. A: Type A: Gastric pits appeared as round spot, B: Type B: Gastric pits appeared as short rod, C: Type C: Gastric pits appeared as branched, D: Type D: Gastric pits appeared as reticular, E: Type E: Gastric pits appeared as villus, F: CAG: Decrease and disappearance of gastric pits.

more easily found in severe CAG, but it was hard to identify them in mild CAG. However, under magnifying endoscope, remarkably characteristic changes of CAG could be seen. With a comparatively low magnifying power, obvious red-white mucosa and increased white areas could be identified. When with enhanced magnifying power, disordered structures, decrease in quantity and even disappearance of pits as scar-like change could be observed in white areas (Figure 1-F).

Thirty-five patients with different grades of gastric mucous atrophy were confirmed by pathological examination in 140 patients, in which 27 in gastric antrum, 5 in gastric angle, 3 in gastric corpus, 16 with mild atrophy, 7 with moderate atrophy and 12 with severe atrophy. By routine endoscopy, only 8 patients (2 with moderate atrophy, 6 with severe atrophy), but by magnifying endoscopy, CAG-related changes were found in 33 patients (14 with mild atrophy, 7 with moderate atrophy, 12 with severe atrophy). The detection rates of atrophic gastritis by routine endoscopy and magnifying endoscopy were 22.9 %(8/35) and 94.3 %(33/35) respectively and significant difference was found by comparison of the two kinds of endoscopy (P<0.01).

Features of intestinal metaplasia under magnifying endoscope It was reported that characteristic changes such as light yellow or ivory-white nodosity-like, fishscale-like and diffusing granule-like appearances of IM in gastric mucosa could be found under routine endoscopy[37]. In this study, by analysis of magnifying endoscopy images of 31 patients with IM, we found that there were mainly three patterns of gastric pits in IM mucosal areas: type C (5 cases), type D (8cases) and type E (18cases). Particularly, very high specificity was found in type E. IM was confirmed pathologically in all the samples of 18 patients with type E. After classification of all the samples with IM by mucous histochemical staining, a certain relation was found between the patterns of gastric pits and classification of IM mucin phenotypes, as was shown in Table 1. Fourteen out of 18 patients (77.8 %) with complete type (type I) of IM appeared as type E of pit patterns, whereas only 4 of 13 (30.8 %) patients with incomplete type (types II and III) of IM appeared as the same type of pit patterns (P<0.05).

Table 1 Relation between IM pit patterns and IM mucin phenotypes

Pit patterns	Cases	Type I IM	Type II IM	Type III IM
Type C	5	2	3	0
Type D	8	2	5	1
Type E	18	14	3	1
Total	31	18	11	2

Architecture of collecting venules and H pylori infection

With reference to Yagi's literature[26], we classified the architecture of collecting venules into the following three types: type R (regular type) with diameter of minor venules being 0.4-0.5 mm and regular spider-like and jellyfish-like arrangement, type I (irregular type) in which decrease in quantity of collecting venules could be unclearly found with irregular arrangement, and type D (disappeared) in which collecting venules could not be found under magnifying endoscope (Figure 2).

When the patients in which positive *H pylori* was confirmed by both rapid urease test and Warrthin-Starry staining were regarded as being infected by *H pylori*, the *H pylori* infection rates in the patients with regular (R), irregular (I) and disappeared (D) types of collecting venules were 12.2 %, 60 % and 84.3 %, respectively. Statistical analysis revealed that *H pylori* infection rates in the patients with types D and I were markedly higher than those in patients with type R (P<0.01), but there was no significance between type I and type D (P>0.05). A comparison of different types of collecting venules by the corresponding rapid urease test and by Warrthin-Starry staining is shown in Table 2.

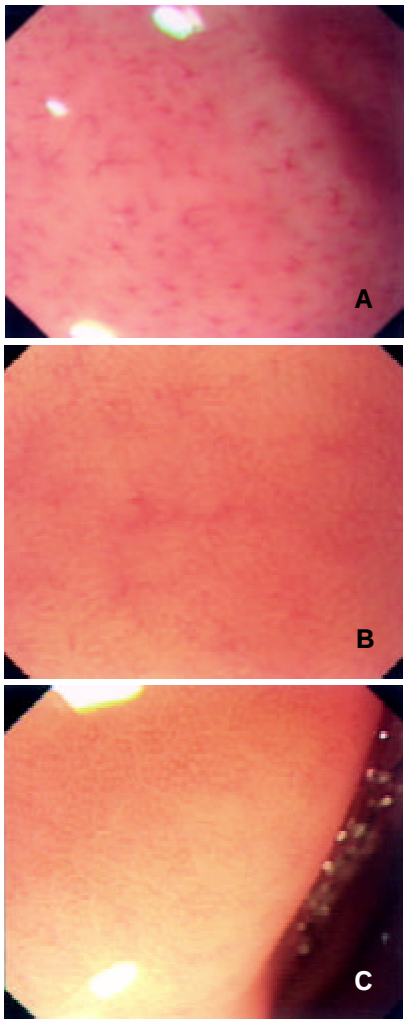

Figure 2 Architecture of collecting venules under magnifying endoscope. A: Type R: Regular spider-like arrangement of collecting venules, B: Type I: Unclear irregular arrangement of collecting venules, C: Type D: Disappearance of collecting venules.

Table 2 Relation of different architectures of collecting venules and *H pylori* infection

Collecting venules	Cases	Rapid urease test (+)	W-S staining (+)	Both methods(+)
Type R	74	9(12.2 %)	13(17.6 %)	9(12.2 %)
Type I	15	11(73.3 %)	9(60 %)	9 (60 %)
Type D	51	43(84.3 %)	45(86.3 %)	43(84.3 %)

DISCUSSION

The pit patterns observed on the mucosal surface are considered to reflect the arrangement and structure of surface epithelia, morphology, number, distribution, and function of glands, mucosal edema and inflammation, and vascular morphology, arrangement, number and distribution. The basic units of the microstructures on the surface of gastric mucosa are countless gastric pits that form gastric areas separated by minor gastric grooves (also called interval grooves). As the openings of glands, gastric pits are the first to have changes of the structures due to gastric mucosal lesions. Magnifying endoscope can be

used to observe the minute architecture of gastric pits because it has the similar magnifying power to that of stereomicroscope.

In this research, we studied the correlation of magnifying endoscopic patterns and histopathology, *Helicobacter pylori* infection of the gastric mucosa in 140 patients with chronic gastritis. There has been no widely accepted standard to the classification of gastric pits under magnifying endoscope, so the classification method, we used, was based on the analysis of our recorded static and successive images by magnifying endoscopy in the 140 patients and referred to Guelrud' s study on mucosal patterns of Barrett' s esophagus with enhanced magnification endoscopy[18]. Type A and type B represented the manifestation of normal gastric pits in gastric corpus and antrum, which concerned the distribution of gastric glands. Single tabular glands with short and fine neck were found in the gastric corpus and fundus, so gastric pits were presented with round spots as the openings of the gastric glands. Glands in frontal area of pyloric ostium and in gastric antrum were of multi-branches and curvatures and 3-5 glands often shared the same opening in one pit, thus the pits in frontal area of pyloric ostium and gastric antrum were short rod-like and deeper and longer than those of type A. Types C and D were formed by the enlargement, elongation, tortuosity of pits and connection of pits due to the pathological changes as inflammation and edema but type E might be the characteristic changes of intestinal metaplasia. Studies by Endo *et al.* of the mucosa with intestinal metaplasia in Barret esophagus in gastric cardia also revealed that villus-like pits were the characteristic change due to intestinal metaplasia[15].

Gastric mucosal atrophy could be identified by routine endoscopy usually when it was at more severe grade. Under magnifying endoscopy, disordered structures, deficiency and even disappearance of gastric pits were of high detection rate and accuracy for atrophic gastritis. As to mild and moderated grades of atrophy, the diagnostic sensitivity by magnifying endoscopy was higher than that by routine endoscopy. The decrease and disappearance of gastric pits due to atrophy were different from mucosal defect due to erosion in which there usually smooth-edged pits belonging to types C and D.

It was reported that characteristic changes such as light yellow or ivory-white nodosity-like, fishscale-like and diffusing granule-like appearances of intestinal metaplsia in gastric mucosa could be found under routine endoscopy[37]. The intestinal metaplasia could be classified into complete and incomplete types according to the histological structures and the properties of mucus excreted by cells[36]. In our study, the pit patterns of 31 patients with intestinal metaplasia appeared as type E in 18 (58.1 %), type D in 8 (25.8 %) and type C in 5 (16.1 %). Fourteen out of 18 patients (77.8 %) with complete type (type I) of intestinal metaplasia appeared as villus-like and finger-like changes (type E) of pit patterns, whereas only 4 out of 13 (30.8 %) patients with incomplete type (types II and III) of intestinal metaplasia appeared as the same type of pit patterns ($P<0.05$), suggesting type E of gastric pits was the result of characteristic change of complete intestinal metaplasia. In addition, our study also reveals that pits of incomplete intestinal metaplasia mainly belonged to types C and D (9/13, 69.2 %). Nevertheless, the above studies were still at preliminary stage with a small number of samples and further studies should be conducted to draw the final conclusion.

Collecting venules are tiny venules in gastric mucosa directly connected with capillary vessels. A few reports have been made on the architecture of collecting venules in gastric mucosa by magnifying endoscopy in which it was regarded as having certain specificity and feasibility to detect *Helicobacter pylori* infection[25,26]. It has also been verified by our study that *Helicobacter pylori* infection rate of patients with type R collecting venules was significantly lower than that with types I and D, suggesting that magnifying endoscopy was of high value in the diagnosis of *Helicobacter pylori* infection in gastric mucosa. As to the causes leading to the changes of collecting venules when *Helicobacter pylori* infection occurs, it has been reported that they were found in types I and D, in which remarkable increase of infiltration of neutrophils and monocytes was found and the architecture of collecting venules might be affected by edema of mucosa due to *Helicobacter pylori* infection[25,26]. However, further studies of the precise mechanism should be conducted because there are some other causes resulting in edema of mucosa.

In conclusion, it is a novel topic in the field of digestive endoscopy to diagnose minute lesions in gastric mucosa by magnifying endoscopy. Our preliminary study has shown that magnifying endoscopy is of high value in the diagnosis of gastric mucosal atrophy, intestinal metaplasia and *Helicobacter pylori* infection. However, the pit patterns of gastric mucosa, particularly those under magnifying chromoendoscopy are very complicated and there has been no widely accepted standard on the classification. Therefore, further studies are suggested on the clinicopathological significance of different patterns of gastric pits, particularly the characteristic changes of gastric pits and microvessels of intramucosal gastric carcinomas.

REFERENCES

1 **Makin GB**, Breen DJ, Monson JR. The impact of new technology on surgery for colorectal cancer. *World J Gastroenterol* 2001; **7**: 612-621

2 **Peitz U**, Malfertheiner P. Chromoendoscopy: from a research tool to clinical progress. *Dig Dis* 2002; **20**: 111-119

3 **Tamura S**, Furuya Y, Tadokoro T, Higashidani Y, Yokoyama Y, Araki K, Onishi S. Pit pattern and three-dimensional configuration of isolated crypts from the patients with colorectal neoplasm. *J Gastroenterol* 2002; **37**: 798-806

4 **Tonooka T**, Sano Y, Fujii T, Kato S, Yoshino T, Fu KI, Hironaka S, Ochiai A, Yoshida S. Adenocarcinoma in solitary large hyperplastic polyp diagnosed by magnifying colonoscope: report of a case. *Dis Colon Rectum* 2002; **45**: 1407-1411

5 **Morita T**, Tamura S, Miyazaki J, Higashidani Y, Onishi S. Evaluation of endoscopic and histopathological features of serrated adenoma of the colon. *Endoscopy* 2001; **33**: 761-765

6 **Matsumoto T,** Hizawa K, Esaki M, Kurahara K, Mizuno M, Hirakawa K, Yao T, Iida M. Comparison of EUS and magnifying colonoscopy for assessment of small colorectal cancers. *Gastrointest Endosc* 2002; **56**: 354-360

7 **Hurlstone DP**, Fujii T, Lobo AJ. Early detection of colorectal cancer using high-magnification chromoscopic colonoscopy. *Br J Surg* 2002; **89**: 272-282

8 **Tung SY**, Wu CS, Su MY. Magnifying colonoscopy in differentiating neoplastic from nonneoplastic colorectal lesions. *Am J Gastroenterol* 2001; **96**: 2628-2632

9 **Kato S**, Fujii T, Koba I, Sano Y, Fu KI, Parra-Blanco A, Tajiri H, Yoshida S, Rembacken B. Assessment of colorectal lesions using magnifying colonoscopy and mucosal dye spraying: can significant lesions be distinguished? *Endoscopy* 2001; **33**: 306-310

10 **Bruno MJ.** Magnification endoscopy, high resolution endoscopy, and chromoscopy; towards a better optical diagnosis. *Gut* 2003; **52**(Suppl 4): iv7-11

11 **Kudo S**, Kashida H, Tamura T, Kogure E, Imai Y, Yamano H, Hart AR. Colonoscopic diagnosis and management of nonpolypoid early colorectal cancer. *World J Surg* 2000; **24**: 1081-1090

12 **Nagata S**, Tanaka S, Haruma K, Yoshihara M, Sumii K, Kajiyama G, Shimamoto F. Pit pattern diagnosis of early colorectal carcinoma by magnifying colonoscopy: clinical and histological implications. *Int J Oncol* 2000; **16**: 927-934

13 **Inoue H**. Magnification endoscopy in the esophagus and stomach. *Digestive Endoscopy* 2001; **13**(Suppl): S40-S41

14 **Sharma P**, Weston AP, Topalovski M, Cherian R, Bhattacharyya A, Sampliner RE. Magnification chromoendoscopy for the detection of intestinal metaplasia and dysplasia in Barrett's oesophagus. *Gut* 2003; **52**: 24-27

15 **Endo T**, Awakawa T, Takahashi H, Arimura Y, Itoh F, Yamashita K, Sasaki S, Yamamoto H, Tang X, Imai K. Classification of Barrett's epithelium by magnifying endoscopy. *Gastrointest Endosc* 2002; **55**: 641-647
16 **Kumagai Y**, Inoue H, Nagai K, Kawano T, Iwai T. Magnifying endoscopy, stereoscopic microscopy, and the microvascular architecture of superficial esophageal carcinoma. *Endoscopy* 2002; **34**: 369-375
17 **Guelrud M**, Herrera I, Essenfeld H, Castro J, Antonioli DA. Intestinal metaplasia of the gastric cardia: A prospective study with enhanced magnification endoscopy. *Am J Gastroenterol* 2002; **97**: 584-589
18 **Guelrud M**, Herrera I, Essenfeld H, Castro J. Enhanced magnification endoscopy: a new technique to identify specialized intestinal metaplasia in Barrett's esophagus. *Gastrointest Endosc* 2001; **53**: 559-565
19 **Yao K**, Oishi T. Microgastroscopic findings of mucosal microvascular architecture as visualized by magnifying endoscopy. *Digestive Endoscopy* 2001; **13**(Suppl): S27-S33
20 **Tajiri H,** Matsuda K, Fujisaki J. What can see with the endoscope? Present status and future perspectives. *Digestive Endoscopy* 2002; **14**: 131-137
21 **Miwa H,** Sato N. Shed light again on magnifying endoscopy for diagnosis of early gastric cancer. *Digestive Endoscopy* 2001; **13**: 127-128
22 **Niwa Y,** Goto H, Ohmiya N, Ohtsuka Y, Ando N. Magnifying endoscopy for the diagnosis of early gastric cancer. *Digestive Endoscopy* 2002; **14**(Suppl): S70-S71
23 **Tajiri H**, Doi T, Endo H, Nishina T, Terao T, Hyodo I, Matsuda K, Yagi K. Routine endoscopy using a magnifying endoscope for gastric cancer diagnosis. *Endoscopy* 2002; **34**: 772-777
24 **Yao K**, Oishi T, Matsui T, Yao T, Iwashita A. Novel magnified endoscopic findings of microvascular architecture in intramucosal gastric cancer. *Gastrointest Endosc* 2002; **56**: 279-284
25 **Yagi K,** Nakamura A, Sekine A. Comparison between magnifying endoscopy and histological, culture and urease test findings from the gastric mucosa of the corpus. *Endoscopy* 2002; **34**: 376-381
26 **Yagi K,** Nakamura A, Sekine A. Characteristic endoscopic and magnified endoscopic findings in the normal stomach without *Helicobacter pylori* infection. *J Gastroenterol Hepatol* 2002; **17**: 39-45
27 **Cales P,** Oberti F, Delmotte JS, Basle M, Casa C, Arnaud JP. Gastric mucosal surface in cirrhosis evaluated by magnifying endoscopy and scanning electronic microscopy. *Endoscopy* 2000; **32**: 614-623
28 **Fujiya M,** Saitoh Y, Nomura M, Maemoto A, Fujiya K, Watari J, Ashida T, Ayabe T, Obara T, Kohgo Y. Minute findings by magnifying colonoscopy are useful for the evaluation of ulcerative colitis. *Gastrointest Endosc* 2002; **56**: 535-542
29 **Jiang B.** Chromoendoscopy and high-magnification colonoscopy in early detection of colorectal cancer. *Diyi Junyi Daxue Xuebao* 2002; **22**: 385-387
30 **Shi HX,** Wu YL. Distinguishing colorectal minute lesions by high-resolution video endoscope with indigo carmine dye spray. *Zhonghua Xiaohua Neijing Zazhi* 1999; **16**: 135-137
31 **Li ZX**, Zhang XR, An DL, Chen FL, Gong JZ. Diagnosis and treatment of early colorectal cancer. *Zhonghua Waike Zazhi* 2000; **38**: 352-354
32 **Yu YZ,** Wang QH, Yu ZL. The gastric mucosal features of *Helicobacter pylori* associated gastritis evaluated by high-resolution magnifying endoscopy. *Zhonghua Xiaohua Neijing Zazhi* 2002; **19**: 274-277
33 **Chen X,** Cen R, Xu FX, Xia J, Luo C, Cheng FL. Pathological analysis with new magnifying endoscopic classification of the gastric mucosal pattern. *Zhongguo Neijing Zazhi* 2002; **8**: 37-38
34 **Gao HJ**, Yu LZ, Bai JF, Peng YS, Sun G, Zhao HL, Miu K, Lu XZ, Zhang XY, Zhao ZQ. Multiple genetic alterations and behavior of cellular biology in gastric cancer and other gastric mucosal lesions: *H pylori* infection, histological types and staging. *World J Gastroenterol* 2000; **6**: 848-854
35 **Chinese Society of Gastroenteroloy, Chinese Medical Association**. Common opinions on chronic gastritis of China. *Zhonghua Xiaohua Zazhi* 2000; **20**: 199-201
36 **Liu YQ**, Zhao H, Ning T, Ke Y, Li JY. Expression of 1A6 gene and its correlation with intestinal gastric carcinoma. *World J Gastroenterol* 2003; **9**: 238-241
37 **Zhou LY**, Li JH, Lin SR, Jin Z, Ding SG, Huang XP, Xia ZW. Endoscopic diagnosis of intestinal metaplasia in gastric mucosa. *Zhonghua Xiaohua Neijing Zazhi* 2001; **18**: 84-86

Edited by Xia HHX and Wang XL

P.O.Box 2345, Beijing 100023,China
Fax: +86-10-85381893
E-mail: wjg@wjgnet.com www.wjgnet.com

World J Gastroenterol 2003;9(11):2557-2560
World Journal of Gastroenterology
 ISSN 1007-9327

• CLINICAL RESEARCH •

Regional variations in mortality rates of pancreatic cancer in China: Results from 1990-1992 national mortality survey

Ke-Xin Chen, Peizhong Peter Wang, Si-Wei Zhang, Lian-Di Li, Feng-Zhu Lu, Xi-Shan Hao

Ke-Xin Chen, Xi-Shan Hao, Tianjin Cancer Institute and Hospital, Tianjin Medical University, Tianjin, 300060, China
Peizhong Peter Wang, Department of Community Health, University of Toronto, Canada
Si-Wei Zhang, Lian-Di Li, Feng-Zhu Lu, Office of Cancer Prevention and Control in China, Beijing, 100021, China
Supported by the National Medical Science and Technology Foundation during the 8th Five-Year Plan Period, No. 85-914-01-07
Correspondence to: Dr. Ke-Xin Chen, Department of Epidemiology, Tianjin Cancer Institute and Hospital, Huanhu Xi Road, Ti Yuanbei, He Xi District, Tianjin, 300060, China. chenkexin@21cn.com
Telephone: +86-22-23359929 Ext 226 **Fax:** +86-22-23359984
Received: 2003-05-10 **Accepted:** 2003-06-04

Abstract

AIM: To examine the regional variations in mortality rates of pancreatic cancer in China.

METHODS: Aggregated mortality data of pancreatic cancer were extracted from the 1990-1992 national death of all causes and its mortality survey in China. Age specific and standardized mortality rates were calculated at both national and provincial levels with selected characteristics including sex and residence status.

RESULTS: Mortality of pancreatic cancer ranked the ninth and accounted for 1.38 percent of the total malignancy deaths. The crude and age standardized mortality rates of pancreatic cancer in China in the period of 1990-1992 were 1.48/100 000 and 1.30/100 000, respectively. Substantial regional variations in mortality rates across China were observed with adjusted mortality rates ranging from 0.43/100 000 to 3.70/100 000 with an extremal value of 8.7. Urban residents had significant higher pancreatic mortality than rural residents.

CONCLUSION: The findings of this study show different mortality rates of this disease and highlight the importance of further investigation on factors, which might contribute to the observed epidemiological patterns.

Chen KX, Wang PP, Zhang SW, Li LD, Lu FZ, Hao XS. Regional variations in mortality rates of pancreatic cancer in China: Results from 1990-1992 national mortality survey. *World J Gastroenterol* 2003; 9(11): 2557-2560
http://www.wjgnet.com/1007-9327/9/2557.asp

INTRODUCTION

Pancreatic cancer is a relatively common malignant disease in the world, both its incidence and mortality rate are ranked in the first ten cancers[1,2]. Especially in recent years, a gradually increased tendency of the disease has been found[3-6]. About 200 000 new cases of pancreatic cancer are reported worldwide annually. Despite the overall improvement in cancer diagnosis and treatment in the past half century, there has been little change in the survival of pancreatic cancer patients. The reported worldwide annual incidence accounts for 2 % of all malignant tumors and is associated with about 196 000 deaths from the disease[7-11]. Though pancreatic cancer is relatively uncommon in China, but it still accounts for substantial cancer related deaths because of its dismal survival rate. Thus, the mortality rate of this disease serves as a mirror for its incidence. Notwithstanding previous studies in China have shown that there were significant geographic variations for several cancer sites, such as liver and esophagus, little is known for pancreatic cancer[12-14]. As the causes of pancreatic cancer are largely unknown, epidemiological studies on regional mortality rate variations may shed light on seeking possible modifiable factors associated with this disease.

MATERIALS AND METHODS

Data source

1990-1992 national mortality survey As China does not have a centralized vital statistics system and cancer registration, national level information on disease specific mortality is often based on periodic national mortality surveys (NMS), the first of which was initiated in the early 1970s. Its purpose was to generate nationally representative estimates of mortality due to various health conditions, such as cancer, heart disease and stroke. The more recent one was conducted between 1990 and 1992 with the primary focus on malignant tumors, which was the data source for this study.

Briefly, the 1990-1992 NMS was a two-stage stratified probability survey. At the first stage, each of the 22 provinces, 5 autonomous regions, and 3 municipatities directly administrated cities under the Central Government (Beijing, Shanghai, and Tianjin) represented one of 30 strata. For the ease of the presentation, we referred to the 30 strata as "areas". The second stratum was formed at county or district level according to the cancer mortality levels (2-3 levels from low to high) from the previous survey. Thus, the primary sampling unit for this survey was county or district (for Beijing, Shanghai and Tianjin). Overall, the sample size for this survey was designed to cover 10 % of all deaths or 242 million baseline person years during the study period. Detailed information can be found from the National Mortality Survey Manual. With respect to pancreatic cancer, samples from 8 of the first level strata did not have sufficient number of cases to generate meaningful estimates, thus the mortality estimates were only applicable to 22 of the first level strata. Specifically, the 22 areas were Beijing, Tianjin, Hebei, Shanxi, Neimeng, Liaoning, Jilin, Heilongjiang, Shanghai, Jiangsu, Anhui, Jiangxi, Fujian, Henan, Hunan, Hainan, Guangxi, Sichuan, Yunnan, Guizhou, Gansu, and Ningxia.

Case assessment and baseline population All death certificates were retrieved from the local death registration offices for the sampled counties or districts. Local neighborhood representatives were also interviewed to further verify each deceased person for possible misreporting and discover deaths not reflected at death registration offices. Causes of deaths obtained from death certificates were checked with clinical records. When clinical records were missing or

not available, possible diagnoses were solicited from the medical professionals who had once treated the case. Each reported cause of death was further converted into 3-digit ICD-9 codes and pancreatic cancer was determined for ICD-9 157. Age-sex specific population data for each surveyed county or district were derived from interpolation using the data from the two most recent censuses conducted in 1982 and 1990.

Statistical analysis

Both crude and age-sex adjusted mortality rates were calculated both at provincial and national levels. In order to make the estimates comparable to reported mortality data from other populations, two standard populations were used: the 1980 Chinese population and the world standard population. The extremal quotient (EQ) was used to quantify regional variation[15]. The EQ is the ratio of the mortality from area with the highest level relative to the area with the lowest level. Age standardised mortality rates from each individual area (defined by resident status) were derived and compared with the corresponding national mean and median using the 1990-1992 NMS. In addition to assessing differences in mortality rate among areas and national levels, we also juxtaposed pancreatic cancer with other leading cancers, such as lung and breast cancers in terms of their relative ranking.

RESULTS

In total, pancreatic cancer deaths were identified from the 181 primary sampling units (counties or districts), among which 54 and 127 were considered as urban and rural respectively.

Table 1 displays the crude and standardized mortality rates of pancreatic cancer. As shown in this table, the crude and Chinese population adjusted mortality rates were 1.29 and 1.08 per 100 000 person-year during the study period.

Table 1 Selected indices derived from pancreatic cancer mortality (1/100 000) in China, 1990-1992

	Crude rate	ASMR1	ASMR2	Mortality proportion to all cancer death (%)
Total	1.48	1.30	1.74	1.38
Male	1.65	1.52	2.03	1.25
Female	1.29	1.08	1.46	1.62

ASMR: Age adjusted mortality rate, 1=the Chinese population in 1980, 2=world population.

Table 2 compares the mortality of pancreatic cancer with other leading cancers in terms of standardized rates, mortality proportion, and relative ranking. Overall, the mortality of pancreatic cancer ranked the 9th and accounted for 1.38 % of total cancer deaths after colon cancer.

While pancreatic cancer could occur at any age, its mortality varied greatly among different age groups. The mortality remained low and did not increase until age 45, there was a steep increase in both males and females from age 45 to age 75 before it reached a plateau around 75. There seemed to be a mortality drop in males after age 75. Pancreatic cancer mortality rates were apparently higher in males than in females, with the ratio 1.4:1.

Regional comparisons (Table 3) suggested that a substantial variation in pancreatic cancer mortality across the 22 regions and standardized mortality rates varied from the lowest 0.47/100 000 person-year in Hunan Province to the highest 3.73/100 000 person year in Shanghai with an extremal quotient of 8.76. Using the national average level as a standard, eight provinces had a rate higher than average and they were Shanghai, Tianjin, Liaoning, Heilongjiang, Jiangsu, Jilin, Beijing, and Ningxia. However, there was little variation in terms of mortality, sex ratios varying between 1.07 and 2.3, most of the values were around 1.5.

Table 3 Distribution of pancreatic cancer mortality in 22 provinces, cities, and autonomous regions in 1990-1992

Regions	Males		Females		Total		M/F
	CR	ASR	CR	ASR	CR	ASR	ratio
Hunan	0.57	0.54	0.36	0.32	0.47	0.43	1.69
Guangxi	0.73	0.73	0.40	0.36	0.58	0.55	2.03
Hainan	0.86	0.76	0.47	0.48	0.67	0.65	1.58
Gansu	0.85	0.87	0.46	0.49	0.66	0.69	1.78
Guizhou	0.97	0.99	0.52	0.51	0.75	0.76	1.94
Jiangxi	0.89	0.92	0.62	0.62	0.76	0.78	1.48
Henan	0.99	0.98	0.68	0.60	0.84	0.78	1.63
Sichuan	1.07	0.99	0.76	0.63	0.92	0.79	1.57
Fujian	1.32	1.36	0.69	0.60	1.01	0.96	**2.27**
Neimenggu	1.72	1.16	0.84	0.81	1.31	0.99	1.43
Shanxi	1.34	1.21	1.02	0.89	1.19	1.04	1.36
Yunnan	1.38	1.24	0.99	0.87	1.19	1.05	1.43
Hebei	1.49	1.37	0.95	0.81	1.23	1.08	1.69
Anhui	1.50	1.44	1.20	0.96	1.36	1.20	1.50
Ningxia	1.85	1.68	1.17	1.06	1.52	1.38	1.58
Beijing	3.21	2.28	1.97	1.25	2.59	1.75	1.82
Jilin	2.07	1.98	1.80	1.85	1.94	1.91	**1.07**
Jiangsu	3.29	2.62	3.29	2.20	3.29	2.40	1.19
Heilongjiang	2.52	2.57	2.26	2.38	2.40	2.47	1.08
Liaoning	3.71	3.16	2.76	2.38	3.24	2.78	1.33
Tianjin	5.68	3.80	4.53	2.91	5.10	3.34	1.31
Shanghai	7.55	**4.22**	6.87	**3.26**	7.21	**3.70**	1.29

Table 2 Age-standardized mortality rates and proportion of major malignant cancers in China

Type of tumor	Males			Females			Total		
	ASR	P(%)	Rank	ASR	P (%)	Rank	ASR	P (%)	Rank
Stomach	30.78	25.10	1	14.52	21.80	1	22.51	23.93	1
Liver	25.73	21.42	2	9.55	14.00	3	17.75	18.74	2
Esophagus	20.22	16.45	4	10.32	15.50	2	15.15	16.11	4
Lung	21.68	17.73	3	9.03	13.46	4	15.23	16.18	3
Rectum	3.60	2.94	5	2.55	3.80	7	3.06	3.29	5
Leukemia	3.46	2.67	6	2.86	3.70	8	3.16	3.04	6
Breast				2.93	4.24	6			
Brain& nervous system	2.01	1.63	7	1.48	2.02	9	1.74	1.77	7
Cervix	-	-	-	3.16	4.62	5	-	-	
Colon	1.49	1.21	9	1.19	1.80	10	1.34	1.43	8
Pancreas	1.52	1.25	8	1.08	1.62	11	1.30	1.38	9
Total	122.35	100.00		67.61	100.00		94.58	100.00	

These comparisons further indicated that urban residents had a significant higher mortality than their rural counterparts. These differences existed in both males and females (Table 4, Figure1) across age groups.

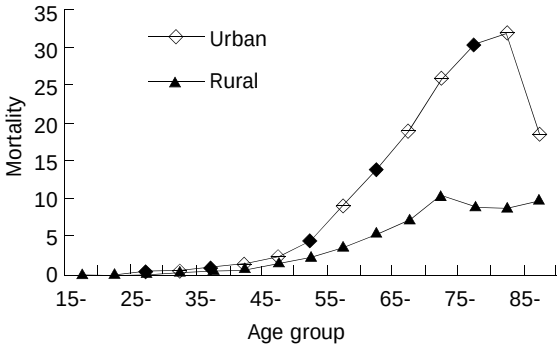

Figure 1 Comparison of age-specific mortality of pancreatic cancer between urban and rural areas, 1990-1992

Table 4 Comparison of pancreatic cancer mortality between urban and rural areas in China, 1990-1992

Region	Sex	CR	ASR
Total	Urban	2.83	2.27
	Rural	1.05	0.95
	U/R ratio	2.67	2.39
Male	Urban	3.16	2.68
	Rural	1.17	1.11
	U/R ratio	2.70	2.41
Female	Urban	2.47	21.89
	Rural	0.92	0.80
	U/R ratio	2.68	2.36

DISCUSSION

In this study, we described some epidemiological characteristics of pancreatic cancer using the most recent Chinese mortality survey data. Compared with other previous studies in China, the age standardized mortality rates from this study appeared to be higher than those reported previously. This may suggest that the mortality rate of pancreatic cancer is increasing.

Ecological studies[16-24] found as shown in Figures 2-3 that the mortality of pancreatic cancer seemed to be correlated with the level of economic development. Developed countries, such as Japan and the United States[25-29] had a higher pancreatic cancer mortality than that of less developed countries, such as some African countries[30-33]. China is a big country with unbalanced economic development and diverse lifestyles. The economic developmental gaps between urban and rural areas seen in China are greater than those in the developed countries. Findings from this study suggest substantial regional variations in the mortality rates of pancreatic cancer and in general, economically more developed regions have higher mortality rates than that of less developed regions. For example, Beijing, Shanghai, and Tianjin shared the 3 highest mortality rates. Thus, results from this study are in accord with previous observations.

The use of a population based national representative sample in the present study was unique in its reliability. Also, in this study most death certificates were crossly validated and consequently the reported causes of death were more believable. Furthermore, as all studied areas used uniform standards, the mortality rate estimates across areas had a good comparability. However, there were also limitations associated with this study. First, all information used in this study was derived from the survey, thus the case assessment method could not be compared with clinical diagnosis. Second, since this survey did not collect life style information (such as smoking and diet) for the deceased subjects, we were restricted from further exploring the impact of potential risk factors on this condition. Lastly, only aggregated data were available to the authors, we were unable to calculate the variances for the estimated mortality rates. As a result, we could only provide point estimates without 95 % confidence intervals.

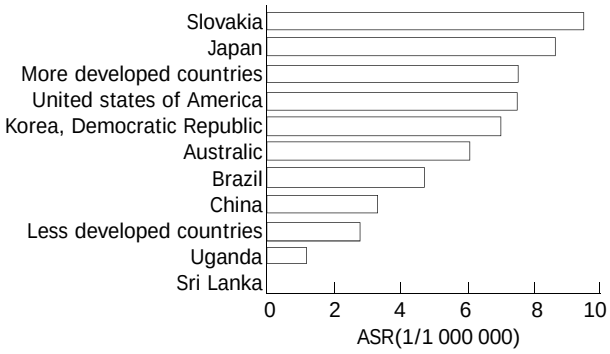

Figure 2 World pancreatic cancer mortality in different countries (male).

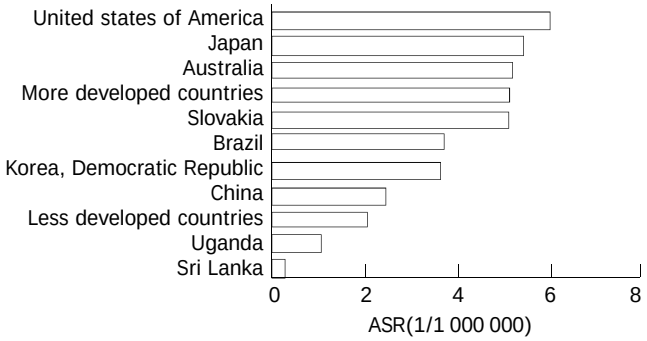

Figure 3 World pancreatic cancer mortality in different countries (female).

In conclusion, we have demonstrated a substantial variation in pancreatic cancer mortality rates across the Mainland China. The results reported in this study beg for answers to the observed differences. As pancreatic cancer is a fast growing disease associated with high fatality, more in-depth epidemiological studies on identifying modifiable risk factors are warranted.

ACKNOWLEGEMENTS

We are grateful to all medical workers from 22 provinces (cities, districts) in China for our data collection and preparation. We want to thank Tianjin Cancer Institute and Hospital for its financial support.

REFERENCES

1 **Levi F**, Lucchini F, Negri E, Boyle P, La Vecchia C. Mortality from major cancer sites in the European Union, 1955-1998. *Ann Oncol* 2003; **14**: 490-495

2 **Remontet L**, Esteve J, Bouvier AM, Grosclaude P, Launoy G, Menegoz F, Exbrayat C, Tretare B, Carli PM, Guizard AV, Troussard X, Bercelli P, Colonna M, Halna JM, Hedelin G, Mace-Lesec'h J, Peng J, Buemi A, Velten M, Jougla E, Arveux P, Le Bodic L, Michel E, Sauvage M, Schvartz C, Faivre J. Cancer incidence and mortality in France over the period 1978-2000. *Rev Epidemiol Sante Publique* 2003; **51**(1Pt 1): 3-30

3 **Fernandez E**, La Vecchia C, Porta M, Negri E, Lucchini F, Levi F. Trends in pancreatic cancer mortality in Europe, 1955-1989. *Int J Cancer* 1994; **57**: 786-792

4 **Vutuc C**, Waldhoer T, Haidinger G. Impact of non-invasive imaging techniques on the trend of pancreatic cancer mortality in Austria. *Wien Med Wochenschr* 1996; **146**: 258-260

5 **Lin RS**, Lee WC. Mortality trends of pancreatic cancer: an affluent type of cancer in Taiwan. *J Formos Med Assoc* 1992; **91**: 1148-1153

6 **Yang CY**, Chiu HF, Cheng MF, Tsai SS, Hung CF, Tseng YT. Pancreatic cancer mortality and total hardness levels in Taiwan's drinking water. *J Toxicol Environ Health A* 1999; **56**: 361-369

7 **Bakkevold KE**, Kambestad B. Morbidity and mortality after radical and palliative pancreatic cancer surgery. Risk factors influencing the short-term results. *Ann Surg* 1993; **217**: 356-368

8 **Riggs JE**. Longitudinal Gompertzian analysis of pancreatic cancer mortality in the U.S., 1962-1987: distinguishing between competitive and environmental influences upon evolving mortality patterns. *Mech Ageing Dev* 1991; **61**: 197-208

9 **Binstock M**, Krakow D, Stamler J, Reiff J, Persky V, Liu K, Moss D. Coffee and pancreatic cancer: an analysis of international mortality data. *Am J Epidemiol* 1983; **118**: 630-640

10 **Calle EE**, Murphy TK, Rodriguez C, Thun MJ, Heath CW Jr. Diabetes mellitus and pancreatic cancer mortality in a prospective cohort of United States adults. *Cancer Causes Control* 1998; **9**: 403-410

11 **Pickle LW**, Gottlieb MS. Pancreatic cancer mortality in Louisiana. *Am J Public Health* 1980; **70**: 256-259

12 **Boffetta P**, Burstyn I, Partanen T, Kromhout H, Svane O, Langard S, Jarvholm B, Frentzel-Beyme R, Kauppinen T, Stucker I, Shaham J, Heederik D, Ahrens W, Bergdahl IA, Cenee S, Ferro G, Heikkila P, Hooiveld M, Johansen C, Randem BG, Schill W. Cancer mortality among European asphalt workers: an international epidemiological study. II. Exposure to bitumen fume and other agents. *Am J Ind Med* 2003; **43**: 28-39

13 **Gapstur SM**, Gann PH, Lowe W, Liu K, Colangelo L, Dyer A. Abnormal glucose metabolism and pancreatic cancer mortality. *Jama* 2000; **283**: 2552-2558

14 **Ghadirian P**, Thouez JP, PetitClerc C. International comparisons of nutrition and mortality from pancreatic cancer. *Cancer Detect Prev* 1991; **15**: 357-362

15 **Neoptolemos JP**, Russell RC, Bramhall S, Theis B. Low mortality following resection for pancreatic and periampullary tumours in 1026 patients: UK survey of specialist pancreatic units. UK Pancreatic Cancer Group. *Br J Surg* 1997; **84**: 1370-1376

16 **Ghadirian P**, Lynch HT, Krewski D. Epidemiology of pancreatic cancer: an overview. *Cancer Detect Prev* 2003; **27**: 87-93

17 **Coughlin SS**, Calle EE, Patel AV, Thun MJ. Predictors of pancreatic cancer mortality among a large cohort of United States adults. *Cancer Causes Control* 2000; **11**: 915-923

18 **Imaizumi Y**. Longitudinal Gompertzian analysis of mortality from pancreatic cancer in Japan, 1955-1993. *Mech Ageing Dev* 1996; **90**: 163-181

19 **Bardin JA**, Eisen EA, Tolbert PE, Hallock MF, Hammond SK, Woskie SR, Smith TJ, Monson RR. Mortality studies of machining fluid exposure in the automobile industry. V: A case-control study of pancreatic cancer. *Am J Ind Med* 1997; **32**: 240-247

20 **Clary T**, Ritz B. Pancreatic cancer mortality and organochlorine pesticide exposure in California, 1989-1996. *Am J Ind Med* 2003; **43**: 306-313

21 **Inoue M**, Tajima K, Takezaki T, Hamajima N, Hirose K, Ito H, Tominaga S. Epidemiology of pancreatic cancer in Japan: a nested case-control study from the Hospital-based Epidemiologic Research Program at Aichi Cancer Center (HERPACC). *Int J Epidemiol* 2003; **32**: 257-262

22 **Kauppinen T**, Heikkila P, Partanen T, Virtanen SV, Pukkala E, Ylostalo P, Burstyn I, Ferro G, Boffetta P. Mortality and cancer incidence of workers in Finnish road paving companies. *Am J Ind Med* 2003; **43**: 49-57

23 **Mohan AK**, Hauptmann M, Freedman DM, Ron E, Matanoski GM, Lubin JH, Alexander BH, Boice JD Jr, Doody MM, Linet MS. Cancer and other causes of mortality among radiologic technologists in the United States. *Int J Cancer* 2003; **103**: 259-267

24 **Konner J**, O'Reilly E. Pancreatic cancer: epidemiology, genetics, and approaches to screening. *Oncology (Huntingt)* 2002; **16**: 1615-1622, 1631-1632

25 **Lee WC** , Lin RS. Age-period-cohort analysis of pancreatic cancer mortality in Taiwan, 1971-1986. *Int J Epidemiol* 1990; **19**: 839-847

26 **Mulder I**, Hoogenveen RT, van Genugten ML, Lankisch PG, Lowenfels AB, de Hollander AE, Bueno-de-Mesquita HB. Smoking cessation would substantially reduce the future incidence of pancreatic cancer in the European Union. *Eur J Gastroenterol Hepatol* 2002; **14**: 1343-1353

27 **Newnham A**, Quinn MJ, Babb P, Kang JY, Majeed A. Trends in oesophageal and gastric cancer incidence, mortality and survival in England and Wales 1971-1998 / 1999. *Aliment Pharmacol Ther* 2003; **17**: 655-664

28 **Lee IM**, Sesso HD, Oguma Y, Paffenbarger RS Jr. Physical activity, body weight, and pancreatic cancer mortality. *Br J Cancer* 2003; **88**: 679-683

29 **Zervos EE**, Norman JG, Gower WR, Franz MG, Rosemurgy AS. Matrix metalloproteinase inhibition attenuates human pancreatic cancer growth *in vitro* and decreases mortality and tumorigenesis *in vivo*. *J Surg Res* 1997; **69**: 667-671

30 **Muirhead CR**, Bingham D, Haylock RG, O'Hagan JA, Goodill AA, Berridge GL, English MA, Hunter N, Kendall GM. Follow up of mortality and incidence of cancer 1952-98 in men from the UK who participated in the UK's atmospheric nuclear weapon tests and experimental programmes. *Occup Environ Med* 2003; **60**: 165-172

31 **Corella Piquer D**, Cortina Greus P, Coltell Simon O. Nutritional factors and geographic differences in pancreatic cancer mortality in Spain. *Rev Sanid Hig Publica* 1994; **68**: 361-376

32 **Olsen GW**, Lacy SE, Bodner KM, Chau M, Arceneaux TG, Cartmill JB, Ramlow JM,Boswell JM. Mortality from pancreatic and lymphopoietic cancer among workers in ethylene and propylene chlorohydrin production. *Occup Environ Med* 1997; **54**: 592-598

33 **Pasquali C**, Sperti C, Filipponi C, Pedrazzoli S. Epidemiology of pancreatic cancer in Northeastern Italy: incidence, resectability rate, hospital stay, costs and survival (1990-1992). *Dig Liver Dis* 2002; **34**: 723-731

Edited by Xu JY and Wang XL

P.O.Box 2345, Beijing 100023,China
Fax: +86-10-85381893
E-mail: wjg@wjgnet.com www.wjgnet.com

World J Gastroenterol 2003;9(11):2561-2564
World Journal of Gastroenterology
 ISSN 1007-9327

• CLINICAL RESEARCH •

Intensity modulated radiation therapy and chemotherapy for locally advanced pancreatic cancer: Results of feasibility study

Yong-Rui Bai, Guo-Hua Wu, Wei-Jian Guo, Xu-Dong Wu, Yuan Yao, Yin Chen, Ren-Hua Zhou, Dong-Qin Lu

Yong-Rui Bai, Guo-Hua Wu, Xu-Dong Wu, Yuan Yao, Yin Chen, Ren-Hua Zhou, Dong-Qin Lu, Department of Radiation Oncology, Xinhua Hospital of Shanghai Second Medical University, Shanghai 200092, China
Wei-Jian Guo, Department of Oncology, Xinhua Hospital of Shanghai Second Medical University, Shanghai 200092, China
Supported by Health Bureau of Shanghai City, No. 00436
Correspondence to: Dr. Yong-Rui Bai, Department of Radiation Oncology, Xinhua Hospital of Shanghai Second Medical University, Shanghai 200092, China. baiyongrui@online.sh.cn
Telephone: +86-21-65790000 **Fax:** +86-21-65030840
Received: 2003-06-16 **Accepted:** 2003-07-24

Abstract

AIM: To explore whether intensity modulated radiation therapy (IMRT) in combination with chemotherapy could increase radiation dose to gross tumor volume without severe acute radiation related toxicity by decreasing the dose to the surrounding normal tissue in patients with locally advanced pancreatic cancer.

METHODS: Twenty-one patients with locally advanced pancreatic cancer were evaluated in this clinical trial. Patients would receive the dose of IMRT from 21Gy to 30Gy in 7 to 10 fractions within two weeks after conventional radiotherapy of 30Gy in 15 fractions over 3 weeks. The total escalation tumor dose would be 51, 54, 57, 60Gy, respectively. 5-fluororacil (5-FU) or gemcitabine was given concurrently with radiotherapy during the treatment course.

RESULTS: Sixteen patients who had completed the radiotherapy plan with doses of 51Gy (3 cases), 54Gy (3 cases), 57Gy (3 cases) and 60Gy (7 cases) were included for evaluation. The median levels of CA19-9 prior to and after radiotherapy were 716 U/ml and 255 U/ml respectively ($P<0.001$) in 13 patients who demonstrated high levels of CA19-9 before radiotherapy. Fourteen patients who suffered from pain could reduce at least 1/3-1/2 amount of analgesic intake and 5 among these patients got complete relief of pain. Ten patients improved in Karnofsky performance status (KPS). The median follow-up period was 8 months and one-year survival rate was 35 %. No patient suffered more than grade III acute toxicities induced by radiotherapy.

CONCLUSION: Sixty Gy in 25 fractions over 5 weeks with late course IMRT technique combined with concurrent 5-FU chemotherapy can provide a definitely palliative benefit with tolerable acute radiation related toxicity for patients with advanced pancreatic cancer.

Bai YR, Wu GH, Guo WJ, Wu XD, Yao Y, Chen Y, Zhou RH, Lu DQ. Intensity modulated radiation therapy and chemotherapy for locally advanced pancreatic cancer: Results of feasibility study. *World J Gastroenterol* 2003; 9(11): 2561-2564
http://www.wjgnet.com/1007-9327/9/2561.asp

INTRODUCTION

The incidence of pancreatic carcinoma has been continuously increasing worldwide in recent years. The incidence in Shanghai of China has increased to 9.6 per 100 000 for males and 9.2 per 100 000 for females. Most patients have locally advanced unresectable disease at the time of initial diagnosis because of lacking clinical symptoms and signs. Without treatment intervention, the mean time of survival was approximately 4 to 6 months[1]. Although surgery was considered to be the only curative treatment method, there were only 10-20 % patients who had resectable tumors suitable for radical resection and 30-85 % patients would have local recurrences[2].

At present, there are no satisfactory treatment modalities for patients with advanced pancreatic carcinoma. Adenocarcinoma of pancreas is a disease characterized by resistance to cytotoxic therapy including chemotherapy and radiotherapy. Treatment response of systemic chemotherapy is relatively poor with only 20 % response rate, which would last only a short time and most of the treatment effects are partial response. Meanwhile, the conventional radiation dose to gross tumor volume is not large enough to cure patients with pancreatic carcinoma because of the limited tolerant dose to the surrounding normal tissues such as gastrointestinal tract and kidneys. Many studies have shown that the local control and survival would be maximized if patients with pancreatic carcinoma were treated by surgery combined with chemoradiation therapy[3-6]. There were full laboratory and clinical evidences of potent radiosensitizing properties and significant systemic activity of 5-fluorouracil (5-FU) and/or gemcitabine (GEM) used in combination with radiothetapy in pancreatic carcinoma[7-12].

In addition, since 1990' s, radiation treatment equipments and related techniques have been developed dramatically. Especially, more attention has been paid to intensity modulated radiation therapy (IMRT), which is an approach with the aid of modern computer treatment planning system to conformal radiation therapy that conforms a high dose to the target (tumor) volume while restricting dose to the surrounding sensitive structures, and encouraging results have been achieved in clinical trials in head and neck carcinoma and thoracic carcinoma.

However, conventional radiotherapy can not give a higher dose needed to eradicate pancreatic carcinoma cells which are moderately sensitive to radiation due to the dose limited tissues adjacent to pancreas. In general, the dose adopted in conventional radiotherapy was approximately or less than 50Gy in 25 fractions over 5 weeks[5,11,12]. But the optimal dose of IMRT to treat patients with pancreatic carcinoma has not been established, especially in combination with chemotherapies such as 5-FU or GEM.

In this study, we reported our experience in the combination of IMRT and chemotherapy with 5-FU or GEM in a group of patients with locally advanced nonresectable pancreatic carcinoma. Our goal was to determine the feasibility of this treatment modality by evaluating the acute radiation toxicity and the treatment efficacy in this dose escalating trial. A second

purpose was to determine the palliation of symptoms, response rate and survival in this group of patients.

MATERIALS AND METHODS

Eligibility

From November 2001 to December 2002, patients with histologically proved pancreatic adenocarcinoma were enrolled into this study. Eligible patients included those with locally unresectable disease due to vascular invasion or extensive regional adenopathy, partial resection or local recurrence after operation. Patients with known metastasis to distant organs, ascites, Karnofsky performance status less than 70 were excluded. Required laboratory parameters included white blood cell count $\geqslant 4\times10^9$/L, platelet count $\geqslant 100\times10^9$/L, creatinine $\leqslant 264$ μmol/L. Patients with biliary or gastroduodenal obstruction must have had prior drainage before radiotherapy and chemotherapy were started. A complete history and physical examination were performed in all patients prior to scheduled treatment. Height, weight, performance status, tumor stage and serum level of tumor markers including carbohydrate antigen (CA) 19-9 were recorded. Required examinations for staging studies included a chest radiograph and abdominal computed tomographic (CT) scan or magnetic resonance image (MRI) scan, abdominal type B ultrosound and sometimes bone isotopic examination. All patients were required to sign a written informed consent according to national and institutional guidelines.

Radiotherapy

Patients were CT simulated and treated in the supine position with their arms overhead. In order to make it easier to define tumor target volume from the stomach and duodenum, 300 ml of oral CT contrast with 2 % gastrografin solution was administered respectively one hour and half an hour before starting CT simulation scan with ACQsim spiral CT. For immobilization, a customed thermoplastic cast extending from the mid-thoracic spine to the mid-pelvis was made. Each patient was scanned from the upper dome of the right diaphragm (approximately at the level of T9-T10) to the bottom of the L4 vertebral body. The patient was imaged with overlapping CT slices that were 5 mm thick at 3 mm intervals. Center of CT scanning was marked on the thermoplastic cast. The gross tumor volume (GTV) and the surrounding critical structures of concern including the liver, kidneys, stomach, small intestine and spinal cord were defined after the data of CT scan were sent to the workstation of ACQsim (version 4.3) CT simulation software system. GTV represents tumor in the pancreas, the surrounding tissue infiltrated and adjacent lymph node metastasis. The clinical target volume (CTV) includes GTV plus any microscopic extension of disease that is suspected around GTV. The planning target volume (PTV) represents CTV plus any additional margins that are required to compensate for daily setup variations. Isocenter coordinate of radiotherapy was marked on the thermoplastic cast with the help of a laser mark system. Cadplan treatment plan system using Helios reverse treatment planning software was adopted to optimize the dose distribution after the images of CT scan and digitally reconstructed radiographs were transmitted. Then, the treatment data were sent to Varian 2100C/D accelerator by Varis network. Port films were taken at the first time and once every week of treatment to verify the radiation position.

Radiotherapy was divided into two phases. Conventional radiotherapy was delivered to a total of 30Gy in 15 fractions of 2Gy per fraction to the initial fields including the primary tumor plus the regional peripancreatic, celiac, and porta hepatis lymph nodes at the first phase. IMRT was given at the second phase and GTV was covered by the 95 % prescribed isodose curve. The dose of IMRT ranged from 21Gy to 30Gy in 7-10 fractions of 3Gy per fraction. The total dose escalation levels were 51Gy, 54Gy, 57Gy and 60Gy respectively. Three patients were needed for each dose level. Dose-limiting toxicity (DLT) from radiotherapy was defined as grade IV hematologic toxicity or grade III nonhematologic toxicity according to common toxicity criteria (CTC, 2.0 version). Dose escalation continued to the next dose level if no patients suffered from DLT. Two or more instances of DLT among 3 patients occurred in the preceding dose level would declare it as the maximum tolerant dose (MTD). Another 3 patients would be needed for observation if one of them had DLT at a certain dose escalation level. If no one had DLT in these additional 3 patients, dose escalation would continue. However, if one patient developed DLT among the added 3 patients, the preceded dose level would be the MTD. In this study, the maximum escalation dose level was 60Gy.

Chemotherapy

Gemcitabine (GM), 150 mg/d, was administered daily prior to radiotherapy on weeks 1, 3, 5, or 5-fluorouracil (5-FU), 250 mg/d, was given every week from Monday to Friday during the days of whole radiotherapy course.

Toxicity and response evaluation

Toxicity was evaluated according to common toxicity criteria: version 2.0 (CTC 2.0)[13]. Hematologic parameters were assessed weekly, and all other adverse reactions were evaluated during the course of radiotherapy. Analgesic intake and weight were recorded at initial consultation and weekly during radiation therapy. Karnofsky performance status (KPS) was estimated prior to radiotherapy and recorded as it was improved, stable, or deteriorated after treatment. Weight change was classified as weight gain/loss if there was a weight increase/decrease $\geqslant$5 % over baseline value, otherwise it was classified as stable. Pain control was recorded when it was improved/deteriorated if there was a $\geqslant$50 % increase/decrease respectively in the daily intake of equivalent analgesic dose at least lasting for 4 weeks. The clinical response index was defined as a sustained improvement in at least one parameter (among three factors as KPS, weight and pain control) without the other two factors worsening for more than 4 weeks. Tumor volume response was assessed based on the tumor size pre- and postradiation CT scans. A complete response (CR) was defined as the disappearance of all clinical evidences of tumor without appearance of new lesions for more than 4 weeks. A partial response (PR) required a 50 % decrement in the maximal perpendicular tumor measurements, with no new lesion appearance for at least 4 weeks. No change (NC) was defined as less than 50 % reduction and less than 25 % increase of measurable tumor lesions. Progressive disease (PD) was defined as more than 25 % increase of measurable tumor lesions or new lesion developed. Response rate included the patients with CR and PR. Survival rate was calculated by the method of Kaplan Meier with the statistic software SPSS (version 9.0).

RESULTS

Dose escalation

Twenty-one patients were enrolled in this clinical study, 15 were unresectable as a result of major vascular invasion, 2 patients had partial tumor resected and other 4 patients had local recurrence at the primary site. Twelve were males and 9 females, and the median age of all patients was 64 years (range: 46-72 years).

Among these twenty-one patients, the primary lesions were

located at the head of 13 patients, at the body or tail of pancreas in 8 patients. Sixteen out of 21 patients completed the whole course of radiotherapy. The number of patients treated with different dose levels of 51Gy, 54Gy, 57Gy, 60Gy were 3, 3, 3 and 7 cases respectively. Dose volume histogram demonstrated that the median percentage of volume of small intestine received 80 % and 90 % of the prescribed dose was 10 % and 6 % respectively. Five out of 21 patients gave up the plan of radiotherapy because 4 patients had hepatic metastasis or ascites and another one had high fever, grade IV hematologic toxicity at the time of administration of GEM with a dose of 200 mg for the second time.

Clinical benefit

Sixteen patients were analyzed. CA19-9 levels prior to radiotherapy were elevated in 13 patients with a median value of 716 U/ml. At the end of radiotherapy, the levels of CA19-9 decreased significantly with a median value of 255 U/ml (P<0.001). Compared with that before radiotherapy, the value of CA19-9 decreased more than half after radiation treatment in 10/13 patients. Fourteen out of 16 patients suffered from pain at the start of chemoradiation had a decrease of oral analgesic consumption at the end of radiotherapy by more than 1/3 of the total amount before treatment. Ten out of 14 patients had a reduction of analgesic consumption more than 50 % and 5 patients were virtually painless. KPS was improved in 10/16 patients while 4 patients deteriorated during treatment, the other 2 patients remained unchanged. Only one patient (1/16) gained weight $\geqslant$5 % during treatment and maintained it for more than four weeks. Nine patients suffered from weight loss in excess of 5 % of their pretreatmeant weight. The other 6 patients remained stable in weight during the treatment. In total, seven patients were improved in at least one parameter of KPS, analgesic consumption or weight without simultaneous deterioration of any other parameters. So the clinical benefit ratio was 33 % (7/21). If the 5 patients who did not complete the radiation schedule were excluded, the benefit ratio increased to 44 % (7/16).

Radiological examination and survival rate

CT scanning after completion of radiotherapy demonstrated that no patient acquired CR, 5 out of 16 patients attained PR. Therefore, the response rate was 31 %. The median follow-up time was 8 months (range 3-17 months). One-year survival rate was 35 %.

Toxicity

No patient had radiation-induced acute reactions such as nausea, vomiting, diarrhea of greater than grade II. Among the six patients (6/21) who received chemotherapy with GEM as radiosensitizer, 3 patients had grade II neutropenia, 1 patients had grade IV neutropenia, and one patient had grade IV hematologic toxicities of neutropenia, thrombocytopenia and anemia. The latter was excluded from the dose escalation study. For patients receiving 5-FU as a radiosensitizer, only 3 patients had grade II neutropenia and two other patients had grade II abnormal liver function. All of them were able to complete the radiotherapy schedule with the support of some medication.

DISCUSSION

Locally advanced, surgically unresectable pancreatic carcinoma is a highly lethal disease. Its one-year survival rate is less than 10 %. Since diagnosis is usually made too late in the course of development of the disease to the chance of radical surgical resection, most patients experience progressive symptoms of pain, jaundice, weight loss, nausea, vomiting, or anorexia. An effective locoregional treatment would be the only chance for such patients. GEM and 5-FU have been studied in clinical trials by Radiation Therapy Oncology Group (RTOG) as radiation sensitizers in pancreatic cancer[14,15]. Studies of 5-FU and radiation have demonstrated that 5-FU was an effective radiation sensitizer by inhibiting tumor cell DNA synthesis. Gemcitabine (GEM) is also a radiosensitizer. It requires intracellular phosphorylation resulting in accumulation of difluorodeoxycytidine triphosphate (dFdCTP). dFdCTP competed with deoxycytidine triphosphate (dCTP) for incorporation into DNA and subsequently inhibited DNA synthesis and decreased intracellular deoxynucleoside triphosphate pools by curbing ribonucleotide reductase[14,15]. Both 5-FU and GEM have significant radiosensitization effect on tumor cells in which DNA band breakage induced by radiation is more difficult to be repaired. The severe toxicity reported by Crane *et al*[16] was significantly higher in patients treated with gemcitabine-based chemoradiation than in those treated with 5-FU-based chemoradiation, in which 12 out of 53 patients (23 %) treated with gemcitabine and one out of 61 patients (2 %) treated with 5-FU suffered from severe acute toxicity (P<0.001). But in a phase II trial of protracted 5-fluorouracil (200 mg/m^2/day) with concurrent radiotherapy, grade III or worse toxicity was observed in 20 % (4/20) patients[17]. In this study, among the 6 patients who were given GEM as a radiosensitizer with a dose of 200 mg/d on weeks 1, 3, 5, grade IV hematologic toxicities were found in two (33 %) patients. However, no one had acute toxicity greater than grade III in patients receiving 5-FU as a radiosensitizer. Therefore, in our study, 5-FU was the only drug used as a radiosensitizer at the later period of all cases. Boz *et al*[8] reported that it was relatively safe to use 5-FU through a central venous catheter at a dose of 300 mg/m^2/d, 7 d/wk, from the first day of external beam radiotherapy throughout the entire course of radiation treatment. In our study, only 5 patients who received 5-FU had grade II acute reaction and it was considered safe to combine the treatment with radiotherapy. No patient had radiotherapy induced severe acute reactions that interrupted the completion of radiotherapy.

Most cases in our study were patients with locally advanced unresectable pancreatic carcinoma. The aim of this study was to find the optimal maximum dose of external beam radiation using IMRT technique, which would not result in severe acute reaction induced by radiotherapy while improving the life quality and prolonging the survival as long as possible. Among the patients who received a total dose of 60Gy, no one suffered from dose-limiting toxicities resulted from radiotherapy. However, the dose greater than 60Gy was not given because of the possible occurrence of severe late toxicities due to radiation to normal tissue. Therefore, this study did not acquire the MTD of radiotherapy. Normalized with conventional dose 2Gy per fraction, the biological equivalent dose of 60Gy with IMRT technique for the early response tissues and the late response tissues were 62.2Gy and 66Gy respectively (for early response tissue: α/β=10Gy, for late response tissue: α/β=3Gy). Consequently, this study suggested that the IMRT adopted in this trial surely could improve the biological dose to tumor volume. The analysis of dose volume histogram (DVH) showed that the median volume of small intestine receiving 80 % and 90 % prescribed dose was 10 % and 6 % respectively. Moreover, late complications of gastrointestinal tract such as intestinal perforation, hemorrhage and obstruction were not found during follow-up. But we were not sure that patients given total dosage of 60Gy would not have severe complications in the future even the expected survival was relatively short. Therefore, our maximum escalation dose was limited to 60Gy. The tolerance of the patients were quite good in terms of normal tissue acute toxicities induced by radiation

when 30Gy was given in 10 fractions with IMRT technique (PTV margin was 5 mm from GTV) in addition to the conventional dose of 30Gy over 15 fractions.

A recent study by Crane *et al*[16] demonstrated that weekly administration of GEM combined with radiation led to 1-year survival rate of 42 % and median survival duration of 11 months. The response rate and 1-year survival rate of this series were 31 % and 35 % respectively. The difference between our results compared with that in literature may be due to discrepancy of patient' s selection. Up to now, no randomized prospective study in patients with pancreatic carcinoma compared the toxicities in gemcitabine-based *versus* 5-FU-based chemoradiation. Although the case number in our present study was relatively small, the primary results of our study indicated that the tolerance to 5-FU based chemoradiotherapy was much better than GEM based chemoradiotherapy.

In conclusion, for locally unresectable or recurrent pancreatic disease, this dose escalation clinical trial demonstrates that the dose level of 60Gy in 25 fractions over 5 weeks with IMRT technique combined with concurrent 5-FU is effective in improving survival, decreasing pain and the level of CA19-9 and promoting clinical benefit index without radiation-induced severe acute toxicities. Long term treatment effects and late toxicities remain to be evaluated.

REFERENCES

1 **Shankar A**, Russell RC. Recent advances in the surgical treatment of pancreatic cancer. *World J Gastroenterol* 2001; **7:** 622-626

2 **Ghaneh P**, Slavin J, Sutton R, Hartley M, Neoptolemos JP. Adjuvant therapy in pancreatic cancer. *World J Gastroenterol* 2001; **7:** 482-489

3 **Shinchi H**, Takao S, Noma H, Matsuo Y, Mataki Y, Mori S, Aikou T. Length and quality of survival after external-beam radiotherapy with concurrent continuous 5-fluorouracil infusion for locally unresectable pancreatic cancer. *Int J Radiat Oncol Biol Phys* 2002; **53:** 146-150

4 **Fisher BJ,** Perera FE, Kocha W, Tomiak A, Taylor M, Vincent M, Bauman GS. Analysis of the clinical benefit of 5-fluorouracil and radiation treatment in locally advanced pancreatic cancer. *Int J Radiat Oncol Biol Phys* 1999; **45:** 291-295

5 **Kornek GV,** Potter R, Selzer E, Schratter A, Ulrich-Pur H, Rogy M, Kraus G, Scheithauer W. Combined radiochemotherapy of locally advanced unresectable pancreatic adenocarcinoma with mitomycin C plus 24-hour continuous infusional gemcitabine. *Int J Radiat Oncol Biol Phys* 2001; **49:** 665-671

6 **Andre T,** Balosso J, Louvet C, Hannoun L, Houry S, Huguier M, Colonna M, Lotz JP, De Gramont A, Bellaiche A, Parc R, Touboul E, Izrael V. Combined radiotherapy and chemotherapy (cisplatin and 5-fluorouracil) as palliative treatment for localized unresectable or adjuvant treatment for resected pancreatic adenocarcinoma: results of a feasibility study. *Int J Radiat Oncol Biol Phys* 2000; **46:** 903-911

7 **Symon Z,** Davis M, McGinn CJ, Zalupski MM, Lawrence TS. Concurrent chemoradiotherapy with gemcitabine and cisplatin for pancreatic cancer: from the laboratory to the clinic. *Int J Radiat Oncol Biol Phys* 2002; **53:** 140-145

8 **Boz G,** De Paoli A, Innocente R, Rossi C, Tosolini G, Pederzoli P, Talamini R, Trovo MG. Radiotherapy and continuous infusion 5-fluorouracil in patients with nonresectable pancreatic carcinoma. *Int J Radiat Oncol Biol Phys* 2001; **51:** 736–740

9 **Yavuz AA,** Aydin F, Yavuz MN, Ilis E, Ozdemir F. Radiation therapy and concurrent fixed dose amifostine with escalating doses of twice-weekly gemcitabine in advanced pancreatic cancer. *Int J Radiat Oncol Biol Phys* 2001; **51:** 974-981

10 **Rich TA.** Chemoradiation for pancreatic and biliary cancer: current status of RTOG studies. *Ann Oncol* 1999; **10**(Suppl 4): 231-233

11 **Katz A**, Hanlon A, Lanciano R, Hoffman J, Coia L. Prognostic value of CA19-9 levels in patients with carcinoma of the pancreas treated with radiotherapy. *Int J Radiat Oncol Biol Phys* 1998; **41:** 393-396

12 **Tokuuye K**, Sumi M, Kagami Y, Murayama S, Ikeda H, Ikeda M, Okusaka T, Ueno H, Okada S. Small-field radiotherapy in combination with concomitant chemotherapy for locally advanced pancreatic carcinoma. *Radiother Oncol* 2003; **67:** 327-330

13 **Trotti A,** Byhardt R, Stetz J, Gwede C, Corn B, Fu K, Gunderson L, McCormick B, Morrisintegral M, Rich T, Shipley W, Curran W. Common toxicity criteria: version 2.0. An improved reference for grading the acute effects of cancer treatment: impact on radiotherapy. *Int J Radiat Oncol Biol Phys* 2000; **47:** 13-47

14 **Safran H,** Dipetrillo T, Iannitti D, Quirk D, Akerman P, Cruff D, Cioffi W, Shah S, Ramdin N, Rich T. Gemcitabine, paclitaxel, and radiation for locally advanced pancreatic cancer: a phase I trial. *Int J Radiat Oncol Biol Phys* 2002; **54:** 137-141

15 **Burris HA 3rd**, Moore MJ, Andersen J, Green MR, Rothenberg ML, Modiano MR, Cripps MC, Portenoy RK, Storniolo AM, Tarassoff P, Nelson R, Dorr FA, Stephens CD, Von Hoff DD. Improvements in survival and clinical benefit with gemcitabine as first-line therapy for patients with advanced pancreas cancer: a randomized trial. *J Clin Oncol* 1997; **15:** 2403-2413

16 **Crane CH,** Abbruzzese JL, Evans DB, Wolff RA, Ballo MT, Delclos M, Milas L, Mason K, Charnsangavej C, Pisters PW, Lee JE, Lenzi R, Vauthey JN, Wong AB, Phan T, Nguyen Q, Janjan NA. Is the therapeutic index better with gemcitabine-based chemoradiation than with 5-fluorouracil-based chemoradiation in locally advanced pancreatic cancer? *Int J Radiat Oncol Biol Phys* 2002; **52:** 1293-1302

17 **Ishii H**, Okada S, Tokuuye K, Nose H, Okusaka T, Yoshimori M, Nagahama H, Sumi M, Kagami Y, Ikeda H. Protracted 5-fluorouracil infusion with concurrent radiotherapy as a treatment for locally advanced pancreatic carcinoma. *Cancer* 1997; **79:** 1516-1520

Edited by Xu JY and Wang XL

P.O.Box 2345, Beijing 100023,China
Fax: +86-10-85381893
E-mail: wjg@wjgnet.com www.wjgnet.com

World J Gastroenterol 2003;9(11):2565-2569
World Journal of Gastroenterology
 ISSN 1007-9327

• CLINICAL RESEARCH •

Therapeutic efficacy of high-dose vitamin C on acute pancreatitis and its potential mechanisms

Wei-Dong Du, Zu-Rong Yuan, Jian Sun, Jian-Xiong Tang, Ai-Qun Cheng, Da-Ming Shen, Chun-Jin Huang, Xiao-Hua Song, Xiao-Feng Yu, Song-Bai Zheng

Wei-Dong Du, Zu-Rong Yuan, Jian Sun, Jian-Xiong Tang, Ai-Qun Cheng, Da-Ming Shen, Xiao-Hua Song, Chun-Jin Huang, Department of Surgery, Huadong Hospital, Shanghai 200040, China
Xiao-Feng Yu, Song-Bai Zheng, Department of Digestive Internal Medicine, Huadong Hospital, Shanghai 200040, China
Correspondence to: Dr. Wei-Dong Du, Department of Surgery, Huadong Hospital, No. 221, Yanan Xilu, Shanghai 200040, China. duzhuyi@sh163.net
Telephone: +86-21-62483180 **Fax:** +86-21-62483180
Received: 2002-12-22 **Accepted:** 2003-02-16

Abstract

AIM: To observe the therapeutic efficacy of high-dose Vitamin C (Vit. C) on acute pancreatitis (AP), and to explore its potential mechanisms.

METHODS: Eghty-four AP patients were divided into treatment group and control group, 40 healthy subjects were taken as a normal group. In the treatment group, Vit. C (10 g/day) was given intravenously for 5 days, whereas in the control group, Vit. C (1 g/day) was given intravenously for 5 days. Symptoms, physical signs, duration of hospitalization, complications and mortality rate were monitored. Meanwhile, serum amylase, urine amylase and leukocyte counts were also determined. The concentration of plasma vitamin C (P-VC), plasma lipid peroxide (P-LPO), plasma vitamin E (P-VE), plasma β-carotene (P-β-CAR), whole blood glutathione (WB-GSH) and the activity of erythrocyte surperoxide dimutase (E-SOD) and erythrocyte catalase (E-CAT) as well as T lymphocyte phenotype were measured by spectrophotometry in the normal group and before and after treatment with Vit. C in the treatment and the control group.

RESULTS: Compared with the normal group, the average values of P-VC, P-VE, P-β-CAR, WB-GSH and the activity of E-SOD and E-CAT in AP patients were significantly decreased and the average value of P-LPO was significantly increased, especially in severe acute pancreatitis (SAP) patients (P <0.05. P-VC, P =0.045; P-VE, P =0.038; P =0.041; P-β-CAR, P =0.046; WB-GSH, P =0.039; E-SOD, P =0.019; E-CAT, P =0.020; P-LPO, P =0.038). Compared with the normal group, CD_3 and CD_4 positive cells in AP patients were significantly decreased. The ratio of CD_4/CD_8 and CD_4 positive cells were decreased, especially in SAP patients (P<0.05. CD_4/CD_8, P =0.041; CD_4, P =0.019). Fever and vomiting disappeared, and leukocyte counts and amylase in urine and blood become normal quicker in the treatment group than in the control group. Moreover, patients in treatment group also had a higher cure rate, a lower complication rate and a shorter in-ward days compared with those in he control group. After treatment, the average value of P-VC was significantly higher and the values of SIL-2R, TNF-α, IL-6 and IL-8 were significantly lower in the treatment group than in the control group (P<0.05 P-VC, P =0.045; SIL-2R, P =0.012; TNF-α, P =0.030; IL-6, P =0.015; and IL-8, P =0.043). In addition, the ratio of CD_4/CD_8 and CD4 positive cells in the patients of treatment group were significantly higher than that of the control group after treatment (P<0.05. CD_4/CD_8, P =0.039; CD_4, P =0.024).

CONCLUSION: High-dose vitamin C has therapeutic efficacy on acute pancreatitis. The potential mechanisms include promotion of anti-oxidizing ability of AP patients, blocking of lipid peroxidation in the plasma and improvement of cellular immune function.

Du WD, Yuan ZR, Sun J, Tang JX, Cheng AQ, Shen DM, Huang CJ, Song XH, Yu XF, Zheng SB. Therapeutic efficacy of high-dose vitamin C on acute pancreatitis and its potential mechanisms. *World J Gastroenterol* 2003; 9(11): 2565-2569
http://www.wjgnet.com/1007-9327/9/2565.asp

INTRODUCTION

In the occurrence and progress of acute pancreatitis (AP), system inflammatory response syndrome (SIRS) often appears as a complication, and may result in pyemia and multiple organ dysfunction (MODS), and death may be the last consequence[1,2]. Many investigations have made it clear that over-activation of leucocytes and their cytokines, the imbalance between release and clearance of free radicals and other pathophysiological changes play important roles in this progress[3-5]. The prognosis of AP patients has a close correlation with infection and pyemia, whereas the occurrence and progress of infection and pyemia also have a correlation with the changes of host immune function[6]. It has been confirmed that vitamin C is an important antioxidant which protects the body from damage of inflammation[7,8], and high-dose vitamin C can improve the immune function[9]. In the present, randomized control study, we observed the clinical efficacy on a high-dose of vitamin C (10 g/day, intravenously) on AP and also monitored its influence on plasma vitamin C (P-VC), plasma lipid peroxide (P-LPO) and other biochemical and immunological markers in order to explore its underlying mechanisms.

MATERIALS AND METHODS

Patients

Based on the AP diagnostic criteria worked out by the Pancreatic Surgery Subgroup of Chinese Medical Association, we selected 84 cases of AP patients. They included 53 males and 31 females, and were aged from 25 to 71 (mean ± SD, 42±13) years. Patients with serious diseases in main visceral organs such as the heart, brain, liver and kidney, peptic ulcer disease, diabetes mellitus, auto-immune diseases ,and tumors were excluded. According to the classification criteria (2nd edition 1996), 70 patients were mild AP (MAP) cases, 14 patients were severe (SAP) cases. Forty healthy volunteers (male 26, female 14, age 28-66 (47±14) years old) were included in the study as a normal group. There was no

significant difference in age and gender between AP patients and healthy volunteers (P>0.05).

Methods

Treatment regimen the routine therapy was used in both treatment and control groups, which consisted of pancreatic excretion inhibition, anti-spasm, analgesia, maintenance of the water-electrolyte balance, prevention and cure of infection and other complications, and if necessary, fasting and gastrointestinal decompression. The patients were randomly divided into two groups. In the treatment group (n=40), vitamin C (10 g/day) was given intravenously for 5 days, while in the control group (n=44), vitamin C (1 g/day) was given intravenously for 5 days. There was no significant difference in age (40±12 *vs*. 43±14 years old), gender (M/F, 25/15 *vs*. 28/16) and disease severity (MAP/SAP, 33/7 *vs*. 37/7) between the treatment and control groups (all P>0.05).

Detection of clinical, biochemical and immunological markers Symptoms such as abdominal pain, fever, vomiting, and hospitalization duration were monitored. Serum amylase, urine amylase, leukocyte counts, concentrations of plasma vitamin c (P-VC), plasma lipid peroxide (P-LPO), plasma vitamin E (P-VE), plasma β-carotene (P-β-CAR), whole blood glutathione (WB-GSH) and the activity of erythrocyte surperoxide dimutase (E-SOD), erythrocyte catalase (E-CAT), serum interleukin-2 receptor (SIL-2R), tumor necrosis factor-alpha (TNF-α), IL-6, IL-8 and complement reaction protein (CRP), as well as T lymphocyte phenotypes CD_3, CD_4, and CD_8 were measured. P-VC and P-VE (μmol/L) were measured by spectrometry using ferrocyanide. P-LPO (μmol/L) was measured by spectrometry using sulfbarbitone. P-β-CAR (μmol/L) was measured with alcohol-petroleum ether spectrometer. WB-GSH (mmol/L) was measured by spectrometry using disulfhydry-dinitrobenzoic acid. E-SOD (U/g*Hb) was measured by spectrometry using pyrocatechol. E-CAT (K/g*Hb) was measured by spectrometryusing oxydol-acetic diachromic acid potassium. SIL-2R, TNF-α, IL-6 and IL-8 (pmol/L) were measured by enzyme-linked immunosorbent assays (ELISA). All reagents were supplied by the Roche Company (Swiss). CRP (mg/L) was measured by the quick immune extinction spectrometry. T-lymphocytephenotypes (%) were determined by spectrometry using anti-AKP monoclonal antibody AKP.

Clinically, cure of the disease was defined if symptoms such as abdominal pain, vomiting and fever disappeared, serum amylase, urine amylase and leukocyte counts returned to normal, and imaging examinations showed no abnormality. Improvement of the disease was defined if symptoms relieved or disappeared, and laboratory examinations showed almost normal results. The disease was defined to be unchanged if symptoms, physical signs and laboratory examinations had remained unchanged since hospitalization, and to be deteriorated if patient' s condition was getting worse, with occurrence of severe complications and death.

Statistics analysis

All the data were expressed as mean ± SD, when appropriate. SPSS 10.0 statistical package was used for statistical analysis. T-test and χ^2-test were used for the analysis, and P<0.05 was regarded as statistically significant.

RESULTS

Comparison of the results between patients and healthy volunteers

As shown in tables 1, 2 and 3, the serum levels of SIL-2R, TNF-α, IL-6, IL-8 and CRP in AP patients were much higher than those in healthy volunteers (P<0.05 or P<0.01). The average contents of P-VC, P-VE, P-β-CAR, WB-GSH, E-SOD and E-CAT were significantly lower, while the level of P-LPO was significantly higher in patients than in healthy volunteers. More importantly, all the above variables were higher in SAP patients than in MAP patients (P<0.05). The percentage of CD_3 and CD_4 positive cells in AP cases was significantly lower in AP patients compared to the healthy group (both P<0.05), CD_4 and the ratio of CD_4/CD_8 were much lower in SAP patients than in healthy group (both P<0.05).

Table 1 Comparison of cytokines between patients and healthy volunteers

	Patients (n=84)	Healthy volunteers (n=40)	P
SIL-2R (pmol/L)	213.42±54.68	72.34±23.17	<0.01
TNF-α (pmol/L)	3.67±1.01	0.58±0.15	<0.01
IL-6 (pmol/L)	92.43±25.67	29.57±11.64	<0.01
IL-8 (pmol/L)	267.58±121.88	60.49±25.35	<0.01
CRP (mg/L)	18.30±7.35	8.34±4.17	<0.01

Table 2 Comparison of oxidation and anti-oxidation levels between patients and healthy volunteers

	Patients (n=84)		Healthy volunteers (n=40)
	MAP (n=70)	SAP (n=14)	
P-VC(μmol/L)	32.56±6.73	43.51±2.15	55.12±13.24
P-VE(μmol/L)	19.21±1.75	13.26±3.14	24.01±5.28
P-LPO(μmol/L)	12.95±3.91	15.41±2.15	11.21±2.76
P-β-CAR(μmol/L)	1.38±0.25	0.94±0.11	1.61±0.23
WB-GSH(mmol/L)	1.08±0.27	0.70±0.33	1.21±0.21
E-SOD(U/g*Hb)	1 804.42±100.14	1 495.27±152.87	2 084.39±191.53
E-CAT(K/g*Hb)	221.54±20.47	174.76±34.56	280.42±77.26

Comparison between patients and healthy volunteers and between mild acute panceatitis (MAP) and severe acute panceatitis (SAP), all P<0.05.

Table 3 Comparison of cellular immunity between patients and healthy volunteers ($\bar{x}$±s)

	MAP (n=70)	SAP (n=14)	Healthy group (n=40)
CD_3(%)	46.73±10.15	45.23±12.24[a]	57.65±10.28
CD_4(%)	34.27±9.52[a]	23.65±7.53[ab]	43.23±7.65
CD_8(%)	22.32±7.29	27.18±4.56	26.18±4.79
CD_4/CD_8	1.84±0.78	0.80±0.67[ab]	2.13±0.66

[a]P<0.05 *vs* healthy volunteers, [b]P<0.05 *vs* MAP.

Table 4 Comparison of clinical symptoms and laboratory examinations between treatment and control groups ($\bar{x}$±s, h)

	Treatment group (n=40)	Control group (n=44)	P
Disappearance of fever	65.75±14.26	89.71±16.25	<0.05
Release of abdominal pain	23.43±5.66	25.31±6.37	>0.05
Disappearance of abdominal pain	55.23±10.08	54.23±11.73	>0.05
Disappearance of vomiting	43.19±12.65	51.67±10.93	<0.05
Normalization of serum amylase	79.14±19.64	91.45±10.45	<0.05
Normalization of urine amylase	100.22±19.22	122.38±13.56	<0.05
Normalization of leucocyte counts	69.59±15.41	81.34±14.05	<0.05

Table 5 Comparison of clinical efficacy between treatment and control groups (day, %)

	Case	Cure	Improvement	No change	Deterioration	Hospitalization
Treatment group	40	30 (75.00)	4(10.00)	4 (10.00)	2 (5.00)	9.34±4.24
Control group	44	18 (40.91)	10(22.73)	6 (13.64)	6 (13.64)	13.45±3.21
P		<0.05	<0.05	<0.05	<0.05	<0.05

Table 6 Comparison of cytokines between treatment and control groups before and after therapy ($\bar{x}\pm s$)

	Treatment group (*n*=40)		Control group (*n*=44)	
	Before therapy	After therapy	Before therapy	After therapy
SIL-2R (pmol/L)	221.67±87.30	118.37±43.68[a]	196.52±63.28	178.84±30.56
TNF-α (pmol/L)	3.65±1.25	1.52±0.78[b]	3.99±1.34	2.46±1.04
IL-6 (pmol/L)	95.58±18.64	39.53±10.36[b]	89.22±12.03	59.83±9.48
IL-8 (pmol/L)	273.49±88.50	127.35±49.86[a]	261.47±64.97	198.31±28.50
CRP (mg/L)	19.19±9.37	8.70±4.65	17.56±5.62	9.42±5.84

Before therapy: $P>0.05$ for each index in the two group. After therapy: [a]$P<0.05$, [b]$P<0.01$ *vs* treatment and control groups.

Table 7 Comparison of oxidation and anti-oxidation between treatment and control groups before and after therapy

	Treatment group (*n*=40)		Control group (*n*=44)	
	Before therapy	After therapy	Before therapy	After therapy
P-VC(μmol/L)	41.54±2.91	53.25±10.11[a]	41.78±1.96	45.21±9.25[1)]
P-VE(μmol/L)	18.47±3.45	19.97±4.26[b]	18.67±2.13	19.24±2.46[2)]
P-LPO(μmol/L)	13.53±2.12	11.54±1.45[a]	13.68±2.31	12.98±2.75[1)]
P-β-CAR(μmol/L)	1.25±0.17	1.37±0.71[b]	1.28±0.21	1.34±0.65[2)]
WB-GSH(mmol/L)	0.97±0.18	1.39±0.41[a]	0.98±0.21	1.04±0.35[1)]
E-SOD(U/g*Hb)	1 749.01±50.55	1 997.42±145.33[1)]	1 726.28±71.37	1 807.22±120.21[1)]
E-CAT(K/g*Hb)	217.34±19.51	269.52±65.32[1)]	220.18±20.14	239.17±70.15[1)]

Before therapy: each index in the two group, $P>0.05$. After therapy: [a]$P<0.05$, [b]$P<0.01$ *vs* treatment and control groups.

Comparison of results between treatment and control groups

As shown in in tables 4 and 5, except for abdominal pain, all symptoms disappeared and serum and urine amylase normalized at a much faster speed in the treatment group than in control group (all $P<0.05$). The treatment group had a higher cure rate and lower deterioration rate than the control group 5 days after therapy (both $P<0.05$).

Comparison of cytokines between treatment and control groups before and after therapy

There was no significant difference in the levels of SIL-2R, TNF-α, IL-6, IL-8 and CRP between the two groups before treatment (all $P>0.05$) (Table 6). However, the levels of cytokines decreased significantly 5 days after therapy in both groups ($P<0.05$), although they were still higher compared with the healthy group. The contents of SIL-2R, TNF-α, IL-6 and IL-8 were significantly lower in the treatment group than in the control group (all $P<0.05$) 5 days after therapy. The CRP level was lower compared with the control group, but the difference was not statistically significant ($P>0.05$, Table 6).

Comparison of oxidation and anti-oxidation levels between treatment and control groups before and after therapy

No notable difference in levels of P-VC, P-VE, P-LPO, P-β-CAR, WB-GSH, E-SOD and E-CAT was observed between the two groups ($P>0.05$) before treatment (Table 7). The average concentration of P-VC, WB-GSH, E-SOD and E-CAT was elevated significantly and P-LPO level was decreased in treatment group 5 days after therapy compared with the control group (all $P<0.05$, Table 7). The contents of P-VE and P-β-CAR had no remarkable difference between the two groups ($P>0.05$).

Comparison of cellular immunity between MAP cases in treatment and control groups before and after therapy

There was no significant difference in CD_3, CD_4 CD_8 and the ratio of CD_4/CD_8 between the MAP patients in the two groups before treatment (Table 8). The mean count of CD_3 and CD_4 and the ratio of CD_4/CD_8 were higher 5 days after treatment than those before treatment in both groups (all $P<0.05$). As far as the comparison of the CD_3 and CD_4 positive cells and the ratio of CD_4/ CD_8 between these two group was concerned, the levels in the former group were slightly higher than that in the latter group ($P>0.05$, Table 8).

Table 8 Immunity change before and after therapy in MAP cases of two groups ($\bar{x}\pm s$)

	Treatment group (*n*=33)		Control group (*n*=37)	
	Before therapy	After therapy	Before therapy	After therapy
CD_3(%)	45.99±9.75	52.34±6.87	47.48±10.35	50.18±7.10
CD_4(%)	36.43±8.56	38.79±7.65	36.01±9.47	37.25±6.92
CD_8(%)	21.98±6.85	20.46±3.53	22.45±7.11	21.33±4.88
CD_4/CD_8	1.88±0.64	1.97±0.74	1.75±0.76	1.85±0.43

Before therapy: $P>0.05$ *vs* the two groups. After therapy: $P>0.05$ *vs* the two groups.

Comparison of cellular immunity between SAP cases treatment and control groups before and after therapy

There was no significant difference in CD_3, CD_4 CD_8 and the ratio of CD_4/CD_8 between the MAP patients in the two groups before treatment (Table 9). The mean count of CD_3 and CD_4 and the ratio of CD_4/CD_8 were higher 5 days after treatment than those before treatment in both groups (all $P<0.05$).

Moreover, the CD_3 and CD_4 positive cells and the ratio of CD_4/CD_8 were remarkably higher in the treatment group than in the control group (all $P<0.05$).

Table 9 Immunity changes in SAP cases of two groups before and after therapy ($\bar{x}\pm s$)

	Treatment group (n=7)		Control group (n=7)	
	Before therapy	After therapy	Before therapy	After therapy
P-VC(μmol/L)	31.93±7.21	49.27±10.12[a]	32.89±2.17	38.17±9.41[a]
CD_3(%)	45.65±11.18	51.39±7.17	44.90±10.47	47.45±10.72
CD_4(%)	22.48±6.35	36.93±8.51[a]	23.85±7.52	25.67±7.57[a]
CD_8(%)	23.32±6.43	23.64±5.50	26.84±5.92	22.58±6.74
CD_4/CD_8	0.85±0.23	1.41±0.47[a]	0.86±0.45	1.17±0.52[a]

Before therapy: $P>0.05$ *vs* the two groups. After therapy: [a]$P<0.05$ *vs* the two groups.

DISCUSSION

Many free radicals are produced in body metabolic procedure. It is estimated that oxygen-derived free radicals account for 95 %. They are cleaned by antioxidants and antioxidases rapidly, and thus the production and clearance keep a homeostasis in normal conditions. Free radicals could exert physiological functions to some degree, such as taking part in biosynthesis, detoxification and microorganism clearance[10,11]. However, overdose free radicals could lead to tissue and cell injuries in pathologic conditions through different approaches[12]: (1) Free radicals attacked bio-membrane, which led to unsaturated fatty acid lipid peroxidation (LPO) and affected the function of membrane of cells and cell organelle. (2) Free radicals might destroy the major enzymes and other molecules, making them lose their functions. (3) Free radicals might disturb the synthesis and replication of DNA. (4) LPO could produce more toxic substances and free radicals. Usually the free radicals produced in metabolism can be cleared by the defence system of anti-oxidation. This system is mainly composed of anti-oxidases and antioxidants. These materials catch and clear the excessive free radicals, prevent the chain reaction of a serial of free radicals from pathologic acceleration and keep the homeostasis of antioxidation from imbalance. Vit. C, Vit. E and β-CAR were the most important anti-oxidases and antioxidants, and played an important role in anti-infection[7-9].

The occurrence and development of acute pancreatitis were related to the disturbance in release and clearance of free radicals, which resulted in the imbalance between oxidation and anti-oxidation[13]. Many studies have indicated that excessive free radicals could lead to tissue and cellular injury in pathological conditions[11]. Free radicals took part in the edema of AP, and probably in the necrosis process[13]. When AP happened, vitamin C was depleted at first by reacting with superoxide, anion hydroperoxide anion and hydroxylperoxide anion, and then by forming vitamin C free radicals to prevent DNA and membrane lipid from damage[14]. The concentration of vitamin C in AP cases decreased to various extents[15], reached the lowest level in the first 1-5 days of the disease course, and the vitamin C level correlated with the severity of the disease[16]. The output of free radicals was increased, and peroxidation reaction was reinforced, therefore a large amount of vitamin C, vitamin E, β-CAR, WB-GSH, E-SOD and E-CAT were depleted so that they could hardly prevent pancreas and other organs from damage caused by lipid peroxidation. Furthermore, the elevation of cytokines is a frequent phenomenon and the extention was closely associated with the severity of AP[17]. The reason why MAP developed into SAP was a chain and amplification reaction (so-called waterfall effect) of inflammatory agents that led to SIRS and MODS[18]. Therefore, the serum levels of cytokines SIL-2R, TNF-α, IL-6, IL-8 and CRP could be regarded as the biomarkers of therapeutic efficacy[19].

Recent studies have shown that the prognosis of AP is closely associated with infection and pyemia. At the same time, the occurrence, development and conversion of infection and pyemia were intimately associated with the changes of immune function[20,21]. Because histamine, bradykinin and many other cytokines produced in AP progression could inhibit the immune function in AP cases, especially in those with SAP, the injuries of immune function took place. Theses injuries included decreased proliferation of T cells, especially Th cells, decreased IL-2 level, reduced monocytes in peripheral blood and increased prostaglandin E2 from monocytes[22-24]. Our study indicated that cellular immune function damage took place in AP patients. The percentage of CD_3 and CD_4 positive lymphocytes was higher in treatment group than in control group after treatment, while that of CD_4 positive lymphocytes and the ratio of CD_4/CD_8 were lower in SAP than in MAP[25]. CD_4 positive T-lymphocytes could excrete IL-2, which stimulated the silent T-lymphocytes to express IL-2 receptor, and thus IL-2 conjugated its receptor, leading to a series of immune reactions and increased DNA synthesis[26]. Therefore, the decrease of CD_4 positive T-lymphocytes certainly influenced the body immune function and resistibility, and the susceptibility to infection increase[27].

We found that the average concentration of P-VC, P-VE, β-CAR, WB-GSH, E-SOD and E-CAT was significantly lower while P-LPO level was significantly higher in AP patients than in healthy volunteers. All these indicate that free radical reaction and lipid peroxidation, and disturbance can speed up free radical elimination and anti-oxidation. We also found that high-dose of vitamin C at early stage could contribute to the improvement of the levels of P-VC, P-VE, WB-GSH, E-SOD and E-CAT, which took part in eliminating injurious free radicals and protecting cells from damage by the free radicals. Simultaneously, the P-LPO level was lower in treatment group than in control group, further confirming the preventive effect of high-dose vitamin C against lipid peroxidation. It was also revealed that there was no significant difference in CD4/CD8 ratio between the MAP patients and the control group. The possible reason is that the immune system of MAP cases has not been seriously impaired, so that the immune adjusting mechanism is able to adjust the CD_8 cells to keep the CD_4/CD_8 ratio at a normal level. However, in SAP patients this mechanism was seriously impaired and could no longer keep the CD_4/CD_8 ratio. Vitamin C could improve the immune function by increasing CD_3, CD_4 and the CD_4/CD_8 ratio, and decreasing CD_8[28], elevating transformation efficiency of lymphocytes, stimulating the production of IL-1, IL-2, IL-6 and other cytokines, and reinforcing cell-mediated immune reaction parameters[29]. In the present study, the percentage of CD4 positive lymphocytes and CD_4/CD_8 ratio in SAP cases were much lower compared with the healthy volunteers, but these indices were significantly higher than those of control group after high-dose vitamin C application. These findings indicate that severe cellular immune defection exists in SAP cases. However, high-dose vitamin C can not only eliminate free radicals and reduce the damage of lipid peroxidation, but also improve the cellular immune function in SAP patients, and thus is useful in reducing the incidence and mortality of pyemia and MODS. SIL-2R, TNF-α, IL-6, IL-8 and CRP concentrations in AP patients were significantly higher than those in healthy volunteers. However, SIL-2R, TNF-α, IL-6 and IL-8 levels decreased significantly after high-dose of vitamin C application, and were significantly lower than those in the control group. It took a shorter time to cure or improve

the clinical symptoms (fever, abdominal pain and vomiting) and to normalize serum amylase, urine amylase and leukocyte counts in patients taking high dose of vitamin C, compared with those taking low dose of vitamin C. Thus, the therapeutic efficacy of high dose of vitamin C was much better than that of low dose of vitamin C. Therefore, we conclude that high-dose vitamin C has therapeutic efficacy on acute pancreatitis. The potential mechanisms include promotion of anti-oxidizing ability of AP patients, blocking of lipid peroxidation in the plasma, and improvement of cellular immune function.

REFERENCES

1 **Huis M**, Balija M, Lojna-Funtak I, Stulhofer M. Acute pancreatitis in the Zabok General Hospital. *Acta Med Croatica* 2001; **55**: 81-85

2 **Hirota M,** Nozawa F, Okabe A, Shibata M, Beppu T, Shimada S, Egami H, Yamaguchi Y, Ikei S, Okajima T, Okamoto K, Ogawa M. Relationship between plasma cytokine concentration and multiple organ failure in patients with acute pancreatitis. *Pancreas* 2000; **21**: 141-146

3 **Schulz HU,** Niederau C, Klonowski-Stumpe H, Halangk W, Luthen R, Lippert H. Oxidative stress in acute pancreatitis. *Hepatogastroenterology* 1999; **46**: 2736-2750

4 **Chen CC**, Wang SS, Lee FY, Chang FY, Lee SD. Proinflammatory cytokines in early assessment of the prognosis of acute pancreatitis. *Am J Gastroenterol* 1999; **94**: 213-218

5 **Tsai K,** Wang SS, Chen TS, Kong CW, Chang FY, Lee SD, Lu FJ. Oxidative stress: animportant phenomenon with pathogenetic significance in the progression of acute pancreatitis. *Gut* 1998; **42**: 850-855

6 **Lankisch PG,** Mahlke R, Blum T, Bruns A, Bruns D, Maisonneuve P, Lowenfels AB. Hemoconcentration: an early marker of severe and/or necrotizing pancreatitis? Acritical appraisal. *Am J Gastroenterol* 2001; **96**: 2081-2085

7 **Scott P,** Bruce C, Schofield D, Shiel N, Braganza JM, McCloy RF. Vitamin C status in patients with acute pancreatitis. *Br J Surg* 1993; **80:** 750-754

8 **Bonham MJ,** Abu-Zidan FM, Simovic MO, Sluis KB, Wilkinson A, Winterbourn CC, Windsor JA. Early ascorbic acid depletion is related to the severity of acute pancreatitis. *Br J Surg* 1999; **86:** 1296-1301

9 **Cartmell MT,** Kingsnorth AN. Acute pancreatitis. *Hosp Med* 2000; **61:** 382-385

10 **Braganza JM,** Scott P, Bilton D, Schofield D, Chaloner C, Shiel N, Hunt LP, Bottiglieri T. Evidence for early oxidative stress in acute pancreatitis. Clues for correction. *Int J Pancreatol* 1995; **17:** 69-81

11 **Wereszczynska-Siemiatkowska,** Dabrowski A, Jedynak M, Gabryelewicz A. Oxidative stress as an early prognostic factor in acute pancreatitis (AP): its correlation with serum phospholipase A2 (PLA2) and plasma polymorphonuclear elastase (PMN-E) in different-severity forms of human AP. *Pancreas* 1998; **17:** 163-168

12 **Kruse P,** Anderson ME, Loft S. Minor role of oxidative stress during intermediate phase of acute pancreatitis in rats. *Free Radic Biol Med* 2001; **30**: 309-317

13 **Jurkowska G,** Rydzewska G, Gabryelewicz A, Dzieciol J. The role of nitric oxide in caerulein-induced acute pancreatitis and the recovery process after inflammatory damage. *Eur J Gastroenterol Hepatol* 1999; **11:** 1019-1026

14 **Abu-Zidan FM,** Bonham MJ, Windsor JA. Severity of acute pancreatitis: a multivariate analysis of oxidative stress markers and modified Glasgow criteria. *Br J Surg* 2000; **87:** 1019-1023

15 **Sweiry JH,** Shibuya I, Asada N, Niwa K, Doolabh K, Habara Y, Kanno T, Mann GE. Acute oxidative stress modulates secretion and repetitive $Ca2^{+}$ spiking in rat exocrine pancreas.*Biochim Biophys Acta* 1999; **1454:** 19-30

16 **Simovic MO,** Bonham MJ, Abu-Zidan FM, Windsor JA. Manganese superoxide dismutase: a marker of ischemia-reperfusion injury in acute pancreatitis? *Pancreas* 1997; **15:** 78-82

17 **Mayer J,** Rau B, Gansauge F, Beger HG. Inflammatory mediators in human acute pancreatitis: clinical and pathophysiological implications. *Gut* 2000; **47:** 546-552

18 **Lipsett PA.** Serum cytokines, proteins, and receptors in acute pancreatitis: mediators, markers, or more of the same? *Crit Care Med* 2001; **29:** 1642-1644

19 **Brivet FG,** Emilie D, Galanaud P. Pro- and anti-inflammatory cytokines during acute severe pancreatitis: an early and sustained response, although unpredictable of death. Parisian Study Group on Acute Pancreatitis. *Crit Care Med* 1999; **27:** 749-755

20 **Kouris GJ,** Liu Q, Rossi H, Djuricin G, Gattuso P, Nathan C, Weinstein RA, Prinz RA. The effect of glucagon-like peptide 2 on intestinal permeability and bacterial translocation in acute necrotizing pancreatitis. *Am J Surg* 2001; **181:** 571-575

21 **Yekebas EF,** Eisenberger CF, Ohnesorge H, Saalmuller A, Elsner HA, Engelhardt M, Gillesen A, Meins J, The M, Strate T, Busch C, Knoefel WT, Bloechle C, Izbicki JR. Attenuation of sepsis-related immunoparalysis by continuous veno-venous hemofiltration in experimental porcine pancreatitis. *Crit Care Med* 2001; **29:** 1423-1430

22 **Bhatnagar A,** Wig JD, Majumdar S. Expression of activation, adhesion molecules and intracellular cytokines in acute pancreatitis. *Immunol Lett* 2001; **77:** 133-141

23 **Powell JJ,** Siriwardena AK, Fearon KC, Ross JA. Endothelial-derived selectins in the development of organ dysfunction in acute pancreatitis. *Crit Care Med* 2001; **29:** 567-572

24 **Berney T,** Gasche Y, Robert J, Jenny A, Mensi N, Grau G, Vermeulen B, Morel P. Serum profiles of interleukin-6, interleukin-8, and interleukin-10 in patients with severe and mild acute pancreatitis. *Pancreas* 1999; **18:** 371-377

25 **Inagaki T,** Hoshino M, Hayakawa T, Ohara H, Yamada T, Yamada H, Iida M, Nakazawa T, Ogasawara T, Uchida A, Hasegawa C, Miyaji M, Takeuchi T. Interleukin-6 is a useful marker for early prediction of the severity of acute pancreatitis. *Pancreas* 1997; **14**: 1-8

26 **Powell JJ,** Fearon KC, Siriwardena AK, Ross JA. Evidence against a role for polymorphisms at tumor necrosis factor, interleukin-1 and interleukin-1 receptor antagonist gene loci in the regulation of disease severity in acute pancreatitis. *Surgery* 2001; **129:** 633-640

27 **Cook JW,** Karakozis S, Kim D, Provido H, Gongora E, Kirkpatrick JR. Interleukin-10 attenuates proinflammatory cytokine production and improves survival in lethal pancreatitis. *Am Surg* 2001; **67:** 237-241

28 **Hartwig W,** Jimenez RE, Fernandez-del Castillo C, Kelliher A, Jones R, Warshaw AL. Expression of the adhesion molecules Mac-1 and L-selectin on neutrophils in acute pancreatitis is protease- and complement-dependent. *Ann Surg* 2001; **233:** 371-378

29 **Mandi Y,** Farkas G, Takacs T, Boda K, Lonovics J. Diagnostic relevance of procalcitonin, IL-6, and sICAM-1 in the prediction of infected necrosis in acute pancreatitis. *Int J Pancreatol* 2000; **28:** 41-49

Edited by Xa HHX and Wang XL

P.O.Box 2345, Beijing 100023,China
Fax: +86-10-85381893
E-mail: wjg@wjgnet.com www.wjgnet.com

World J Gastroenterol 2003;9(11):2570-2573
World Journal of Gastroenterology
 ISSN 1007-9327

• CLINICAL RESEARCH •

Organ failure associated with severe acute pancreatitis

Ai-Jun Zhu, Jing-Sen Shi, Xue-Jun Sun

Ai-Jun Zhu, Jing-Sen Shi, Xue-Jun Sun, Department of General surgery, The First Hospital of Xi' an Jiaotong University, Xi' an 710061, Shaanxi Province, China
Correspondence to: Dr. Ai-Jun Zhu, Department of General surgery, The First Hospital of Xi' an Jiaotong University, No.1 Jiankang Lu, Xi' an 710061, Shaanxi Province, China. zhaj_1023@163.com
Telephone: +86-29-5323527
Received: 2003-03-20 **Accepted:** 2003-04-11

Abstract

AIM: To investigate the relationship between severe acute pancreatitis (SAP) and organ failure.

METHODS: Clinical data of 74 cases of SAP from Jan. 1993 to Dec. 2002 were retrospectively reviewed, and the relationship between organ failure and age, gender, etiology, extent of necrosis, infection of necrosis and mortality was analyzed.

RESULTS: A total of 47 patients (63.5 %) showed organ failure, 20 patients (27.0 %) multiple organ failure, whereas 27 patients (36.5 %) with dysfunction of a single organ system. Pulmonary failure was the most common organ dysfunction (23.0 %) among single organ failures. There were no significant differences in age, gender and gallstone pancreatitis among patients with or without organ failure ($P>0.05$). The incidence of organ failure in infected necrosis was not higher compared with sterile necrosis, and patients with increased amount of necrosis did not have an increased prevalence of organ failure ($P>0.05$). Patients with organ failure had a higher mortality rate compared with those without organ failure ($P<0.05$). The death of SAP was associated with multiple organ failure ($P<0.005$), pulmonary failure ($P<0.005$), cardiovascular dysfunction ($P<0.05$) and gastrointestinal dysfunction ($P<0.05$).

CONCLUSION: Organ failure is common in patients with SAP, and patients with multiple organ failure and pulmonary failure have a higher mortality rate. Prevention and active treatment of organ failure can improve the outcome of patients with SAP.

Zhu AJ, Shi JS, Sun XJ. Organ failure associated with severe acute pancreatitis. *World J Gastroenterol* 2003; 9(11): 2570-2573
http://www.wjgnet.com/1007-9327/9/2570.asp

INTRODUCTION

Severe acute pancreatitis (SAP), as a common acute abdomen, is characterized by complicated causes, lots of morbidities, difficulties in the treatment, and high mortality[1-8]. The natural course of SAP progresses in two phases. The first 14 days are characterized by systemic inflammatory response syndrome resulted from the release of inflammatory mediators. In patients with SAP, organ failure is common and often occurs in the absence of infection. The second phase, beginning approximately 2 weeks after the onset of the disease, is dominated by sepsis-related complications resulted from infection of pancreatic necrosis. This is associated with multiple systemic complications, such as pulmonary, renal, and cardiovascular failure[9-18]. Despite considerable improvements in understanding of the pathophysiologic mechanisms and management of these patients, mortality of SAP remains between 15-50 %[19-22]. Organ failure is a severe complication of SAP and death occurs usually only in patients with SAP and is commonly associated with failure of at least one organ system[23-25]. From Jan. 1993 to Dec. 2002, a total of 74 patients with a diagnosis of SAP were admitted to Department of Hepatobiliary Surgery, the First Hospital of Xi' an Jiaotong University, 12 patients died in hospital. The aim of this study was to analyze the relationship between extent of necrosis, pancreatic infection, hospital death due to organ failure.

MATERIALS AND METHODS

Patients

From Jan. 1993 to Dec. 2002, a total of 74 patients with a diagnosis of SAP were admitted to Department of Hepatobiliary Surgery, the First Hospital of Xi' an Jiaotong University. Pancreatic necrosis was defined by findings on CT scan or in operation. There were 40 men and 34 women with a ratio of 1.18:1, the average age of the patients was 49.3 years (range 14-94). The presence of infected necrosis was determined by bacterial culture of CT or ultrasonography-guided percutaneous aspiration and pancreatic tissues debrided at surgery. Organ failure was defined according to the Criteria of Clinical Diagnosis and Classification System for Acute Pancreatitis (the second project, 1996, Pancreatic Surgery Association of CMA)[26]. Causes of SAP were identified as gallstone and non-gallstone. Initial management of these patients included bowel rest, gastric secretions, intravenous fluid resuscitation, suppression of pancreatic external secretion, and use of prophylactic antibiotics. The indication for surgical treatment was difined in the following instances, such as infection of necrosis, pancreatic abscesses, cholangitis, obstructive jaundice and pseudocyst formation for a long time.

Methods

The patients were divided into two groups according to patients with or without organ failure within 2 weeks after admission. The differences of age, gender, gallstone pancreatitis, APACHE II scores, and mortality were analyzed. According to the results of CT scan and findings in operation, the extent of pancreatic necrosis was estimated to be (1) <33 %, (2) 33-50 %, (3) >50 %. The relationship of organ failure to the extent of pancreatic necrosis and infection of necrosis was analyzed. Finally, the relationship between multiple organ failure and specific single organ failure with infected necrosis and mortality was evaluated.

Statistics

Continuous data were evaluated by *t* test, and categorized data were analyzed by Chi-square test. Significance was defined by $P<0.05$.

RESULTS

There were no significant differences in age, sex, gallstone

pancreatitis. Mortality and APACHE II scores were significantly higher in patients with organ failure than in those without organ failure (P<0.05 and P<0.001, respectively) (Table 1).

Table 1 Characteristics of 74 patients with or without organ failure

	Organ failure (n=47)	No organ failure (n=27)	Sig.
Age (Y)	48±15	49±15	NS
Gender (M/F)	26/21	14/13	NS
Etiology			
Gallstones	21	11	NS
Non-gallstones	26	16	
APACHE II scores	29±7	23±3	<0.001
Mortality (%)	12/47(25.5)	0	<0.05

Among the 74 patients, 20 patients (27.0 %) showed multiple organ failure (maximum 5 organ systems) and 9 of them died, 27 patients showed single organ failure. In patients suffering from single organ failure, 17 patients (23.0 %) had pulmonary failure and 3 patients (17.6 %) died, 7 patients showed hepatic failure and 3 patients showed gastrointestinal failure, but none of these patients died. No patient in this group was accompanied by cardiovascular failure, renal failure, or neurologic failure (Table 2).

Table 2 Number of patients with organ failure in 74 patients

Organ failure	Morbidity(%)	Mortality(%)
Multiple organ failure	20(27.0 %)	9(45 %)
Specific single organ failure		
Pulmonary failure	17(23.0 %)	3(17.6 %)
Renal failure	0	0
Cardiovascular failure	0	0
Hepatic failure	7(9.4 %)	0
Neurologic failure	0	0
Gastrointestinal failure	3(4.1 %)	0

As for the frequency of different specific single organ failure, pulmonary failure occurred in 45.9 % (34/74), renal failure in 16.2 % (12/74), cardiovascular failure in 17.6 % (13/74), hepatic failure in 18.9 % (14/74), neurologic failure in 5.4 % (4/74) and gastrointestinal failure in 10.8 % (8/74) (Table 3).

Table 3 Frequency of organ failure in 74 patients

Organ failure	No. organ failure	Frequency (%)
Multiple organ failure	20	27.0
Pulmonary failure	34	45.9
Renal failure	12	16.2
Cardiovascular failure	13	17.6
Hepatic failure	14	18.9
Neurologic failure	4	5.4
Gastrointestinal failure	8	10.8

No relationship was found between organ failure to the extent of necrosis and infected necrosis (Tables 4, 5). No difference was found between patients with infected necrosis and those with sterile necrosis in the development of multiple organ failure and specific organ failure (Table 6). Nevertheless patients died in hospital had a significantly higher incidence rate of multiple organ failure, pulmonary failure, cardiovascular failure and gastrointestinal failure compared with survivors (Table 7).

Table 4 Relationship between infected versus sterile necrosis and organ failure in 74 patients

	Organ failure (%)	No. organ failure (%)
Sterile necrosis	31(66.0)	16(34.0)
Infected necrosis	16(59.3)	11(40.7)

Note: χ^2=0.3320, P>0.05.

Table 5 Relationship between amount of necrosis and organ failure in 74 patients

Amount of necrosis (%)	Organ failure (n=47)	No. organ failure (n=27)
<33 %	21(55.3 %)	17(44.7 %)
33-50 %	11(64.7 %)	6(35.3 %)
>50 %	15(78.9 %)	4(21.1 %)

Note: χ^2=3.0784, P>0.05.

Table 6 Relationship between infected versus sterile necrosis and single organ failure in 74 patients

Organ failure (%)	Sterile necrosis (n=47)	Infected necrosis (n=27)	χ^2	Sig.
Multiple organ failure	13(27.7 %)	7(25.9 %)	0.0261	NS
Pulmonary failure	24(51.1 %)	10(37.0 %)	1.3585	NS
Renal failure	6(12.8 %)	6(22.2 %)	1.1287	NS
Cardiovascular failure	10(21.3 %)	3(11.1 %)	1.2237	NS
Hepatic failure	7(14.9 %)	7(25.9 %)	1.3607	NS
Neurologic failure	4(8.5 %)	0		NS[a]
Gastrointestinal failure	4(8.5 %)	4(14.8 %)	0.7068	NS

a: Fisher's exact probabilities test.

Table 7 Relationship between hospital death and organ failure in 74 patients

Organ failure	Survivor (n=62)	Nonsurvivor (n=12)	χ^2	P value
Multiple organ failure	11(17.7 %)	9(75 %)	16.7130	<0.005
Pulmonary failure	22(35.5 %)	12(100 %)	16.8501	<0.005
Renal failure	8(12.9 %)	4(33.3 %)	1.7680	NS
Cardiovascular failure	8(12.9 %)	5(41.7 %)	3.9295	<0.05
Hepatic failure	11(17.7 %)	3(25 %)	0.0342	NS
Neurologic failure	0	4(33.3 %)		NS[a]
Gastrointestinal failure	4(6.5 %)	4(33.3 %)	5.0050	<0.05

a: Fisher's exact probabilities test.

DISCUSSION

Most of SAP mortality is associated with organ failure. In the early courses, organ failure is resulted from inflammatory mediator released by systemic inflammatory response syndrome even if in the absence of infection. In the septic phase, organ failure occurs because of sepsis, so organ failure is common in SAP. Previous study showed that in SAP, organ failure occurred in 72-90.3 %, single organ failure in 24.7-37 %, multiple organ failure in 35-65.6 %. Among the single organ failures, pulmonary failure was the most commonly organ failure (39.1-63 %), followed by cardiovascular failure (23-37.7 %), hepatic failure (20.7 %), renal failure (8.5-13 %)[27,28]. The present data showed that organ failure occurred in 63.5 % (47/74), multiple organ failure in 27.0 % (20/74), single organ failure in 36.5 % (27/74) (Table 2). No relationship existed between organ failure and age, sex, gallstone pancreatitis,

but the severity (APACHE II scores) and mortality were significantly higher in patients with organ failure than in those without organ failure (Table 1). Pulmonary failure was the most common single organ failure (23.0 %, 17/74) in SAP. The mortality rate in patients with single pulmonary failure was 17.6 % (3/17), followed by hepatic and gastrointestinal failure. No patient in this group was accompanied by single renal failure, or cardiovascular organ failure, or encephalic failure (Table 2). Among all the organ failures, pulmonary failure was the most frequent organ failure (45.9 %), the second was multiple organ failure (Table 3).

Conflicting results about the relation between extent of necrosis, infected necrosis and organ failure have been reported[28-31]. The present study demonstrated that although the incidence of organ failure in sterile necrosis was slightly higher than that in infected necrosis (66.0 % *vs* 59.3 %), there was no difference in the prevalence of organ failure in sterile necrosis compared with infected necrosis (Table 4). The incidence of organ failure increased with increased extent of necrosis, but patients with increased amounts of necrosis did not have increased prevalence of organ failure (Table 5).

As to the relation between specific single organ failure and sterile and infected necrosis, previous study showed that the incidence of pulmonary failure was increased in infected necrosis compared with sterile necrosis, and there was no difference in the prevalence of renal failure, cardiovascular failure in infected necrosis compared with sterile necrosis[31]. Our study showed that there was no difference in the prevalence of specific single organ failure in infected necrosis compared with sterile necrosis (Table 6).

The mortality rate was 30 % in patients with multiple organ failure, and was 8 % in those with single organ failure[31]. Our data showed the mortality rate was 45 % (9/20) in patients with multiple organ failure, and was 11 % (3/27) in those with single organ failure (Table 2). Halonen *et al*[32] compared multiple organ dysfunction (MOD) score, sequential organ failure assessment (SOFA) score, and logistic organ dysfunction (LOD) score in predicting hospital mortality rates of 178 SAP patients. The results demonstrated that three different multiple organ dysfunction scores showed good accuracy and were comparable with APACHE II in predicting hospital mortality. In multiple logistic regression analysis, only hepatic, renal, and cardiovascular failures were independent risk factors for hospital mortality. Our study revealed that non survivors had a significantly higher morbidity of multiple organ failure, pulmonary failure, cardiovascular failure and gastrointestinal failure compared with survivors, there was no difference in the morbidity of renal failure, hepatic failure and neurologic failure in nonsurvivors and survivors (Table 7). The results demonstrated that the hospital mortality of SAP was associated with multiple organ failure, pulmonary failure, cardiovascular failure and gastrointestinal failure. Therefore, prophylactic and active treatment of these organ failures are very important in the treatment of SAP. Recently, hemoconcentration (hematocrit $\geqslant$44 % and/or failure of admission hematocrit to decrease at approximately 24 hours)[33,34], plasma concentrations of sTNF-Rs[35], activated polymorphonuclear leucocytes-elastase (PMN-E) and IL-6[36] have been reported as early markers for organ failure and necrotic pancreatitis. Patients coincident with this standard should be treated with strong fluid resuscitation and closely monitored in intensive care units, and new approaches have to be found to counteract these severe complications.

REFERENCES

1 **Wu XN**. Management of severe acute pancreatitis. *World J Gastroenterol* 1998; **4:** 90-91

2 **Qin RY,** Zou SQ, Wu ZD, Qiu FZ. Experimental research on production and uptake sites of TNFα in rats with acute hemorrhagic necrotic pancreatitis. *World J Gastroenterol* 1998; **4:** 144-146

3 **Zhao LG,** Wu XX, Han EK, Chen YL, Chen C, Xu DQ. Protective effect of YHI and HHI-I against experimental acute pancreatitis in rabbits. *World J Gastroenterol* 1998; **4:** 256-259

4 **Robert JH,** Frossard JL, Mermillod B, Soravia C, Mensi N, Roth M, Rohner A, Hadengue A, Morel P. Early prediction of acute pancreatitis: prospective study comparing computed tomography scans, Ranson, Glascow, Acute Physiology and Chronic Health Evaluation II scores, and various serum markers. *World J Surg* 2002; **26:** 612-619

5 **Wu XN.** Treatment revisited and factors affecting prognosis of severe acute pancreatitis. *World J Gastroenterol* 2000; **6:** 633-635

6 **Chen DL,** Wang WZ, Wang JY. Epidermal growth factor prevents gut atrophy and maintains intestinal integrity in rats with acute pancreatitis. *World J Gastroenterol* 2000; **6:** 762-765

7 **Mao EQ,** Tang YQ, Zhang SD. Effects of time interval for hemofiltration on the prognosis of severe acute pancreatitis. *World J Gastroenterol* 2003; **9:** 373-376

8 **Zhou ZG,** Chen YD, Sun W, Chen Z. Pancreatic microcirculatory impairment in experimental acute pancreatitis in rats. *World J Gastroenterol* 2002; **8:** 933-936

9 **Norman J.** The role of cytokines in the pathogenesis of acute pancreatitis. *Am J Surg* 1998; **175:** 76-83

10 **Yi Y,** Gao NR, Li ZL. Protective effects of ulinostatin on acute lung injury induced by acute necrotizing pancreatitis in rats. *Shijie Huaren Xiaohua Zazhi* 2002; **10**: 558-561

11 **Knoefel WT,** Kollias N, Warshaw AL, Waldner H, Nishioka NS, Rattner DW. Pancreatic microcirculatory changes in experimental pancreatitis of graded severity in the rat. *Surgery* 1994; **116:** 904-913

12 **He L,** Chen SF, Cao XH, Zhang LD, Pan LL, Zhou Z. Changes of serum level of IL-15, IL-18 and sTNF-1R in patients with acute pancreatitis. *Shijie Huaren Xiaohua Zazhi* 2003; **11:** 57-60

13 **Schmid SW,** Uhl W, Friess H, Malfertheiner P, Buchler MW. The role of infection in acute pancreatitis. *Gut* 1999; **45:** 311-316

14 **Berger HG,** Rau B, Mayer J, Pralle U. Natural course of acute pancreatitis. *World J Surg* 1997; **21:** 130-135

15 **Wu XZ.** Therapy of acute severe pancreatitis awaits further improvement. *World J Gastroenterol* 1998; **4:** 285-286

16 **Wu XN.** Current concept of pathogenesis of severe acute pancreatitis. *World J Gastroenterol* 2000; **6:** 32-36

17 **Slavin J,** Ghaneh P, Sutton R, Hartley M, Rowlands P, Garvey C, Hughes M, Neoptolemos J. Management of necrotizing pancreatitis. *World J Gastroenterol* 2001; **7:** 476-481

18 **Isenmann R,** Rau B, Berger HG. Early severe acute pancreatitis: characteristics of a new subgroup. *Pancreas* 2001; **22:** 274-278

19 **Abu-Zidan FM,** Bonham MJ, Windsor JA. Severity of acute pancreatitis:a multivariate analysis of oxidative stress markers and modified Glasgow criteria. *Br J Surg* 2000; **87:** 1019–1023

20 **Luo Y,** Yuan CX, Peng YL, Wei PL, Zhang ZD, Jiang JM, Dai L, Hu YK. Can ultrasound predict the severity of acute pancreatitis early by observing acute fluid collection? *World J Gastroenterol* 2001; **7:** 293-295

21 **Pezzilli R,** Mancini F. Assessment of severity of acute pancreatitis: a comparison between old and most recent modalities used to evaluate this perennial problem. *World J Gastroenterol* 1999; **5:** 283-285

22 **Shi X,** Gao NR, Guo QM, Yang YJ, Huo MD, Hu HL, Friess H. Relationship between overexpression of NK-1R, NK-2R and intestinal mucosal damage in acute necrotizing pancreatitis. *World J Gastroenterol* 2003; **9:** 160-164

23 **Baron TH,** Morgan DE. Acute necrotizing pancreatitis. *N Engl J Med* 1999; **340:** 1412-1417

24 **Yuan YZ,** Gong ZH, Lou KX, Tu SP, Zhai ZK, Xu JY. Involvement of apoptosis of alveolar epithelial cells in acute pancreatitis-associated lung injury. *World J Gastroenterol* 2000; **6:** 920-924

25 **Blum T,** Maisonneuve P, Lowenfels AB, Lankisch PG. Fatal outcome in acute pancreatitis: its occurrence and early prediction. *Pancreatology* 2001; **1:** 237-241

26 **Pancreatic Surgery Association of CMA.** The Criteria of Clinical Diagnosis and Classification System for Acute Pancreatitis (the second project, 1996,). *Zhonghua Waike Zazhi* 1997;

35: 773-775

27 **Buchler MW,** Gloor B, Muller CA, Friess H, Seiler CA, Uhl W. Acute necrotizing pancreatitis: Treatment strategy according to the status of infection. *Ann Surg* 2000; **232:** 619-626

28 **Gotzinger P,** Sautner T, Kriwanek S, Beckerhinn P, Barlan M, Armbruster C, Wamser P, Fugger R. Surgical treatment for severe acute pancreatitis: extent and surgical control of necrosis determine outcome. *World J Surg* 2002; **26:** 474-478

29 **Lankisch PG,** Pflichthofer D, Lehnick D. No strict correlation between necrosis and organ failure in acute pancreatitis. *Pancreas* 2000; **20:** 319-322

30 **Tenner S,** Sica G, Hughes M, Noordhoek E, Feng S, Zinner M, Banks PA. Relationship of necrosis to organ failure in severe acute pancreatitis. *Gastroenterology* 1997; **133:** 899-903

31 **Isenmann R,** Rau B, Beger HG. Bacterial infection and extent of necrosis are determinants of organ failure in patients with acute necrotizing pancreatitis. *Br J Surg* 1999; **86:** 1020-1024

32 **Halonen KI,** Pettila V, Leppaniemi AK, Kemppainen EA, Puolakkainen PA, Haapiainen RK. Multiple organ dysfunction associated with severe acute pancreatitis. *Crit Care Med* 2002; **30:** 1274-1279

33 **Brown A,** Orav J, Banks PA. Hemoconcentration is an early marker for organ failure and necrotizing pancreatitis. *Pancreas* 2000; **20:** 367-372

34 **Jiang CQ**, Ai ZL, Liu ZS, He YM, Sun Q, Xu R, Fan LF. Hemoconcentration as an early risk factor for severe acute pancreatitis. *Zhongguo Shiyong Waike Zazhi* 2001; **21:** 666-667

35 **Hirota M,** Nozawa F, Okabe A, Shibata M, Beppu T, Shimada S, Egami H, Yamaguchi Y, Ikei S, Okajima T, Okamoto K, Ogawa M. Relationship between plasma cytokine concentration and multiple organ failure in patients with acute pancreatitis. *Pancreas* 2000; **21**: 141-146

36 **Ikei S,** Ogawa M, Yamaguchi Y. Blood concentrations of polymorphonuclear leucocyte elastase and interleukin-6 are indicators for the occurrence of multiple organ failures at the early stage of acute pancreatitis. *J Gastroenterol Hepatol* 1998; **13:** 1274-1283

Edited by Zhao M and Wang XL

P.O.Box 2345, Beijing 100023,China
Fax: +86-10-85381893
E-mail: wjg@wjgnet.com www.wjgnet.com

World J Gastroenterol 2003;9(11):2574-2578
World Journal of Gastroenterology
 ISSN 1007-9327

• CLINICAL RESEARCH •

Grading and staging of hepatic fibrosis, and its relationship with noninvasive diagnostic parameters

Lun-Gen Lu, Min-De Zeng, Mo-Bin Wan, Cheng-Zhong Li, Yi-Min Mao, Ji-Qiang Li, De-Kai Qiu, Ai-Ping Cao, Jun Ye, Xiong Cai, Cheng-Wei Chen, Ji-Yao Wang, Shan-Ming Wu, Jin-Shui Zhu, Xia-Qiu Zhou

Lun-Gen Lu, Min-De Zeng, Yi-Min Mao, Ji-Qiang Li, De-Kai Qiu, Ai-Ping Cao, Shanghai Institute of Digestive Disease, Renji Hospital, Shanghai Second Medical University, Shanghai 200001, China
Mo-Bin Wan, Cheng-Zhong Li, Department of Infectious Diseases, Changhai Hospital, Shanghai 200433, China
Jun Ye, Department of Infectious Diseases, Putou District Central Hospital, Shanghai 200062, China
Xiong Cai, Department of Infectious Diseases, Changzheng Hospital, Shanghai 200003, China
Cheng-Wei Chen, Shanghai Liver Diseases Research Center, Nanjing Military Command, Shanghai 200233, China
Ji-Yao Wang, Department of Gastroenterology, Zhongshan Hospital, Shanghai 200032, China
Shan-Ming Wu, Shanghai Infectious Hospital, Shanghai 200085, China
Jin-Shui Zhu, Department of Gastroenterology, Shanghai NO.6 Hospital, Shanghai 200233, China
Xia-Qiu Zhou, Department of Infectious Diseases, Ruijin Hospital, Shanghai 200025, China
Supported by the Key Project of Shanghai Medical Development Foundation, No.99ZDI001
Correspondence to: Lun-Gen Lu, MD, Shanghai Institute of Digestive Disease, Renji Hospital, Shanghai Second Medical University, Shanghai 200001, China. lulungen@online.sh.cn
Telephone: +86-21-33070834 **Fax:**+86-21-63364118
Received: 2003-04-02 **Accepted:** 2003-06-19

Abstract

AIM: To explore the grade and stage of pathology and the relationship between grading and staging of hepatic fibrosis and noninvasive diagnostic parameters.

METHODS: Inflammatory activity and fibrosis of consecutive liver biopsies from 200 patients with chronic liver disease were determined according to the Diagnostic Criteria of Chronic Hepatitis in China, 1995. A comparative analysis was made in these patients comparing serum markers, Doppler ultrasonography, CT and/or MR imaging with the findings of liver biopsy.

RESULTS: With increase of inflammatory activity, the degree of fibrosis also rose. There was a close correlation between liver fibrosis and inflammatory activity. AST, GGT, albumin, albumin/globulin, ALP, AFP, hyaluronic acid, N-terminal procollagen III(P III NP), collagen type IV(Col IV), tissue inhibitors of metalloproteinases-1(TIMP-1), alpha-2-macroglobulin, natural killer cells(NK), some parameters of Doppler ultrasonography, CT and/or MR imaging were all related to the degree of inflammatory activity. GGT, albumin, albumin/globulin, ALP, AFP, hyaluronic acid, Col IV, TIMP-1, alpha-2- macroglobulin, transforming growth factor-beta 1(TGFβ1), NK, some parameters of Doppler ultrasonography, CT and/or MR imaging were all related to the staging of fibrosis. By regression analysis, the parameters used in combination to differentiate the presence or absence of fibrosis were age, GGT, the parameter of blood flow of portal vein per minute, the maximum oblique diameter of right liver by B ultrasound, the wavy hepatic surface contour by CT and/or MR. The sensitivity, specificity and accuracy of the above parameters were 80.36 %, 86.67 %, and 81.10 %, respectively.

CONCLUSION: There is close correlation between liver fibrosis and inflammatory activity. The grading and staging of liver fibrosis are related to serum markers, Doppler ultrasonography, CT and/or MR imaging. The combination of the above mentioned noninvasive parameters are quite sensitive and specific in the diagnosis of hepatic fibrosis.

Lu LG, Zeng MD, Wan MB, Li CZ, Mao YM, Li JQ, Qiu DK, Cao AP, Ye J, Cai X, Chen CW, Wang JY, Wu SM, Zhu JS, Zhou XQ. Grading and staging of hepatic fibrosis, and its relationship with noninvasive diagnostic parameters. *World J Gastroenterol* 2003; 9(11): 2574-2578

http://www.wjgnet.com/1007-9327/9/2574.asp

INTRODUCTION

Hepatic fibrosis has been a common response to chronic liver injury and might result in potentially lethal sequelae[1-3]. In chronic liver diseases, determination of stage and activity of the fibrotic process and evaluation of anti-fibrotic treatment required accurate variables, the commonly so-called ' fibrotic markers' [4-11]. Since the value of laboratory test to diagnose liver fibrosis was limited, biopsy has been still the golden criterion of the diagnosis of liver fibrosis and cirrhosis at present[12,13]. But it is an invasive diagnostic method, so its application and further propagation are somewhat limited. Searching for a noninvasive diagnostic approach is an interesting subject both at home and abroad. Although some parameters have been found to have important values in iconography and laboratory tests, they are still far from satisfactory. So it is of great realistic value to explore a credible, specific, and noninvasive diagnostic parameter of liver fibrosis for the prevention and treatment of chronic liver disease[14-28]. Therefore, on the basis of histology of chronic liver diseases, this study was designed to explore the relationship between the grade and stage of pathology, and noninvasive diagnostic parameters. We hoped that we could provide the basis for the noninvasive diagnosis of liver fibrosis, so as to improve the prevention and treatment of liver fibrosis.

MATERIALS AND METHODS

Selection of patients

The study was organized and carried out by Shanghai Cooperative Group of Hepatic Fibrosis Project. The Cooperaitive Group was led by Renji Hospital and Changhai Hospital in Shanghai. Cases collected by the Cooperative Group were 37 from Changhai Hospital, 36 from Renji Hospital, 30 from Putuo District Central Hospital, 22 from Shanghai Liver Disease Center of Nanjing Military Command, 20 from Changzheng Hospital, 14 from Zhongshan Hospital,

11 from Huashan Hospital, 9 from Shibei Hospital, 8 from Shanghai No.6 Hospital, 6 from Shanghai Infectious Disease Hospital, 3 from Ruijin Hospital, 3 from Shanghai No.9 hospital, and 1 from Shanghai No.1 hospital. A total of 200 patients were collected between July and October in 1999 according to both clinical and pathological criteria. There were 156 males and 44 females with an average age of 34 years (range 15-60).

Histological examination

One week after admission, all patients underwent liver puncture biopsy under the guide of B type ultrasound with the 14G Quick-cut needle (8-Light Company, Japan) or Menghini needle. The length of liver specimen was more than 1 cm. The samples were fixed with 10 % formaldehyde, paraffin slides were made and stained with hematoxylin-eosin, reticular fiber and collagen fiber according to the grading and staging of Diagnostic Criteria of Chronic Hepatitis in China in 1995[29]. Eleven patients were graded and staged for inflammatory activity and liver fibrosis. Three pathologists read the slide independently. The results were checked with Kappa test by statistical experts. It was shown that the coherence of grading and staging of hepatitis fibrosis was excellent. The pathological diagnosis of liver biopsy was finally made by the Department of Pathology , Medical Collage of Fudan University.

Laboratory tests

Blood and urine routine tests: α-fetoprotein(AFP) and prothrombin time were examined by the Cooperative Units.

Serum biochemical tests: Total bilirubin, indirect bilirubin, alanine aminotransferase (ALT), aspartate aminotransferase (AST), AST/ALT, γ-glutamyl transpeptidase(GGT), alkaline phosphatase(ALP), albumin, albumin/globulin, blood urea nitrogen(BUN), creatinine(Cr), triglyceride, cholersterol, high density lipoprotein and low density lipoprotein were all measured by Shanghai Institute of Digestive Disease.

Markers of hepatitis virus and immunological parameter: HBsAg, Anti-HBs, HBeAg, Anti-HBe, Anti-HBc, HBV- DNA, Anti-HCV, HCV- RNA, $CD3^+$, $CD4^+$, $CD8^+$, natural killer cell (NKC), interleukin-2 (IL-2), and interferon-γ (IFN-γ) were detected by Shanghai Institute of Digestive Disease.

Related liver fibrosis markers: α-2-macroglobulin(α-MA), transferrin, apolipoproteinA1, hyaluronic acid (HA), laminin, N-terminal procollagen III(PIIINP), 7S collagen IV (7S-IV), and transforming growth factor-β1(TGF-β1) were detected by the Clinical Immunology Center of Changzheng Hospital in Shanghai.

Tissue inhibitor of metalloproteinase-1(TIMP-1) were assayed by Shanghai Hongqiao Medical Reagent Institute.

B ultrasound examination

All B ultrasound examinations of the patients were carried out in Shanghai Institute of Digestive Disease. The patients had empty stomach for 14 hours before examination. Two skillful doctors performed the examination with color Doppler ultrasonic instrument(HDI 5000). The results were saved in compact disk, three experts judged the examination results and made the final reports.

CT and/or MR imaging

All CT and/or MR examinations were performed by Ruijin Hospital, Changzheng Hospital, Changhai Hospital, Zhongshan Hospital, and Shanghai No.6 Hospital in the Cooperative Group. CT scanners with PQ-2000 and/or PQ-5000 (Picker Company), Plus-s (Siemens Company), Hispeed Adv (GE Company), and MR scanners with Cyroscan T10-NT (Philips Company),Vision Plus and Magnetron Impact (Siemens Company) were used.

Statistical analysis

All the data were analyzed with SAS software by Statistical Department in Shanghai Second Medical University.

RESULTS

Histological examinations

It was revealed that there was a significantly positive correlation between the inflammatory activity and the staging of liver fibrosis. With increase of inflammatory activity, liver fibrosis became more serious (Table 1).

Table 1 Pathological diagnostic results of 200 liver biopsy samples

Staging of fibrosis	Grading of inflammation					value	
	1	2	3	4	Total	χ^2-value	*P*-value
0	18	2	0	0	20	278.3	1E-04
1	42	22	0	0	64		
2	6	33	26	0	64		
3	9	2	19	4	25		
4	0	0	3	23	26		
Total	66	59	48	27	200		

Laboratory examinations

Relationship between serum biochemical parameters and the grading of inflammation: Only serum biochemical parameters related to liver inflammation are listed in Table 2.

Table 2 Relationship between serum biochemical parameters and grading of inflammation

Parameter	Comparision among groups of inflammation grading					
	1-2	1-3	1-4	2-3	2-4	3-4
RBC			b		b	b
PLT			b		b	b
AST		b	b	a	b	
GGT	a	b	b	b	b	
Albumin			b		b	b
Albumin / globulin			b		b	b
ALP			b		b	
AFP	b	b	b	b	b	b
HA	b	b	b	b	b	b
PIIINP			b		b	
7S-IV		a	b	a	b	
TIMP-1		a	a			
α-MA			b		a	
NK			b		a	a
IgG			b		b	b
IgG+IgA+IgM			b		b	b

$^aP<0.05$, $^bP<0.01$.

Relationship between serum biochemical parameters and staging of liver fibrosis: Only the serum biochemical parameters related to liver fibrosis are listed in Table 3.

B ultrasound examinations

Comparison between parameters of ultrasonic 2-D and color Doppler flow image and the groups of inflammation grading: Only the parameters of ultrasonic 2-D and color Doppler flow image related with the groups of inflammation grading are listed in Table 4.

Comparison between parameters of ultrasonic 2-D and color Doppler flow image and groups of liver fibrosis staging: Only the parameters of ultrasonic 2-D and color Doppler flow image related with the groups of liver fibrosis staging are listed in Table 5.

CT and/or MR imaging examination

Among the 200 patients who received liver biopsy, 192 patients had CT and/or MR imaging examintion. Twenty cases (10.4 %) received both CT and MR imaging examination, 92cases (47.9 %) received only CT examination, 80 cases (41.7 %)

Table 3 Relationship between serum biochemical parameters and staging of liver fibrosis

Parameter	Comparision among groups of liver fibrosis staging									
	0-1	0-2	0-3	0-4	1-2	1-3	1-4	2-3	2-4	3-4
RBC				a			a		a	a
GGT		b	b	b	b	b	b			
Albumin				b			b		b	b
Albumin / globulin				b			b		b	b
ALP				b			a			
AFP			b	b		b	b		b	
HA		b	b	b	b	b	b		b	b
7S-IV				a			a		a	
TIMP-1			a	b		a	a			
α-MA				a			b		a	
TGFβ-1	a	a	a	a						
IgG				b			b		b	b
IgG+IgA+IgM				b			b		b	b

[a]$P<0.05$, [b]$P<0.01$.

Table 4 Comparison between parameters of ultrasonic 2-D and color Doppler flow image and groups of inflammation grading

Parameter	Comparision among groups of inflammation grading					
	1-2	1-3	1-4	2-3	2-4	3-4
Inner diameter of left portal vein		a				
Inner diameter of middle liver vein			a		a	
Inner diameter of right liver vein			b		a	
Thickness of gallbladder wall		a	b	a	b	
Shape of gallbladder			b		b	
Vertical diameter of spleen		a	b	a	b	a
Thickness of spleen		a	b	a	b	
Diameter of spleen vein			b		a	
Thickening of the light dots in liver substance			b		b	
Movement degree along with breath			b		a	
Movement degree along with heart beat			b		a	
Blood stream velocity in constriction phase of liver artery		a				
Blood stream velocity in dilation phase of liver artery			a			

[a]$P<0.05$, [b]$P<0.01$.

Table 5 Comparison between parameters of ultrasonic 2-D and color Doppler flow image and groups of liver fibrosis staging

Parameter	Comparision among groups of liver fibrosis staging									
	0-1	0-2	0-3	0-4	1-2	1-3	1-4	2-3	2-4	3-4
Thickness of liver capsule				a						
Maximum oblique diameter of right liver	a	b	b	b						
Tube diameter of portal vein trunk		a		a						
Inner diameter of left portal vein	a	b	b	a						
Inner diameter of right portal vein	a	a	a	a						
Thickness of gallbladder wall				b			b		a	a
Shape of gallblader				b			a		a	a
Diameter of splenic vein				b			a			a
Vertical diameter of spleen			a	b			b		a	
Thickness of spleen				a						
Thickening of the light dots in liver substance		a		b			a			
Movement degree along with breath				b			a			
Movement degree along with heart beat									b	a
Parameter of blood flow of portal vein per minute	a	a	a	a						

[a]$P<0.05$, [b]$P<0.01$.

received only MR examination.

The results demonstrated that the longitudinal diameter of the left lobe, volume index, the wavy hepatic surface contour, liver crack widening, size of the gallbladder, thickening of the gallbladder wall, changes like little bursa of peri-gallbladder tube, to and fro diameter of the spleen, and thickness of the spleen were all correlated with the grading of inflammation. The wavy hepatic surface contour, changes like little bursa of peri-gallbladder tube, and the to and fro diameter of the spleen were correlated with the staging of liver fibrosis.

DISCUSSION

At present, the diagnosis of liver fibrosis still depends on pathological examination of liver puncture tissue. Since the procedure is invasive, its application and extensive use in clinical practice are still limited. So great attention has been paid to search for and clinical study of a non-invasive diagnostic parameter for liver fibrosis[15,27,28]. It would not only speed up the study of basic medical theory about liver disease, but also be of value[1,3].

In 1995, a new pathological classification method was carried out in our country[29]. The criteria were established respective to distinguish inflammation from liver fibrosis by grading and staging. Both of them have quantified parameters, which are convenient for statistical analysis. Following these criteria, we compared pathological classification with some non-invasive parameters (serologic and imaging parameters), so as to evaluate the value and significance of different parameters in reflecting pathological changes. In the liver puncture tissue of 200 patients with chronic hepatitis, there was a significant positive correlation between inflammatory activity and staging of liver fibrosis. With the increase of inflammatory activity, liver fibrosis became more serious.

In serology, RBC, PLT, AST, GGT, albumin, albumin/globulin, ALP, AFP, HA, PIIINP, 7S-IV, TIMP-1, α2-MA, NK, *etc*. had a relationship with inflammatory activity, but GGT, albumin, albumin/globulin, ALP, AFP, HA, 7S-IV, and α2-MA had a relationship with liver fibrosis. So these latter parameters might be used as the parameters of liver fibrosis[5,10,30-34]. With the development of inflammation and fibrosis, the level of HA and 7S-IV rose gradually in different inflammatory grading and liver fibrosis staging. In pathological diagnosis, Stage 1 and Stage 2 indicated mild fibrosis, Stage 3 and Stage 4 indicated severe fibrosis. The accuracy, specificity and sensitivity of HA were 82.9 %, 93 %, and 56 %, respectively. The accuracy, specificity and sensitivity of 7S-IV were 72.4 %, 94.3 %, and 18 %, respectively. To some extent, PIIINP might reflect mild and severe changes of inflammation, but it might not reflect the fibrotic changes. This study revealed that laminin had no diagnostic value either in inflammation or in fibrotic changes. It was found that the level of TGFβ1 and TIMP-1 increased more significantly in inflammation and early stage of fibrosis, indicating that they could reflect the changes of liver inflammation and fibrosis[35-38]. In this study, PIIINP, laminin, transferrin, and apoproteinA1 which were known to have significant diagnostic value, were not confirmed. So, we should do more work to probe into their diagnostic significance. In the following study, we would increase the number of cases to further study the diagnostic value of the related parameters in liver fibrosis and evaluate the efficacy of anti-fibrotic drugs, so as to provide a sound basis for the reasonable combined use of the different parameters, and to improve the specificity, accuracy and sensitivity of noninvasive diagnostic tests for liver fibrosis[3,15,19,28].

With the development of modern medical imaging techniques, ultrasound, CT and MR would be widely used. These methods could significantly improve the diagnosis and differential diagnosis of liver disease[17,18,20-26]. In this study, ultrasound examination indicated that the thickness of liver capsule, maximum oblique diameter of right liver, tube diameter of portal vein trunk, diameter of left portal vein, diameter of right portal vein, thickness of gallbladder wall, thickness of spleen, diameter of splenic vein, parameter of blood stream quantity per minute in portal vein, light dot shape, and shape of gallbladder were correlated with the staging of liver fibrosis. CT and/or MR imaging only revealed that the volume of spleen was correlated with liver fibrosis. The results demonstrated that B ultrasound had more value than CT and/or MR imaging in the diagnosis of liver fibrosis. This of course needs further study. It should be noted that factors such as individual variation, nature of the instrument used, patient' s condition at the time of examination and difference of the performer' s skill might affect the evaluation of the result[21-24]. At the same time, we should carry out quantitative and/or semi-quantitative research on ultrasonic two-dimensional imaging and Doppler blood stream, so as to increase the sensitivity, specificity and accuracy of the diagnostic parameters.

REFERENCES

1 **Botta F**, Giannini E, Romagnoli P, Fasoli A, Malfatti F, Chiarbonello B, Testa E, Risso D, Colla G, Testa R. MELD scoring system is useful for predicting prognosis in patients with liver cirrhosis and is correlated with residual liver function: a European study. *Gut* 2003; **52**: 134-139

2 **Yang C**, Zeisberg M, Mosterman B, Sudhakar A, Yerramalla U, Holthaus K, Xu L, Eng F, Afdhal N, Kalluri R. Liver fibrosis: insights into migration of hepatic stellate cells in response to extracellular matrix and growth factors. *Gastroenterology* 2003; **124**: 147-159

3 **Oberti F**, Valsesia E, Pilette C, Rousselet MC, Bedossa P, Aube C, Gallois Y, Rifflet H, Maiga MY, Penneau-Fontbonne D, Cales P. Noninvasive diagnosis of hepatic fibrosis or cirrhosis. *Gastroenterology* 1997; **113**: 1609-1116

4 **Guechot J**, Serfaty L, Bonnand AM, Chazouilleres O, Poupon RE, Poupon R. Prognostic value of serum hyaluronan in patients with compensated HCV cirrhosis. *J Hepatol* 2000; **32**: 447-452

5 **Hayasaka A**, Saisho H. Serum markers as tools to monitor liver fibrosis. *Digestion* 1998; **59**: 381-384

6 **Ninomiya T**, Yoon S, Hayashi Y, Sugano M, Kumon Y, Seo Y, Shimizu K, Kasuga M. Clinical significance of serum hyaluronic acid as a fibrosis marker in chronic hepatitis C patients treated with interferon-alpha: histological evaluation by a modified histological activity index scoring system. *J Gastroenterol Hepatol* 1998; **13**: 68-74

7 **George DK**, Ramm GA, Walker NI, Powell LW, Crawford DH. Elevated serum type IV collagen: a sensitive indicator of the presence of cirrhosis in haemochromatosis. *J Hepatol* 1999; **31**: 47-52

8 **Murawaki Y**, Koda M, Okamoto K, Mimura K, Kawasaki H. Diagnostic value of serum type IV collagen test in comparison with platelet count for predicting the fibrotic stage in patients with chronic hepatitis C. *J Gastroenterol Hepatol* 2001; **16**: 777-781

9 **Wang T**, Wang B, Liu X. Correlation of serum markers with fibrosis staging in chronic viral hepatitis. *Zhonghua Binglixue Zazhi* 1998; **27**: 185-190

10 **Zheng M**, Cai W, Weng H, Liu R. Determination of serum fibrosis indexes in patients with chronic hepatitis and its significance. *Chin Med J* 2003; **116**: 346-349

11 **McHutchison JG**, Blatt LM, de Medina M, Craig JR, Conrad A, Schiff ER, Tong MJ. Measurement of serum hyaluronic acid in patients with chronic hepatitis C and its relationship to liver histology. Consensus Interferon Study Group. *J Gastroenterol Hepatol* 2000; **15**: 945-951

12 **Gabrielli GB**, Capra F, Casaril M, Squarzoni S, Tognella P, Dagradi R, De Maria E, Colombari R, Corrocher R, De Sandre G. Serum laminin and type III procollagen in chronic hepatitis C. Diagnostic value in the assessment of disease activity and fibrosis. *Clin Chim Acta* 1997; **265**: 21-31

13 **Castera L**, Hartmann DJ, Chapel F, Guettier C, Mall F, Lons T, Richardet JP, Grimbert S, Morassi O, Beaugrand M, Trinchet JC.

Serum laminin and type IV collagen are accurate markers of histologically severe alcoholic hepatitis in patients with cirrhosis. *J Hepatol* 2000; **32**: 412-418

14 **Stickel F**, Urbaschek R, Schuppan D, Poeschl G, Oesterling C, Conradt C, McCuskey RS, Simanowski UA, Seitz HK. Serum collagen type VI and XIV and hyaluronic acid as early indicators for altered connective tissue turnover in alcoholic liver disease. *Dig Dis Sci* 2001; **46**: 2025-2032

15 **Pilette C**, Rousselet MC, Bedossa P, Chappard D, Oberti F, Rifflet H, Maiga MY, Gallois Y, Cales P. Histopathological evaluation of liver fibrosis: quantitative image analysis vs semi-quantitative scores. Comparison with serum markers. *J Hepatol* 1998; **28**: 439-446

16 **Persico M**, Palmentieri B, Vecchione R, Torella R, De SI. Diagnosis of chronic liver disease: reproducibility and validation of liver biopsy. *Am J Gastroenterol* 2002; **97**: 491-492

17 **Wachsberg RH**, Bahramipour P, Sofocleous CT, Barone A. Hepatofugal flow in the portal venous system: pathophysiology, imaging findings, and diagnostic pitfalls. *Radiographics* 2002; **22**: 123-140

18 **Colli A**, Fraquelli M, Andreoletti M, Marino B, Zuccoli E, Conte D. Severe liver fibrosis or cirrhosis: accuracy of US for detection-analysis of 300 cases. *Radiology* 2003; **227**: 89-94

19 **Tran A**, Hastier P, Barjoan EM, Demuth N, Pradier C, Saint-Paul MC, Guzman-Granier E, Chevallier P, Tran C, Longo F, Schneider S, Piche T, Hebuterne X, Benzaken S, Rampal P. Non invasive prediction of severe fibrosis in patients with alcoholic liver disease. *Gastroenterol Clin Biol* 2000; **24**: 626-630

20 **Aube C**, Oberti F, Korali N, Namour MA, Loisel D, Tanguy JY, Valsesia E, Pilette C, Rousselet MC, Bedossa P, Rifflet H, Maiga MY, Penneau-Fontbonne D, Caron C, Cales P. Ultrasonographic diagnosis of hepatic fibrosis or cirrhosis. *J Hepatol* 1999; **30**: 472-478

21 **Murakami T**, Mochizuki K, Nakamura H. Imaging evaluation of the cirrhotic liver. *Semin Liver Dis* 2001; **21**: 213-224

22 **Laghi A**, Iannaccone R, Catalano C, Carbone I, Ferrari R, Mangiapane F, Passariello R. Multiphase multislice spiral CT for liver assessment: optimization in cirrhotic patients. *Radiol Med* 2002; **103**: 188-195

23 **Bernatik T**, Strobel D, Hahn EG, Becker D. Doppler measurements: a surrogate marker of liver fibrosis? *Eur J Gastroenterol Hepatol* 2002; **14**: 383-387

24 **Martinez-Noguera A**, Montserrat E, Torrubia S, Villalba J.Doppler in hepatic cirrhosis and chronic hepatitis. *Semin Ultrasound CT MR* 2002; **23**: 19-36

25 **Kok T**, van der Jagt EJ, Haagsma EB, Bijleveld CM, Jansen PL, Boeve WJ. The value of Doppler ultrasound in cirrhosis and portal hypertension. *Scand J Gastroenterol Suppl* 1999; **230**: 82-88

26 **Lonjedo E**, Ripolles T. Vascular imaging and interventional procedures in hepatic cirrhosis. *Semin Ultrasound CT MR* 2002; **23**: 130-140

27 **Thabut D**, Simon M, Myers RP, Messous D, Thibault V, Imbert-Bismut F, Poynard T. Noninvasive prediction of fibrosis in patients with chronic hepatitis C. *Hepatology* 2003; **37**: 1220-1221

28 **Myers RP**, Ratziu V, Imbert-Bismut F, Charlotte F, Poynard T. Biochemical markers of liver fibrosis: a comparison with historical features in patients with chronic hepatitis C. *Am J Gastroenterol* 2002; **97**: 2419-2425

29 Prevention and treatment projects of virus hepatitis (tryout). *Chin J Intern Med* 1995; **34**: 788-791

30 **Flisiak R**, Maxwell P, Prokopowicz D, Timms PM, Panasiuk A. Plasma tissue inhibitor of metalloproteinases-1 and transforming growth factor beta 1-possible non-invasive biomarkers of hepatic fibrosis in patients with chronic B and C hepatitis. *Hepatogastroenterology* 2002; **49**: 1369-1372

31 **Murawaki Y**, Nishimura Y, Ikuta Y, Idobe Y, Kitamura Y, Kawasaki H. Plasma transforming growth factor-beta 1 concentrations in patients with chronic viral hepatitis. *J Gastroenterol Hepatol* 1998; **13**: 680-684

32 **Walsh KM**, Timms P, Campbell S, MacSween RN, Morris AJ. Plasma levels of matrix metalloproteinase-2 (MMP-2) and tissue inhibitors of metalloproteinases -1 and -2 (TIMP-1 and TIMP-2) as noninvasive markers of liver disease in chronic hepatitis C: comparison using ROC analysis. *Dig Dis Sci* 1999; **44**: 624-630

33 **Kanzler S**, Baumann M, Schirmacher P, Dries V, Bayer E, Gerken G, Dienes HP, Lohse AW. Prediction of progressive liver fibrosis in hepatitis C infection by serum and tissue levels of transforming growth factor-beta. *J Viral Hepat* 2001; **8**: 430-437

34 **Pohl A**, Behling C, Oliver D, Kilani M, Monson P, Hassanein T. Serum aminotransferase levels and platelet counts as predictors of degree of fibrosis in chronic hepatitis C virus infection.*Am J Gastroenterol* 2001; **96**: 3142-3146

35 **Giannini E**, Risso D, Botta F, Chiarbonello B, Fasoli A, Malfatti F, Romagnoli P, Testa E, Ceppa P, Testa R. Validity and clinical utility of the aspartate aminotransferase-alanine aminotransferase ratio in assessing disease severity and prognosis in patients with hepatitis C virus-related chronic liver disease.*Arch Intern Med* 2003; **163**: 218-224

36 **Wong VS**, Hughes V, Trull A, Wight DG, Petrik J, Alexander GJ. Serum hyaluronic acid is a useful marker of liver fibrosis in chronic hepatitis C virus infection. *J Viral Hepat* 1998; **5**: 187-192

37 **Zheng M**, Cai WM, Weng HL, Liu RH. ROC curves in evaluation of serum fibrosis indices for hepatic fibrosis. *World J Gastroenterol* 2002; **8**: 1073-1076

38 **Chen YP**, Feng XR, Dai L, Ding HB, Zhang L. Screening and evaluation of non-invasive diagnosis markers for compensated liver cirrhosis in patients with chronic hepatitis B. *Zhonghua Ganzangbing Zazhi* 2003; **11**: 225-227

Edited by Xu JY and Wang XL

P.O.Box 2345, Beijing 100023,China
Fax: +86-10-85381893
E-mail: wjg@wjgnet.com www.wjgnet.com

World J Gastroenterol 2003;9(11):2579-2582
World Journal of Gastroenterology
 ISSN 1007-9327

• CLINICAL RESEARCH •

Expression of Bcl-2 and Bax in extrahepatic biliary tract carcinoma and dysplasia

Sheng-Mian Li, Shu-Kun Yao, Nobuyoshi Yamamura, Toshitsugu Nakamura

Sheng-Mian Li, Shu-Kun Yao, Department of Internal Medicine, the Fourth Hospital of Hebei Medical University, Shijiazhuang 050011, Hebei Province, China
Nobuyoshi Yamamura, Department of Internal Medicine, Suwa Red Cross Hospital, 5-11-50 Kogan-dori, Suwa 392-8510, Japan
Toshitsugu Nakamura, Department of Pathology, Suwa Red Cross Hospital, 5-11-50 Kogan-dori, Suwa 392-8510, Japan
Correspondence to: Dr. Sheng-Mian Li, Department of Internal Medicine, the Fourth Hospital of Hebei Medical University, Shijiazhuang 050011, China. kyc@hbmu.edu
Telephone: +86-311-6033946 Ext 302
Received: 2003-05-12 **Accepted:** 2003-06-12

Abstract

AIM: To compare the difference of expression of Bcl-2 and Bax in extrahepatic biliary tract carcinoma and dysplasia, and to analyze the role of Bcl-2 and Bax proteins in the progression from dysplasia to carcinoma and to evaluate the correlation of Bcl-2/Bax protein expression with the biological behaviors.

METHODS: Expressions of Bcl-2 and Bax were examined immunohistochemically in 27 cases of extrahepatic biliary tract carcinomas (bile duct carcinoma: n=21, carcinoma of ampulla of Vater: n=6), and 10 cases of atypical dysplasia. Five cases of normal biliary epithelial tissues were used as controls. A semiquantitative scoring system was used to assess the Bcl-2 and Bax reactivity.

RESULTS: The expression of Bcl-2 was observed in 10 out of 27 (37.0 %) invasive carcinomas, 1 out of 10 dysplasias, none out of 5 normal epithelial tissues. Bax expression rate was 74.1 % (20/27) in invasive carcinoma, 30 % (3/10) in dysplasia, and 40 % (2/5) in normal biliary epithelium. Bcl-2 and Bax activities were more intense in carcinoma than in dysplasia, with no significant difference in Bcl-2 expression (P=0.110), and significant difference in Bax expression (P=0.038). Level of Bax expression was higher in invasive carcinoma than in dysplasia and normal tissue (P=0.012). Bcl-2 expression was correlated to Bax expression (P=0.0059). However, Bcl-2/Bax expression had no correlation with histological subtype, grade of differentiation, or level of invasion.

CONCLUSION: Increased Bcl-2/Bax expression from dysplasia to invasive tumors supports the view that this is the usual route for the development of extrahepatic biliary tract carcinoma. Bcl-2/Bax may be involved, at least in part, in the apoptotic activity in extrahepatic biliary carcinoma.

Li SM, Yao SK, Yamamura N, Nakamura T. Expression of Bcl-2 and Bax in extrahepatic biliary tract carcinoma and dysplasia. *World J Gastroenterol* 2003; 9(11): 2579-2582
http://www.wjgnet.com/1007-9327/9/2579.asp

INTRODUCTION

Extrahepatic biliary tract carcinoma is a relatively rare disease[1], and its mortality is 5 % of all deaths from malignant neoplasms in Japan[2] and its prognosis is poor[3,4]. Its pathogenic mechanisms remain unknown. Genetic and some risk factors contribute to its pathogenesis[1]. It has been suggested that invasive carcinoma of extrahepatic biliary tract is preceded by dysplasia[1,5], which provides a good model for the study of genetic abnormalities and neoplastic progression.

Genetic control of cell death (apoptosis or programmed cell death) and cell survival play a crucial role in tumor growth[6]. Among the molecules related to the apoptotic process, Bcl-2 family proteins are important and critical regulators in a variety of physiological and pathological contexts[6-10]. Bcl-2 and Bax are members of the Bcl-2 family. Bcl-2 prevents cells from death through a variety of mechanisms, whereas overexpression of Bax protein increases the susceptibility of cells to apoptosis[11]. Although Bax and Bcl-2 have different functions, they share similar structures. Bax is a homologue protein of Bcl-2 and possesses two conserved regions, BH1 and BH2 that appear to be important for Bax/Bcl-2 binding[10]. Bax and Bcl-2 may form homodimers (Bax/Bax, or Bcl-2/Bcl-2) or heterodimers (Bax/Bcl-2). The balance of Bcl-2 and Bax determines survival or death of cells exposed to apoptotic stimuli[12] and relates with chemotherapeutic response and prognosis in some diseases[11].

Expressions of Bcl-2 and Bax in intrahepatic bile duct have been studied extensively by immunohistochemical methods[12-18], but little is known about extrahepatic biliary tract carcinoma and dysplasia. In this study, we attempted to clarify the difference of Bcl-2/Bax protein expression between extrahepatic biliary tract carcinoma and dysplasia, to analyze the role of Bcl-2/Bax proteins in the progression from dysplasia to carcinoma, and to evaluate the correlation of Bcl-2/Bax protein expression and biological behaviors.

MATERIALS AND METHODS

Specimens

Pathological slides of surgically removed extrahepatic biliary tract carcinoma were retrieved from a database file at Department of Pathology, Suwa Red Cross Hospital, Nagano, Japan, from 1993 to 2000. The slides stained with hemaloxylin and eosin (H&E) were reviewed, and slides in 27 cases were selected for this study. These 27 cases composed of 21 biliary duct carcinomas and 6 carcinomas of ampulla of Vater. Histological criteria for diagnosis of dysplasia have been described[1], that is, dysplasia is characterized by cuboidal or columnar cells showing mild to moderate nuclear dysplasia, with or without pseudostratification, loss of polarity, and occasional mitotic figures. Slides in 3 cases had both dysplasia and carcinoma, and other 7 dysplasia lesions were obtained from the margins of malignant tissue. In all, dysplasia (Figure A) was observed in 10 (37.1 %) of invasive carcinomas. As non-neoplastic controls, 5 cases of normal epithelial tissue adjacent to the lesions were used. The histopathological diagnosis was made according to literature[1] using the specimens stained with H&E. There were 17 cases of well-differentiated adenocarcinoma (17/27, 63.0 %), 7 moderately differentiated (7/27, 25.9 %), and 3 poorly differentiated (3/

27, 11.1 %). Clinical stages were determined according to Union International Centre le Cancer (UICC) classification[19]. The numbers of cases in stages I, II, III and IV were 4, 9, 10 and 4, respectively.

Immunohistochemistry

All specimens were fixed in 10 % buffered formalin and embedded in paraffin. The deparaffinized sections were treated in 0.3 % hydrogen peroxide in methanol for 30 minutes to eliminate endogenous peroxidase activity. Retrieval of antigenecity was performed by microwave. Slides were placed in 10 mmol/l citrate buffer (pH 6.0), boiled for 15 min in a microwave oven, cooled for 15 min, and rinsed in distilled water. Anti-Bcl-2 antibody (Clone 124, DAKO Corporation, Glostrup, Denmark, 1:40 dilution) or anti-Bax antibody (Clone 4F11, Immunotech, Marseille, France, pre-diluted) was applied and incubated for 1 hour at room temperature. Each antigen was detected by LSAB-2 kit (DAKO) with 3, 3-diaminobenzidine and hydrogen peroxide and the sections were finally counterstained with hematoxylin. For positive controls, mature lymphocytes in the sections were stained positively for Bcl-2 and neutrophils for Bax.

The results of Bcl-2 and Bax immunostains were scored as described previously[20]. The percentage of positive tumor cells was graded as follows: 0: 0 %, 1: 1-25 %, 2: 26-50 %, 3: more than 50 %. Immunostaining intensity was rated as follows, 0: none, 1: weak, 2: moderate, 3: intense. When a score of intensity multiplying percentage of positive cells is equal to or more than 1, the specimen was considered as immunopositive. Only cytoplasmic staining was evaluated and nuclear reaction was interpreted to be nonspecific staining.

Statistical analyses

Fisher' s exact test was used for statistical analysis. Spearman relation analysis was used for comparison of Bcl-2 and Bax expression. All statistical analyses were performed using STATA software (STATA Inc, Texas, USA). $P<0.05$ was considered as significant.

RESULTS

Bcl-2 and Bax protein expression

The results of immunostaining are shown in Table 1.

Significant Bcl-2 protein expression was observed in 9 out of 21 (42.9 %) bile duct carcinomas and 1 out of 6 (16.7 %) carcinomas of ampulla of Vater. The immunoreactive cases showed diffuse cytoplasmic staining (Figure 1 B). There was no significant difference according to the primary site of carcinoma (P=0.363). On the other hand, only one case out of 10 dysplasia was stained (Figure 1 C). Although there was an increasing tendency of Bcl-2 positive cases from normal to dysplasia and carcinoma, no statistical significance was observed among these three groups (P=0.110).

For Bax expression, the positive cases showed a granular cytoplasmic staining pattern. The positive rate of Bax expression was 17 out of 21 (81.0 %) cases of bile duct carcinoma (Figure 1D) and 3 out of 6 (50.0 %) carcinomas of ampulla of Vater, without statistical significance (P=0.290). Bax was positively stained in 3 out of 10 cases of dysplasia, and 2 out of 5 normal epithelia. There was a significant difference among these three groups (P=0.038), the Bax expression in invasive carcinoma was more obvious than that in dysplasia and normal group when further compared (P=0.012).

Table 1 Expression of Bcl-2 and Bax in biliary tract carcinoma and dysplasia lesions

Lesions	Bcl-2 expression			Bax expression		
	No. positive/tested	%	*P*	No. positive/tested	%	*P*
Invasive carcinoma	10/27	37.0		20/27	74.1	
Bile duct	9/21	42.9		7/21	81.0	
Ampulla of Vater	1/6	16.7	0.363	3/6	50.0	0.290
Dysplasia	1/10	10.0		3/10	30.0	
Normal	0/5	0	0.110	2/5	40.0	0.038[a]

a: Further compared, it was shown that the difference of Bax expression between dysplasia and normal epithelium was not significant (P=1.00), but Bax expression of carcinoma differed from that in dysplasia and normal tissues significantly (P=0.012).

Table 2 Comparison of Bcl-2/Bax protein expression with histological features or clinical stages in biliary tract carcinoma

Histological features	Bcl-2 expression			Bax expression		
	No.positive/tested	%	*P*	No.positive/tested	%	*P*
Differentiation grade						
Well	7/17	41.18		13/17	76.48	
Moderately	2/7	28.57		5/7	71.43	
Poorly	1/3	33.33	0.846	2/3	66.67	1.000
Perineural invasion						
No	4/9	44.44		7/9	77.78	
Yes	6/18	33.33	0.236	13/18	72.22	0.209
Vascular invasion						
No	8/19	42.11		15/19	78.95	
Yes	2/8	25.00	0.666	5/8	62.50	0.633
Lymph node metastasis						
No	7/14	50.00		12/14	85.71	
Yes	3/13	23.08	0.683	8/13	61.54	1.000
Stages						
I+II	5/13	38.46		10/13	76.92	
III+IV	5/14	35.70	1.000	10/14	71.431	1.000

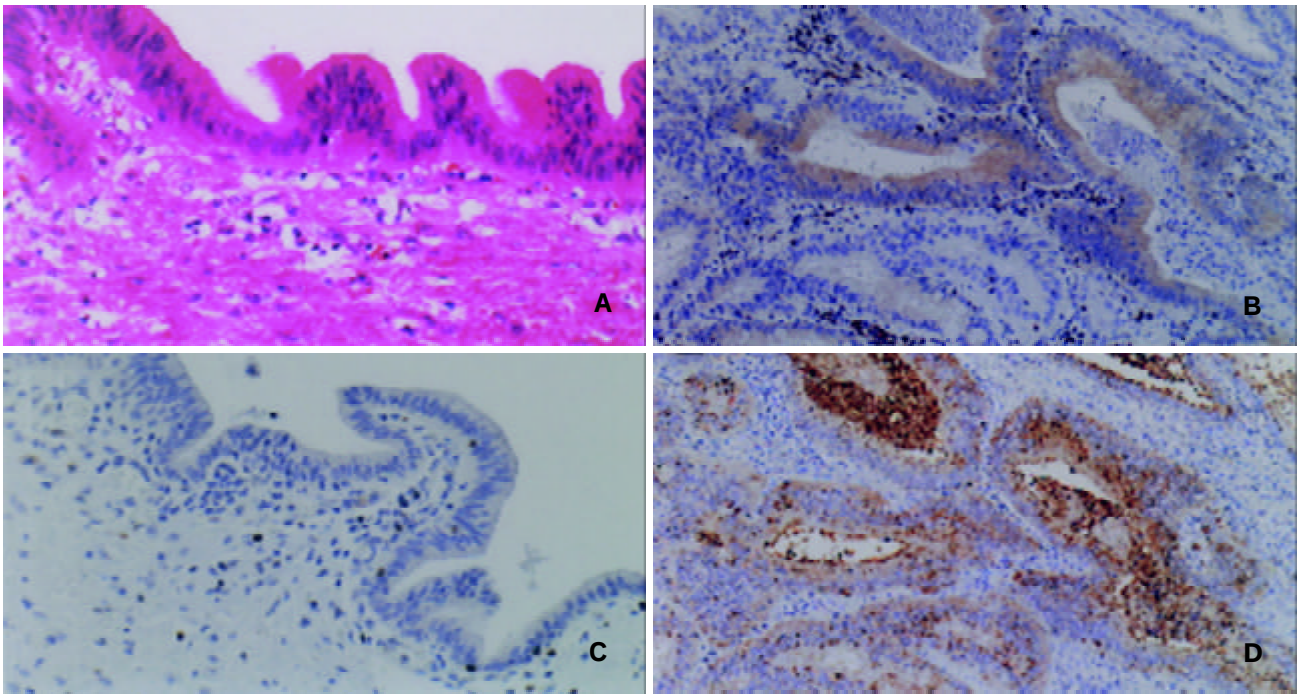

Figure 1 A: Cytological features of dysplasia (Hematoxylin-eosin stain, original ×100 magnification). B: Cytoplasmic expression of Bcl-2 in 1 % to 25 % cells in carcinoma (original magnification ×100). C: Bcl-2 expression in dysplasia with weak staining (original magnification ×100). D: Cytoplasmic expression of Bax in more than 50 % cells in carcinoma stained as intense granular patterns (original magnification ×100. B, D: serial sections).

Comparison between positive expression of Bcl-2/Bax protein and histological characteristics in carcinoma tissue

The results are shown in Table 2.

Out of 27 specimens with invasive carcinoma, the positive rate of Bcl-2/Bax expression was higher in well differentiated type than in poorly differentiated one, and higher in cases without invasion of vessels and lymph nodes than in those with tumor invasion with statistical significance, and higher in cases at stages I and II than in those at stages III and IV without statistical significance.

Correlation of Bcl-2 and Bax protein expression

Expression of Bcl-2 had a significant correlation with that of Bax in malignant tissues, dysplasia and normal epithelium (P=0.0059). Six invasive carcinomas expressed both Bcl-2 and Bax, 5 cases expressed only Bcl-2 protein, 10 cases expressed only Bax protein, 6 cases expressed neither Bcl-2 nor Bax.

DISCUSSION

Dysplasia-carcinoma sequence was regarded as a usual pathway in the development of invasive carcinoma of extrahepatic biliary tract[1]. The foci of dysplasia are multicentric in most cases, which probably explain the high incidence of local recurrence. Laitio [21] and Davis *et al*[22]. noted dysplasia in 45 % and 30 % of extrahepatic bile duct carcinomas, respectively. Suzuki *et al*[23]. found high grade dysplasia in 75 % of invasive carcinoma. In our study, dysplasia accounted for 37 % (10/27) of invasive carcinomas in extrahepatic bile duct and ampulla of Vater, which could be interpreted as an evidence for the theory that dysplasia is a precursor lesion of invasive carcinoma of biliary tract.

Apoptosis has caused great interest in many fields in recent years. Apoptosis-related genes such as p53, bcl-2, bax, c-myc, and bcl-x influence the susceptibility of normal and neoplastic cells to apoptosis[11]. High expression of Bcl-2 protein inhibited apoptosis of cells subjected to chemotherapy, irradiation, and nutritional withdrawal, whereas overexpression of Bax protein facilitated cell death[11]. In this study, we investigated the expression of Bcl-2 and Bax protein in 27 cases of biliary tract carcinoma and found that Bcl-2 protein was expressed in 37 % cases. Previous study showed that varying amounts of Bcl-2 protein were expressed in intrahepatic bile duct[24], while Okaro [14] and Arora[25] reported none of cholangiocarcinoma samples examined expressed Bcl-2 protein. For extrahepatic bile duct carcinoma, Ito *et al*[26]. reported Bcl-2 expression in 17 out of 38 (44.7 %) cases, which was similar to our result (10/27, 37.0 %). On the other hand, Bax was diffusely expressed along the intrahepatic biliary tree[15]. In biliary epithelial cells of rats the expression of Bax protein was visualized by immunohistochemistry and quantified stereologically[12], but in human extrahepatic biliary epithelium, Bax protein expression has not been reported. We observed Bax expression in 74 % cases of extrahepatic biliary carcinoma. Moreover, intensity of Bax staining was generally stronger than that of Bcl-2. Although further studies should be performed, our results suggest that both Bcl-2 and Bax play a role in regulating apoptosis in extrahepatic biliary tract carcinoma. Whether there is a difference of expression of Bcl-2 and Bax between carcinomas of intrahepatic and extrahepatic biliary tract should be clarified in the future.

Our study also showed that Bcl-2 protein expressed in 10 % biliary dysplasia, and no expression of Bcl-2 in 5 normal biliary epithelial cells. These findings were consistent with the results described by Okaro *et al*[14]. Bax protein expression rate was 30 % in dysplasia and 40 % in normal biliary epithelium. Incidence of Bcl-2 and Bax expression in invasive carcinoma was higher than that in dysplasia and normal tissue. Expression of Bax but not Bcl-2 showed a statistically significant difference among the malignant tissue, peri-cancerous tissue and normal one. Previously we demonstrated that Bcl-2 expression in premalignant lesions was an early event in the carcinogenesis of colorectal, gastric and cervix glandular tumors[27]. However, this was not true for biliary tract tumors. Bcl-2 and Bax might play some roles in the development from dysplasia to carcinoma. As the number of cases in each group was too small for statistical analysis, further studies are needed.

The ratio of anti-apoptotic to pro-apoptotic Bcl-2 family proteins appeared to control the relative sensitivity or resistance of many types of cells to apoptotic stimuli[15]. In our study, Bcl-2 expression was related to Bax protein expression in malignant, dysplasia and normal lesions. This finding was consistent with the conclusion of Harada *et al*[28], and supported that Bcl-2 and Bax were involved in the apoptotic activity in the development of extrahepatic biliary tract carcinomas as a couple of contrary functions.

There was a tendency that the low expression of Bcl-2/Bax was found in less differentiated and more advanced cases with metastasis of lymph node and perineural and vascular invasion, although statistical analysis revealed no significance. The impact of Bcl-2 expression on clinical outcome was demonstrated by Ito *et al*[29], who showed that Bcl-2 expression was inversely related to the incidence of apoptosis, and that Bcl-2 expression was more frequently absent in cases of advanced stages, lymph node metastasis, and perineural invasion (inverse relationship). On the other hand, previous study showed that Bax expression might be involved in tumor differentiation/histological types and metastatic progression in colorectal cancer[30], no reports on Bax expression/Bcl-2 in extrahepatic biliary tract tumor has been published yet. The study could not show any distinct correlation between Bcl-2/Bax expression and clinical stage or aggression, and a larger number of cases may be required to clarify this issue.

In conclusion, the increased incidence of Bcl-2/Bax expression observed from dysplasia to invasive tumor supports that this is the usual route for the development of extrahepatic biliary carcinoma. Bcl-2/Bax may be involved in the pathogenesis of extrahepatic biliary carcinoma and there is a correlation between Bcl-2 and Bax protein expression, suggesting that Bcl-2 and Bax regulate the apoptotic activity in extrahepatic biliary carcinoma as a couple of opposite functions.

ACKNOWLEDGMENT

The authors thank Mr. M.Yajima, Mr. M. Shimomura, Ms. H. Yabusaki, and Ms. R. Komatsu for their excellent technical assistance, and Ms. LM. Tang for her help with statistical analysis.

REFERENCES

1 **Albores-saavedra J**, Henson DE, Klimstra DS. Tumors of the gallbladder, extrahepatic bile ducts, and ampulla of Vater. Atlas of tumor pathology, third series, fascicle 27. *Washington, DC: Armed Forces Institute of Pathology* 2000: 181-191
2 **Yamamoto M,** Nakadaira H, Nakamura K. Biliary tract cancer. *Gan To Kagaku Ryoho* 2001; **28**: 155-158
3 **Ichikawa K,** Imura J, Kawamata H, Takeda J, Fujimori T. Down-regulated p16 expression predicts poor prognosis in patients with extrahepatic biliary tract carcinomas. *Int J Oncol* 2002; **20**: 453-461
4 **Niiyama H,** Mizumoto K, Kusumoto M, Ogawa T, Suehara N, Shimura H, Tanaka M. Activation of telomerase and its diagnostic application in biopsy specimenes from biliary tract neoplasms. *Cancer* 1999; **85**: 2138-2143
5 **Hoang MP,** Murakata LA, Padilla-Rodriguez AL, Albores-Saavedra J. Metaplastic lesions of the extrahepatic bile ducts: a morphologic and immunohistochemical study. *Mod Pathol* 2001; **14**: 1119-1123
6 **Adams J,** Cory S. The Bcl-2 protein family: Arbiters of cell survival. *Science* 1998; **281**: 1322-1326
7 **Kluck RM,** Bossy-Wetzed E, Green DR, Newmeyer DD. The release of cytochrome C from mitochondria: a primary site for Bcl-2 regulation of apoptosis. *Science* 1997; **275**: 1132-1136
8 **Yang J,** Liu X, Bhalla K, Kim CN, Ibrado AM, Cai J, Peng TI, Jones DP, Wang X. Prevention of apoptosis by Bcl-2: release of cytochrome c from mitochondria blocked. *Science* 1997; **275**: 1129-1132
9 **Boise LH,** Gonzalez-Garcia M, Postema CE, Ding L, Lindsten T, Turka LA, Mao X, Nunez G, Thompson CB. bcl-x, a bcl-2-related gene that functions as a dominant regulator of apoptotic cell death. *Cell* 1993; **74**: 597-608
10 **Yang E,** Zha J, Jockel J, Boise LH, Thompson CB, Korsmeyer SJ. Bad, a heterodimeric parter for Bcl-X_L and Bcl-2, displaces Bax and promotes cell death. *Cell* 1995; **80**: 285-291
11 **Wheaton S,** Netser J, Guinee D, Rahn M, Perkins S. Bcl-2 and Bax protein expression in indolent versus aggressive B-cell non-Hodgkins lymphomas. *Hum Pathol* 1998; **29**: 820-825
12 **Stahelin BJ,** Marti U, Zimmermann H, Reichen J. The interaction of Bcl-2 and Bax regulates apoptosis in biliary epithelial cells of rats with obstructive jaundice. *Virchows Arch* 1999; **434**: 333-339
13 **Korsmeyer SJ.** Bcl-2 initiates a new category of oncogenes: regulators of cell death. *Blood* 1992; **80**: 879-886
14 **Okaro AC,** Deery AR, Hutchins RR, Davidson BR. The expression of antiapoptotic proteins Bcl-2, Bcl-X(L), and Mcl-1 in benign , dysplastic and malignant biliary epithelium. *J Clin Pathol* 2001; **54**: 927-932
15 **Iwata M,** Harada K, Kono N, Kaneko S, Kobayashi K, Nakanuma Y. Expression of Bcl-2 familial proteins is reduced in small bile duct lesions of primary biliary cirrhosis. *Hum Pathol* 2000; **31**: 179-184
16 **Bergquist A,** Glaumann H, Stal P, Wang GS, Broome U. Biliary dysplasia, cell proliferation and nuclear DNA-fragmentation in primary sclerosing cholangitis with and without cholangiocarcinoma. *J Intern Med* 2001; **249**: 69-75
17 **Harnois DM,** Que FG, Celli A, LaRusso NF, Gores GJ. Bcl-2 is overexpressed and alters the threshold for apoptosis in a cholangiocarcinoma cell line. *Hepatology* 1997; **26**: 884-890
18 **Nakopoulou L,** Stefanaki K, Vourlakou C, Manolaki N, Gakiopoulou H, Michalopoulos G. Bcl-2 protein expression in acute and chronic hepatitis, cirrhosis and hepatocellular carcinoma. *Pathol Res Pract* 1999; **195**: 19-24
19 **Sobin LH,** Fleming ID. TNM classification of malignant tumors, fifth edition (1997). Union internationale contre le cancer and the american joint committee on cancer. *Cancer* 1997; **80**: 1803-1804
20 **Krajewska M,** Krajewski S, Epstein JI, Shabaik A, Sauvageot J, Song K, Kitada S, Reed JC. Immunohistochemical analysis of bcl-2, bax, bcl-X and mcl-1 expression in prostate cancers. *Am J Pathol* 1996; **48**: 1567-1576
21 **Laitio M.** Carcinoma of extrahepatic bile duct: a histopathologic study. *Pathol Res Pract* 1983; **178**: 67-72
22 **Davis RI,** Sloan JM, Hood JM, Maxwell P. Carcinoma of the extrahepatic biliary tract: a clinicopathological and immunohistochemical study. *Histopathology* 1988; **12**: 623-631
23 **Suzuki M,** Takahashi T, Ouchi K, Matsuno S. The development and extension of hepatohilar bile duct carcinoma. A three-dimensional tumor mapping in the intrahepatic biliary tree visualized with the aid of a graphic computer system. *Cancer* 1989; **64**: 658-666
24 **Skopelitou A,** Hadjiyannakis M, Alexopoulou V, Krikoni O, Kamina S, Agnantis N. Topographical immunohistochemical expression of bcl-2 protein in human liver lesions. *Anticancer Res* 1996; **16**: 975-978
25 **Arora DS,** Ramsdale J, Lodge JP, Wyatt JI. p53 but bcl-2 is expressed by most cholangiocarcinomas: a study of 28 cases. *Histopathology* 1999; **34**: 497-501
26 **Ito Y,** Takeda T, Sakon M, Tsujimoto M, Matsuura N. Expression and clinical implications of bcl-2 in extrahepatic bile duct carcinoma: its relationship with biological features. *Anticancer Res* 2000; **20**: 3891-3895
27 **Nakamura T,** Nomura S, Sakai T, Nariya S. Expression of Bcl-2 oncoprotein in gastrointestinal and uterine carcinomas and their premalignant lesion. *Hum Pathol* 1997; 28: 309-315
28 **Harada K,** Iwata M, Kono N, Koda W, Shimonishi T, Nakanuma Y. Distribution of apoptotic cells and expression of apoptosis–related proteins along the intrahepatic biliary tree in normal and non-biliary disease liver. *Histopathology* 2000; **37**: 347-354
29 **Ito Y,** Takeda T, Sasaki Y, Sakon M, Monden M, Yamada T, Ishiguro S, Imaoka S, Tsujimoto M, Matsuura N. Bcl-2 expression in cholangiocellular carcinoma is inversely correlated with biologically aggressive phenotypes. *Oncology* 2000; **59**: 63-67
30 **Jansson A,** Sun XF. Bax expression decreases significantly from primary tumor to metastasis in colorectal cancer. *J Clin Oncol* 2002; **20**: 811-816

Edited by Ren SY and Wang XL

P.O.Box 2345, Beijing 100023,China
Fax: +86-10-85381893
E-mail: wjg@wjgnet.com www.wjgnet.com

World J Gastroenterol 2003;9(11):2583-2586
World Journal of Gastroenterology
 ISSN 1007-9327

• CLINICAL RESEARCH •

Effect of a single oral dose of rabeprazole on nocturnal acid breakthrough and nocturnal alkaline amplitude

Jin-Yan Luo, Chun-Yan Niu, Xue-Qin Wang, You-Ling Zhu, Jun Gong

Jin-Yan Luo, Chun-Yan Niu, Xue-Qin Wang, You-Ling Zhu, Jun Gong, Department of Gastroenterology, The Second Hospital of Xi' an Jiaotong Uuniversity, Xi' an 710004, Shanxi Province, China
Correspondence to: Dr. Jin-Yan Luo, The Second Hospital of Xi' an Jiaotong University, Xi' an 710004, Shanxi Province, China. ljy18272@163.com
Telephone: +86-29-7678758 **Fax:** +86-29-7678758
Received: 2002-10-05 **Accepted:** 2003-04-05

Abstract

AIM: To study the effect of rabeprazole (RAB) on nocturnal acid breakthrough (NAB) and nocturnal alkaline amplitude (NAKA) and to compare it with omeprazole (OME) and pantoprazole (PAN).

METHODS: By an open comparative study, forty patients with active peptic ulcer were randomly assigned to receive one of the three PPIs (proton pump inhibitor) with a single oral dose. They were divided into RAB group (10 mg), OME group(20 mg) and PAN group (40 mg). Twenty healthy volunteers were enrolled to the control group (without taking any drug). Intragastric pH monitoring was then performed 1 hour before and 24 hours after the dose was given.

RESULTS: No clinically undesirable signs and symptoms possibly attributed to the administration of RAB or OME and PAN were recognizable throughout the study period. All subjects completed the study according to the protocol. All data were processed by a computer using the Student *t* test or *t* ' test followed by an analysis of covariance. $P<0.05$ was considered to have statistical significance. The intragastric pH of NAB was significantly higher in RAB group (1.84±0.55) than in either OME group (1.15±0.31) or PAN group (1.10±0.30) (both $P<0.01$). RAB produced a longer sustaining time (4.65±1.22 h) on NAKA than OME (3.22±1.89 h) ($P<0.05$), PAN (3.15±1.92 h) ($P<0.05$), and the sustaining time of NAKA in RAB group was longer than that in the healthy control group ($P<0.01$) too. In addition, RAB produced a much higher pH on NAKA (6.41±0.45) in comparison with PAN (6.01±0.92) ($P<0.05$).

CONCLUSION: A single oral dose of 10 mg RAB may increase the pH of NAB and shorten the sustaining time of NAB, and it may increase the pH of NAKA as well as prolong the sustaining time of NAKA.

Luo JY, Niu CY, Wang XQ, Zhu YL, Gong J. Effect of a single oral dose of rabeprazole on nocturnal acid breakthrough and nocturnal alkaline amplitude. *World J Gastroenterol* 2003; 9 (11): 2583-2586
http://www.wjgnet.com/1007-9327/9/2583.asp

INTRODUCTION

The first-generation proton pump inhibitors (PPIs) (such as omeprazole, lansoprazole and pantoprazole) have been considered to be the most primary and potent treatments of acid-related diseases since they were put into clinical application, and their efficacy and safety have been well-documented and widely recognized. However, researches during the last 10 years have shown that, despite the multiple treatment modalities such as modifying administer methods, increasing the dosages or adding H_2 receptor antagonist, the first-generation PPIs can not suppress the nocturnal acid secretion successfully especially NAB[1,2]. The objective in designing this trial was to observe the effect of the newer-generation of PPI rabeprazole on NAB (nocturnal acid breakthrough) and NAKA (nocturnal alkaline amplitude).

MATERIALS AND METHODS

Subjects and grouping

Forty patients with endoscopically proven active gastric or duodenal ulcer at our hospital from June, 2001 to May, 2002 entered into the study. They were randomly assigned to three groups: RAB group (n=15), OME group (n=15) and PAN group (n=10). The male/female ratio of patients was 9:6, 8:7, 6:4 in the three groups respectively. Their age (mean) was 20-61 (34.5±7.8)years, 22-60(30.6±6.7)years and 25-59(29.3±6.5) years respectively. Twenty healthy volunteers (10 men and 10 women) were enrolled as the control group, aged from 18 to 60 years (mean 25.7±9.5).

Methods

Administering method This study was an open comparative trial. With a single oral dose, every one was administered 10 mg RAB, 20 mg OME or 40 mg PAN respectively, ambulatory intragastric pH measurements were then performed. All subjects ceased the drugs that might affect acid secretion and gastrointestinal motility 2 weeks before the study.

Instruments and processes[3] Portable pH recorder (DIGITRAPPER MKIII, CTD Co., Sweden). After fasted for 12 hours, an electrode was placed via a nostril into the stomach at 8 am, to record the baseline pH for an hour, a dose of drug was given to one patient at 9 am, pH was recorded continuously for hours. All participants kept their normal daily activities and consumed their customary diet, except to abstain from drinking acid and alkali beverages during the test period. The pH electrode was withdrawn at the following morning 9 am, pH data were downloaded onto a computer for analysis.

Measuring indicator The impact of the three agents on NAB (identifying criterion[4]: Intragastric pH dropped to <4 and remained below that level for at least 1 hour during the 12 hours of night sleeping period after the dose of PPI). The impact of the three agents on NAKA (identifying criterion[5]: The time that intragastric pH remained >4 lasted for>1 hour from 0:00 to 8 am).

Statistical analysis

All data were processed by a computer. Data were presented as the mean ±SD. Comparisons between two groups and among three groups were made using the Student *t* test or *t*' test followed an analysis of covariance. $P<0.05$ was considered to have statistical significance.

Table 1 Effect of single dose of PPI on NAB

PPI group	*n*	Occurring cases(%)	Time range	pH($\bar{x}$±s)	Persisting time ($\bar{x}$±s)(h)
RAB10 mg	15	9(60 %)	0:00-4:0	1.84±0.55[ac]	4.10±2.38
OME20 mg	15	9(60 %)	20:00-2:0	1.15±0.31	5.40±2.73
PAN40 mg	10	8(80 %)	20:00-6:0	1.10±0.30	5.71±2.60

[a]*P*<0.05 *vs* OME, [c]*P*<0.05 *vs* PAN.

Table 2 Effect of single dose of PPI on NAKA

PPI group	*n*	Occurring cases (%)	Time range	pH($\bar{x}$±s)	Persisting time ($\bar{x}$±s) (h)
RAB10 mg	15	9(60 %)	2.0-7.0	6.41±0.45[cb]	4.65±1.22[acb]
OME20 mg	15	8(53.3 %)	1.0-7.0	6.51±0.82[b]	3.22±1.89
PAN40 mg	10	5(50 %)	2.0-6.0	6.01±0.92	3.15±1.92
Control group	20	9(45 %)	1.0-6.0	5.30±0.47	2.25±1.23

[a]*P*<0.05 *vs* OME, [c]*P*<0.05 *vs* PAN, [c]*P*<0.05 *vs* healthy control group.

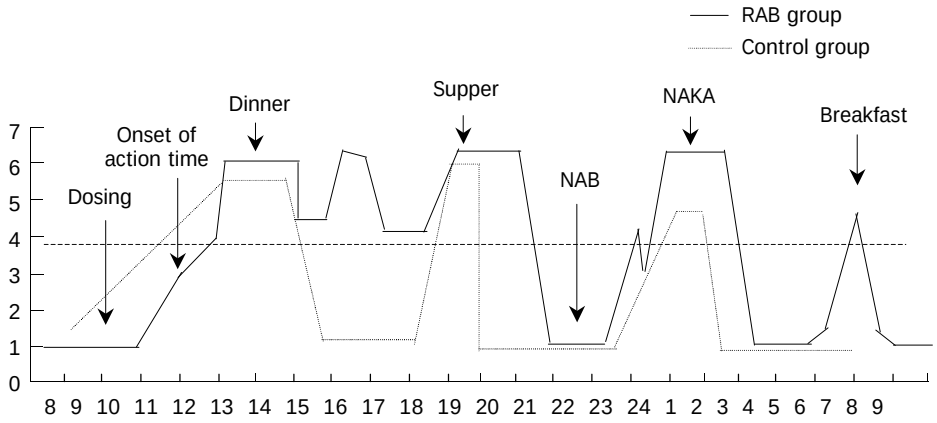

Figure 1 Simulating figure of NAB and NAKA. NAB and NAKA all occurred after midnight, and NAKA always appeared after NAB. Compared with the control group (didn't receive either PPI or placebo), RAB increased the pH of NAKA as well as prolonged the persisting time of NAKA.

RESULTS

Impacts of RAB, OME and PAN on NAB (Table 1)

NAB often occurs after 8 pm. Of the 40 patients, 26 (65 %) exhibited NAB, which occurred mostly from 8 pm to 4-6 am next morning. The results showed that RAB increased pH of NAB significantly (1.84±0.55) than OME and PAN (*P*<0.05), it also shortened persisting time of NAB. NAB occurred frequently in PAN group.

Impacts of RAB, OME and PAN on NAKA (Table 2)

Compared with the healthy group, all three PPIs could increase pH of NAKA and prolong the sustaining time of NAKA. The persisting time that pH>4 of NAKA in RAB group was longer than that in the other three groups (*P*<0.05, <0.05, <0.01), intragastric pHs in RAB group and OME group were all higher than that in the healthy control group (*P*<0.01) (Table 2).

DISCUSSION

NAB and NAKA are two common clinical phenomena, but the developing mechanisms are remain unclear. Our attention was to investigated the effects of PPIs on NAB and NAKA.

NAB was defined as the occurrence of intragastric pH dropped to below 4 and remained below that level for at least 1 hour during the 12 hours of night sleeping period (typically the second 6-hours) after the dose of PPI[1,4]. This study showed that the pH(1.84±0.55) of NAB was significantly higher in RAB group than in OME group and PAN group (*P*<0.05), the persisting time of NAB was shortened. Additionally, the occurrence of NAB was lower in RAB group than in PAN group. The above results suggested that RAB had an advantage over OME and PAN on suppressing NAB, which was consistent with other reports[6,7]. It might contribute to the pharmacological features of RAB such as longer half-life, rapid onset of action, acid-stability, no influences on foods, dosing time or patterns[8-10]. NAB had a high occurrence after midnight and typically in the second 6-hours during night sleeping[1,4,11]. NAB after taking PPIs was first reported by Peghini and Katz[4]. Peghini *et al.* considered that NAB could be explained by food-related factors (for example, the absence of the buffering effect of meals after midnight) which resulted in weakened acid-inhibiting efficacy of PPIs and increased night acid production. This might help to explain why the acid-suppressing effect of PPIs during daytime was greater than that during nighttime[12]. According to the fact that adding a dose of H_2RA at bed time could produce a much better controllable action than that of PPIs on NAB. Peghini *et al*. suggested that histamine played a major role in nocturnal acid secretion[4,13,14]. A study revealed that 70 % of patients with gastro-oesophageal reflux disease (GERD) receiving PPIs had NAB which was often accompanied by esophageal acid exposure. The prevalence of ineffective esophageal motility and low LES pressure was significantly higher in refluxers than in non-refluxers[15], so GERD was considered to correlate with NAB closely. This might be the result of gastric acid secretion following a circadian profile

which was characterized by an increase in the evening , with a peak at about midnight[16]. This might explain why only some refluxers developed esophagitis. There was another opinion that eradication of *H pylori* appeared to be closely related to the occurrence of nocturnal NAB when a dose of PPI was given[17]. There were important clinical implications of NAB, because there existed a close relationship between night acid-control and GERD as well as peptic ulcer. Esophageal protective mechanism was decreased during this time and it was unbeneficial for ulceric mucosa to restore[18,19]. It was thought that NAB might be particularly injurious to the esophageal mucosa and might arise lasting nocturnal heartburn or acid regurgitation and even respiratory complaints. Hence, there was a clinical rationale and greater importance for reducing or abolishing nocturnal acid secretion and increasing intragastric pH or intra-esopgageal pH in treatment of acid-related disorders to promote the healing of peptic ulcer, severe GER and Barrett' s esophagus in order to improve the quality of life[20]. But NAB was also reckoned to prove reversely the safety of PPI (i.e it was extremely difficult to render achlorhydric)[11]. Many studies supported that the addition of a low dose of H_2RA did enhance the control effect on NAB of PPIs because H_2RAs reduced basal gastric acid secretion, H_2RA nizatidine has been known to stimulate gastric emptying and elevate LES pressure and therefore decrease NAB as well as nightly reflux[21], low dose of H_2RA following a provocative dinner or a large fatty meal might effectively reduce esophageal acid exposure. Being prone to produce a tolerance to H_2RA due to its long-term intaking, an intermittent dosing fashion might be an optimal approach[22].

NAKA was also termed as "spontaneous nocturnal gastric alkalinization" (SNGAK), "spontaneous nocturnal alkalinization" (SNA), "nocturnal anhydrochloric wave" and "inversion of gastric pH"[23-25], which was defined as a phenomenon that an abrupt physiological or pathological raise of intragastric pH to above 4 to 6 after sleeping (mostly in the early morning). The prevalence of NAKA ranged between 40-80 % in normal populations, mostly beginning in the latter part of the night. Bianco *et al*[25] found that SNA lasted for 87.82±12.47min/time in normal volunteers and for 3.27±1.62 min/time in patients with duodenal ulcer. Ke *et al*[26]. reported that NAKA presented in 67 % of normal group, lasting for 169.7±40.2 min (total), and raised in 70 % of patients with duodenal ulcer, lasting for 57.6±12.0 min (total). In this study, NAKA presented in 45 %(9/20) of normal subjects, which sustained for 135.0±73.8 min (total), and in 55 %(22/40) of patients with duodenal ulcer. The results were lower than the above, the mean sustaining time of NAKA was 220.4±100.6 min (total) in patients with duodenal ulcer after a single administration of PPI. These findings indicated that RAB might increase the pH of NAKA and prolong persisting time of NAKA. We have previously conducted a simultaneous monitoring of intragastric pH and bile in normal subjects and patients with duodenal gastric reflux (DGR), and found that the pH and cholerythrin exhibited 2 models and 4 types[27]. The 2 models were simultaneous and non-simultaneous raise of pH and cholerythrin, and the 4 types were simultaneouse raise and drop of pH and cholerythrin. pH raised alone and cholerythrin raised alone. The test of neutralizing bile with gastric juice *in vitro* showed that until the absorbency had already raised to 0.900 when bile concentration was 20 %, while pH remained at 1 or so. Furthermore, only when bile concentration raised to >60 %, did gastric pH begin to raise to >4, suggesting that it was not until bile reached to a considerable level when it had an influence on intragastric pH. As bile is nocuous to esophageal mucosa, so only a solitary pH raise produces a protective action. NAKA was proposed by Bianco *et al*. at first in 1970s, there were several opinions about its pathophysiological mechanism. NAKA appeared to be a kind of self-protective mechanism for gastric mucosa against the damages of acid and mucosa-injuring agents, and helping expulse H^+ to gastric cavity continuously so as to relieve clinical symptoms[28]. In this trial, all 3 PPIs increased peak value and persisting time of NAKA(there was a significant difference in comparison with the control). The increase was more prominent for RAB than for OME and PAN, one likely explanation was that H^+-K^+ATPase was inhibited much more. Further investigation is needed. Based on earlier studies[23,27,29], we hypothesed that NAKA was related to DGR, this hypothesis was supported by conclusions of other countries[30,31]. Alkali reflux mostly occurred during MMC phase II and phase III, suggesting that NAKA together with duodenal uncoordinated motor activity could lead to the reflux of duodenal juice (not always bile) into gastric cavity and hence antrum "alkalinization" state at the end of phase III. NAKA was thought to be strongly related to sleeping and interrupted by waking up[31]. Some investigators deduced that NAKA correlated with reduced vagal tension and chlecystectomy as well as modulation of gastric secretions[24,32]. There were evidences that ulcer patients did not show SNA phenomenon before treatment, but the therapy led it to recurrence, and the lack of SNA in duodenal ulcer patients was so frequent that its absence might be a diagnostic sign of peptic ulcer (positively predictive value 82 %)[25,33]. In addition, we had an interesting observation that NAKA always appeared following NAB (Figure 1). There have been no findings concerning this phenomenon yet, and its etiology needs to be identified.

NAB is the most notable limitation of PPIs used at present. By comparison we can understand that available PPIs are unable to resolve the problem of NAB, including rabeprazole. In summary, we have shown that a single dose of 10 mg rabeprazole can achieve a much superior acid-suppressing efficacy as compared to omeprazole and pantoprazole. It can elevate pH of NAB, shorten persisting time of NAB, increase pH as well as sustaining time of NAKA. These findings show that rabeprazole may provide a profound control on nocturnal gastric acid secretion. However, there remain problems demanding further evaluations. For example, whether it is beneficial by increasing the dose or administering time of rabeprazole (i.e twice daily) or an on-demand treatment[19] should be given to enhance the acid-inhibiting efficacy of rabeprazole, whether the onset of NAKA correlates with more effective inhibiting on H^+-K^+ATPase of rabeprazole, etiology and clinical implications of NAB and NAKA, and why NAKA is always present after NAB.

REFERENCES

1 **Tytgat GNJ.** Shortcomings of the first-generation proton pump inhibitors. *Eur J Gastroenterol Hepatol* 2001; **13**(Suppl 1): S29-S33

2 **Sachs G.** Improving on PPI-based therapy of GORD. *Eur J Gastroenterol Hepatol* 2001; **13**(Suppl 1): S35-S41

3 **Gong J,** Zhu YL, Luo JY, Wang XQ. The acid-inhibiting effect of famotidine with a single dose by injection in musle. *Zhonghua Yixue Zazhi* 1998; **37**: 762-765

4 **Peghini PL,** Katz PO, Bracy NA, Castell DO. Nocturnal recovery of gastric acid secretion with twice-daily dosing of proton pump inhibitors. *Am J Gastroenterol* 1998; **93**: 763-767

5 **Bianco A,** Cagossi M, Piraccini R, Castrucci G, Greco AV. The nightly spontaneous alkalinization of the stomach. *Riv Eur Sci Med Farmacol* 1993; **15**: 17-27

6 **Robinson M**. New-generation proton pump inhibitors:overcoming the limitations of early-generation agents. *Eur J Gastroenterol Hepatol* 2001; **13**(Suppl 1): S43-S47

7 **Katz PO,** Frissora C. The pharmacology and clinical relevance of proton pump inhibitors. *Curr Gastroenterol Rep* 2002; **4**: 459-462

8 **Williams MP**, Pounder RE. Review article: the pharmacology of rabeprazole. *Aliment Pharmacol Ther* 1999; **13**(Suppl 3): 3-10

9 **Williams MP,** Sercombe J, Hamilton MI, Pounder RE. A placebo-controlled trial to assess the effects of 8 days of dosing with rabeprazole versus omeprazole on 24-h intragastric acidity and plasma gastrin concentrations in young healthy male subjects. *Aliment Pharmacol Ther* 1998; **12**: 1079-1089

10 **Skoczylas T,** Sarosiek I, Sostarich S, McElhinney C, Durham S, Sarosiek J. Significant enhancement of gastric mucin content after rabeprazole administration: its potential clinical significance in acid-related disorders. *Dig Dis Sci* 2003; **48**: 322-328

11 **Fackler WK,** Ours TM, Vaezi MF, Richter JE. Long-term effect of H_2RA therapy on nocturnal gastric acid breakthrough. *Gastroenterology* 2002; **122**: 625-632

12 **Chiverton SG,** Howden CW, Burget DW, Hunt RH. Omeprazole (20mg) daily given in the morning or evening: a comparison of effects on gastric acidity, and plasma gastrin and omeprazole concentration. *Aliment Pharmacol Ther* 1992; **6:** 103-111

13 **Peghini PL,** Katz PO, Castell DO. Ranitidine controls nocturnal gastric acid breakthrough on omeprazole: a controlled study in normal subjects. *Gastroenterology* 1998; **115**: 1335-1339

14 **Xue S,** Katz PO, Banerjee P, Tutuian R, Castell DO. Bedtime H2 blockers improve nocturnal gastric acid control in GERD patients on proton pump inhibitors. *Aliment Pharmacol Ther* 2001; **15**: 1351-1356

15 **Fouad YM,** Katz PO, Castell DO. Oesophageal motility defects associated with nocturnal gastro-oesophageal reflux on proton pump inhibitors. *Aliment Pharmacol Ther* 1999; **13**: 1467-1471

16 **Wolfe MM,** Soll AH. The physiology of gastric acid secretion. *N Engl J Med* 1988; **319**: 1707-1715

17 **Katsube T,** Adachi K, Kawamura A, Amano K, Uchida Y, Watanabe M, Kinoshita Y. *Helicobacter pylori* infection influences nocturnal gastric acid breakthrough Aliment. *Pharmacol Ther* 2000; **14**: 1049-1056

18 **Katz PO,** Anderson C, Khoury R, Castell DO. Gastro-oesophageal reflux associated with nocturnal gastric acid breakthrough on proton pump inhibitors *Aliment Pharmacol Ther* 1998; **12**: 1231-1234

19 **Holtmann G.** Reflux disease: the disorder of the third millennium. *Eur J Gastroenterol Hepatol* 2001; **13**(Suppl 1): S5-S11

20 **Galmiche JP,** Blum A. Editorial. *Eur J Gastroenterol Hepatol* 2001; **13**(Suppl 1): S1-S13

21 **Kurosawa S.** Maintenance therapy of mild form of GERD by H2 receptor antagonists. *Nippon Rinsho* 2000; **58**: 1859-1864

22 **Orr WC,** Harnish MJ. Sleep-related gastro-oesophageal reflux: provocation with a late evening meal and treatment with acid suppression. *Aliment Pharmacol Ther* 1998; **12**: 1033-1038

23 **Gong J,** Zhang Q, Zhang Y, Zhu YL, Wang XQ, Luo JY. The study of rhythm of 24h gastric pH. *Xi'an Yike Daxue Xuebao* 1999; **20**: 326-328

24 **Brown TH,** Walton G, Cheadle WG, Larson GM. The alkaline shift in gastric pH after cholecystectomy. *Am J Surg* 1989; **157**: 58-65

25 **Bianco A,** Cagossi M, Piraccini R, Greco AV. Human duodenogastric reflux, retroperistalsis, and MMC. *Riv Eur Sci Med Farmacol* 1992; **14**: 281-291

26 **Ke MY**, Lan Y, Wang ZF, Xing JH. Character of 24-hour intragastric pH change in patients with functional dyspepsia. *Linchuang Xiao huabing Zazhi* 1995; **7**: 97

27 **Gong J,** Zhang R, Luo JY, Zhu YL, Wang XQ. The effect of bile reflux on the intragastric pH. *Xi'an Yike Daxue Xuebao* 2001; **22**: 25-27

28 **Dalenback J,** Abrahamson H, Bjornson E, Fandriks L, Mattsson A, Olbe L, Svennerholm A, Sjovall H. Human duodenogastric reflux, retroperistalsis and MMC. *Am J Physiol* 1998; **275**(3Pt2): R762-769

29 **Gong J,** Zhang R, Luo JY, Zhu YL, Wang XQ. A study on the etiology of the spontaneous nocturnal gastric alkalinization. *Xi'an Yike Daxue Xuebao* 2001; **22**: 230-232

30 **Bjornsson ES,** Abrahamsson H. Nocturnal antral pH rises are related to duodenal phase III retroperistalsis. *Dig Dis Sci* 1997; **42:**2432-2438

31 **Dai F,** Gong J, Zhang R, Luo JY, Zhu YL, Wang XQ. Assessment of duodenogastric reflux by combined continuous intragastric pH and bilirubin monitoring. *World J Gastroenterol* 2002; **8**: 382-384

32 **Bianco A,** Cagossi M, Piraccini R, Castrucci G, Greco AV. The nightly spontaneous alkalinization of the stomach. *Riv Eur Sci Med Farmacol* 1993; **15**: 17-27

33 **Bianco A,** Cagossi M, Piraccini R, Greco AV. Twenty-four-hour intragastric pH-metry: H_2-receptor antagonist restoration of nightly gastric spontaneous alkalinization in duodenal ulcer healing. *Riv Eur Sci Med Farmacol* 1992; **14**: 281-291

Edited by Zhao M and Wang XL

P.O.Box 2345, Beijing 100023,China
Fax: +86-10-85381893
E-mail: wjg@wjgnet.com www.wjgnet.com

World J Gastroenterol 2003;9(11):2587-2591
World Journal of Gastroenterology
 ISSN 1007-9327

• CLINICAL RESEARCH •

Long-term effect of stent placement in 115 patients with Budd-Chiari syndrome

Chun-Qing Zhang, Li-Na Fu, Lin Xu, Guo-Quan Zhang, Tao Jia, Ji-Yong Liu, Cheng-Yong Qin, Ju-Ren Zhu

Chun-Qing Zhang, Li-Na Fu, Lin Xu, Ji-Yong Liu, Cheng-Yong Qin, Ju-Ren Zhu, Department of Gastroenterology, Shandong Provincial Hospital, Jinan 250021, Shandong Province, China
Guo-Quan Zhang, Tao Jia, Department of Ultrasound, Shandong Provincial Hospital, Jinan 250021, Shandong Province, China
Correspondence to: Chun-Qing Zhang, M.D, Department of Gastroenterology, Shandong Provincial Hospital, Jinan 250021, Shandong Province, China. chunqing9@hotmail.com
Telephone: +86-531-7938911-2350
Received: 2002-11-06 **Accepted:** 2002-12-16

Abstract

AIM: To report the long-term effect of stent placement in 115 patients with Budd-Chiari syndrome (BCS).

METHODS: One hundred and fifteen patients with BCS were treated by percutaneous stent placement. One hundred and two patients had IVC stent placement, 30 patients had HV stent placement, 17 of them underwent both IVC stent and HV stent. All the procedures were performed with guidance of ultrasound.

RESULTS: The successful rates in placing IVC stent and HV stent were 94 % (96/102) and 87 % (26/30), respectively. Ninety-seven patients with 112 stents (90 IVC stents, 22 HV stents) were followed up. 96.7 %(87/90) IVC stents and 90.9 %(20/22) HV stents remained patent during follow up periods (mean 49 months, 45 months, respectively). Five of 112 stents in the 97 patients developed occlusion. Absence of anticoagulants after the procedure and types of obstruction (segmental and occlusive) before the procedure were related to a higher incidence of stent occlusion.

CONCLUSION: Patients with BCS caused by short length obstruction can be treated by IVC stent placement, HV stent placement or both IVC and HV stent placement depending on the sites of obstruction. The long-term effect is satisfactory. Anticoagulants are strongly recommended after the procedure especially for BCS patients caused by segmental occlusion.

Zhang CQ, Fu LN, Xu L, Zhang GQ, Jia T, Liu JY, Qin CY, Zhu JR. Long-term effect of stent placement in 115 patients with Budd-Chiari syndrome. *World J Gastroenterol* 2003; 9(11): 2587-2591
http://www.wjgnet.com/1007-9327/9/2587.asp

INTRODUCTION

Budd-Chiari syndrome (BCS) is characterized by obstruction of outflow in hepatic vein (HV) and inferior vena cava (IVC) leading to hepatomegaly, portal hypertension, impaired liver function, formation of communicating channel, and edema in lower extremities. Various patterns of vascular obstruction can be seen in BCS. The most common type in the orient is short length obstruction (membranous and segmental) in IVC and/or in the ostium of main hepatic vein (HV), and most of them are chronic and idiopathic[1-3]; whereas thrombotic obstruction is the the most common cause in Western country[4,5].

The optimal management of BCS is difficulty, surgical shunting has been recommended as the most appropriate choice to relieve symptoms in most instances[6,7]. But the long-term patency of these shunts varied with high morbidity and mortality[7-9]. Orthotopic liver transplantation has been used to treat BCS cases, but it was mainly for patients with fulminant hepatic failure caused by acute BCS and those with end stage of cirrhosis[10,11]. Recently, the transjugular intrahepatic portosystemic shunt (TIPS) has been reported as an effective therapeutic method for BCS[12,13]. But primary TIPS shunt dysfunction occurred in 60 % of patients with TIPS stent modifications, and angioplasties were required to keep a long-term patency[13,14].

With the development of percutaneous transluminal angioplasty (PTA) and stent placement in the 1990's, a pseudosurgical technique has been employed as an alternative to the major portosystemic shunts[15]. This procedure, applied by Furuil for the first time in a case of BCS in 1990[16], has shown beneficial results. Up to now, almost all of the reports were based on small numbers of patients without long-term follow-up. PTA and stent placement were limited to case report especially for patients with hepatic vein occlusion[17,18]. The role of these therapies in the overall management of BCS has not been clearly established.

From 1994, we have performed percutaneous IVC stent placement in 102 patients and HV stent placement in 30 patients with BCS, 17 out of 102 were treated with combined IVC and HV stent placement. Different from the other reports, all procedures were performed under ultrasound guidance instead of x-ray guidance. Our previous reports demonstrated the safety and advantages of IVC and/or HV stent placement under ultrasound guidance[19,20]. In this study, the long-term effects of stent placement in BCS were reported. The large series of patients enabled us to evaluate the outcome of stent placement and to establish protocol for management of BCS.

MATERIALS AND METHODS

Patients

From April 1994 to June 2001, 115 patients with BCS underwent stent placement in our hospital (All were performed by Dr. Chunqing). There were 65 males and 50 females. The average age was 37.3±12.7 years (SD, range 17-67). The duration of the illness ranged from 3 months to 17 years. Underlying etiological factors for BCS were identified in 5 patients. Two patients had a history of tuberculosis infection, 2 patients took oral contraceptives, 1 patient was pregnant. No patients were examined for the levels of antithrombin-III, protein C and protein S. The main clinical features are listed in Table 1 according to the site of obstruction (see below). Patients manifested mainly as abdominal fullness, weakness, hepato-splenomegaly and ascites.

All patients underwent gray-scal sonography and colour Doppler sonography prior to the stent placement. Ultrasound scanning could identify the site, degree and extent of obstruction of hepatic IVC and hepatic veins, while colour

Doppler could demonstrate the altered hemodynamic within the IVC and HV. In our early study only 11 patients underwent venography.

Based on the findings by ultrasound, colour Doppler and the subsequent probing of the lesions with a guide wire or a 5F-cathetor during the interventional procedure, the patients were divided into obstruction of inferior vena cava with at least one patent hepatic vein (IVC group, *n*=85 patients), obstruction of three main hepatic veins (HV group, *n*=13 patients), obstruction of both inferior vena cava and three main hepatic veins (Combined group, *n*=17 patients). IVC stent were placed in both IVC group and combined group (102 patients). HV stent placement were performed in both HV group and combined group (30 patients). Of the102 patients who underwent IVC stent placement, 49 patients had membranous obstruction, and 53 patients had IVC segmental obstruction (range 1.0-7.6 cm, Table 2). While in 30 patients who underwent HV stent placement, 17 patients had membranous obstruction in HV and 13 patients had segmental obstruction in HV(range 1-4 cm, Table 2).

During the same period, sonography did not reveal hepatic IVC and the main hepatic vein in 30 patients, patients with thrombosis below the obstruction were excluded from this study.

Table 1 Clinical features and choice of management in 115 patients with Budd-Chiari Syndrome

	Site of obstruction		
	IVC (*n*=85)	HV (*n*=13)	Combined (*n*=17)
Symptoms			
Abdominal fullness	79	13	17
Weakness	71	13	17
Abdominal pain	58	13	15
Low extremities edema	53	3	13
Gastrointestinal bleeding	9	4	8
Jaundice	5	4	7
Hepatic encephalopathy	3	2	3
Signs			
Hepatomegaly	80	13	17
Splenomegaly	77	13	17
Ascites	36	10	12
Distended abdominal veins	55	3	5
Leg ulcer	21	0	3
Management	IVC stent	HV stent	IVC and HV stent

Table 2 Types of obstruction in the IVC and HV in 115 patients

	Membraneous	Segmental (extent, cm)
IVC Stenosis (*n*=54)	30	24 (1-7.6)
Occlusion (*n*=48)	19	29 (1-7.2)
HV Stenosis (*n*=11)	6	5 (1-4.5)
Occlusion (*n*=19)	11	8 (1-4.0)

IVC=IVC group + combined group, HV=HV group + combined group.

Methods

All the procedures were performed under ultrasound guidance[19,20]. Before the procedure, all the patients were given cisapride 10 mg and pipemidic acid 0.5 three times daily for 3 days. They were fasted and asked to have bed rest for 12 hours to reduce intestinal tympanites and to keep a clear image of ultrasound. In patients with massive ascites, before the procedure a therapeutic paracentesis was performed followed by intravenous administration of albumin. The methods were approved by the ethic committee of our hospital.

IVC stent placements: Briefly, the transducer of ultrasound unit was positioned in the infrasternal angle to show the longitudinal axis of hepatic IVC, the lesion and interventional devices. Though the right femoral vein, a 14F sheath was advanced over a guide wire into the IVC. Echo contrast in 5-10 ml normal saline was injected through the sheath. The soft end of a guide wire or a 5F-catheter was then introduced to probe the lesion under US guidance. If the obstruction was incompletely, the guide wire could easily cross the narrowed part of IVC into the right atrium. For complete obstruction, an 8-F Teflon catheter and its appropriate metal cannula were inserted through the sheath and were pushed carefully into the occluded IVC. If necessary, a Brockenbrough needle was inserted to cut through the lesion. Once the catheter or the needle was placed into right atrium, its strong rebound echo could be shown on US and blood return could be obtained. Then, a balloon catheter with a 1.8-2.4 cm diameter was inserted to dilate the IVC. At the end, under US guidance, the stent (Gianturco stent, Jayu Medical Equipment, Shenyang, China) was pushed into the obstructive part of IVC where it could completely support the obstructive portion after deployment.

HV stent placement: The procedures were performed by percutaneous and transhepatic route. Under ultrasound guidance, a 16-gauge needle was inserted into the hepatic vein via either an intracostal (for right HV) or infrasternal (for middle and left HV) approach. Then over a guide wire, a 10F sheath was put into HV, and all other operations were done thought the sheath to prevent damage of hepatic parenchyma. In patients with partially obstructed HV, the guide wire could cross the entrance of hepatic vein into IVC and finally into the right atrium. Otherwise, a Brockenbrough needle was used to make a tract from the hepatic vein into IVC. Then, the obstructive hepatic vein was dilated by a 1.0-1.2 cm diameter balloon catheter, and a metallic stent (Giantureco Z stent or Wallstent, Jayu Medical Equipment, Shenyang, China) was placed through the 10F catheter to support the hepatic vein. At the end, the 10-F sheath was withdrawn under guidance of ultrasound, and pieces of gelatin sponge were placed over the sheath to plug the tract.

After the procedure, antibiotics were given to all patients. Intravenous heparin was given for for 1 week and followed by aspirin (75-100 mg per day) at least for 6 months to prevent stent thrombosis.

Follow-up

During the follow-up period, manifestations of BCS were evaluated and the liver function was valued, and Doppler duplex ultrasonography was obtained to assess patency of the stent and the hemodynamics in HV and IVC. All patients underwent these examinations before discharge, and then they were seen at 3-6 month intervals, or when they had recurrence of symptoms of BCS.

Statistical analysis

Results were expressed as mean ± SD, range or absolute numbers. Chi-square test, Wilcoxon' s, or Student' s *t* test was used. $P<0.05$ was considered statistically significant.

RESULTS

IVC stent placement

IVC stent was placed successfully in 94 %(95 /102) of patients (IVC group and HV group). The procedure failed in 6 patients (all in IVC group) with segmental occluded IVC (3-4 cm). Pericardial effusion occurred in 3 patients and inferior infarction in 1 patient during dilatation of the occluded IVC with balloon, the Brockenbrough needle failed to cut through

the hard occlusive segment of IVC in 2 patients. Stent migrated into right atrium in one patient who had mesoatrial shunt with the stent fixed to the wall of right atrium and no procedural death occurred.

Hemodynamic features in patients with successful stent placement improved significantly, the inferior vena cava pressure below the obstruction decreased from 29±12.7 cm H_2O to 11.5±7.3 cm H_2O (P<0.05), and satisfactory antegrade flow in IVC was observed with a normal flow spectrum in colour Doppler ultrasound. All patients in IVC group improved clinically. Ascites, hepatomegaly, lower extremity edema, and distended abdominal veins disappeared or diminished at discharge.

Seventy-nine patients in IVC group were followed for 12-84 months (mean 58 months). Four patients were lost in follow-up. Of the remaining 75 patients, 48 had no symptoms, 24 improved clinically, but they still had mild weakness or abdominal swelling on physical examination. On the latest follow up, 68 patients were employed or engaged in full house keeping (Table 3). Of the 17 patients in combined group, 2 were lost to follow-up, the other 15 patients had no symptoms of IVC obstruction.

Thirty-four of the 90 patients (75 in IVC group and 15 in combined group) were followed up for 5 years, 31 patients for 3 years, 25 patients for 1 year. Doppler ultrasonography showed that IVC stent was patent and worked effectively in 87 patients. The overall IVC stent patency rate was 96.6 % (87/90). Stent occlusion occurred in 3 patients at 12-24 months (mean 19 months) following stent placement, these 3 patients had recurrence of abdominal fullness and edema of lower extremity, and 1 patient had ascites. Two patients underwent caval-portal shunt and the others were treated with diuretics and anticoagulants.

Table 3 Long term results of Stent placement in 97 follow up patients

	IVC group	HV group	Combined group
Number of patients	75	7	15
Follow-up (months)			
Mean	49	45	45
Range	7-84	9-78	9-78
Ascites			
Before procedure	29	7	11
Disappeared	21	5	8
improved	7	2	3
Hepatomegaly			
Before procedure	73	7	15
Disappeared	38	3	6
Improved	33	3	7
Splenomegaly			
Before procedure	67	7	15
Disappeared	9	1	3
Improved	46	3	8
Abnormal liver function test			
Before procedure	53	7	15
Disappeared	21	3	4
Improved	29	3	9
Employed or housekeeping	68	6	14
Stent occlusion	3	1	1

HV stent placement

Hepatic vein stent was placed in 30 patients, including 13 patients in HV group and 17 in combined group. In HV group, the patients had hepatic vein stent placement alone, although some patients had narrowed IVC pressed by enlarged caudate lobe. In combined group, successful IVC stent placement resulted in disappearance of all symptoms of IVC obstruction. However, ascites, and hepatosplenomegaly were not alleviated. Therefore, hepatic vein stent was placed 1 week after IVC stent placement.

HV stent were successfully placed in 86.6 % (26/30) patients. Four patients in HV group failed due to a long occluded hepatic vein (3.0-3.5 cm), which was difficult to cut through. All but one of the 26 successful patients had hemodynamic improvement immediately after the procedure. HV pressure dropped from 36.5±16.4 cm H_2O to 12.7±9.5 cm H_2O and satisfactory antegrade flow was noted with a normal phasic flow spectrum in the stented HV. At the time of discharge, 10 patients were free of ascites, the massive ascites decreased without diuretics, and hepato-splenomegaly disappeared or diminished obviously in 25 patients.

Early stent occlusion occurred in one patient of HV group on the third day after the procedure, because the stent immigrated into the hepatic vein and the ostium of hepatic vein was not support by the stent. The patient was treated with repeated paracentesis, intravenous albumin, and a portocaval shunt. Severe haemorrhage from the unplugged transhepatic access occurred in one patient in our early study. Emergent surgical haemostasis was performed, and the patient survived well with a patent hepatic vein stent. One patient with peritonitis and ascitis was treated with paracentesis and parenteral antibiotics. Two patients experienced pleural effusion resolved within 2 weeks. No other major complications occurred.

During a mean follow-up period of 53 months (range 15-78 months), three patients missed the follow-up (1 in HV group, 2 in combined group). Of the 22 follow-up patients (7 in HV group, 15 in combined group), 7 patients were followed up for 5 years, 11 for 3 years, 4 for 1 year. Clinical symptoms and signs of BCS patients improved (Table 3). In these patients, ascites disappeared or decreased, hepatomegaly and splenomegaly were greatly alleviated or dissapeared. Periodic liver function tests were consistent normal or improved. Colour Doppler ultrasonography examinations demonstrated patency of the stents in hepatic vein in 20 patients. The overall HV stent patency rate was 90.9 % (20/22). All were gainfully employed and leading productive lives of good quality. One woman married, pregnant and delivered a healthy baby.

Ascites recurred in 1 patient in combined group at 6 months after the procedure, varices bleeding occurred in 1 patient in HV group at 12 months after the stent placement. Doppler ultrasonography confirmed the stent occlusion and dysfunction in 2 patients. One patient underwent mesocaval shunt, the other was treated with diuretics.

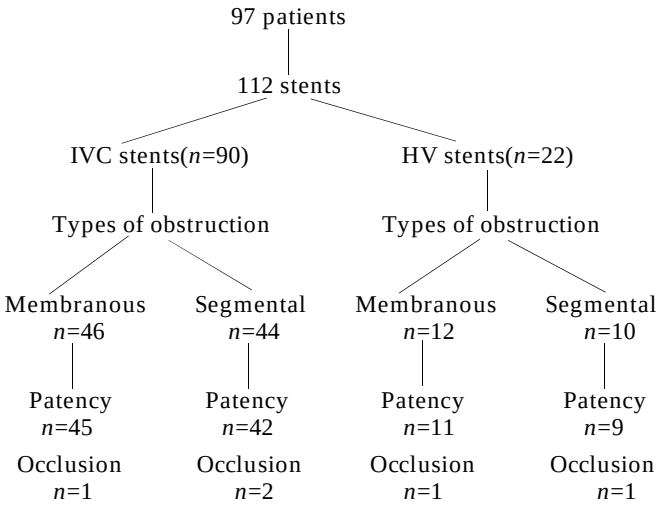

Table 4 The results of 112 stents in 97 follow patients.

Evaluation of risk of stent reocclusion

Of the 112 stents in 97 follow-up patients, occlusion was observed in 5 (4.5 %) stents (3 in IVC stents, 2 in HV stents) (Table 4). Risks of stent occlusion were evaluated (Table 5), and stent occlusion in HV stents (9.1 %) was more common than that in IVC stents (3.3 %) ($P<0.05$). Absence of long-term anticoagulants was related to stent occlusion, stent occlusion was observed in 3 out of 25 (12 %) stents in patients without anticoagulant therapy *versus* 2 of 87 (2.3 %) stents in patients with at least 6 months of anticoagulants for.

No significant difference was found between stent occlusion and severity of obstruction (Table 5). Stent occlusion occurred in 11 % (3/27) patients with segmental obstruction and occlusion *versus* 2.9 % (1/34) patients without them, the difference was significant ($P<0.05$).

Table 5 Analysis of factors influencing stent occlusion in 112 stents of 97 patients

	Number of stents	Number of occlusion	*P* valve
Total	112	5	
Site of stents			
IVC	90	3	
HV	22	2	<0.05
Degrees of obstruction			
Stenosis	60	2	
Occlusion	52	3	>0.05
Types of obstructon			
Membraneous	58	2	
Segmental	54	3	>0.05
Anticoagulants at least 6 months			
Yes	87	2	
No	25	3	<0.05

DISCUSSION

Since the location, extent and rapidity of venous obstruction are highly variable, a range of clinical presentations necessitates an individualized therapeutic strategy. The management of BCS has traditionally been classified as medical, surgical and radical. Conventional medical therapy with diuretics and anticoagulation has been reported to be of limited value in relieving hepatic venous outflow obstruction[21]. The use of fibrinolytic therapy might be of benefit for patients at early stage of acute thrombosis[23]. Surgical treatment was the most frequently reported approach for BCS[6,7]. When venous obstruction is limited to the main HV without serious involvement of IVC, a portacaval shunt or a mesocaval shunt is proposed. In cases of BCS complicated with obstruction of IVC, the mesoatrial shunt may be used to allow the portal flow to drain directly into the right atrium. Liver transplantation as the second surgical option for BCS was indicated for BCS in acute or chronic liver failure in the Western world[23,24]. Radiological interventions including balloon angioplasty, stent insertion and transjugular intrahepatic portosystemic shunts have been shown to be effective for selected patients with BCS during the past 10 years[11,25], but these results were confined to small series of patients with short term follow up.

In this series, all BCS patients were caused by short length obstruction of the hepatic IVC and/or of the main HV. Most patients were chronic and idiopathic. Our series was the largest report to date for the use of stent placement in BCS. The results demonstrated the long-term efficacy of stent placement for BCS.

In this series, stent placement was performed based on the locations of vascular obstruction.

IVC obstruction with short length lesion was a common cause for BCS in the Eastern countries including China[2,3,26]. Although balloon angioplasty has been regarded as the first choice for patients with IVC obstruction, restenosis and redilitation was reported[2,27], even in patients with membranous obstruction[28]. In our study, the residual membrane in most cases was often pushed back into the lumen of IVC once the balloon catheter moved back. This might be a cause of reccurrence of BCS. Therefore, stents were placed in the restricted part in all patients whether the lesion was a membraneous or a segmental obstruction. During a period of 12-84 months follow-up, 87 out of 90 (96.7 %) IVC stents remained patent and functioned well, the manifestions of BCS disappeared or improved in all the patients. The results demonstrate that IVC stent placement is effective and reliable in management of BCS and has a satisfactory long-term patency.

HV obstructon was one of the main causes of BCS, both in Eastern and in Western countries[2,29]. However, treatment of HV obstruction has been challenging. Usually the hepatic vein angioplasty or stent were performed under x-ray guidance via the jugular vein or both transhepatic and jugular veins. Under this condition, the ostium of hepatic vein could not be revealed directly. Thus, it was very difficult to cut through the occluded orifice of the hepatic vein from the vena cava, cardiac perforation or IVC rupture was reported during the procedure[30,31]. Up to now, reports on treatment on HV obstruction were limited with a small number of patients, and its successful rate was low[2,25]. We performed percutanous hepatic vein recanalization, dilation and stent placement in 26 out of 30 patients with a success rate of 86.7 %. This was a report involving the treatment of BCS with short length hepatic vein obstruction. All the patients had three obstructed hepatic veins, we chose to place stent in one of them. By intrahepatic communicating channels of hepatic veins, the stent was sufficient to drain the entire liver. During a period of 15-78 months follow-up, 90.9 % (20/22) patients had patent stents, the clinical manifestations of BCS improved obviously or disappeared. The long term stent patency was rather good compared with PTA of hepatic vein that had a high incidence of restenosis[31]. In our study, percutanous trashepatic hepatic vein stent placement was the first choice in the treatment of BCS caused by short length hepatic vein obstruction.

For the treatment of HV obstruction, percutanous transhepatic route was safe if the tract was plugged with gelatin sponge before removal of the sheath. Patients with short length HV obstruction should be treated by stent placement instead of simple angioplasty, because hepatic vein webs were more likely to restenose compared with caval webs following angioplasty[31]. Performance under ultrasound guidance contributed to a high success rate and low morbidity, reducing intestinal tympanites and ascites before the procedure was necessary for a clean image of ultrasound.

Combined IVC and HV obstruction was a special kind of BCS consisting of 15 % of our patients. Management of these patients was usually difficult[2,6,7]. When the procedures were divided into 2 steps, the treatment became simple. In 17 patients, the IVC stent were placed first, and the HV stent was placed one week later. During a long-term follow-up, only one patient developed HV stent occlusion, and all IVC stents worked well. The results showed that the combined procedure was an advisable choice for BCS patients with both IVC and HV obstruction.

The total stent occlusion rate was 4.5 % during the follow-up. The long term results were satisfactory. The stent occlusion was more likely to occurred in BCS patients with segmental and occluded obstruction than in patients with membraneous and stenosis obstruction, the stent occlusion rate was higher in patients without anticoagulants after operation than that in

patients with anticoagulants at least for 6 months. Stent occlusion occurred more likely at HV (9.1 %) than at IVC (3.3 %). Therefore, we suggest that anticoagulants should be used routinely after the procedure, especially for patients with segmental and occluded obstruction, and for patients having HV stent placement.

In conclusion, IVC and HV stents or combined IVC and HV stent can be applied to BCS patients with short length obstruction depending on the sites of obstruction. The stents can be placed under ultrasound guidance with a high successful rate and a low morbidity. Excellent long-term results can be obtained in IVC and HV stents as well as in combined stents. Anticoagulants are strongly recommended for at least 6 months after the procedure.

REFERENCES

1 **Okuda H**, Yamagata H, Obata H, Iwata H, Sasaki R, Imai F, Okudaira M, Ohbu M, Okuda K. Epidemiological and clinical features of Budd-Chiari syndrome in Japan. *J Hepatol* 1995; **22**: 1-9

2 **Kohli V**, Pande GK, Dev V, Reddy KS, Kaul U, Nundy S. Management of hepatic venous outflow obstruction. *Lancet* 1993; **18**: 718-722

3 **Dilawari JB**, Bambery P, Chawla Y, Kaur U, Bhusnurmath SR, Malhotra HS, Sood GK, Mitra SK, Khanna SK, Walia BS. Hepatic outflow obstruction (Budd-Chiari syndrome). Experience with 177 patients and a review of the literature. *Medicine (Baltimore)* 1994; **73**: 21-36

4 **Mahmoud AE**, Mendoza A, Meshikhes AN, Olliff S, West R, Neuberger J, Buckels J, Wilde J, Elias E. Clinical spectrum, investigations and treatment of Budd-Chiari syndrome. *QJM* 1996; **89**: 37-43

5 **Mitchell MC**, Boitnott JK, Kaufman S, Cameron JL, Maddrey WC. Budd-Chiari syndrome: etiology, diagnosis and management. *Medicine (Baltimore)* 1982; **61**: 199-218

6 **Slakey DP**, Klein AS, Venbrux AC, Cameron JL. Budd-Chiari syndrome: current management options. *Ann Surg* 2001; **233**: 522-527

7 **Orloff MJ**, Daily PO, Orloff SL, Girard B, Orloff MS. A 27-year experience with surgical treatment of Budd-Chiari syndrome. *Ann Surg* 2000; **232**: 340-352

8 **Panis Y**, Belghiti J, Valla D, Benhamou JP, Fekete F. Portosystemic shunt in Budd-Chiari syndrome: long-term survival and factors affecting shunt patency in 25 patients in Western countries. *Surgery* 1994; **115**: 276-281

9 **Bismuth H**, Sherlock DJ. Portasystemic shunting versus liver transplantation for the Budd-Chiari syndrome. *Ann Surg* 1991; **214**: 581-589

10 **Klein AS**, Sitzmann JV, Coleman J, Herlong FH, Cameron JL. Current management of the Budd-Chiari syndrome. *Ann Surg* 1990; **212**: 144-149

11 **Tilanus HW**. Budd-Chiari syndrome. *Br J Surg* 1995; **82**: 1023-1030

12 **Ganger DR**, Klapman JB, McDonald V, Matalon TA, Kaur S, Rosenblate H, Kane R, Saker M, Jensen DM. Transjugular intrahepatic portosystemic shunt (TIPS) for Budd-Chiari syndrome or portal vein thrombosis: review of indications and problems. *Am J Gastroenterol* 1999; **94**: 603-608

13 **Perello A**, Garcia-Pagan JC, Gilabert R, Suarez Y, Moitinho E, Cervantes F, Reverter JC, Escorsell A, Bosch J, Rodes J. TIPS is a useful long-term derivative therapy for patients with Budd-Chiari syndrome uncontrolled by medical therapy. *Hepatology* 2002; **35**: 132-139

14 **Cejna M**, Peck-Radosavljevic M, Schoder M, Thurnher S, Bassalamah A, Angermayr B, Kaserer K, Pokrajac B, Lammer J. Repeat interventions for maintenance of transjugular intrahepatic portosystemic shunt function in patients with budd-Chiari syndrome. *J Vasc Interv Radiol* 2002; **13**: 193-199

15 **Carrasco CH**, Charnsangavej C, Wright KC, Wallace S, Gianturco C. Use of the Gianturco self-expanding stent in stenoses of the superior and inferior venae cavae. *J Vasc Interv Radiol* 1992; **3**: 409-419

16 **Furui S**, Sawada S, Irie T, Makita K, Yamauchi T, Kusano S, Ibukuro K, Nakamura H, Takenaka E. Hepatic inferior vena cava obstruction: treatment of two types with Gianturco expandable metallic stents. *Radiology* 1990; **176**: 665-670

17 **Weernink EE**, Huisman AB, ten Napel CH. Treatment of Budd-Chiari syndrome by insertion of wall-stent in hepatic vein. *Lancet* 1991; **338**: 644

18 **Dolmatch BL**, Cooper BS, Chang PP, Gray RJ, Horton KM. Percutaneous hepatic venous reanastomosis in a patient with Budd-Chiari syndrome. *Cardiovasc Intervent Radiol* 1995; **18**: 46-49

19 **Zhang C**, Fu L, Zhang G, Xu L, Shun H, Wang Z, Zhu J. Ultrasonically guided inferior vena cava stent placement: experience in 83 cases. *J Vasc Interv Radiol* 1999; **10**: 85-91

20 **Chunqing Z**, Lina F, Guoquan Z, Lin X, Zhaohai W, Tao J, Chengyong Q, Juzhen Z. Ultrasonically guided percutaneous transhepatic hepatic vein stent placement for Budd-Chiari syndrome. *J Vasc Interv Radiol* 1999; **10**: 933-940

21 **McCarthy PM**, van Heerden JA, Adson MA, Schafer LW, Wiesner RH. The Budd-Chiari syndrome. Medical and surgical management of 30 patients. *Arch Surg* 1985; **120**: 657-662

22 **Mitchell MC**, Boitnott JK, Kaufman S, Cameron JL, Maddrey WC. Budd-Chiari syndrome: etiology, diagnosis and management. *Medicine (Baltimore)* 1982; **61**: 199-218

23 **Hemming AW**, Langer B, Greig P, Taylor BR, Adams R, Heathcote EJ. Treatment of Budd-Chiari syndrome with portosystemic shunt or liver transplantation. *Am J Surg* 1996; **171**: 176-180

24 **Rao AR**, Chui AK, Gurkhan A, Shi LW, Al-Harbi I, Waugh R, Verran DJ, McCaughan GW, Koorey D, Sheil AG. Orthotopic liver transplantation for treatment of patients with Budd-Chiari syndrome: a Singe-center experience. *Transplant Proc* 2000; **32**: 2206-2207

25 **Pisani-Ceretti A**, Intra M, Prestipino F, Ballarini C, Cordovana A, Santambrogio R, Spina GP. Surgical and radiologic treatment of primary Budd-Chiari syndrome. *World J Surg* 1998; **22**: 48-53

26 **Singh V**, Sinha SK, Nain CK, Bambery P, Kaur U, Verma S, Chawla YK, Singh K. Budd-Chiari syndrome: our experience of 71 patients. *J Gastroenterol Hepatol* 2000; **15**: 550-554

27 **De BK**, Biswas PK, Sen S, Das D, De KK, Das U, Mandal SK, Majumdar D. Management of the Budd-Chiari syndrome by balloon cavoplasty. *Indian J Gastroenterol* 2001; **20**: 151-154

28 **Hung WC**, Fang CY, Wu CJ, Lo PH, Hung JS. Successful metallic stent placement for recurrent stenosis after balloon angioplasty of membranous obstruction of inferior vena cava. *Jpn Heart J* 2001; **42**: 519-523

29 **Valla D**, Hadengue A, el Younsi M, Azar N, Zeitoun G, Boudet MJ, Molas G, Belghiti J, Erlinger S, Hay JM, Benhamou JP. Hepatic venous outflow block caused by short-length hepatic vein stenoses. *Hepatology* 1997; **25**: 814-819

30 **Lois JF**, Hartzman S, McGlade CT, Gomes AS, Grant EC, Berquist W, Perrella RR, Busuttil RW. Budd-Chiari syndrome: treatment with percutaneous transhepatic recanalization and dilation. *Radiology* 1989; **170**: 791-793

31 **Fisher NC**, McCafferty I, Dolapci M, Wali M, Buckels JA, Olliff SP, Elias E. Managing Budd-Chiari syndrome: a retrospective review of percutaneous hepatic vein angioplasty and surgical shunting. *Gut* 1999; **44**: 568-574

Edited by Ren SL and Wang XL

P.O.Box 2345, Beijing 100023,China
Fax: +86-10-85381893
E-mail: wjg@wjgnet.com www.wjgnet.com

World J Gastroenterol 2003;9(11):2592-2595
World Journal of Gastroenterology
 ISSN 1007-9327

• CLINICAL RESEARCH •

Detection of type IV collagenase activity in malignant ascites

Xiao-Min Sun, Wei-Guo Dong, Bao-Ping Yu, He-Sheng Luo, Jie-Ping Yu

Xiao-Min Sun, Wei-Guo Dong, Bao-Ping Yu, He-Sheng Luo, Jie-Ping Yu, Department of Gastroenterology, Renmin Hospital, Wuhan University, Wuhan 430060, Hubei Province, China
Supported by the Natural Science Foundation of Hubei Province, No. 99J163
Correspondence to: Dr. Wei-Guo Dong, Department of Gastroenterology, Renmin Hospital, Wuhan University, Wuhan 430060, Hubei Province, China. dongwg@public.wh.hb.cn
Telephone: +86-27-88041911 **Fax:** +86-27-88042292
Received: 2003-05-11 **Accepted:** 2003-06-02

Abstract

AIM: Type IV collagenase participates in invasion and metastasis of cancer cells. Malignant ascites is a manifestation of advanced malignant disease that is associated with invasion and metastasis of the peritoneal cavity. Thus, it is reasonable to hypothesize that type IV collagenase is linked to malignant ascites. The purpose of our study was to detect type IV collagenase activity in malignant ascites so as to provide the scientific basis for clinic diagnosis and treatment of malignant ascites.

METHODS: Cirrhotic ascites (n=36), tuberculous ascites (n=8) and malignant ascites (n=23) from patients with gastric cancer (n=6), colon cancer (n=5), ovarian cancer (n=8) and other cancers (n=4), including 2 hepatocellular cancers, 1 pancreatic cancer, 1 primary peritoneal carcinoma were collected by paracentesis. The ascites were made cell-free by centrifugation and stored frozen at -70 ℃ before determination. Type IV collagenase activity was determined by gelatin zymography.

RESULTS: The activity of matrix metalloproteinases-2 and -9 could not be detected in ascites of hepatic cirrhosis and tuberculous peritonitis but could be detected in 20 and 18 out of 23 malignant ascites respectively. The positive rate of type IV collagenase (MMP-2, 87.0 % and MMP-9, 78.3 %) was higher than that by routine ascites tests (P<0.01) in malignant ascites. Furthermore, the activity of MMP-2 was higher than that of MMP-9 (P=0.022<0.05).

CONCLUSION: Type IV collagenase is positive in malignant ascites. Detection of type IV collagenase activity is useful in qualitative diagnosis of ascites. Type IV collagenase may play an important role in malignant ascites formation.

Sun XM, Dong WG, Yu BP, Luo HS, Yu JP. Detection of type IV collagenase activity in malignant ascites. *World J Gastroenterol* 2003; 9(11): 2592-2595
http://www.wjgnet.com/1007-9327/9/2592.asp

INTRODUCTION

Although tumor invasion and metastasis are considered to be a dynamic, complex and multi-step process, proteolytic degradation of the extracellular matrix (ECM) made of interstitial matrix and basement membrane is the essential step[1-4]. The basement membrane, a specialized ECM containing large amounts of type IV collagen and laminin, serves a barrier function separating epithelial cells from the underlying stroma. For the occurrence of metastasis, a tumor cell must repeatedly cross this basement membrane barrier, a process for which proteolysis of ECM components is required[5,6]. It is reasonable to hypothesize that proteolysis of ECM also plays a key role in intraperitoneal metastasis of tumor cells, such as in disruption of the mesothelial cell layer, during extension of the implanted tumor through the submesothelial basement membrane into the visceral organ stroma, and importantly, in gaining access to the host vascular supply, a necessary step in progression of the implant.

In disruption of the ECM, the contribution of matrix metalloproteinases (MMPs) of proteolytic enzymes is direct and important in that it catalyzes the hydrolysis of numerous ECM molecules[7-11]. While in the matrix metalloproteinase, type IV collagenase, one of the most important members of MPPs family, including a 72 kD enzyme resembling matrix metalloproteinase-2 (MMP-2), also named gelatinase A and a 92 kD enzyme resembling matrix metalloproteinase-9 (MMP-9), also named gelatinase B, has been demonstrated to be closely associated with several tumor systems and linked to invasive potential of tumor cells[12-16]. Type IV collagenase can degrade not only interstitial matrix, but also basement membrane, and malignant ascites is the direct and prominent manifestation of advanced malignant disease that is associated with invasion and metastasis of peritoneal cavity by tumor cells. Thus it is possible and feasible to detect type IV collagenase in malignant ascites. In the present study, we detected type IV collagenase activity in various kinds of ascites by gelatin zymography so as to explore the relationship between type IV collagenase and malignant ascites, and to provide the scientific basis for clinic diagnosis and treatment of malignant ascites.

MATERIALS AND METHODS

Reagents and instruments

The common reagents and principal apparatus used in SDS-PAGE were provided by the Biochemical Laboratory, Medical College, Wuhan University. Gelatin was purchased from Sigma Co. Type IV collagenase was the product of Invitrogen. Matrix metalloproteinase inhibitor, 1,10-phenanthroline, was purchased from Sangon, Shanghai, China.

Clinical specimems

Sixty-seven inpatients with ascites were recruited respectively at Renmin Hospital of Wuhan University, Zhongnan Hospital of Wuhan University and Tumor Hospital of Hubei Province from July 2002 to March 2003. The ascites were obtained by therapeutic or diagnostic paracentesis. In all cases, informed consent of the patient and approval of the hospital were obtained prior to collection of ascites and medical records. All the diagnoses were confirmed by cytologic examination of the ascites, biopsy for pathological examination, B-ultrasound and CT scan. Details of the patient data are shown in Table 1. The ascites were made cell-free by centrifugation at 3 000 rpm for 15 min and stored frozen at -70 ℃ before determination. At the same time, the protein content of the ascites was measured.

Table 1 Patient data

Characteristics	*n*
Number of patients	67
Male	38
Female	29
Median age (y)	
Male	50.68
Female	48.60
Disease categories	
Cirrhotic ascites	36
Tuberculous ascites	8
Malignant ascites	23
Ovarian cancer	8
Gastric cancer	6
Colon cancer	5
Hepatocellular cancer	2
Pancreatic cancer	1
Primary peritoneal carcinoma	1

Sodium dodecyl sulfate-polyacrylamide gel electrophoresis (SDS-PAGE) zymography

Samples were analyzed by SDS-PAGE zymography according to the method of Kleiner and settler-Stevenson[17] to determine the molecular weights and relative abundance of the gelatinases present. Samples containing 70 μg of protein were incubated for 40 min at 37 ℃ and electrophoresed without reduction (no DTT) on 8 % SDS polyacrylamide gels copolymerized with 0.1 % gelatin. Electrophoresis was performed at 4 ℃ at a constant current of 20 mA. When the tracking dye at the front reached the bottom of the gel, the gel was removed and shaken gently for 45 min in 2.5 % Triton x-100 to remove SDS. Then, the gel slabs were transferred to a bath (without Triton x-100) and washed for 20 min to remove Triton x-100. The above operation was repeated twice both at 4 ℃. Next, the gels were incubated and shaken for 60 h in 0.1 mol/L glycine, 50 mmol/L Tris-HCl, 5 mmol/L $CaCl_2$, 1 μmol/L $ZnCl_2$, 0.5 mol/L NaCl, pH 8.3 , at 37 ℃. At last, following staining with 0.075 % Coomassie blue for 3 h, regions of proteolytic activity were visualized as clear zones against a blue background. Gelatinolytic bands were assessed for semiquantitative analysis using an arbitrarily graded scale. Scale categories were defined as follows: +/-, faint band detected, <1.0 mm in width: 1+, clear band detected, 1.0-1.5 mm in width: 2+, intense band detected, 1.5-3.0 mm in width.

Matrix metalloproteinase inhibition test[18]

In order to verify that the clear zones resembled matrix metalloproteinase, 2.5 mmol/L 1,10- phenanthroline was added into the samples before electrophoresis to inhibit matrix metalloproteinase activities.

Detection of LDH, cytologic examination of ascites and serum complex index

Detection of LDH, cytologic examination of ascites and serum complex index were performed by the Department of Clinical Laboratory and Pathology.

Statistical analysis

Chi-square test and Fisher' s exact probabilities test were used for statistical analysis. Differences were considered significant when *P* value was less than 0.05.

RESULTS

Metalloproteinase inhibition test

Except that when 2.5 mmol/L 1,10-phenanthroline was added to the sample prior to electrophoresis, the result of electrophoresis for the identical samples was negative, indicating what we had detected was matrix metalloproteinase (Figure 1).

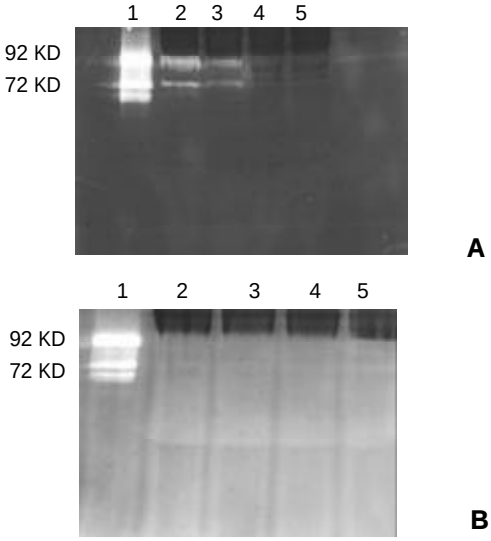

Figure 1 Results of SDS-PAGE zymography. A, Lane 1: type IV collagenase as marker, Lanes 2, 3: cancerous ascites, Lane 4: cirrhotic ascites (no bright bands), Lane 5: tuberculous ascites (no bright bands). B, Lane 1: Marker, Lanes 2-5: identical samples with A, except the addition of 2.5 mmol/L 1,10-phenanthroline. The result was negative.

Qualitative analysis of type IV collagenase activity in various kinds of ascites

Type IV collagenase activity could not be detected in ascites of hepatic cirrhosis and tuberculous peritonitis but could be detected in majority of malignant ascites (Table 2, Figure 1A).

Table 2 Qualitative analysis of type IV collagenase activity in various kinds of ascites

Ascites type	MMP-2 (Positive cases)	MMP-9 (Positive cases)
Cirrhotic ascites	0	0
Tuberculous ascites	0	0
Malignant ascites	20	18
Gastric cancer	5	5
Colon cancer	3	5
Hepatocellular cancer	2	1
Pancreatic cancer	1	0
Ovarian cancer	8	6
Primary peritoneal carcinoma	1	1

Table 3 Semi-quantitative analysis of MMP-2, MMP-9 activity in different kinds of malignant ascites

Type	Case (*n*)	MMP-2 activity (*n*)			MMP-9 activity (*n*)		
		+/-	1+	2+	+/-	1+	2+
Gastric cancer	6	1	4	0	3	2	0
Colon cancer	5	1	2	0	4	1	0
Hepatocellular cancer	2	1	1	0	0	1	0
Pancreatic cancer	1	0	1	0	0	0	0
Ovarian cancer	8	1	5	2	3	1	2
Primary peritoneal carcinoma	1	0	0	1	0	0	1

+/-, faint band detected, <1.0 mm in width; 1+, clear band detected, 1.0-1.5 mm in width; 2+, intense band detected, 1.5-3.0 mm in width.

Table 4 Comparison of detection of type IV collagenase and other indexes in malignant ascites

	Type IV collagenase		LDH in ascites / serum LDH (>1: positive)	Cytologic examination	Serum complex indexes (AFP, CEA, CA)
	MMP-2	MMP-9			
Positive numbers	20	18	10	11	13
Positive rates	87.0 %	78.3 %	43.4 %	47.8 %	56.5 %

Semi-quantitative analysis of type IV collagenase in different kind of cancerous ascites

Gelatinolytic bands were assessed for semiquantitative analysis using an arbitrary grade scale as described in Materials and Methods. The 72 kD MMP-2 was detected in 87.0 % of malignant ascites (n=23), with 80.0 % being scaled >1+; and the 92 kD MMP-9 was found in 78.3 %, with 44.4 % scaled >1+. The activity of MMP-2 was higher than that of MMP-9 ($0.01<P=0.022<0.05$). Additionally, three cases had the highest type IV collagenase activity (2+) for MMP-2 and MMP-9 respectively. Both included one primary peritoneal carcinoma, and two ovarian cancers (Table 3).

Comparison of detection of type IV collagenase and other indexes in malignant ascites

In 23 cases of carcinoma ascites, MMP-2 was found in 20 (87.0 %), significantly higher than that by routine ascites tests (including LDH, cytologic examination of ascites and complex indexes in serum) ($P<0.01$, respectively). MMP-9 was detected in 18 (78.3 %), higher than that by LDH and cytologic examination. However, compared with the two detection methods of type IV collagenase and serum complex indexes, there was no significant difference ($P>0.05$) (Table 4).

DISCUSSION

Type IV collagenase is closely linked with malignant ascites

Overexpression of type IV collagenase has been demonstrated in a variety of cancers, including colorectal cancer, gastric cancer, and breast cancer. Substantial evidences indicate that type IV collagenase activity or concentration was increased in plasma of patients with advanced carcinoma[19-24]. Recently, some researches found that type IV collagenase activity was increased in urine of patients with metastatic breast cancers[25,26] and in cerebrospinal fluid of patients with brain tumors[27]. However, few reports on type IV collagenase activity in ascites could be seen[18,21]. In the present study, we found that type IV collagenase activity could not be detected in ascites of hepatic cirrhosis and tuberculous peritonitis but could be detected in malignant ascites. At the same time, MMP-2 activity was higher than MMP-9 activity in malignant ascites, which might be attributed to the difference of expression of MMP-2 and MMP-9 in ascites of different kinds of tumor. Furthermore, the detection rate of type IV collagenase in ascites of malignant tumor was higher than that by routine ascites tests. Additionally, 2 out of 4 unidentified cases of ascites were identified by peritoneal biopsy. One was metastatic ovarian cancer, the other was primary peritoneal carcinoma. In these two cases, the activity of MMP-2 and MMP-9 was positive, and scale categories all exceeded 1+. Another 2 cases, gastric cancer and colon cancer, were identified by gastroscopy and colonoscopy respectively. The activity of MMP-2 and MMP-9 in these 2 cases was positive also. It was suggested that the peritoneal implants of tumors might secrete type IV collagenase (MMP-2 and/or MMP-9) into peritoneal cavity. Type IV collagenase activity in ascites reflects tumor biological behavior to some extent and is related with malignant ascites. So detection of type IV collagenase activity may probably provide a new approach with high sensitivity and specificity for differential diagnosis of benign and malignant ascites.

Type IV collagenase is correlated with malignant ascites formation

Some reports demonstrated that MMPs played a key role in intraperitoneal metastasis[21]. Others found metalloproteinase inhibitor could reduce ascites in patients with advanced malignant disease[28-30]. Our experiments indicated no expression of type IV collagenase in nonmalignant ascites. On the contrary, majority of malignant ascites showed higher activity of type IV collagenase. Thus, it is reasonable to infer that type IV collagenase is associated with malignant ascites formation to some extent. The probable mechanism of inducing malignant ascites formation by type IV collagenase may be explained as follows[31-37]: breakdown of apparent physical barriers to metastasis of peritoneal cavity, role of MMPs in angiogenesis, formation of new blood vessels which increases overall capillary membrane surface available for fluid filtration, inducing fluid accumulation. These new observations indicate that use of metalloproteinase inhibitors may offer a novel treatment of malignant ascites.

ACKNOWLEDGEMENTS

The authors are grateful to teachers of the Biochemical Laboratory, Medical College, Wuhan University, especially Xiao-Ming Li, Hong Yu and Chun-Yan He, and thank Dr. Hui-Lan Lu from the Department of Clinical Laboratory for their suggestions, advice, and cooperation in this study.

REFERENCES

1 **Meyer T**, Hart IR. Mechanisms of tumor metastasis. *Eur J Cancer* 1998; **34**: 214-221
2 **Kleiner DE**, Stetler-Stevenson WG. Matrix metalloproteinases and metastasis. *Cancer Chemother Pharmacol* 1999; **43**: S42-51
3 **Conway JG**, Trexler SJ, Wakefield JA, Marron BE, Emerson DL, Bickett DM, Deaton DN, Garrison D, Elder M, McElroy A, Willmott N, Dockerty AJ, McGeehan GM. Effect of matrix metalloproteinase inhibitors on tumor growth and spontaneous metastasis. *Clin Exp Metastasis* 1996; **14**: 115-124
4 **Heppner KJ**, Matrisian LM, Jensen RA, Rodaers WH. Expression of most matrix metalloproteinase family members in breast cancer represents a tumor-induced host response. *Am J Pathol* 1996; **149**: 273-282
5 **Ara T**, Fukuzawa M, Kusafuka T, Komoto Y, Oue T, Inoue M, Okada A. Immunohistochemical expression of MMP-2, MMP-9, and TIMP-2 in neuroblastoma: Association with tumor progression and clinical outcome. *J Pediatr Surg* 1998; **33**: 1272-1278
6 **Ellenrieder V**, Alber B, Lacher U, Hendler SF, Menke A, Boeck W, Wagner M, Wilda M, Friess H, Buchler M, Adler G, Gress TM. Role of MT-MMPs and MMP-2 in pancreatic cancer progression. *In J Cancer* 2000; **85**: 14-20
7 **Stracke JO**, Hutton M, Stewart M, Pendas AM, Smith B, Lopez-Otin C, Murophy G, Knauper V. Biochemical characterization of the catalytic domain of human matrix metalloproteinase 19. Evidence for a role as a potent basement membrane degrading enzyme. *J Biol Chem* 2000; **275**: 14809-14816
8 **Uria JA**, Lopez-Otin C. Matrilysin-2, a new matrix metalloproteinase expressed in human tumors and showing the minimal organization required for secretion, latency, and activity. *Cancer Res* 2000; **60**: 4745-4751
9 **Stock UA**, Wiederschain D, Kilroy SM, Shum-Tim D, Khalil PN,

Vacanti JP, Mayer Jr JE, Moses MA. Dynamics of extracellular matrix production and turnover in tissue engineered cardiovascular structures. *J Cell Biochem* 2001; **81**: 220-228

10 **Lauer-Fields JL**, Tuzinski KA, Shimokawa K, Nagase H, Fields GB. Hydrolysis of triple-helical collagen peptide models by matrix metalloproteinases. *J Biol Chem* 2000; **275**: 13282-13290

11 **Jiang ZS**, Gao Y. Biological feature of matrix metalloproteinase and its action in metastasis of liver cancer. *Shijie Huaren Xiaohua Zazhi* 2000; **8**: 1403-1404

12 **Wang ZN**, Xu HM. Relationship between collagen IV expression and biological behavior of gastric cancer. *World J Gastroenterol* 2000; **6**: 438-439

13 **Ji F**, Wang WL, Yang ZL, Li YM, Huang HD, Chen WD. Study on the expression of matrix metalloproteinase-2mrna in human gastric cancer. *World J Gastroenterol* 1999; **5**: 455-457

14 **He YD**, Zhao YW, Kong LF, Yin PZ. Activity alternating of matrix metalloproteinase-2 in hepatocellular carcinoma. *Shijie Huaren Xiaohua Zazhi* 2000; **8**: 952-953

15 **Tryggvason K**, Hoyhtya M, Pyke C. Type IV collagenases in invasive tumors. *Breast Cancer Res Treat* 1993; **24**: 209-218

16 **Zhu ZY**, Du Z, Wang YJ, Zhang W, Sun BC. Examination of E-cadherin and matrix metalloproteinases and its significance in primary HCC. *Shijie Huaren Xiaohua Zazhi* 2001; **9**: 839-840

17 **Kleiner DE**, Stetler-Stevenson WG. Quantitative zymography: detection of picogram quantities of gelatinases. *Anal Biochem* 1994; **218**: 325-329

18 **Young TN**, Rodriguze GC, Rinehart AR, Bast RC Jr, Pizzo SV, Stack MS. Characterization of gelatinases linked to extracellular matrix invasion in ovarian adenocarcinoma: purification of matrix metalloproteinase 2. *Gynecol Oncol* 1996; **62**: 89-99

19 **Sato H**, Takino T, Okada Y, Cao J, Shinagawa A, Yamamoto E, Seiki M. A matrix metalloproteinase expressed on the surface of invasive tumor cells. *Nature* 1994; **370**: 61-65

20 **Torii A**, Kodera Y, Uesaka K, Hirai T, Yasui K, Morimoto T, Yamamura Y, Kato T, Hayakawa T, Fujimoto N, Kito T. Plasma concentration of matrix metalloproteinase 9 in gastric cancer. *Br J Surg* 1997; **84**: 133-136

21 **Fishman DA**, Bafetti LM, Banionis S, Kearns AS, Chilukuri K, Stack MS. Production of extracellular matrix-degrading proteinases by primary cultures of human epithelial ovarian carcinoma cells. *Cancer* 1997; **80**: 1457-1463

22 **Ylisirnio S**, Hoyhtya M, Turpeenniemi-Hujanen T. Serum matrix metalloproteinase -2, -9 and tissue inhibitors of metalloproteinase -1, -2 in lung cancer-TIMP-1 as a prognostic marker. *Anticancer Res* 2000; **20**: 1311-1316

23 **Gohji K**, Fujimoto N, Hara I, Fujii A, Gotoh A, Okada H, Arakawa S, Kitazawa S, Miyake H, Kamidono S, Nakajima M. Serum matrix metalloproteinase –2 and its density in men with prostate cancer as a new predictor of disease extension. *Int J Cancer* 1998; **79**: 96-101

24 **Waas ET**, Lomme RM, DeGroot J, Wobbes T, Hendriks T. Tissue levels of active matrix metalloproteinase-2 and -9 in colorectal cancer. *Br J Cancer* 2002; **86**: 1876-1883

25 **Moses MA**, Wiederschain D, Loughlin KR, Zurakowski D, Lamb CC, Freeman MR. Increased incidence of matrix metalloproteinase in urine of cancer patient. *Cancer Res* 1998; **58**: 1395-1399

26 **Zhang Q**, Chen LB, Zang J, Chu XY. Detection of matrix metalloproteinases in urine of breast cancer patients with zymography. *Nanjing Daxue Xuebao* 2002; **38**: 192-195

27 Gao Y, Li XN, Li SY, Zong ZH, Wang XR, Yu BZ. Zymographic analysis of MMPs in human cerebrospinal fluid with brain tumor. *Zhongguo Yike Daxue Xuebao* 2000; **29**: 10-12

28 **Macaulay VM**, O'Byrne KJ, Saunders MP, Braybrooke JP, Long L, Gleeson F, Mason CS, Harris AL, Brown P, Talbot DC. Phase 1 study of intrapleural batimastat (BB-94), a matrix metalloproteinase inhibitor, in the treatment of malignant pleural effusions. *Clin Cancer Res* 1999; **5**: 513-520

29 **Beattie GJ**, Smyth JF. Phase I study of intraperitoneal metalloproteinase inhibitor BB94 in patients with malignant ascites. *Clin Cancer Res* 1998; **4**: 1899-1902

30 **Parsons SL**, Watson SA, Steele RJ. Phase I/II trial of batimastat, a matrix metalloproteinase inhibitor, in patients with malignant ascites. *Eur J Surg Oncol* 1997; **23**: 526-531

31 **Parsons SL**, Watson SA, Brown PD, Collins HM, Steele RJ. Matrix metalloproteinases. *Br J Surg* 1997; **84**: 160-166

32 **Ray JM**, Stetler-Stevenson WG. The role of matrix metalloproteinase and their inhibitors in tumor invasion, metastasis and angiogenesis. *Eur Respir J* 1994; **7**: 2062-2072

33 **O'Reilly MS**, Holmgren L, Shing Y, Chen C, Rosenthal RA, Moses M, Lane WS, Cao Y, Sage EH, Folkman J. A novel angiogenesis inhibitor that mediates the suppression of metastases by a Lewis lung carcinoma. *Cell* 1994; **79**: 315-328

34 **Giannelli G**, Falk-Marzillier J, Schiraldi O, Stetler-Stevenson WG, Quaranta V. Induction of cell migration by matrix metalloproteinase-2 cleavage of laminin-5. *Science* 1997; **277**: 225-228

35 **Chambers AF**, Matrisian LM. Changing views of the role of matrix metalloproteinases in metastasis. *J Natl Cancer Inst* 1997; **89**: 1260-1270

36 **Tamsma JT**, Keizer HJ, Meinders AE. Pathogenesis of malignant ascites: Starlings law of capillary hemodynamics revisited. *Ann Oncol* 2001; **12**: 1353-1357

37 **Aslam N**, Marino CR. Malignant ascites: new concepts in pathophysiology, diagnosis, and management. *Arch Intern Med* 2001; **161**: 2733-2737

Edited by Zhu LH and Wang XL

P.O.Box 2345, Beijing 100023,China
Fax: +86-10-85381893
E-mail: wjg@wjgnet.com www.wjgnet.com

World J Gastroenterol 2003;9(11):2596-2600
World Journal of Gastroenterology
 ISSN 1007-9327

• CLINICAL RESEARCH •

Role of VEGF and CD44v6 in differentiating benign from malignant ascites

Wei-Guo Dong, Xiao-Min Sun, Bao-Ping Yu, He-Sheng Luo, Jie-Ping Yu

Wei-Guo Dong, Xiao-Min Sun, Bao-Ping Yu, He-Sheng Luo, Jie-Ping Yu, Department of Gastroenterology, Renmin Hospital, Wuhan University, Wuhan 430060, Hubei Province, China
Supported by Natural Science Foundation of Hubei Province, No. 99J163
Correspondence to: Dr. Wei-Guo Dong, Department of Gastroenterology, Renmin Hospital, Wuhan University, Wuhan 430060, Hubei Province, China. dongwg@public.wh.hb.cn
Telephone: +86-27-88041911 **Fax:** +86-27-88042292
Received: 2003-06-05 **Accepted:** 2003-07-24

Abstract

AIM: To detect the vascular endothelial growth factor (VEGF) and soluble splice variant 6 of CD44 (sCD44v6) levels in ascites and to explore their role in differentiating benign from malignant ascites.

METHODS: Cirrhotic ascites (n=36), tuberculosis ascites (n=8) and malignant ascites (n=23) were collected and studied. Concentrations of soluble VEGF and sCD44v6 in various kinds of ascites (n=67) were measured using a sandwich enzyme-linked immunoadsorbent assay.

RESULTS: VEGF and sCD44v6 levels in malignant ascites were 640.74±264.81 pg/ml and 89.22±38.20 ng/ml, respectively, both of which were significantly higher than those in cirrhotic ascites and tuberculous ascites (q=18.98, 11.89 and q=8.92, 5.09; P<0.01). However, the levels of VEGF and sCD44v6 in cirrhotic and tuberculous ascites had no significant difference (q=0.48, 0.75; P>0.05). Furthermore, VEGF levels in malignant ascites in patients with ovarian cancer were higher than those with gastric and colon cancer (q=5.03, 6.79; P<0.01, respectively). But differences of VEGF levels between gastric and colon cancer were not significant (q=1.90, P>0.05). Whereas, sCD44v6 levels in malignant ascites from patients with ovarian, gastric and colon cancer had no significant difference (q=0.06, 0.91, 0.35; P>0.05, respectirely). In comparison with cirrhotic and tuberculous ascites, when the upper limit of its VEGF mean levels 119.44 pg/ml (70.90±48.54) and sCD44v6 mean levels 63.59 ng/ml (44.42±19.17) was taken as the minimum cutoff limit, the sensitivity and specificity of VEGF and sCD44v6 of this assay to the diagnos is of malignant ascites were 91.3 %, 90.9 % and 73.9 %, 88.7 % respectively.

CONCLUSION: Elevated levels of VEGF and sCD44v6 may be useful in differential diagnosis of benign and malignant ascites.

Dong WG, Sun XM, Yu BP, Luo HS, Yu JP. Role of VEGF and CD44v6 in differentiating benign from malignant ascites. *World J Gastroenterol* 2003; 9(11): 2596-2600
http://www.wjgnet.com/1007-9327/9/2596.asp

INTRODUCTION

Angiogenesis is an absolute requirement for neoplastic growth of solid tumors after tumors reach a critical size of 1-2 mm^3[1], and is also essential for tumor invasion and metastasis, facilitates the shedding of tumor cells into surrounding blood vessels. Tumor cells have been shown to secrete a variety of angiogenic factors and thereby induce local formation of new blood capillaries. Among these factors, vascular endothelial growth factor (VEGF), also called vascular permeability factor (VPF), is a bifunctional cytokine and has the role in enhancing vascular permeability and stimulating endothelial growth[2-5], and is recognized as one of the most important molecules in the growth, invasion, metastasis and recurrence of human tumors[6-9].

However, tumor invasion and metastasis are considered to be a complex and multi-step process. Since the initial observation that a splice variant of CD44 (CD44v) could endow non-metastasizing cells with metastasis potential[10]. Many studies have demonstrated that CD44v, especially splice variant 6 of CD44 (CD44v6), probably promoting cancer cells to adhere to vascular endothelium and base membranes and enhancing moving ability of cancer cells, is most likely responsible for the invasion and metastasis of several tumor systems[11-15].

Malignant ascites is the direct and prominent manifestation of advanced carcinoma metastasized to the peritoneum[16]. Thus it is reasonable to hypothesize that VEGF and CD44v6 can be detected in malignant ascites. In the present study, we measured the concentration of VEGF and soluble CD44v6 (sCD44v6) using an enzyme-linked immunoadsorbent assay (ELISA) in various kinds of ascites in order to assess the value of VEGF and CD44v6 in identifying benign and malignant ascites.

MATERIALS AND METHODS

Patients

A total of 67 inpatients with ascites were collected at Renmin Hospital of Wuhan University, Zhongnan Hospital of Wuhan University and Tumor Hospital in Hubei Province from July 2002 to March 2003(Table 1). Informed consent of the patient and approval of the hospital were provided prior to collection of samples and medical records. All the cases were confirmed by cytologic examination of ascites, pathological examination, B-ultrasound and CT scan, etc.

Table 1 Patient characteristics

Diagnosis	No. of Patients	Mean age (range)	Female / male
Ascite	67	47(19-86)	26 / 41
Cirrhotic ascites	36	48(30-86)	10 / 26
Tuberculous ascites	8	28(19-33)	4 / 4
Carcinoma ascites	23	66(35-76)	12 / 11
Ovarian cancer	8	60(35-70)	8 / 0
Gastric cancer	6	68(38-74)	1 / 5
Colon cancer	5	64(48-71)	2 / 3
Hepatocellular cancer	2	-	0 / 2
Pancreatic cancer	1	-	0 / 1
Primary peritoneal carcinoma	1	-	1 / 0

Sample processing

Ascites samples were collected during therapeutic or diagnostic paracentesis and centrifuged at 3 000 rpm for 15 minutes at 4 ℃. Cell free supernatants were collected and aliquots were stored at -70 ℃ before determination.

Experimental groups

Cirrhotic, tuberculous and malignant ascites were defined as groups 1, 2 and 3, respectively. Malignant ascites from patients with ovarian, gastric and colon cancer were grouped as groups A, B and C, respectively.

Immunoassay for human VEGF

Concentrations of VEGF in ascites were determined with an ELISA kit (R & D Systems) following the manufacturer' s guidelines. All samples were analyzed in the laboratory of the Department of Gastroenterology, Renmin Hospital, Wuhan University. For determination of VEGF, samples were analyzed in duplicate, human recombinant $VEGF_{165}$ was diluted in series and used as a standard. VEGF concentrations were measured according to the standard curve. Samples with VEGF values beyond the standard curve were diluted and reanalyzed.

ELISA for human sCD44v6

Levels of sCD44v6 in ascites were measured with a sCD44v6 ELISA kit (Bender MedSystems, Austria). Briefly, monoclonal antibody against CD44v6, VFF-7, was absorbed by microwells in 96-well microtiter plates. sCD44v6 in the sample or in the standard bound to antibodies was adsorbed by each microwell. Horseradish peroxidase-conjugated monoclonal antibody against CD44v6 was then added and bound to the sCD44v6 that had been captured by the first antibody. After incubation, unbound enzyme conjugated antibodies were removed by washing and a substrate solution was added to each well. A colorful reactive product was formed , the reaction was terminated by addition of acid, and absorbance was measured at 450 nanometers. A standard curve was prepared from six standard dilutions of sCD44v6, which allowed determination of the levels of sCD44v6 in our samples.

Statistical analysis

The data were presented as $\bar{x}\pm s$. One-way analysis of variance was used for statistical analysis. Differences were considered significant when P value was less than 0.05.

RESULTS

Concentrations of VEGF in ascites

Figure 1 shows VEGF levels in malignant ascites (640.74± 264.81 pg/ml), which were significantly higher than those in cirrhotic ascites (67.05±51.91 pg/ml), tuberculous ascites (88.25±24.12 pg/ml) (P<0.01). However, there was no significant difference of VEGF levels between cirrhotic and tuberculous ascites (P>0.05).

Levels of sCD44v6 in ascites

sCD44v6 levels in malignant ascites (89.22±38.20 ng/ml) were higher than those in cirrhotic ascites (44.79±18.02 ng/ml), tuberculous ascites (50.25±12.57 ng/ml) (P<0.01). But the difference of sCD44v6 levels in cirrhotic and tuberculous ascites was not statistically significant (P>0.05) (Figure 2). We found both VEGF and sCD44v6 levels were increased in malignant ascites.

Comparison of VEGF and sCD44v6 levels in different kinds of malignant ascites

Statistical comparison of VEGF and sCD44v6 levels in these kinds of malignant ascites was not performed due to the limited number of hepatocellular cancer (n=2), pancreatic cancer (n=1) and primary peritoneal carcinoma (n=1).

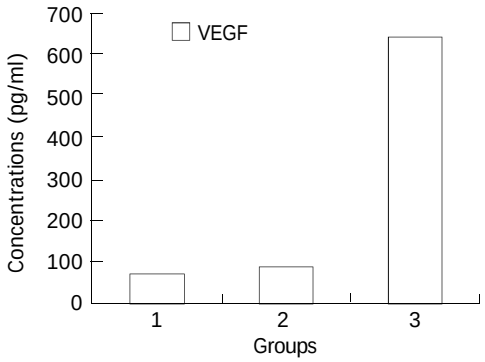

Figure 1 Comparison of VEGF concentrations in different kinds of ascites. Group 1: cirrhotic ascites, Group 2: tuberculous ascites, Group 3: malignant ascites.

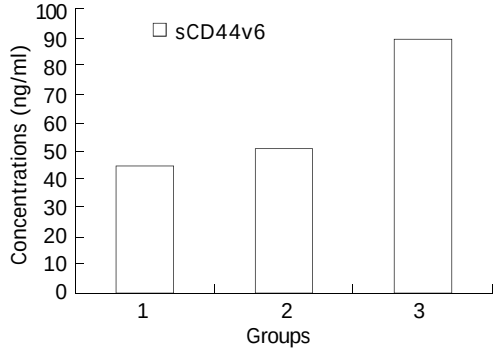

Figure 2 Comparison of sCD44v6 concentrations in different kinds of ascites. Group 1: cirrhotic ascites, Group 2: tuberculous ascites, Group 3: malignant ascites. Concentrations of sCD44v6 in group 3 were significantly higher than those in groups 1 and 2 (P<0.01).

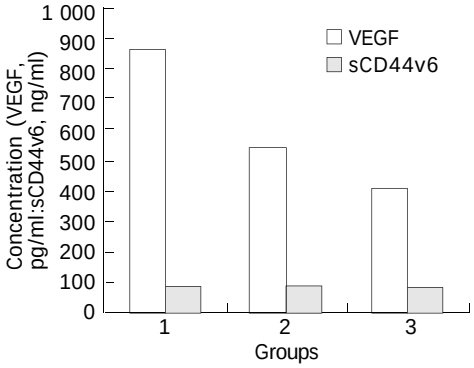

Figure 3 Concentrations of VEGF and sCD44v6 in different kinds of malignant ascites. Group A: ovarian cancer, Group B: gastric cancer, Group C: colon cancer. Concentrations of VEGF in group A were higher than those in groups B and C (P<0.01), while the difference of CD44v6 levels among groups A, B and C was not statistically significant (P>0.05).

Figure 3 shows VEGF levels in ascites from patients with ovarian cancer (866.25±208.46 pg/ml), which were higher than those with gastric cancer (541.30±123.17 pg/ml) and colon cancer (402.80±140.10 pg/ml), respectively (P<0.01). There was no significant difference of VEGF levels between gastric and colon cancer (P>0.05). Whereas, no statistical difference of sCD44v6 levels in ascites of patients with ovarian cancer

(89.42±25.70 ng/ml), gastric cancer (83.91±32.62 ng/ml) and colon cancer (80.10±9.97 ng/ml) was found (P>0.05).

Additionally, in our study, 2 out of 4 unidentified ascites cases were identified by peritoneum biopsy as metastatic ovarian cancer and primary peritoneal carcinoma. In these two cases, the levels of VEGF exceeded 1 200 pg/ml, and sCD44v6 levels exceeded 100 ng/ml. Another 2 cases of gastric and colon cancer, were identified by gastroscopy and colonoscopy, respectively. The concentration of VEGF and sCD44v6 in these 2 cases exceeded 650pg/ml and 80ng/ml respectively.

Sensitivity and specificity of VEGF and sCD44v6 levels to diagnosis of malignant ascites

Using benign ascites including cirrhotic and tuberculous ascites as control, and the upper limit of its VEGF mean levels, 119.44 pg/ml (70.90±48.54), as positive boundary value, 21 out of 23 malignant ascites cases and 4 out of 44 benign ascites cases exceeded the boundary line. So the sensitivity and specificity of this assay to the diagnosis of malignant ascites were 91.3 % (21/23) and 90.9 %(40/44), respectively, and calculated positive value, negative value and accurate rate were 84.0 %(21/25), 95.2 %(40/42) and 91.0 %(61/67), respectively. With same method, the sensitivity, specificity, positive value, negative value and accurate rate of sCD44v6 to the diagnosis of malignant ascites were 73.9 %(17/23), 88.7 % (39/44), 77.3 %(17/22), 86.4 %(39/45) and 83.4 % (56/67), respectively.

DISCUSSION

Human VEGF could be expressed in at least 5 isoforms, which have 206, 189, 165, 145 and 121 amine acids, respectively[17]. It is a multifunctional cytokine that has potent angiogenic activity and enhances microvascular permeability by direct action on vascular endothelium, promoting tumor growth and metastasis[18,19]. Strong VEGF expression has been demonstrated in various solid tumor types, including gastric[20-24], colorectal[25,26] and ovarian carcinomas[27,28]. Recently, substantial evidences indicated that serum concentration of VEGF was increased in cancerous patients[29-32]. Although some studies showed that VEGF levels were high in malignant ascites[30,33], its value to the diagnosis of malignant ascites has not been elucidated.

In the present study, we found that VEGF protein levels in malignant ascites were markedly higher than those in benign ascites, which were consistent with the previous results[30,33], and possessed a high sensitivity and specificity to the diagnosis of malignant ascites. Meanwhile, we also found that VEGF levels in malignant ascites in patients with ovarian cancer were higher than those in patients with gastric or colon cancer. No significant difference of VEGF levels was observed among those with gastric and colon cancer. Additionally, although the number of cases studied in our experiment was small, extremely increased VEGF levels in ascites of patients with ovarian cancer (n=8) and primary peritoneal carcinoma (n=1) could be measured. These data suggested that VEGF levels in ascites could reflect tumor biological behavior to a great extent, and cells of ovarian cancer and primary peritoneal carcinoma might secrete VEGF into peritoneal cavity directly[27]. Most importantly, detection of VEGF levels could provide a new approach for differential diagnosis of benign and malignant ascites, which remains a knotty problem all the time[34,35]. Moreover, detecting VEGF levels may contribute to the diagnosis of primary cancer that causes malignant ascites to a certain extent.

CD44 is an integral cell membrane glycoprotein, and is known to function in homing of lymphocytes, cell adhesion, activation of leukocytes and migration of cells. At least 20 variants (v) of CD44 have been reported due to the alternative splicing of 10 exons (v1-v10) that encode the membrane's proximal portion of the extracellular domain[36-38]. NH2-terminal function area of CD44 on the surface of cells could join the hyaluronate in the basement membrane to extracellular matrix, thus regulate the movement and function of cells. By this mechanism, neoplastic cells could adhere to the extracellular matrix and basement membrane of the host cell, resulting in invasion and metastasis of malignancy. On the other hand, the degraded products of hyaluronic acid could motivate the growth of local vessels, providing the basis for invasion and metastasis[39,40]. Many studies have reported that expression of CD44v, especially CD44v6, was correlated with invasion and metastasis of certain type of human cancer[11,40-47], including gastric cancer[48-50], colorectal cancer[51-53], ovarian cancer[54] and prostate cancer[55]. Furthermore, serum concentrations of sCD44v6 were found to be significantly increased in patients with advanced carcinoma[13,15,56]. To our knowledge, however, concentration of sCD44v6 has not been examined in malignant ascites, this might be the first study to document sCD44v6 in malignant ascites.

We found sCD44v6 levels were high in malignant ascites, and relatively low in nonmalignant ascites. It implies that elevated CD44v6 appears to be correlated to the invasion and metastasis of cancer cells into peritoneal cavity. But it is unclear why CD44v6 is closely associated with malignant ascites. The ability of CD44v6 to bind peritoneal mesothelial surfaces of abdominal cavity, and a subsequent cancer cell implantation may contribute to it. At the same time, our results showed a higher sensitivity and specificity of sCD44v6 to the diagnosis of malignant ascites. However, no evidence is available to show that detection of sCD44v6 could contribute to the determination of a potential primary cancer causing malignant ascites. It is reasonable to consider sCD44v6 may be a diagnostic index of malignant ascites.

In summary, VEGF and sCD44v6 are detectable in ascites and are significantly elevated in malignant ascites. Prospective monitoring of VEGF and sCD44v6 levels in ascites would be helpful in differential diagnosis of benign and malignant ascites.

REFERENCES

1 **Folkman J**, Watson K, Ingber D, Hanahan D. Induction of angiogenesis during the transition from hyperplasia to neoplasia. *Nature* 1989; **339**: 58-61

2 **Masood R**, Cai J, Zheng T, Smith DL, Hinton DR, Gill PS, Folkman J. Vascular endothelial growth factor (VEGF) is an autocrine growth factor for (VEGF) receptor-positive human tumors. *Blood* 2001; **98**: 1904-1913

3 **Leung DW**, Cachianes G, Kuang WJ, Goeddel DV, Ferrara N. Vascular endothelial growth factor is a secreted angiogenic mitogen. *Science* 1989; **246**: 1306-1309

4 **Senger DR**, Galli SJ, Dvorak AM, Perruzzi CA, Harvey VS, Dvorak HF. Tumor cells secreted a vascular permeability factor that promotes accumulation of ascitic fluid. *Science* 1983; **219**: 983-985

5 **Connolly DT**, Heuvelman DM, Nelson R, Olander JV, Eppley BL, Delfino JJ, Siegel NR, Leimgruber RM, Feder J. Tumor vascular permeability factor stimulates endothelial cell growth and angiogenesis. *J Clin Inves* 1989; **84**: 1470-1478

6 **Che X**, Hokita S, Natsugoe S, Tanabe G, Baba M, Takao S, Aikou T. Tumor angiogenesis related to growth pattern and lymph node metastasis in early gastric cancer. *Chin Med J* 1998; **111**: 1090-1093

7 **Erenoglu C**, Akin ML, Uluutku H, Tezcan L, Yildirim S, Batkin A, Erenogku C. Angiogenesis predicts poor prognosis in gastric carcinoma. *Dig Surg* 2000; **17**: 581-586

8 **Yoshikawa T**, Yanoma S, Tsuburaya A, Kobayashi O, Sairenji

M, Motohashi H, Noguchi Y. Angiogenesis inhibitor, TNP-470, suppresses growth of peritoneal disseminating foci. *Hepatogastroenterology* 2000; **47**: 298-302

9 **Xiangming C**, Hokita S, Natsugoe S, Tanabe G, Baba M, Takao S, Kuroshima K, Aikou T. Angiogenesis as an unfavorable factor related to lymph node metastasis in early gastric cancer. *Ann Surg Oncol* 1998; **5**: 585-589

10 **Gunthert U**, Hofmann M, Rudy W, Reber S, Zoller M, Haussmann I, Matzku S, Wenzel A, Ponta H, Herrlich P. A new variant of glycoprotein CD44 confers metastatic potential to rat carcinoma cells. *Cell* 1991; **65**: 13-24

11 **Sleeman J**, Moll J, Sherman L, Dall P, Pals ST, Ponta H, Herrlich P. The role of CD44 splice variants in human metastatic cancer. *Ciba Found Symp* 1995; **189**: 142-156

12 **Harn HJ**, Ho LI, Chang JY, Wu CW, Jing SY, Lee HS, Lee WH. Differential expression of the human metastasis adhesion molecule CD44V in normal and carcinomatous stomach mucosa of Chinese subjects. *Cancer* 1995; **75**: 1065-1071

13 **Harn HJ**, Ho Li, Shyu RY. Soluble CD44 isoforms in serum as potential markers of metastatic gastric carcinoma. *J Clin Gastroenterol* 1996; **22**: 107-110

14 **Fichtner I**, Dehmel A, Naundorf H, Finker LH. Expression of CD44 standard and isoforms in human breast cancer xenografts and shedding of soluble forms into serum of nude mice. *Anticancer Res* 1997; **17**: 3633-3645

15 **Zeimet AG**, Widschwendter M, Uhl-Steidl M, Muller-Holzner E, Daxenbichler G, Marth C, Dapunt O. High serum levels of soluble CD44 variant isoform are associated with favorable clinical outcome in ovarian cancer. *Br J Cancer* 1997; **76**: 1646-1651

16 **Enck RE**. Malignant ascites. *Am J Hosp Palliat Care* 2002; **19**: 7-8

17 **Neufeld G**, Cohen T, Gengrinovitch S, Poltorak Z. Vascular endothelial growth factor (VEGF) and its receptors. *FASEB J* 1999; **13**: 9-22

18 **Roussea S**, Houle F, Landry J, Huot J. P38MAP kinase activation by vascular endothelial growth factor mediates actin reorganization and cell migration in human endothelial cells. *Oncogene* 1997; **15**: 2169-2177

19 **Brock TA**, Dvorak HF, Senger DR. Tumor-secreted vascular permeability factor increased cytosolic Ca^{++} AND Von Willebrand factor release in human endothelial cells. *Am J Pathol* 1991; **138**: 213-221

20 **Tao HQ**, Lin YZ, Wang RN. Significance of vascular endothelial growth factor messenger RNA expression in gastric cancer. *World J Gastroenterol* 1998; **4**: 10-13

21 **Konno H**, Baba M, Tanaka T, Kamiya K, Ota M, Oba K, Shoji A, Kaneko T, Nakamura S. Overexpression of vascular endothelial growth factor is responsible for the hematogenous recurrence of early-stage gastric carcinoma. *Eur Surg Res* 2000; **32**: 177-181

22 **Ichikura T**, Tomimatsu S, Ohkura E, Mochizuki H. Prognostic significance of vascular endothelial growth factor (VEGF) and VEGF-C in gastric carcinoma. *J Surg Oncol* 2001; **78**: 132-137

23 **Kabashima A**, Maehara Y, Kakeji Y, Sugimachi K. Overexpression of vascular endothelial growth factor C is related to lymphogenous metastasis in early gastric carcinoma. *Oncology* 2001; **60**: 146-150

24 **Tian XJ**, Wu J, Meng L, Dong ZW, Shou CC. Expression of VEGF-121 in gastric carcinoma MGC803 cell line. *World J Gastroenterol* 2000; **6**: 281-283

25 **Zhao MF**, Mao H, Zhen JX, Yuan YW. Effect of vascular endothelial growth factor on adhesion of large intestine cancer cell HT-29. *Shijie Huaren Xiaohua Zazhi* 2000; **8**: 646-649

26 **Ishigami SI**, Arii S, Furutani M, Niwano M, Harada T, Mizumoto M, Mori A, Onodera H, Imamura M. Predictive value of vascular endothelial growth factor in metastasis and prognosis of human colorectal cancer. *Br J Cancer* 1998; **78**: 1379-1384

27 **Santin AD**, Hermonat PL, Ravaggi A, Cannon MJ, Pecorelli S, Parham GP. Secretion of vascular endothelial growth factor in ovarian cancer. *Eur J Gynaecol Oncol* 1999; **20**: 177-181

28 **Yamamoto S**, Konishi I, Mandai M, Kuroda H, Komatsu T, Nanbu K, Sakahara H, Mori T. Expression of vascular endothelial growth factor (VEGF) in epithelial ovarian neoplasms: correlation with clinicopathology and patient survival, and analysis of serum VEGF levels. *Br J Cancer* 1997; **75**: 1221-1227

29 **Dirix LY**, Vermeulen PB, Pawinski A, Prove A, Benoy I, De Pooter C, Martin M, Van Oosterom AT. Elevated levels of the angiogenic cytokines basic fibroblast growth factor and vascular endothelial growth factor in sera of cancer patients. *Br J Cancer* 1997; **78**: 238-243

30 **Kraft A**, Weindel K,Ochs A, Marth C, Zmija J, Schumacher P, Unger C, Marme D, Gastl G. Vascular endothelial growth factor in the sera and effusion of patients with malignant and nonmalignant disease. *Cancer* 1999; **85**: 178-187

31 **Zhang HT**, Hu S. Relationship between VEGF in the sera and invasion and metastasis of gastric cancer. *Shijie Huaren Xiaohua Zazhi* 2003; **11**: 344-345

32 **Mao ZB**, Xiao MB, Huang JF, Ni HB, Ni RZ, Wei Q, Zhang H. Expression of VEGF in the sera of patients with gastric cancer. *Shijie Huaren Xiaohua Zazhi* 2002; **10**: 1220-1221

33 **Zebrowski BK**, Liu W, Ramirez K, Akagi Y, Mills GB, Ellis LM. Markedly elevated levels of vascular endothelial growth factor in malignant ascites. *Ann Surg Oncol* 1999; **6**: 373-378

34 **Aslam N**, Marino CR. Malignant ascites: new concepts in pathophysiology, diagnosis, and management. *Arch Intern Med* 2001; **161**: 2733-2737

35 **Tamsma JT**, Keizer HJ, Meinders AE. Pathogenesis of malignant ascites: Starling's law of capillary hemodynamics revisited. *Ann Oncol* 2001; **12**: 1353-1357

36 **Screaton GR**, Bell MV, Jackson CG, Cornelis FB, Ferth U, Bell JI. Genomic structure of DNA encoding the lymphocyte homing receptor CD44 reveals at least 12 alternatively spliced exons. *Proc Natl Acad Sci U S A* 1992; **89**: 12160-12164

37 **Harn HJ**, Isola N, Cooper DL. The multispecific cell adhesion molecule CD44 is represented in reticulocyte cDNA. *Biochem Biophys Res Commun* 1991; **178**: 1127-1134

38 **Herrlich P**, Zoller M, Pals ST, Ponta H. CD44 splice variants: metastases meet lymphocytes. *Immunol Today* 1993; **14**: 395-399

39 **Strobel T**, Swanson L, Cannistra SA. *In vivo* inhibition of CD44 limits intra-abdominal spread of a human ovarian cancer xenograft in nude mice. *Cancer Res* 1997; **57**: 1228-1232

40 **Weber GF**, Bronson RT, Ilagan J, Cantor H, Schmits R, Mak TW. Absence of the CD44 gene prevents sarcoma metastasis. *Cancer Res* 2002; **62**: 2281-2286

41 **Chen GY**, Wang DR. The expression and clinical significance of CD44v in human gastric cancers. *World J Gastroenterol* 2000; **6**:125-127

42 **Xin Y**, Zhao FK, Zhang SM, Wu DY, Wang YP, Xu L. Relationship beteeen CD44v6 expression and prognosis in gastric carcinoma patients. *Shijie Huaren Xiaohua Zazhi* 1999; **7**: 210-214

43 **Gu HP**, Ni CR, Zhang RZ. Relationship of expressions of CD15, CD44v6 and nm23 H1 mRNA with metastasis and prognosis of colon carcinoma. *Shijie Huaren Xiaohua Zazhi* 2000; **8**: 887-891

44 **Mi JQ**, Zhang ZH, Sheng MC. Significance of CD44v6 protein expression in gastric carcinoma and precancerous lesions. *Shijie Huaren Xiaohua Zazhi* 2000; **8**: 156-158

45 **Liu YH**, Liu JZ, Xiao B, Wang SX. The clinical significance of CD44v6 abnormal expression in gastric cancer. *Shijie Huaren Xiaohua Zazhi* 2001; **9**: 89-90

46 **Wu LY**, Hao YD, Shi ML. Relationship between CD44v6 expression and biological behavior of gastric cancer. *Shijie Huaren Xiaohua Zazhi* 1999; **7**: 1034

47 **Xiao CZ**, Dai YM, Yu HY, Wang JJ, Ni CR. Relationship between expression of CD44v6 and nm23-H1 and tumor invasion and metastasis in hepatocellular carcinoma. *World J Gastroenterol* 1998; **4**: 412-414

48 **Yamaguchi A**, Coi T, Yu J, Hirono Y, Ishida M, Lida A, Kimura T, Takeuchi K, Katayama K, Hirose K. Expression of CD44v6 in advanced gastric cancer and its relationship to hematogenous metastasis and long-term prognosis. *J Surg Oncol* 2002; **79**: 230-235

49 **Sun XW**, Shen BZ, Shi MS, Dai XD. Relationship between CD44v6 expression and risk factors in gastric carcinoma patients. *Shijie Huaren Xiaohua Zazhi* 2002; **10**: 1129-1132

50 **Chen ZF**, Deng CS, Xia B, Zhu YQ, Zeng J, Gong LL. Expression of heat shock protein 60, CD44v6 splice variant in human gastric cancer. *Shijie Huaren Xiaohua Zazhi* 2001; **9**: 988-991

51 **Masaki T**, Goto A, Sugiyama M, Matsuoka H, Abe N, Sakamoto A, Atomi Y. Possible contribution of CD44 variant 6 and nuclear beta-catenin expression to the formation of budding tumor cells in patients with T1 colorectal carcinoma. *Cancer* 2001; **92**: 2539-2546

52 **Xu SH**, Feng JG, Li DC, Mou HZ, Lou RC. Relationship between CD44 in the peripheral blood of patients with colorectal cancer and clinicopathological features. *Shijie Huaren Xiaohua Zazhi* 2000; **8**: 432-435

53 **Cai Q**, Lu HF, Sun MJ, Du X, Fan YZ, Shi DR. Expression of CD44 v3 and v6 proteins in human colorectal carcinoma and its relevance with prognosis. *Shijie Huaren Xiaohua Zazhi* 2000; **8**: 1255-1258

54 **Schiffenbauer YS**, Meir G, Maoz M, Even-Ram SC, Bar-shavit R, Neeman M. Gonadotropin stimulation of MLS human epithelial ovarian carcinoma cells augments cell adhesion mediated by CD44 and by alpha (v)-integrin. *Gynecol Oncol* 2002; **84**: 296-302

55 **Ekici S**, Ayhan A, Kendi S, Ozen H. Determination of prognosis in patients with prostate cancer treated with radical prostatectomy: prognostic value of CD44v6 score. *J Urol* 2002; **167**: 2037-2041

56 **Saito H**, Tsujitani S, Katano K, Ikeguchi M, Maeta M, Kaibara N. Serum concentration of CD44 variant 6 and its relation to prognosis in patients with gastric carcinoma. *Cancer* 1998; **83**: 1095-1101

Edited by Ren SY and Wang XL

P.O.Box 2345, Beijing 100023,China
Fax: +86-10-85381893
E-mail: wjg@wjgnet.com www.wjgnet.com

World J Gastroenterol 2003;9(11):2601-2604
World Journal of Gastroenterology
 ISSN 1007-9327

• CLINICAL RESEARCH •

Effects of bowel rehabilitation and combined trophic therapy on intestinal adaptation in short bowel patients

Guo-Hao Wu, Zhao-Han Wu, Zhao-Guang Wu

Guo-Hao Wu, Zhao-Han Wu, Zhao-Guang Wu, Department of General Surgery, Zhongshan Hospital, Fu Dan University, Shanghai, 200032, China
Correspondence to: Guo-Hao Wu, Department of General Surgery, Zhongshan Hospital, Fu Dan University, Shanghai 200032, China. wugh@zshospital.net
Telephone: +86-21-64041990 Ext 2365 **Fax:** +86-21-64038472
Received: 2003-03-12 **Accepted:** 2003-05-11

Abstract

AIM: To evaluate the effects of bowel rehabilitation and combined trophic therapy on intestinal adaptation in short bowel patients.

METHODS: Thirty-eight patients with severe short-bowel syndrome (SBS) were employed in the present study, whose average length of jejunum-ileum was 35.8±21.2 cm. The TPN treatment was initiated early to attain positive nitrogen balance and prevent severe weight loss. The TPN composition was designated to be individualized and altered when necessary. Enteral feeding was given as soon as possible after resection and increased gradually. Meals were distributed throughout the day. Eight patients received treatment of growth hormone (0.14 mg/kg.day) and glutamine (0.3 g/kg.day) for 3 weeks. D-xylose test, ^{15}N-Gly trace test and ^{13}C-palmitic acid breath test were done to determine the patients' absorption capability.

RESULTS: Thirty-three patients maintained well body weight and serum albumin concentration. The average time of follow-up for 33 survival patients was 5.9±4.3 years. Twenty-two patients weaned from TPN with an average TPN time of 9.5±6.6 months. Two patients, whose whole small bowel, ascending and transverse colon were resected received home TPN. An other 9 patients received parenteral or enteral nutritional support partly as well as oral diet. Three week rhGH+GLN therapy increased nutrients absorption but the effects were transient.

CONCLUSION: By rehabilitation therapy, most short bowel patients could wean from parenteral nutrition. Dietary manipulation is an integral part of the treatment of SBS. Treatment with growth hormone and glutamine may increase nutrients absorption but the effects are not sustained beyond the treatment period.

Wu GH, Wu ZH, Wu ZG. Effects of bowel rehabilitation and combined trophic therapy on intestinal adaptation in short bowel patients. *World J Gastroenterol* 2003; 9(11): 2601-2604
http://www.wjgnet.com/1007-9327/9/2601.asp

INTRODUCTION

Short-bowel syndrome (SBS) is resulted from extensive small bowel resection due to infarction of the mesenteric vessels, intestinal volvulus, trauma, malignancy, or from complications of Crohn's disease, and is defined as the manifestations of signs, symptoms and complications associated with the inadequate absorptive surface area of functional bowel[1]. It is usually characterized by severe diarrhea, malabsorption, dehydration, electrolyte and metabolic disturbances, and progressive malnourishment.

The pathophysiological consequences following extensive intestinal resection depend on the length and site of resection and the extent of adaptation of the remaining intestine[2-4]. Patients often have to be supported with total parenteral nutrition (TPN) until maximal adaptation of the residual small bowel is complete. This process can take place for up to a year and sometimes longer. Certain patients may require lifelong TPN support depending on the length and health of the residual small bowel. TPN is associated with certain complications, which include catheter sepsis and liver failure[5-8]. It is therefore important for dietary management and pharmacological treatment in the short bowel patients hopefully to wean from TPN. Dietary management and some trophic factors are important in promoting intestinal adaptation after resection. The aim of the study was to define the role of bowel rehabilitation, trophic factors in intestinal adaptation in short bowel patients.

MATERIALS AND METHODS

Patients

Thirty-eight patients (28 men, 10 women; mean age 38.0±16.0 years, range 7-68 years) with severe short-bowel syndrome were eligible for this study. All patients had previously undergone extensive bowel resection for intestinal volvulus, mesenteric infarction or inflammatory bowel disease with or without colonic resection. The average length of jejunum-ileum, as determined from operative reports and confirmed by perioperative radiographs, was 35.8±21.2 cm (range, 0-110 cm) in all patients. Two patients had entire jejunum, ileum and right colon resected. The ileocecal valve and a portion of colon were resected in 13 patients, and 25 patients had intact colon (Table 1). The patients were clinically stable, and did not demonstrate evidence of infection, or extradigestive organ failure. In addition, they did not have a history of cancer. The protocol for the present study was approved by the Ethics Committee of Zhongshan Hospital.

Bowel rehabilitation

Clinical management Massive fluid and electrolyte losses were noted due to transient gastric hypersecretion and profound diarrhea during the initial postoperative periods. So, initial postoperative treatment was designed to maintain adequate fluid and electrolyte balance. TPN began early to attain positive nitrogen balance and to prevent severe weight loss. It should continue until the adaptive processes were complete or indefinitely, if clinically indicated. The composition of TPN was individualized and altered when necessary. Caloric requirements were delivered in accordance with the resting energy expenditure of patients, and it was reassessed often as the patient's clinical condition warranted. As the patient's oral

intake increased, the amount of TPN was reduced, the frequency of TPN was reduced to every other day in the first week, three times in the next week, and twice during the third week. If the patient lost 1 kg/week or more or if diarrhea exceeded 600 g/day or if laboratory abnormalities developed, then the patients were placed back on TPN. If the patient's eventual adaptation was insufficient to allow survival on oral/enteral feeding alone, the patients usually required lifelong TPN support.

Patients with SBS received at least some enteral feeding as soon as possible after resection. Usually this was administered for a postoperative period of 7-10 days. The ideal composition of enteral formulas for patients with SBS was also dependent upon the length of the small bowel and the presence of a colon. Originally, elemental and peptide based enteral formulas were favored for patients with SBS. Gradually, the diet with intact protein nutrient formulas and dietary fiber was given in accordance with the patients' need. Meals were distributed throughout the day.

Combined trophic therapy

Eight patients (4 males, 4 females, mean age 36±8 years) with severe SBS (mean jejunoileal length 44 cm, range 0 to 80 cm)

Table 1 Patient characteristics and status

Patient No.	Gender	Age(a)	Cause of resection	Jejunum-ileum(cm)	Colon	TPN(a)	Current status	Survival time(a)
1	F	28	Small bowel volvulus	0	ACR	17	HPN	17
2	M	7	Small bowel volvulus	0	ACR	7.6	HPN	7.6
3	M	41	Small bowel volvulus	35	All	0.8	Normal oral diet	13.5
4	M	61	SMA thrombosis	30	All	1.6	Died	2.2
5	M	62	SMA thrombosis	30	All	2.0	Died	2.6
6	M	33	Small bowel volvulus	28	All	1.2	Normal oral diet	14.4
7	M	24	Small bowel volvulus	18	All	1.8	PN+EN	1.8
8	M	35	Small bowel volvulus	45	All	0.5	Died	6.2
9	F	52	Small bowel volvulus	55	ICV(-)	0.3	Died	7.4
10	F	68	SMA thrombosis	70	ICV(-)	0.6	Normal oral diet	9.5
11	F	44	Small bowel obstruction	100	All	0.2	Normal oral diet	9.6
12	M	22	Crohn's disease	80	ICV(-)	0.5	Normal oral diet	12.2
13	M	15	Small bowel volvulus	20	ICV(-)	5.2	Died	5.4
14	M	50	Small bowel obstruction	60	ICV(-)	1.2	Normal oral diet	9.0
15	F	42	Small bowel volvulus	28	All	2.2	PN+oral diet	8.5
16	F	44	Small bowel volvulus	35	ICV(-)	1.0	Normal oral diet	10.8
17	M	59	Small bowel volvulus	30	All	1.2	Normal oral diet	6.4
18	F	50	SMA thrombosis	60	ICV(-)	0.4	Normal oral diet	5.4
19	M	55	SMA thrombosis	40	ICV(-)	1.0	Normal oral diet	7.6
20	M	56	Small bowel volvulus	30	All	0.8	PN+oral diet	4.5
21	M	26	Small bowel volvulus	30	All	1.0	Normal oral diet	8.8
22	M	40	Small bowel obstruction	50	ICV(-)	0.6	Normal oral diet	6.0
23	M	16	Small bowel volvulus	30	All	1.5	Normal oral diet	12.5
24	M	28	Small bowel volvulus	30	All	2.0	Normal oral diet	5.5
25	M	57	SMA thrombosis	45	All	0.3	Normal oral diet	6.5
26	M	34	Crohn's disease	60	All	0.5	Normal oral diet	4.0
27	M	41	Crohn's disease	70	All	0.4	Normal oral diet	2.0
28	M	30	Small bowel volvulus	40	All	0.2	Normal oral diet	1.8
29	M	62	SMA thrombosis	50	ICV(-)	0.8	EN+ oral diet	1.6
30	F	45	Small bowel volvulus	30	All	0.5	EN+ oral diet	1.5
31	M	18	Small bowel volvulus	30	All	0.4	Normal oral diet	2.0
32	M	20	Small bowel volvulus	30	All	0.5	Normal oral diet	2.0
33	M	16	Small bowel volvulus	20	All	1.0	EN+ oral diet	1.5
34	M	36	Small bowel volvulus	30	All	0.4	EN+ oral diet	1.2
35	M	18	Small bowel volvulus	18	All	0.6	HPN+ oral diet	2.6
36	F	46	SMA thrombosis	40	ICV(-)	0.5	EN+ oral diet	0.5
37	M	32	Small bowel volvulus	35	All	0.3	Normal oral diet	1.8
38	F	30	Small bowel volvulus	30	All	0.2	Normal oral diet	1.0
Mean		38±16		35.8±21.2		9.5±6.6		5.9±4.3

ACR=ascending colon resection, ICV(-)=without ileal cecal valve, HPN=home parenteral nutrition, PN=parenteral nutrition, EN=enteral nutrition, a=year.

Table 2 Absorption capability of patients before and after treatment with GH+GLN

	Baseline	End of therapy	One week after therapy
D-xylose test (%)	5.4±2.1	7.6±1.8[a]	6.0±2.0[b]
^{15}N-Gly trace test (%)	62.4±14.2	73.2±15.3[a]	58.4±11.8[b]
^{13}C-palmitic acid breath test (%)	55.3±8.8	64.5±11.2[a]	62.6±10.4[b]

Values are mean ±SEM, [a]$P<0.05$ *vs* baseline, [b]$P>0.05$ *vs* baseline.

who previously adapted to the provision of TPN and enteral feedings were admitted for 0.8±0.5 years in the study after surgical resection. The first week served as a control period when nutritional (parenteral and enteral) and medical managements were delivered as the routine therapy. Thereafter, the patients who received treatment of subcutaneous recombinant human growth hormone (rhGH) (0.14 mg/kg.day; Saizen, Serono Co., Switzerland) were divided into two daily injections, intravenous alanyl-glutamine solution (0.3 g/kg.day, Dipeptiven, Fresenius Co., Germany) was delivered daily for 3 weeks. D-xylose test, ^{15}N-Gly trace test and ^{13}C-palmitic acid breath test were done respectively before, at the end of therapy and one week after treatment to determine the patients' absorption capability.

Statistical analysis

Data were analyzed using standard statistical software (SPSS 10.0). For normally distributed data, a paired Student' s *t* test was used for statistical analysis. A probability value less than or equal to 0.05 was considered statistically significant. Data are expressed as mean ±SEM.

RESULTS

Thirty-eight patients were admitted and received nutritional support and rehabilitation therapy, among them 2 died of severe malnutrition 2 years after treatment because they failed to receive nutritional therapy, 2 died of accidental event, 1 died of liver failure 5 years later. Thirty-three patients maintained well body weight and serum albumin concentration. The average time of follow-up for 33 survival patients was 5.9±4.3 years (range, 0.5-17 years). Twenty-two patients weaned from TPN, their average TPN time was 9.5±6.6 months. They maintained their nutritional status well on normal oral diet. Two patients, whose whole small bowel, ascending and transverse colon were resected received home TPN. An other 9 patients received parenteral or enteral nutritional support partly as well as oral diet (Table 1). Eight patients developed gall bladder stones. Cholecystectomy was performed for three patients.

For the eight patients, the 3 week rhGH+GLN therapy resulted in weight gain, and stool output dramatically decreased. Three patients weaned from TPN completely after the treatment period, 3 patients reduced TPN requirements, and 2 patients failed the therapy. The absorption capability of D-xylose, ^{15}N-Gly and ^{13}C-palmitic acid in these SBS patients was much lower than normal level. After 3 week rhGH+GLN therapy, the absorption capability of D-xylose, ^{15}N-Gly and ^{13}C-palmitic acid improved. However, it dropped to the level of baseline at one week after treatment (Table 2).

DISCUSSION

After extensive resection of the small intestine, the remaining bowel, to some degree, had a significant adaptation response to resection. Bowel adaptation, characterized by epithelial hyperplasia and increase in villus diameter, height, and crypt depth, occurred weeks to months after resection[9-11]. Various nutritional and medical therapies can be tried to improve bowel absorptive capacity. TPN is the most important factor responsible for prolonging the lives of patients with SBS. In the initial stages after massive resection of bowel, TPN should begin early to attain positive nitrogen balance and to prevent severe weight loss[12,13]. TPN has been shown to greatly increase the chances of long-term survival. It should be delivered until the adaptive processes were complete or indefinitely, if clinically indicated[14]. This process can take place for up to a year and sometimes longer. Long-term TPN resulted in small bowel mucosa atrophy and was associated with certain complications, such as catheter sepsis and liver failure[15]. So, oral diet is encouraged, if there is any absorptive capacity of the remaining bowel, bowel adaptation should be promoted. An enteral tube feeding might be used to supplement the diet in an effort to wean patients from TPN[16]. At first, diluted solutions of chemically defined diets containing simple amino acids and short-chain peptides were offered. Gradually, the diet with intact protein nutrient formulas and dietary fiber was given in accordance with the patients' need. The parenteral supply had to be adjusted according to the oral intake. As the patient' s oral intake increased, the amount of TPN was reduced, the frequency of TPN was reduced to every other day for 1 week, three times in the next week, and twice during the third week or weaned from TPN at last[17]. If the patient lost or more 1 kg/week of body weight or more, if diarrhea exceeded 600 g/day or if laboratory abnormalities developed, then the patients were placed back on TPN[18]. In our group, 22 patients weaned from TPN among the 33 survived patients after receiving rehabilitation therapy. They maintained their nutritional status well on normal oral diet. It indicated that rehabilitation therapy for SBS played important roles in the intestinal adaptation.

Combination of glutamine, human recombinant growth hormone has been shown to influence bowel adaptation[19-24]. The study by Byrne *et al*[25,26] indicated that at one year of follow-up 40 % of treated patients were able to reduce or discontinue parenteral nutrition. Patients in the study were also receiving other medical therapy, including medications known to slow down intestinal motility and oral rehydration solutions. It is not clear whether glutamine, growth hormone, diet, or other factors contributed to the favorable outcome. It did not necessarily mean that fluid and nutrients absorption was increased because absorptive studies were not performed. Szkudlarek *et al*[27] reported in a randomized control study of eight short-bowel patients the combination of growth hormone and glutamine for 28 days did not result in a significant increase in fluid or nutrient absorption. In our clinical trial, we used D-xylose test, ^{15}N-Gly trace test and ^{13}C-palmitic acid breath test to determine the patients' nutrient absorption capability. The results showed that the absorption of carbohydrates (from 5.4 % to 7.6 %), protein (from 62.4 % to 73.2 %) and fat (from 55.3 % to 64.5 %) increased. Weight gain was observed and stool output dramatically decreased. Three patients weaned from TPN completely after the treatment period and 3 patients reduced TPN requirements. However, the absorption capability dropped to the level of baseline at one week after treatment. We found that the treatment with growth hormone and glutamine might increase absorption of nutrients but the effect seemed to be transient with no long term improvement in gut function when treatment was discontinued. This has been supported by recent clinical studies[28-30].

In conclusion, by rehabilitation therapy, most short bowel patients could wean from parenteral nutrition. Dietary manipulation is an integral part of the treatment of SBS. Treatment with growth hormone and glutamine may increase nutrients absorption but the effects are not sustained beyond the treatment period. Therapeutic efficacy can be achieved only when the treatment plan is tailored to meet individual need.

REFERENCES

1 **Thompson JS**. Comparison of massive vs. repeated resection leading to short bowel syndrome. *J Gastrointest Surg* 2000; **4**: 101-104
2 **Jeppesen PB**, Mortensen PB. Enhancing bowel adaptation in short bowel syndrome. *Curr Gastroenterol Rep* 2002; **4**: 338-347
3 **Welters CF**, Dejong CH, Deutz NE, Heineman E. Intestinal

adaptation in short bowel syndrome. *ANZ J Surg* 2002; **72**: 229-236
4 **Wasa M**, Takagi Y, Sando K, Harada T, Okada A. Intestinal adaptation in pediatric patients with short-bowel syndrome. *Eur J Pediatr Surg* 1999; **9**: 207-209
5 **Sondheimer JM**, Asturias E, Cadnapaphornchai M. Infection and cholestasis in neonates with intestinal resection and long-term parenteral nutrition. *J Pediatr Gastroenterol Nutr* 1998; **27**: 131-137
6 **Burstyne M**, Jensen GL. Abnormal liver functions as a result of total parenteral nutrition in a patient with short-bowel syndrome. *Nutrition* 2000; **16**: 1090-1092
7 **Terra RM**, Plopper C, Waitzberg DL, Cukier C, Santoro S, Martins JR, Song RJ, Gama-Rodrigues J. Remaining small bowel length: association with catheter sepsis in patients receiving home total parenteral nutrition: evidence of bacterial translocation. *World J Surg* 2000; **24**: 1537-1541
8 **Candusso M**, Faraguna D, Sperli D, Dodaro N. Outcome and quality of life in paediatric home parenteral nutrition. *Curr Opin Clin Nutr Metab Care* 2002; **5**: 309-314
9 **Schulzke JD**, Schmitz H, Fromm M, Bentzel CJ, Riecken EO. Clinical models of intestinal adaptation. *Ann N Y Acad Sci* 1998; **859**: 127-138
10 **Kvietys PR**. Intestinal physiology relevant to short-bowel syndrome. *Eur J Pediatr Surg* 1999; **9**: 196-199
11 **Welters CF**, Dejong CH, Deutz NE, Heineman E. Intestinal function and metabolism in the early adaptive phase after massive small bowel resection in the rat. *J Pediatr Surg* 2001; **36**: 1746-1751
12 **Platell CF**, Coster J, McCauley RD, Hall JC. The management of patients with the short bowel syndrome. *World J Gastroenterol* 2002; **8**: 13-20
13 **Sundaram A**, Koutkia P, Apovian CM. Nutritional management of short bowel syndrome in adults. *J Clin Gastroenterol* 2002; **34**: 207-220
14 **Messing B**, Crenn P, Beau P, Boutron-Ruault MC, Rambaud JC, Matuchansky C. Long-term survival and parenteral nutrition dependence in adult patients with the short bowel syndrome. *Gastroenterolog* 1999; **117**: 1043-1050
15 **Howard L**, Ashley C. Management of complications in patients receiving home parenteral nutrition. *Gastroenterology* 2003; **124**: 1651-1661
16 **Vanderhoof JA**, Matya SM. Enteral and parenteral nutrition in patients with short-bowel syndrome. *Eur J Pediatr Surg* 1999; **9**: 214-219
17 **Buchman AL**. The clinical management of short bowel syndrome: steps to avoid parenteral nutrition. *Nutrition* 1997; **13**: 907-913
18 **Gouttebel MC**, Saint Aubert B, Colette C, Astre C, Monnier LH, Joyeux H. Intestinal adaptation in patients with short bowel syndrome. Measurement by calcium absorption. *Dig Dis Sci* 1989; **34**: 709-715
19 **Gu Y**, Wu ZH. The anabolic effects of recombinant human growth hormone and glutamine on parenterally fed, short bowel rats. *World J Gastroenterol* 2002; **8**: 752-757
20 **Zhou X**, Li YX, Li N, Li JS. Effect of bowel rehabilitative therapy on structural adaptation of remnant small intestine: animal experiment. *World J Gastroenterol* 2001; **7**: 766-773
21 **Ukleja A**, Scolapio JS, Buchman AL. Nutritional management of short bowel syndrome. *Semin Gastrointest Dis* 2002; **13**: 161-168
22 **Seguy D**, Vahedi K, Kapel N, Souberbielle JC, Messing B. Low-dose growth hormone in adult home parenteral nutrition-dependent short bowel syndrome patients: a positive study. *Gastroenterolog* 2003; **124**: 293-302
23 **Li-Ling L**, Irving M. The effectiveness of growth hormone, glutamine and a low-fat diet containing high-carbohydrate on the enhancement of the function of remnant intestine among patients with short bowel syndrome: a review of published trials. *Clin Nutr* 2001; **20**: 199-204
24 **Scolapio JS**, Ukleja A. Short-bowel syndrome. *Curr Opin Clin Nutr Metab Care* 1998; **1**: 391-394
25 **Byrne TA**, Morrissey TB, Nattakom TV, Ziegler TR, Wilmore DW. Growth hormone, glutamine, and a modified diet enhance nutrient absorption in patients with severe short bowel syndrome. *J Parenter Enteral Nutr* 1995; **19**: 296-302
26 **Byrne TA**, Persinger RL, Young LS, Ziegler TR, Wilmore DW. A new treatment for patients with short- bowel syndrome. Growth hormone, glutamine, and a modified diet. *Ann Surg* 1995; **222**: 243-254
27 **Szkudlarek J**, Jeppesen PB, Mortensen PB. Effect of high dose growth hormone with glutamine and no change in diet on intestinal absorption in short bowel patients: a randomized, double blind, crossover, placebo controlled study. *Gut* 2000; **47**: 199-205
28 **Scolapio JS**, McGreevy K, Tennyson GS, Burnett OL. Effect of glutamine in short-bowel syndrome. *Clin Nutr* 2001; **20**: 319-323
29 **Jeppesen PB**, Szkudlarek J, Hoy CE, Mortensen PB. Effect of high-dose growth hormone and glutamine on body composition, urine creatinine excretion, fatty acid absorption, and essential fatty acids status in short bowel patients: a randomized, double-blind, crossover, placebo-controlled study. *Scand J Gastroenterol* 2001; **36**: 48-54
30 **Scolapio JS**. Effect of growth hormone, glutamine, and diet on body composition in short bowel syndrome: a randomized, controlled study. *J Parenter Enteral Nutr* 1999**; 23**: 309-312

Edited by Zhu LH and Wang XL

P.O.Box 2345, Beijing 100023,China
Fax: +86-10-85381893
E-mail: wjg@wjgnet.com www.wjgnet.com

World J Gastroenterol 2003;9(11):2605-2608
World Journal of Gastroenterology
 ISSN 1007-9327

• BRIEF REPORTS •

Restenosis following balloon dilation of benign esophageal stenosis

Ying-Sheng Cheng, Ming-Hua Li, Ren-Jie Yang, Hui-Zhen Zhang, Zai-Xian Ding, Qi-Xin Zhuang, Zhi-Ming Jiang, Ke-Zhong Shang

Ying-Sheng Cheng, Ming-Hua Li, Qi-Xin Zhuang, Ke-Zhong Shang, Department of Radiology, Sixth People' s Hospital, Shanghai Jiaotong University, Shanghai 200233, China
Ren-Jie Yang, Department of Interventional Diagnosis and Therapy, Clinical Oncology College of Beijing University, Beijing 100036, China
Hui-Zhen Zhang, Zhi-Ming Jiang, Department of Pathology, Sixth People' s Hospital, Shanghai Jiaotong University, Shanghai 200233, China
Zai-Xian Ding, Department of Animal Experiment, Sixth People' s Hospital, Shanghai Jiaotong University, Shanghai 200233, China
Supported by the National Key Technologies Research and Development Program of China During the 9th Five-Year Plan Period, No.96-907-03-04
Correspondence to: Dr. Ying-Sheng Cheng, Department of Radiology, Sixth People' s Hospital, Shanghai Jiaotong University, Shanghai 200233, China. chengys@sh163.net
Telephone: +86-21-64368920 **Fax:** +86-21-64701361
Received: 2003-05-13 **Accepted:** 2003-06-02

Abstract

AIM: To elucidate the mechanism of restenosis following balloon dilation of benign esophageal stenosis.

METHODS: A total of 49 rats with esophageal stenosis were induced in 70 rats using 5 ml of 50 % sodium hydroxide solution and the double-balloon method, and an esophageal restenosis (RS) model was developed by esophageal stenosis using dilation of a percutaneous transluminal coronary angioplasty (PTCA) balloon catheter. These 49 rats were divided into two groups: rats with benign esophageal stricture caused by chemical burn only (control group, *n*=21) and rats with their esophageal stricture treated with balloon catheter dilation (experimental group, *n*=28). Imaging analysis and immunohistochemistry were used for both quantitative and qualitative analyses of esophageal stenosis and RS formation in the rats, respectively.

RESULTS: Cross-sectional areas and perimeters of the esophageal mucosa layer, muscle layer, and the entire esophageal layers increased significantly in the experimental group compared with the control group. Proliferating cell nuclear antigen (PCNA) was expressed on the 5th day after dilation, and was still present at 1 month. Fibronectin (FN) was expressed on the 1st day after dilation, and was still present at 1 month.

CONCLUSION: Expression of PCNA and FN plays an important role in RS after balloon dilation of benign esophageal stenosis.

Cheng YS, Li MH, Yang RJ, Zhang HZ, Ding ZX, Zhuang QX, Jiang ZM, Shang KZ. Restenosis following balloon dilation of benign esophageal stenosis. *World J Gastroenterol* 2003; 9 (11): 2605-2608
http://www.wjgnet.com/1007-9327/9/2605.asp

INTRODUCTION

Balloon catheter dilation is a common nonsurgical treatment for benign esophageal stricture. Its short-term effect is good, but its long-term effect is not so good, because esophageal restenosis is a major complication. The underlying mechanism of esophageal restenosis has not been understood yet. To study this mechanism, we established a benign esophageal stricture model and restenosis model in Sprague-Dawley (SD) rats. We performed quantitative histopathological image analysis of sections of the rat esophagus, and qualitative immunohistochemical analysis of the related indicators of proliferation and restenosis of mucous and striated muscle layers of rat esophagus dilated by a balloon catheter at different time points. This provided us with an effective experimental model for investigation of the causes of restenosis.

MATERIALS AND METHODS

Materials

All protocols used for animal experiment and maintenance were approved by the Animal Ethics Committee in our university and conformed to the highest international standards of humane care.

70 male Sprague-Dawley (SD) rats weighing 305±50 g were obtained from the Shanghai Experimental Animal Center (Shanghai, China). The animals were weighed on day 0 and then 1 day before sacrifice. After anesthesia with 10 % ketamine (80 mg/kg) by abdominal injection, the animals were placed in a supine position and stabilized on an operating table. A 3F segmental epidural catheter was inserted into the mouth, and 10 ml of edible vinegar was injected into the stomach. The epidural catheter was then replaced by two 3F percutaneous transluminal coronary angioplasty (PTCA) balloon catheters at the mid-to-lower segment of the esophagus. The two balloons were at least 2 cm apart. These balloons were simultaneously inflated with air until they expanded to cling to the wall of the esophagus. Then 5 ml of a freshly prepared 50 % sodium hydroxide solution was injected through the orifice of the balloon catheter. After three minutes the air was released from the balloon. Distilled water was injected repeatedly through the same orifice for rinsing for 1 minute. The balloon catheters were removed and the animals returned to their cages for feeding. An esophageal barium-contrast examination was performed 2 and 4 weeks later to ascertain whether benign esophageal strictures had formed. We achieved 49 animal models from the 70 rats. These 49 rats were divided into two groups: rats with benign esophageal stricture caused by chemical burn only (control group, *n*=21) and rats with their esophageal stricture treated with balloon catheter dilation (experimental group, *n*=28).

Samples were collected at different times for immunohistochemical assay. We divided rats in both groups into seven subgroups according to the time after the dilation procedure when the samples were collected on day 1, 3, 5, 7, 14, 21 and 30. At the time of sacrifice, samples were fixed in 4 % buffered formaldehyde solution.

Table 1 Source of antigens and their effective concentrations

First antibody			Second antibody		
Goat antihuman PDGF	Promega	1:40	Biotinylated house antigoat IgG	Vector	1:200
Mouse antihuman FN	Life	1:20	Biotinylated house antimouse IgG	Vector	1:200
Mouse antihuman PCNA	Maxim	1:20	Biotinylated house antimouse IgG	Maxim	1:200

Statistical analysis: Data were expressed as the mean±SD. Statistical analysis was performed using the unpaired or paired *t*-test. A probability value less than 0.05 was considered significant.

Methods

Image analysis: Esophageal sections were stained with hematoxylin and eosin, and images were taken by a CCD camera (JVC, Osaka, Japan) and analyzed by a VIDAS imaging system (Carl Zeiss, Germany). The indicators used comprised the cross-sectional areas and perimeters of esophageal mucous layer, esophageal muscle layer, and the entire esophageal layers.

Immunohistochemical staining: ABC methods and SP methods were performed following the manufacturer's instructions using an ABC kit (Vector, USA) and an SP immunochemistry kit (Zymed Maxim, USA). The source of antibodies and their effective concentrations are listed in Table 1. The presence of platelet-derived growth factor (PDGF) and fibronectin (FN) was tested by the ABC method, and proliferating cell nuclear antigen (PCNA) was tested by the SP method.

RESULTS

Models of benign esophageal stricture and esophageal restenosis

Of the 49 model rats with benign esophageal stricture, 28 rats with esophageal restenosis were established.

Morphologic changes in benign esophageal stricture and esophageal restenosis

The control group showed chemical-burn lesions with an inflammatory reaction on the mucous layer of the esophagus, and comparatively slight thickening on the muscle layer of the esophagus. No broken regions were found in the muscle layer of the esophagus, and the esophageal wall was intact. Besides chemical-burn lesions, the experimental group showed mechanical damage in the mucosa of the esophagus. The muscle layer of the esophagus was thickened and broken, with accompanying inflammatory reactions (Figure 1). On the 5th day after the procedure, the broken section of the muscle layer of the esophagus became thickening, and 14 days later the degree of thickening was obvious. The changes in the cross-sectional areas and perimeters of mucosa, muscle layers, and the entire esophagus wall are listed in Table 2.

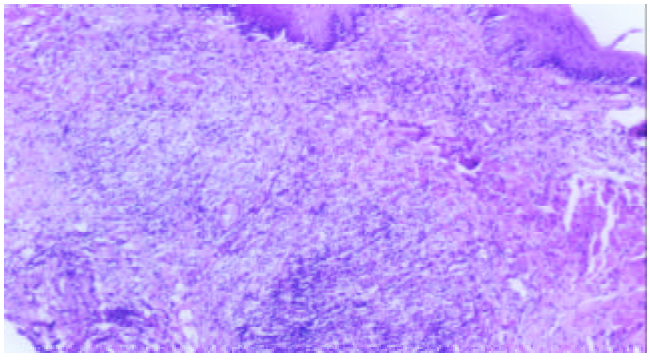

Figure 1 In the experimental group, on the 5th day after the procedure, muscle layers of the rat esophagus exhibited an inflammatory reaction. H&E stain, ×4.

Table 2 Morphologic changes in benign esophageal stricture and esophageal restenosis (area, mm^2; perimeter, mm)

	Control group	Experimental group
A1	0.49±0.14	0.75±0.18[b]
A2	1.70±0.42	1.97±0.33[a]
A3	2.20±0.45	2.72±0.46[a]
P1	4.83±1.52	6.65±1.22[b]
P2	6.89±1.96	8.80±1.67[b]
P3	9.86±2.25	14.19±2.89[b]

[b]$P<0.01$, [a]$P<0.05$ *vs* control group and experimental group. Abbreviations: A1: cross-sectional area of mucosa of esophagus, A2: cross-sectional area of muscle layer of esophagus, A3: cross-sectional area of entire esophagus wall, P1: perimeter of mucosa of esophagus, P2: perimeter of muscle layer of esophagus, P3: perimeter of entire esophagus wall.

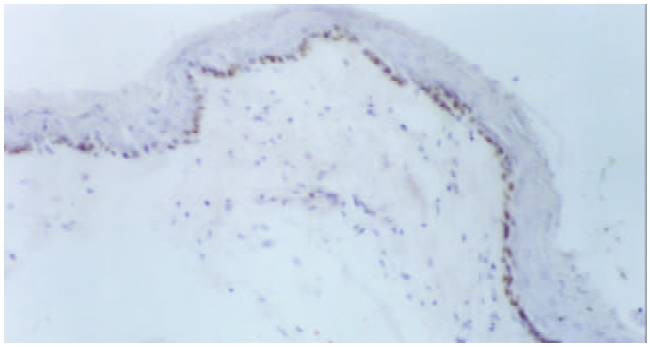

Figure 2 In the experimental group, on the 5th day after the procedure, the basal cells of the squamous epithelium in rat esophagus exhibited strong PCNA expression. Immunostaining, ×4.

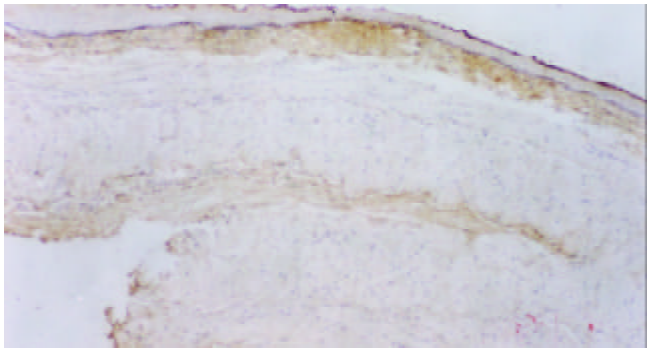

Figure 3 In the experimental group, on the 30th day after the procedure, the substratum of the rat esophageal mucosa and muscle layers exhibited strong FN expression. H&E stain, ×4.

Immunohistochemical staining of benign esophageal stricture and esophageal restenosis: In the control group, basal cells of the squamous epithelium and striated-muscle cells of the esophagus exhibited no PCNA expression. Five days after the dilation procedure, PCNA expression became obvious in

basal cells of the squamous epithelium, and this positive expression lasted for 30 days (Figure 2). In the control group, 3-7 days after the dilation procedure, the basal layer of the esophagus exhibited weak positive expression. Fourteen days later there was no FN expression in the basal layer. In the experimental group, on the 1st day after the procedure, the collagen fibers in submucosa and in the striated-muscle layer of esophagus were positive for FN, and this was still the case on the 14th day. After 1 month, FN positive expression was still reasonably strong (Figure 3). PDGF was not expressed at all in striated-muscle cells from the 1st to the 30th day in both control and experimental groups.

DISCUSSION

Models of benign esophageal stricture and esophageal restenosis

The causes of benign esophageal stricture are numerous and complicated, and hence the models thereof are difficult to reproduce consistently. However, benign esophageal stricture eventually manifests as thickened scars and reduced luminal sizes. We used chemical burns to develop the model of benign esophageal stricture because it allowed timing to be controlled and exhibited a high rate of success. Early in the 1970s, Przymanowski *et al*[1] used sodium hydroxide to establish a model of benign esophageal stricture. Their method was to perform an abdominal midsection on rats, thereby exposing the lower segment of the esophagus. They used surgical thread to tightly tie the region 2-cm either side of the lower segment of the esophagus. They then inserted a stomach tube via the mouth until it reached the tied point. Sodium hydroxide solution was injected, and then rinsed out three times for 3 minutes with distilled water later. Then they withdrew the tube, cut the threads, and closed the abdomen. Based on their procedure, we developed a nonsurgical method to establish a model of benign esophageal stricture. Since our method did not involve surgery, it was simpler and faster. Our experimental observations demonstrated that the model was satisfactorily established. Our use of two balloon catheters made manipulation somewhat difficult. We intended to make a single catheter with two balloons, but this was found to be too difficult since the rats had a narrow esophagus that demanded fine catheters and balloons. In contrast, a double-balloon catheter with a larger caliber was easy to be constructed. Therefore, the double-balloon method was used to establish the model of benign esophageal stricture.

The technique used to establish the model of esophageal restenosis is easier. After ascertaining the stricture position by esophageal visualization, we performed balloon catheter dilation under X-ray. In this way, the esophageal restenosis model was established. In a very few cases of severe stricture, the restenosis model could not be produced due to the catheters being unable to pass through.

Morphological changes in benign esophageal stricture and esophageal restenosis

After the benign esophageal stricture formed, its morphology was relatively stable. It manifested as thickened muscle layers, reduced luminal sizes, and inelastic lumens. Thus it caused dysphagia. The esophageal morphology was altered by balloon catheter dilation. The esophageal mucosa exhibited not only chemical-burn lesions, but also lesions caused by mechanical damage. The thickened muscle layer of the esophagus was torn or broken, causing the areas of mucosal and muscle layers of the esophagus to increase siginficantly in the experimental group. Significant differences were also observed in the perimeters of the mucosal and muscle layers of the esophagus and in the perimeter of the entire esophagus wall. Within the same group, after the dilation procedure the areas of each layer increased rather than decreased, whilst the perimeters also increased. This indicated that dysphagia improvement was due to an enlargement of the lumen of the esophagus after dilation. Up to a certain time, these new scar tissues would further contract and cicatrize. As a result, the duct lumen was further reduced and lacked elasticity. This was one of the key factors in esophageal restenosis. This also illustrated that if there was no treatment plan after balloon dilation in benign esophageal stricture, esophageal restenosis could not be resolved[2-28].

Immunohistochemical observation of benign estophageal stricture and estophageal restenosis

PCNA is a type of nuclear protein equivalent to the binding protein of DNA polymerase. It coordinates the synthesis of DNA up and down strands. The quantity of PCNA is minimal in normal cells at the G_0, whereas at the M stage the quantity of PCNA in transforming cells changes dramatically. The quantity of PCNA mostly declines at stage G_0/G_1. This quantative change coincides with DNA synthesis. Therefore, PCNA is used as an indicator to assess cell proliferation. There were a number of reports on the application of immunohistochemical methods to the study of tumor-cell proliferation[29]. In our study, we used the new method involving PCNA to investigate the basal-cell proliferation of the squamous epithelium in benign esophageal stricture by the procedure of balloon dilation. We found that there was no PCNA expression in the control group in basal cells of the squamous epithelium of the esophagus. However, in the experimental group, PCNA was expressed strongly from day 5 onwards 30 days later, PCNA expression was still positive. This consistently high proliferation of basal cells illustrated their importance in the development of esophageal restenosis.

FN was a glucoprotein with multiple functions[30]. As a noncollagenous substance in the extracellular matrix, it participates in various reactions between cells as well as between cells and the extracellular matrix, including adhesion, migration, injury, restoration, and tumor metasis. FN has two forms: a soluble dimerization in humor and a barely soluble polymerization in the extracellular matrix. After combining with its receptor through a tripeptide sequence Arg-Gug-(RGD), FN transmits cellular signals and facilitates cells' interfacing and kinetics. The study of FN expression in the lesion of benign estophageal stricture caused by balloon dilation is therefore helpful to elucidate the mechanism of proliferation and migration of cells. In the control group, we noticed that the expression of FN in the basal mucosa of the esophagus was weak, which indicates that FN expression after a chemical burn is related to the esophageal stricture. In the experimental group, soon after the procedure the squamous epithelium and striated-muscle cells expressed a large amount of FN. This reaction might be related to regulated cellular proliferation and chemotaxis. Previous studies have shown that FN has the similar function to growth factor in fibroblast cells. Even in small doses it can accelerate proliferation. An *in vitro* study has also shown that fibroblasts could adhere directly to the FN matrix or adhere to collagen through FN. FN can also facilitate unfolding of cells that adhere to the matrix. We also noticed that in the experimental group, FN was strongly expressed at both early and later stages after the procedure. This illustrates that FN is one of the key factors in the production of esophageal restenosis, especially at the late stage.

PDGF could stimulate the proliferation of fibroblasts *in vitro*[31-38]. Initially it was found in platelet granules, and afterwards its secretion was also found in normal cells and transformed cells. It exists in three biologically active isoforms: PDGF-AB, PDGF-AA, and PDGF-BB; comprising PDGF-A and PDGF-B polypeptide chains. It acts on target cells through receptors consisting of two subunits, α and β. PDGF-AB

combines αα and ββ functions. In our experiment, PDGF was not expressed in striated muscle cells of the esophagus, which indicates that PDGF is not a key factor in esophageal restenosis produced by balloon dilated esophageal stricture. However, the enhanced expression of PDGF was involved in the proliferation of smooth-muscle cells. In the study of restenosis, PDGF was regarded as a strong split promoter and chemotactic factor, playing an important role in the formation of blood vessel restenosis. The full length of the esophagus in SD rats (as used in our experiments) comprised striated muscle, and hence PDGF and its function could not be shown in esophageal restenosis in these rats. Besides, in clinical settings, relatively severe chemical burns of the esophagus are usually located at the middle and lower segments of the esophagus, while the upper segment is rarely involved. The middle and lower segments of the esophagus comprise smooth muscle, while the upper segment is striated muscle. This indirectly demonstrates that PDGF expressed in smooth-muscle cells plays a greater role than that in striated-muscle cells in the formation of benign esophageal stricture and restenosis.

REFERENCES

1 **Przymanowski Z.** Dilatational treatment of the esophageal constriction after burning in the light of experimental investigations and clinical observations (author's transl). *Acta Biol Med* 1970; **15**: 55-116
2 **London RL**, Trotman BW, DiMarino AJ Jr, Oleaga JA, Freiman DB, Ring EJ, Rosato EF. Dilatation of severe esophageal strictures by an inflatable balloon catheter. *Gastroenterology* 1981; **80**: 173-175
3 **Chang TS**, Wang W, Huang OL. One-stage reconstruction of esophageal defect by free transfer of jejunum: treatment and complications. *Ann Plast Surg* 1985; **15**: 492-496
4 **Kochhar R,** Nagi B, Mehta SK. Balloon catheter dilatation of esophageal strictures. *Indian J Gastroenterol* 1988; **7**: 97-98
5 **Othersen HB Jr**, Parker EF, Smith CD. The surgical management of esophageal stricture in children. A century of progress. *Ann Surg* 1988; **207**: 590-597
6 **Shemesh E**, Czerniak A. Comparison between Savary-Gilliard and balloon dilatation of benign esophageal strictures. *World J Surg* 1990; **14**: 518-522
7 **Wang C,** Wang CL, Chen CX. Four-year experience in the treatment of upper gastrointestinal strictures with balloon dilatation. *Chin Med J* 1991; **104**: 114-118
8 **Strautman PR,** Dorfman GS. Use of metallic stents to salvage and maintain patency in surgically created esophagocutaneous fistulas. *J Vasc Interv Radiol* 1992; **3**: 131-133
9 **Davies RP,** Linke RJ, Davey RB. Retrograde esophageal balloon dilatation: salvage treatment of caustic-induced stricture. *Cardiovasc Intervent Radiol* 1992; **15**: 186-188
10 **Song HY,** Han YM, Kim HN, Kim CS, Choi KC. Corrosive esophageal stricture: safety and effectiveness of balloon dilation. *Radiology* 1992; **184**: 373-378
11 **Chen PC.** Endoscopic balloon dilation of esophageal strictures following surgical anastomoses, endoscopic variceal sclerotherapy, and corrosive ingestion. *Gastrointest Endosc* 1992; **38**: 586-589
12 **Broor SL,** Lahoti D. Balloon dilation of corrosive esophageal strictures. *Gastrointest Endosc* 1993; **39**: 597-598
13 **De Wilde I,** Pieper CH, Moore SW, Hoffman B. Oesophageal stricture caused by washing powder ingestion. *S Afr Med J* 1995; **85**: 121
14 **Sinha KN**. Foley catheter self dilatation for strictures of the upper end of oesophagus. *Indian J Chest Dis Allied Sci* 1996; **38**: 91-93
15 **Hwang TL,** Chen MF. Surgical treatment of gastric outlet obstruction after corrosive injury-can early definitive operation be used instead of staged operation? *Int Surg* 1996; **81**: 119-121
16 **Panieri E,** Millar AJ, Rode H, Brown RA, Cywes S. Iatrogenic esophageal perforation in children: patterns of injury, presentation, management, and outcome. *J Pediatr Surg* 1996; **31**: 890-895
17 **Fan S,** Jiang Y, Li Z. Intraluminal stent and balloon of intraluminal stent for prevention of esophageal stenosis due to alkali corrosive injury: experimental and clinical studies. *Zhonghua Waike Zazhi* 1996; **34**: 170-172
18 **Cheng YS,** Shang KZ, Zhuang QX, Li MH, Xu JR, Yang SX. Interventional therapy and cause of restenosis of esophageal benign stricture. *Huaren Xiaohua Zazhi* 1998; **6**: 791-794
19 **Kadakia SC,** Wong RKH. Graded pneumatic dilation using Rigiflex achalasia dilators in patents with primary esophageal achalasia. *Am J Gastroenterol* 1993; **88**: 34-38
20 **Misra SP,** Dwivedi M. Entrapment of guide-wire during oesophageal dilation. *Trop Gastroenterol* 1997; **18**: 117-118
21 **De Peppo F,** Zaccara A, Dall'Oglio L, Federici di Abriola G, Ponticelli A, Marchetti P, Lucchetti MC, Rivosecchi M. Stenting for caustic strictures: esophageal replacement replaced. *J Pediatr Surg* 1998; **33**: 54-57
22 **Karnak I,** Tanyel FC, Buyukpamukcu N, Hicsonmez A. Esophageal perforations encountered during the dilation of caustic esophageal strictures. *J Cardiovasc Surg* 1998; **39**: 373-377
23 **Al-Jadaan S,** Bass J. Retrograde esophageal balloon dilatation for caustic stricture in an outpatient clinic setting. *Can J Surg* 1999; **42**: 48-50
24 **Hunt DR,** Wills VL, Weis B, Jorgensen JO, DeCarle DJ, Coo IJ. Management of esophageal perforation after pneumatic dilation for achalasia. *J Gastrointest Surg* 2000; **4**: 411-415
25 **Huang YC,** Chen SJ, Hsu WM, Li YW, Ni YH. Balloon dilation of double strictures after corrosive esophagitis. *J Pediatr Gastroenterol Nutr* 2001; **32**: 496-498
26 **Wilsey MJ Jr,** Scheimann AO, Gilger MA. The role of upper gastrointestinal endoscopy in the diagnosis and treatment of caustic ingestion, esophageal strictures, and achalasia in children. *Gastrointest Endosc Clin N Am* 2001; **11**: 767-787
27 **Gehanno P,** Guedon C. Inhibition of experimental esophageal lye strictures by penicillamine. *Arch Otolaryngol* 1981; **107**: 145-147
28 **Rivera EA,** Maves MD. Effects of neutralizing agents on esophageal burns caused by disc batteries. *Ann Otol Rhinol Laryngol* 1987; **96**: 362-366
29 **Alexandrov VA,** Novikov AI, Zabezhinsky MA, Stolyarov VI, Petrov AS. The stimulating effect of acetic acid, alcohol and thermal burn injury on esophagus and forestomach carcinogenesis induced by N-nitrososarcosin ethyl ester in rats. *Cancer Lett* 1989; **47**: 179-185
30 **Demirbilek S,** Bernay F, Rizalar R, Baris S, Gurses N. Effects of estradiol and progesterone on the synthesis of collagen in corrosive esophageal burns in rats. *J Pediatr Surg* 1994; **29**: 1425-1428
31 **Takagi K,** Tashiro T, Yamamori H, Mashima Y, Nakajima N, Sunaga K. Recombinant human growth hormone and protein metabolism of burned rats and esophagectomized patients. *Nutrition* 1995; **11**: 22-26
32 **Yoshikawa T**, Asai S, Takekawa Y, Kida A, Ishikawa K. Experimental investigation of battery-induced esophageal burn injury in rabbits. *Crit Care Med* 1997; **25**: 2039-2044
33 **Bingol-Kologlu M,** Tanyel FC, Muftuoglu S, Renda N, Cakar N, Buyukpamukcu N, Hicsonmez A. The preventive effect of heparin on stricture formation after caustic esophageal burns. *J Pediatr Surg* 1999; **34**: 291-294
34 **Kaygusuz I**, Celik O, Ozkaya OO, Yalcin S, Keles E, Cetinkaya T. Effects of interferon-alpha-2b and octreotide on healing of esophageal corrosive burns. *Laryngoscope* 2001; **111**(11 Pt1): 1999-2004
35 **Wornat MJ,** Ledesma EB, Sandrowitz AK, Roth MJ, Dawsey SM, Qiao YL, Chen W. Polycyclic aromatic hydrocarbons identified in soot extracts from domestic coal-burning stoves of Henan Province, China. *Environ Sci Technol* 2001; **35**: 1943-1952
36 **Arzbaecher R,** Jenkins JM. A review of the theoretical and experimental bases of transesophageal atrial pacing. *J Electrocardiol* 2002; **35**(Suppl): 137-141
37 **Trevisani M,** Smart D, Gunthorpe MJ, Tognetto M, Barbieri M, Campi B, Amadesi S, Gray J, Jerman JC, Brough SJ, Owen D, Smith GD, Randall AD, Harrison S, Bianchi A, Davis JB, Geppetti P. Ethanol elicits and potentiates nociceptor responses via the vanilloid receptor-1. *Nat Neurosci* 2002; **5**: 546-551
38 **Demirbilek S**, Aydin G, Yucesan S, Vural H, Bitiren M. Polyunsaturated phosphatidylcholine lowers collagen deposition in a rat model of corrosive esophageal burn. *Eur J Pediatr Surg* 2002;**12**: 8-12

Edited by Zhang JZ and Wang XL

P.O.Box 2345, Beijing 100023,China
Fax: +86-10-85381893
E-mail: wjg@wjgnet.com www.wjgnet.com

World J Gastroenterol 2003;9(11):2609-2611
World Journal of Gastroenterology
 ISSN 1007-9327

• BRIEF REPORTS •

Follow-up evaluation for benign stricture of upper gastrointestinal tract with stent insertion

Ying-Sheng Cheng, Ming-Hua Li, Wei-Xiong Chen, Qi-Xin Zhuang, Ni-Wei Chen, Ke-Zhong Shang

Ying-Sheng Cheng, Ming-Hua Li, Qi-Xin Zhuang, Ke-Zhong Shang, Department of Radiology, Sixth People' s Hospital, Shanghai Jiaotong University, Shanghai 200233, China
Wei-Xiong Chen, Ni-Wei Chen, Department of Gastroenterology, Sixth People' s Hospital, Shanghai Jiaotong University, Shanghai 200233, China
Supported by National Key Technologies Research and Development Program of China during 9th Five-Year Plan Period, No.96-907-03-04; Shanghai Nature Science Funds, No.02Z1314073; Shanghai Medical Development Funds, No.00419
Correspondence to: Dr. Ying-Sheng Cheng, Department of Radiology, Sixth People' s Hospital, Shanghai Jiaotong University, Shanghai 200233, China. chengys@sh163.net
Telephone: +86-21-64368920 **Fax.:** +86-21-64701361
Received: 2003-05-13 **Accepted:** 2003-06-02

Abstract

AIM: To determine the best mothod for benign stricture of the upper gastrointestinal tract (UGIT) with stent insertion by follow-up evaluation.

METHODS: A total of 110 stents insertions were performed in 110 cases of benign stricture of the UGIT. Permanent (group A) and temporary (group B) placement of an expandable metal stent in 30 cases and 80 cases respectively. All cases were completed under fluoroscopy.

RESULTS: In group A, 30 uncovered or antireflux covered or partially covered expandable metal stents were placed permanently. In group A, 5 cases (16.7 %) in 3-months, 5 cases (20.0 %) in 6-months, 6 cases (25 %) in the 1st year, 6 cases (50 %) in the 3rd year, and 4 cases (80 %) in the 5th year exhibited dysphagia relapse. In group B, a partially-covered expandable metal stent was temporarily placed in each patient and removed after 3-7 days via gastroscopy. Follow-up data in this group showed that 8 cases (7.5 %) in 3-months, 9 cases (12.0 %) in 6-months,10 cases (15.4 %) in the 1st year, 6 cases (20 %) in the 3rd year, and 3 cases (25 %) in the 5th year exhibited dysphagia relapse. The placement and withdrawal of all stents were all performed successfully. The follow-up of all cases lasted for 3-99 months (mean 41.6±19.7 months).

CONCLUSION: The best mothod for benign stricture of UGIT with stent insertion is temporary placement of a partially-covered expandable metal stent.

Cheng YS, Li MH, Chen WX, Zhuang QX, Chen NW, Shang KZ. Follow-up evaluation for benign stricture of upper gastrointestinal tract with stent insertion. *World J Gastroenterol* 2003; 9(11): 2609-2611
http://www.wjgnet.com/1007-9327/9/2609.asp

INTRODUCTION

Benign stricture of the upper gastrointestinal tract (UGIT) refers to stenosis caused by benign pathological changes in the pharynx, esophagus, stomach, and duodenum. Such stenosis includes marginal stricture after surgery, chemical-burn-related stricture, simple scar-related stricture after radiation therapy for tumor, digestive stricture, and functional stricture (achalasia). Since July 1994 , 110 cases with benign stricture of the UGIT have been treated with stent insertion and followed-up. We herein report our experiences.

MATERIALS AND METHODS

Materials

Our subjects were 110 patients with benign stricture of the UGIT (61 males, 49 females; age 18-84 years, mean 53.9 years). Sequential trials were adopted for these cases who were nonrandomly divided into the following two groups according to the method of stent insertion: 30 cases with permanent uncovered or antireflux covered or partially covered metal stent dilation (group A), and 80 cases with temporary partially covered metal stent dilation (group B). In group A there were 6 cases of simple cicatricial stricture after radiation therapy for esophageal carcinoma, 8 cases of achalasia, 13 cases of esophageal and esophagogastric marginal stricture, 2 cases of gastroduodenal marginal stricture, and 1 case of esophageal chemical-burn-related stricture. The mean diameter of the strictured UGIT was 3.2±2.3 mm before stent placement and 17.8±2.4 mm after stent placement. In group B there were 2 cases of simple scar-related stricture after radiation therapy for esphageal carcinoma, 67 cases of achalasia, 9 cases of esophageal and esophagogastric marginal stricture,and 2 cases of esophageal chemical burn. The mean diameter of the strictured UGIT was 3.3±2.1 mm before stent placement and 22.3±2.7 mm after stent placement. All cases had dysphagia grades 2-4 before stent insertion and dysphagia grades 0-2 after stent insertion. All casess were examined by barium-meal radiography of the UGIT and gastroscopy.

Methods

It involved an empty stomach for at least 4 h and examination of the normal bleeding and clotting time. Two types of metal stent were used: covered stainless steel wire Z-stent (COOK, USA), and partially covered or uncovered or antireflux covered nitinol stent (Zhiye Medical Equipment Research Institute, Changzhou, China; and Youyan Yijin Advanced Materials Co. Ltd, Beijing, China). The COOK stents were constructed from multiple fragments, each fragment was typically 2-cm long. The stent was completely coated on the outer layer and mounted with a metal barb. The diameter of the stent body was 18 mm and that of the horn was 25 mm. The body of the partially covered metal stents was coated with intracavity silica gel. The areas within 2 cm of both ends of the stents were not covered. Stents were 4-14 cm in length and 16-30 mm in diameter. They had single or double horns, the horn diameter was 20-35 mm.

The different types of metal stents were placed differently. For example, placement of the partially-covered nitinol internal stent used in groups B and C firstly involved spraying the

pharynx with 1% lidocaine (as a mist) for anesthesia. When a stent was a placed, the patients were placed in a sitting position or lying on the side, and where applicable with their false teeth removed and a teeth bracket mounted. A 260-cm-long guidewire was first led into the distal end of the benign stricture. The stent was mounted on the propeller whose front end was coated with sterilized liquid paraffin. Guided by the wire, the propeller on which the stent was mounted was moved through the strictured section. Under fluoroscopic control, the outer sheath was slowly withdrawn and the stent expanded under its own tension. After the stent was placed, radiography was performed to observe the patency of the UGIT. In group B, 500-1 000 ml of ice-cold water was injected 3-7 days after stent placement via a bioptic hole under gastroscopy, which caused the stent to reduce its diameter. Bioptic pliers were then used to withdraw the stent using a gastroscope. Gastroscopy was performed again in the UGIT to detect complications, such as bleeding, mucosal tearing, or perforation of the UGIT. The patients returned to the ward and consumed cold drinks and snacks for 2 days before resuming a normal diet. It was preferable for patients to eat solid food since the natural expansion caused by ingesting food reduced the retraction of the UGIT.

Criteria for therapeutic efficacy included diameter of the most-strictured section of the UGIT before and after dilation, and dysphagia score before and after dilation.

After stent placement barium-meal radiography was performed to observe patency of the UGIT. The patients ate semifluid food on the day after surgery, and were treated with antibiotics, antacids, and antireflux drugs. One week after stent removal, barium-meal radiography of the UGIT was performed to observe patency of the UGIT. The patients went to a clinic or were followed-up by telephone at the 3rd, 6th months, 1st, 3rd and 5th year.

RESULTS

In group A, 30 uncovered or antireflux covered or partially-covered stents were placed. Stent placement was successful in all the cases. In group B, 80 partially- covered stents were placed and removed under gastroscopy guidance 3-7 days after stent insertion. The successful rate of stent placement and extraction was 100 %. Relapse rate of dysphagia treated with stent insertion during follow-up is shown in Table 1.

DISCUSSION

Since Domschke *et al*[1] reported the first successful treatment of malignant esophageal strictures with an uncovered expandable metal stent in 1990, placement of covered or uncovered or antireflux covered expandable UGIT metal stents has been shown to be a safe, easy, and effective treatment for malignant UGIT strictures. Cwikiel *et al*[2] reported the first successful treatment of benign esophageal strictures in 1993. Cheng *et al*[3] reported the first successful treatment of benign esophageal strictures with temporary partially covered stent in 1999. Many patients with benign UGIT strictures have received treatment with uncovered or covered or temporary partially covered metal stents[4-26]. Permanent uncovered metal stent insertion for benign functional stricture in the UGIT had poor mid-term and long-term therapeutic efficiency, mainly due to frequent severe gastroesophageal reflux and restenosis (hyperplasia of granulation tissue). After a 12-month follow-up, three uncovered metal stents could not be removed in three cases of achalasia, and we had to resect and reconstruct the esophageal cardia. Therefore, permanent uncovered metal stent dilation is not suitable for cases of functional stricture of the UGIT. Permanent partially covered metal stent dilation had poor mid-term and long-term therapeutic efficiency, mainly due to reflux and stent migration[27-37].

Temporary partially-covered metal stent dilation was used for benign stricture of the UGIT with both excellent immediate and mid- and long-term therapeutic efficacy. Firstly, the design of the stent coincided with the specific anatomy of the UGIT and pathological manifestations of benign stricture. If a stent was not well designed, it did not exhibit therapeutic efficacy, and was also associated with a higher frequency of complications such as stent migration. With the aim of solving these problems, we designed a special stent for benign stricture of the UGIT. The stent was partially covered. A membrane covered the inner wall of the stent, with the area within 2 cm of the stent orifice not covered. The upper orifice of the stent was a large horn, which increased the stability of the stent but made it difficult to withdraw. Secondly, the diameter of the stents used in this group was 16-30 mm. By dilating the stent, the stricture could almost be returned to the maximum diameter of a normal strictured UGIT. What the diameter of a stent is most appropriate is that the stent should expand the strictured part without complications. We found that the bigger the diameter of stents was, the better the mid- and long-term therapeutic efficacy was ,but the ideal size still needs to be further investigated.

The further development of biologically degraded stents for the gastrointestinal tract would provide advantages of a very long retention time without the necessity to remove the stent[38]. This would provide potentially superior stent insertion for cases of benign stricture of the UGIT. In the treatment of UGIT benign stricture with stent insertion, temporary partially-covered metal stent dilation will gradually replace others and become the preferred method for the nonsurgical treatment of

Table 1 Relapse rate of dysphagia treated with stent insertion

Group	Follow-up >3 months (*n*)	Dysphagia relapse (*n*)	Dysphagia relapse rate (%)	Follow-up >6 months year (*n*)	Dysphagia relapse (*n*)	Dysphagia relapse rate (%)
A	30	5	16.7%	25	5	20.0%
B	80	8	7.5%	75	9	12.0%

Group	Follow-up>1st year (*n*)	Dysphagia relapse (*n*)	Dysphagia relapse rate (%)
A	24	6	25.0 %
B	65	10	15.4 %

Group	Follow-up >3rd year (*n*)	Dysphagia relapse (*n*)	Dysphagia relapse rate (%)	Follow-up >5th year (*n*)	Dysphagia relapse (*n*)	Dysphagia relapse rate (%)
A	12	6	50.0 %	5	4	80.0%
B	30	6	20.0 %	12	3	25.0%

benign stricture in gastrointestinal tract due to its superior mid-term and long-term therapeutic efficacy[39,40].

According to our experiences in the treatment of 110 casess of benign stricture of the UGIT with stent insertion, we consider that the method chosen for an individual case should be based on the nature of the stricture, course of disease, and complications. Moreover, long-term therapeutic efficacy and medical expense need to be comprehensively assessed. Finally, other combined therapies should be carried out concurrently both before and after the treatment in order to achieve a high therapeutic efficacy.

REFERENCES

1 **Domschke W,** Foerster EC, Matek W, Rodl W. Self-expanding mesh stent for esophageal cancer stenosis. *Endoscopy* 1990; **22**: 134-136
2 **Cwikiel W,** Willen R, Stridbeck H, Liool -Cil R, Von Holstein CS. Self-expanding stent in the treatment of benign esophageal stricture:experimental study in pigs and presentation of clinical cases. *Radiology* 1993; **187**: 667-671
3 **Cheng YS,** Yang RJ, Shang KZ, Li MH, Chen WX, Zhuang QX, Xu JR, Chen NW, Yang SX. Esophageal benign structure with temporary stent insertion. *Jieru Fangshexue Zazhi* 1999; **8**: 32-34
4 **Song HY,** Choi KC, Kwon HC, Yang DH, Cho BH, Lee ST. Esophageal strictures: treatment with a new design of modified Gianturco stent. Work in progress. *Radiology* 1992; **184**: 729-734
5 **Cwikiel W,** Willen R, Stridbeck H, Lillo-Gil R, von Holstein CS. Self-expanding stent in the treatment of benign esophageal strictures: experimental study in pigs and presentation of clinical cases. *Radiology* 1993; **187**: 667-671
6 **Song HY,** Do YS, Han YM, Sung KB, Choi EK, Sohn KH, Kim HR, Kim SH, Min YI. Covered, expandable esophageal metallic stent tubes: experiences in 119 patients. *Radiology* 1994; **193**: 689-695
7 **Foster DR.** Use of a Strecker oesophageal stent in the treatment of benign oesophageal stricture. *Australas Radiol* 1995; **39**: 399-400
8 **Profili S,** Bifulco V, Demelas P, Migaleddu V, Meloni GB. Possibility of using self-expanding uncoated stents in benign esophageal stenosis. Experience in a case of post-irradiation stenosis. *Radiol Med* 1995; **89**: 171-173
9 **Strecker EP,** Boos I, Vetter S, Strohm M, Domschke S. Nitinol esophageal stents: new designs and clinical indications. *Cardiovasc Intervent Radiol* 1996; **19**: 15-20
10 **De Gregorio BT,** Kinsman K, Katon RM, Morrison K, Saxon RR, Barton RE, Keller FS, Rosch J. Treatment of esophageal obstruction from mediastinal compressive tumor with covered, self-expanding metallic Z-stents. *Gastrointest Endosc* 1996; **43**: 483-489
11 **Moores DW,** Ilves R. Treatment of esophageal obstruction with covered, self-expanding esophageal Wallstents. *Ann Thorac Surg* 1996; **62**: 963-967
12 **Song HY,** Park SI, Do YS, Yoon HK, Sung KB, Sohn KH, Min YI. Expandable metallic stent placement in patients with benign esophageal strictures: results of long-term follow-up. *Radiology* 1997; **203**: 131-136
13 **Foster DR.** Self-expandable oesophageal stents in the management of benign peptic oesophageal strictures in the elderly. *Br J Clin Pract* 1997; **51**: 199
14 **Tan BS,** Kennedy C, Morgan R, Owen W, Adam A. Using uncovered metallic endoprostheses to treat recurrent benign esophageal strictures. *Am J Roentgenol* 1997; **169**: 1281-1284
15 **Sheikh RA,** Trudeau WL. Expandable metallic stent placement in patients with benign esophageal strictures: results of long-term follow-up. *Gastrointest Endosc* 1998; **48**: 227-229
16 **Neuhaus H,** Schumacher B. Use of metal stents in gastroenterology. *Z Gastroenterol* 1998; **36**: 121-134
17 **Sheikh RA,** Trudeau WL. Expandable metallic stent placement in patients with benign esophageal strictures: results of long-term follow-up. *Gastrointest Endosc* 1998; **48**: 227-229
18 **Wengrower D,** Fiorini A, Valero J, Waldbaum C, Chopita N, Landoni N, Judchack S, Goldin E. EsophaCoil: Long-term results in 81 patients. *Gastrointest Endosc* 1998; **48**: 376-382
19 **Sandha GS,** Marcon NE. Expandable metal stents for benign esophageal obstruction.*Gastrointest Endosc Clin N Am* 1999; **9**: 437-446
20 **Boulis NM,** Armstrong WS, Chandler WF, Orringer MB. Epidural abscess: a delayed complication of esophageal stenting for benign stricture. *Ann Thorac Surg* 1999; **68**: 568-570
21 **Fiorini A,** Fleischer D, Valero J, Israeli E, Wengrower D, Goldin E. Self-expandable metal coil stents in the treatment of benign esophageal strictures refractory to conventional therapy: a case series. *Gastrointest Endosc* 2000; **52**: 259-262
22 **Macdonald S,** Edwards RD, Moss JG. Patient tolerance of cervical esophageal metallic stents. *J Vasc Interv Radiol* 2000; **11**: 891-898
23 **Lee JG,** Hsu R, Leung JW. Are self-expanding metal mesh stents useful in the treatment of benign esophageal stenoses and fistulas? An experience of four cases. *Am J Gastroenterol* 2000; **95**: 1920-1925
24 **Song HY,** Jung HY, Park SI, Kim SB, Lee DH, Kang SG, Min Y. Covered retrievable expandable nitinol stents in patients with benign esophageal strictures: initial experience. *Radiology* 2000; **217**: 551-557
25 **Cordero JA Jr,** Moores DW. Self-expanding esophageal metallic stents in the treatment of esophageal obstruction. *Am Surg* 2000; **66**: 956-959
26 **Ackroyd R,** Watson DI, Devitt PG, Jamieson GG. Expandable metallic stents should not be used in the treatment of benign esophageal strictures. *J Gastroenterol Hepatol* 2001; **16**: 484-487
27 **Dormann AJ,** Deppe H, Wigginghaus B. Self-expanding metallic stents for continuous dilatation of benign stenoses in gastrointestinal tract - first results of long-term follow-up in interim stent application in pyloric and colonic obstructions. *Z Gastroenterol* 2001; **39**: 957-960
28 **Profili S,** Meloni GB, Feo CF, Pischedda A, Bozzo C, Ginesu GC, Canalis GC. Self-expandable metal stents in the management of cervical oesophageal and/or hypopharyngeal strictures. *Clin Radiol* 2002; **57**: 1028-1033
29 **Yates MR 3rd,** Morgan DE, Baron TH. Palliation of malignant gastric and small intestinal strictures with self-expandable metal stents. *Endoscopy* 1998; **30**: 266-272
30 **Mauro MA,** Koehler RE, Baron TH. Advances in gastrointestinal intervention: the treatment of gastroduodenal and colorectal obstructions with metallic stents. *Radiology* 2000; **215**: 659-669
31 **DePalma GD,** Catanzano C. Removable self-expanding metal stents: a pilot study for treatment of achalasia of the esophagus. *Endoscopy* 1998; **30**: S95-96
32 **Ell C,** May A, Hahn EG. Self-expanding metal endoprosthesis in palliation of stenosing tumors of the upper gastrointestinal tract. Comparison of experience with three stent types in 82 implantations. *Dtsch Med Wochensch* 1995; **120**: 1343-1348
33 **Smout AJ.** Back to the Whale bone? *Gut* 1999; **44**: 149-150
34 **Mumtaz H,** Barone GW, Ketel BL, Ozdemir A. Successful management of a nonmalignant esophageal perforation with a coated stent. *Ann Thorac Surg* 2002; **74**: 1233-1235
35 **Acunas B,** Poyanli A, Rozanes I. Intervention in gastrointestinal tract: the treatment of esophageal, gastroduodenal and colorectal obstructions with metallic stents. *Eur J Radiol* 2002; **42**: 240-248
36 **Petruzziello L,** Costamagna G. Stenting in esophageal strictures. *Dig Dis* 2002; **20**: 154-166
37 **Catnach S,** Barrison I. Self-expanding metal stents for the treatment of benign esophageal strictures. *Gastrointest Endosc* 2001; **54**: 140
38 **Fry SW,** Fleischer DE. Management of a refractory benign esophageal stricture with a new biodegradable stent. *Gastrointest Endosc* 1997; **45**: 179-182
39 **Catnach S,** Barrison I. Self-expanding metal stents for the treatment of benign esophageal strictures. *Gastrointest Endosc* 2001; **54**: 140
40 **Therasse E,** Oliva VL, Lafontaine E, Perreault P, Giroux MF, Soulez G. Balloon dilation and stent placement for esophageal lesions: indications, methods, and results. *Radiographics* 2003; **23**: 89-105

Edited by Zhang JZ and Wang XL

P.O.Box 2345, Beijing 100023,China
Fax: +86-10-85381893
E-mail: wjg@wjgnet.com www.wjgnet.com

World J Gastroenterol 2003;9(11):2612-2615
World Journal of Gastroenterology
 ISSN 1007-9327

• BRIEF REPORTS •

Relationship between genetic polymorphism of cytochrome P450IIE1 and fatty liver

Yun-Feng Piao, Jing-Tao Li, Yang Shi

Yun-Feng Piao, Jing-Tao Li, Yang Shi, Department of Gastroenterology, First Hospital, Jilin University, Changchun 130021, Jilin Province, China
Correspondence to: Dr. Yang Shi, Department of Gastroenterology, First Hospital, Jilin University, 1 Xinmin Road, Changchun 130021, Jilin Province, China. shiyangwhy@163.com
Telephone: +86-431-5612242 **Fax:** +86-431-5612542
Received: 2003-03-29 **Accepted:** 2003-05-17

Abstract

AIM: To study the correlation between genetic polymorphism of cytochrome P450IIE1 (CYPIIE1) and fatty liver.

METHODS: Peripheral blood mononuclear cells were collected in 56 patients with fatty liver, 26 patients without fatty liver and 20 normal controls. Then PCR-RFLP was used to analyze genetic polymorphism of CYPIIE1 in monocytes on the region of Pst I and Rsa I.

RESULTS: The frequency of homozygotic C1 gene in patients with alcoholic fatty liver (28.6 %), obese fatty liver (38.5 %), or diabetic fatty liver (33.3 %) was significantly lower than that of the corresponding patients without fatty liver (100 %, 100 % and 80 % respectively), while the frequency of C2 genes, including C1/C2 and C2/C2, was significantly higher (71.4 %/0 %, 61.5 %/0 %, and 66.7 %/20 %) (P<0.01). The frequency distribution of the above genes of non-fatty liver patients (100 %/0, 100 %/0, and 80 %/20 %) was not significantly different from that of the normal controls (85 %/15 %) (P>0.05).

CONCLUSION: The genetic polymorphism of CYPIIE1 on the position of Pst I and Rsa I is related to the susceptibility of fatty liver. Besides, C2 gene may play a key role in the pathogenesis of fatty liver.

Piao YF, Li JT, Shi Y. Relationship between genetic polymorphism of cytochrome P450IIE1 and fatty liver. *World J Gastroenterol* 2003; 9(11): 2612-2615

http://www.wjgnet.com/1007-9327/9/2612.asp

INTRODUCTION

Cytochrome P450 (CYP) is a group of isoenzymes encoded by genes with similar structure and function, whose molecular weight is 40-60KD. CYP is a kind of monooxygenase, located in the smooth endoplasmic reticulum of cells. According to the similarity of amino acid sequence, CYP is divided into CYPI, CYPII, CYPIII, and CYPIV gene families. The subfamily is named alphabetically, and every enzyme is named in number order. Cytochrome P450IIE1 (CYPIIE1) is a N-nitrosodimethylamine demethylase, which is mainly expressed in the liver with an evident racial and individual difference in activity. It not only takes part in the metabolism of drugs, but also activates a lot of precarcinogens and prepoison[1-4]. Human CYPIIE1 is located in 10q2403-qter. It is 1104Kb consisting of 9 extrons and 8 introns, encoding a 493-amino acid protein[5]. The polymorphism of CYPIIE1 gene is significantly different among races and individuals. It may be related to some genetic factors. CYPIIE1 has 6 restriction fragment length polymorphisms (RFLP), among which 5' -flanking region of Pst I and Rsa I affects CYPIIE1 expression at the transcription level. C2 allelic gene can enhance the transcription, which causes the different activities of CYPIIE1[6-11].

Fatty liver is common and is resulted frequently from alcohol excess, obesity, diabetes or drugs[12-17]. Its pathogenesis remains unclear. Studies on the relationship between genetic polymorphisms of CYPIIE1 and the development of alcoholic fatty liver has been reported, but the results are disputable[17-21]. In this study, we used PCR-RFLP to study the relationship between genetic polymorphisms of CYPIIE1 and alcoholic or non-alcoholic fatty liver.

MATERIALS AND METHODS

Reagents

Heparin and lymphocyte separation medium were purchased from Tianjin Hematologic Institution of Chinese Academy of Medical Sciences. The primers of CYPIIE1, PCR buffer, dNTP, and Taq enzyme were obtained from Roche (America). Restriction endonucleases (PstIand RsaI), their buffer, and pUC19-DNA marker were obtained from MBI Ferments.

Patients and controls

From October 1998 to January 2001, 82 patients from several hospitals in Jilin Province were studied, among them 28 cases had alcoholic fatty liver, 8 cases had alcoholism but no liver disease, 13 cases had obese fatty liver, 8 cases had obesity but no fatty liver, 15 cases had diabetic fatty liver, and 10 cases had diabetes but no fatty liver. Twenty health blood donors were used as normal controls. The standard of alcoholism for female was drinking alcohol >40 g/d, for male drinking alcohol >80 g/d, for at least 5 years. The age and sex distribution of the two groups were similar. Five ml venous blood was taken from every person and anticoagulated with heparin.

PCR-RFLP

Peripheral blood mononuclear cells (PBMC) were separated by density gradient centrifugation. Then DNA was extracted. The two primers of CYPIIE1 were 5' -ccagtcgagtctacattgtca-3' (1 370-1 349) and 5' -ttcattctgtcttctaactgg-3' (999-978) respectively. PCR was conducted for 40 cycles with denaturing at 94 ℃ for 1 min, annealing at 50 ℃ for 1 min, extending at 72 ℃ for 1 min, and then designed to extend at 72 ℃ for 10 min. The PCR products were digested with Pst I or Rsa I at 37 ℃ for 2 hours, then loaded onto a 20 g/L agarose gel for electrophoresis. At last, the DNA fragments were observed under ultraviolet lamp.

Statistical analysis

Analysis of data was performed using χ^2 test. P<0.05 was considered to be statistically significant.

RESULTS

Genetic polymorphism of CYPIIE1

The PCR products were fragments of 410 bp (Figure 1). After digestion with restriction enzyme Pst I or Rsa I, CYPIIE1 was divided wild type homozygote group (C1/C1, type A), heterozygote group (C1/C2, type B) and mutant homozygote group (C2/C2, type C) (Figure 2). C1 referred to wild type gene (PstI+, RsaI-), and C2 referred to mutant gene (PstI-,RsaI+).

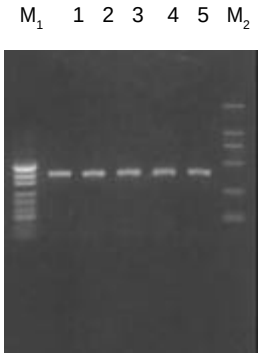

Figure 1 Electrophoregram of PCR products (Lanes 1-5). The signals of pUC19-DNA marker (M_1) present 489 bp, 404 bp, 331 bp, 242 bp, 190 bp, 147 bp and 110 bp from up to bottom. The signals of DL2000-DNA marker (M_2) present 2 000 bp, 1 000 bp, 750 bp, 500 bp, 250 bp and 100 bp from up to bottom.

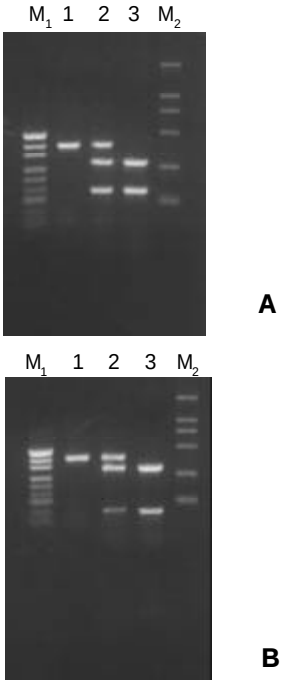

Figure 2 After digested with restriction enzyme PstI(A) or RsaI (B), CYPIIE1 was divided into three types, namely wild type homozygote (C1/C1) (Lane 1), heterozygote (C1/C2)(Lane 2) and mutant homozygote (C2/C2)(Lane 3). C1 means wild type gene (PstI+, RsaI-), and C2 mutant gene (PstI-, RsaI+). pUC19-DNA marker (M_1) and DL2000-DNA marker (M_2).

Genotype distribution

The genotype distribution of each group of patients and controls are presented in Table 1.

Comparison of gene frequency

The frequency of homozygotic C1 gene in patients with alcoholic, obese, or diabetic fatty liver was significantly lower than that of patients with corresponding diseases but without fatty liver, while the frequency of C2 genes, including C1/C2 and C2/C2, was significantly higher (P<0.01) (Table 2). Compared with healthy controls, the frequency of homozygotic C1 gene of the patients with alcoholic, obese, or diabetic fatty liver was apparently lower and the frequency of C2 gene was apparently higher (P<0.01). At the same time, there was no obvious difference in homozygotic C1 gene or C2 gene between healthy controls and patients with alcoholism, obesity or diabetes but without fatty liver (P>0.05).

Table 1 Genotype distribution of each group of patients and controls

Group	*n*	A (C1/C1)	B (C1/C2)	C (C2/C2)
Patients with alcoholic fatty liver	28	8	14	6
Patients with alcoholism but without liver diseases	8	8	0	0
Patients with obese fatty liver	13	5	6	2
Patients with obese but without fatty liver	8	8	0	0
Patients with diabetic fatty liver	15	5	8	2
Patients with diabetes but without fatty liver	10	8	2	0
Healthy controls	20	17	3	0

Table 2 Comparison of gene frequency of each group (%)

Group	A	B	C	C2 frequency
Patients with alcoholic fatty liver	28.6	50.0	21.4	71.4
Patients with alcoholism but without liver diseases	100	0	0	0
Patients with obese fatty liver	38.5	46.1	15.4	61.5
Patients with obese but without fatty liver	100	0	0	0
Patients with diabetic fatty liver	33.3	53.4	13.3	66.7
Patients with diabetes but without fatty liver	80	20	0	20
Healthy controls	85	15	0	15

DISCUSSION

There are three metabolic pathways of ethanol in the liver, alcohol dehydrogenase (ADH) in cytoplasm, microsomal ethanol oxidazing system (MEOS) in smooth endoplasmic reticulum, and catalase in peroxidase. The major component of MEOS is CYPIIE1[22,23]. When concentration of ethanol in blood and liver tissue is low, most of ethanol is oxidized by ADH. While for the alcoholism or the people in whose liver tissue the concentration of ethanol is higher than 10 mmol/L, the activation of MESO plays a key role in metabolism of ethanol. In the pathogenesis of alcoholic fatty liver, the function of CYPIIE1 was mainly to take part in lipid peroxidation (LOP) reaction and to increase the contents of microsomal oxygen and carbonyl free radical[16,24,25]. It has been proved in rat models that generation of microsomal oxygen and carbonyl free radical formed from oxidated ethanol was related to CYPIIE1[26,27]. It was presumed that these oxygen-derived free radicals might impair the liver by directly damaging liver cells, affecting the sensititity of the liver to LPO, and inducing antibody-dependent cytotoxic effect through combination with CYPIIE1 on the cell membrane[28-30]. Not every alcoholic abuser could inevitably induce liver injury. Iwahashi K and colleagues[31] reported that in the people who had C2 allele, CYPIIE1 activity was much

higher, and metabolic ability on ethanol was much stronger. Our results showed that homozygotic C1 gene frequency of the patients with alcoholic fatty liver was significantly lower than that of the controls or the patients with alcoholism but without fatty liver, while C2 gene frequency was much higher. It suggested that C2 gene might induce the expression of CYPIIE1 and facilitate genesis of alcoholic fatty liver.

LPO also took part in the pathogenesis of non-alcoholic fatty liver induced by obese or diabetes[32,33]. Now the precise stimulator of LPO reaction is unclear. The expression of CYPIIE1 in the animal models and patients with nonalcoholic fatty liver might be related to the induction of acetone and fatty acid[34,35]. It has been proved that the level of CYPIIE1 in the rats with obesity was four times as high as that of the rats without obesity[36]. The rising concentration of fatty acid and pyruvic acid in the liver might be a risk factor in pathogenesis of nonalcoholic fatty liver. When the increased fatty acid concentration in blood of patients with obesity could not be oxidated by mitochondria completely, CYPIIE1 would have the ability to oxidize fatty acid and in turn is activated by it so as to strengthen the oxidation ability. During oxidation of fatty acid, high reactivity carbonyl free radicals would be produced, which then stimulated the production of LPO, at last injured the liver[37]. In patients with diabetes, the ketone bodies produced by the liver could not be totally utilized by extrahepatic tissues, and the level of acetone would rise in the liver. The acetone could not only induce CYPIIE1 activation, but also be resolved by it. A great many of free radicals were produced, thus injuring the liver[38]. Not all patients with obesity or diabetes suffer from fatty liver. Our results showed that C2 gene frequency in patients with obese fatty liver or diabetic fatty liver was obviously higher than that of the patients without fatty liver. In conclusion, C2 gene frequency in patients with alcoholic or nonalcoholic fatty liver is much higher than that of controls. So C2 gene may be important for the pathogenesis of fatty liver.

REFERENCES

1 **Koop DR.** Oxidative and reductive metabolism by cytochrome P4502E1. *FASEB J* 1992; **6**: 724-730
2 **Gonzalez FJ**, Gelboin HV. Transcriptional and posttranscriptional regulation of CYP 2E1, an N-nitrosodimethylamine demethylase. *Princess Takamatsu Symp* 1990; **21**: 157-164
3 **Ramaiah SK**, Apte U, Mehendale HM. Cytochrome P450 2E1 induction increases thioacetamide liver injury in diet-restricted rats. *Drug Metab Dispos* 2001; **29**: 1088-1095
4 **Zangar RC**, Benson JM, Burnett VL, Springer DL. Cytochrome P450 2E1 is the primary enzyme responsible for low-dose carbon tetrachloride metabolism in human liver microsomes. *Chem Biol Interact* 2000; **15**: 233-243
5 **Umeno M**, McBride OW, Yang CS, Gelboin HV, Gonzalez FJ. Human ethanol-inducible P450IIE1: complete gene sequence, promoter characterization, chromosome mapping, and cDNA-directed expression. *Biochemistry* 1988; **27**: 9006-9013
6 **Han XM**, Zhou HH. Polymorphism of CYP450 and cancer susceptibility. *Acta Pharmacol Sin* 2000; **21**: 673-679
7 **Snawder JE**, Lipscomb JC. Interindividual variance of cytochrome P450 forms in human hepatic microsomes: correlation of individual forms with xenobiotic metalolism and implications in risk assessment. *Regul Toxical Pharmacol* 2000; **32**: 200-209
8 **Stephens EA**, Taylor JA, Kaplan N, Yang CH, Hsieh LL, Lucier GW, Bell DA. Ethnic variation in the CYPE1 gene polymorphism analysis of 695 African-Americans, European-Americans and Taiwanese. *Pharmacogenetics* 1994; **4**: 185-192
9 **Watanabe J**, Hayashi S, Kawajiri K. Different regulation and expression of the human CYP2E1 gene due to the Ras I polymrophim in the 5'-flanking region. *J Biochem* 1994; **116**: 321-326
10 **Hu Y**, Hakkola J, Oscarson M, Ingelman-Sundberg M. Structural and functional characterization of the 5'-flanking region of the rat and human cytochrome P4502E1 genes: indentification of a polymorphic repeat in the human gene. *Biochem Biophys Res Commun* 1999; **263**: 286-293
11 **Hayashi SI**, Watanabe J, Kawajiri K. Genetic polymorphisms in the 5'-flanking region change transcriptional regulation of human cytochrome P450IIE1. *J Biochem* 1991; **110**: 559-565
12 **Farrell GC**. Drugs and steatohepatitis. *Semin Liver Dis* 2002; **22**: 185-194
13 **Niemela O**, Parkkila S, Juvonen RO, Viitala K, Gelboin HV, Pasanen M. Cytochromes P450 2A6, 2E1, and 3A and production of protein-aldehyde adducts in the liver of patients with alcoholic and non-alcoholic liver diseases. *J Hepatol* 2000; **33**: 893-901
14 **Pirttiaho HI**, Salmela PI, Sotaniemi EA, Pelkonen RO, Pitkanen U, Luoma PV. Drug metabolism in diabetic subjects with fatty livers. *Br J Clin Pharmacol* 1984; **18**: 895-899
15 **Karvonen I**, Stengard JH, Huupponen R, Stenback FG, Sotaniemi EA. Effects of enzyme induction therapy on glucose and drug metabolism in obese mice model of non-insulin dependent diabetes mellitus. *Diabetes Res* 1989; **10**: 85-92
16 **Yang S**, Zhu H, Li Y, Lin H, Gabrielson K, Trush MA, Diehl AM. Mitochondrial adaptations to obesity-related oxidant stress. *Arch Biochem Biophys* 2000; **378**: 259-268
17 **Vidali M**, Stewart SF, Rolla R, Daly AK, Chen Y, Mottaran E, Jones DE, Leathart JB, Day CP, Albano E. Genetic and epigenetic factors in autoimmune reactions toward cytochrome P4502E1 in alcoholic liver disease. *Hepatology* 2003; **37**: 410-419
18 **Robertson G**, Leclercq I, Farrell GC. Nonalcoholic steatosis and steatohepatitis. II. Cytochrome P-450 enzymes and oxidative stress. *Am J Physiol Gastrointest Liver Physiol* 2001; **281**: 1135-1139
19 **Sinclair JF**, Szakacs JG, Wood SG, Walton HS, Bement JL, Gonzalez FJ, Jeffery EH, Wrighton SA, Bement WJ, Sinclair PR. Short-term treatment with alcohols causes hepatic steatosis and enhances acetaminophen hepatotoxicity in Cyp2e1 (-/-) mice. *Toxicol Appl Pharmacol* 2000; **168**: 114-122
20 **Jarvelainen HA**, Fang C, Ingelman-Sundberg M, Lukkari TA, Sippel H, Lindros KO. Kupffer cell inactivation alleviates ethanol-induced steatosis and CYP2E1 induction but not inflammatory responses in rat liver. *J Hepatol* 2000; **32**: 900-910
21 **Agundez J**, Ladero J, Diaz-Rubio M, Benitez J. Rsa I polymorphism at the cytochrome P4502E1 locus is not related to the risk of alcohol-related severe liver disease. *Liver* 1996; **16**: 380-383
22 **Donohue TM Jr**, Clemens DL, Galli A, Crabb D, Nieto N, Kato J, Barve SS. Use of cultured cells in assessing ethanol toxicity and ethanol-related metabolism. *Alcohol Clin Exp Res* 2001; **25**: 87S-93S
23 **Kunitoh S**, Imaoka S, Hiroi T, Yabusaki Y, Monna T, Funae Y. Acetaldehyde as well as ethanol is metabolized by human CYPIIE1 . *J Pharmacol Exp Ther* 1997; **280**: 527-532
24 **Ingelman-Sundberg M**, Ronis MJ, Lindros KO, Eliasson E, Zhukov A. Ethanol-inducible cytochrome P4502E1: regulation, enzymology and molecular biology. *Alcohol Alcohol Supl* 1994; **2**: 131-139
25 **Maher J**. The CYP2E1 knockout delivers another punch: first ASH, now NASH. Alcoholic steatohepatitis. Nonalcoholic steatohepatitis. *Hepatology* 2001; **33**: 311-312
26 **Ekstrom G**, Ingelman-Sundberg M. Rat liver nicrosomal NADPH-supported oxidase activity and peroxidation dependent on ethanol-inducible cytochrom P450. *Biochem Pharmacol* 1989; **38**: 1313-1319
27 **Albano E**, Clot P, Morimoto M, Tomasi A, Ingelman-Sundberg M, French SW. Role of cytochrome-P4502E1-dependent formation of hydroxyethyl free radical in the development of liver damage in rats intragstrically fed with ethanol. *Hepatology* 1996; **23**: 155-163
28 **Clot P**, Albano E, Eliasson E, Tabone M, Arico S, Israel Y, Moncada C, Ingelman-Sundberg M. Cytochrome P4502E1 hydroxyethyl radical adducts as the major antigen in autoantibody formation among alcoholics. *Gastroenterology* 1996; **111**: 206-216
29 **Albano E**, French SW, Ingelman-Sundberg M. Hydroxyethyl radical in ethanol hepatotoxicity. *Front Biosci* 1999; **4**: 533-540
30 **Britton RS**, Bacon BR. Role of free radical in liver diseases and hepatic fibrosis. *Hepatogastroenterology* 1994; **41**: 343-348

31 **Iwahashi K**, Miyatake R, Suwaki H, Kinoshita H, Ameno K, Ijiri I, Ishikawa Y, Matsuo Y. Blood ethanol levels and CYPIIE1 allele. *Arukoru Kenkyuto Yakubutsu Ison* 1994; **29**: 190-194
32 **Leclercq IA**, Farrell GC, Field J, Bell DR, Gonzalez FJ, Robertson GR. CYP2E1 and CYP4A as microsomal catalysts of lipid peroxides in murine nonalcoholic steatohepatitis. *J Clin Invest* 2000; **105**: 1067-1075
33 **Letteron P**, Fromenty B, Terris B, Degott C, Pessayre D. Acute and chronic hepatic steatosis lead to in vivo lipid peroxidation in mice. *J Hepatol* 1996; **24**: 200-208
34 **Weltman MD**, Farrell GC, Hall P, Ingelman-Sundberg M, Liddle C. Hepatic cytochrome P4502E1 is increased in patients with non-alcoholic steatohepatitis. *Hepatolygy* 1998; **27**: 128-133
35 **Weltman MD**, Farrell GC, Liddle C. Increased CYP2E1 expression in a rat nutritional model of hepatic steatosis with inflammation. *Gastroenterology* 1996; **111**: 1645-1653
36 **Raucy JL**, Lasker JM, Kraner JC, Salazar DE, Lieber CS, Corcoran GB. Introduction of cytochrome P450IIE1 in the obese overfed rat. *Mol Pharmacol* 1991; **39**: 275-280
37 **Osmundsen H**, Bremer J, Pedersen JI. Metabolic aspects of peroxisomal-oxidation. *Biochim Biophys Acta* 1991; **1085**: 141-158
38 **Zangar RC**, Novak RF. Effects of fatty acids and ketone bodies on cytochromes P450 2B, 4A and 2E1 expression in primary cultured rat hepatocytes. *Arch Biochem Biophys* 1997; **337**: 217-224

Edited by Zhang JZ and Wang XL

P.O.Box 2345, Beijing 100023,China
Fax: +86-10-85381893
E-mail: wjg@wjgnet.com www.wjgnet.com

World J Gastroenterol 2003;9(11):2616-2618
World Journal of Gastroenterology
 ISSN 1007-9327

• BRIEF REPORTS •

Significance of expression of heat shock protein90α in human gastric cancer

Dong-Sheng Zuo, Jie Dai, Ai-Hua Bo, Jie Fan, Xiu-Ying Xiao

Dong-Sheng Zuo, Ai-Hua Bo, Jie Fan, Xiu-Ying Xiao, Department of Pathology, Zhangjiakou Medical College, Zhangjiakou 075029, Hebei Province, China
Jie Dai, Capital University of Medical Sciences, Beijing 100054, China
Supported by the Natural Science Fundation of Hebei Province, No. 301427
Correspondence to: Dong-Sheng Zuo, Department of Pathology, Zhangjiakou Medical College, Zhangjiakou 075029, Hebei Province, China. dshz2003@yahoo.com.cn
Telephone: +86-313-8041652 **Fax:** +86-313-8041652
Received: 2003-04-08 **Accepted:** 2003-05-19

Abstract

AIM: To evaluate the significance of hsp90α expression in human gastric cancer tissues.

METHODS: Immunohistochemical staining was used in clinical specimens from 33 cases of gastric cancer and 33 cases of gastritis with rabbit anti-human hsp90α multi-clonal antibody in order to explore the relationship between the expression of hsp90α in gastric carcinoma tissue and gastritis tissue as well as in mucous membrane adjacent to cancer and lymph node metastasis.

RESULTS: Hsp90α was detected in 88 % of gastric carcinoma cases and 55 % of gastritis cases. The hsp90α positive rate in gastric cancer group was significantly higher than that in gastritis group ($P<0.01$, $P=0.005$). The hsp90α positive rate in gastric cancer and in mucous membrane adjacent to cancer was 88 % and 55 % respectively ($P<0.01$,$P=0.005$). The hsp90α positive rate in lymph node metastasis group and non-lymph node metastasis group was 100 % and 60 % respectively, and a significant correlation between hsp90α expression and lymph node metastasis was shown ($P<0.01$, $P=0.005$).

CONCLUSION: The hsp90α expression rate in gastric cancer group was significantly higher than that in gastritis group as well as that in the group of mucous membrane adjacent to cancer. The hsp90α expression in lymphatic node metastasis group was higher than that in non-lymphatic node metastasis group. The results indicate that increased hsp90α expression has a close relationship with occurrence and lymph node metastasis of gastric cancer.

Zuo DS, Dai J, Bo AH, Fan J, Xiao XY. Significance of expression of heat shock protein90α in human gastric cancer. *World J Gastroenterol* 2003; 9(11): 2616-2618
http://www.wjgnet.com/1007-9327/9/2616.asp

INTRODUCTION

Heat shock protein90α, commonly known as heat stress protein, is a highly conserved cytosolic protein during the evolution of living things. It extensively exists in the living organisms and has many important biological functions such as enhancing cellular tolerance to stress and maintaining cellular homeostasis, etc. There are two forms of hsp90 in the advanced organisms, i.e. α form and β form. Under stress, the synthesis of hsp90 increases. For example, high temperature and infection can induce increase of hsp90 synthesis. However, different inducers play different roles in inducing hsp90 synthesis. hsp90α is more sensitive to heat induction, hsp90β is more sensitive to mitosis induction[1]. Recent studies showed that hsp90 had a close relationship with carcinoma. It was highly expressed in cancer tissue[2]. hsp90 combines with many transformed proteins to form complexes that are transported into intracellular special sites and correlated with cancer cell proliferation and differentiation[3,4]. There is a close relationship between the occurrence of gastric cancer and the synthesis of heat shock protein. At present there have been few reports on the study of hsp90 expression during the genesis of gastric cancer. In our study, we used immunohistochemical staining SP method to detect the expression of hsp90α in gastric cancer, gastritis, mucous membrane adjacent to cancer and gastric cancer tissue with or without lymph node metastasis in order to explore the relationships among them and their clinical significances,as well as the roles of hsp90α expression in the genesis and development of gastric cancer. Our study showed that the hsp90α expression rate in gastric cancer group was significantly higher than that in gastritis group, and in group of mucous membrance adjacent to cancer, hsp90α expression in the lymphatic node metastasis group was higher than that in the non-lymphatic node metastasis group.

MATERIALS AND METHODS

Samples collection

A total of 66 samples were collected from our hospital which were cut off from the stomach after operation, including 33 cases of gastric cancer and 33 cases of gastritis. Twenty-three of the 33 cases of gastric cancer had lymph nodes metastases and 10 cases had no lymph node metastasis. The samples were fixed in 10 % formaldehyde, dehydrated and embedded in paraffin. Five μm-thick sections were sliced. All samples were confirmed by pathological diagnosis.

Immunohistochemistry reagents

Rabbit anti-human hsp90α multi-clonal antibody (650-871-1919 CA, U.S.A), immunohistochemical staining S-P kit and DAB were purchased from Maixin LTD.

Methods

Immunohistochemical SP staining method was used in our experiment. The conventional staining procedures were carried out. The main procedures were as follows. The tissue sections were routinely dewaxed and hydrated, then treated with 3 % peroxide for 10 minutes. Antigen restoration was carried out by heating in citrate buffer, blocked with normal goat serum, incubated overnight with anti-human hsp90α multi-clonal antibody at 4 ℃, washed three times with PBS, treated with antibody II for 30 minutes at 37 ℃ and then with antibody III

for 30 minutes at 37 ℃. Color was displayed with DAB. Negative control was designed with PBS instead of antibody I. The known positive tissue sections were used as positive control.

Statistic analysis

SPSS10.0 software was used for statistical analysis.

RESULTS

Evaluation standard

Under light-microscope the hsp90α immunoreactive products showed as granules with brown color. These granules were mainly located in cytoplasm, only a few in nuclei. According to the amount and color density of granules, the staining was divided into three grades: +: few granules, canary color; ++: lots of granules filled cytoplasm, brown color ; +++: cytoplasm was filled with brown-black granules. The granules were also found in nucleoli. Detailed expressions of hsp90α in tissues of gastric cancer, gastritis and lymph nodes are shown in Tables 1, 2 and 3.

Table 1 Hsp90α expression in tissues of gastric cancer and gastritis

Pathologic types	*n*	Grade of hsp90α expression				Positive rate (%)
		-	+	++	+++	
Gastric cancer	33	4	23	4	2	88
Gastritis	33	15	13	4	1	55

[b]$P<0.01$ *vs* group of Gastritis, $\chi^2=8.943$.

Table 2 Hsp90α expression in gastric cancer tissues and tissues adjacent to cancer

Pathologic types	*n*	Grade of hsp90α expression				Positive rate (%)
		-	+	++	+++	
Gastric cancer	33	4	23	4	2	88
Tissues adjacent to cancer	33	15	17	1	0	55

[b]$P<0.01$ *vs* group of tissue adjacent to cancer, $\chi^2=8.943$.

Table 3 Hsp90α expression in tissues of gastric cancer with and without lymph node metastasis

Pathologic types	*n*	Grade of hsp90α expression				Positive rate (%)
		-	+	++	+++	
With lymph node metastasis	23	0	17	4	2	100
Without lymph node metastasis	10	4	5	1	0	60

[b]$P<0.01$ *vs* group without ymph node metastasis, $\chi^2=10.469$.

The hsp90α immunoreactive signals in gastric cancer were mostly strong or very strong. The positive rate was 88 %. However, in gastritis samples, the positive rate of hsp90α immunoreactive signals was 55 %, most of which were weakly positive. There was a significant difference between gastric cancer and gastritis ($P<0.01$). The hsp90α immunoreactive positive rates in gastric cancer or in mucous membrane adjacent to cancer were 88 % and 55 % respectively. There was also a significant difference between them ($P<0.01$). A significant difference also existed between gastric cancer with lymph node metastasis (100 %) and that without lymph node metastasis (62.5 %) ($P<0.01$).

DISCUSSION

The expression of hsp90α in normal cells is controlled by cell cycle[5], but it can continuously express at high level in tumor cells without heat stimulation. The existence of mutant or abnormal proteins also stimulates HSPs synthesis[6-9]. Heat shock proteins can maintain oncogene products in inactive state[10]. On the other hand, it has the functions of transportation and transfer. In tumor cells, the expression of hsp90α is higher than that in normal cells. An increasing trend of hsp90α expression was seen in virus-transformed and chemical-induced tumor cells[11,12]. In pancreatic cancer, hsp90α showed a selective expression at high level. Jamell[13] found that hsp90α expressed in all human breast cancers and hsp90α expression was higher in malignant breast tissue[14]. An increased expression of hsp90α mRNA was also found in ovary cancer and the more serious the disease was, the higher the expression of hsp90α mRNA was[1]. It was also found that hsp90α showed a high expression in 29 % of endometrium cancer. Yano' s research[1] showed that the hsp90α mRNA level in breast cancer was higher than that in non-cancer tissues[14,15]. The expression of hsp90α mRNA has a close correlation with proliferating cell nuclear antigen labeling index (PCNA LI), indicating that high expression of hsp90α mRNA should have an important role in cell proliferation. It was identified in our study that the expression of hsp90α in gastric cancer was obviously higher than that in gastritis and mucous membrane adjacent to cancer.

HSPs take part in cell growth and proliferation by several means such as signal transduction and cell cycle regulation. HSPs express highly in germ cells and embryonic cells, but express lowly in aging cells. This suggests that the increase of protein synthesis in proliferating cells needs much more HSPs to take part in the formation of protein activities. Because tumor cells are a group of high proliferation heteromorphic cells, they may need much more HSPs to sustain their proliferation[16,17]. Our results also showed that the expression of hsp90α in gastric cancer with lymph node metastasis was higher than that without lymph node metastasis. All of these were consistent with the results from Jamell' s report that the higher the breast cancer malignancy is, the higher the hsp90α expresses. This indicats increase of hsp90α expression probably has some relationship with genesis, development, invasion and lymph node metastasis of gastric cancer.

Under various stimulations, gastric mucous membrane can transcript and translate high levels of HSPs that can change the metabolism and functions of cells in order to alleviate the damage caused by deleterious factors including exogenous stimulants such as heat, chemicals and ethanol, and endogenous stimulants such as acid, local ischemia, hypoxia. In this case, gastric mucous membrane should synthesize HSP rapidly to exert the protecting role for gastric mucous cells[1]. The genesis of gastric cancer is a gradual process under the long-term influence of various stimulants as well as other factors. During the process, HSPs synthesis increases gradually[16]. This viewpoint was confirmed by our results that hsp90α positive rate in gastric cancer was higher than that in gastritis and gastric tissues adjacent to cancer. The discovery of our study may provide some useful clues for early detection and clinical diagnosis of gastric cancer.

REFERENCES

1 **Yano M**, Naito Z, Tanaka S, Asano G. Expression and roles of heat shock proteins in human breast cancer. *Jpn J Cancer Res* 1996; **87**: 908-915

2 **Gress TM**, Muller-Pillasch F, Weber C, Lerch MM, Friess H, Buchler M, Beger HG, Adler G. Differential expression of heat shock proteins in pancreatic carcinoma. *Cancer Res* 1994; **54**: 547-551

3 **Pratt WB**. The hsp90-based chaperone system: involvement in

signal transduction from a variety of hormone and growth factor receptors. *Proc Soc Exp Biol Med* 1998; **217**: 420-434

4 **Whitesell L,** Mimnaugh EG, De Costa B, Myers CE, Neckers LM. Inhibition of heat shock Protein HSP90-PP60v-src heteroprotein complex formation by benzoquinone ansamycins: essential role for stress proteins in oncogenic transformation. *Proc Natl Acad Sci U S A* 1994**; 91**: 8324-8328

5 **Liu XL,** Xiao B, Yu ZC, Guo JC, Zhao QC, Xu L, Shi YQ, Fan DM. Down-regulation of HSP90 could change cell cycle distribution and increase drug sensitivity of tumor cells. *World J Gastroenterol* 1999; **5**: 199-208

6 **Maloney A**, Workman P. HSP90 as a new therapeutic target for cancer therapy: the story unfolds. *Expert Opin Biol Ther* 2002; **2**: 3-24

7 **Neckers L,** Mimnaugh E, Schulte TW. HSP90 as an anti-cancer target. *Drug Resist Updat* 1999; **2**: 165-172

8 **Darimont BD.** The Hsp90 chaperone complex-A potential target for cancer therapy? *World J Gastroenterol* 1999; **5**: 195-198

9 **Neckers L**. Hsp90 inhibitors as novel cancer chemotherapeutic agents. *Trends Mol Med* 2002; **8**(4 Suppl): S55-61

10 **Nagata Y,** Anan T, Yoshida T, Mizukami T, Taya Y, Fujiwara T, Kato H, Saya H, Nakao M. The stabilization mechanism of mutant-type p53 by impaired ubiquitination: the loss of wild-type p53 function and the HSP90 association. *Oncogene* 1999; **18**: 6037-6049

11 **Srivastava PK,** Vdono H. Heat shock protein-peptide complexes in cancer immunotherapy. *Curr Opin Immunol* 1994**; 6**: 728-732

12 **Cho G,** Park SG, Jung G. Localization of HSP90 binding sites in the human hepatitis B virus polymerase. *Biochem Biophys Res Commun* 2000**; 269**: 191-196

13 **Jameel A**, Skilton RA, Campbell TA. Clinical and biological significance of HSP89α in human breast cancer. *Int J Cancer* 1992; **50**: 409-415

14 **Munster PN,** Basso A, Solit D, Norton L, Rosen N. Modulation of HSP90 function by ansamycins sensitizes breast cancer cells to chemotherapy-induced apoptosis in an RB- and schedule-dependent manner. See: E. A. Sausville, Combining cytotoxics and 17-allylamino, 17-demethoxygeldanamycin: sequence and tumor biology matters, Clin. Cancer Res., **7**: 2155-2158, 2001. *Clin Cancer Res* 2001; **7**: 2228-2236

15 **Sausville EA**. Combining cytotoxics and 17-allylamino, 17-demethoxygeldanamycin: sequence and tumor biology matters. Commentary re: P. Munster *et al*, Modulation of HSP90 function by ansamycins sensitizes breast cancer cells to chemotherapy-induced apoptosis in an RB- and schedule-dependent manner. Clin. Cancer Res., **7**: 2228-2236,2001. *Clin Cancer Res* 2001; **7**: 2155-2158

16 **Zhang XY.** The basic research and clinic of gastric cancer. *Beijing Scientific Press* 1996: 32

17 **Kazlauskas A,** Sundstrom S, Poellinger L, Pongratz I. The hsp90 chaperone complex regulates intracellular localization of the dioxin receptor. *Mol Cell Biol* 2001; **21**: 2594-2607

Edited by Zhu LH and Wang XL

P.O.Box 2345, Beijing 100023,China
Fax: +86-10-85381893
E-mail: wjg@wjgnet.com www.wjgnet.com

World J Gastroenterol 2003;9(11):2619-2621
World Journal of Gastroenterology
 ISSN 1007-9327

• BRIEF REPORTS •

Prevention and therapy of fungal infection in severe acute pancreatitis: A prospective clinical study

Yue-Ming He, Xin-Sheng Lv, Zhong-Li Ai, Zhi-Su Liu, Qun Qian, Quan Sun, Ji-Wei Chen, Dao-Xiong Lei, Cong-Qing Jiang, Yu-Fong Yuan

Yue-Ming He, Xin-Sheng Lv, Department of General Surgery, Xiangya Hospital, Central South University, Changsha 410008, Hunan Province, China
Zhong-Li Ai, Zhi-Su Liu, Qun Qian, Quan Sun, Ji-Wei Chen, Dao-Xiong Lei, Cong-Qing Jiang, Yu-Fong Yuan, Department of General Surgery, Zhongnan Hospital, Wuhan University, Wuhan 430071, Hubei Province, China
Correspondence to: Dr. Yue-Ming He, Department of General Surgery, Zhongnan Hospital, Wuhan University, 169 Donghu Road, Wuhan 430071, Hubei Province, China. heym@medmail.com.cn
Telephone: +86-27-67813297 **Fax:** +86-27-87330795
Received: 2003-05-10 **Accepted:** 2003-06-02

Abstract

AIM: To investigate the prevention and therapy of fungal infection in patients with severe acute pancreatitis (SAP).

METHODS: Seventy patients with SAP admitted from Jan. 1998 to Dec. 2002 were randomly divided into garlicin prevention group, fluconazole (low dosage) prevention group and control group. The incidence of fungal infection, the fungal clearance and mortality after treatment were compared.

RESULTS: The incidence of fungal infection in garlicin group and fluconazole group was lower than that in control group (16 % *vs* 30 %, $P<0.05$ and 9 % *vs* 30 %, $P<0.01$, respectively). Amphotericin B or therapy-dose fluconazole had effects on patients with fungal infection in garlicin group and control group, but had no effects on patients with fungal infection in fluconzole group.

CONCLUSION: Prophylactic dosage of antifungal agents (garlicin or low dosage fluconazole) can reduce the incidence of fungal infection in patients with SAP. But once fungal infection occurs, amphotericin B should be used as early as possible if fluconazole is not effective.

He YM, Lv XS, Ai ZL, Liu ZS, Qian Q, Sun Q, Chen JW, Lei DX, Jiang CQ, Yuan YF. Prevention and therapy of fungal infection in severe acute pancreatitis: A prospective clinical study. *World J Gastroenterol* 2003; 9(11): 2619-2621
http://www.wjgnet.com/1007-9327/9/2619.asp

INTRODUCTION

Severe acute pancreatitis (SAP) accounts for about 20 % of acute pancreatitis. With understanding of the natural course of SAP and advances in critical care medicine, most SAP patients can survive systemic inflammatory response syndrome and accompanying dysfunction of important organs such as the heart, lung, kidney, etc[1]. The major complication in the middle and later phases of SAP is infection, its incidence is 40-50 % and its mortality is 10-20 %. About 80 % of mortality at the later phase of SAP is caused by infection[2]. For the time being, drug resistant bacteria infection, especially fungal infection is obviously increasing, and has become one of the major difficulties in the treatment of SAP[3]. In order to prevent and treat the deep fungal infection of SAP, this clinical research was conducted on fungal infection prevention and treatment by adopting garlicin, fluconazole and amphotericin B for SAP patients admitted from Jan. 1998 to Dec. 2002.

MATERIALS AND METHODS

Selection of cases

The selected cases accorded with the clinical diagnosis criteria proposed by the Pancreas Surgery Group of the Chinese Medical Association in 1997[4], and were complicated with one of the following predisposing factors of deep fungal infections[5-8], such as gerontism, history of diabetes, dysfunction of one or more organs, non-iatrogenic fasting hyperglycemia ($\geqslant$9 mmol/L), central venous catheter, TPN, retaining urethral catheterization, operation, gastrointestinal fistula, ICU, breathing machine supported$\geqslant$5d, user of glucocorticoid$\geqslant$5d, administration of broad spectrum antibiotics$\geqslant$5d or super broad spectrum antibiotics (such as Tienam, etc.)$\geqslant$3d.

Groups and methods

A total of 70 cases conforming to the above criteria were randomly divided into 3 groups. The garlicin group (25 patients) was given venous instillation of 120 mg garlicin one time per day plus routine treatment. The fluconazole group (22 patients) was given venous instillation of 100 mg fluconazole one time per day plus routine treatment. The control group (23 patients) received routine treatment only. The prophylactic medication for the garlicin and fluconazole groups was applied until relief of the predisposing factors (except gerontism and history of diabetes). The fungal infection treatment protocol was applied when the patients showed signs of deep fungal infection. The clinical data of these three groups are shown in Table 1.

Monitoring

Smears from peritoneal permeated liquid, pus of the infected wounds, throat specimen, sputum, urine and stool were prepared for fungus detection or/and fungal cultivation 2 times per week. If there was fungal infection, smears from the above sources were prepared for fungal identification 3 times per week. If the central venous catheter was suspected as the infection source, it was removed and cultured for fungi. Incidence and mortality of the patients with SAP complicated with deep fungal infection were observed.

Statistics analysis

All data were analyzed with SPSS11.0 software package, and a P value <0.05 was considered statistically significant. The average age, hospitalization duration, APACHE II grading etc, were displayed by $\bar{x}\pm s$, and differences were analysed using analysis of viariance and F test. Sex, etiological factor, death, fungal infection and number of cleared fungi and other data were analyzed using χ^2 or Fisher' s exact test.

Table 1 General clinical data of three groups

Group	Cases		Age	Etiological factor				APACHII
	Male:	Female		Biliary	Alcoholemia	Injury	Others	
Garlicin	12:	13	51.4±15.2	14	6	1	4	11.8±3.8
Fluconazole	12:	10	48.7±17.3	11	6	-	5	13.2±2.5
Control	13:	10	50.5±20.1	11	7	1	4	11.6±4.7

There were no statistically significant differences in three groups.

RESULTS

Incidence rate of fungal infection

Diagnostic criteria for SAP deep fungal infection[5,6] Doubtful clinical manifestations were fever after the broad spectrum antibiotics treatment with no drug resistant bacteria infection, cough, glue-like mucus or blood streak sputum, pseudo-membrane of the oral cavity or oral ulceration and symptoms of urinary tract stimulation, diarrhea with brown or/and jam-like feces, consciousness changes with unknown reasons, or bleedings irrelevant to pancreatitis such as fistula bleeding of the biliary and digestive tracts.Pathogenic evidences of fungi included positive fungal cultivation of blood, central venous catheter, smears of the fine-needle aspiration before operation, aspiration ascites or necrotic pancreas tissue during the operation, and drained bile, samples of sputum, peritoneal permeated fluid, pus of the infected wounds, throat specimen, sputum, urine and stool. Deep fungal infection could be diagnosed according to the suspicious clinical manifestations together with the same fungi existed in two or more systems.

Incidence rate of fungal infection The SAP patients infected with fungi in the garlicin and fluconazole groups were obviously less than those in the control group, and the number infected by fungi was the fewest in the fluconazole group (Table 2).

Table 2 Incidence rate of fungal infection in 3 groups

Group	Cases	Rate of fungal infection	Times of fungal infection after SAP(d)
Garlicin	25	4(16%)[a]	39-57
Fluconazole	22	2(9 %)[b]	35-62
Control	23	7(30 %)	24-183

[a]$P<0.05$, [b]$P<0.01$ *vs* control.

Treatment results of fungal infection

Protocol of treatment For highly suspicious pathogenic proofs of fungi or those with fungal infection, fluconazole was intravenous used to treat fungal infection, 200 mg (double dosage for the initial injection) once per day until the fungi were cleared. Amphotericin B was used for those with fungal infection in the fluconazole group. The dosage was started from 0.1 $mg.kg^{-1}$, and increased by 5 mg daily according to the patient's tolerance, and the treatment was continued till the dosage reached to 0.6 $mg.kg^{-1}$, the total accumulated amount reached 1.5-2 g. If the patients in garlicin and control groups were not sensitive to fluconazole, amphotericin B was then used.

Treatment results The fluconazole group had the lowest incidence of fungal infection, and the shortest hospital stay, but amphotericin B could not clear the fungi in fluconazole group, in which the patients were once complicated with fungal infection, they would inevitably died. When fungal infection occurred, the garlicin group had the highest clearance rate of fungi after treatment, and its mortality and average hospital stay were obviously lower or shorter than those in the control group. In the garlicin and control groups, each had one patient infected with fungi who was not cured by fluconazole therapy for 3 days, and their fungi were cleared when they changed to receive amphotericin B and they finally recuperated (Table 3).

Table 3 Treatment results of fungal infection in 3 groups

Group	Rate of fungal clearance	Mortality[#]	Times of Hospitalization
Garlicin	3(75 %)[a]	1(25 %)[a]	48.1±30.7[a]
Fluconazole	-	2(100 %)	43.3±26.9[b]
Contrast	4(57%)	3(43 %)	57.4±27.3

Note: # Mortality is the percentage (%) of patients who died of fungal septicemia. [a]$P<0.05$, [a]$P<0.01$ *vs* control.

DISCUSSION

Deep fungal infection often occurs in patients with impaired immunity, e.g. diabetes, AIDS, malignant tumor and organ transplantation, etc. In recent years, the incidence of SAP deep fungal infection has obviously increased. Before routine administration of prophylactic antibiotics for SAP, the proportion of fungi was 7 % in the bacteria spectrum of SAP infection[9]. After that, the incidence of fungal infection in SAP has increased to 12-41 %[2,3,5,6,8,10-14], which has become an important cause for death and mutilation by SAP[3,5,6,8,10-14]. Since lack of specific manifestations, unrecongizability of symptoms, a long time for fungal cultivation, and apparent relevance between the fungal infection and prognosis, active and effective measures to prevent SAP deep fungal infection will contribute to further decreasing the mortality of SAP.

It has been reported[7] that prophylactic application of fluconazole in patients after bone marrow transplantation or chemotherapy could reduce the incidence of fungal infection. But there was not any systematic or prospective study in preventing SAP fungal infection. This study initially showed that prophylactic application of anti-fungi garlicin or fluconazole could significantly reduce the incidence of deep fungal infection of SAP patients who had some predisposing factors. Garlicin is cheap but good in quality, which not only has anti-fungi effects, but also anti-bacteria and anti-viral effects. The normal prophylactic dosage of garlicin is 1-2 $mg.kg^{-1}.d^{-1}$. With respect to prevention alone, fluconazole is better than garlicin, but we have noticed that once those who used fluconazole to prevent infection were indeed infected by fungi, their treatment might become more difficult and the prognosis was much worse. Once fungal infection occurred, an in-time use of fluconazole could quickly clear fungi, and significantly improve prognosis. Low dosage (100-150 mg/d) of fluconazole is often used in prevention while high dosage (200-600 mg/d) is often used in treatment.

About 80 % of the fungal strains in SAP fungal infection are candida[3,5,6,10-14]. Once fungal infection has been ascertained, anti-fungal drugs should be applied in time. Besides direct application of amphotericin B for mucor infection, fluconazole has be the priority for other fungal infections. Like maphotericin B[15], fluconazole has a good permeability in pancreas. If

fluconazole is not effective, it should change for amphotericin B in time or combined medication. In this research, two patients with fungal infection died in fluconazole group possibly due to delayed treatment besides drug resistance.

Deep fungal infection is different from shallow one, sometimes its diagnosis depends on biopsy, because it is hard to differentiate "passenger" bacterial parasites from real infection under many circumstances. As shown by autopsy statistics, only less than 20 % of the patients with fungal infection received anti-fungal treatment[16]. It is believed that for SAP patients, even "passenger" bacterial parasites may probably develop into infection, the finding of fungi in extra-peritoneal positions has provided clues to fungal infection within abdominal cavity, especially when fungi have been cultured from the peritoneal draining liquid. Hoerauf *et al*[12] reported that anti-fungi chemotherapy could increase survival rate. Aloia *et al*[11] suggested small dosage and short course amphotericin B treatment. Grewe *et al*[10] and Gotzinger *et al*[13] reported that although amphotericin B could quickly clear fungi, it could not improve prognosis. This might be related to the fact that anti-fungi treatment was only started when the blood cultivation became positive. The authors agree with Keiser' s viewpoint[17] that the failure of treatment was unable to be realized in time because the fungi were the pathogenic bacteria, instead they were often regarded as pollution and "passenger" in the infection course of surgery, therefore treatment was delayed.

SAP complicated with fungal infection could be classified into primary infection (fungus found in samples of fine-needle aspiration before operation or the first operation) and secondary infection (no fungus found in samples of fine-needle aspiration before operation or the first operation, and fungal infection happens later)[10,13]. In time clearing and draining of the necrotic tissues should be done for primary fungal infection, conservative treatment is mainly for the secondary infection, operation should be done actively if there is a fungal abscess formation. There is no special clinical manifestation in fungal infection, and repeated fungal cultivation on sputum, urine, stool and peritoneal permeated liquid and blood sample can contribute to in-time diagnosis and treatment. Zhang[18] reported that it was helpful to rapid diagnosis of fungal infection in patients with severe acute pancreatitis by PCR using universal primers targeting the 18s rRNA gene of fungus.

REFERENCES

1 **Beger HG,** Rau B, Mayer J, Pralle U. Natural course of acute pancreatitis. *World J Surg* 1997; **21**: 130-135

2 **Ho HS,** Frey CF. The role of antibiotic prophylaxis in severe acute pancreatitis. *Arch Surg* 1997; **132**: 487-493

3 **Gloor B**, Muller CA, Worni M, Stahel PF, Redaelli C, Uhl W, Buchler MW. Pancreatic infection in severe pancreatitis: the role of fungus and multiresistant organisms. *Arch Surg* 2001; **136**: 592-596

4 **Pancreas Surgery Group of China Medical Association**. Clinical diagnosis and classify standard of acute pancreatitis. *Zhonghua Waike Zazhi* 1997; **35**: 773-775

5 **Lei RQ**, Liu W, Qu HP, Tang YQ, Yuan ZR, Han TQ, Zhang SD. Diagnosis and prophylaxis of fungi infection in severe acute pancreatitis. *Zongguo Shiyong Waike Zazhi* 1999; **19**: 544-545

6 **He YM**, Lu XS, Huang JH, Ai ZL, Liu ZS, Lei DX, Qian Q, Sun Q, Wang BY, Jiang CQ, Yuan YF. Fungal infection in severe acute pancreatitis (a report of 40 cases). *Zhongguo Putong Waike Zazhi* 2002; **11**: 135-138

7 **Edwards JE Jr**, Bodey GP, Bowden RA, Buchner T, de Pauw BE, Filler SG, Ghannoum MA, Glauser M, Herbrecht R, Kauffman CA, Kohno S, Martino P, Meunier F, Mori T, Pfaller MA, Rex JH, Rogers TR, Rubin RH, Solomkin J, Viscoli C, Walsh TJ, White M. International conference for the development of a consensus on the management and prevention of severe candidal infections. *Clin Infect Dis* 1997; **25**: 43-59

8 **Qin S**, Tang YQ, Qu HP, Liu W, Mao EQ. Study on the risk factors of fungal infection in severe acute pancreatitis. *Waike LiLun yu Shijian* 2001; **6**: 96-99

9 **Beger HG,** Bittner R, Block S, Buchler M. Bacterial contamination of pancreatic necrosis: A prospective clinical study. *Gastroenterology* 1986; **91**: 433-438

10 **Grewe M,** Tsiotos GG, Luque de-Leon E, Sarr MG. Fungal infection in acute necrotizing pancreatitis. *J Am Coll Surg* 1999; **188**: 408-414

11 **Aloia T**, Solomkin J, Fink AS, Nussbaum MS, Bjornson S, Bell RH, Sewak L, Mc Fadden DW. Candida in pancreatic infection: a clinical experience. *Am Surg* 1994; **60**: 793-796

12 **Hoerauf A,** Hammer S, Muller-Myhsok B, Rupprecht H. Intra-abdominal Candida infection during acute necrotizing pancreatitis has a high prevalence and is associated with increased mortality. *Crit Care Med* 1998; **26**: 2010-2015

13 **Gotzinger P**, Wamser P, Barian M, Sautner T, Jakesz R, Fugger R. Candida infection of local necrosis in severe acute pancreatitis is associated with increased mortality. *Shock* 2000; **14**: 320-324

14 **Isenmann R**, Schwarz M, Rau B, Trautmann M, Schober W, Beger HG. Characteristics of infection with Candida species in patients with necrotizing pancreatitis. *World J Surg* 2002; **26**: 372-376

15 **Shrikhande S**, Friess H, Issenegger C, Martignoni ME, Yong H, Gloor B, Yeates R, Kleeff J, Buchler MW. Fluconazole penetration into the pancreas. *Antimicrob Agents Chemother* 2000; **44**: 2569-2571

16 **Du B**, Zhang H, Chen D. Invasive fungal infection in 3447 autopsy cases. *Zhonghua Yixue Zazhi* 1996; **76**: 352-354

17 **Keiser P,** Keay S. Candidal pancreatic abscesses: report of two cases and review. *Clin Infect Dis* 1992; **14**: 884-888

18 **Zhang WZ**, Han TQ, Tang YQ, Zhang SD. Rapid diagnosis of fungal infection in patients with acute necrotizing pancreatitis by polymerase chain reaction. *Asian J Surg* 2002; **25**: 209-213

Edited by Zhang JZ and Wang XL

P.O.Box 2345, Beijing 100023,China
Fax: +86-10-85381893
E-mail: wjg@wjgnet.com www.wjgnet.com

World J Gastroenterol 2003;9(11):2622-2626
World Journal of Gastroenterology
 ISSN 1007-9327

• BRIEF REPORTS •

Formalized therapeutic guideline for hyperlipidemic severe acute pancreatitis

En-Qiang Mao, Yao-Qing Tang, Sheng-Dao Zhang

En-Qiang Mao, Yao-Qing Tang, Sheng-Dao Zhang, Department of Surgery, Ruijin Hospital, Shanghai Second Medical University, Shanghai 200025, China
Correspondence to: Dr. En-Qiang Mao, Department of Surgery, Ruijin Hospital, Shanghai Second Medical University, Shanghai 200025, China. maoeq@yeah.net
Telephone: +86-21-64370045 Ext 666014
Received: 2003-06-10 **Accepted:** 2003-08-16

Abstract

AIM: To investigate a formalized therapeutic guideline for hyperlipidemic severe acute pancreatitis (HL-SAP).

METHODS: Thirty-two consecutive patients with severe acute pancreatitis were included in the clinical trial. All of them met the following five criteria for admission to the study, namely the Atlanta classification and stratification system for the clinical diagnosis of SAP, APACHEII score more than 8, time interval for therapeutic intervention less than 72 hours after onset of the disease, serum triglyceride (TG) level 6.8 mmol/l or over, and exclusion of other etiologies. They were divided into severe acute pancreatitis group (SAP, 22 patients) and fulminant severe acute pancreatitis group (FSAP, 10 patients). Besides the conventional therapeutic measures, *Penta-association therapy* was also applied in the two groups, which consisted of blood purification (adsorption of triglyceride and hemofiltration), antihyperlipidemic agents (fluvastatin or lipanthyl), low molecular weight heparin (fragmin), insulin, topical application of Pixiao (a traditional Chinese medicine) over the whole abdomen. Serum triglyceride, pro-inflammatory cytokines and anti-inflammatory cytokines were determined before blood purification (PF), at the end of blood purification (AFE) and on the 7th day after onset of the disease (AF7) respectively. Simultaneously, severity of the diseases was assessed by the APACHE II system. Prognosis was evaluated by non-operation cure rate, absorption rate of pseudocyst, time interval pseudocyst absorption, hospital stay and survival rate.

RESULTS: Serum triglyceride level (mmol/L), TNFα (U/ml) concentration and APACHE II score were significantly decreased ($P<0.05$) at AFE and AF7, as compared with PF. However, serum IL-10 concentration (pg/ml) was increased significantly ($P<0.001$) at AFE, and decreased significantly ($P<0.05$) at AF7 when compared with PF. Operations: The First surgical intervention time was 55.8±42.6 days in SAP group (5 patients) and 12.2±6.6 days in FSAP group (7 patients), there was a significant difference between the two groups ($P=0.02$). The number of operations in the two groups was 1.33±0.5 *vs* 3.5±1.2 ($P=0.0037$), respectively. Prognosis: Non-operation cure rate, absorption rate of pseudocyst, hospital stay and survival rate in SAP group and FSAP group were 100 % (22/22) *vs* 11.1 % (1/9), 77.3 % (17/22) *vs* 11.1 % (1/9), 54.2±35.9 *vs* 99.1±49.5 days ($P=0.008$) and 100 % (22/22) *vs* 66.7 % (6/9) ($P=0.0044$). The time for absorption of pseudocyst was 135.1±137.5 days in SAP group.

CONCLUSION: *Penta-association therapy* is an effective guideline in the treatment of hyperlipidemic severe acute pancreatitis at its early stage (within 72 hours).

Mao EQ, Tang YQ, Zhang SD. Formalized therapeutic guideline for hyperlipidemic severe acute pancreatitis. *World J Gastroenterol* 2003; 9(11): 2622-2626
http://www.wjgnet.com/1007-9327/9/2622.asp

INTRODUCTION

Currently, cholilithiasis, alcohol abuse, hyperlipidemia and other specific factors, are the main causues of acute pancreatitis. The morbidity of severe acute pancreatitis secondary to hyperlipidemia (HL) has been apparently increased in recent years, acute pancreatitis occurred in 12-38 % of hyperlipidemic patients[1,2]. Hypertriglyceridemia (HTG) was the second cause of acute pancreatitis in our specialty center. However, this is in contrast with Yadav' s views point[3] that it was a rare cause of severe acute pancreatitis, obviously different from our situation.

Serum triglyceride (TG) level more than 10 to 20 mmol/l in patients with types I, IV, or V hyperlipidemia (Fredrickson' s classification) might lead to acute pancreatitis, so it has been considered as an identifiable risk factor[3]. It was reported that the mechanism leading to severe acute pancreatitis was that combining capacity of albumin surpassed by over production of free fatty acid would cause tissue toxicity. Thus, pancreatic acinar cells and microvessels were injured[4-8]. The main treatment for hyperlipidemic severe acute pancreatitis (HL-SAP) is to decrease serum triglyceride level and to prevent systemic inflammatory response. Although serum triglyceride could be decreased by plasmapheresis[9], there has been no formal therapeutic strategy to treat HL-SAP at present. We retrieved references about the treatment of HL-SAP from MEDLINE during 1966-2003 using severe acute pancreatitis and hyperlipidemia as the key words, and found that reports were all case reports of single treatment measure[10-12]. No formalized therapeutic strategy was found. Therefore, we prospectively treated patients with HL-SAP by *Pent-association therapy* which consisted of purification, antihyperlipidemic agents, insulin, heparin and topical application of Pixiao (a traditional Chinese medicine) over the whole abdomen to observe its therapeutic effects and influence on prognosis.

MATERIALS AND METHODS

Patients and groups

Patient Thirty-two consecutive patients with SAP admitted to Department of Surgical Intensive Care Unit, Ruijin Hospital, Shanghai, China, from April 2000 to March 2003 were included in the clinical trial. Therapeutic strategies to all patients were determined by a group of doctors from SICU and Department of Surgery.

Groups Five entry criteria for admission to the study were the Atalanta classification system to stratify patients with acute

pancreatitis (1992)[13], APACHEII score more than 8, within 72 hours after onset of the disease, serum triglyceride level more than 6.8 mmol/L, and exclusion of other etiologies.

The diagnosis of fulminant severe acute pancreatitis (FSAP) was made according to the following criteria.

FSAP was diagnosed by meeting one or more of the following indices within 72 hours after onset of the disease with adequate fluid resuscitation such as APACHEII score 20 or more, acute renal failure, ARDS, DIC, and Glasgow score less than 8.

According to the aforementioned criteria, 32 patients were divided into SAP group (22 patients) and FSAP group (10 patients). Of the FSAP group, one patient was excluded from the clinical trial due to giving up of the therapy. The patient did not undergo triglyceride adsorption and hemofiltration, and thus developed ARDS and acute renal failure within 48 hours. According to theoretical speculation and references, the *Penta-association therapy* might have some positive effects on patients. Therefore, we did not set control group in the present study. In addition, patients and/or their family were told about the trial in details. We were thus authorized to perform the study.

Etiology This included uncontrolled diabetes mellitus, long period alcohol abuse, heredity, pregnancy, obesity, *etc*. Among them, 23 men aged 45±9.4 years, 9 women aged 41.9±14.9 years.

Methods

Thearpy Conventional therapy: It included appropriate fluid resuscitation, fasting, gastrointestinal decompression, use of pancreatic enzyme inhibitors, prophylactic antibiotics, decoction of raw rhubarb poured into stomach via gastric tube, enteral nutrition and operation if necessary.

Specific therapy (Penta-association therapy) This included blood purification (adsorption of triglyceride and hemofiltration), triglyceride decreasing antihyperlipidemic agents (fluvastatin sodium capsules 40 mg, qn, P.O; lipanthyl, 200 mg qn, P.O), low molecular weight heparin (fragmin 5 000 IU, subcutaneous injection, qd, for 3 days), insulin by intravenous infusion (blood sugar controlled to less than 200 mg/dl), topical application of Pixiao over the whole abdomen.

Adsorption of triglyceride and hemofiltration Blood purification was performed using Diapact CRRT machine (B. Braun Co., Germeny). Polysulfone filters were used (Cut-off-point 30 000 Dalton, AV 600S, Fresenius Medical Care). Systemic anticoagulation was undergone with low molecular weight heparin (fragmin, 5 000 IU/ampule) at a dose of 100-140 IU/kg for bolus injection. Ultrafiltrate was replaced with substitutes made according to patient' s electrolyte and blood glucose. Pre-dilution mode was used. Extracoporeal blood flow ranged from 250 to 360 ml/min. Ultrafiltrating rate was controlled within 50-500 ml/h. In order to remove triglyceride rapidly, we changed the filter every 4 hours.

Indications for stopping blood purification Short veno-venous hemofiltration was stopped when the abdominal symptoms and signs disappeared, or the heart rate was less than 90 beats/min and the respiration rate was 20 times/min, respectively. Continuous veno-venous hemofiltration was stopped if the renal function was recovered and/or heart rate was less than 90 beats/min and the respiration rate was 20 times/min respectively.

Determination of Indices Serum levels of triglyceride, TNFα and IL-10 were determined before blood purification (PF), at the end of therapy (AFE) and on the 7th day (AF7) after onset of the disease. APACHE II scores were evaluated simultaneously. Activity of TNFα was assessed in the L929 cell line. IL-10 was tested using a commercially available ELISA kit (From Endogen Company, USA.).

Follow-up Enhanced CT scan of abdomen was performed every month for the patients with successful conservative treatment, and intra- and extra-pancreatic radiological changes were observed.

Prognosis Non-operation curative rate, survival rate, hospital stay, absorption rate of pseudocyst, time of first operation and total operation time were calculated and compared between the two groups.

Statistics

Data were reported as mean ± standard deviation, and analyzed using Student' s *t* and or chi square test.

RESULTS

Serum level of triglyceride, cytokine and APACHEII score

Serum concentrations of triglyceride and TNFα, and APACHE II scores were significantly decreased at AFE (t=5.687, P<0.001; t=6.342, P<0.001; t=12.12, P<0.001) and AF7 (t=7.576, P<0.001; t=10.19, P<0.001; t=15.09, P<0.001) compared with PF. Serum triglyceride level was decreased to safe range within 10 hours after the beginning of blood purification, and to normal range at AF7 when triglyceride was decreased as well as heparin and insulin were used continuously. But serum level of IL-10 at AFE was significantly increased compared with PF (t=19.21, P<0.001). However, it was significantly decreased (t=9. 87, P<0.001) at AF7 compared to PF.

Thus, serum triglyceride and pro-inflammatory cytokines were decreased, and anti-inflammatory cytokine was increased through blood purification (hemofiltration and adsorption of triglyceride), and severity of the disease was significantly decreased (Table 1).

Table 1 Levels of serum triglyceride, cytokines and APACHE II score

	PF	AFE	AF7
Serum triglyceride (mmol/L)	13.1±8.1	4.5±2.3	2.02±0.83
APACHE II score	18.4±4.4	7.38±2.5	5.8±1.5
TNFα (u/ml)	43.1±12.7	26.3±7.5	17.7±5.6
IL-10 (pg/ml)	72.1±20.0	179.6±23.9	31.2±11.5

Time duration for blood purification and number of filters used

Systemic inflammatory response syndrome (SIRS) was prevented through adsorption of triglyceride and short veno-venous hemofiltration in SAP group, but long time blood purification and/or drainage of large amounts of exudates from abdominal cavity and retroperitoneal space were needed in FSAP group. The number of filters used and time duration for blood purification in SAP group and FSAP group were 2.6±1.3 *vs* 2.9±1.5 h, 6.5 ±2.7 *vs* 48±62 h, respectively.

Surgical intervention

Time interval from onset of the disease to the first operation was significantly longer in SAP group (5 patients) than in FSAP group (7 patients) (t=2.715, P=0.02). Debridement of pancreatic necrosis and internal drainage of pseudocyst were performed in SAP group. Only debridement of pancreatic necrosis was performed in FSAP group, but operation number was more than that in SAP group (t=3.775, P=0.0037). This indicated that *Penta-association therapy* had better results in hyperlipidemic SAP than in FSAP group (Table 2).

Prognosis

We compared the results from this clinical trial with 283 patients treated with conventional therapy in our hospital, and found that non-operation cure rate was 100 %(22/22) in the present

SAP group, and was 43.5 % in our previous group (123/283) (χ^2=26.16, P=3.3×10^{-7}). The survival rate was 100 %(22/22) and was 84.1 % in our previous group (238/283) (χ^2=4.104, P=0.043). In SAP group, pancreatic pseudocysts were resolved spontaneously in 17 patients, with an absorption rate of 77.3 % (17/22), and surgical intervention was thus avoided. Absorption time was 135.1±137.5 days with a variation constant of 102 %.

In FSAP group, only one patient was cured through conservative treatment, its time interval for absorption of pseudocyst was 96 days. Another patient died without operation. Surgical drainage and debridement of pancreatic necrosis were done for the rest of 7 patients within 2 weeks after onset of the disease. The survival rate of 66.7 %(6/9) was slightly higher than 58 % (27/47) from Beger' s report[14] [χ^2=0.2653, P=0.61] without significant difference.

Absorption rate of pseudocyst, non-operation cure rate and survival rate in SAP group were higher than those in FSAP group. Hospital stay was also shortened compared to FSAP group (P=0.008, Table 3).

Table 2 Surgical intervention

	SAP	FSAP
Number of cases	5	7
Time of first operating (days)	55.8±42.6	12.2±6.6
Surgical procedures	Debridement and gastro-or jejuno-pancreatic anastomosis for pseudocyst	Debridement with drainage and nutritional jejunostomy
Number of operation	1.33±0.5	3.5±1.2

Table 3 Prognosis of SAP and FSAP

	SAP group	FSAP group
Number of cases	22	9
Rate of adsorption of pseudocyst	77.3 %(17 / 22)	11.1 %(1 / 9)
Time interval for absorption of pseudocyst	135.1±137.5	96
Non-operation cure rate	100 %(22 / 22)	11.1 %(1 / 9)
Hospital stay (days)	54.2±35.9	99.1±49.5
Survival rate	100 %(22 / 22)	66.7 %(6 / 9)

DISCUSSION

With an increased incidence of hyperlipidemia and its complication, acute pancreatitis also increased accordingly. SAP secondary to hypertriglyceridemia (HTG), presented typically as an episode of SAP, rarely as chronic pancreatitis. A level of serum triglyceride (TG) more than 6.8 mmol/L in patients with types I, IV, or V hyperlipidemia (Fredrickson' s classification) is an identifiable risk factor. The typical clinical profiles of hyperlipidemic pancreatitis were a patient with a preexisting lipid abnormality along with the presence of a secondary factor (e.g., poorly controlled diabetes, alcohol abuse or a medication) that could induce HTG[15]. Patients with isolated hyperlipidemia (type V or I) without a precipitating factor would rarely have pancreatitis. Interestingly, serum pancreatic enzymes might be normal or only minimally elevated even in the presence of SAP as diagnosed by imaging studies. The clinical course of HL-SAP was not different from severe acute pancreatitis caused by other causes. Although conventional management of SAP caused by hyperlipidemia is similar to that by other causes, but it still needs some specific management. So we did this clinical trial to investigate systematically how to manage HL-SAP within 72 hours after onset of the disease.

Formation of therapeutic regimen and its mechanism

At present, there have no formalized therapeutic strategies for the treatment of HL-SAP in the literature, besides single case report or the use of certain measures. In 2000, our Pancreatic Disease Therapy Center considered a therapeutic strategy aiming at HL-SAP that was based on the concepts that hyper-triglyceride, fatty acid and inflammatory mediators were the pathological mechanism of deterioration of HL-SAP[8,16-19]. A prospective investigation was thus carried out. Principles of the strategy included r*apid lowering serum triglyceride, blocking of induction pancreatic damage by pro-inflammatory mediators, preventing recurrence by the use of antihyperlipidemic agents, promoting self- absorption of pancreatic pseudocyst.* Concrete measures could be found in the details of *Penta-association therapy*, which included blood purification (adsorption of triglyceride and hemofiltration), fluvastatin (40 mg, qn, P.O) or lipanthyl (200 mg, qn, P.O), low molecular weight heparin (fragmin, 5 000 IU subcutaneous injection, qd, for three days.), insulin (intravenous infusion, blood sugar level controlled well below 200 mg/dl), and topical application of Pixiao (Chinese traditional medicine) over the whole abdomen. Hyperchylomicronemia caused by hyperlipidemia could lead to not only pulmonary edema[20] and systemic microcirculatory dysfunction, but also release of fatty acids, which would play an important role in causing pancreatic injury[8,17]. Thus, the first item of the therapeutic regimen was adsorption of serum triglyceride, and it was essential to lower blood triglyceride level within the safe range. Simultaneously, heparin could stimulate lipoprotein-lipase activity and accelerate chylomicron degradation[9]. It could also contribute to the decrease of serum triglyceride level. Besides this effect on blood triglyceride, it could also improve microcirculation and prevent activation of neutrophils activity[21]. Polymorphonuclear cells (PMN) could play an important role in the deterioration of severe acute pancreatitis, especially release of elastase (PMNE), which would lead to persistent pancreatic necrosis and acute lung injury[22]. Insulin could not only decrease blood sugar, but also accelerate degradation of chylomicrons[9]. Therefore insulin was given to control blood sugar well below 200 mg/dL. Simultaneously, fluvastatin sodium or lipanthyl was given to decrease blood lipid in order to avoid recurrence of acute pancreatitis.

Though the etiologies of patients with acute pancreatitis could be different, but their pathophysiological changes were just the same[23]. Activated enzymes and oxygen free radicals injured the acinar cells and caused release of cytokines and vasoactive mediators, attracted inflammatory cells and activated vascular endothelium as well as the expression of adhesion molecules. The disturbance of pancreatic microcirculation could induce progression from edematous to necrotizing pancreatitis independent of the early intracellular events, including protease activation. Specific therapy must be directed towards microperfusion failure as the secondary pathogenetic step, since the initial enzyme activation and cytokine release were irreversible by the time of clinical presentation. In experiments comparable to the clinical situation, following therapeutic principles have been proven to be beneficial: increase of blood fluidity, inhibition of leukocyte-endothelium interaction and blockade of systemic inflammatory response. As we know, Short time veno-venous hemofiltration could significantly decrease circulatory TNFα level and increase circulatory IL-10 level[24]. This could block systemic inflammatory response and pancreatic necrosis. Due to dynamic balance of pro-inflammatory and anti-inflammatory cytokines, long time hemofiltration was prohibited to avoid creation of new imbalance in SAP[25]. However, FSAP usually resulted in Ultra-SIRS (systemic inflammatory response syndrome), thus continuous veno-venous hemofiltration and

drainage of abdominal, retroperitoneal toxic exudates were essential to prevent recurrence of Ultra-SIRS. Based on this concept, hemofiltration could be used as a specific measure to treat HL-SAP.

After acute response phase, emphasis should be put on the prevention of infection, rapid subsidence of fluid accumulation in the third space as well as promotion absorption of pancreatic pseudocyst. Topical application of Pixiao (Chinese traditional medicine) over the whole abdomen could ameliorate tissue edema including that of abdominal wall, peritoneum and intestinal wall, and accelerate absorption of pancreatic pseudocyst. Therefore, Pixiao was used through out the whole course of the disease in order to relieve tissue edema and resolve pancreatic pseudocyst spontaneously. When patients were discharged with pancreatic pseudocyst, application of Pixiao was continued until it no longer absorbed fluid and became dry. Though the effect of this measure was slow, but it played an important role in decreasing operation rate.

Efficacy and prognosis

Although *Penta-association therapy* is far from perfect, especially for the prevention of recurrence of the disease, but good clinical efficacy has been obtained by these specific measures in the acute response phase of the episode.

In acute pancreatitis, medications, such as heparin and insulin *etc*. decreased trigylceride levels to less than 10 mmol/L within 2.8 days (1 to 6), the amylase and lipase levels returned to normal after 3 and 4 days respectively, and the abdominal pain was resolved[9,10]. Also, it was reported that plasmapheresis removed blood triglyceride[26-31] and got good results. Clinically, this method could not be propagated to wider use due to the problems of equipments and the need for large amounts of plasma. So we adopted the present measure to adsorb triglyceride. Within 72 hours after onset of the disease, serum triglyceride concentration was decreased to 6.8 mmol/l within 10 hours. At this time, abdominal pain was resolved in 31 patients. So adsorption of triglyceride can not only decrease triglyceride level rapidly, but also resolve abdominal pain and prevent deterioration of the disease. This has been regarded as a necessary measure in the treatment of HL-SAP at its early stage. As to the safe range of blood triglyceride level, it was reported that the level should be decreased to 5.65 mmol/L[32], but in our series when it was below 6.8 mmol/l, abdominal pain in 31 patients was resolved. This discrepancy might be due to different etiologies of hypertriglyceridemia or different preexisting factors. All the patients received insulin, heparin and antilipidemic agents to prevent deterioration of the disease by controlling serum triglyceride level at normal range 7 days after onset of the disease. Even though etiologies resulting in each SAP patients might be different, but pathophysiological lesions were just the same, such as overproduction of cytokines, microcirculation failure and over-activated neutrophils. Therefore, hemofiltration was continued after lipid adsorption to regulate the balance between proinflammatory and anti-inflammatory cytokines. This caused decrease of proinflammatory cytokines as well as temporary increase of anti-inflammatory cytokines with APACHEII score decreased. Our results were in accordance with the report in the literature[24]. Thus, hemofiltration used in the early treatment of HL-SAP was of important clinical significance.

Five patients with SAP underwent the first operation on the 56th day after onset of the disease. Surgical modalities used coincided with literature reports[31]. The major methods were debridement and drainage of pancreatic necrosis as well as internal drainage of pancreatic pseudocyst. But FSAP group underwent the first operation on the 12th day after onset of the disease. The first operation time was earlier than that of SAP group (P<0.01). Surgical methods in FSAP group were mainly debridement and drainage. Furthermore, the number of operations was also increased (P<0.01).

Non-operation cure rate and survival rate were both 100 % in SAP group, they were increased significantly compared with non-operation rate of 43.5 % and survival rate of 84.1 % in 283 patients with SAP in our hospital in the past. Meanwhile, the survival rate of 100 % was higher than that of 62 % (8/13) in literature report[31] [χ^2=9.872, P=0.002]. Incidence of pseudocyst in SAP group was 81.8 % (18/22) which was significantly higher than that of 37 % in literature report of[33]. Pseudocysts in 17 patients resolved spontaneously without operation. The reason why the morbidity and absorption rate of pseudocyst were very high was that the full-blown summit of SAP was at 72 hours, so pancreatic microcirculation was compromised, and ischemia occurred in the pancreas within 72 hours. Thirty-one patients were treated on time within 72 hours, thus pancreatic necrosis was prevented. After onset of the disease, the whole abdomen was covered with Pixiao (rough-wrought Glauber' s salt) until it could not be moistened. This treatment could accelerate absorption of pseudocyst. Ischemia occurred in the major component of Pixiao (rough-wrought Glauber' s salt) is Glauber' s salt, additionally, it contains magnesium sulfate, calcium chloride, magnesium chloride *etc*. and acts on inflammatory mass by the effect of shrinkage, anti-inflammation, dehydration and others. Based on the aforementioned results, we think that *Penta-association therapy* has quite good clinical efficacy, and should be regarded as a specific measure in the treatment of HL-SAP.

HL-FSAP is a sub-type of HL-SAP. Although we applied the same conservative therapeutic measures as those of SAP, but the efficacy was not the same. Only one patient recovered through conservative treatment. It took 96 days for the pseudocyst to resolve spontaneously. Another patient died. If conservative treatment could not control the disease, it was taken as the indication for operation in FSAP. Seven of them underwent debridement and drainage of abdominal and/or retroperitoneal exudates through laparotomy within 2 weeks after onset of the disease. Although its cure rate was 66.7 %, it was still higher than Beger' s 58 %[14] and Bosscha' s 61 %[34], the percentage of mortality was still 33 %. According to our data and literature data[34], survival rate has not been improved through early enthusiastic operation and surgical drainage. This demonstrated that conventional treatment and *Penta-association therapy*, optimal surgical indication, proper timing of operation and choice of drainage method, such as laparoscopy, drainage through single lumen catheter puncture guided by ultrasound, play an important role on survival rate in the treatment of HL-FSAP. Although the viewpoint that conservative treatment should be applied to treat FSAP during it' s early stage (within 2 weeks)[35] was controversial, it is advisable to apply cautiously drainage through laparotomy in the treatment of FSAP during its early stage, and this could achieve curing rate. Some authors suggested that management and clinical surveillance required specific expertise, and management of these patients was best undertaken in specialized centers.

It is thus evident that *Penta-association therapy* upon the basis of conventional therapy for HL-SAP can give good clinical results, but its efficacy in treating FSAP needs to be further improved.

Recommendation of formalized therapeutic regimen

Efforts has been made by the pancreatic disease specialists all over the world in the past hundred years, the therapy of acute pancreatitis has been basically formalized, and therapeutic principles were also basically established. Thus, the cure rate of SAP has reached 80 %. But there were still 20 % of patients who could not be cured. Among them, 15 % were still SAP,

5 % were another subtype - FSAP. Regardless of the etiologies of SAP, their pathophysiological changes were identical, and this determined the accordance of their management. But why there were still 15 % of these patients who could not be cured? Based upon our experimental results, we think some of them were not treated appropriately with regard to their etiologies during early stage (within 72 hours). Although pancreatic lesions could not be prevented from progression even after the etiologies were resolved, continuing existence of the etiological factors would aggravate the disease, such as choledocholithiasis and hyperlipidemia. At present, there are a lot of measures to treat biliary acute pancreatitis, such as EST, ENBD or surgical operation. Nevertheless, there is no formalized regimen to manage HL-SAP. On account of this, our Pancreatic Disease Therapy Center has suggested a formulated specific regimen to treat HL-SAP in order to save some of the 15 % patients. In the present study, from the standpoint of cure rate, almost all the patients were recovered from the disease. Based upon our results, we suggest that it is important to determine whether hyperlipidemia is existent or not by history and laboratory examinations or simply by the presence of chylous blood. Once the diagnosis of HL-SAP is established, besides the conventional therapy, *Penta-association therapy* should be given immediately to mange HL-SAP.

Additionally, 5 % of the patients belonged to FSAP. Although the therapeutic efficacy of HL-FSAP in the present group was somewhat improved, but it was not significant. This should be further investigated.

In summary, HL-SAP has not only the general characteristics of severe acute pancreatitis, but also some specific characteristics. So, besides conventional therapy of SAP, specific strategy should be taken into consideration. *Penta-association therapy* is not a perfect regimen, further refinement, especially to treatment for FSAP, is urgently required.

REFERENCES

1 **Toskes PP.** Hyperlipidemic pancreatitis. *Gastroenterol Clin North Am* 1990; **19:** 783-791
2 **Searles GE,** Ooi TC. Underrecognition of chylomicronemia as a cause of acute pancreatitis. *CMAJ* 1992; **147:** 1806-1808
3 **Yadav D,** Pitchumoni CS. Issues in hyperlipidemic pancreatitis. *J Clin Gastroenterol* 2003; **36:** 54-62
4 **Thompson GR.** Primary hyperlipidaemia. *Br Med Bull* 1990; **46:** 986-1004
5 **Havel RJ.** Pathogenesis, differentiation and management of hypertriglyceridemia. *Adv Intern Med* 1969; **15:** 117-154
6 **Nagai H,** Henrich H, Wunsch PH, Fischbach W, Mossner J. Role of pancreatic enzymes and their substrates in autodigestion of the pancreas. *In vitro* studies with isolated rat pancreatic acini. *Gastroenterol* 1989; **96:** 838-847
7 **Kimura W,** Mossner J. Role of hypertriglyceridemia in the pathogenesis of experimental acute pancreatitis in rats. *Int J Pancreatol* 1996; **20:** 177-184
8 **Domschke S,** Malfertheiner P, Uhl W, Buchler M, Domschke W. Free fatty acids in serum of patients with acute necrotizing or edematous pancreatitis. *Int J Pancreatol* 1993; **13:** 105-110
9 **Berger Z,** Quera R, Poniachik J, Oksenberg D, Guerrero J. Heparin and insulin treatment of acute pancreatitis caused by hypertriglyceridemia. Experience of 5 cases. *Rev Med Chil* 2001; **129:** 1373-1378
10 **Henzen C,** Rock M, Schnieper C, Heer K. Heparin and insulin in the treatment of acute hypertriglyceridemia-induced pancreatitis. *Schweiz Med Wochenschr* 1999; **129:** 1242-1248
11 **Routy JP,** Smith GH, Blank DW, Gilfix BM. Plasmapheresis in the treatment of an acute pancreatitis due to protease inhibitor-induced hypertriglyceridemia. *J Clin Apheresis* 2001; **16:** 157-159
12 **Lechleitner M,** Ladner E, Seyr M, Hoppichler F, Foger B, Hackl JM. Hypertriglyceridemia and acute pancreatitis. *Acta Med Austriaca* 1994; **21:** 125-128
13 **Bradley EL 3rd.** A clinically based classification system for acute pancreatitis. Summary of the international symposium on acute pancreatitis. Atlanta, Ga, September 11 through 13, 1992. *Arch Surg* 1993; **128:** 586-590
14 **Isenmann R,** Rau B, Beger HG. Early severe acute pancreatitis: characteristics of a new subgroup. *Pancreas* 2001; **22:** 274-278
15 **Pfau J.** Acute pancreatitis and hypertriglyceridemia. *Rev Med Chil* 1989; **117:** 907-909
16 **Saharia P,** Margolis S, Zuidema GD, Cameron JL. Acute pancreatitis with hyperlipemia: studies with an isolated perfused canine pancreas. *Surgery* 1977; **82:** 60-67
17 **Hofbauer B,** Friess H, Weber A, Baczako K, Kisling P, Schilling M, Uhl W, Dervenis C, Buchler MW. Hyperlipaemia intensifies the course of acute oedematous and acute necrotising pancreatitis in the rat. *Gut* 1996; **38:** 753-758
18 **Norman J.** The role of cytokines in the pathogenesis of acute pancreatitis. *Am J Surg* 1998; **175:** 76-83
19 **Van Laethem JL,** Eskinazi R, Louis H, Rickaert F, Robberecht P, Deviere J. Multisystemic production of interleukin 10 limits the severity of acute pancreatitis in mice. *Gut* 1998; **43:** 408-413
20 **Warshaw AL,** Lesser PB, Rie M, Cullen DJ. The pathogenesis of pulmonary edema in acute pancreatitis. *Ann Surg* 1975; **182:** 505-510
21 **Capecchi PL,** Ceccatelli L, Laghi Pasini F, Di Perri T. Inhibition of neutrophil function in vitro by heparan sulfate. *Int J Tissue React* 1993; **15:** 71-76
22 **Mao EQ,** Han TQ, Tang YQ, Zhang SD, Zhang SD. Polymorphonuclear elastase is the major causative factor in acute lung injury complicating severe acute pancreatitis in rats. *Zhonghua Xiaohua Zazhi* 1998; **18:** 207-209
23 **Klar E,** Werner J. New pathophysiologic knowledge about acute pancreatitis. *Chirurg* 2000; **71:** 253-264
24 **Mao E,** Tang Y, Han T, Zhai H, Yuan Z, Yin H, Zhang S. Effects of short veno-venous hemofiltration on severe acute pancreatitis. *Zhonghua Waike Zazhi* 1999; **37:** 141-143
25 **Mao EQ,** Tang YQ, Zhang SD. Effects of time interval for hemofiltration on the prognosis of severe acute pancreatitis. *World J Gastroenterol* 2003; **9:** 373-376
26 **Perrone G,** Critelli C. Severe hypertriglyceridemia in pregnancy. A clinical case report. *Minerva Ginecol* 1996; **48:** 573-576
27 **Mayan H,** Gurevitz O, Mouallem M, Farfel Z. Multiple spurious laboratory results in a patient with hyperlipemic pancreatitis treated by plasmapheresis. *Isr J Med Sci* 1996; **32:** 762-766
28 **Majlis S,** Anguita T, Weishaupt R, Socias M. Plasmapheresis in acute pancreatitis secondary to familial hyperlipidemia in a pregnant woman. *Rev Med Chil* 1989; **117:** 1275-1278
29 **Schranz W,** Bartels O. Early plasma exchange in acute pancreatitis. A successful therapeutic principle in extreme hyperlipidemia. *Fortschr Med* 1986; **104:** 530-532
30 **Sunamura M,** Yamauchi H, Takeda K, Suzuki T, Abe R, Oikawa S, Sano R. A case of acute pancreatitis associated with hyperlipidemia and pregnancy with reference to plasma exchange as a therapeutic intervention. *Nippon Shokakibyo Gakkai Zasshi* 1985; **82:** 2139-2143
31 **Ohmoto K,** Neishi Y, Miyake I, Yamamoto S. Severe acute pancreatitis associated with hyperlipidemia: report of two cases and review of the literature in Japan. *Hepatogastroenterology* 1999; **46:** 2986-2990
32 **Nair S,** Yadav D, Pitchumoni CS. Association of diabetic ketoacidosis and acute pancreatitis: observations in 100 consecutive episodes of DKA. *Am J Gastroentero l* 2000; **95:** 2795-2800
33 **Fortson MR,** Freedman SN, Webster PD 3rd. Clinical assessment of hyperlipidemic pancreatitis. *Am J Gastroenterol* 1995; **90:** 2134-2139
34 **Bosscha K,** Hulstaert PF, Hennipman A, Visser MR, Gooszen HG, van Vroonhoven TJ, vd Werken C. Fulminant acute pancreatitis and infected necrosis: results of open management of the abdomen and "planned" reoperations. *J Am Coll Surg* 1998; **187:** 255-262
35 **Gronroos JM,** Nylamo EI. Mortality in acute pancreatitis in Turku University Central Hospital 1971-1995. *Hepatogastroenterology* 1999; **46:** 2572-2574

Edited by Xu JY and Wang XL

P.O.Box 2345, Beijing 100023,China
Fax: +86-10-85381893
E-mail: wjg@wjgnet.com www.wjgnet.com

World J Gastroenterol 2003;9(11):2627-2631
World Journal of Gastroenterology
 ISSN 1007-9327

• BRIEF REPORTS •

Correlation between metastatic potential and variants from colorectal tumor cell line HT-29

Min Wang, Ilka Vogel, Holger Kalthoff

Min Wang, Department of Surgical Oncology, First Affiliated Hospital of Medical College, Zhejiang University, Hangzhou 310003, Zhejiang Province, China
Ilka Vogel, Holger Kalthoff, Molecular Oncology Research Laboratory, Clinic for General and Thoracic Surgery, Christian-Albrechts-University, 24105 Kiel, Germany
Supported by the Scientific Research Foundation for Returned Overseas Chinese Scholars, Personnel Affairs Bureau of Zhejiang Province
Correspondence to: Dr. Min Wang, Department of Surgical Oncology, First Affiliated Hospital of Medical College, Zhejiang University, 79 Qingchun Road, Hangzhou 310003, Zhejiang Province, China. pfeng@mail.hz.zj.cn
Telephone: +86-571-7236880 **Fax:** +86-571-7236628
Received: 2003-04-12 **Accepted:** 2003-05-19

Abstract

AIM: To evaluate the relationship between uPA, PAI-1, CEA, PI3K and metastatic potential in three colorectal tumor cell lines.

METHODS: Metastatic model in nude rats was established by variants HT-29c and HT-29d cell lines and the metastatic potential of two tumor cell variants was compared. Urokinase-type plasminogen activator (uPA) and plasminogen activator inhibitor type 1 (PAI-1) were determined using ELISA in colorectal carcinoma WiDr, HT-29 and HT-29d cell lines with different metastatic potentials. Expression of carcinoembryonic antigen (CEA) and phosphoinositide 3-kinase (PI3-Kinase) was analyzed using immunohistochemistry (IHC) in these cell lines *in vitro* and *in vivo*. CEA expression was compared using fluorescence activated cell sorter (FACS) *in vitro*.

RESULTS: The number of HT-29d cells arrested in liver dramatically decreased within the initial 24 hours after injection. The taking rate of liver metastases in the variant HT-29d increased as compared with parental HT-29 cells (70 % versus 50 %) and a variant HT-29b cells (70 % versus 60 %), and extensive organs were synchronously involved in metastases. The uPA concentration of variant HT-29d cell line was significantly higher than that of the non-metastatic WiDr and the low metastatic HT-29 cell lines. The variant HT-29d cells produced stronger PI3-kinase expression as compared with the non-metastatic WiDr cells and the low metastatic HT-29 cells *in vivo*.

CONCLUSION: The selected variant HT-29d cell exhibited an enhanced metastatic potential. The level of uPA and PAI-1 is positively correlated with the metastatic capacity of tumor cells. The expression of PI3-kinase correlates with tumor development and metastasis.

Wang M, Vogel I, Kalthoff H. Correlation between metastatic potential and variants from colorectal tumor cell line HT-29. *World J Gastroenterol* 2003; 9(11): 2627-2631
http://www.wjgnet.com/1007-9327/9/2627.asp

INTRODUCTION

The malignancy of a solid tumor is due to its ability to invade and metastasize. Metastasis is a major cause of cancer death. Cancer metastasis consists of multiple sequential and selective steps. The aggressiveness of a tumor is primarily dependent on its ability to invade adjacent tissues and to metastasize to distant sites. In recent years special attention has been paid to tumor-associated protease systems, such as urokinase-type plasminogen activator (uPA)[1]. A role of uPA in regulating tumor cell invasiveness has been proposed on the basis of generally increased uPA activity in several metastatic tumors[2,3]. For many malignant tumors, there is a significant correlation between the production of uPA and tumor invasion[4,5]. The activation of uPA is controlled by well-characterized plasminogen activator inhibitors: type 1 (PAI-1). Numerous studies have shown that PAI-1 antigen levels in primary tumor with lymph node involvement were significantly higher than those in cancers without lymph node involvement[6,7], and in metastatic lymph nodes their levels were also increased compared to primary tumors[8].

Carcinoembryonic antigen (CEA) is one of the most common tumor-associated substances produced by colorectal carcinoma, and it has been used in numerous studies as a tumor marker. Although the functional role of CEA in liver metastasis from colorectal carcinomas has been assumed to be an adhesion factor or receptor binding to Kupffer cells[9,10], a conclusive evidence *in vivo* has not been clarified yet.

Phosphoinositide 3-kinase (PI3-kinase) is a key signaling enzyme implicated in a variety of receptor-stimulated cell responses[11]. This lipid product is believed to act as the second messenger in a variety of signaling processes including cell survival and migration[12,13]. Numerous studies have implicated PI3K in signal transduction pathways correlated with cell proliferation, cell cycle progression, cell apoptosis, tumorigenesis, tumor angiogenesis and tumor invasiveness[14,15].

In this study, uPA, PAI-I, CEA and PI3K were determined in three colorectal cancer cell lines with different metastatic capacities *in vitro* and *in vivo*, and the relationship between metastatic potential and these biological factors in colorectal tumor was investigated.

MATERIALS AND METHODS

Experimental animals

Three-week old male athymic Rowett nude rats (Hsd:RH-nu/nu) were obtained from Harlan/Winkelmann (Borchen, Germany). All rats were housed under special pathogen-free conditions in a laminar flow cabinet (EHRET, DIPL.-ING. W. EHRET GmbH, Germany) with constant temperature (24-26 ℃), humidity (40-50 %) and 12-hour light/12-hour dark cycle. The rats were fed with standard rat food and water. All cages, bedding and operative equipments were autoclaved at 121 ℃ for 30 minutes. The nude rats were stabilized for one week in the laboratory before the experiments were started.

Cell lines and cell culture

Human colonic adenocarcinoma cell lines WiDr and HT-29

as well as their variants HT-29c and HT-29d were used in the present study. WiDr cell line was established from a moderately differentiated human primary rectosigmoid adenocarcinoma with non-distasnt metastatic capability and obtained from American Type Culture Collection (ATCC, Rockville, MD, USA). HT-29 cell line was established from a moderately differentiated human colon adenocarcinoma and was a gift of Dr. Dippold (Mainz, Germany). HT-29c and HT-29d cell lines were two variant cell lines after three and four cycles of selection of liver metastases from parental HT-29 cells[16].

All the cell lines were grown in RPMI-1640 medium (Life Technologies, Eggenstein, Germany) plus 10 % fetal bovine serum (FCS, Life Technologies) supplemented with 2 mM L-glutamine and 1 mM sodium pyruvate (Life Technologies) and maintained in a 37 ℃ incubator (Heraeus, Germany) with 100 % relative humidity and 5 % CO_2. Cells were seeded and grown as monolayers in 75 cm^2 culture flasks (Falcon, England).

Establishment of metastatic model

Cells were harvested from exponential growth phase by brief trypsinization. The number of cell concentration was determined using a hemocytometer (Marienfeld, Germany). The cell suspensions were resuspended in HBSS at a final concentration of 4×10^7 cells/ml. A toal of 12 rats were anesthetized, an abdominal incision about 2 cm long was made in midline and the portal vein and mesenteric vein were isolated and exposed. Single-cell suspension of 0.5 ml containing 2×10^7 cells of HT-29c or HT-29d was injected into the mesenteric vein of 2 or 10 rats, respectively. The rats were explored for the first time about 4 weeks after injection and killed and autopsied at 6-10 weeks or when moribund after injection. The liver, lung and other organs were removed and frozen in liquid nitrogen, then stored at -80 ℃ for IHC.

To investigate the distribution and fate of tumor cells in the liver at the initial 48 hours after injection, 3-4 rats were killed at 1, 24, 48 hours after injection, respectively. The livers were removed, frozen in liquid nitrogen immediately, then the liver tissues were sliced at 5 μm cryosections and analysed for tumor cells by IHC with anti-CK mAb KL-1.

Quantitative detection of uPA and PAI-1

Six-well tissue culture plates were used. The single cell suspension of WiDr cells, HT-29 cells and HT-29d cells containing 3×10^5 tumor cells in supplemented RPMI-1640 was seeded into each well, respectively, and incubated at 37 ℃ in a humidified 5 % CO_2 incubator. After incubation for 24 hours, the medium of each well was sucked away and freshly supplemented RPMI-1640 medium (1.5 ml/per well) was added. The cells were incubated under the same conditions as above for 24 and 48 hours, respectively. Then the medium of each well was removed into Eppendorf tubes and centrifuged at 10 000 rpm for 15 minutes at 4 ℃. The supernatant was for detection of uPA and PAI-1. To measure the concentration of uPA and PAI-1 antigen in tumor cell culture supernatants, the uPA and PAI-1 ELISA kits (Imubind, American Diagnostica, Greenwich, CT, USA) were used. The sample value was multiplied by the dilution factor to determine the uPA and PAI-1 concentration of the cell culture supernatant. Meanwhile, the cells in six-well tissue culture plates were harvested by brief trypsinization and cell number was determined using a hemocytometer.

Determination of PI3-kinase expression

Tumor cells were seeded on 10-well mask slides at a density of 2×10^5 cells/ml supplemented medium and incubated at 37 ℃ in an incubator with 100 % relative humidity and 5 % CO_2 as described above. 48 hours later, the slides were washed twice with PBS and fixed in cold acetone for 5 minutes. Tumor tissue samples were cut into 5 μm cryosections and placed on microscope slides. The 10-well mask cell slides or tissue cryosections were fixed in cold acetone (4 ℃) for 5 minutes. The rabbit polyclonal antibody against PI3-kinase p85α and P110α (Santa Cruz Biotechnology) was used for immunohistochemical evaluation. The standard ABC immunostaining method was employed as immunohistochemical staining with ABC kit (Vector Laboratories, CA, USA). A semiquantitated score of 5 categories based on color intensity was assigned as -: no reaction, +: weak positive reaction, ++: moderate positive reaction, +++: strong positive reaction. The percentage of positive tumor cells was determined by calculating 1 000 tumor cells in 5 random areas of one section.

CEA determination

FACS analysis of cell lines WiDr, HT-29 and HT-29d cells were harvested from exponential growth phase with 0.002 % EDTA in PBS and inactivated with supplemented medium, then centrifuged at 1 410 rpm for 5 minutes. The pellet was washed in Na-azide-PBS (7.5 mM) at 4 ℃, and cells were counted with 5×10^5 cells removed to each FACS tube. The cells were washed in 1 ml Na-azide-PBS and centrifuged again. The supernatant was sucked away, primary mAb to human CD66e (clone 85A12, 100 μg/ml, Cymbus Biotechnology, Chandlers Ford, Hants, UK) was diluted (2:3) with 3 % BSA in azide-PBS and added to each tube. The tube was vortexed and incubated on ice at 4 ℃ for 1 hour. One ml azide-PBS was added for inactivation and the cells were centrifuged. The supernatant was sucked away, the second antibody of dichlorotriazinyl amino fluorescein (DTAF)-conjugated affinipure goat anti-mouse IgG+IgM (1.3 mg/ml, Dianova, Hamburg, Germary) diluted (1:100) with 3 % BSA in azide-PBS was added to each tube. The tube was vortexed and incubated on ice in the dark at 4 ℃ for 30 minutes. One ml azide-PBS was added for inactivation and the cells were centrifuged. The supernatant was sucked away, 300 μl of azide-PBS was added to each tube and vortexed, then 100 μl of 4 % paraformaldehyde was added. The samples were stored at 4 ℃ in the dark for FACS analysis. The primary antibody and secondary antibody were replaced by 3 % BSA in azide-PBS as negative controls, the primary antibody was replaced by 3 % BSA in azide-PBS as the second antibody control.

Immunohistochemistry analysis To investigate the CEA expression of different cell lines, s.c tumor and liver metastasis tumor, mouse monoclonal antibody to human CD66e were used for immunohistochemical evaluation. The standard ABC immunostaining method and a semiquantitated score were performed as described above.

Statistical analysis

The data were presented as mean ± standard deviation. Statistical analyses were performed using the F test and χ^2 test. Differences were considered significant if the P-values were <0.05.

RESULTS

Phenotype of HT-29 variants with enhanced tumorigenicity in vivo

The distribution and fate of tumor cells HT-29d in the liver at the initial phase after inoculation were observed in the rats of each group at different time intervals, respectively. The number of HT-29d cells arrested in the liver was dramatically decreased within the initial 48 hours after injection. By 1 hour after mesenteric vein injection, many tumor cells could be found in

Table 1 Macroscopical pattern of HT-29c/d cell metastases

Cell	Hepatic metastasis				Lung metastasis			Other organs
	No of metast[a]	I	II	III	No of metast[a]	I	II	
HT-29c	1/2	0/2	0/2	1/2	1/2	1/2	0/2	2/2
HT-29d	7/10	2/10	3/10	2/10	3/10	1/10	2/10	9/10

a: metastasis.

the livers, with a mean of 14.7 tumor cells/mm^2, and the single and clustered cells in the liver were located surrounding portal vein and in hepatic sinusoids. By 24 hours, however, the number of tumor cells surviving in the liver was significantly decreased. Only a few cells were found, with a mean of 2.3 tumor cells/mm^2 (range, 0-9 tumor cells/mm^2), and the cells were located mostly in parenchyma of the liver. At 48 hours after injection, a similar tumor cell distribution was found.

Metastatic potential of HT-29c and HT-29d cells was studied by injecting tumor cells into the mesenteric vein of nude rats. All rats survived the surgery and tumor-cell injection. Exploration was performed at the fourth week after injection. The rats were killed 8 to 10 weeks after injection or when moribund. The metastases were determined either by macroscopy or by microscopy. Liver tumor burden was evaluated based on the number of lesions as Class I: histological evidence of tumor growth, Class II: <10 tumor foci (macroscopically), Class III: >10 tumor foci (macroscopically). Lung metastasis was evaluated as Class I: histological evidence of tumor growth, Class II: macroscopically positive. The results are shown in Table 1. One of the two rats injected HT-29c cells developed extensive hepatic metastases, in which 60 % of the right liver was occupied by tumor tissue. The other developed micrometastases in the lung, diaphragm, left kidney with hemorrhagic ascites. The two rats developed mesenteric metastases. Seven of the ten rats (70 %) injected HT-29d cells had either liver macrometastases or micrometastases. Still three of the ten rats (30 %) had lung metastasis, of which two developed extensively dispersed metastatic nodules in their lungs. Three of the ten rats (30 %) developed metastatic tumors in their thoracic cavity. Five developed metastatic tumors in the diaphragm. Two produced hemorrhagic ascites. Nine developed extensive mesenteric metastases within 8 to 10 weeks after injection of HT-29d. One suffered from hindlegs paralysis at day 30 after injection.

Level of uPA and PAI-1

The concentrations of uPA and PAI-I in cell supernatants were statistically significantly different among WiDr, HT-29 and HT-29d cells. The uPA and PAI-I concentrations of variant HT-29d cell line were significantly higher than those of HT-29 and WiDr cell lines at 24 hours (F value was 17.4, P=0.03) and at 48 hours (F value was 98.3, P=0.001). The uPA and PAI-I concentration of variant HT-29 cell line was also higher than that of WiDr cell line (Table 2).

Expression of CEA in cell lines and tumor tissues

The results by FACS showed that mAb CD66e could react with CEA on the surface of cells *in vitro*, but no differences were observed between WiDr, HT-29 and HT-29d cell lines. Their fluorescence intensities were 212, 215 and 207, respectively, (F value was 0.07, P=0.93).

CEA expressions among WiDr, HT-29 and HT-29d cell lines *in vitro* by IHC were not significantly different (χ^2 value was 2.311, P=0.315). However, HT-29d showed a slightly higher ratio of positive cells and stronger staining compared with WiDr and HT-29 in s.c. tumor, without significant difference (χ^2 value was 4.397, P=0.111). The ratio of positive cells and staining intensity showed no significant difference in liver metastases between HT-29 and HT-29d (χ^2 value was 0.823, P=0.364) (Table 3).

Expression of PI3-kinase

For detection of expression of PI3-kinase, we stained PI3-kinase with Abs against p85α and p110α subunits of PI3-kinase in WiDr, HT-29 and HT-29d cell lines. Immunochemical reactivity with polycolonal antibodies p85α and p110α subunits of PI3-kinase was present among all tumor cell lines *in vitro*. No significant difference was observed in positive cell ratio and staining intensity among WiDr, HT-29 and HT-29d cell lines (χ^2 value was 2.041, P=0.360).

PI3-kinase expression of HT-29d showed stronger staining intensity compared to WiDr and HT-29 in s.c tumor, and the ratio of positive cells of HT-29 and HT-29d was significantly higher than that of WiDr (χ^2 value was 6.161, P=0.046). HT-29d cells exhibited stronger staining and a slightly higher ratio than that of the parental HT-29 in liver metastatic tumor using mAb p85α and p110α (Table 3).

Table 2 uPA and PAI-1 level of different cell lines at 24 h

Cell	Level(pg/10^5 ell)	
	uPA($\bar{x}\pm s$)	PAI-1($\bar{x}\pm s$)
WiDr	16.7±5.8	1 613±90
HT-29	80.01±8.1[a]	2 650±1154[a]
HT-29d	87.0±20.8[b]	9 707±2450[b]

[a]P<0.05 *vs* WiDr, [b]P<0.05 *vs* HT-29.

Table 3 Expression of CEA and PI3-Kinase *in vitro* and *in vivo*

Cell lines and tumor	CEA		PI3-Kinase	
	Positive cell(%)	Intensity	Positive cell (%)	Intensity
WiDr	93±4.4	+++	99±0.8	++
HT-29	90±2.1	+++	98±1.6	++
HT-29d	94±3.0	+++	97±3.6	++
WiDr s.c[a].	29±2.6	++	14±0.8	+
HT-29 s.c.	31±4.6	++	22±0.8	+
HT-29d s.c.	40±6.0	+++	23±2.2	++
HT-29 Lm[b]	71±7.9	+++	28±0.8	+
HT-29d Lm	66±7.0	+++	34±0.8	++

a: s.c.: s.c. tumor, b: Lm: liver metastases.

DISCUSSION

Tumor metastasis in the liver is a complex process of tumor-cell invasion into normal tissue on the one hand and the anti-invasive mechanisms of host defense system on the other hand. Lodgment of tumor cells in a blood vessel is an important step of tumor cell invasion. The survival of cancer cells after they enter the circulation depends upon their abilities to successfully reach the microcirculation, invade the capillary endothelium, establish a microenvironment for subsequent vascularization and growth. In the present study the capacity of arrested tumor

cells in the liver was observed in HT-29d cell line. One hour after tumor cell injection via the mesenteric vein, the number of tumor cells arrested in the liver was very high. Most tumor cells were located in the portal vein and its surrounding hepatic sinusoids. Furthermore, at 24 hours, the number of tumor cells surviving in the liver was significantly decreased, most tumor cells had been removed from the liver, the survived cells were located mostly in parenchyma of the liver. The remaining tumor cells were likely to be able to proliferate and to develop metastatic colonies. The results suggested that not all cells that entered the liver via hematogenous dissemination produced metastasis, the majority of circulating tumor cells died and only a minority of the cells escaped from host defense systems (e.g. NK cell activity in nude rats), arrested and survived in the liver could develop metastasis.

Neoplasms are heterogeneous with regard to invasion and metastasis, they contain a variety of subpopulations of cells with different metastatic potentials[17]. The outcome of metastasis is to a large extent dependent on a selection process that favors the survival and growth of a special subpopulation of cells. Isolation of clonal populations of cells that differed from the parent neoplasm in their metastatic capacity supported the hypothesis that not all the cells in a primary tumor could successfully disseminate[18]. The liver is the first and primary site affected by the hematogenous spread in colorectal carcinoma. In the present study, although only two rats were injected variant HT-29c cells with three selections *in vivo* into the mesenteric vein, still they showed a higher metastatic potential. One of the two rats developed extensive hepatic metastases, and the other developed synchronous multiple organ metastases. Both rats developed mesenteric metastases. The variant HT-29d with four-cycle selections had a higher metastatic efficiency in nude rats. The taking rate of liver metastases was increased as compared with parental HT-29 cells (70 % versus 50 %), and variant HT-29b cells with two-cycles selections (70 % versus 60 %)[16]. Three of the ten rats developed lung metastasis, and extensive organs were synchronously involved in metastases. The results showed that HT-29d cells had more extensive metastatic potential than parental HT-29, variant HT-29b and HT-29c. The present study supported the hypothesis of metastatic heterogeneity. Pre-existing tumor cell subpopulations with heterogeneous metastatic capacity could be isolated from their parental neoplasms by means of cycles of selection *in vivo*. The availability of selected human colorectal cell lines and the *in vivo* model of metastasis in rats allows to search for the molecular determinants of human colorectal cancer metastases and for the establishment of relevant models to test novel therapeutic agents against colorectal cancer metastasis.

uPA is a serine protease with multiple actions that could enable it to play a role in cellular migration, tissue remodeling, and cancer spread[19]. Some investigators reported that patients with a high uPA or high PAI-1 level had a poorer prognosis for relapse than those with a low uPA or low PAI-1 antigen level. It was concluded that uPA and PAI-1 antigen levels in tumor tissue were an independent and useful prognostic marker in a variety of malignancies[20,21], especially breast cancer[22,23]. However, there have been no studies concerning the relation between uPA as well as PAI-1 level of high-metastatic cells and low-metastatic cells or non-metastatic cells. We analyzed the difference of uPA and PAI-1 level produced by WiDr (non-metastatic), HT-29 (low metastatic) and variant HT-29d cells (highly metastatic) in their supernatants by ELISA. It showed that variant HT-29d cells produced higher a levels of uPA and PAI-1 as compared with non-metastatic WiDr cells and low metastatic HT-29 cells. HT-29 cells produced higher levels of uPA and PAI-1 as compared with WiDr cells. uPA might act as an offensive mechanism for tumor cell invasion and metastasis. Although the functional role of PAI-1 in tumor biology has been unknown, PAI-1 might play a role in enhancing tumor spread by mechanisms involving in angiogenesis or promote tumor cell division[24]. Since PAI-1 is present in endothelial cells and platelets of normal tissues, increased PAI-1 levels may reflect a high degree of angiogenesis, which offers the possibility of tumor spread and metastasis. Our results showed that levels of uPA and PAI-1 in variant HT-29d cells were higher than that in HT-29 cells, suggesting that the process of metastasis might depend on the selection of tumor cell clones with increased expression of plasminogen activator, which was positively correlated with the metastatic potential of colorectal carcinoma cells in this study.

CEA has been implicated in the development of hepatic metastases from colorectal cancers, and has been described as an adhesion molecule either by Ca^{2+}-independent homophilic binding or heterophilic binding. The present results showed that CEA levels on cell surfaces *in vitro* were not different among WiDr, HT-29 and HT-29d cells. In CEA immunostaining, no difference was observed among the cell lines, s.c. tumor and liver metastases of WiDr, HT-29 and HT-29d cells, repectively. These results showed that CEA surface expression might not be correlated with the metastastic potential in this model. However, the secretion of CEA was significantly altered in metastatic cells. Moreover, other members of the CEA family might also be differently expressed in metastatic cells.

PI3-kinase is a heterodimer consisting of an 85-kDa regulatory subunit (p85), and a 110-kDa catalytic subunit (p110). The role of PI3-kinase in growth factor signaling pathways has been studied intensively[25]. Several reports have shown PI3-kinase was involved in signal transduction pathways associated with cell growth regulation, cell cycle progression, and cell survival[26]. Some studies showed increased cellular content of PI3-kinase products and also physical association of the enzyme with transmembrane receptor tyrosine kinases following stimulation by various growth factors, including hepatocyte growth factor[27,28] and insulin-like growth factor[29]. A recent research indicated the importance of PI3-kinase in increased cell motility stimulated by growth factors such as PDGF and hepatocyte growth factor[30]. However, these data do not indicate whether expression of PI3-kinase is associated with the metastatic potential of colorectal carcinoma cells. In this study, we investigated the PI3-kinase expression in colorectal carcinoma cell lines WiDr, HT-29 and HT-29d *in vitro* and in s.c. tumors and liver metastases of rats immunohistochemically. *In vitro*, non-metastatic WiDr cells, metastatic HT-29 cells and highly-metastatic vairant HT-29d cells all expressed PI3-kinase. No significant differences were found in positive cell ratio and staining intensity. In s.c. tumors, highly metastatic vairant HT-29d cells showed a stronger PI3-kinase expression in staining intensity and a higher ratio of positive cells compared to WiDr and HT-29 cells. In liver metastases, vairant HT-29d cells showed a stronger staining intensity and a higher positive ratio than that of parental HT-29 cells. These results suggest metastatic potential may positively correlate with synthesis of PI3-kinase in this *in vivo* model. The highly-metastatic HT-29d variant highly expresses PI3-kinase. The expression of PI3-kinase correlates with tumor development and metastasis, and it may be a late event of tumor development of colorectal carcinoma and may correlate with an invasive stage of cancer.

REFERENCES

1 **Schmitt M,** Wilhelm O, Janicke F, Magdolen V, Reuning U, Ohi H, Moniwa N, Kobayashi H, Weidle U, Graeff H. Urokinase-type plasminogen activator (uPA) and its receptor (CD87): a new target in tumor invasion and metastasis. *J Obstet Gynaecol* 1995; **21**: 151-165

2 **Gershtein ES,** Kushlinskii NE. Urokinase and tissue plasminogen activators and their inhibitor PAI-1 in human tumors. *Bull Exp Biol Med* 2001; **131**: 67-72

3 **Yamamoto M,** Ueno Y, Hayashi S, Fukushima T. The role of proteolysis in tumor invasiveness in glioblastoma and metastatic brain tumors. *Anticancer Res* 2002; **22**: 4265-4268

4 **Cho JY,** Chung HC, Noh SH, Roh JK, Min JS, Kim BS. High level of urokinase-type plasminogen activator is a new prognostic marker in patients with gastric carcinoma. *Cancer* 1997; **79**: 878-883

5 **Qin LX,** Tang ZY. The prognostic molecular markers in hepatocellular carcinoma. *World J Gastroenterol* 2002; **8**: 385-392

6 **Duffy MJ.** Urokinase plasminogen activator and its inhibitor, PAI-1, as prognostic markers in breast cancer: from pilot to level 1 evidence studies. *Clin Chem* 2002; **48**: 1194-1197

7 **Bouchet C,** Hacene K, Martin PM, Becette V, Tubiana-Hulin M, Lasry S, Oglobine J, Spyratos F. Breast cancer: Prognostic value of a dissemination index based on 4 components of the urokinase-type plasminogen activator system. *Pathol Biol (Paris)* 2000; **48**: 825-831

8 **Schmalfeldt B,** Kuhn W, Reuning U, Pache L, Dettmar P, Schmitt M,Janicke F, Hofler H, Graeff H. Primary tumor and metastasis in ovarian cancer differ in their content of urokinase-type plasminogen activator, its receptor, and inhibitors types 1 and 2. *Cancer Res* 1995; **55**: 3958-3963

9 **Minami S,** Furui J, Kanematsu T. Role of carcinoembryonic antigen in the progression of colon cancer cells that express carbohydrate antigen. *Cancer Res* 2001; **61**: 2732-2735

10 **Duffy MJ.** Carcinoembryonic antigen as a marker for colorectal cancer: is it clinically useful? *Clin Chem* 2001; **47**: 624-630

11 **Katada T,** Kurosu H, Okada T, Suzuki T, Tsujimoto N, Takasuga S, Kontani K, Hazeki O, Ui M. Synergistic activation of a family of phosphoinositide 3-kinase via G-protein coupled and tyrosine kinase-related receptors. *Chem Phys Lipids* 1999; **98**: 79-86

12 **Krasilnikov MA.** Phosphatidylinositol-3 kinase dependent pathways: the role in control of cell growth, survival, and malignant transformation. *Biochemistry (Mosc)* 2000; **65**: 59-67

13 **Khwaja A,** Lehmann K, Marte BM, Downward J. Phosphoinositide 3-kinase induces scattering and tubulogenesis in epithelial cells through a novel pathway. *J Biol Chem* 1998; **273**: 18793-18801

14 **Besson A,** Robbins SM, Yong VW. PTEN / MMAC1 / TEP1 in signal transduction and tumorigenesis. *Eur J Biochem* 1999; **263**: 605-611

15 **Keely PJ**, Westwick JK, Whitehead IP, Der CJ, Parise LV. Cdc42 and Rac 1 induce integrin- mediated cell motility and invasiveness through PI(3)K. *Nature* 1997; **390**: 632-636

16 **Vogel I**, Shen Y, Soeth E, Juhl H, Kremer B, Kalthoff H, Henne-Bruns D. A human carcinoma model in athymic rats reflecting solid and disseminated colorectal metastases. *Langenbecks Arch Surg* 1998; **383**: 466-473

17 **Morikawa K,** Walker SM, Nakajima M, Pathak S, Jessup JM, Fidler IJ. Influence of organ environment on the growth, selection, and metastasis of human colon carcinoma cells in nude mice. *Cancer Res* 1988; **48**: 6863-6871

18 **Dinney CP**, Fishbeck R, Singh RK, Eve B, Pathak S, Brown N, Xie B, Fan D, Bucana CD, Fidler IJ. Isolation and characterization of metastatic variants from human transitional cell carcinoma passaged by orthotopic implantation in athymic nude mice. *J Urol* 1995; **154**: 1532-1538

19 **Yamamoto M,** Ueno Y, Hayashi S, Fukushima T. The role of proteolysis in tumor invasiveness in glioblastoma and metastatic brain tumors. *Anticancer Res* 2002; **22**: 4165-4268

20 **Duffy MJ,** Maguire TM, McDermott EW, O'Higgins N. Urokinase plasminogen activator: a prognostic marker in multiple types of cancer. *J Surg Oncol* 1999; **71**: 130-135

21 **Duffy MJ.** Urokinase-type plasminogen activator: a potent marker of metastatic potential in human cancers. *Biochem Soc Trans* 2002; **30**: 207-210

22 **Gandolfo GM,** Conti L, Vercillo M. Fibrinolysis components as prognostic markers in breast cancer and colorectal carcinoma. *Anticancer Res* 1996; **16**: 2155-2159

23 **Janicke F,** Prechtl A, Thomssen C, Harbeck N, Meisner C, Untch M, Sweep CG, Selbmann HK, Graeff H, Schmitt M. Randomized adjuvant chemotherapy trial in high-risk, lymph node-negative breast cancer patients indentified by urokinase-type plasminogen activator and plasminogen activator inhibitor type 1. *J Natl Cancer Inst* 2001; **93**: 913-920

24 **Kaneko T,** Konno H, Baba M, Tanaka T, Nakamura S. Urokinase-type plasminogen activator expression correlates with tumor angiogenesis and poor outcome in gastric cancer. *Cancer Sci* 2003; **94**: 43-49

25 **Varticovski L,** Harrison-Findik D, Keeler ML, Susa M. Role of PI 3-kinase in mitogenesis. *Biochim Biophys Acta* 1994; **1226**: 1-11

26 **Divecha N,** Irvine RF. Phospholipid signaling. *Cell* 1995; **80**: 269-278

27 **Qiao H,** Saulnier R, Patryzkat A, Rahimi N, Raptis L, Rossiter J, Tremblay E, Elliott B. Cooperative effect of hepatocyte growth factor and fibronectin in anchorage-independent survival of mammary carcinoma cells: requirement for phosphatidylinositol 3-kinase activity. *Cell Growth Differ* 2000; **11**: 123-133

28 **Fan S,** Ma YX, Wang JA, Yuan RQ, Meng Q, Cao Y, Laterra JJ, Goldberg ID, Rosen EM. The cytokine hepatocyte growth factor / scatter factor inhibits apoptosis and enhances DNA repair by a common mechanism involving signaling through phosphatidyl inositol 3' kinase. *Oncogene* 2000; **19**: 2212-2223

29 **Gentilini A,** Marra F, Gentilini P, Pinzani M. Phosphatidylinositol-3 kinase and extracellular signal-regulated kinase mediate the chemotactic and mitogenic effects of insulin-like growth factor-I in human hepatic stellate cells. *J Hepatol* 2000; **32**: 227-234

30 **Yao J,** Morioka T, Oite T. PDGF regulates gap junction communication and connexin43 phosphorylation by PI 3-kinase in mesangial cells. *Kidney Int* 2000; **57**: 1915-1926

Edited by Zhu LH and Wang XL

P.O.Box 2345, Beijing 100023,China
Fax: +86-10-85381893
E-mail: wjg@wjgnet.com www.wjgnet.com

World J Gastroenterol 2003;9(11):2632-2634
World Journal of Gastroenterology
 ISSN 1007-9327

• CASE REPORT •

A case report of localized gastric amyloidosis

Dan Wu, Jian-Ying Lou, Jian Chen, Lun Fei, Gui-Jie Liu, Xiao-Yu Shi, Han-Ting Lin

Dan Wu, Jian-Ying Lou, Jian Chen, Lun Fei, Gui-Jie Liu, Xiao-Yu Shi, Han-Ting Lin, Department of General Surgery, Second Affiliated Hospital, Medical College of Zhejiang University, Hangzhou 310009, Zhejiang Province, China
Correspondence to: Dr. Dan Wu, Department of General Surgery, Second Affiliated Hospital, Medical College of Zhejiang University, Hangzhou 310009, Zhejiang Province, China. loujianying@163.com
Telephone: +86-571-87783580
Received: 2003-06-17 **Accepted:** 2003-07-15

Abstract

AIM: To elucidate the clinical and laboratory features of localized gastric amyloidosis via a rare report along with a review of related literatures.

METHODS: The clinical manifestations, laboratory results and surgical treatment of a female patient with localized gastric amyloidosis in our hospital were summarized. The relevant literatures were reviewed on the etiology, clinical features, diagnosis, treatment and prognosis of this disease.

RESULTS: The patient was lack of specific clinical manifestations and positive laboratory results. Prior to the treatment, she was suspected to be of malignization from gastric ulcer by both gastroscopy and endoscopic ultrasonography, which was denied by the gastric biopsy. The patient was treated with subtotal gastrectomy and clearance of perigastric lymph nodes. The postoperative pathological diagnosis determined the lesion to be the deposition of amyloid materials in the gastric mucosa, submucosa and blood vessel walls with intestinal metaplasia and atrophy of the gastric glands, in which no malignant tumor was found. Congo red staining with prior potassium permanganate incubation confirmed the AA type of amyloid in this case. Multiple biopsies from esophagus, remnant stomach, duodenum, colon and bone marrow in the follow-up survey showed no amyloidal deposition in these tissues and organs. Up to the present, no signs of recurrence have been found in this patient.

CONCLUSION: Localized gastric amyloidosis, being rare in incidence, should be considered in the differentiation of gastric tumors, in which biopsy is the only means to confirm the diagnosis. Currently, surgical resection of pathological tissue and circumambient lymph nodes may be a preferable therapeutic strategy for the localized amyloidosis to prevent possible complications. Although with a benign prognosis, gastric amyloidosis possesses a recurrent tendency as suggested by the literatures.

Wu D, Lou JY, Chen J, Fei L, Liu GJ, Shi XY, Lin HT. A case report of localized gastric amyloidosis. *World J Gastroenterol* 2003; 9(11): 2632-2634
http://www.wjgnet.com/1007-9327/9/2632.asp

INTRODUCTION

Amyloidosis is an abnormal intercellular deposition of insoluble proteins that share a remarkably similar and stable core structure of β sheets[1]. It may be resulted from a heterogeneous group of disorders and result in impairment or even dysfunction of involved organs. Generally, amyloidosis is more commonly manifested as a systemic involvement of multiple tissues and organs including the heart, liver, spleen, kidneys, lymph nodes, adrenals, thyroid, as well as many others. In contrast, the clinical implication of a single organ or tissue is relatively rare in this pathological condition[2-6], in which the amyloidal deposit confined to the stomach is extremely scarce in the previous literatures[7-9]. Recently, we have experienced and cured a case of localized gastric amyloidosis and now report it as follows.

CASE REPORT

A 50-year-old female was admitted to our hospital on Aug 23, 2002, with chief complaints of recurrent epigastric discomfort for 10 years and a newly-appeared dull pain in the upper abdomen for 4 months. The Inpatient No of this patient was 370655. Ever since being diagnosed as gastric ulcer and erosive gastritis with intestinal metaplasia 10 years ago by gastroscopy, she has not received any normal treatment except for long-term administration of metronidazole and omeprazole tablets herself. Prior to hospitalization, she was suggested to be of cancerization from gastric ulcer by gastroscopy at another medical institution. On admission, the patient displayed a good general condition and no positive signs including enlargement of superficial lymph node were revealed by physical check-up. Laboratory data showed negative results in the detection of serum anti-streptolysin O, rheumatoid factor and urine Bence-Jones protein. No abnormal signs were found on the chest radiograph. An upper gastrointestinal endoscopy revealed a gastric ulcer of 3 cm×1 cm in size that was located at the posterior wall of small curvature at the inferior part of gastric corpus. The margin of the ulcer was heaped up and rugged, the ambient mucosa was erosive, friable and prone to bleeding. The base of the ulcer was shaggy and covered with fibrinous layers. The malignization of this ulcer was suggested by endoscopic ultrasonography with low echo findings that the sick part of gastric wall was markedly and unevenly thickened, and some parts of the submucosa were infiltrated. On the contrary, a diagnosis of gastric amyloidosis, along with chronic gastritis with intestinal metaplasia, proliferation of lymphatic tissue and negative finding of *Helicobacter pylori*, was made by the biopsy of gastric mucosa. Exploratory laparotomy was carried out on Sep 3, 2002, in which no abnormal signs including enlargement of lymph node were found except that part of tumor-like, stiff and diffusely-thickened gastric wall was recognized at the inferior part of gastric corpus. Subtotal gastrectomy and clearance of perigastric lymph nodes were performed. Final pathological diagnosis determined the lesion to be the deposition of amyloidal materials in the gastric mucosa, submucosa and blood vessel walls with intestinal metaplasia and atrophy of the gastric glands, and no malignancies or other tumors were found. When stained with hematoxylin-eosin (Figure 1) and Congo red (Figure 2) respectively, the amyloidal deposits displayed as amorphous, homogeneous, translucent and acidophilic material under light microscope. The amyloidal protein was further proved to be

the AA type by the fact that it exhibited green birefrigence with Congo red staining under polarized light, which was disappeared when the specimens were pretreated with potassium permanganate. The patient got recovered and no complications occurred after operation. Multiple biopsies from esophagus, remnant stomach, duodenum, colon and bone marrow in the follow-up survey of 5 months post operation showed no amyloidal deposition in these tissues and organs. Up to the present, no signs of recurrence have been found in this patient.

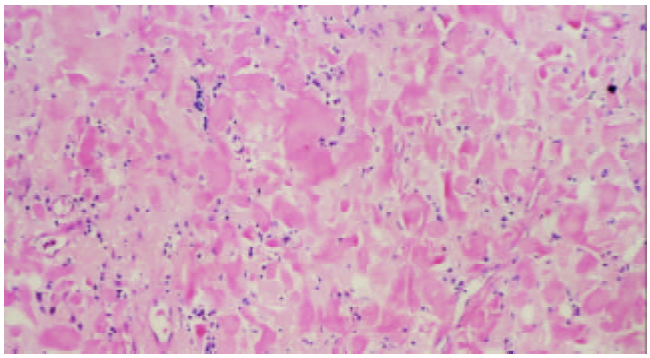

Figure 1 Stained with hematoxylin-eosin, amyloidal deposits in gastric mucosa and submucosa display amorphous, homogeneous, translucent and acidophilic materials under light microscope. (Magnification ×100).

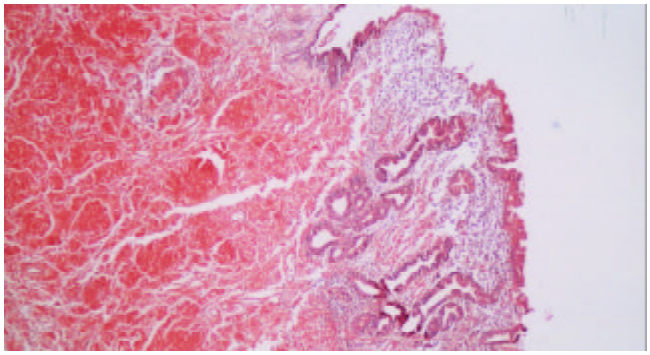

Figure 2 Stained with Congo red, deposition of amyloid could also be observed extending from gastric mucosa to submucosal layer. (Magnification ×50).

DISCUSSION

Amyloidosis, a disorder marked by the deposition of amyloid in various organs and tissues of the body, is usually associated with a variety of chronic diseases such as rheumatoid arthritis, tuberculosis, multiple myeloma and many others. Its classifications have been notoriously unsatisfactory for donkey' s years because the definition of this disorder was initially based on the morphological features, in which the amyloidosis was categorized according to the tissue distribution of amyloid (e.g. systemic versus localized amyloidosis) and the presence or absence of the identifiable predisposing factors (e. g. secondary versus primary amyloidosis). As the unique feature of amyloidal substance was, the component of the precursor protein that forms the fibrillar deposit has been now accepted as the basis for the classification of amyloidosis[10]. Up to the present, several types of the precursor proteins such as serum amyloid A (SAA), amyloid immunoglobulin light chains (AL), abnormal transthyretin (ATTR), β_2 microglobulin (β_2-M), amyloid precursor protein *etc* have been identified in amyloidosis.

Gastrointestinal tract is one of the regions to be commonly involved in the systemic amyloidosis. However, amyloidosis confined to the stomach is a rare occurrence. Although the detailed mechanism for the deposition of amyloidal materials in a specific tissue or organ remains unclear, the excessive accumulation of proteinaceous metabolites in local tissue might be a possible explanation[11]. The patient in our report suffered from gastric ulcer and gastritis for more than 10 years, which might cause a local disorder in protein metabolism and lead to localized deposition of amyloidal materials.

The clinical manifestations of amyloidosis were often uncharacteristic and varied with the involved organs. As for localized gastric amyloidosis, a variety of common gastrointestinal symptoms such as epigastric discomfort, poor appetite, hematemesis, hematochezia and gastric perforation might occur in the process of this disease because of involvement of local autonomic nervous system[7] and gastric wall structure damage[8]. Although localized gastric amyloidosis might associate with gastric malignancies in some cases[6,12,13], its non-tumorous form usually tended to be misdiagnosed as gastric tumors due to the likeness of gross appearance in endoscopic and imaging examinations. In this respect, biopsy has been suggested to be the only means to confirm the diagnosis[15]. The fact that pretreatment with potassium permanganate made biopsy specimens unstained by Congo red is helpful to determine the amyloidal component as AA type rather than AL protein. Scintigraphy with radiolabeled serum amyloid P (SAP) component could provide support for the diagnosis of amyloidosis in patients with negative histological studies[11] and distinguish localized lesion from systemic amyloidosis[14]. Besides, Immunohistochemical staining or immunofixation electrophoresis of biopsy specimens with the specific antibodies might guarantee the accurate classification of this disease[15-17].

The prognosis of amyloidosis depends on both the specific types of lesions and the involved organs. Systemic amyloidosis is usually with an unfavorable prognosis while the localized types of this disease such as the localized gastric amyloidosis have a relatively better outcome. Untreated AL amyloidosis often had the worst prognosis with a median survival time of one to two years[18], especially when cardiac involvement occurred. Patients with ATTR amyloidosis might survive up to 15 years from diagnosis but this time also varies with the specific mutation and the time of diagnosis - the younger the age of presentation the worse the outcome. However, the prognosis of patients with AA type was affected mainly by the underlying conditions[1,15]. Currently, there is no specific therapy for systemic amyloidosis. The treatment strategy has been directed both to support the affected organs and to deal with the underlying specific disease[19] in an attempt to reduce the deposition of amyloidal substances and improve prognosis, in which several supportive protocols and chemotherapeutic drugs including melphalan, iodinated anthracycline 4-iodo-4-deoxydoxorubicin, dimethylsulfoxide and colchicines have been widely used, although their effectiveness in ameliorating this disease has remained to be determined[15]. With the advances in molecular biology, some promising attempts have been made to reduce inflammatory response and amyloidal deposits by blocking the signal conduction of RAGE-NF-κB in monocytes/macrophages[20]. In patients with localized amyloidosis, thorough resection of the foci and their circumambient lymph nodes as performed in our case is probably the preferable therapeutic modality and the key measures to prevent postoperative recurrence. Up to the present, no signs of recurrence have been found in the follow-up survey of our patient.

REFERENCES

1 **Khan MF**, Falk RH. Amyloidosis. *Postgrad Med J* 2001; **77**: 686-693
2 **Kurokawa H**, Takuma C, Tokudome S, Yamashita Y, Kajiyama

M. Primary localization amyloidosis of the sublingual gland. *Fukuoka Igaku Zasshi* 1998; **89**: 216-220
3 **Aouda A**, Toyozaki T, Saito T, Yorimitsu K, Miyazaki A, Deguchi F, Inagaki Y. A case of primary cardiac amyloidosis with amyloid A protein. *Kokyu To Junkan* 1993; **41**: 89-92
4 **Matsui H**, Kato T, Inoue G, Onji M. Amyloidosis localized in the sigmoid colon. *J Gastroenterol* 1996; **31**: 607-611
5 **Hauben E**, Fierens H, Heylen H, Van Marck E. Localized amyloid tumour of the duodenum: a case report. *Acta Gastroenterol Belg* 1997; **60**: 304-305
6 **Aoyagi K**, Koufuji K, Yano S, Murakami N, Miyagi M, Koga A, Takeda J, Shirouzu K. Early gastric carcinoma associated with amyloidosis: a case report. *Kurume Med J* 2002; **49**: 153-156
7 **Zheng W**, Song S, Zhu Q, Tan H, Li P, Jiang Y. Local amyloidosis of stomach. *Zhonghua Waike Zazhi* 1998; **36**: 415-416
8 **Bjornsson S**, Johannsson JH, Sigurjonsson F. Localized primary amyloidosis of the stomach presenting with gastric hemorrhage. *Acta Med Scand* 1987; **221**: 115-119
9 **Macmanus Q**, Okies JE. Amyloidosis of the stomach: report of an unusual case and review of the literature. *Am Surg* 1976; **42**: 607-610
10 **Husby G**. A chemical classification of amyloid. Correlation with different clinical types of amyloidosis. *Scand J Rheumatol* 1980; **9**: 60-64
11 **Tan SY**, Pepys MB. Amyloidosis. *Histopathology* 1994; **25**: 403-414
12 **Goteri G**, Ranaldi R, Pileri SA, Bearzi I. Localized amyloidosis and gastrointestinal lymphoma: a rare association. *Histopathology* 1998; **32**: 348-355
13 **Hayashi I**, Muto Y, Fujii Y, Katsuda Y. Primary amyloidosis associated with early gastric carcinoma (IIb like IIa type) diagnosed by preoperative gastric biopsy-a case report. *Gan No Rinsho* 1983; **29**: 1686-1692
14 **Hachulla E**, Grateau G. Diagnostic tools for amyloidosis. *Joint Bone Spine* 2002; **69**: 538-545
15 **Falk RH**, Comenzo RL, Skinner M. The systemic amyloidoses. *N Engl J Med* 1997; **337**: 898-909
16 **Abraham RS**, Katzmann JA, Clark RJ, Bradwell AR, Kyle RA, Gertz MA. Quantitative analysis of serum free light chains. A new marker for the diagnostic evaluation of primary systemic amyloidosis. *Am J Clin Pathol* 2003; **119**: 274-278
17 **Linke RP**, Nathrath WBJ, Eulitz M. Classification of amyloid syndromes from tissue sections using antibodies against various amyloid fibril proteins: report of 142 cases. In: Glenner GG, Osserman EF, Benditt EP, Calkins E, Cohen AS, Zucker-Franklin D, eds. Amyloidosis, 1986. *New York: Plenum Publishers* 1986: 599-605
18 **Kyle RA**, Gertz MA. Primary systemic amyloidosis: clinical and laboratory features in 474 cases. *Semin Hematol* 1995; **32**: 45-59
19 **Skinner M**. Amyloidosis. In: Lichtenstein LM, Fauci AS, eds. Current therapy in allergy, immunology, and rheumatology. 5th ed. St. *Louis: Mosby-year Book* 1996: 235-240
20 **Yan SD**, Zhu H, Zhu A, Golabek A, Du H, Roher A, Yu J, Soto C, Schmidt AM, Stern D, Kindy M. Receptor-dependent cell stress and amyloid accumulation in systemic amyloidosis. *Nat Med* 2000; **6**: 643-651

Edited by Wang XL